THE UNIVERSITY OF NEWCASTLE UPON TYNE

DEPARTMENT OF MINING ENGINEERING

ROCK CUTTING MECHANICS RELATED TO THE DESIGN OF PRIMARY EXCAVATION SYSTEMS

by

HUW R. PHILLIPS

A thesis submitted for the degree of
Doctor of Philosophy in the Faculty
of Applied Science

OCTOBER, 1975.

CONTENTS

LIST OF ILLUSTRATIONS

ACKNOWLEDGEMENTS

The experimental work described in this thesis was undertaken in the Rock Mechanics Research Laboratories of the Department of Mining Engineering, University of Newcastle upon Tyne and the support and encouragement given by Professor E.L.J. Potts, Head of Department, is acknowledged with gratitude.

Professor F.F. Roxborough, University of New South Wales (formerly Reader in Mining Engineering, University of Newcastle) introduced me to this subject and I thank him for his encouragement and enthusiastic direction of this project.

The valuable assistance provided by Mr. Keith Hewitt, a postgraduate research student in the Department, and by several other colleagues and associates is much appreciated and gratefully acknowledged.

A special word of thanks is due to Mr. Tom Pollock, Workshop Superintendent, who provided both a technical service and a reliable source of advice.

The author would also like to thank Mr. P.A. Gillanders, Laboratory Supervisor, and his staff for their help in the preparation and printing of this thesis.

The research described in this thesis is part of an investigation into the cutting characteristics of several rock formations sponsored by the Transport and Road Research Laboratory of the Department of the Environment.

INTRODUCTION

Estimates of the future need for tunnelling activity in this country are of necessity tenuous, but a recent survey (1) predicts a threefold increase during the next decade. It is reasonable to assume that, where ground conditions permit, the use of mechanised systems to excavate these tunnels will be considered.

The decision to utilize machines in place of labour intensive cyclic tunnelling systems is normally based on their relative costs. A tunnelling machine, while representing a considerable capital investment, eliminates the wages and uncertainties associated with a large labour force. In addition, tunnelling activity within urban areas is subject to environmental constraints. The use of explosives to fragment the rock can cause inconvenience, while the irregular profile obtained, together with the damage caused to adjacent strata, can lead to surface subsidence.

During the last fifteen years machines have, on several occasions, been used to bore development tunnels at metaliferrous mines (2). At the same time the successful introduction of coal winning machinery has ensured the need for, and the acceptance of, mechanised roadway drivages in coal mines.

Although the design of tunnelling machines has developed substantially during the last twenty years a complete understanding of the action on which these designs are based has yet to be achieved.

This thesis is concerned with a detailed investigation into fundamental aspects of excavating Bunter Sandstone and Magnesian Limestone by drag picks and rotary cutters. These rocks were chosen because they appear at shallow depth and in considerable thicknesses throughout large parts of the Midlands and North of England. They are, therefore, of considerable interest to tunnelling engineers operating in these areas.

In order to maintain the experimental work at a manageable size a partial factorial approach, proposed by Protodyakonov (3), is used for the design of the experiments.

Existing theories of rock cutting are reviewed and a simple mathematical model of the action of a disc cutter is proposed. Experimental data from both pick and disc cutting is compared with theoretical predictions.

1. OBJECTIVES OF RESEARCH

Tunnels have already been driven in Bunter Sandstone using machines. Disc cutters were used for boring the Second Mersey Tunnel (4) and drag picks have also been successfully applied to machine drivages in both Birmingham (5) and Liverpool (6). Field trials of the Greenside tunnelling machine were undertaken in Magnesian Limestone at Bullwell Quarry, Nottinghamshire (7) and the initial trials of the 5.5m diameter N.C.B. tunnelling machine were in a hard, partly dolomotised limestone (8). So the applicability of mechanised tunnelling systems to these two rocks is not the primary concern of this study.

While improvements in the design of tunnelling machines have largely been a matter of learning by experience, there is good evidence to show that even a modest research effort can lead to substantial improvements in the design and performance of similar machines (9)(10)(11).

The purpose of this investigation is to provide scientific data of value to the design of rock tunnelling machines. The programme of work involves studies on aspects of rock cutting mechanics known, or believed, to be of a fundamental nature. These are outlined below.

1.1 Drag Picks

The performance of simple chisel picks operating both singly and in array is investigated. From these results it has been possible to establish well founded relationships between accepted parameters of performance and the principal variables. Rock wetness was believed to be important in this study and many of the experiments have been undertaken in both the dry and wet conditions.

These experiments were conducted using sharp picks for each test. This was done to avoid complications in the analysis of data resulting from the consequences of progressive tool wear.

1.2 Drag Picks of a Complex Shape

Tools of simple wedge configuration have been shown by experiment and mathematical analysis to have a higher efficiency than picks of a more complex geometry (12)(13). Yet, the simple wedge is rarely encountered in practice. Tools having a ridged front and vee bottom are more often preferred. The concentration of stress at the point that such a pick type provides must aid its penetration of the rock face. Since most complex shapes of symmetrical profile can be reduced to combinations of different front ridge and vee bottom angles, independent studies of these two shape variables were undertaken. Asymmetry is not usually applied to pick designs, but there have been applications in coal mining of tools having a single side rake. This variable is, therefore, also investigated.

Round nosed picks and other contoured shapes which do find application, are designs which to some extent are a compromise of the wedge and pointed profiles. They do have the further advantage of presenting a more stable shape which suffers less from the effects of wear in an abrasive environment (14).

1.3 Disc Cutters

The performance of disc cutters operating in both the unrelieved and relieved cutting modes is studied. The principal geometrical variables of disc diameter and edge angle are examined together with an operational parameter - cutting speed. In the Bunter Sandstone the tests were all undertaken in both dry and wet rock.

1.4 Disc Malfunction

The operation of a disc cutter relies on a free rolling action, which, if impeded, is likely to produce a definite change in the mode of cutting. A collapsed or siezed bearing could prevent the disc from

rolling and thereby create what is equivalent to a drag pick having a ridged front developing into a negative radiused, back clearance angle.

A disc was deliberately stalled and thereafter used to cut Bunter Sandstone. Its performance is contrasted with that for the free disc. Since it is under such conditions that discs will suffer the greatest damage from abrasion the rate of disc wear during this experiment was noted.

1.5 Roller Cutters

Roller cutters, while being similar in design to disc cutters, are provided with wedge shaped teeth disposed around their circumference. They resemble bevel gear wheels and, as they rotate, each tooth attempts to mesh with the rock. During this process a series of chips are disengaged from the surface of the rock.

The performance of a single roller cutter of fixed geometry working in both the relieved and unrelieved cutting situations is studied.

2. PREVIOUS RESEARCH IN ROCK CUTTING

The mechanical excavation of soft and medium strength rock is normally performed by drag picks, discs or roller cutters. All three types are designed to disengage relatively small pieces from the rock mass.

Most industrialised countries have to some extent engaged in research into improving the performance of rock cutting tools. The nature and extent of tunnelling and mining activity in each country has determined the direction and scope of the individual research programmes.

For example, in Britain the emphasis has been on coal mining and soft ground tunnelling; hence the majority of research effort has been concerned with the design of drag picks.

2.1 Experimental Work with Drag Picks

In this country research into the performance of picks has been carried out at the Mining Research and Development Establishment of the National Coal Board, the Department of Mining Engineering at the University of Newcastle upon Tyne and the Transport and Road Research Laboratory of the Department of the Environment.

Research by the National Coal Board has been conducted in coal and coal measures rock. The effects of varying the rake and clearance angle of a pick have been studied by O'Dogherty (15) and tools of different profiles were tested by Robinson, Pomeroy and Dalziel (16)(17). The operational variables - depth of cut and spacing between adjacent tools have been investigated by Barker (18). Much of this research has been summarised in a monograph by Evans and Pomeroy (19).

Research into the mechanics of rock cutting began at the University of Newcastle upon Tyne with a study of the ploughability of coal (20)(21).

This was followed by a programme of research into the cutting characteristics of several rock types (22). Special emphasis was placed on obtaining an understanding of the mechanisms of tool wear (14)(23). A preliminary study of the mechanical cutting characteristics of the Lower Chalk was undertaken on behalf of the Transport and Road Research Laboratory by Roxborough and Rispin (24).

The Transport and Road Research Laboratory continued this investigation by constructing and operating a 1m diameter, pilot scale tunnel boring machine (25)(26). This provided a link between the laboratory studies at Newcastle and a full scale 5m diameter experimental machine operating at Chinnor, Oxfordshire (27).

Cook, Joughin and Wiebols (28) working in South African have experimented with a variety of tungsten carbide picks. These were used to cut deep and narrow slots in core samples of quartzite. The results of these experiments were used as design data for the prototype of a reef cutting machine. This machine under- and overcuts the gold bearing reef to allow selective removal of rock from the mine.

2.2 Theoretical Models of the Cutting Action of Picks

The cutting action of a pick is to produce a series of rock chips. At the inception of each chip the behaviour of the pick may be likened to that of a wedge penetrating a buttock of rock. Several theories have been postulated to explain the post-penetration failure of this buttock.

Evans (29) has produced an expression relating the penetration force required by a sharp wedge to the tensile strength of the rock and the geometry of the cutting situation. By applying the work of Dalziel and Davies (30) he has extended his theory to include the case of blunt picks (31). In addition, Evans has recently used his tensile theory of failure to estimate the optimum spacing between adjacent tools (32).

Merchant (33) has developed a semi-empirical model to explain the process of machining metals. It is based on the assumption that the material will fail in shear and that the shear plane passes through the tip of the tool. The orientation of this shear plane is determined by the wedge angle of the cutting tool and the coefficient of friction between the tool and the cut material. Shuttleworth (34) used a modified form of Merchant's theory to predict the forces acting on a coal plough. By empirically determining the shear angle for soft coal he obtained a good correlation between theoretical predictions and experimental results. However, observation of the process of cutting the more brittle coals and rocks has shown no sign of the plastic deformation implicit in Merchant's theory (19).

A theory, similar to that of Merchant, has been derived by Nishimatsu (35). Assuming a brittle mode of failure he describes a "primary crushed zone" when the tool first enters the rock and the subsequent failure along a shear plane. The equation for the cutting force contains empirical constants which must be determined for each rock type.

The mechanics of chip formation by drag picks have been studied by Hardy and Fairhurst (36). Using a finite element approach they have predicted the force necessary to initiate failure of the rock and the direction in which cracks will develop. The analysis is dependent on knowing the "work of fracture" and the strain energy release rate of the material being excavated.

2.3 Research into the Performance of Disc Cutters

The effects of varying the geometry of disc cutters have been studied, in this country, by the National Coal Board and the University of Newcastle. Dalziel (37) has carried out experiments in both Darley Dale and Pennant Sandstone and Teale (38) has contrasted the cutting characteristics of disc and roller cutters. Roxborough and Rispin (24), working in chalk, used two discs of different edge angles.

Research in the United States has been concentrated in two centres, i.e. the U.S. Bureau of Mines, Twin Cities, Minnesota and the Colorado School of Mines. Bruce, Morrell and Larson (39)(40) have provided a useful insight into the performance of discs. However their programme of experimental work tended to emphasis rock type rather than disc geometry as the principle variable.

Rad and Olson (41), also working at the Bureau of Mines, have carried out experiments to determine the optimum spacing between adjacent discs operating in an array. Rad has extrapolated the results of these laboratory tests to provide the basis of a simple in-situ measurement of machine performance (42).

Research at the Colorado School of Mines has led to the development of an index of rock machineability. Ross and Hustralid, using a linear cutting machine, have tested a "standard" disc in rock recovered from several machine driven tunnels. Correlation of the laboratory results to the recorded performance of the tunnelling machines has led to the establishment of this index (43).

Laboratory studies of the excavation, by disc cutters, of three types of Japanese rocks have been undertaken (44). A relationship between the measured value of the rolling force applied to the disc and the geometrically calculated arc of contact between disc and rock was obtained.

Although the dynamic behaviour of a disc cutter is complex its primary action is similar to that of a wedge penetrating a rock surface. Hence several of the models proposed for drag picks are also applicable to discs. Evans and Murrell (45) have produced an expression for the thrust required to penetrate coal or weak rock. They assumed the contact pressure on the wedge to be equal to the unconfined compressive strength of the material.

The more difficult problem of discontinuous penetration of a brittle material has been investigated by Paul and Sikarskie (46). They arrived at the conclusion that the thrust on a wedge is proportional to both the

compressive strength of the material and the depth of penetration at the formation of the first chip.

Calculations have been made to determine the energy requirements and optimum ratio of thrust/torque of full face tunnel boring machines. Gaye (47) has derived an expression for the energy required per unit volume of rock excavated by an array of discs. A theoretical analysis, by Ross and Hustralid (48), of the thrust and torque requirements of a machine has shown that for a given diameter of tunnel there is a fixed ratio between the two.

2.4 Previous Research Using Roller (Gear) Cutters

Roller cutters in the form of tri-cone bits, have been extensively used in the drilling of oil-wells. In addition there are several examples of their application in mechanised tunnel drivages (2)(8). However, due to their high cost they have, in general, been replaced by disc cutters and little research has been conducted into their mode of operation or likely performance. Nevertheless roller cutters do have the potential to excavate hard rock, at present beyond the scope of disc cutters.

Roxborough and Rispin (24) have shown that a roller cutter may be just as efficient as a disc when excavating chalk. However, when using roller cutters consideration must be given to the likely change in the mode of operation when the depth of cut exceeds the tooth length. Teale (38) analysed the geometry of simple roller cutters in order to eliminate inefficient tool configurations from his programme of experimental work. Shepherd, O'Dogherty and Price have produced internal reports to the National Coal Board on the forces and energies involved when using roller cutters to fragment both rock and concrete (49)(50).

Takoaka et al (51) have carried out tests using both gear and spherical cutters. The effects of varying the tip pitch and the vertical load were studied. A theoretical analysis of the action of a gear cutter was used to predict the applied tractive force and a good correlation was obtained between the predicted and measured values.

3. SOME GEOLOGICAL FEATURES OF THE PERMO-TRIASSIC SYSTEM

Classification of the New Red Sandstones is difficult hence the rocks which overlie the coal measures and underlie the Jurassic are collectively termed the Permo-Triassic. In Britain these deposits consist of sandstones, pebble beds, marls, some evaporites and the magnesian limestones. The system outcrops over a large part of the Midlands, and as can be seen from Figure 1, divides to the North with a branch lying on each side of the Pennines. There is a further extension of the outcrop towards the South West of England, with a brief coastal occurance in South Wales. Other sporadic outcrops which occur, particularly in the North West, include the well known St. Bees sandstone of Cumberland.

3.1 The Triassic Rocks

The Triassic succession in this country is:-

KEUPER	Rhaetic (shales and thin limestones)
	Keuper Marl
	Lower Keuper Sandstone
BUNTER	Upper Mottled Sandstone
	Pebble Beds
	Lower Mottled Sandstone

The name "Trias", however, implies a threefold arrangement and this is in fact the case on the Continent where a group of limestones, the Muschelkalk, appears.

3.1.1 The Bunter Sandstone

The Bunter occurs in great thicknesses in Shropshire, Cheshire and South West Lancashire where it reaches its maximum thickness of nearly 1000 metres. Variations in thickness are shown in Figure 2. Its distinctive red colouration comes from the presence of iron oxides, a thin film of which coats each constituent quartz grain.

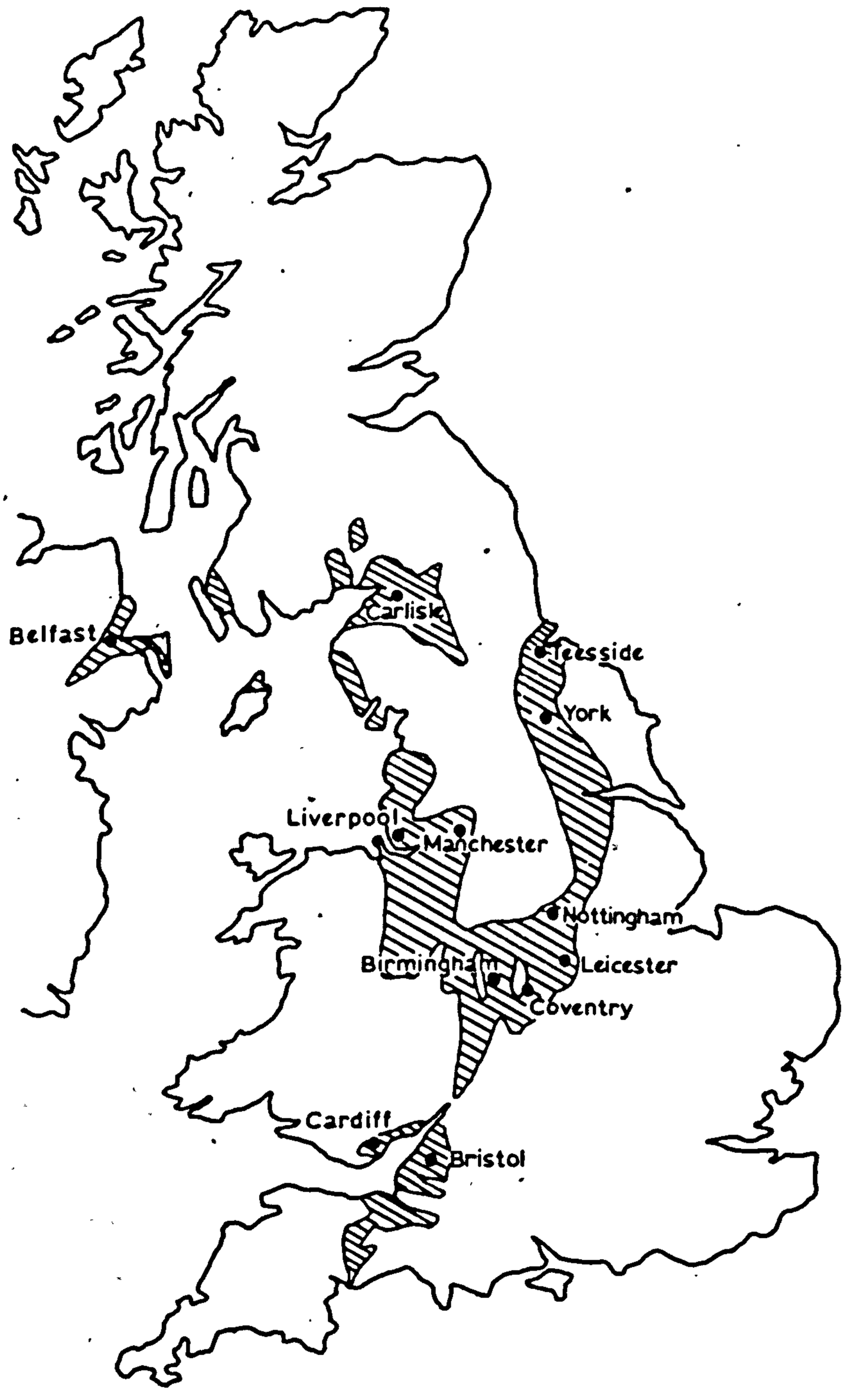

FIGURE 1 - OUTCROP OF THE NEW RED SANDSTONES

The Bunter, apart from providing excellent building stone, forms the most important acquifer of the Midlands. A good general description of the Bunter Sandstone is provided by Blyth's text on Geology for Engineers (52).

3.2 The Permian

The Permian was first classified in the U.S.S.R. and takes its name from the province of Perm in Russia. In central Europe it consists of two sub-systems, the Zechstein and the Rotsliegendes but in Britain only the Zechsteincan be satisfactorily defined. The Permian succession in this country, as given by Rayner (53) is:-

Upper Permian Marls, with evaporites.
Upper Magnesian Limestone.
Middle Permian Marl, with evaporites.
Middle Magnesian Limestone.
Lower Magnesian Limestone.
Marl Slate.
Basal Yellow Sands.

3.2.1. Magnesian Limestone

Magnesian Limestone outcrops in Co.Durham, Yorkshire and Nottinghamshire and forms a narrow band running due south from the mouth of the River Tyne to a point just north of the city of Nottingham. The maximum thickness of 500m occurs in Co.Durham and the beds become progressively thinner towards the south. Indeed the Upper Magnesian Limestone is absent in most of Southern Yorkshire and Nottinghamshire, with the upper portion of the Lower Magnesian Limestone forming the bulk of the division. The Geological Memoirs for Nottinghamshire and South Yorkshire (54)(55) go so far as to consider the Lower Magnesian Limestone of Nottinghamshire to be the direct equivalent of the Upper Limestone of Co.Durham.

FIGURE 2 - BUNTER SANDSTONE ISOPACHYTES (metres)

3.3 Experimental Samples

Acknowledging that for any rock considerable variations in strength and character occur with both depth and location, it was considered essential that the experimental work should be undertaken using samples of consistent quality and strength. Furthermore, the test specimens should represent the rock in something close to its strongest condition, so that experimental data will reflect the probable maximum requirements for mechanical excavation.

Suitable sources of rock, complying with these broad specifications, were found after reference to the following authorities:-

Institute of Geological Sciences.
Institute of Quarrying.
Lancashire County Council.
Mersey and Weaver River Authority.
Messrs. Mott, Hay and Anderson.
National Coal Board.
N.W. Road Construction Unit.
S.E.L.N.E.C. - Passenger Transport Authority.
U.M.I.S.T.
University of Nottingham.
Water Resources Board.

3.3.1. Test Specimens of Bunter Sandstone

Some of the above organisations provided core samples taken from various locations and from different horizons in the Bunter series. Tests, involving standard and well known procedures, were undertaken on fifty six sections of core. From these results, Hewitt (56) has shown that one source of Bunter, the Woolton Quarry of Liverpool Cathedral Contractors Ltd., produces rock which, on all of the strength property bases, is of higher than average strength. The following percentages represent the amount of rock tested which had a lower value for the specified parameter than the Woolton rock:-

Compressive Strength	=	95%
Tensile Strength	=	85%
Cone Indentor Hardness	=	90%
Shore Hardness	=	88%
Average Grain Size	=	87%
Quartz Content	=	89%
Bulk Density	=	50%

Despite the acute shortage of this high quality and durable building stone, the Woolton Quarry (Grid Reference SJ 4230,8700) provided sufficient prepared blocks to complete all the experiments.

3.3.2 Test Specimens of Magnesian Limestone

Since Magnesian Limestone is used extensively for building stone, for the production of lime and, in a crushed form, for road-metal the outcrop abounds with quarries from which blocks of a suitable size can be recovered. Samples of the Upper Magnesian Limestones were rejected as being unsuitable for cutting tests since they contain large calcite crystals. A source of good quality Lower Magnesian Limestone was, however, located at the Vale Road Quarry, Mansfield Woodhouse (Grid Reference SK 5310,6320). Although this rock is normally crushed for road-stone Cast Development Ltd. supplied sufficient blocks for the experimental work to be undertaken.

3.4 Petrography and Mineralogy of the Experimental Samples

Dr. P.K. Harvey of the University of Nottingham has undertaken analyses of rock samples from both the Bunter and Magnesian Limestone quarries. The following comments are abstracted directly from his report.

3.4.1 Petrography of the Bunter Sample

The sample is a water lain deposit and can be classified as a mature lithic arenite in the scheme of Chen (57). It consists

primarily of grains of quartz and feldspar together with rock fragments. These are uniformly distributed to produce a homogeneous rock with an isotropic fabric. The grains are well sorted and sub to well rounded.

The quartz grains are mainly monocrystalline, though some 20% are polycrystalline and frequently show strained and sutured aggregates of quartz exhibiting a planar fabric. The feldspar grains present are mainly orthoclase, though some microcline and albite are also present.

The rock fragments are of two types:-

(i) pollycrystalline quartz grains,
(ii) generally rounded grains of shales or mudstones, some of them up to 1.5mm diameter, together with less common impure siltstones which occur with the original clay matrix recrystallised to sericite.

Accessory minerals include a few detrital muscovite flakes, yellow and green tourmalines, magnetite and rare zircon. When viewed under an electron microscope the rock is seen to be indurated by quartz overgrowths on the quartz grains and feldspar overgrowths on the feldspar. In addition many of the grains are coated with a veneer of limonite.

3.4.2 Petrography of the Magnesian Limestone Sample

This rock is petrographically quite simple, consisting almost entirely of euhedral to sub-hedral grains of pale brown to colourless dolomite. When examined under an electron microscope the faces of the dolomite grains are seen to be well developed and form almost perfect rhombs. Rare quartz grains, a little clay and iron oxides occur as accessory phases, making up less than 5% of the rock.

3.5 Chemistry of the Samples

The major element analyses are given in Table 1, the elements being quoted conventionally in weight percentage of the oxides.

TABLE 1

CHEMICAL COMPOSITION OF THE TWO ROCK SAMPLES

	Bunter Sandstone (%)	Magnesian Limestone (%)
SiO_2	91.07	1.53
Al_2O_3	4.03	1.23
K_2O	2.41	0.10
Fe_2O_3	0.93	0.49
FeO	0.36	-
MgO	0.36	19.56
Na_2O	0.31	0.17
H_2O+	0.15	0.15
TiO_2	0.13	0.02
CaO	0.06	30.78
MnO	0.03	0.11
P_2O_5	0.03	0.01
CO_2	-	45.48
Total	99.87	99.63

All elements except FeO, Na_2O, H_2O+, and Co_2 were determined by X-ray spectrometry using the fusion method of Harvey et al (58). FeO was determined by dichromate titration and Na_2O by X-ray spectrometry using the resin pellet technique of Leake (59). H_2O+ was measured by the Penfield method and Co_2 by stoichiometry assuming all the calcium and magnesium to be bound as carbonates.

3.5.1 Mineral Composition

Direct measurements of the proportions of the different minerals (modal analysis) is complicated by the large number of point counts necessary to determine the minor constituents with any accuracy. Normative estimates, derived from the chemical analysis, are accurate for minerals of fixed composition but are of little value for minerals with non-stoichiometric compositions.

The following mineral and grain composition of Bunter Sandstone, represented in volume percentages, is tentative and based on a combination of both modal and normative analysis.

	%
Monocrystalline Quartz	63
Polycrystalline Quartz	19
Feldspars	12
Shale/Mudstone Fragments	4
Iron Oxides	1.5
Minor Minerals	0.5
	100.0

The chemistry of the Magnesian Limestone confirms, in general, its dolomitic composition. However, the calcium to magnesium ratio is higher than the theoretical value for a true dolomite. Hence this rock may be precisely defined as a dolomitic limestone. The small amounts of silica, aluminium and alkalis indicate some three percent of quartz and clay impurity.

4. MECHANICAL AND PHYSICAL PROPERTIES OF BUNTER SANDSTONE AND MAGNESIAN LIMESTONE

In order to define the properties of the rock on which the main programme of experiments was carried out, specimens recovered from the two chosen quarries have been subjected to a broad range of standard tests. As cutting experiments were undertaken in both dry and wet rock the principal physical tests were also carried out for both rock conditions.

4.1 Moisture Content

Experiments were undertaken to determine the percentage by weight of water in saturated samples of the two rocks. Ten cylindrical specimens of each rock were weighed and measured. The nominal values of diameter and length were 41.3 and 82.6mm respectively. Thereafter they were totally immersed in fresh water under a vacuum of 710mm Hg., until they achieved a constant weight.

TABLE 2

SATURATED MOISTURE CONTENT AND DRY BULK DENSITY

	Bunter Sandstone	Magnesian Limestone
Water Content Wt. (%)	10.26 ± 0.47	6.52 ± 0.42
Dry Bulk Density (g/cc)	2.03 ± 0.02	2.39 ± 0.22

This moisture content, which is on a weight basis, can be used to calculate the Apparent Porosity of the rock by multiplying it by the Dry Bulk Density.

Apparent Porosity of Bunter Sandstone = 20.83%

Apparent Porosity of Magnesian Limestone = 15.59%

4.2 Grain Density and True Porosity

Bulk density does not reflect the density of the basic material from which the rock is composed since integral rock samples include natural voids. Grain density is a measure of the density of the constituent materials and is determined by crushing a rock specimen down to grain size. Thereafter a sample of this material is weighed and its volume calculated.

The Apparent Porosity is a volumetric measure of interconnected voids in the rock. Isolated voids can occur however and the apparent porosity will be less than the true porosity. This latter can be determined from the Grain Density (G) and Bulk Density (B) thus:

$$\text{True Porosity} = 100. \frac{G - B}{G} \%$$

Values quoted in Table 3 are each the mean of three replications.

TABLE 3

GRAIN DENSITY AND TRUE POROSITY

Parameter	Bunter Sandstone	Magnesian Limestone
Grain Density	2.63 g/cc	2.84 g/cc
True Porosity	22.84 %	15.85 %

4.3 Uniaxial Compressive Strength

The strength of rock cannot be defined by a single appropriately dimensioned numerical value. Heterogeneity always exists in small or large measure and therefore a strength value must be statistically qualified. Furthermore the strength of a rock is greatly influenced by the size and to a lesser extent the shape of the test specimen. Test procedures should also be defined since the testing machine platens and the rate of applying the load can have a major influence on measured strength.

It is necessary therefore to undertake a number of tests under standardised conditions to provide a statistically reliable result. The widely accepted standard is to use cylinders of rock having a length to diameter ratio of 2. (61), to use dry steel platens, and to apply the stress at the nominal rate of 100 p.s.i. (0.69 MN/m^2) per second. These standards of procedure were adopted.

Since neither rock exhibited clearly defined bedding planes the test specimens were produced by drilling in random convenient directions. Mean strength values thereby embrace any possible directional influence.

Half of each batch of specimens was oven dried at 105°C for one week and the remainder vacuum saturated for one hour. All specimens were 82.6mm high and 41.3mm in diameter. The results for both dry and saturated conditions are given in Table 4.

TABLE 4

UNIAXIAL COMPRESSIVE STRENGTHS

Bunter Sandstone		Magnesian Limestone	
Dry MN/m^2	Saturated MN/m^2	Dry MN/m^2	Saturated MN/m^2
49.44	41.93	78.3	103.7
49.74	40.44	87.8	87.8
48.68	39.99	61.6	70.0
48.99	39.92	106.0	59.0
49.14	39.70	58.7	56.0
48.10	42.08	115.1	81.6
49.14	40.29	74.9	65.5
50.34	41.93	59.4	56.0
48.54	41.04	97.7	71.9
49.81	42.38	109.0	50.0
Mean 49.20	40.97	84.9	70.2
s.d. ± 0.67	± 1.03	± 21.4	± 16.7

The variation in the results for both dry and saturated Bunter is remarkably low. Bearing in mind that these results also include any influence of direction, the homogeneous and isotropic description offered by Harvey is well confirmed. The greater variation in the results for Magnesian Limestone may, in part, be attributed to the randomly distributed voids caused by the dolomitization of the rock.

In order to give an indication of the relative strength of the test rock, comparative dry strength tests were undertaken on samples recovered from locations of interest. These results are given in Tables 5 and 6.

TABLE 5

A COMPARISON OF THE COMPRESSIVE STRENGTHS OF BUNTER SANDSTONE

Sample Location	Compressive Strength			
	MN/m^2	(± s.d.)	p.s.i.	(± s.d.)
Woolton Quarry	49.2	(0.67)	7,140	(100)
Running Tunnel **	33.3	(0.87)*	4,820	(130)
Escalator Tunnel **	30.3	(1.66)*	4,394	(240)

* 6 specimens.

** Central Station Site, Liverpool Loop Railway Tunnel.

TABLE 6

A COMPARISON OF THE COMPRESSIVE STRENGTHS OF MAGNESIAN LIMESTONE

Sample Location	Compressive Strength			
	MN/m^2	(± s.d.)	p.s.i.	(± s.d.)
Mansfield Quarry	84.9	(21.4)	12,310	(3,100)
Bullwell Quarry *	87.2	(17.6)	12,650	(2,550)
Breedon Quarry **	107.0	(28.5)	15,520	(4,130)

* Site of the Greenside Tunnelling Machine Trials.

** Site of the Bretby Tunnelling Machine Trials.

The effect of specimen size on strength has been investigated using cylindrical specimens of Bunter having a nominal diameter to height ratio of 1. Each result, given in Table 7, is the mean of 5 replications.

TABLE 7

EFFECT OF SPECIMEN SIZE ON COMPRESSIVE STRENGTH

Diameter (mm)	Height (mm)	Compressive Strength MN/m^2 (± s.d.)		p.s.i. (± s.d.)	
28.0	29.0	65.75	(0.67)	9540	(100)
49.5	51.5	64.00	(1.84)	9280	(280)
74.5	74.5	58.38	(1.88)	8470	(270)
99.5	102.0	48.46	(1.28)	7030	(185)

Clearly, as the size of specimen increases so the rock strength is reduced. This is common in rock and complies with the Weakest Link Theory (19). Relationships between strength and the dimensional attributes of diameter, cross sectional area and volume were examined. Linear regression of compressive strength against volume showed the relationship to have the very high correlation coefficient of 0.9997. It must be stressed, however, that it would be wrong to extrapolate the effect of size, since the strength cannot indefinitely continue to reduce linearly with increasing size. It is probable that the linear relationship over this small range of specimen sizes is part of the wider exponential relationship found by Evans, Pomeroy and others.

4.4 Uniaxial Tensile Strength

Tensile strength was measured in two different ways. The Brazilian disc method (62) was used for both dry and saturated rock. Further tensile strength measurements were made, on dry rock only, using the four point beam test.

Discs were 74.5mm in diameter and 32.7mm thick. Diametral loading was applied using dry steel platens at a rate of 100 p.s.i. (0.69 MN/m^2) per second. The results of dry and saturated tests are given in Table 8.

TABLE 8

UNIAXIAL TENSILE STRENGTHS - BRAZILIAN DISC TEST

Bunter Sandstone		Magnesian Limestone	
Dry MN/m^2	Saturated MN/m^2	Dry MN/m^2	Saturated MN/m^2
2.72	1.93	5.64	5.39
2.51	2.04	5.85	5.62
2.77	1.57	6.38	5.78
2.77	2.14	6.65	5.94
2.48	2.01	6.86	6.56
2.72	1.93	6.60	5.71
2.66	1.86	6.15	5.39
2.77	1.41	6.12	6.12
2.69	1.96	4.91	5.21
2.33	1.75	7.25	5.71
Mean 2.64	1.86	6.24	5.73
s.d. 0.15	0.23	0.67	0.39

These results confirm the isotropy of both rocks since no attempt was made to orientate the line of diametral compression in any preferred direction.

Results of the four-point beam test were obtained using dry specimens, each of length 255mm, breadth 70mm and thickness 25.5mm. Because beams of this configuration fail at very low loads, the rate of load application had to be extremely slow.

TABLE 9

TENSILE STRENGTHS - BEAM TEST

Specimen No.	Bunter Sandstone MN/m^2	Magnesian Limestone MN/m^2
1	5.74	7.95
2	5.12	7.91
3	6.09	8.70
4	4.86	7.68
Mean	5.45	8.06
s.d. $\pm$	0.56	0.44

Tensile strength measured by the four-point beam method gives values considerably higher than those obtained from the disc test. This phenomenon has been observed in other rock materials (19)(62) and the general belief is that the higher strength is due to the fact that stress concentrations in the beam test are highly localised, initiating failure in the outer fibres of the beam. The chance of a natural incipient weakness in the rock coinciding with the point of localised stress is such that consistently higher measured tensile strengths are found by this method.

4.5 Shear Strength

This involved the direct measurement of shear load using a double shear box (63). Specimens of 25mm square section and 80mm long provided a good sliding fit into the apparatus, which was symmetrically loaded with no lateral constraint.

For this test 5 specimens were oven dried, 5 saturated and, for Bunter Sandstone only, a further 5 were produced at an average intermediate moisture content of 7.7%. The results for each condition are given in Tables 10 and 11.

TABLE 10

UNIAXIAL SHEAR STRENGTH - BUNTER SANDSTONE

Dry MN/m^2	Intermediate MN/m^2	Saturated MN/m^2
8.08	9.04	6.72
6.48	5.84	8.00
7.68	5.76	7.97
6.88	6.12	6.98
7.60	7.64	9.66
Mean 7.34	6.88	7.85
$\pm$ s.d. 0.26	0.57	0.45

Initially shear strength was measured only at the extreme moisture conditions of dry and saturated. But, unlike the compressive and tensile results, the saturated shear strength of Bunter was found on average to be 6.4% higher than the dry value. On further examination however this was not found to be a statistically significant difference and judging from the scatter of the results there was also less consistency than might have been expected from the compressive and tensile strength values.

TABLE 11

UNIAXIAL SHEAR STRENGTH - MAGNESIAN LIMESTONE

Dry MN/m^2	Saturated MN/m^2
10.48	12.64
12.48	16.04
17.04	8.80
10.32	9.04
9.68	6.80
Mean 12.00	10.66
$\pm$ s.d. 3.01	3.67

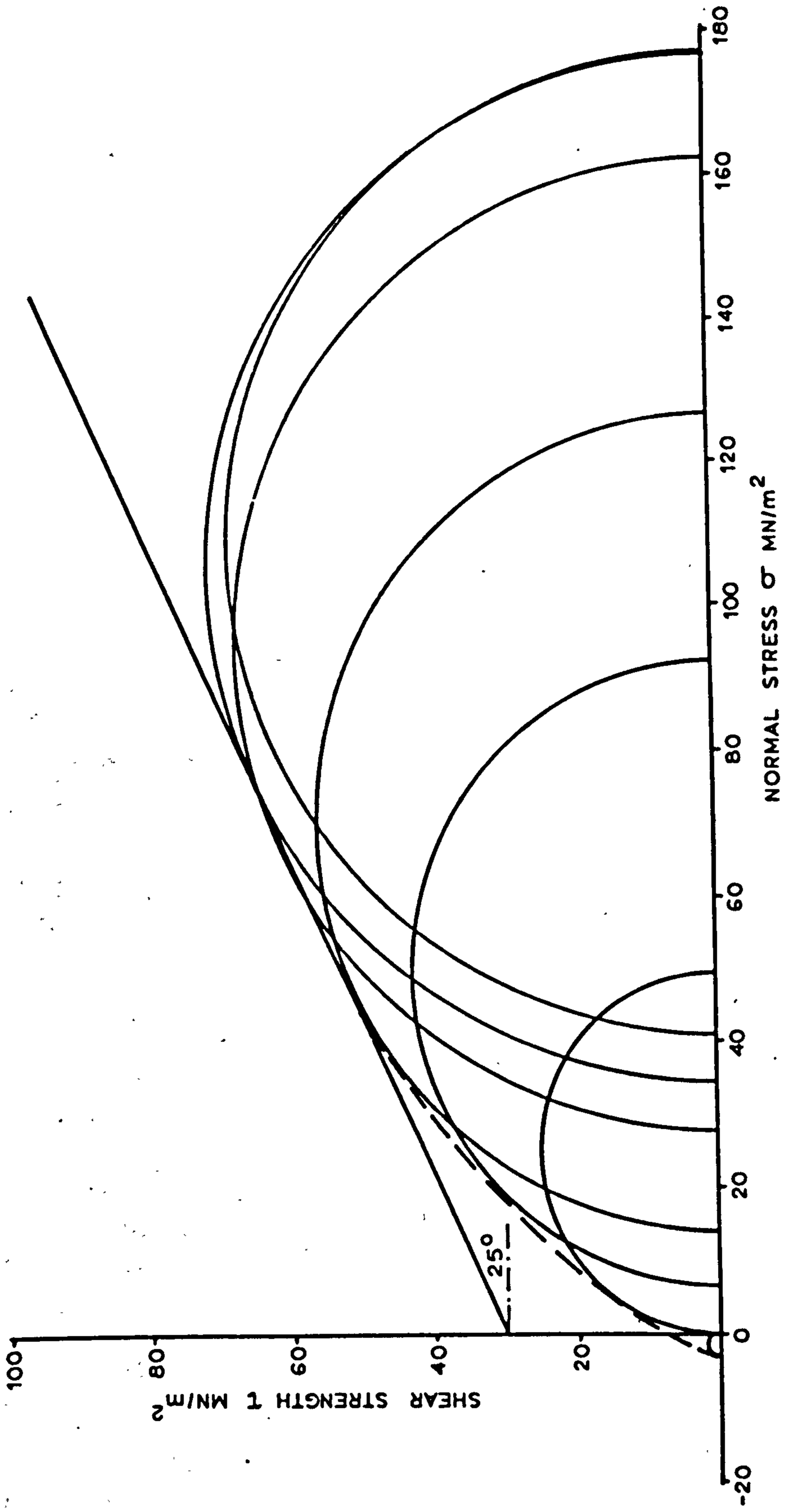

FIGURE 3 - MOHR'S ENVELOPE FOR DRY BUNTER SANDSTONE

The value of rock testing methods which rely on a precisely predetermined line of failure must be dubious. In addition, it was observed on a number of occasions that failure occurred along one predetermined shear plane in advance of the other. This meant that the ensuing failure was under conditions of asymmetrical loading thus introducing a state of complex stress.

4.6 Triaxial Strength

The two moisture conditions of dry and saturated were investigated. Triaxial testing of saturated rock may be undertaken "drained" or "undrained". During the rock cutting process the time taken to reach failure stress is extremely short, and this rapid rate of loading provides inadequate opportunity for the internal water to disperse. The undrained test was, therefore, selected as being the most appropriate to the rock cutting situation.

Tests on cores of 76.2mm diameter and 152.4mm length, were conducted at 7 levels of confinement and each experiment was replicated five times. The uniaxial tensile strengths obtained from the disc test completed the data required for a full triaxial description of the two rocks. The results are given in Tables 12 and 13.

TABLE 12

TRIAXIAL STRENGTH OF BUNTER SANDSTONE

Confining Pressure MN/m^2 (p.s.i.)	Failure Stress (MN/m^2)	
	Dry	Saturated
Uniaxial Tension	2.64	1.86
Uniaxial Compression	44.40	36.97
6.89 (1000)	90.96	55.89
13.69 (2000)	126.91	82.49
20.69 (3000)	146.86	98.30
27.58 (4000)	161.76	106.87
34.48 (5000)	176.89	115.00
41.37 (6000)	176.45*	123.84

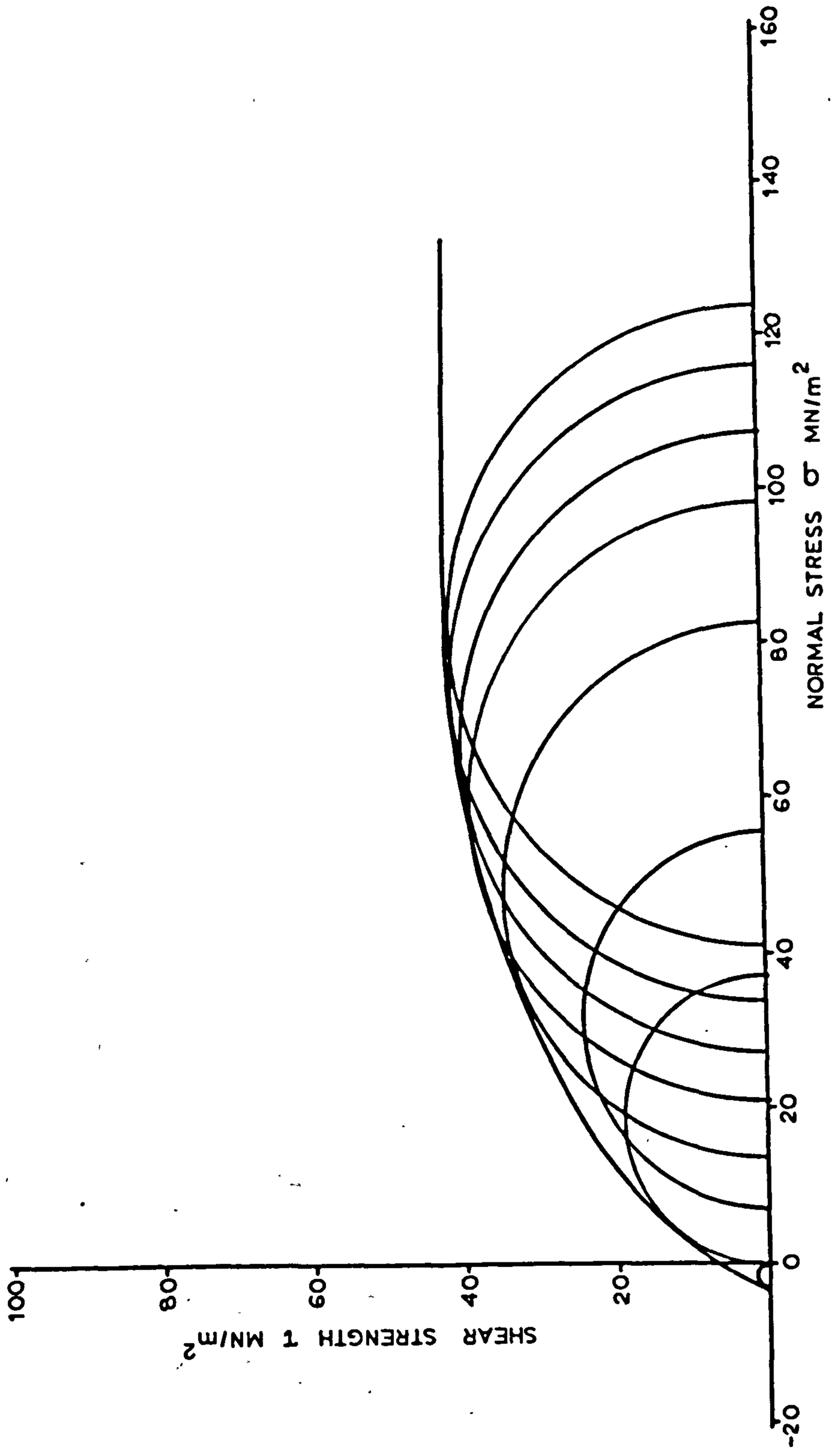

FIGURE 4 - MOHR'S ENVELOPE FOR SATURATED BUNTER SANDSTONE (undrained)

*This value is suspect since it proved difficult to control the confining pressure at 6000 p.s.i.

TABLE 13

TRIAXIAL STRENGTH OF MAGNESIAN LIMESTONE

Confining Pressure MN/m^2 (p.s.i.)	Failure Stress (MN/m^2)	
	Dry	Saturated
Uniaxial Tension	6.24	5.73
Uniaxial Compression	76.93	63.35
6.89 (1000)	82.24	74.34
13.79 (2000)	110.53	103.73
20.69 (3000)	119.09	123.60
27.58 (4000)	137.32	128.42
34.48 (5000)	156.44	136.18
41.37 (6000)	172.59	141.80

These results have been plotted to produce the Mohr Envelopes shown in Figures 3-6. The internal friction of the rock is the slope of the tangent to the envelope at any point. At low confining pressures, internal friction assumes its highest values, reducing as confinement increases to a point beyond which it becomes fairly constant. This is a common feature of rock (64). Approximate values of the slope of the linear portion of the envelope are given below:-

Bunter Sandstone	Dry	=	25^{o}
Bunter Sandstone	Saturated	=	0^{o}
Magnesian Limestone	Dry	=	18^{o}
Magnesian Limestone	Saturated	=	0^{o}

A feature of the triaxial strength in an undrained situation is the negligible value of the internal friction. Since the pore water pressure increases proportionately with confinement the effective stress, which is equivalent to the total stress minus the pore pressure, may be expected to be constant.

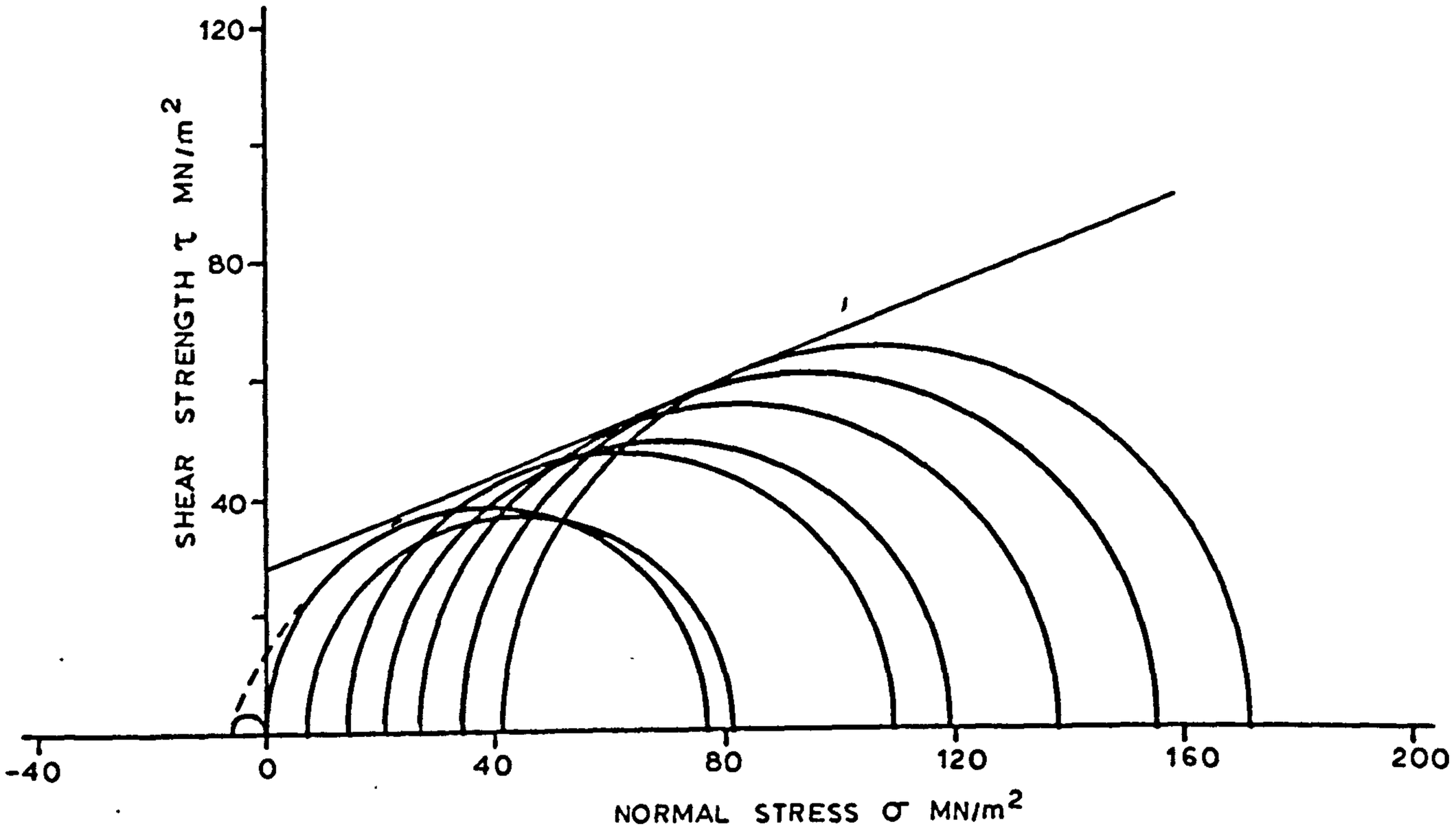

FIGURE 5 — MOHR'S ENVELOPE FOR DRY MAGNESIAN LIMESTONE

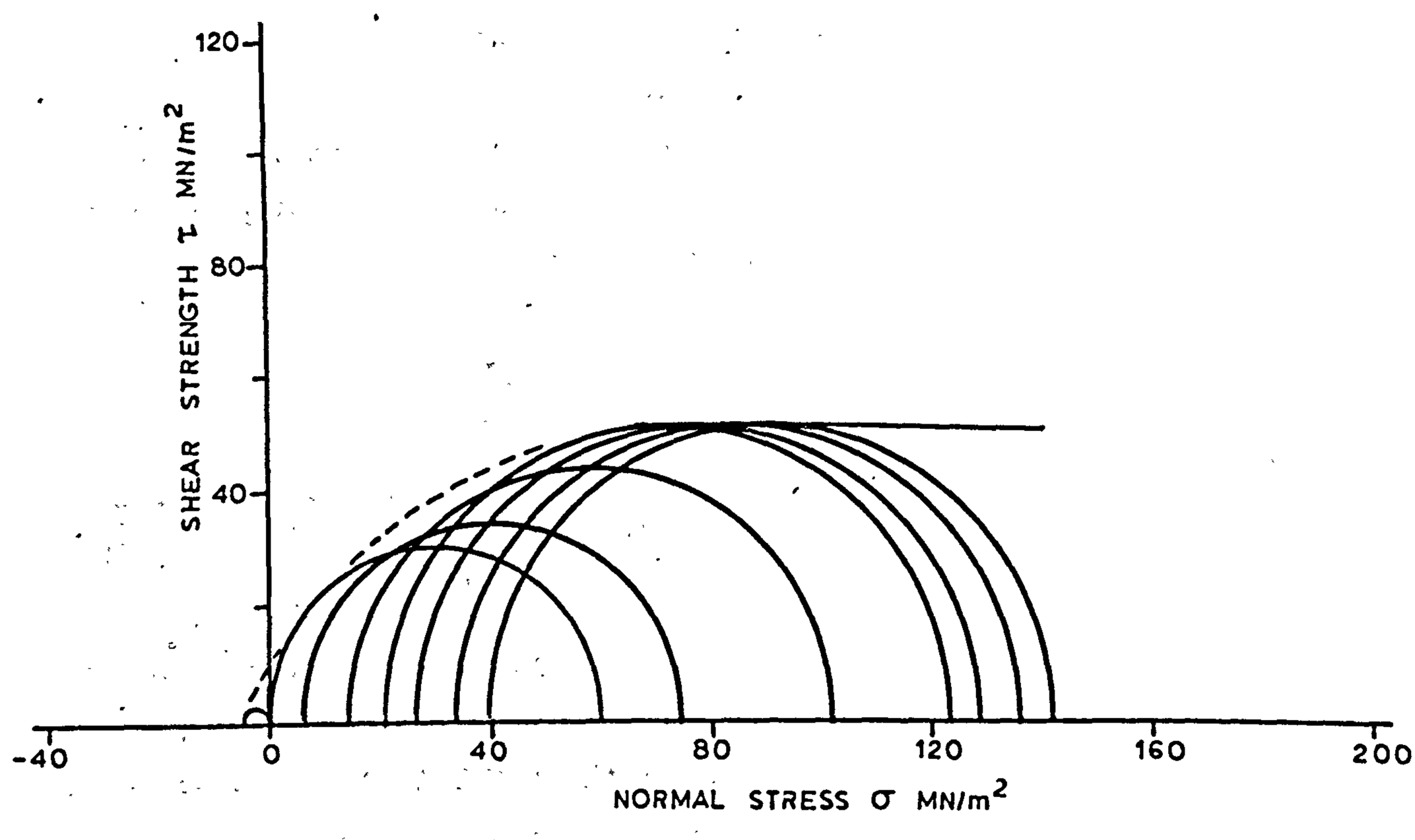

FIGURE 6 — MOHR'S ENVELOPE FOR SATURATED MAGNESIAN LIMESTONE

The intercept of the Mohr Envelope with the ordinate is a measure of the unconfined shear strength. These results conform well with the measured shear strength values in Tables 10 and 11.

4.7 Elastic Properties

Tests were undertaken to examine the stress-strain relationships in uniaxial compression up to failure load. This was done for both the dry and saturated conditions.

The stress-strain curves in Figures 7 and 8 show good linearity up to failure proving both rocks to be brittle and elastic.

From the same data the static modulii can be determined. Dynamic modulii were also measured for dry and saturated rock using "Pundit Sonic Testing Equipment" set for a pulse frequency of 50 k Hz.

The modulii values are presented in Tables 14 and 15.

TABLE 14

ELASTIC MODULII OF BUNTER SANDSTONE

Static ($MN/m^2 \times 10^3$)		Dynamic ($MN/m^2 \times 10^3$)	
Dry	Saturated	Dry	Saturated
10.97	9.42	11.96	11.38
10.70	11.67	11.67	11.57
10.00	11.14	11.87	11.57
9.44	8.45	11.82	12.06
10.17	10.65	11.87	12.67
Mean 10.26	10.27	11.83	11.75
± s.d. 0.6	1.31	0.11	0.33

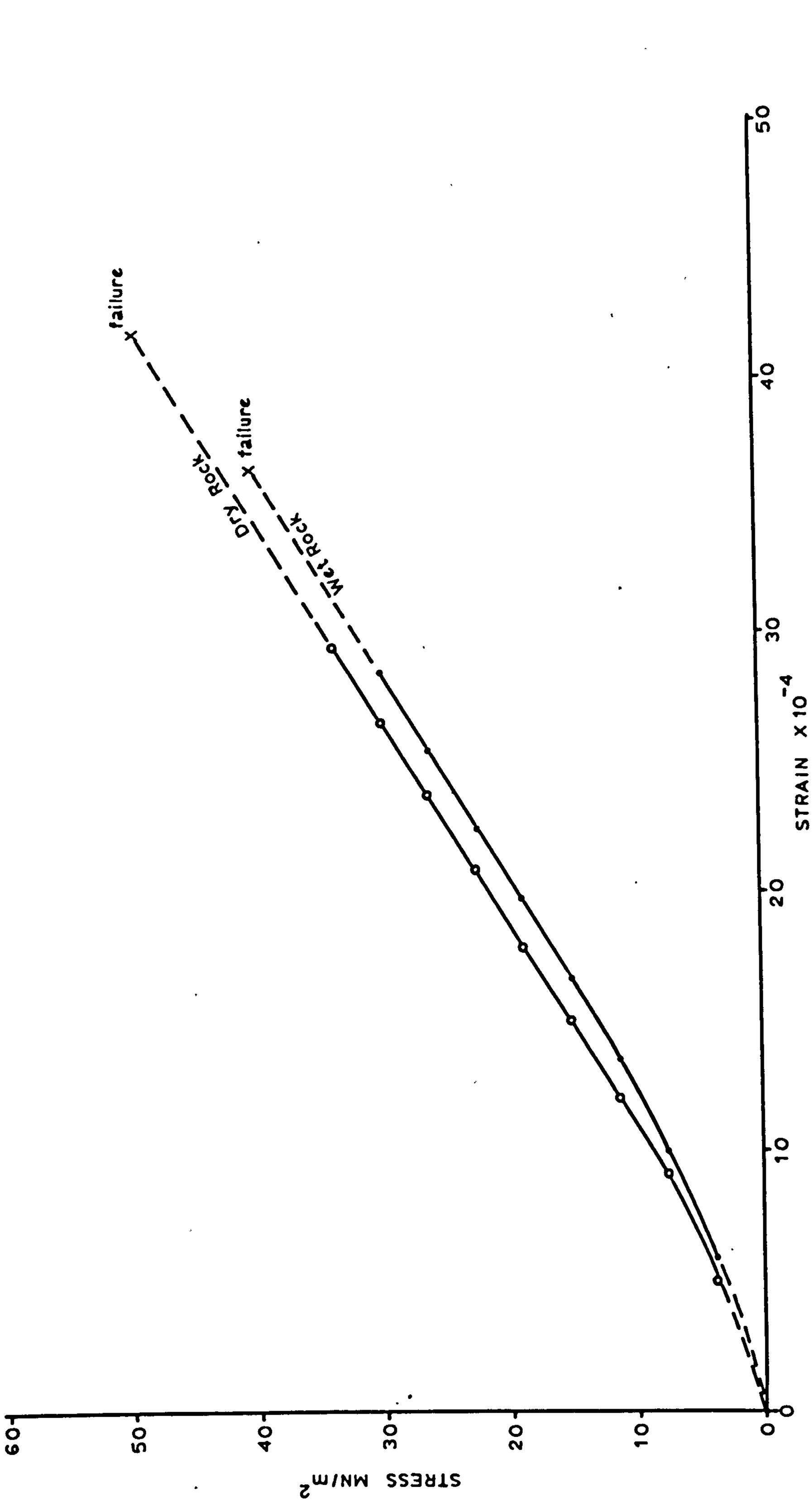

FIGURE 7 - COMPRESSIVE STRESS STRAIN CURVES - BUNTER SANDSTONE

TABLE 15

ELASTIC MODULII OF MAGNESIAN LIMESTONE

Static ($MN/m^2 \times 10^3$)		Dynamic ($MN/m^2 \times 10^3$)	
Dry	Saturated	Dry	Saturated
19.50	19.86	27.18	21.14
21.08	20.93	25.63	20.86
19.03	18.92	20.49	24.54
21.22	22.69	21.78	24.61
22.56	20.54	28.47	24.50
Mean 20.68	20.59	24.71	23.13
± s.d. 1.42	1.40	3.45	1.95

4.8 Sliding Friction

During cutting operations there is a frictional interaction between tool and rock. Throughout the cutting experiments all picks were made of tungsten carbide (CM Grade) and the discs were made of hardened steel.

The coefficients of sliding friction for both materials on the dry and saturated rock surfaces were measured using elementary equipment. Normal loads were applied to the sliding member and the mass required to produce sliding was measured. The resulting friction values are given in Table 16.

TABLE 16

COEFFICIENTS OF SLIDING FRICTION

Rock Condition	Coefficient of Friction	
	Tungsten Carbide	Hardened Steel
Bunter Dry	0.65	0.35
Bunter Saturated	0.55	0.33
Limestone Dry	0.48	0.34
Limestone Saturated	-	-

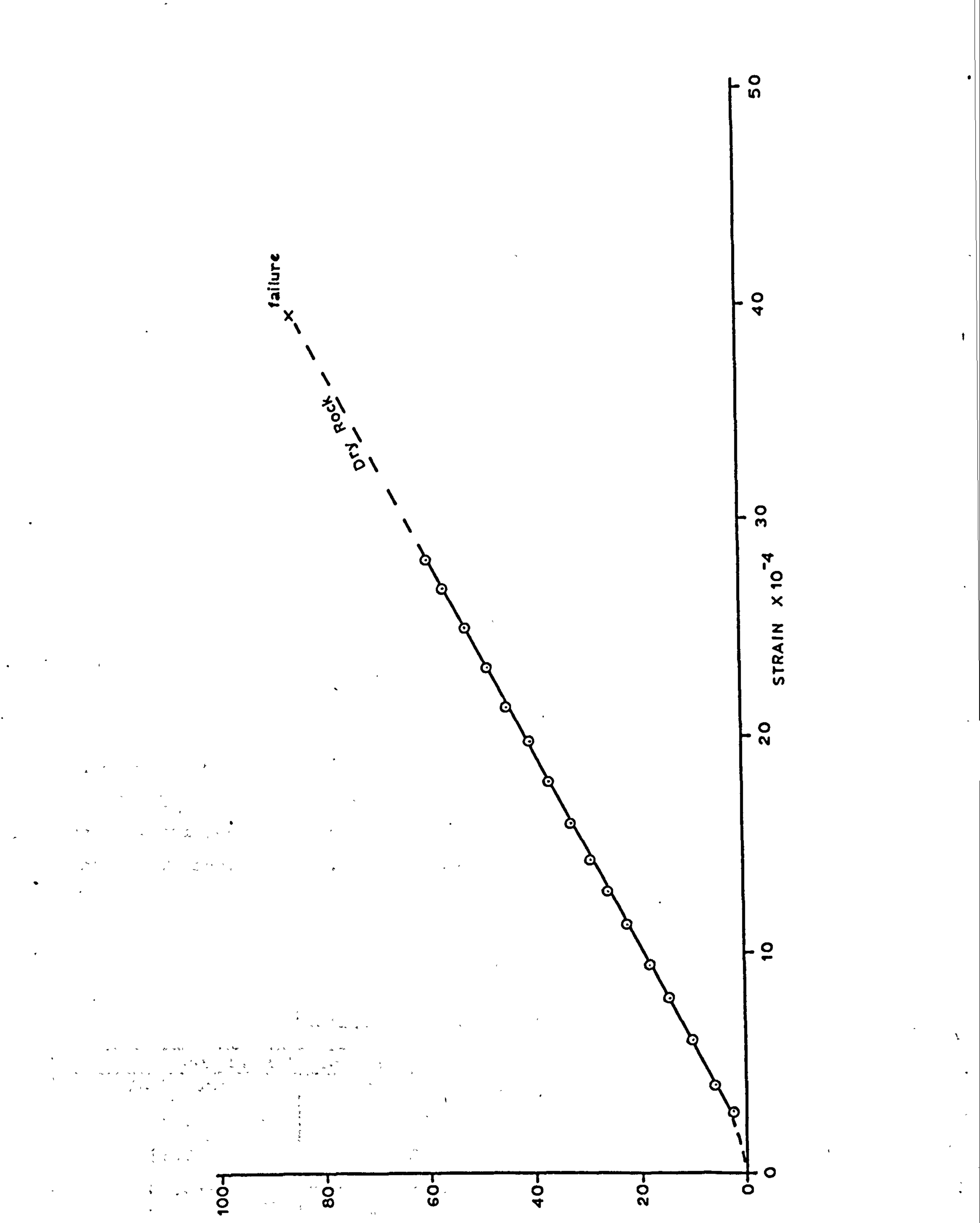

FIGURE 8 - COMPRESSIVE STRESS STRAIN CURVES - MAGNESIAN LIMESTONE

4.9 Indirect Rock Testing

There are several commercially available instruments which are designed to provide a measure of rock hardness or strength. Generally these involve a probe or impact mechanism of simple mechanical and portable construction. The virtue of these instruments is their simplicity of operation and their ability to provide a very large number of results from several locations in a short time. Variations in rock strength that may occur on site are therefore readily assessed using such instruments.

The commonest of these devices have been used to determine appropriate results for both rocks. Because such measures are of considerably less value than the equivalent direct measurements of strength the test results are exclusively for dry rock.

These results, together with appropriate references to the construction and use of the instruments are given in Table 17.

TABLE 17

SUMMARY OF INDIRECT ROCK TESTING RESULTS

	No. of Tests	Bunter Sandstone	Magnesian Limestone
Schmidt Hammer (65)	25	51.7 ± 1.1	40.50 ± 1.7
Shore Hardness (66)	40	37.3 ± 8.2	19.45 ± 3.04
M.R.D.E. Cone Indenter (67)	20	2.12 ± 0.83	1.92 ± 0.44
Impact Strength Index (68)	5	42.1 ± 0.4	84.90 ±10.40
Brinell Hardness (69)	20	97.0 ± 33.8	94.00 ±28.20
Hacksaw Machineability (70)	5	1.10 ± 0.1	20.35 ± 1.8

In general the results of these indirect tests are at variance with those obtained by direct measurement. This is largely due to the small area of rock sampled by these instruments, so that the measured parameter is grain hardness rather than the strength of the specimen.

Hence, although the measured compressive strength of Bunter Sandstone is only about half that of Magnesian Limestone the greater hardness of its constituent quartz grains is reflected in the results of the indirect rock tests.

5. PLANNING OF THE EXPERIMENTS

The main programme of experiments was planned to provide data through which relationships can be established between criteria of cutting performance and the several variables available in drag pick and disc cutter design.

5.1 Parameters and Variables

Parameters of performance, for both types of tool, fall into two categories referred to as "primary" and "secondary". The primary parameters are those quantities capable of being measured directly. Secondary parameters, on the other hand, involve calculations based on the primary values. These are listed separately for picks and discs. Definitions of the parameters are generally well understood and have appeared elsewhere (24). (Appendix XIV).

	Picks		Discs	
PRIMARY	Mean Cutting Force	$\overline{F}_c$	Mean Rolling Force	$\overline{F}_R$
	Mean Peak Cutting Force	F_c	Mean Peak Rolling Force	F_R
	Mean Normal Force	$\overline{F}_N$	Mean Thrust Force	$\overline{F}_T$
	Mean Peak Normal Force	F_N	Mean Peak Rolling Force	F_T
	Rock Yield	Q	Rock Yield	Q
	Coarseness Index	C.I.	Coarseness Index	C.I.
SECONDARY	Mean Resultant Force	F_p	Mean Resultant Force	F_d
	Direction of Resultant	λ_p	Direction of Resultant	λ_d
	Specific Energy	S.E.	Specific Energy	S.E.

This subdivision is not intended to reflect the relative importance of parameters as performance criteria.

The variables available for the main cutting experiments with picks and discs are as follows:-

Picks		Discs	
Front Rake Angle	α	Peripheral Edge Angle	ϕ
Width	w	Diameter	D
Depth of Cut	d	Penetration	p
Cutting Speed	v_p	Cutting Speed	V_d
Spacing	s_p	Spacing	S_d
Rock Moisture Content	m.c.	Rock Moisture Content	m.c.

As will be seen later in this chapter, the special techniques which need to be used for the design of the main experiments are applied to best effect when the number of variables to be studied is kept at four. It was, however, considered necessary to include six variables in the main experimental programme. Since only four, or in the case of discs, five, of these were to be studied at more than two levels, then it was possible to arrange a programme of experiments to provide the required factorial coverage.

In order to establish a reliable relationship between one of the principal variables with each parameter, it has been found necessary to study its effect at not less than 5 levels (24) and that, if possible, the levels should form an arithmetic progression.

Since there is a strong possibility of interaction* between some of these variables, it would normally be necessary to undertake a full factorial experiment, involving all interacting variables. All of the above pick variables, with the exception of cutting speed, are known to interact (24) and the apparent requirement is, therefore, for a full factorial experiment involving 4 variables at 5 levels and 1 variable at 2 levels. Full factorial coverage would, in this case, lead to

$$(5)^4 \times (2)^1 = 1250 \text{ cutting tests}$$

---

*The meaning of interaction is most conveniently explained by example. Suppose a firm relationship was found to exist between say depth of cut and specific energy, and that this was established for a constant rake angle and pick width. It would be wrong to assume that the same relationship held true for all other values of rake and width. If the relationship between depth and specific energy changes at other levels of the other 2 variables, then all 3 variables are said to interact.

If pick speed did interact with the others then the number of tests would increase to 6250. A great deal of previous work on the effect of cutting speed shows that all the parameters, except possibly tool wear rate, are unaffected by speeds well beyond the range used by machines. The influence of speed could therefore be checked in a small independent experiment.

Nevertheless, the 1250 tests required for the other 5 variables provides only 1 result for each condition. Analyses of previous rock cutting data have shown that since every type of rock exhibits some heterogeneity, several replications of a test are required to provide a level of statistical confidence to the value obtained. Results of rock strength tests have revealed that to achieve a given level of statistical confidence for the mean of a set of values, the minimum number of tests required to achieve it can be related to the coefficient of variance (61) thus:-

Coefficient of Variance %	Minimum Number of Tests
30	9
25	6
20	4
15	3

A preliminary series of cutting tests in Bunter showed that the coefficient of variance of cutting and normal forces was usually about 10% and always below 15%. It was decided therefore that each test should be carried out 4 times and represented as a mean value.

Four replications for each of 1250 tests using picks, together with a considerably larger number for discs, would create a workload equivalent to 10 man-years. Clearly, such a task is unmanageable and recourse must therefore be made to techniques for partial factorial planning.

5.2 Partial Factorial Experiments

There are 3 commonly used partial factorial techniques which are briefly outlined

a) Experimenting with only one variable at a time, with the remaining variables held at a constant value. With this approach it is not possible to determine interactions which may exist between it and the other variables.

b) Variables may be grouped in pairs and throughout the experiment the pairs used as if they were single variables in a full factorial experiment. Empirical relationships may be obtained from this method, but it is not possible to isolate the effects of the variables that form a pair.

c) By taking a random sample of levels from the full factorial matrix, in the expectation that abstracting the effects of one particular variable will be at the mean level for all other variables.

Protodyakonov (Sr) (71) using this method as long ago as 1932, recognised the limitations of random selection as being only appropriate to very large experiments. To further develop this approach, however, he suggested that some systematic, as opposed to random, method should be adopted for sampling the full factorial matrix.

Protodyakonov (Jr) and Teder (72) have since developed the concept of random coverage of the matrix in such a way that each level of all variables in the experiment is systematically chosen. This effectively removes the element of chance in achieving a balanced experimental programme. It is an essential feature of the method that each level of a variable appears in only one combination with each level of the other variables. This is apparent from Table 18 and Figure 11 which appear later.

5.3 The Protodyakonov (Jr) Method

There are two techniques available to achieve the required combinations of levels. The combination square method is a graphical approach to selection, which is tedious to apply and becomes progressively more difficult to use as the size of experiment increases. Protodyakonov has provided a full description of this method (3).

An alternative means for achieving the same objective involves a numerical approach, using orthogonal Latin Squares. Since this was the method for planning the main cutting experiments, its application will be described in some detail.

The use of Latin Squares in the planning of experiments is now a well developed technique (73)(74). The definition of two orthogonal Latin Squares is that, when superimposed, each pair of figures occurs once and only once. Similarly when three squares are superimposed, each group of three figures occurs only once. This fulfils the pre-requisite, referred to previously, that each level of a variable should appear in only one combination with each level of the other variables. This concept will become clearer through the following example.

A Latin Square of the same size as the number of levels of each variable, is constructed. If 5 levels are to be attributed to a variable, then it is a pre-requisite that all other variables should appear at 5 levels.
(n.b. This was in fact the principal reason for not including moisture content within a single experiment plan, since 5 levels of moisture could not realistically be provided).

This initial Latin Square is shown in Figure 9a) and further Latin Squares, orthogonal to this one and to each other are constructed, until the number of squares is equal to the number of variables.

For example, consider an experiment to investigate the 3 pick variables of rake angle, width and depth of cut, each being studied at 5 levels. The appropriate construction of orthogonal Latin Squares is shown in Figures 9a), b) and c).

FIG. 9

ORTHOGONAL LATIN SQUARES FOR A 3 VARIABLE, 5 LEVEL EXPERIMENT

a) Rake Angle (α)					b) Width (w)					c) Depth of Cut (d)				
1	1	1	1	1	1	2	3	4	5	1	3	5	2	4
2	2	2	2	2	2	3	4	5	1	2	4	1	3	5
3	3	3	3	3	3	4	5	1	2	3	5	2	4	1
4	4	4	4	4	4	5	1	2	3	4	1	3	5	2
5	5	5	5	5	5	1	2	3	4	5	2	4	1	3

By direct and simultaneous superimposition of squares a), b) and c) the composite square shown in Figure 10 is produced.

FIG. 10

COMPOSITE SQUARE

111	123	135	142	154
222	234	241	253	215
333	345	352	314	321
444	451	413	425	432
555	512	524	531	543

Each of the 25 sets of numbers in Figure 10 may now be taken to represent the levels of the 3 variables at which one test is to be undertaken. For example, the last set in the first row would be a test in which rake angle was at level 1, width at level 5 and depth at level 4.

Suitable values can now be ascribed to these numerical levels.

For example:-

		Level	1	2	3	4	5
Rake Angle	(α) ^{o}		-10	0	10	20	30
Width	(w) mm		10	20	30	40	50
Depth of Cut	(d) mm		3	6	9	12	15

These absolute values taken in conjunction with the composite square in Figure 10 produces the Experimental Plan which is given in Table 18.

TABLE 18

PLAN FOR A 3 VARIABLE - 5 LEVEL EXPERIMENT WITH PICKS

Test No.	Rake Angle ^{o}	Width mm	Depth of Cut mm
1	-10	10	3
2	-10	20	9
3	-10	30	15
4	-10	40	6
5	-10	50	12
6	0	20	6
7	0	30	12
8	0	40	3
9	0	50	9
10	0	10	15
11	10	30	9
12	10	40	15
13	10	50	6
14	10	10	12
15	10	20	3
16	20	40	12
17	20	50	3
18	20	10	9
19	20	20	15
20	20	30	6
21	30	50	15
22	30	10	6
23	30	20	12
24	30	30	3
25	30	40	9

Using this method, the full factorial requirement for a 5 level, 3 variable experiment of 125 tests (without replications), has been reduced to a balanced sample of 25. For experiments involving 4, 5 or 6 variables, the 4th, 5th and 6th orthogonal squares must be constructed. Thereafter the procedure is exactly the same as that described. Superimposition of the 4, 5 or 6 squares also produces 25 sets of numbers but each set now contains 4, 5 or 6 digits.

The number of levels predetermines the number of tests in the experiment irrespective of the number of variables, with the number of tests always being equal to the square of the number of levels chosen. What is important, however, is that the number of variables is limited to the number of orthogonal squares that can be produced.

For instance, a 5 level experiment will always produce a requirement for 25 tests, a 7 level experiment 49 and a 9 level experiment 81. Similarly, because only 6 orthogonal squares can be generated for a 5 level experiment, the maximum number of variables that can be studied in that experiment is also 6. A 7 level experiment will however produce 8 orthogonal squares and allow up to 8 variables. It should be noted that the number of levels chosen must always be odd. For rather complex reasons relating to symmetry, an even number of levels cannot be used.

Having explained in some detail the procedure relating to the generation of a 3 variable - 5 level experiment by the numerical method, the graphical method has been used to produce Figure 11 which is for a 4 variable, 5 level experiment. Each small shaded square represents a single test. Both techniques, in effect, achieve the same result.

Since all of the proposed partial factorial experiments in this project use either 3 or 4 variables, but always at 5 levels, the two plans represented by Table 18 and Figure 11 can be used as master plans throughout. The need for statistical replications is satisfied by executing the same planned programme the required number of times; in this case 4.

PARTIAL FACTORIAL EXPERIMENTAL MATRIX

w \ ∝		I					II					III					IV					V				
	d / s	1	2	3	4	5	1	2	3	4	5	1	2	3	4	5	1	2	3	4	5	1	2	3	4	5
I	1	▨																								
	2														▨											
	3																						▨			
	4										▨															
	5																		▨							▨
II	1																									▨
	2							▨																		
	3																			▨						
	4			▨																						
	5											▨														
III	1																▨									
	2					▨																				
	3													▨												
	4																				▨					
	5								▨																	
IV	1					▨																				
	2																									▨
	3							▨																		
	4																			▨						
	5		▨																							
V	1								▨																	
	2																▨									
	3				▨																					
	4												▨													
	5																									▨

The 5 levels selected for each variable are :

		I	II	III	IV	V
Rake Angle (∝)	:	-10°	0°	10°	20°	30°
Pick Width (w)	:	10	20	30	40	50 mm.
		1	2	3	4	5
Depth of Cut (d)	:	3	6	9	12	15 mm.
Pick Spacing (s)	:	-6	6	18	30	42 mm.

FIGURE 11 - EXPERIMENTAL MATRIX

5.4 Analysis of Experimental Data

It is a feature of such partial factorial programmes that if data is grouped according to the levels of one of the variables, each group will contain data at all the levels of all the other variables.

For example and referring to Table 18. Grouping data according to rake angle, gives the following 5 groups of test numbers : 1 - 5, 6 - 10, 11 - 15, 16 - 20 and 21 - 25. It can be found by inspection, that each of these groups contains, on only one occasion, each level of width and depth. Also the same level of width in each group, corresponds with the 5 different levels of depth. At a width of say 40mm, the depths in Table 18 are found to be 6, 3, 15, 12 and 9mm. This is, in effect, the same as saying that there is nothing unique in grouping according to rake angle as is done in Table 18. Groupings could equally well be based on width or depth of cut.

The objective from this stage onwards is to manipulate the grouped experimental data to yield empirical equations inter-relating parameters and variables. Since the procedure involved is quite complex, a worked example using real data will be followed through in stages.

An experiment undertaken according to the 3 variable plan in Table 18 provided the values of mean cutting force $\overline{F}_c$ given in Table 19.

TABLE 19

MEAN CUTTING FORCE AND ASSOCIATED DATA FOR 3 VARIABLE EXPERIMENT WITH PICKS

Test No	$\overline{F}_c$	d	$\overline{F}_c'$	w	w + 19.16	$\overline{F}_c''$ x 10^{-3}	α	$\overline{F}_c$ (Predicted)
1	0.374	3	.125	10	29.16	4.287	-10	0.393
2	1.890	9	.210	20	39.16	5.363	-10	1.585
3	4.230	15	.282	30	49.16	5.737	-10	3.315
4	1.285	6	.214	40	59.16	3.617	-10	1.595
5	3.856	12	.321	50	69.16	4.642	-10	3.731
6	0.722	6	.120	20	39.16	3.065	0	0.863
7	2.432	12	.203	30	49.16	4.130	0	2.168
8	0.740	3	.246	40	59.16	4.158	0	0.652
9	1.440	9	.160	50	69.16	2.314	0	2.287
10	1.650	15	.110	10	29.16	3.773	0	1.607
11	1.048	9	.116	30	49.16	2.360	10	1.337
12	2.320	15	.155	40	59.16	2.620	10	2.682
13	1.518	6	.253	50	69.16	3.658	10	1.254
14	0.975	12	.081	10	29.16	2.778	10	1.057
15	0.371	3	.124	20	39.16	3.167	10	0.355
16	1.860	12	.155	40	59.16	3.153	20	1.777
17	0.813	3	.271	50	69.16	4.581	20	0.519
18	0.520	9	.058	10	29.16	1.989	20	0.660
19	1.154	15	.077	20	39.16	1.966	20	1.470
20	0.714	6	.119	30	49.16	2.421	20	0.738
21	1.474	15	.098	50	69.16	1.417	30	2.170
22	0.358	6	.059	10	29.16	2.023	30	0.366
23	0.933	12	.077	20	39.16	1.966	30	0.983
24	0.537	3	.179	30	49.16	3.641	30	0.308
25	0.758	9	.084	40	59.16	1.420	30	1.114

From the data in Table 19, the mean value of $\overline{F}_c$ is calculated for each of the groups. In the case of level 1 this mean is 2.327 for rake angle, 0.775 for width and 0.567 for depth, derived as follows:-

Level 1 Rake Angle	Level 1 Width	Level 1 Depth
0.374 kN	0.374 kN	0.374 kN
1.890	1.650	0.740
4.230	0.975	0.371
1.285	0.520	0.813
3.856	0.358	0.537
5|11.635	5|3.877	5|2.835
2.327 kN	0.775 kN	0.567 kN

This procedure, applied to all levels, produces Table 20.

TABLE 20

COLLATED DATA FOR PARTIAL EMPIRICAL RELATIONSHIPS BETWEEN $\overline{F}_c$ AND EACH VARIABLE

	α o	$\overline{F}_c$ kN	w mm	$\overline{F}_c$ kN	d mm	$\overline{F}_v$ kN
Level 1	-10	2.327	10	0.775	3	0.567
Level 2	0	1.397	20	1.014	6	0.919
Level 3	10	1.246	30	1.792	9	1.131
Level 4	20	1.012	40	1.393	12	2.011
Level 5	30	0.812	50	1.821	15	2.166

The variation in $\overline{F}_c$ with rake angle is shown in Figure 12a) and this is appropriate to the mean value of width and cutting depth. Similarly the relationship between $\overline{F}_c$ and w is shown in Figure 12b), which likewise is at mean values of α and d. Finally, the $\overline{F}_c$ relationship with d, shown in Figure 12c) is at mean α and w.

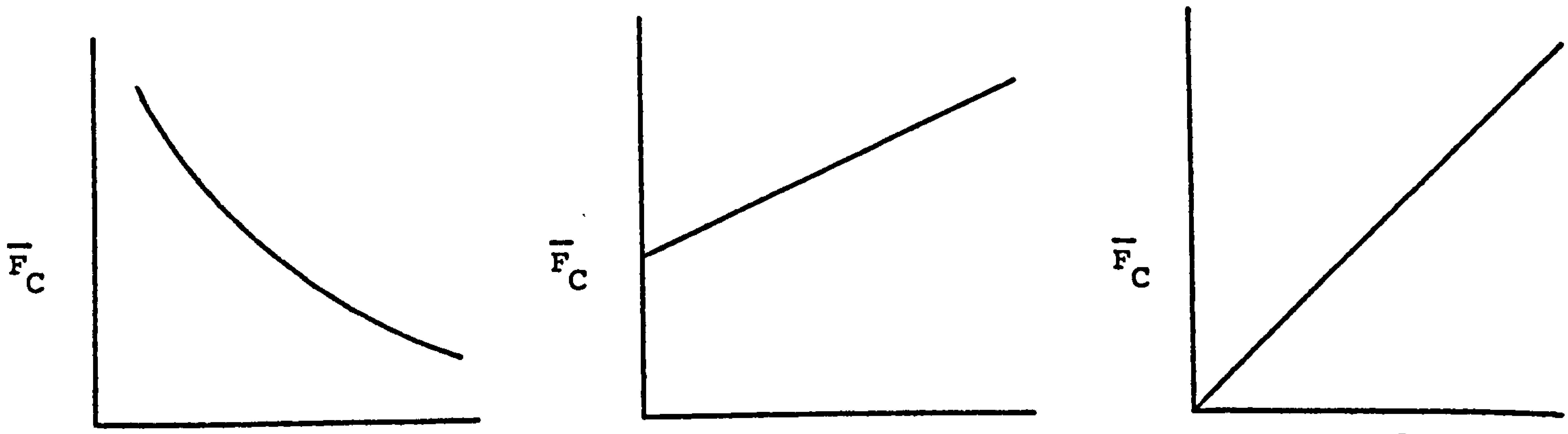

FIGURE 12 - GRAPHS OF VARIABLES AGAINST MEAN CUTTING FORCE

Two of these relationships are clearly linear, one being through the origin. These can therefore be represented by equations of the form:

$$\overline{F}_c = A\,d \qquad \text{.......................................(1)}$$

$$\overline{F}_c = Bw + c \qquad \text{.......................................(2)}$$

The third relationship appears to be exponential and can to a good approximation, be represented by the equation:

$$\overline{F}_c = e^{(D\alpha + E)} + F \qquad \text{.................................(3)}$$

Although technically the letters A - F in the above equations are constants, it must be remembered that these are only partial equations and the constants cannot therefore be single valued. They are in fact functions of the 2 variables not included in the equation.

The purpose is now to combine the partial equations to produce a single general equation relating $\overline{F}_c$ to the 3 variables. Partial equations which all contain a constant term may simply be added together to produce the general equation (3). If, however, one or more does not include a constant term, then the simplest form of the general equation must be a product of the partials (75). Since equation (1) does not, in fact have a constant term, then all 3 partials must be multiplied together,

Thus:

$$\overline{F}_c = f_1(d) \cdot f_2(w) \cdot f_3(\alpha) \quad \ldots\ldots\ldots\ldots\ldots\ldots\ldots\ldots (4)$$

where f_1, f_2 and f_3 are of the forms given by equations (1), (2) and (3) respectively.

The next stage is to determine the constants appropriate to this general equation. Since the general equation is, however, composed of 3 partial equations, there is the possibility that one of the partials will dominate the general relationship. This could mask the secondary, but nevertheless important effect of the other two variables. In the equation (4) and inspecting the "independent" relationships shown in Fig. 12, the partial equation (1) is likely to have the strongest influence.

In order to determine the contribution of the two weaker variables to the general equation, the powerful influence of equation (1) must be neutralised and this is done as follows:-

$$\overline{F}_c' = \frac{\overline{F}_c}{d} = f_2(w) \cdot f_3(\alpha) \quad \ldots\ldots\ldots\ldots\ldots\ldots\ldots\ldots (5)$$

So that, by dividing the mean force value $\overline{F}_c$ by depth of cut d, an intermediate parameter of mean cutting force per unit depth of cut is introduced. The 25 different values which this takes are included in Table 19.

It is now possible to calculate the general constant associated with width. This is done by regrouping values of the intermediate parameter $\overline{F}_c'$ according the levels of width and determining new mean values as follows:-

Level of Width	$\overline{F}_c'$ (kN/mm)					Mean $\overline{F}_c'$
10	0.125	0.110	0.081	0.058	0.059	0.087
20	0.210	0.120	0.124	0.077	0.077	0.122
30	0.282	0.203	0.116	0.119	0.179	0.180
40	0.214	0.246	0.155	0.155	0.084	0.171
50	0.321	0.160	0.253	0.271	0.098	0.221

The mean values for $\overline{F}_c'$ shown above are all appropriate to a mean level of rake angle α, since the 5 values of $\overline{F}_c'$ in a row is each at a different level of α. Since the mean $\overline{F}_c'$ values in the last column are all at the same effective value of α, then the $f_3(\alpha)$ term in equation (5) is constant and may be ascribed the value K_1. Equation (5) can now be re-written:-

$$\overline{F}_c' = f_2(w) \times K_1 \quad \ldots\ldots(6)$$

By now introducing the actual partial for $f_2(w)$, using equation (2), this becomes:

$$\overline{F}_c' = (B_1 w + C_1) \cdot K_1$$

$$= (w + \frac{C_1}{B_1}) \cdot K_2 \quad \ldots\ldots(7)$$

where $K_2 = K_1 \cdot B_1$

By regressing the Mean $\overline{F}_c'$ values against width, $\frac{C_1}{B_1}$ which is the ratio intercept/slope, can be calculated. It must be calculated as a ratio otherwise slope remains as $B_1 \cdot K_1$ and intercept as $C_1 \cdot K_1$, providing only 2 equations to solve for the 3 unknowns B_1, C_1 and K_1.

The value obtained for this ratio is 19.16 giving

$$\overline{F}_c' = (w + 19.16) \cdot f_3(\alpha) \quad \ldots\ldots(8)$$

Now that the role of width in the general equation has been determined, its affect can be isolated, as was the case with depth. So that similarly

$$\overline{F}_c'' = \frac{F_c'}{(w + 19.16)} = f_3(\alpha) = e^{(D_1\alpha + E_1)} + F_1 \quad \ldots\ldots(9)$$

In Table 19, 25 values for $\overline{F}_c''$ have been calculated and listed. Abstracting these, grouped according to the level of α, the following mean values of $\overline{F}_c''$ emerge.

Level of Rake Angle	$\overline{F}_c$" ($\times 10^{-3}$)					Mean
-10°	4.287	5.363	5.737	3.617	4.642	4.729
0°	3.065	4.130	4.158	2.314	3.773	3.488
10°	2.360	2.620	3.658	2.778	3.167	2.917
20°	3.153	4.581	1.989	1.966	2.421	2.822
30°	1.417	2.023	1.966	3.641	1.420	2.093

Using the rake angle and mean $\overline{F}_c$" values, the constants D_1, E_1, and F_1 for a relationship of the form of equation (3) can be determined using graphical or other standard curve fitting methods. These are found to be

$$D_1 = -0.023$$
$$E_1 = -5.753$$
$$F_1 = 5 \times 10^{-4}$$

The general empirical equation for this example can now be written

$$\overline{F}_c = d\{w + 19.16\}\{e^{-(0.023\alpha + 5.753)} + 0.0005\} \quad \ldots\ldots(10)$$

The validity of this equation can be assessed by inserting values of d, w and α appropriate to Table 18 and comparing the 25 results for $\overline{F}_c$ with the corresponding measured values. This has been done and values derived from equation (10) appear in the final column of Table 19. The predicted and measured values are contrasted in Figure 13, which gives a correlation coefficient of 0.94. This measure of reliability for the application of the Protodyakonov method is highly significant.

If, however, the confidence level had not been of a sufficiently high order, then the first approximation of the partial equations should be revised to provide greater accuracy and the subsequent analytical procedure repeated.

5.5 Application of Analytical Procedure

The above example was for a 3 variable 5 level case and considered only one of the parameters. Similar procedures are therefore necessary to determine the relationships for the parameters F_c, F_N, $\overline{F}_N$, Q, C.I. and S.E.

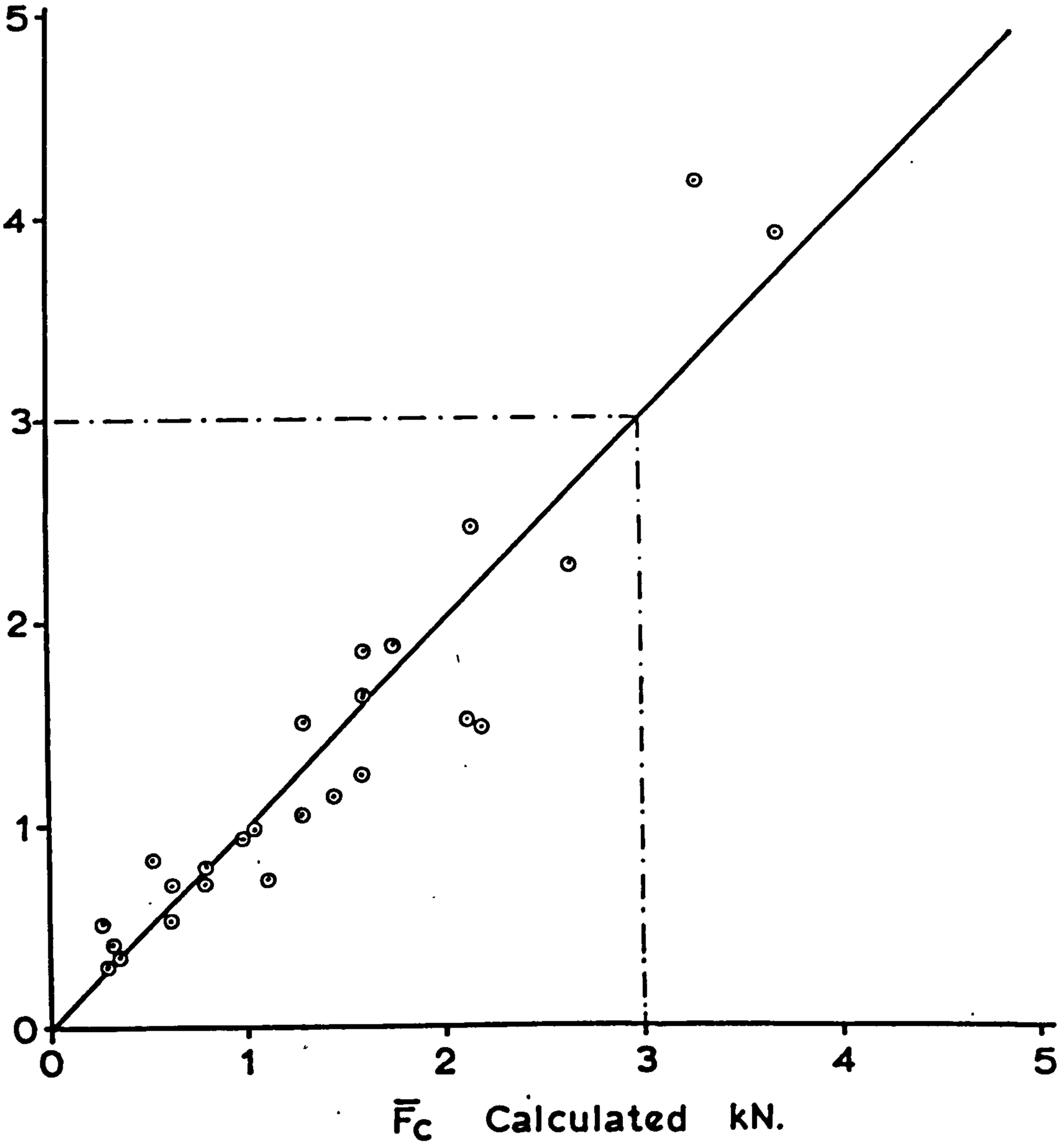

FIGURE 13 - MEASURED & CALCULATED MEAN CUTTING FORCES FOR PICKS (DRY BUNTER SANDSTONE)

The same basic procedure is used when 4 or more variables are under consideration. For 4 variables, however, there will be 4 partial equations for each parameter. Isolating the effect of each variable now becomes a very long process.

It has been found necessary, therefore, to use a computer to perform the many routine calculations. Since a computer had to be involved, it was decided also to use it to provide the best partial equation to fit the appropriate data. Eight basic forms of relationship were stored from which the computer offered the most accurate equation. This was done using a conversational mode.

5.6 Programmes for the Main Cutting Experiments

As was stated in 5.3, all variables in a single planned experiment must be tested at the same number of levels. Since moisture content could only be tested at 2 levels, it was necessary to arrange 2 separate programmes of experiments.

A further important consideration at this stage concerns the inclusion of "spacing" as a variable within the experimental matrix. Although this is possible in both theory and practice, its inclusion eliminates an opportunity to study the absolute performance of picks and discs in isolation. If there is a need to relate tool parameters to rock properties, then it is essential to have programmes of work entirely devoted to picks and discs cutting without relief. There is an additional factor against the inclusion of spacing. It is found that the variables depth, width and spacing not only interact, but their effects are also closely inter-related, as shown by previous relationships which have needed to introduce spacing/ depth ratio as a parameter (18)(76).

With these important factors in mind the programmes for the main cutting experiments were produced. The individual experimental plans are given in the appropriate sections of Chapters 7 and 9.

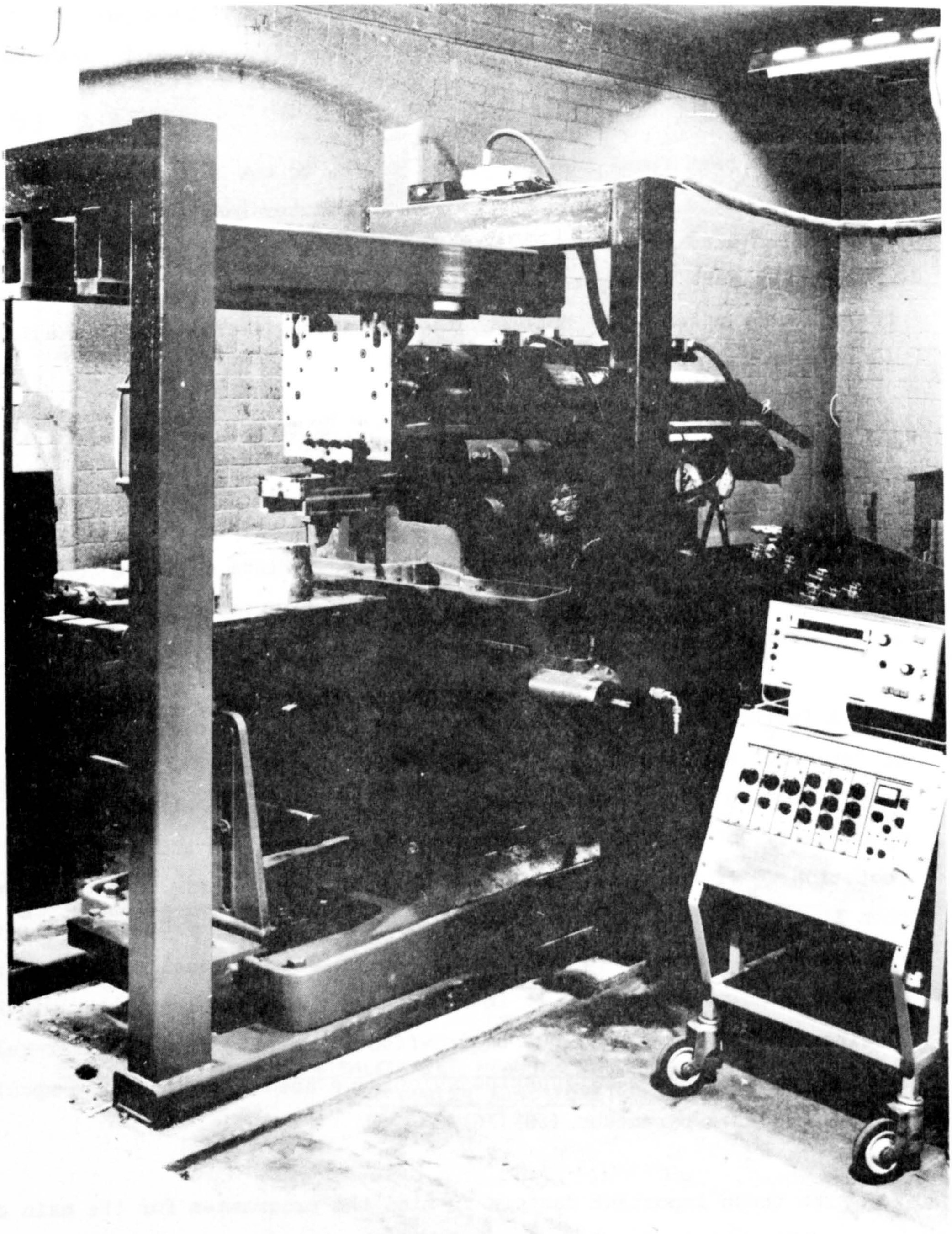

FIGURE 14 MODIFIED KELLY SHAPER WITH INSTRUMENTATION

6. EXPERIMENTAL EQUIPMENT

6.1 Rock Cutting Rigs

The main programme of experiments used two different cutting rigs. For the greater part of the pick cutting programme the rig used was a modified 9 kW Butler Shaping Machine having a stroke of 660mm and maximum in line thrust of 50 kN. Cutting speed was variable between 0.13 and 0.63 m/s.

This particular rig was unsuitable for some of the pick work in Magnesian Limestone, and for all of the disc work, due to its poor vertical constraint. To provide a facility for these experiments a Kelly Shaper, of 800mm stroke was extensively modified. It was fitted with a stiff box-sectioned framework, which provided a track to both constrain and guide the tool during its forward motion. This frame limited the vertical deflection of the tool during cutting to 0.5mm at a load of 50 kN. The arrangement is shown in Figure 14. A further modification was the replacement of the normal driving mechanism by a power pack and hydraulic ram. The ram provided a stroke of 800mm and a maximum thrust of 50 kN. Hydraulic power was provided by a Vickers V.S.G. Swash Plate Pump driven by a 7.5 kW motor and capable of generating speeds of up to 0.2 m/s.

Rock specimens of maximum dimensions 0.5m square by 0.3m high could be accommodated by both the Butler and Kelly rigs. Dry blocks were cemented directly onto a steel plate using Araldite. This assembly was then bolted onto the machine table. This provided an excellent bond and there were no failures of the adhesive. The same method of mounting could not, however, be used for the wet blocks. Although wet setting Araldites and other adhesives were tried, in contact with water they generated heat sufficient to crack the rock. The alternative was, therefore, the use of a welded box-section framework to retain the rock.

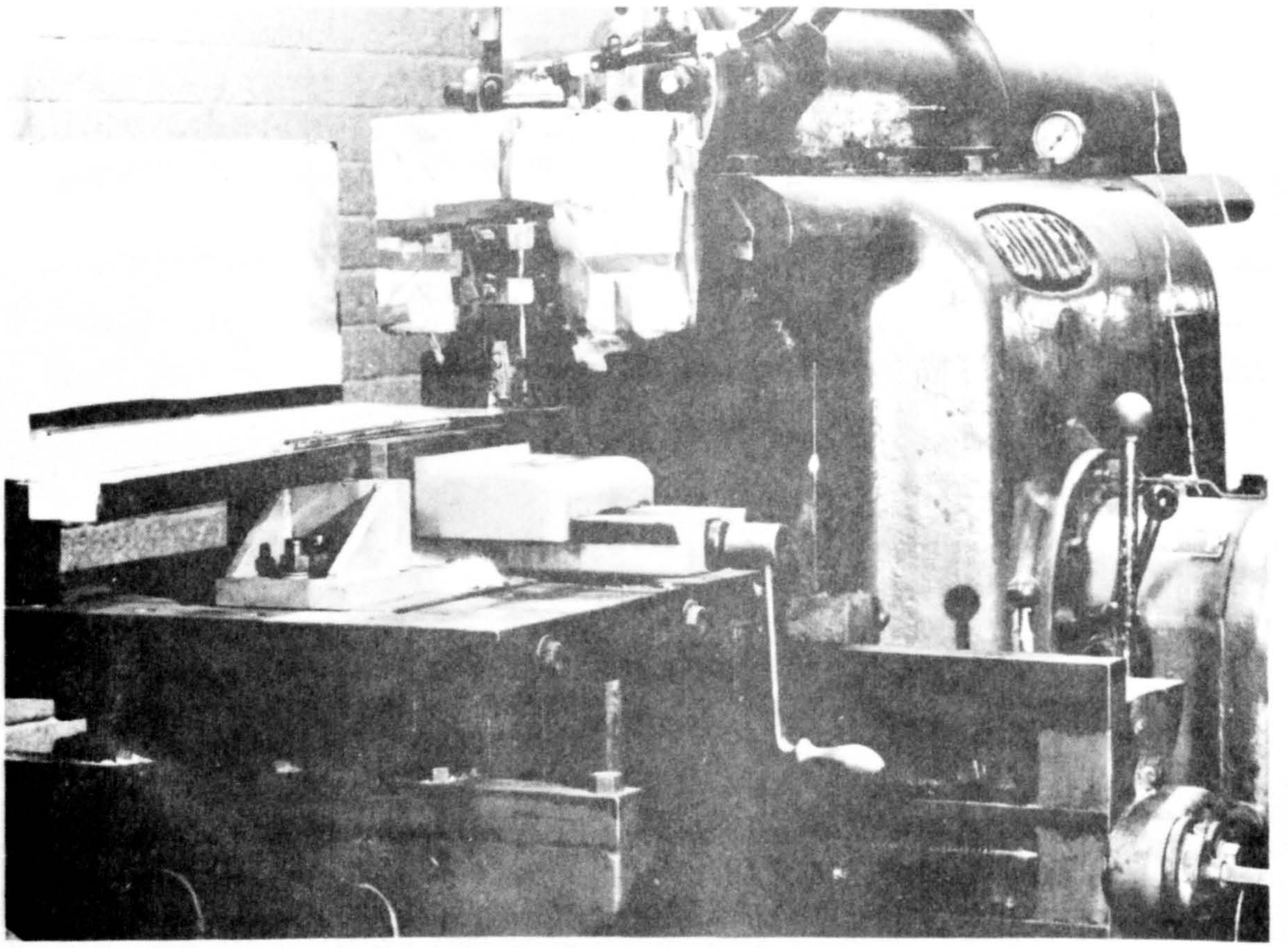

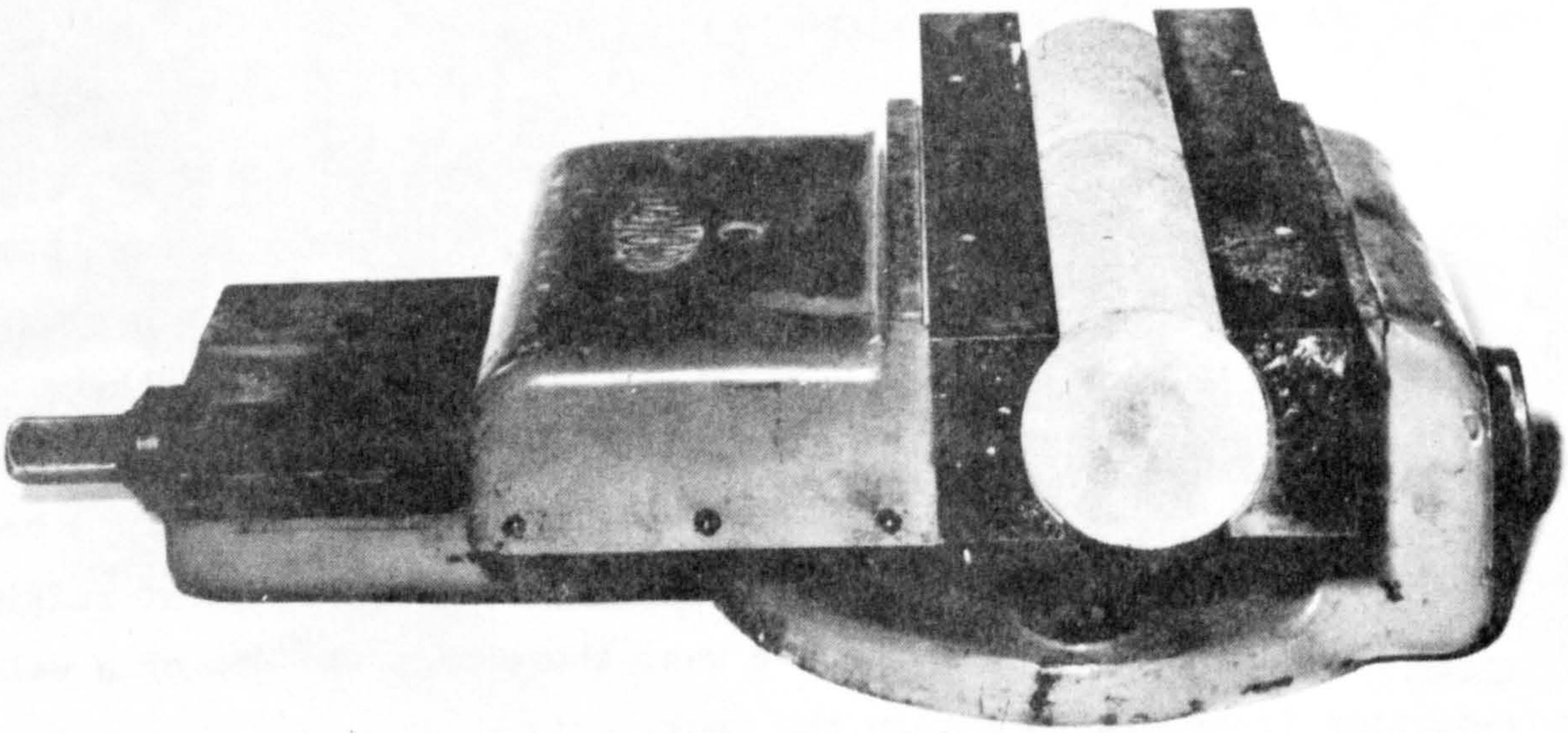

FIGURE 15 RIG ADAPTED FOR CORE CUTTING SHOWING VICE ASSEMBLY

Special reinforcement of both wet and dry blocks was required when using discs at the deeper penetration levels. There was in such cases a tendency for the block to split and this was prevented by applying lateral constraint using six 25mm diameter bolts clamped against steel plates.

During the ancilliary core cutting tests the rock was firmly held in the concave jaws of a vice. The arrangement is shown in Figure 15.

6.2 Instrumentation

Tool forces were resolved into mutually perpendicular components using a solid plate dynamometer furnished with 24 bonded resistance strain gauges mounted as 3 bridge networks. This instrument has been fully described previously (7)(77)(78).

The first dynamometer of this type was made in EN8 steel, which in certain cutting situations has been found lacking in sensitivity. Therefore an instrument of identical design and having the same strain gauge layout was made in HP 15 WP aluminium. Since this produced a five-fold increase in sensitivity, this dynamometer was extensively used to measure pick forces.

The original steel dynamometer was, however, used for the disc cutting experiments to accommodate the anticipated high thrust forces.

Input to both dynamometers was from a 5.8V, 3kHz stabalised A.C. supply. This differs from the original arrangement (7), which used a 12V D.C. supply. The A.C. system is preferred due to its inherent stability thus avoiding the problem of galvanometer drift (79).

The amplified output of the three dynamometer bridge circuits was simultaneously fed to three of the six channels of a S.E. system 3000 U.V. recorder and to three integrating circuits. Signals for the other three channels of the recorder were obtained from the output stages of the integraters. Thus a permanent record of the analogue output of the dynamometer together with an electrically integrated estimate of its mean value was obtained for each cut.

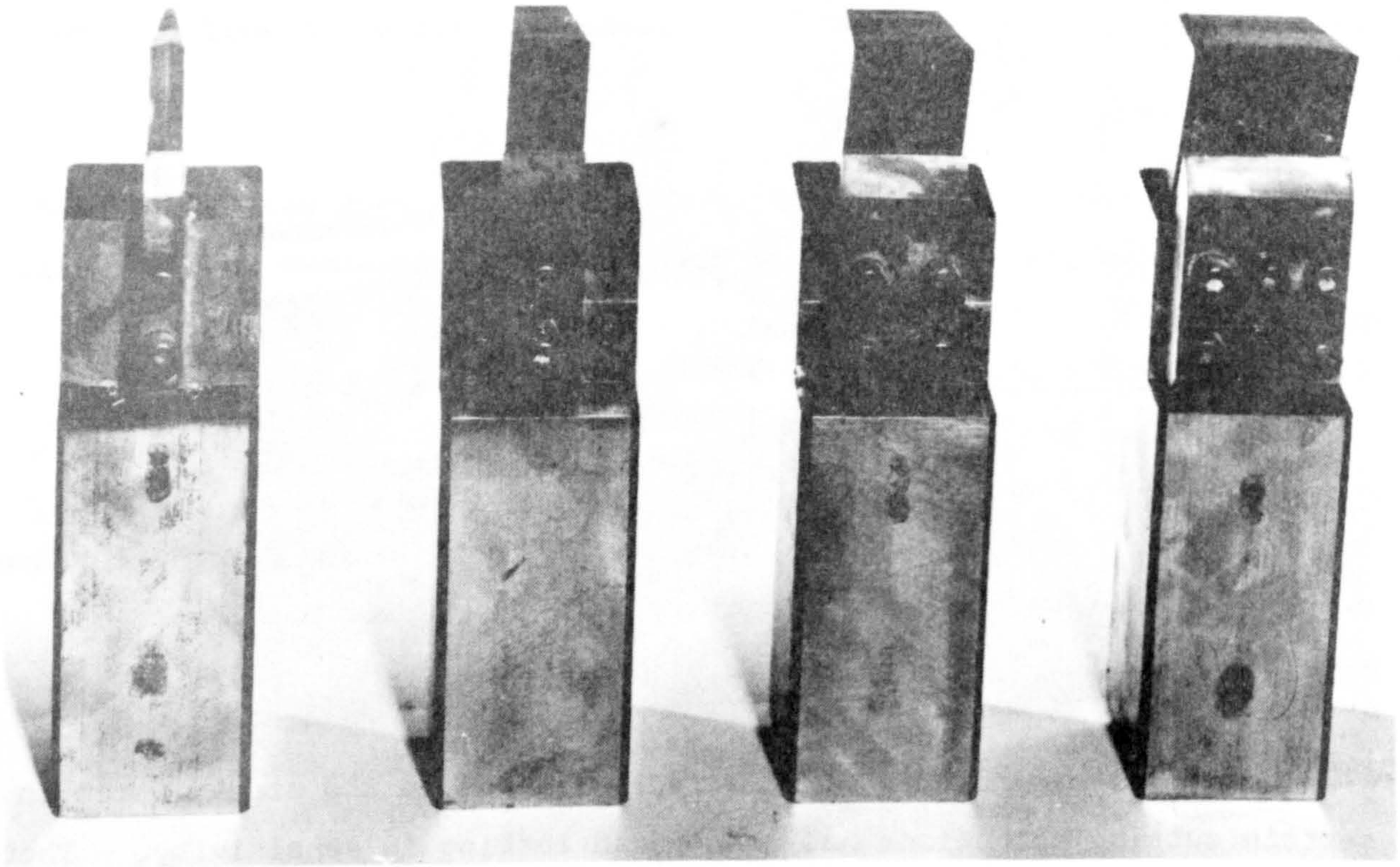

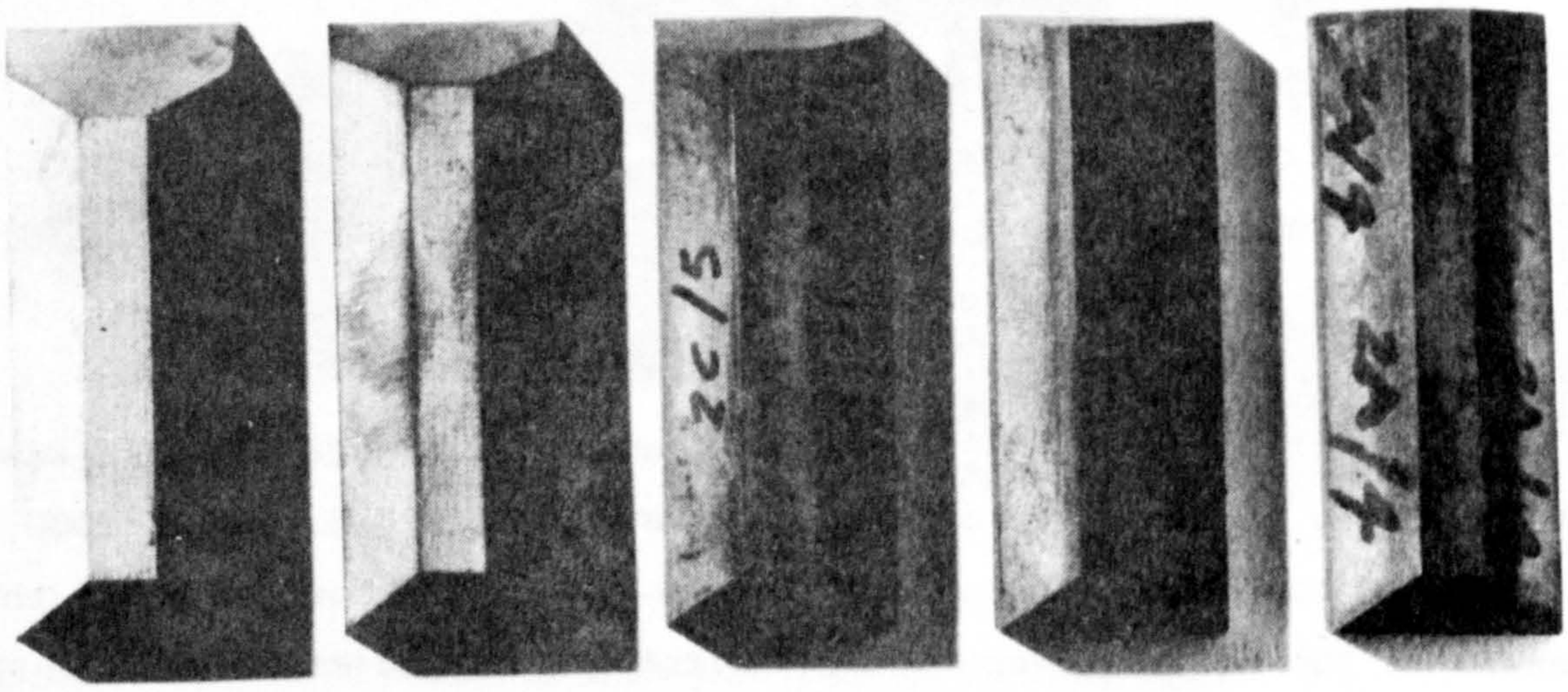

FIGURE 16 SOME TOOLHOLDERS, CLAMPS & TUNGSTEN CARBIDE INSERTS

6.3 Calibration of the Instrumentation

The force recording system was calibrated by applying a known load to the dynamometer and observing the variations in the recorded trace.

A special, spherical-ended, calibration tool was clamped into the dynamometer and loaded by means of a 100 kN hydraulic ram. Pressure was supplied by a hand pump fitted with a helicoid gauge which, together with the ram, had initially been calibrated in a 250 kN Avery Testing Machine. A complete description of the apparatus is given by Allington (7) and Rispin (14).

A wide range of forces up to the design maxima of the dynamometer were applied in the in-line, normal and sideways directions. Irrespective of the direction of the applied force, all three force traces were recorded. This enabled the interactions between the three forces bridges of the dynamometer to be measured. In addition, check calibrations were made with the force applied in arbitrary directions. These forces were resolved by the dynamometer into their orthogonal components and these measured values compared with the equivalent calculated values.

6.4 Cutting Tools

Since the Bunter Sandstone contains a high percentage of quartz and is therefore likely to be highly abrasive, special tools had to be made to minimise the effects of wear.

a) Drag Picks

In the case of picks, this was done by manufacturing a series of toolholders to accommodate replaceable inserts, made of tungsten carbide. Figure 16 shows some of the toolholders, clamps and inserts used for this investigation. In all, 25 different types of toolholder and insert were used for the main programme of tests, being appropriate to 5 different rake angles at 5 different widths. Other special toolholders, of similar design, were made for the programme of work which involved complex shapes of pick.

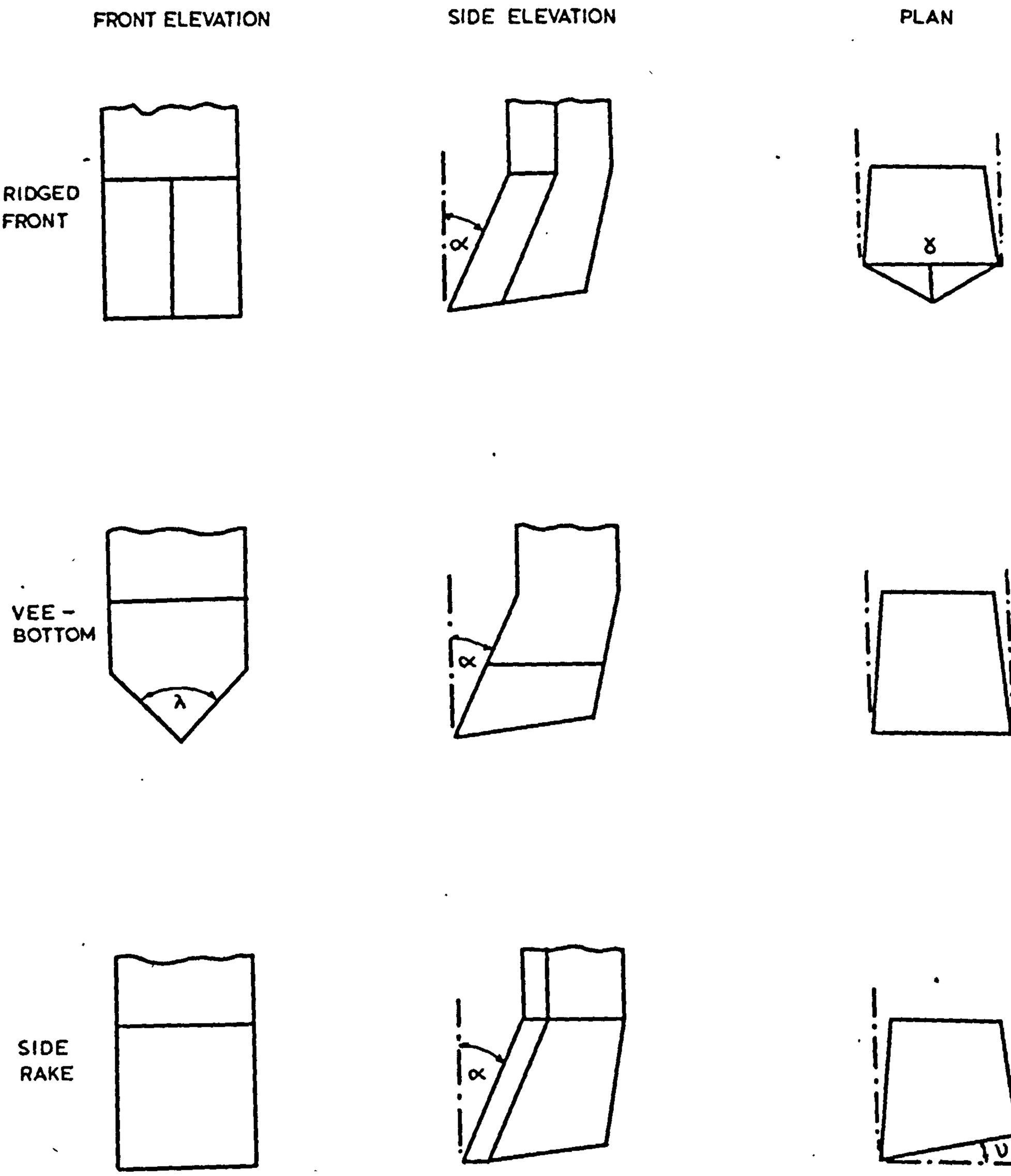

FIGURE 17– COMPLEX TOOL ANGLES

The toolholders and inserts were all designed by the Wolfson Rock Cutting Research Group and their full specification appears elsewhere (80).

With the exception of the complex tool shapes, which used 110B grade of carbide, all the inserts were of the same CM grade. Additional special grades of carbide, CH and CPM are referred to in the section on wear testing of picks.

The grade codings CM, CPM and CH are peculiar to Hoy Carbides Ltd., and 110B to Wickman Wimet Ltd., both of whom manufactured and supplied inserts.

TABLE 21

SPECIFICATIONS OF TUNGSTEN CARBIDE GRADES

Grade	CH	CM	CPM	110 B
Cobalt Content	7%	10%	15%	11%
Nominal Grain Size	3.5μ	3.5μ	3.5μ	2 - 4μ
Hardness V.P.N.	1354	1299	1114	
Density, g/cc	14.82	14.62	14.09	
Coercivity	134	116	90	
Number of Cracks	31	17	2	
Ave. Crack Length	14.0μ	5.8μ	0.4μ	

The crack propagation figures are for 10 diamond impressions (40 corners) on each test piece.

While the shape of the picks was largely determined by the levels of the experimental variables, other geometrical features of these tools were constant throughout, each pick having 10^{o} back clearance and 5^{o} side clearance angles.

The complex pick shapes were of three types:- i) Front Ridge, ii) Vee-Bottom, iii) Side Rake. The angles under consideration are defined in Figure 17. Combinations of these angles were not used, each investigation being independent.

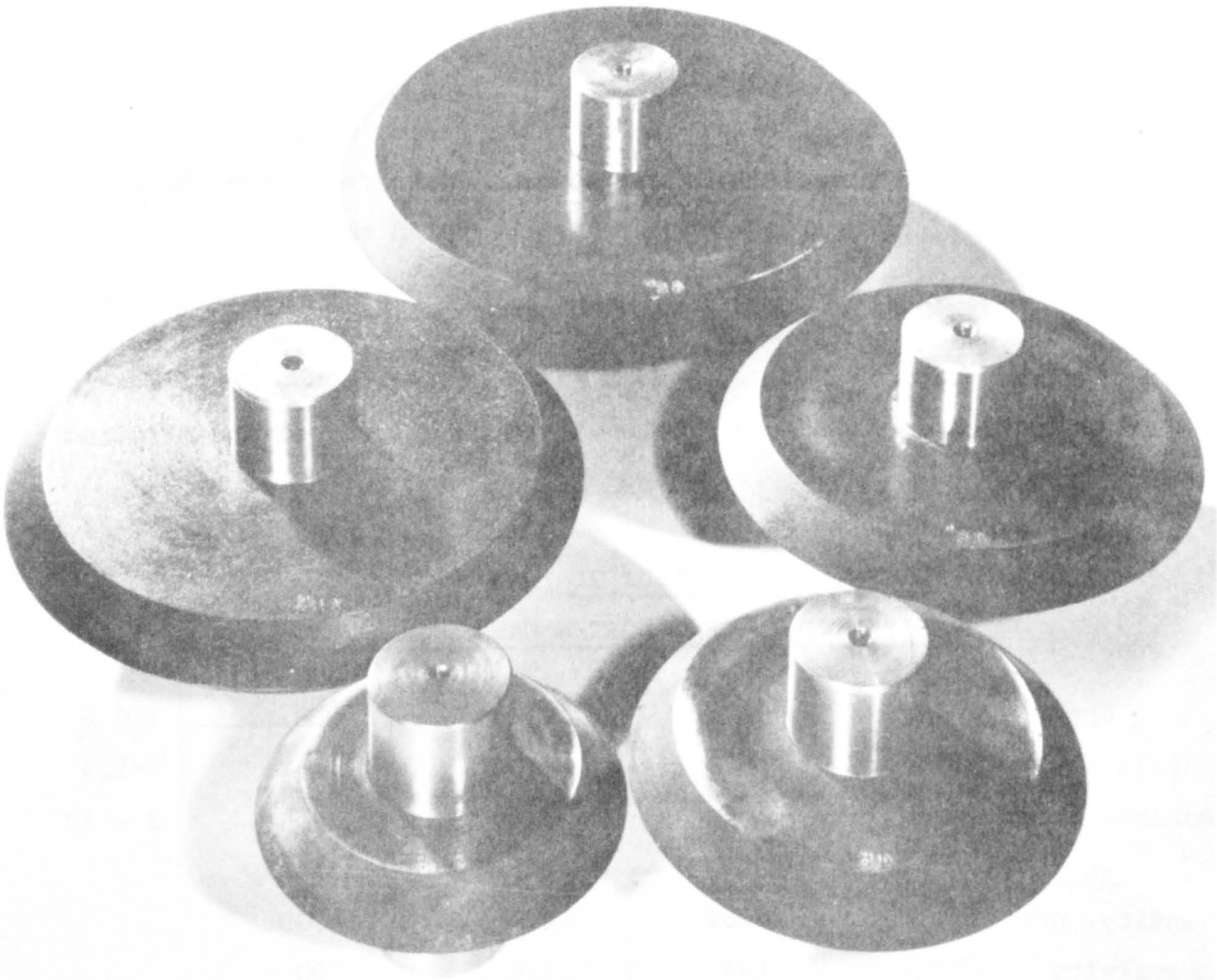

DIAMETERS OF 100 – 200 mm AT 90° EDGE ANGLE

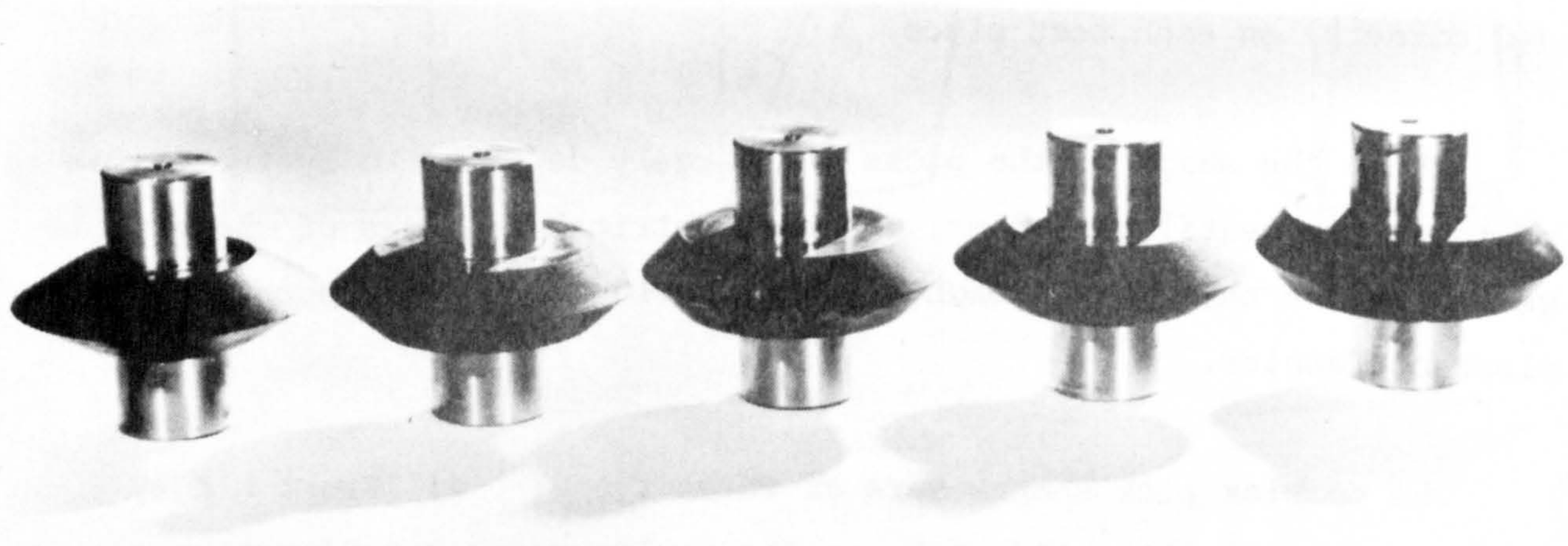

EDGE ANGLES OF 60 – 100° AT 100 mm DIAMETER

FIGURE 18 SOME EXPERIMENTAL DISCS

Front Ridge Angle	(γ)	-	90°	120°	150°	180°
Vee-Bottom Angle	(λ)	60°	90°	120°	150°	180°
Side Rake Angle	(υ)	0°	10°	20°	30°	-

All of these tools had a front rake angle of 10° with a back clearance of 10° and side clearance of 5°.

b) Disc Cutters

All 25 discs were machined from blanks of high carbon, high chrome, non-distorting steel and subsequently heat treated. This involved heating to 950°C followed by oil cooling and then tempered at 250°C. A final surface hardness of 60 RC was thereby achieved.

Each disc had a bearing shaft 40mm diameter and 85mm long. These were made from EN16 high tensile steel which made an interference fit with the disc. By fitting all discs with the same size of shaft, it was necessary to produce only one bearing housing assembly.

Figure 18 shows discs of 5 different diameters and 5 different edge angles at the same diameter. The mounting arrangement for a disc on the modified Kelly machine is seen in Figure 19.

The only supplementary experiment involving discs was an investigation into the performance of a disc cutter operating in the stalled condition. This requirement for preventing the disc from rolling was achieved by drilling a 20mm diameter hole through the disc and inserting a 50mm long, tight fitting rod of high carbon tool steel which, in turn, buttressed against the bearing housing.

The full range of tools used is summarised in Table 22.

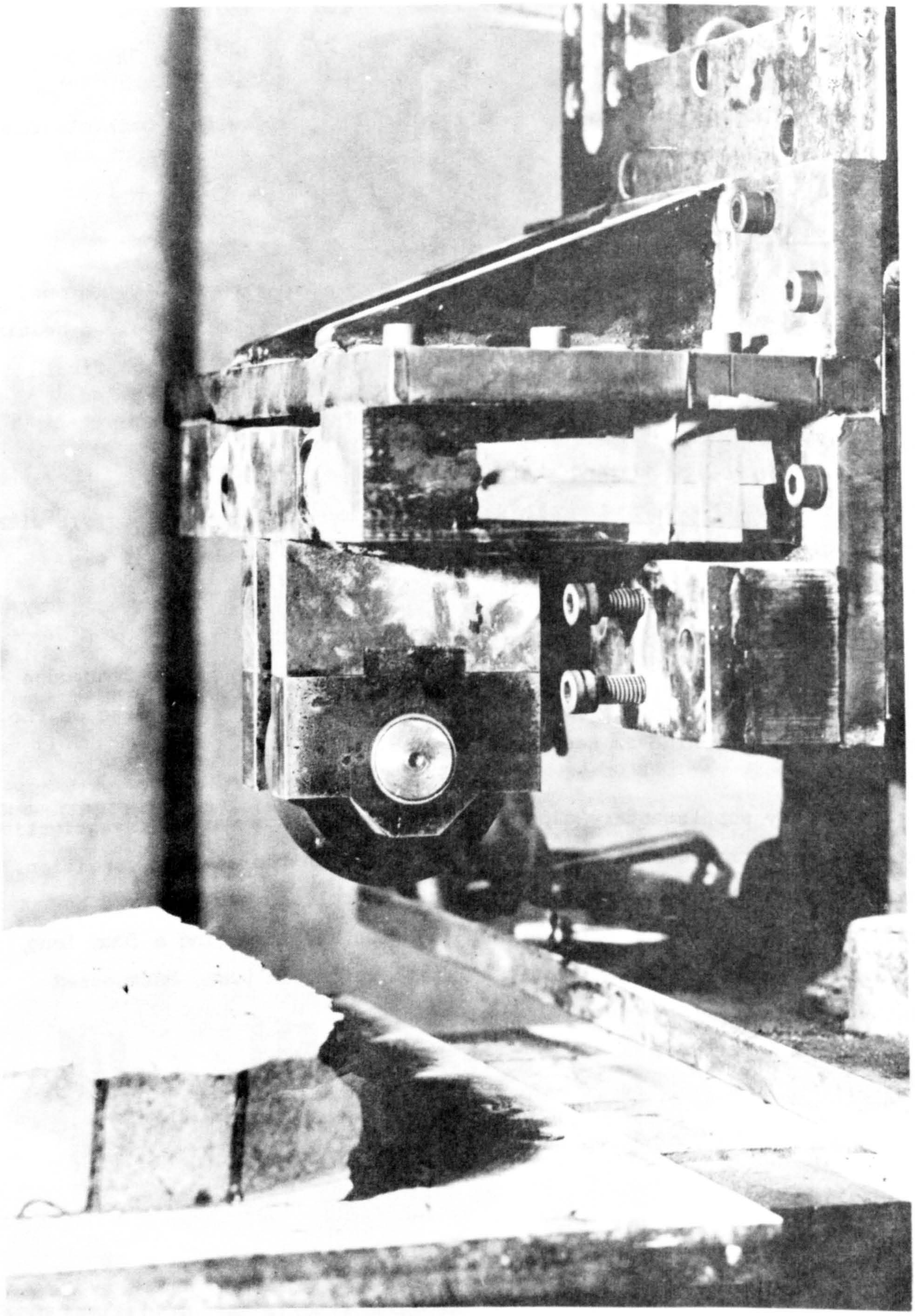

FIGURE 19 DISC MOUNTING ARRANGEMENT

TABLE 22

SUMMARY OF TOOL CONFIGURATIONS

Main Programme Picks	Simple Wedge	Tungsten Carbide CM Grade	25 configs. combining α = -10,0,10,20,30° w = 10,20,30,40,50mm
Main Programme Discs	Plain Symmetrical	High Cr & C steel Heat Treated	25 configs. combining ϕ = 60,70,80,90,100° D = 100,125,150,175,200mm
Front Ridged Picks	Complex Shape	Tungsten Carbide 11OB Grade	4 picks all α=10° w=20mm γ = 90,120,150,180°
Vee-Bottom Picks	Complex Shape	Tungsten Carbide 11OB Grade	5 picks all α=10° w=20mm γ = 60,90,120,150,180°
Side Rake Picks	Complex Shape	Tungsten Carbide 11OB Grade	4 picks all α=10° w=20mm λ = 0,10,20,30°
Core Cutting	Simple Wedge	Tungsten Carbide CM Grade	Standard pick α = -5° w = 12.7mm
Stalled Disc	Plain Symmetrical	High Cr & C steel Heat Treated	1 disc ϕ = 60° D = 200mm

6.5 Data Analysis

Dynamometer output from the cutting rigs is in analogue form and, as described in 6.2, is printed directly onto U.V. sensitive paper.

The typical U.V. recording seen in Figure 20a shows the two force diagrams representing in-line cutting and normal forces generated by a drag pick and Figure 20b, the equivalent trace for a disc cut, shows the thrust and rolling forces.

The mean peak force for a cut is determined by measuring the peak value for each 0.1 sec. interval and averaging. The precise co-ordinates of each peak are obtained using a D-Mac trace analyser which produces punched card output ready for computer analysis (81).

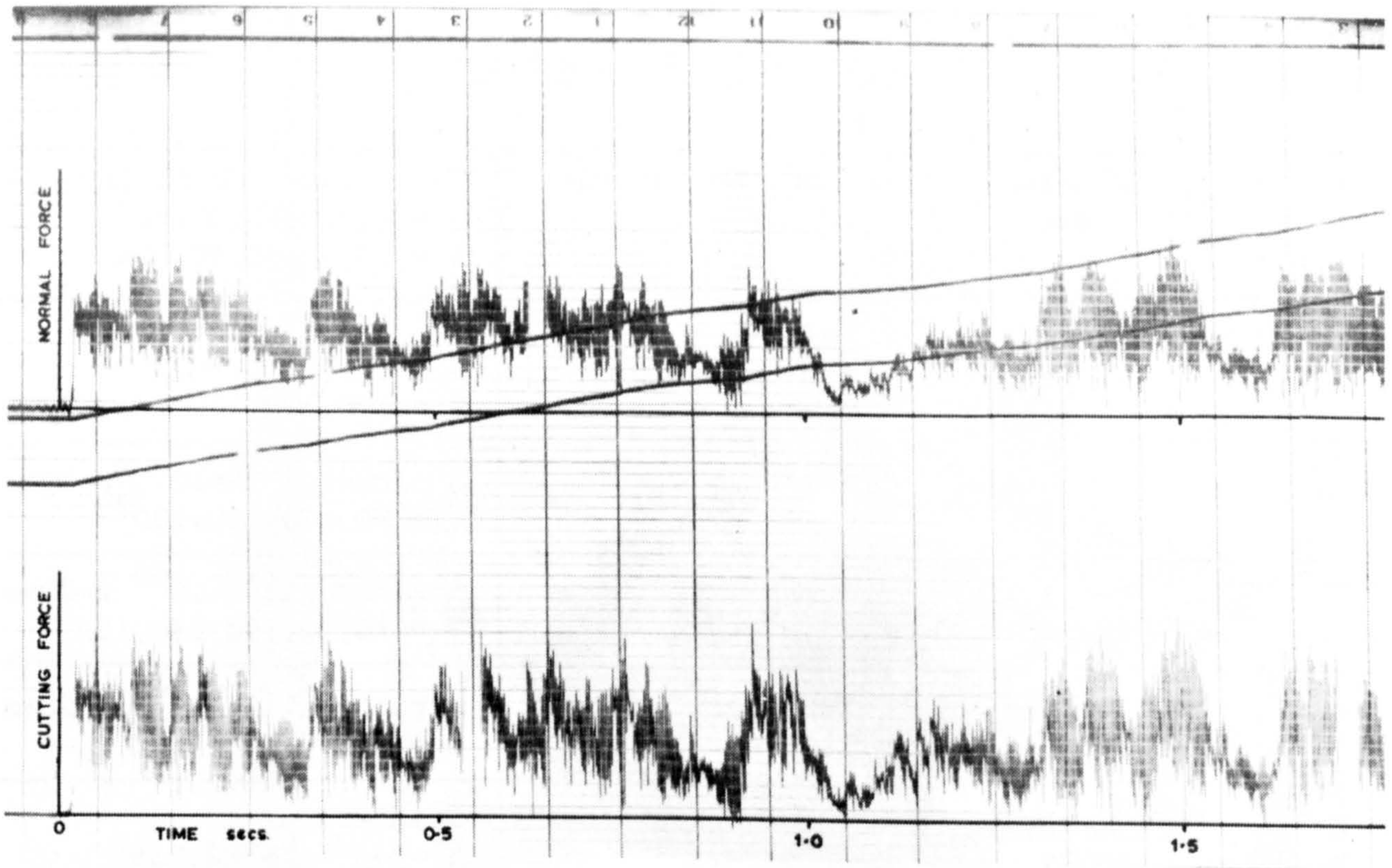

(A) PICK CUTTING

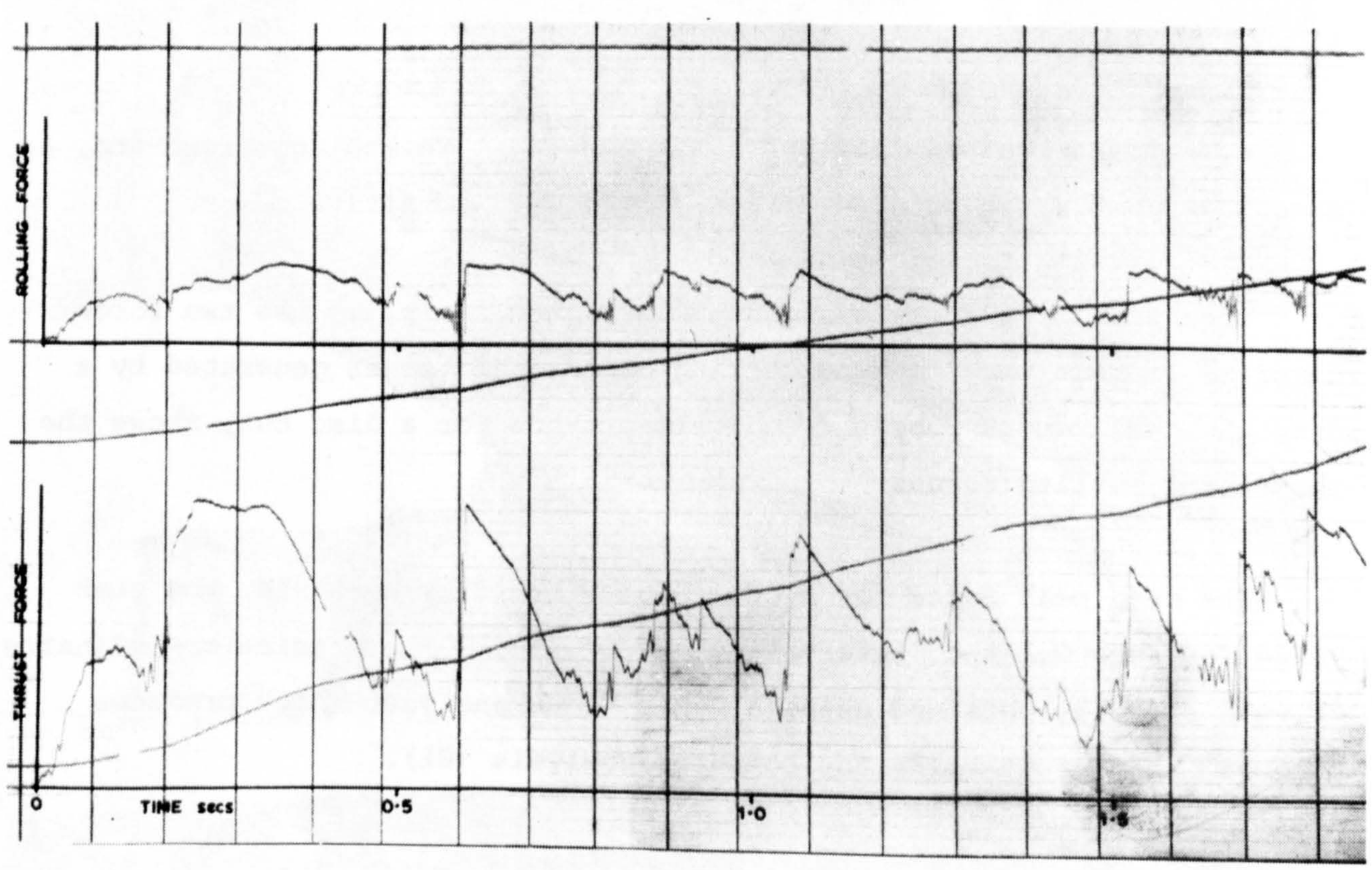

(B) DISC CUTTING

FIGURE 20 TYPICAL U.V. TRACES

Additional measurements also required for computer input include precise depth of cut, rock yield and total cutting length. Rock debris is size analysed using a stack of 6 Endecott sieves. Sieve sizes of +50, 25, 8, 2, 0.5, 0.125, -0.115mm are used.

Programmes have been written to calculate all parameters from the input data (82). They make use of a Wang 720B desk-top computer having a 4K store with magnetic tape input. The development of empirical equations for the partial factorial experiments is undertaken using a Hewlett Packard 2000E, having a 32K store, which is also connected to an I.B.M. 360/67 computer.

7. CUTTING WITH CHISEL PICKS

This chapter is exclusively concerned with picks of a simple wedge (chisel) configuration. Five partial factorial and two auxiliary spacing experiments were undertaken. The effects of wear and cutting speed on tool performance were studied in separate experiments. Chisel picks were also used to cut rock cores drilled from the large blocks of both Bunter and Magnesian Limestone.

7.1 Design of the Pick Cutting Experiments

The planning techniques used for partial factorial experiments were discussed in Chapter 5. The three unrelieved cutting experiments, which each involve 3 variables, followed the master plan shown in Table 18. Experiment I was carried out in dry Bunter, Experiment II in wet Bunter and Experiment III in dry Magnesian Limestone. The two spacing experiments, each involving four variables, used the master plan given in Figure 11. Experiment IV was conducted in dry Bunter and Experiment V in wet Bunter.

7.2 Unrelieved Cutting

It is an implicit feature of all these experiments that the effects of each variable under consideration can be abstracted from the results obtained, to provide graphical data relating an individual variable to the principal parameters of performance.

The graphical relationships which follow have been established in this way. The raw data on which the graphs are based is provided in Appendix I (A - F) and the appropriate grouped data appears in Appendix I (G, H and J).

1. Effect of Rake Angle

Figures 21 and 22 show the effect of changes in front rake angle on the forces and energies involved in cutting both Bunter and Magnesian Limestone. As previously explained in 5.4 these results are for mean pick width and cutting depth.

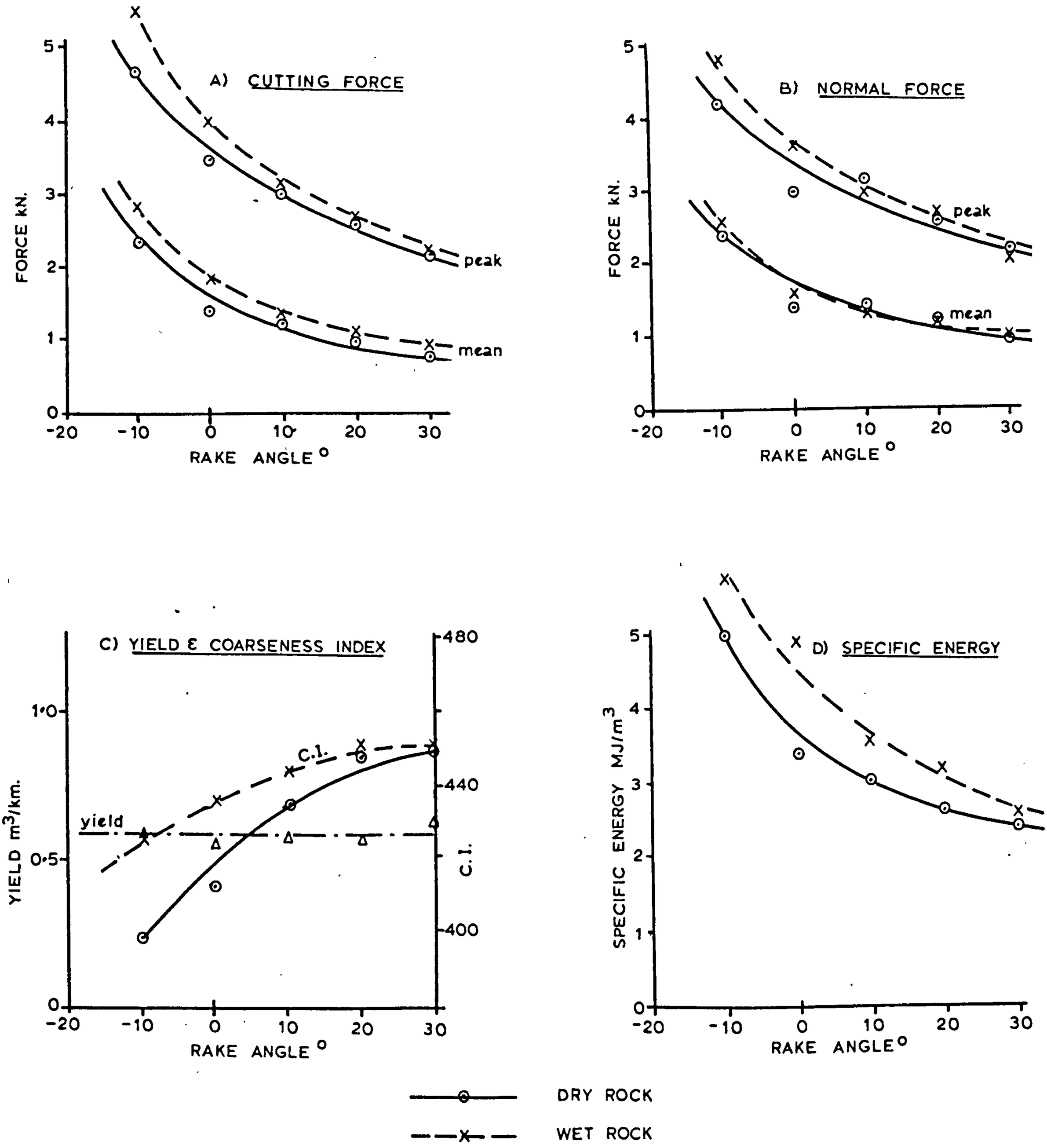

FIGURE 21 - EFFECT OF RAKE ANGLE - BUNTER SANDSTONE

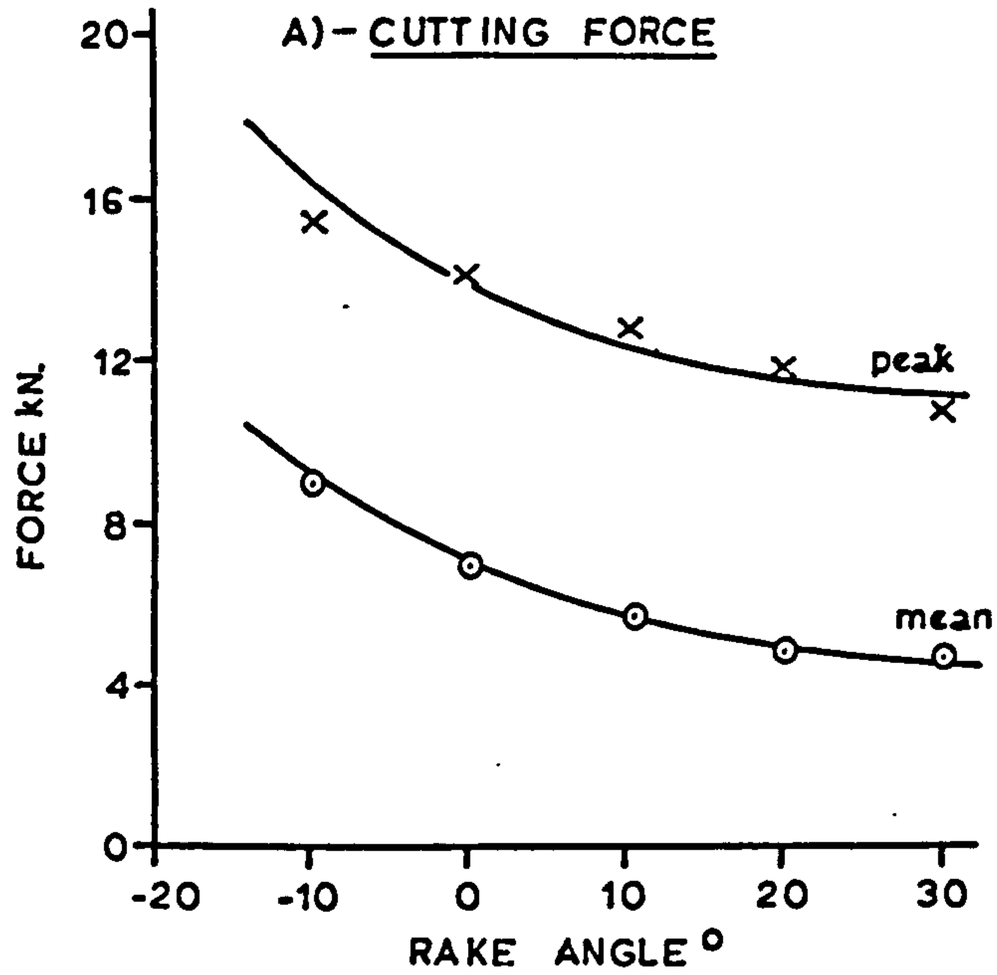

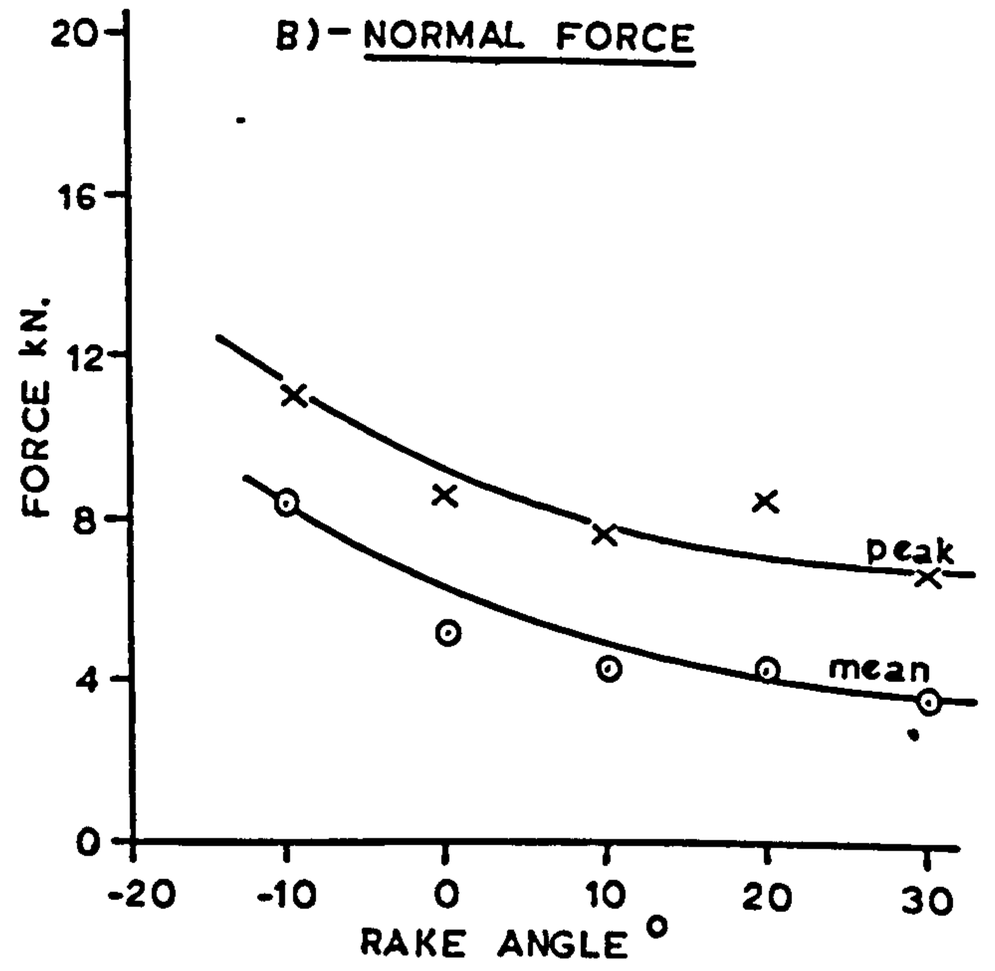

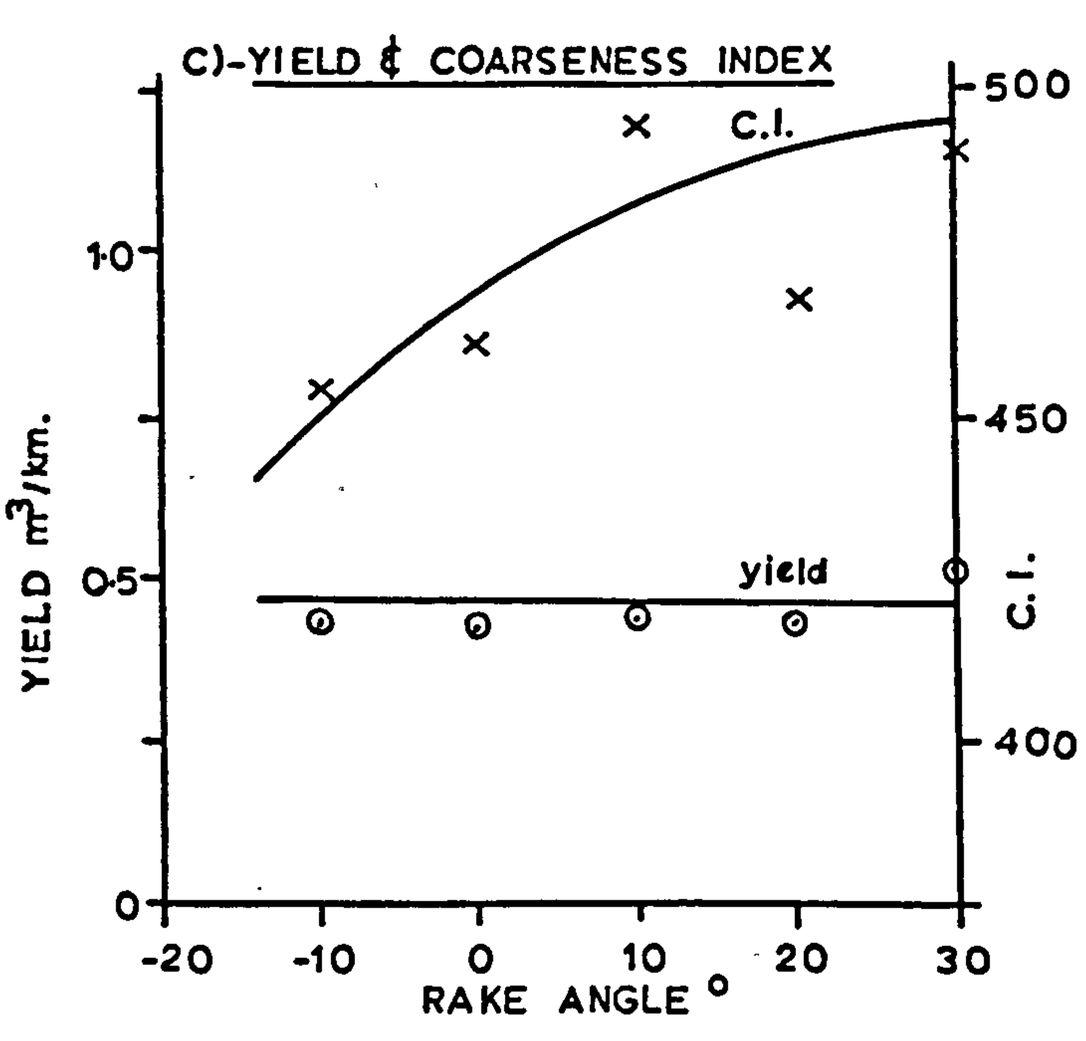

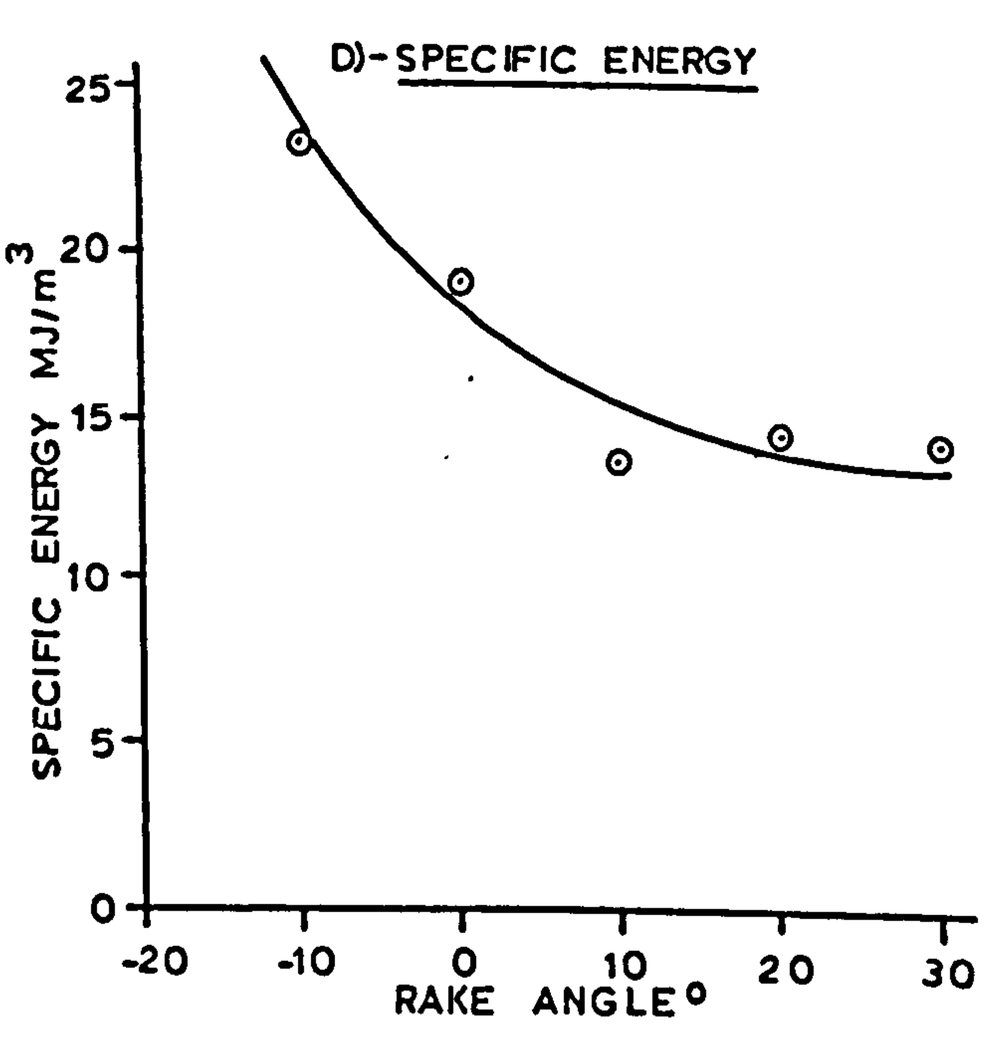

FIGURE 22 - EFFECT OF RAKE ANGLE
- MAGNESIAN LIMESTONE

Cutting forces, normal forces and specific energies are all seen to follow the same general trend. Significant benefits are to be gained from increasing the rake angle, but this requirement must be balanced against the consequential reduction in mechanical strength of the pick. The only damage caused to the picks by the Bunter Sandstone was some sign of abrasive wear but, at depths of cut of 12 and 15mm in Magnesian Limestone, the 30^{o} rake angle tool suffered gross fracturing of the carbide. In order to obtain the repetitions of these tests four carbide inserts were required. As most benefit has, however, been achieved at a rake of 20^{o} and further increases in rake provide only marginal improvements in force and energy levels, few practical applications of 30^{o} rake tools in medium strength rock would be contemplated.

The geometry of the force curves conform to the theoretical predictions of both Evans (83) and Nishimatsu (35) and extrapolation of the experimental trends shows the anticipated levelling off at rake angles above 30^{o}. Theoretical and experimental evidence in some rocks indicates the existance of a negative normal force at the higher rake angles. This was in fact found to be the case with the Lower Chalk (24). Neither of the test rocks exhibit this trend, but the ratio of normal/cutting force in Bunter is much higher than that of Magnesian Limestone. The abrasivity of the Bunter creates a wear flat at the cutting edge, which however small and apparently insignificant, tends to inhibit voluntary increase in cutting depth and increases the normal force disproportionately. A situation can quickly be reached where the normal force exceeds the corresponding cutting force.

Contrasting the difference in pick performance between the dry and wet rock conditions for Bunter, reveals that the forces and energies appear to be consistently higher in the wet rock. The rock is referred to as wet rather than saturated since it proved impossible to fully saturate the large test blocks. To produce this wet condition, blocks were fully immersed in tanks of fresh water for up to 3 months. The block was supported in the tank,

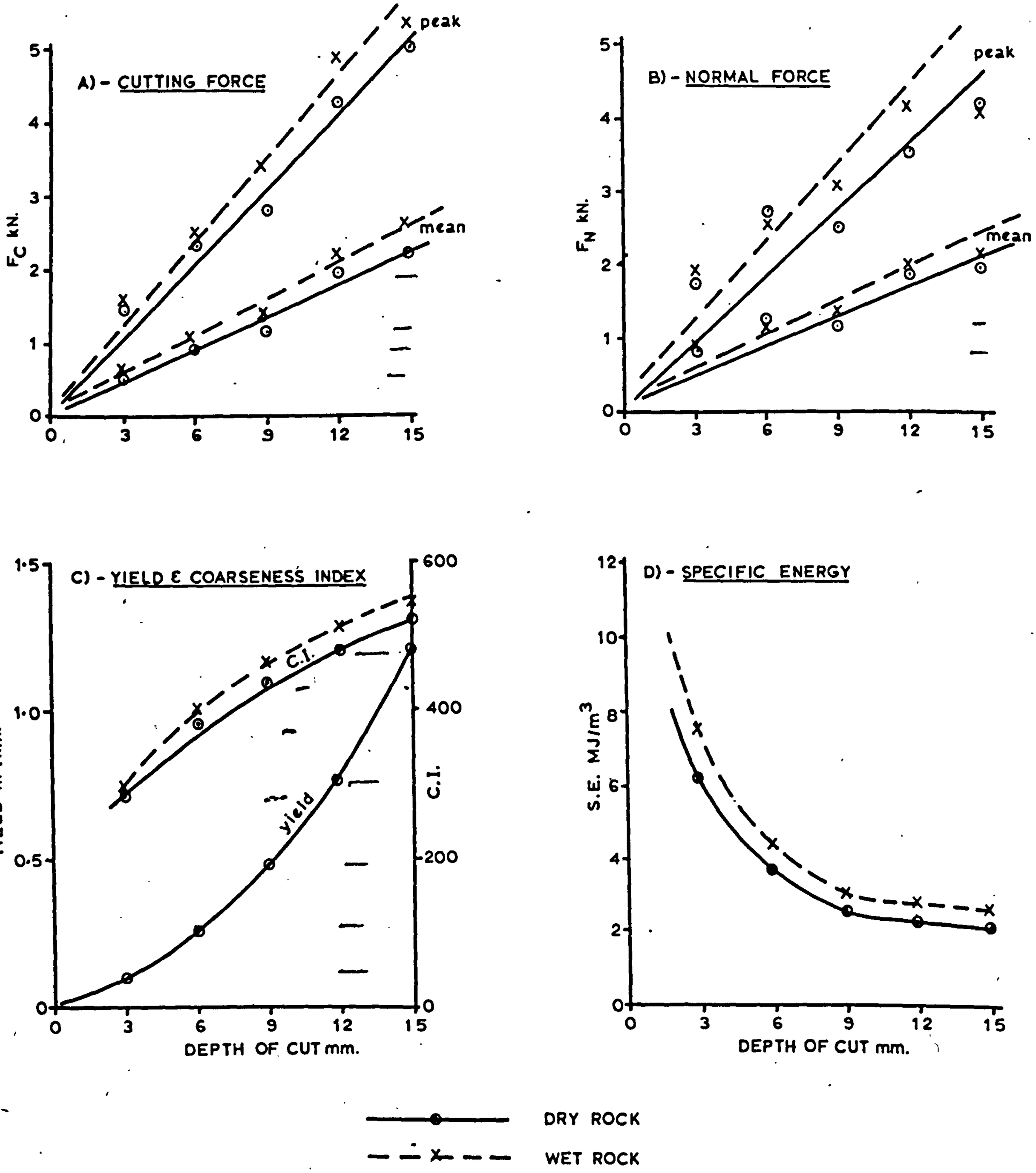

FIGURE 23 - EFFECT OF CUTTING DEPTH - BUNTER SANDSTONE

on 2 narrow beams, to give water access to all 6 faces. Extra test blocks were given exactly the same exposure to water and periodically samples were taken from these in order to determine the moisture content. Such sampling was not confined to the outer extremes of the block but was also carried out well into the centre.

After prolonged immersion the test blocks showed that the water intake stabilised after 3 weeks and further prolonged exposure caused no increase in moisture content.

The stabilisation moisture content of 7.5% was somewhat lower than the saturation level of 10.3%. Doubtless, had it been possible to provide a vacuum during the soaking process, a higher level of moisture content would have been achieved.

The fact that the main cutting experiments were at a moisture level less than saturation is of little consequence, since most "in-situ" wet rock conditions are likely to be nearer the 7.5% than the 10.3% value. What was important, however, was to ensure that the moisture content remained as consistent and constant as possible throughout the wet cutting experiments. Considerable care was therefore taken to monitor rock moisture during cutting tests, using the product from each cut. Also on the completion of a series of tests, the block was immediately returned to the water tank and re-immersed. The results of the moisture determinations are given in Appendix II.

It is of interest to note that rock yield, as shown in Figures 21 and 22, is independent of rake angle and therefore, that breakout angle is similarly unaffected. Coarseness index against rake angle follows the inverse of the force and energy curves. This suggests that the additional force and energy required at lower rake angles is in part simply absorbed in further degradations of the rock debris.

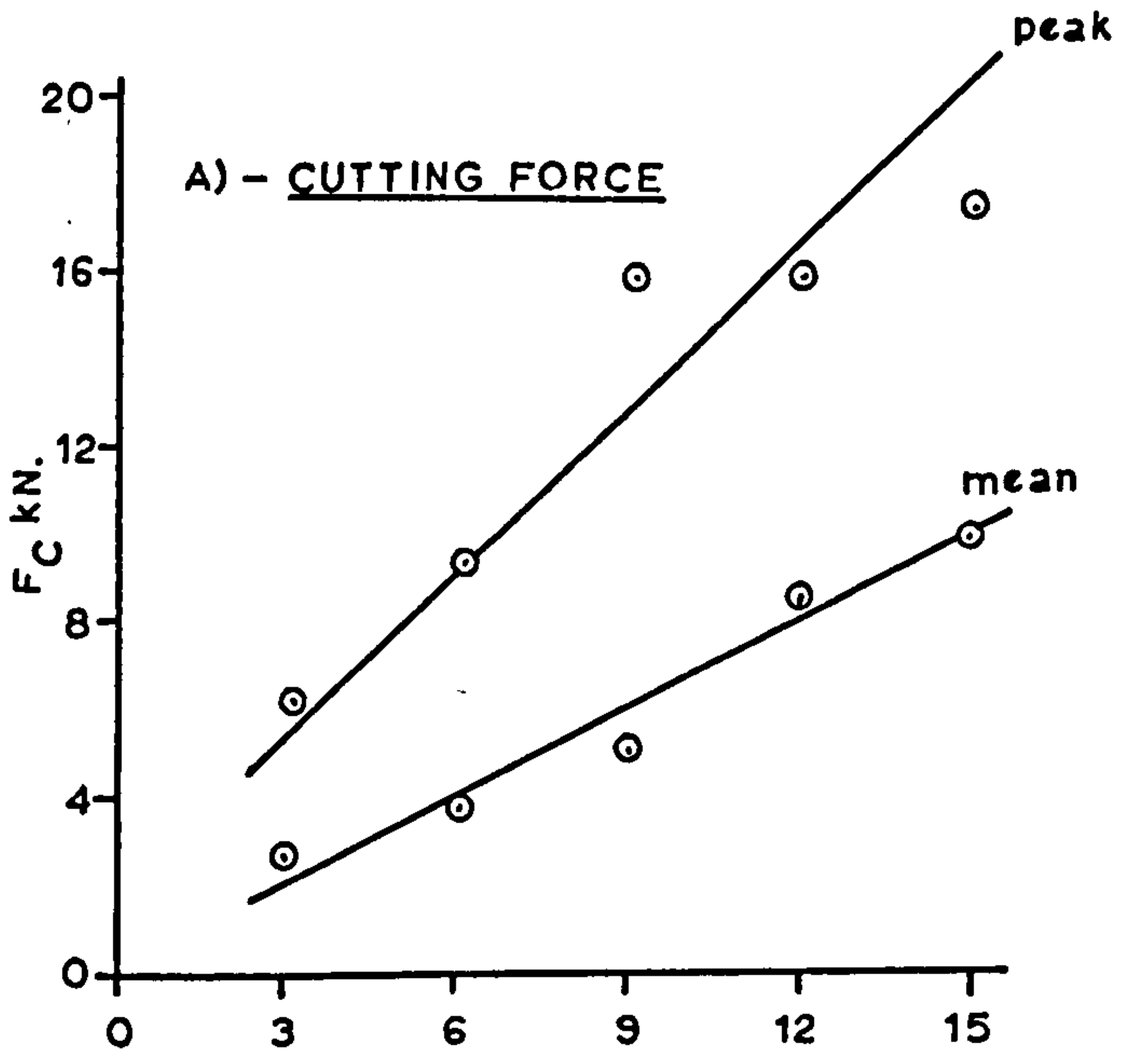

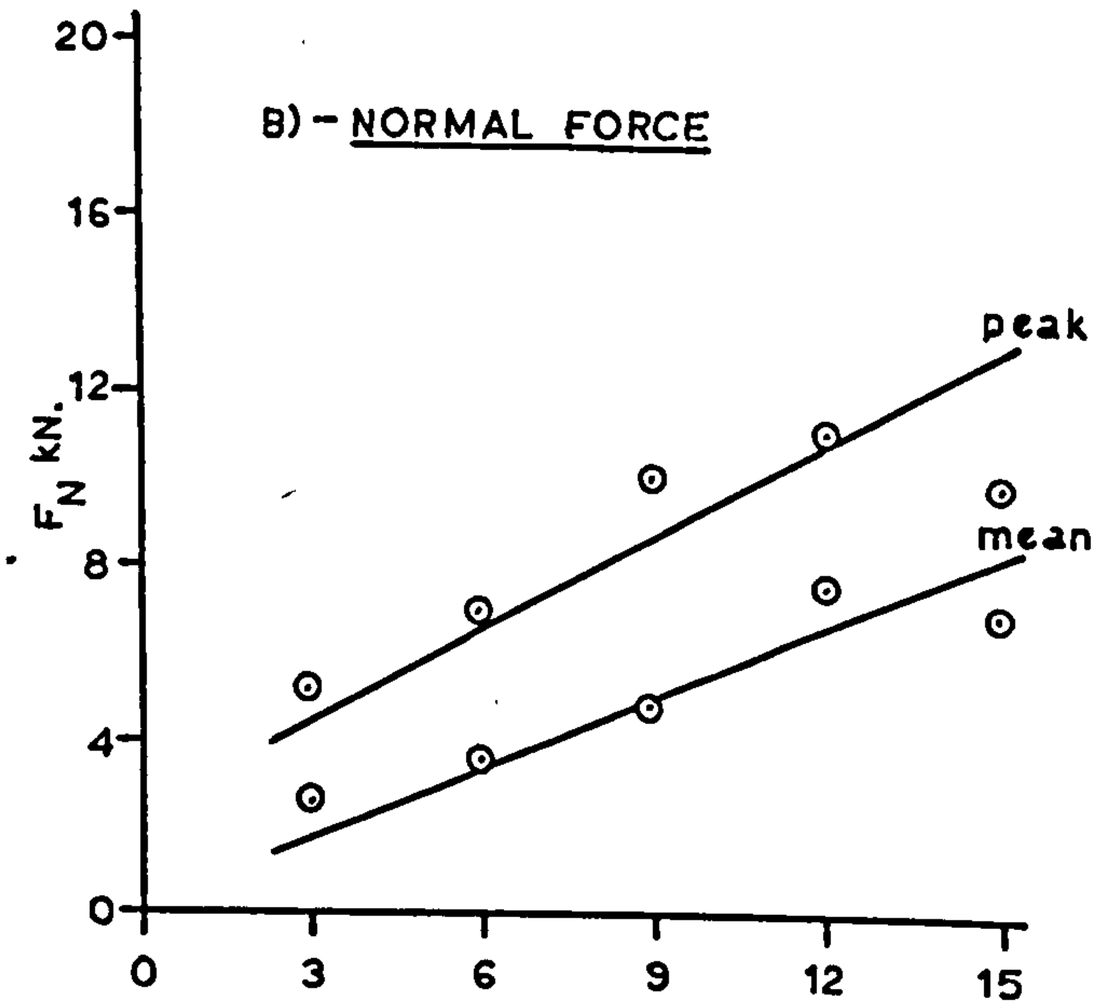

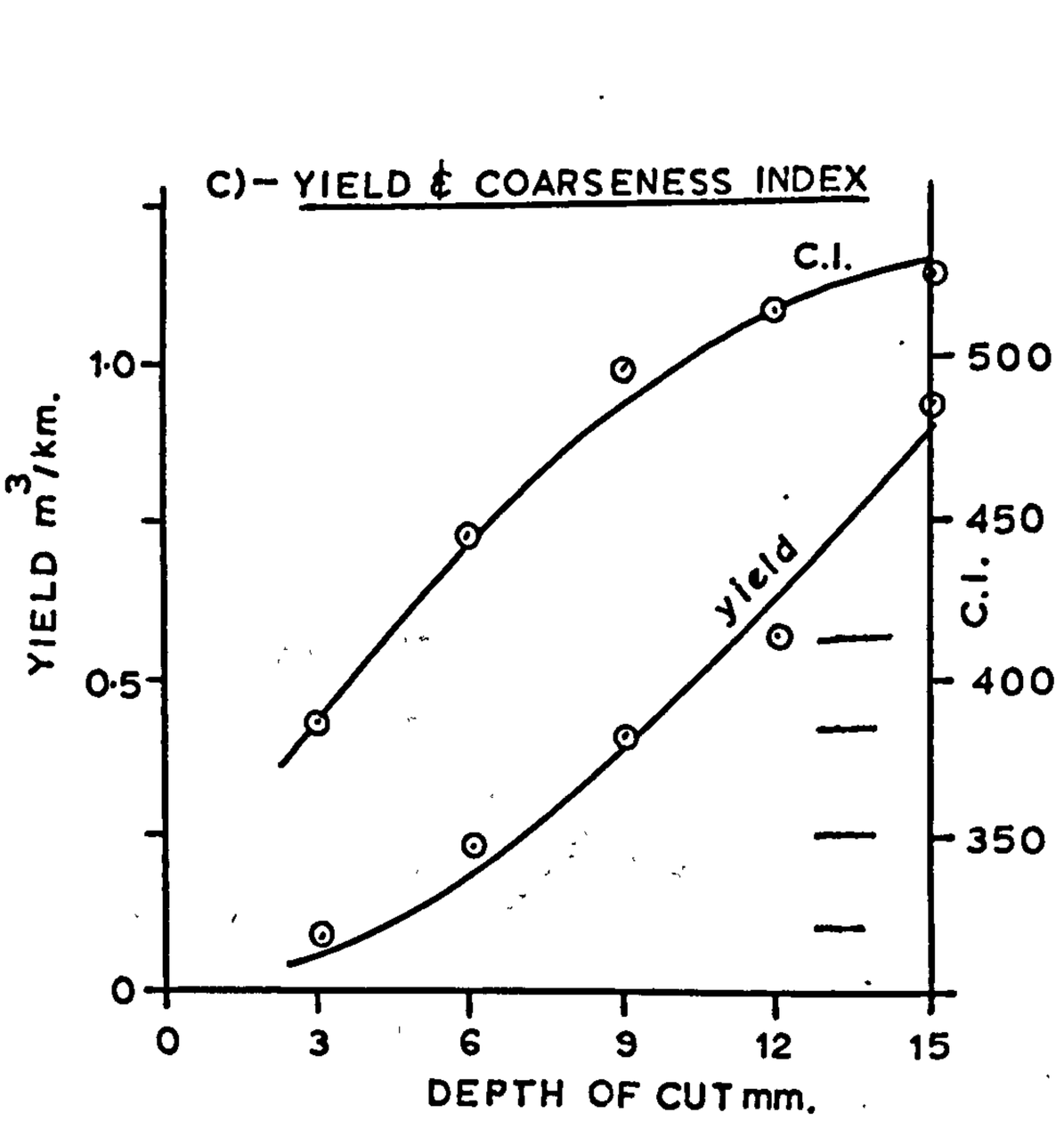

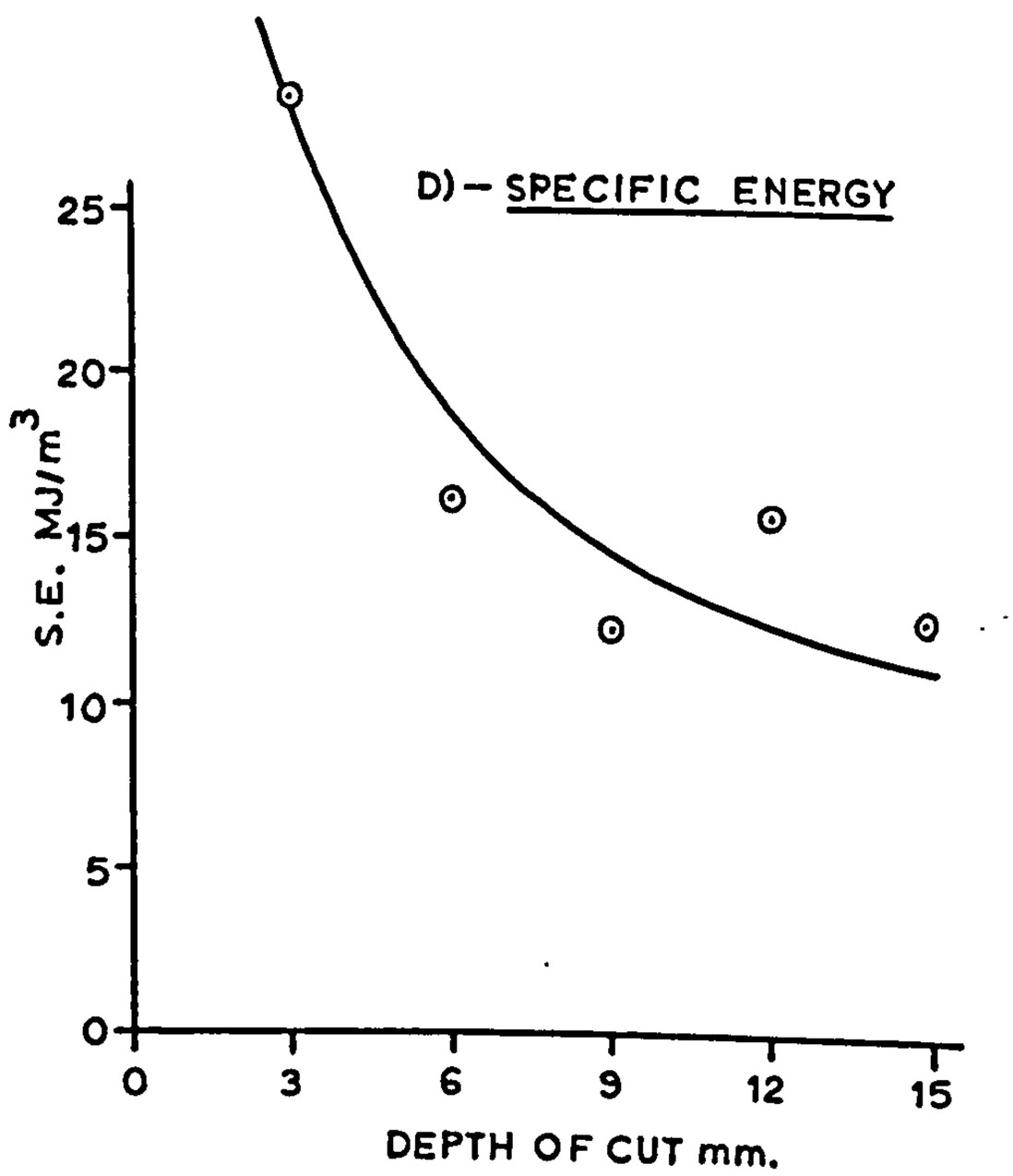

FIGURE 24 – EFFECT OF CUTTING DEPTH
– MAGNESIAN LIMESTONE

2. Effect of Depth of Cut

Figures 23 and 24 show that all pick forces are directly proportional to cutting depth. The origin may be included as a point since zero depth of cut may be defined as one of infinitesimal negative value. As before, these results are at the mean level of the other two variables. The linear proportionality of pick forces and cutting depth is in accordance with a wealth of experience in other rocks (28),(76),(84),(85).

In the sandstone mean and mean peak normal forces are found to be of similar magnitude to the corresponding cutting forces at all depths of cut while in Magnesian Limestone the normal forces are always less than the cutting forces. This conforms with similar observations made in 7.2.1 with respect to rake angle.

Wet Bunter again produces force and energy levels somewhat greater than those found in the dry rock. On average all forces are about 20% higher when cutting in the wet condition. Bearing in mind that the uniaxial compressive and tensile strengths of the saturated Bunter were respectively 17% and 30% less than the corresponding dry strengths, this increase of around 20% in wet cutting forces and energies is surprising. Yield, when considered on a volumetric basis, is unaffected by rock moisture. There is however a yield increase in wet rock of around 8% when calculated on a weight basis. This simply reflects the higher density of the wet rock, there being no discernible change of groove geometry between the wet and dry cutting conditions.

The relationship between yield and cutting depth is found, for both rocks, to follow a square law of the type:-

$$Q = Ad^2 + Bd \qquad \ldots\ldots\ldots (11)$$

This is in exact agreement with geometrical anaylis of the shape of groove, which from Figure 25 can be written

$$Q = d^2 \tan\theta + w\,d \qquad \ldots\ldots\ldots (12)$$

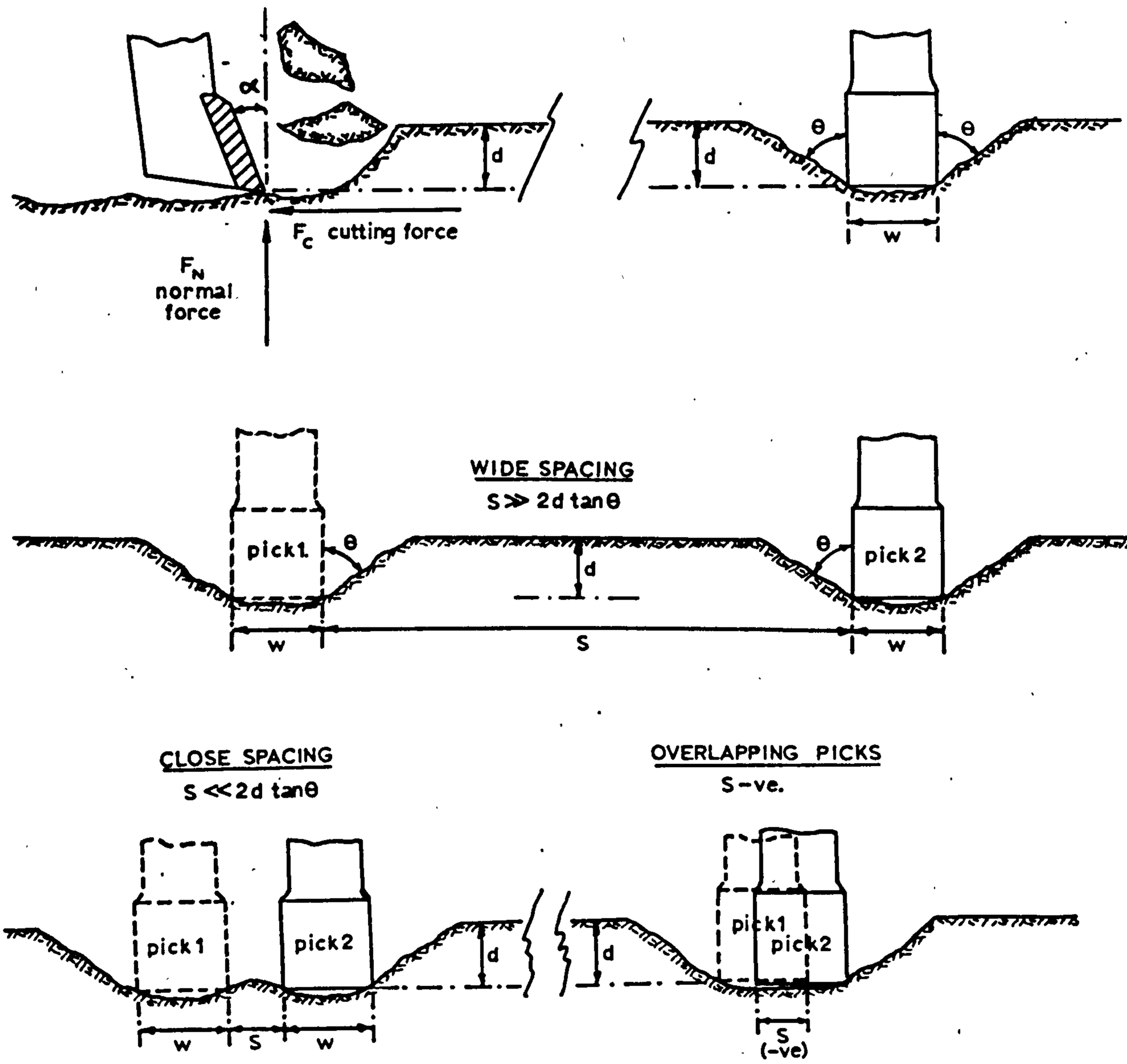

α = RAKE ANGLE

θ = BREAKOUT ANGLE

d = DEPTH OF CUT

w = PICK WIDTH

S = PICK SPACING

FIGURE 25 - GEOMETRY OF CUTTING SITUATIONS

Since specific energy is the quotient of force and yield its relationship with depth of cut at constant width of tool must be of the form:-

$$S.E. = \frac{K\,d}{d^2 \tan\theta + w\,d} \equiv \frac{K_1}{K_2 + d} \qquad \ldots\ldots\ldots (13)$$

The curves for specific energy shown in Figures 23D and 24D are ideally represented by an equation of this form.

In general, shallow cuts are seen to be highly inefficient and considerable improvement is gained by increasing the depth of cut. The benefits in this direction are not, however, unlimited since specific energy appears to be approaching an asymptotic value. Equation (13) implies that specific energy will tend to zero as depth approaches infinity. It has been found, however, in other rocks, that while breakout angle may remain constant over a limited range of cutting depths, a depth will eventually be reached beyond which the groove becomes proportionately narrower (86), (87). In such cases the asymptote can be expected to have a positive value.

Coarseness indeces increase with cutting depth, again following the inverse of the specific energy graphs.

Figure 25 shows the geometry of the cutting situation referred to, including that for relieved cutting.

3. Effect of Pick Widths

Mean and peak cutting and normal forces all increase linearly with pick width, as shown in Figures 26 and 27. Unlike the depth of cut graphs, these all have a definite intercept on the ordinate. These intercepts are highly significant values since they represent the forces involved in cutting with a tool of infinitesimal width. In other words, it defines the amount of cutting force wholly attributable to the production of breakout.

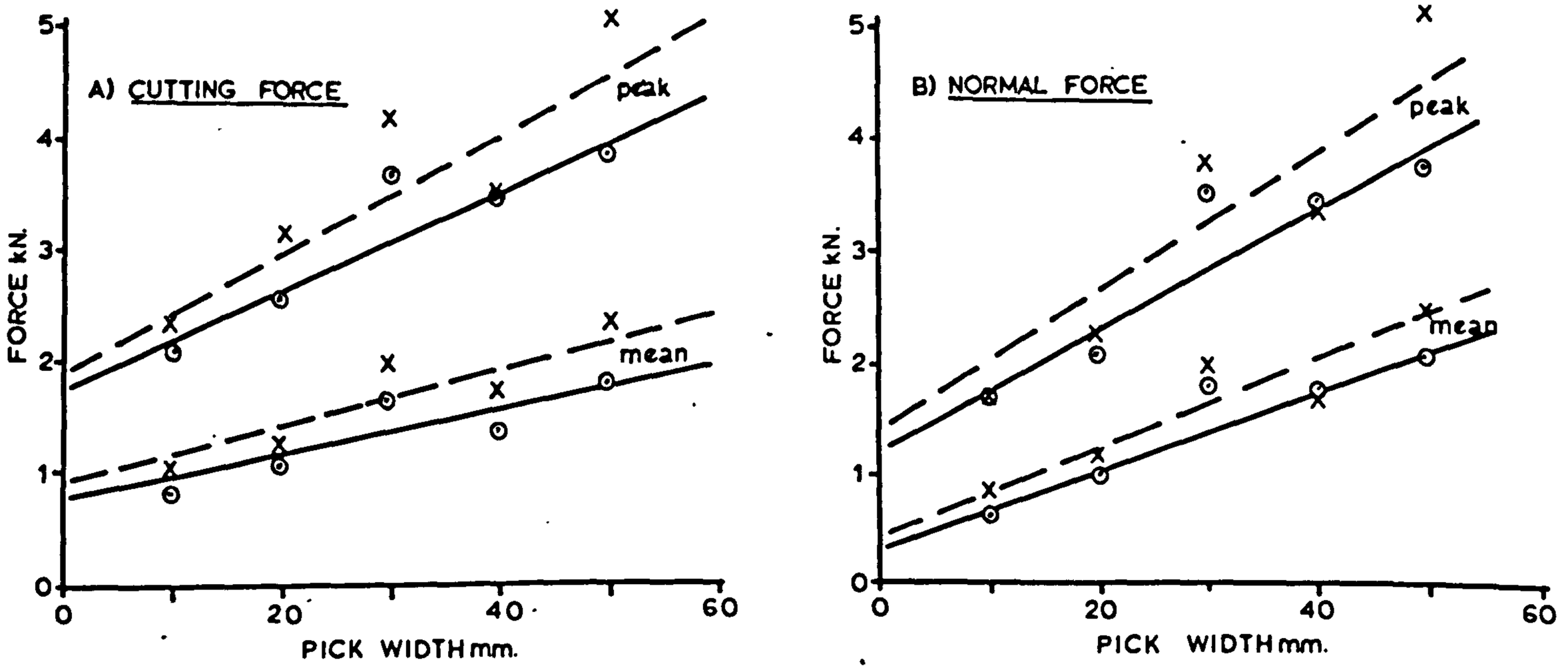

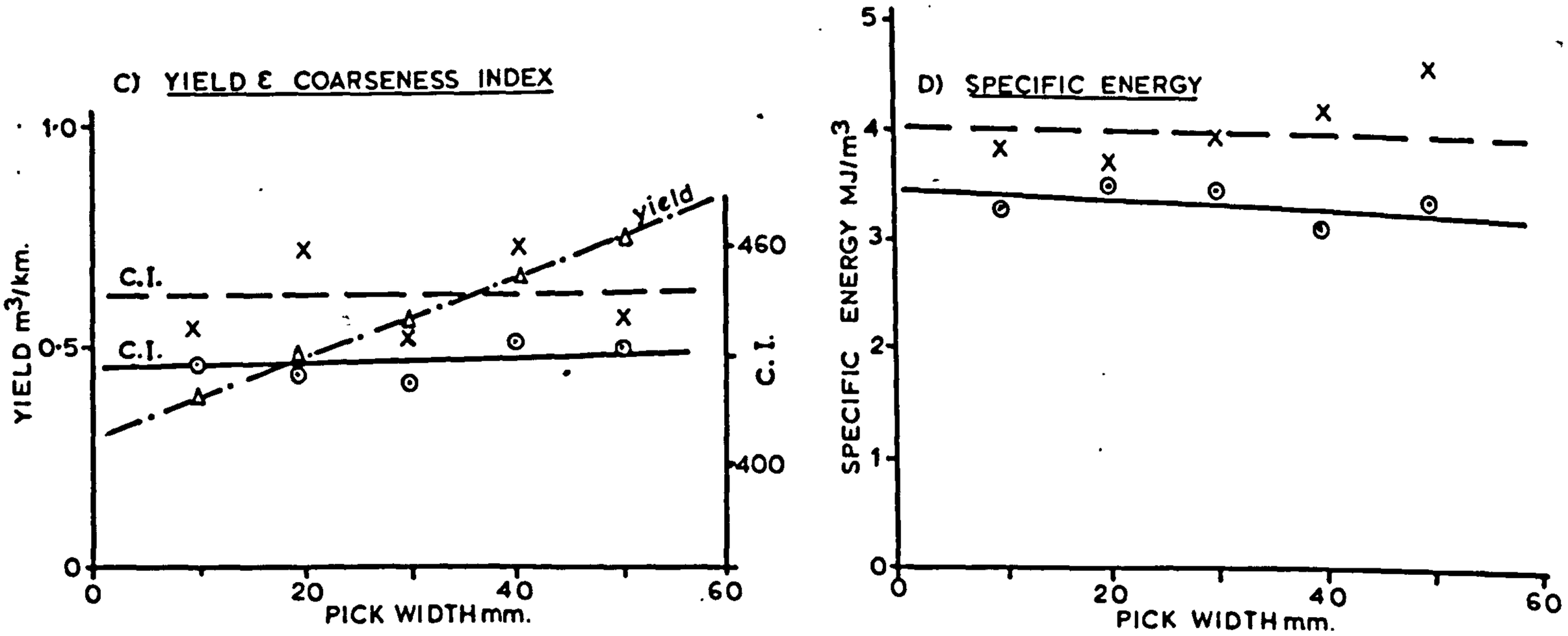

DRY ROCK

WET ROCK

FIGURE 26 - EFFECT OF PICK WIDTH - BUNTER SANDSTONE

It is worthwhile comparing these graphs with those for yield, which are also linear and have finite values at zero width. These values are equivalent to the volume of breakout rock. Contrasting the mean cutting force intercepts with those for yield, provides measures of the energy involved in the production of breakout rock. These work out at 3.2 MN/m^3 for dry Bunter, 3.6 MJ/m^3 for wet Bunter and 14.2 MJ/m^3 for Magnesian Limestone.

As pick width increases in dry Bunter there is no significant change in specific energy. The wet Bunter energy requirements at different widths are less readily defineable. The specific energy values are certainly higher than those for dry rock cutting, but there are indications of an increase in energy needs at the higher tool widths. Since, however, specific energy is found to be independent of pick width when cutting Magnesian Limestone, the best horizontal straight line has been drawn through the wet Bunter specific energy results.

7.3 Relieved Cutting

Partial factorial experiments, using the design referred to in 7.1, were undertaken in dry and wet Bunter. With the experience gained from these two experiments auxiliary spacing tests were designed. These tests, which more readily define optimum spacing between adjacent tools, were undertaken in dry Bunter and Magnesian Limestone. The results of all spacing tests are given in Appendix III.

The test procedure involved cutting a groove, at the appropriate levels of spacing and other defined variables, adjacent to and at the same depth and width as a previously cut groove. This new groove was thereafter used to provide the relief for the next in the series of 4 replications.

Figure 28 illustrates this geometrically and shows a typical relieved cut for a close (negative) spacing situation.

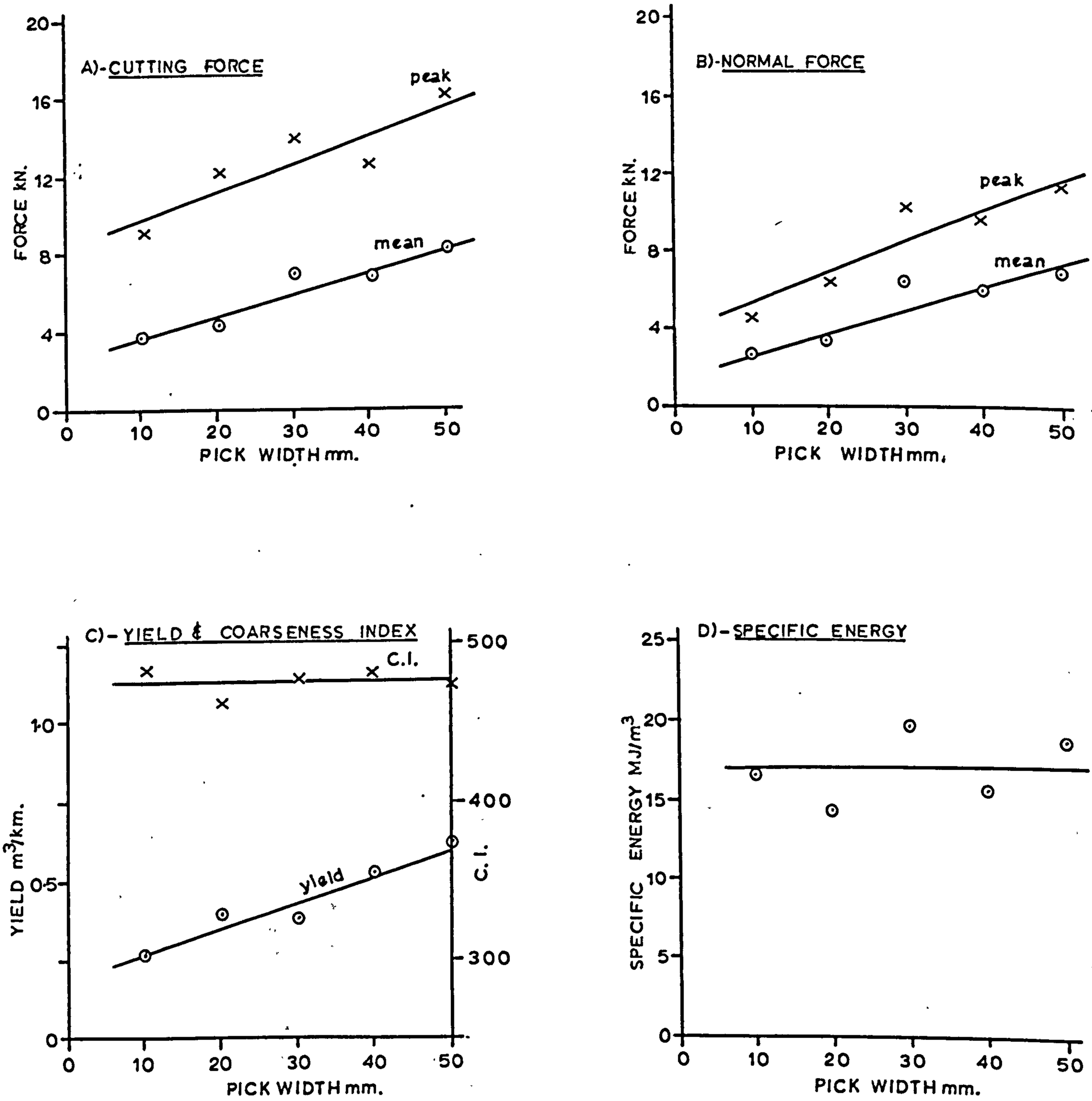

FIGURE 27 – EFFECT OF PICK WIDTH – MAGNESIAN LIMESTONE

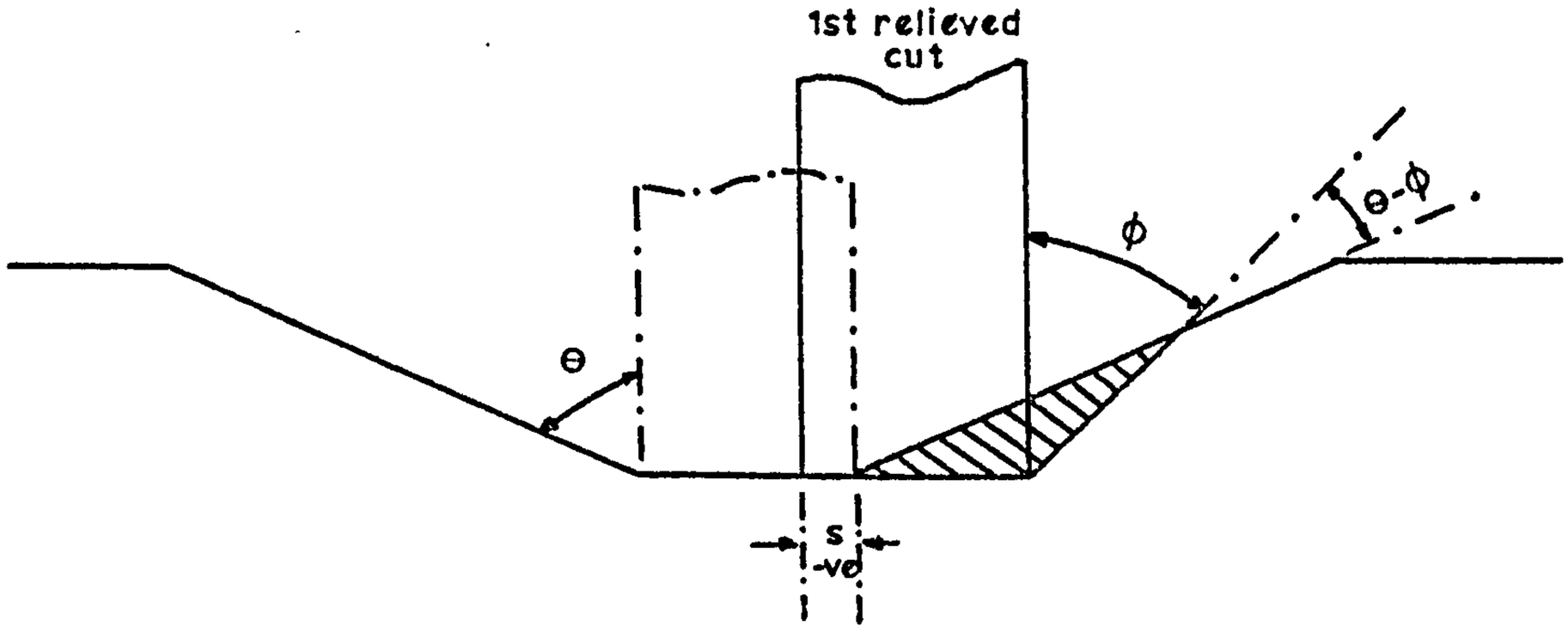

FIGURE 28. RELIEVED CUTTING AT CLOSE SPACING

Whereas such a sequential disposition of relieved cuts parallels some practical cutting situations, it is found to produce irregular patterns of breakout on the unrelieved side of the cut. For example, the breakout angle θ produced by the first unrelieved cut is regular. Thereafter, the first relieved cut, particularly in the negative spacing situation, is found to produce a much lower breakout angle on the unrelieved side, shown above as ϕ. This may persist throughout the ensuing cuts but sometimes, depending on the precise geometry, an intermediate cut in the sequence may re-establish the original breakout angle θ, after which further cuts again return to a low breakout for a time.

It was not possible to fully determine any regularity in this type of sequence since this would have required a large number of consecutive cuts, many more than the physical width of the test block could accommodate.

The shape of the curve relating specific energy with pick spacing can be inferred (76)(86). As shown in Figure 25, at spacings greater than 2d tan θ, there will be no interaction and tools will operate as if in isolation, having a performance equivalent to an unrelieved cutting situation.

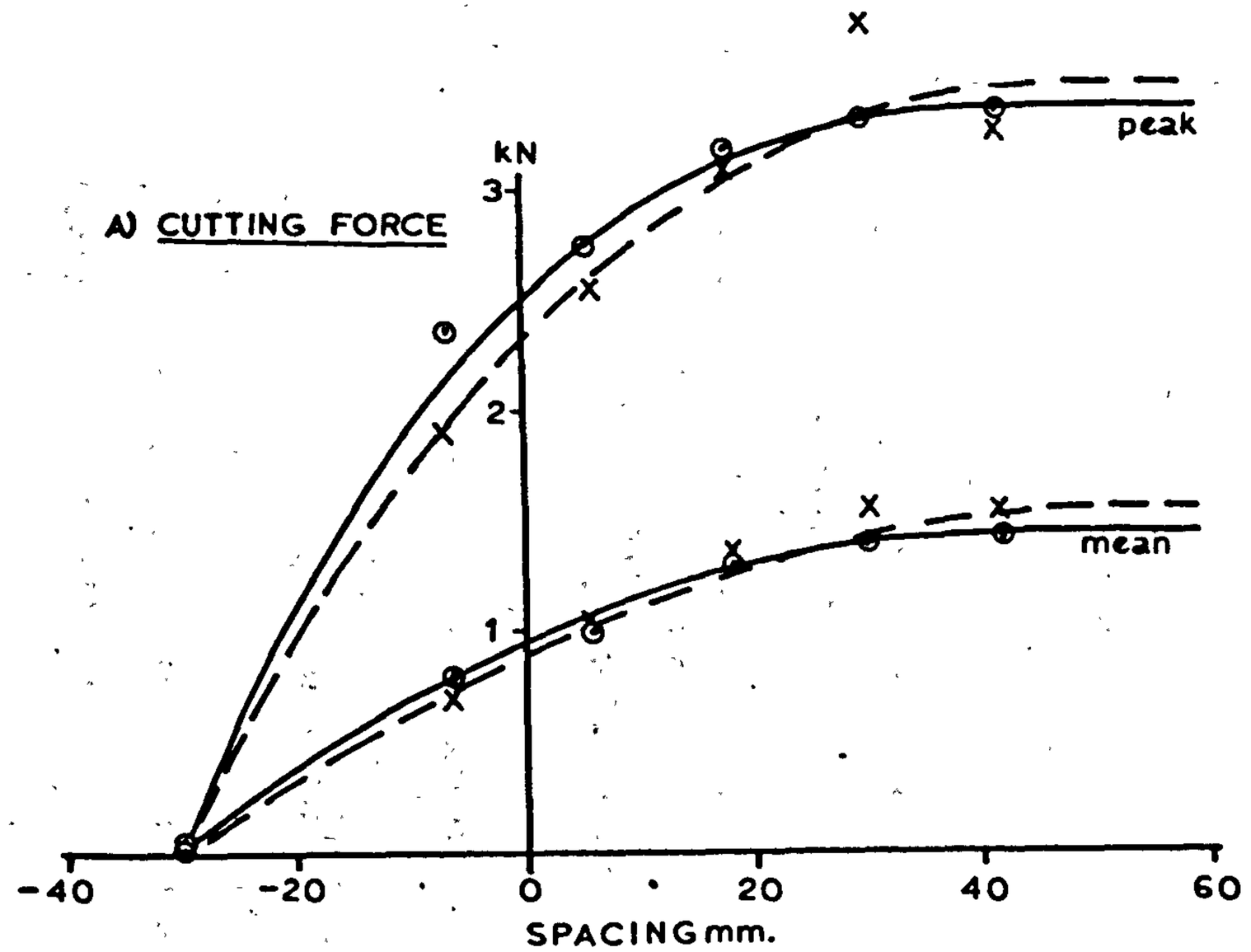

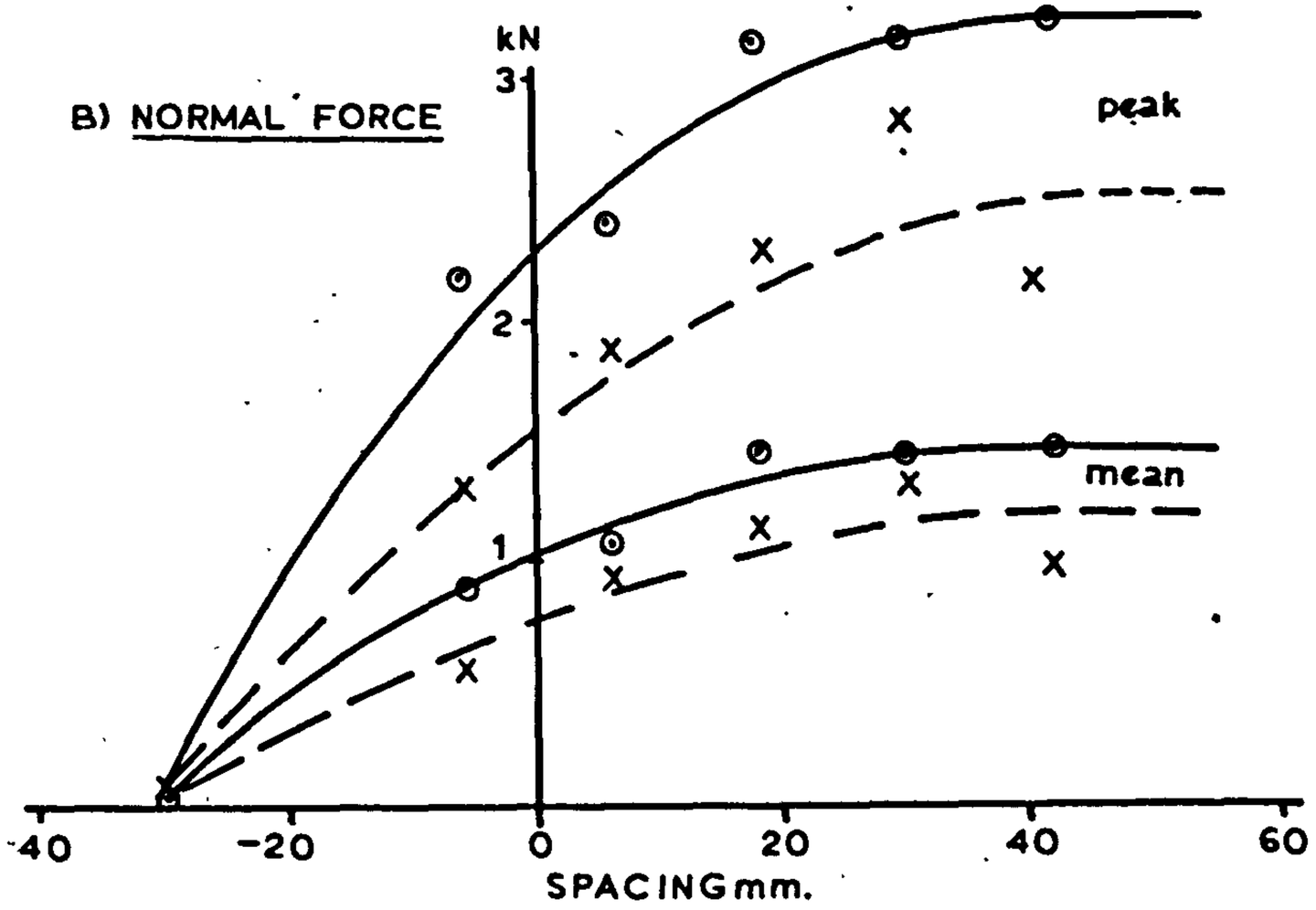

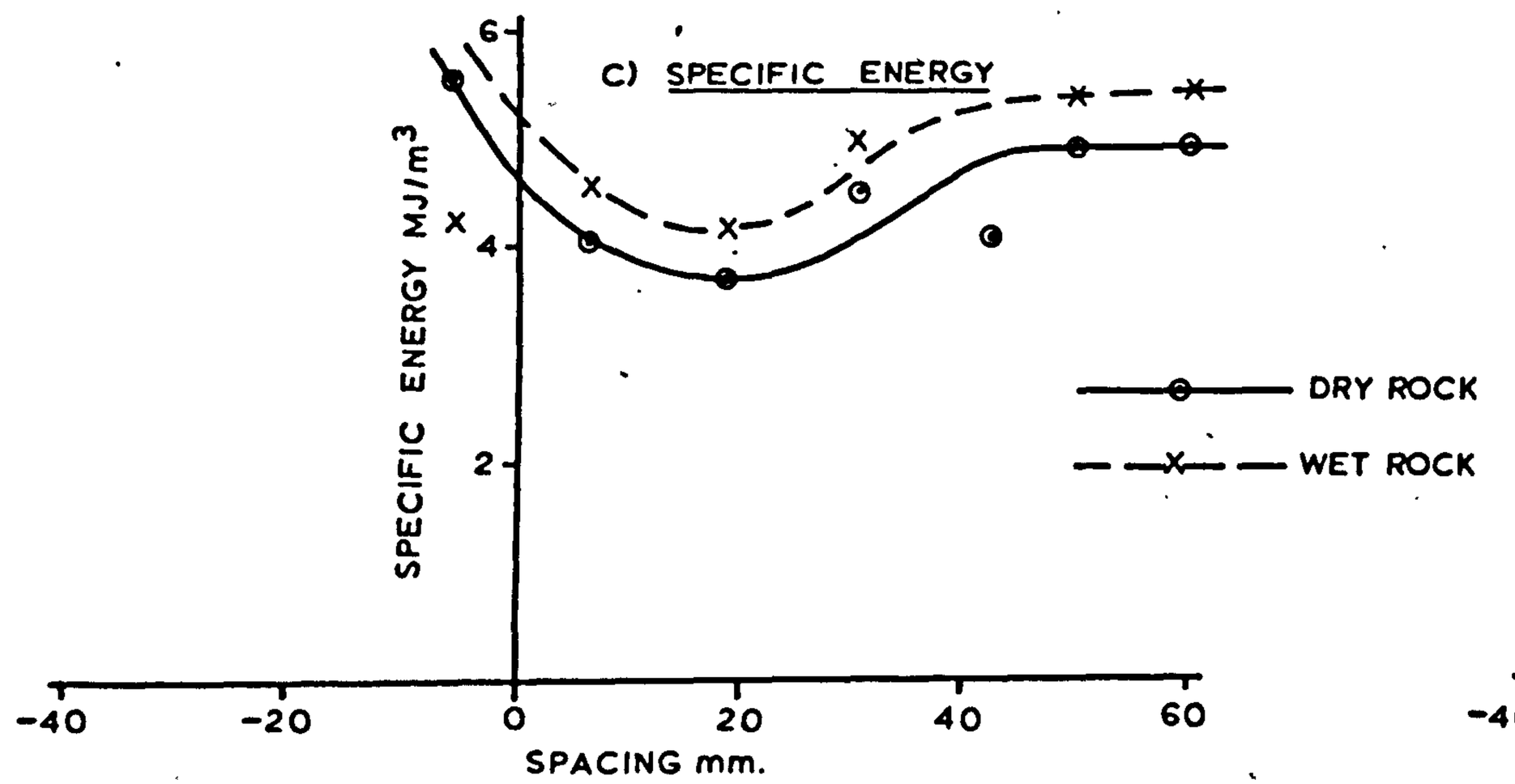

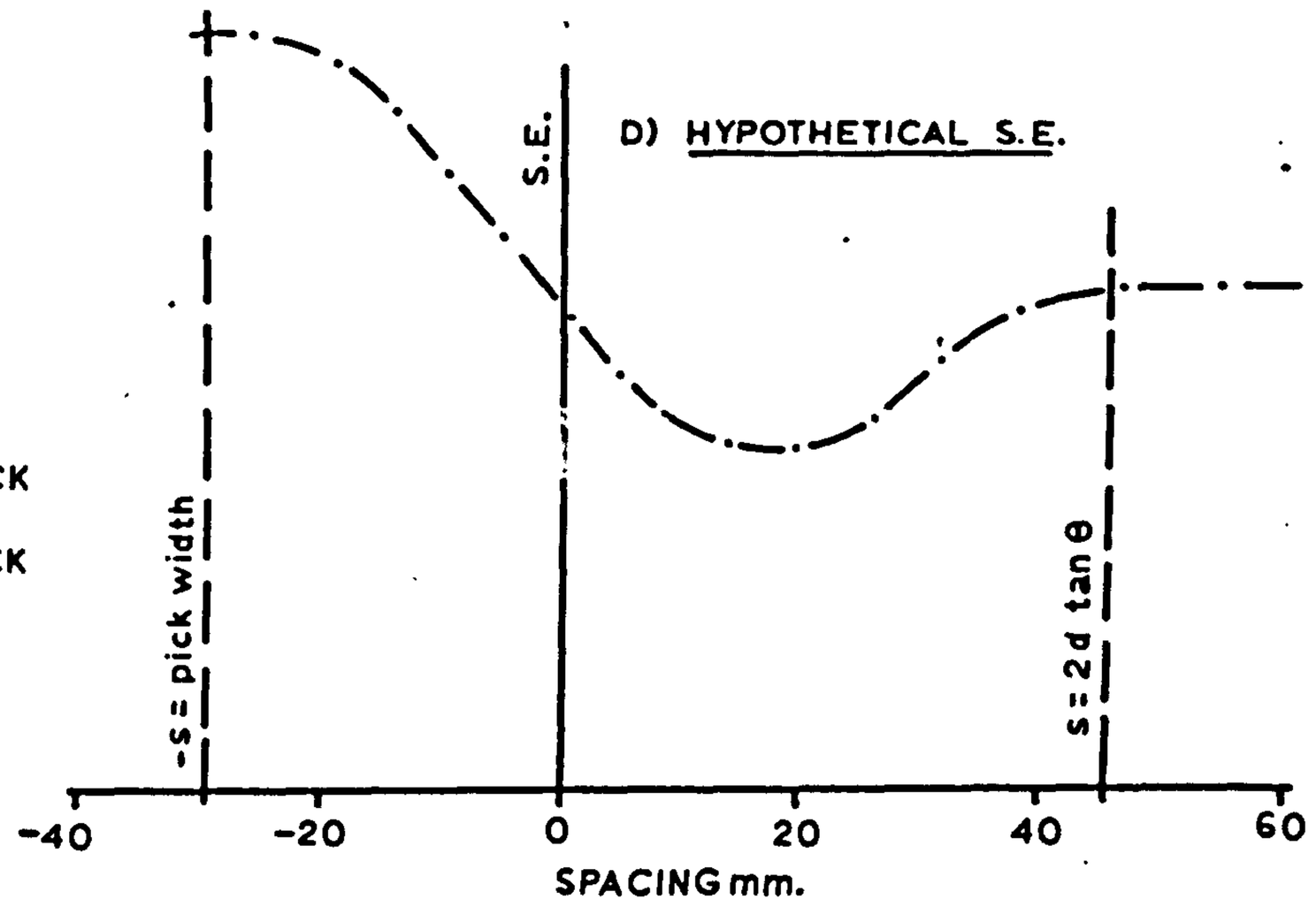

FIGURE 29 - EFFECT OF PICK SPACING - BUNTER SANDSTONE

The other extreme is where the second tool cuts exactly in the shadow of the first, i.e. at a spacing s = -w. It has been shown (76) that this situation represents the limiting condition for equation:-

$$S.E. = \frac{K_1}{K_2 + d} \qquad \ldots\ldots\ldots (14)$$

$$\text{i.e.} \quad \lim_{d \to 0} \frac{K_1}{K_2 + d} = \frac{K_1}{K_2}$$

which gives a finite and maximum value for S.E. at zero depth.

If there is benefit in cutting adjacent to a previously cut groove, then somewhere between these extremes, specific energy will achieve a minimum value. A hypothetical curve based on this reasoning is shown in Figure 29D.

It can similarly be argued that pick forces will reduce from a maximum at $s > 2d \tan \theta$ and tend to zero at $s = -w$.

Figure 29 shows the effect of spacing on forces and specific energy for dry and wet Bunter. As anticipated, all forces increase with spacing to stabilise at maximum values at a spacing greater than $2d \tan \theta$, which for both dry and wet rocks at the mean depth of 9mm is approximately 50mm.

It is interesting to observe that the cutting force in wet rock is less than in the dry at close spacing, but that this situation is reversed at spacings above about 20mm. Again, normal forces are lower in the wet rock but in this case it persists for all values of spacing.

Specific energy curves in both the dry and wet rock conditions provide the expected minima, but these show that the benefits of relief are much less than might have been supposed. There is, however, more scatter in these results than should occur in a balanced and replicated programme of testing.

The reasons for this become clear from further consideration of the irregular breakout found to occur in the close spacing situation shown in Figure 28. These undefined variations in breakout must produce corresponding variations in the measured parameters and thereby contribute to the scatter of results. There is however a further and equally important feature of the interactive groove geometry, shown in Figure 30, which concerns the definition of depth of cut. As the diagram shows, the nominal depth of cut is 'd', the thickness of the layer of rock being removed. The effective depth of cut is of course much less than 'd'. If now the breakout from the second cut is irregular, then the ensuing effective cutting depth must be correspondingly modified and thereby take similarly irregular values. Pick width has, however, a dominant role in this situation since the effective depth taken by a tool at a fixed spacing varies according to its width as shown in Figure 30.

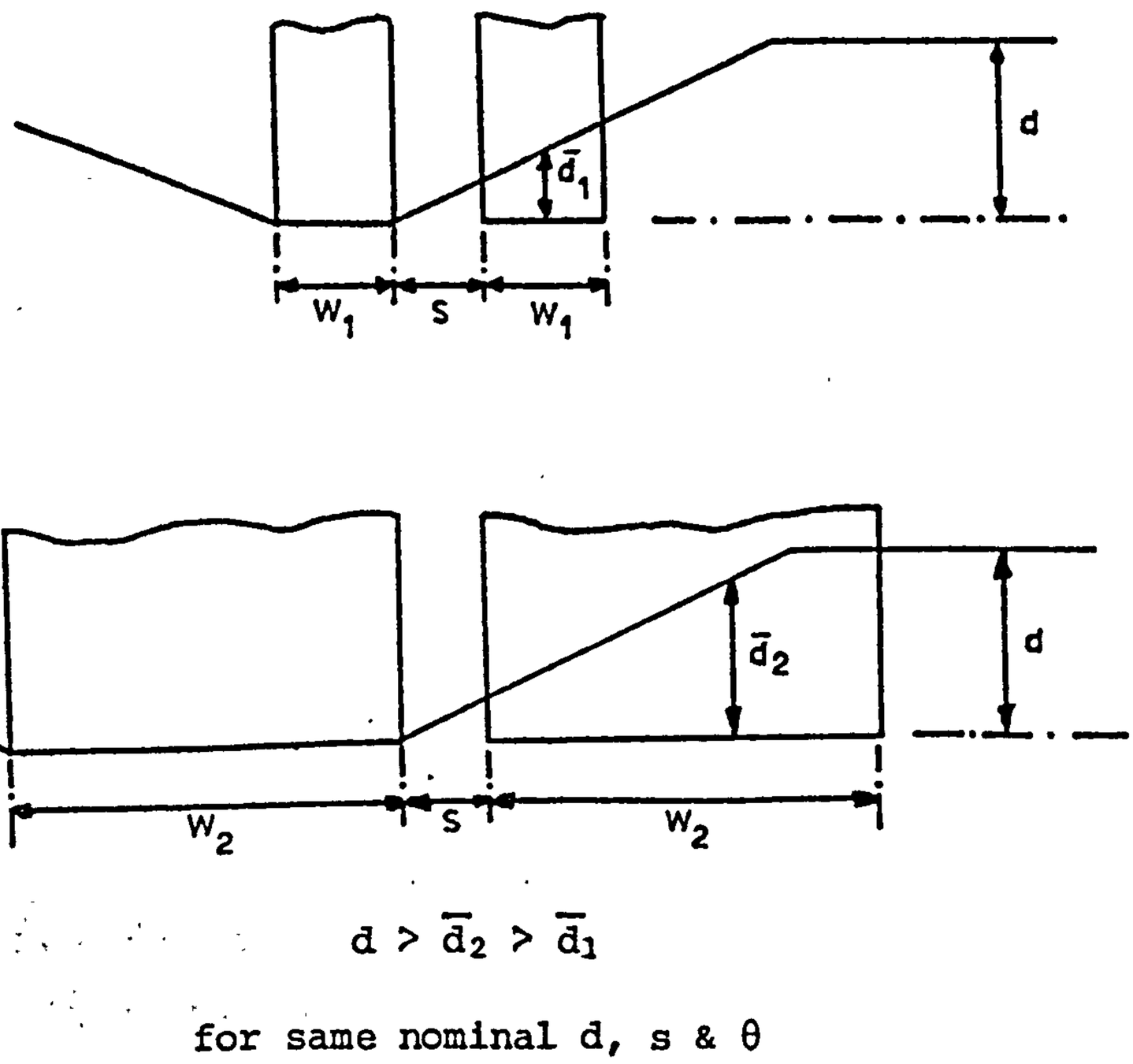

$$d > \bar{d}_2 > \bar{d}_1$$

for same nominal d, s & θ

FIGURE 30. EFFECT OF PICK WIDTH ON SPACING GEOMETRY

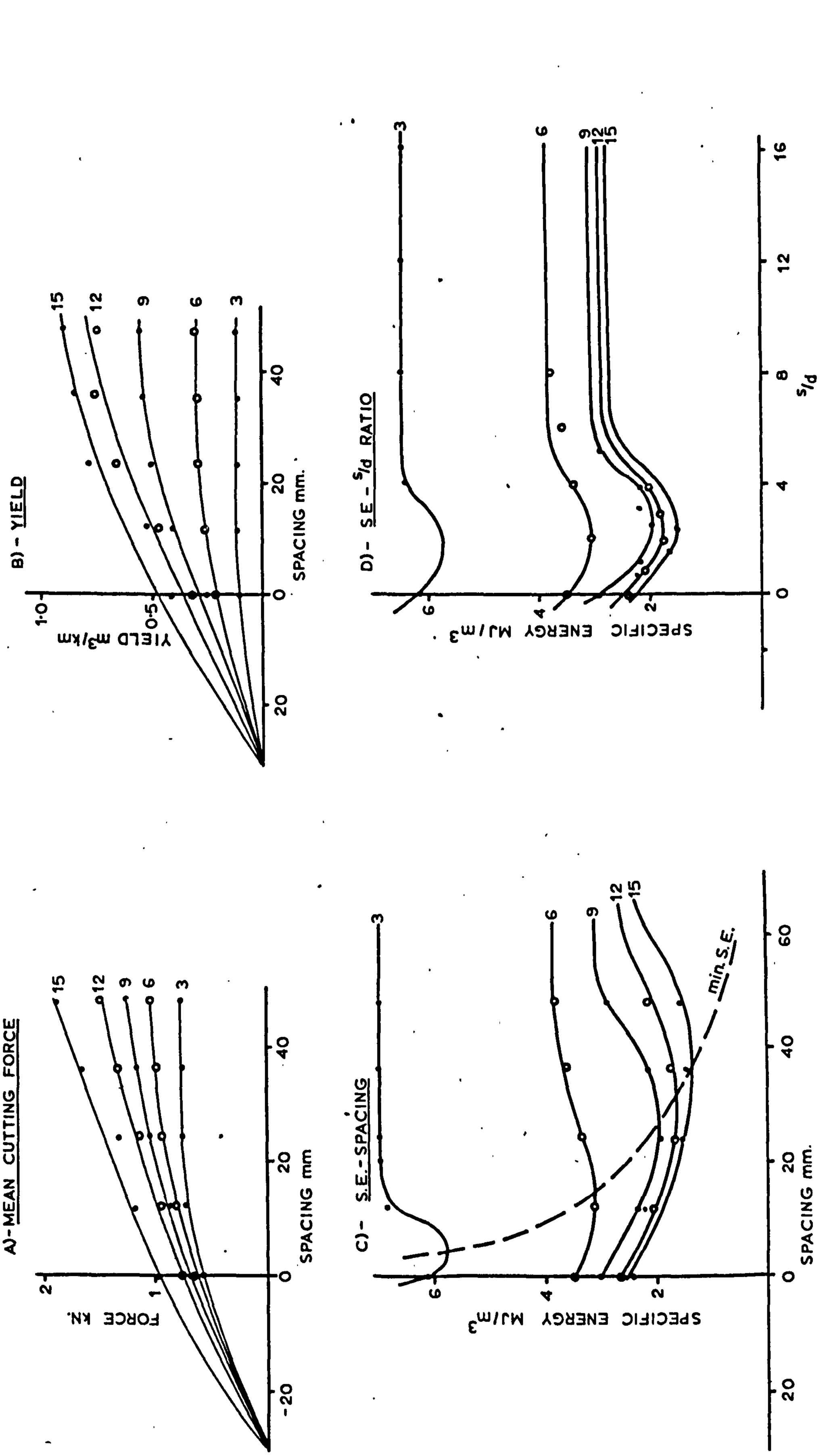

FIGURE 31 - AUXILIARY SPACING EXPERIMENT - BUNTER SANDSTONE

FIGURE 32 AUXILIARY SPACING EXPERIMENT
MAGNESIAN LIMESTONE

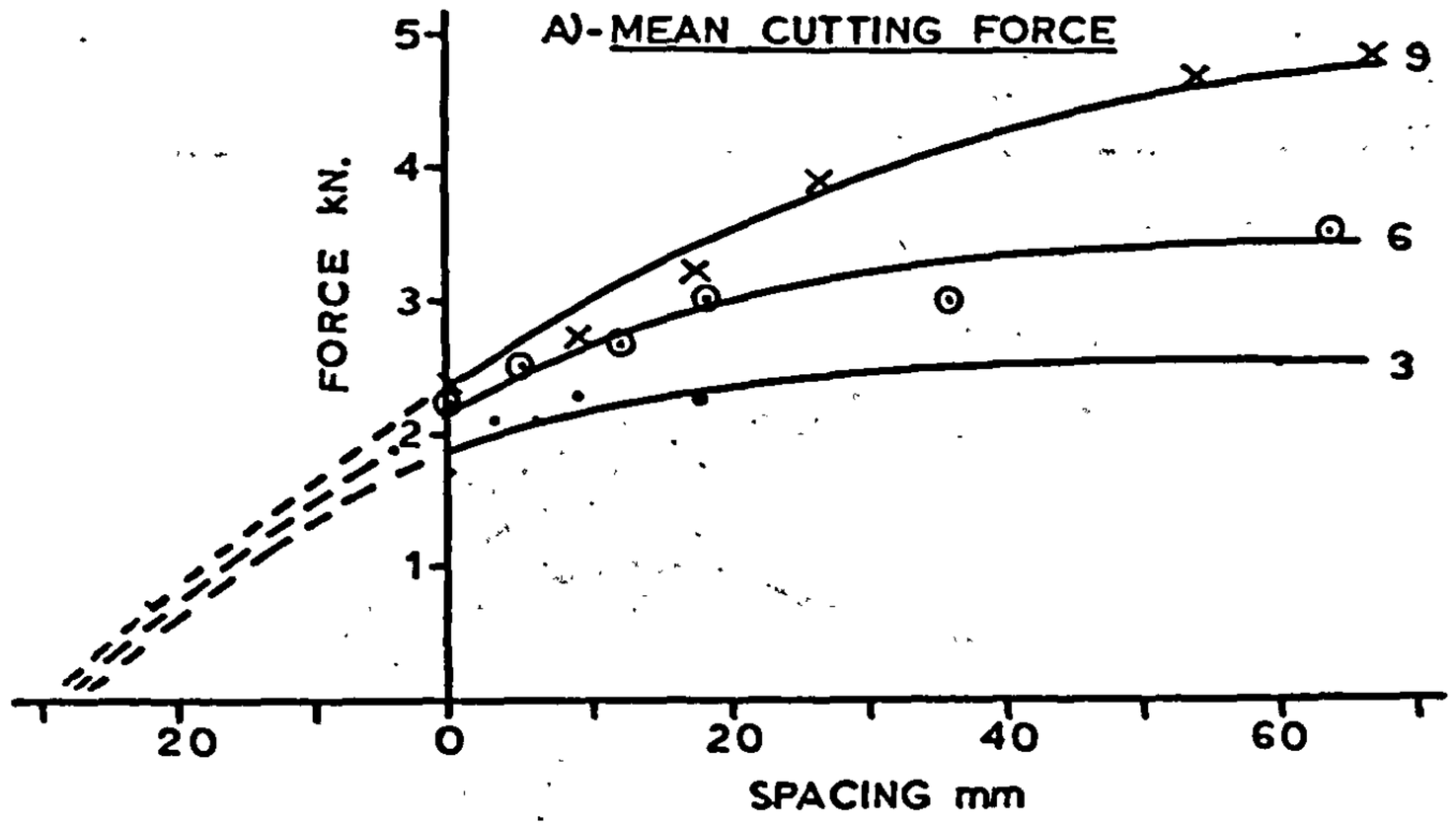

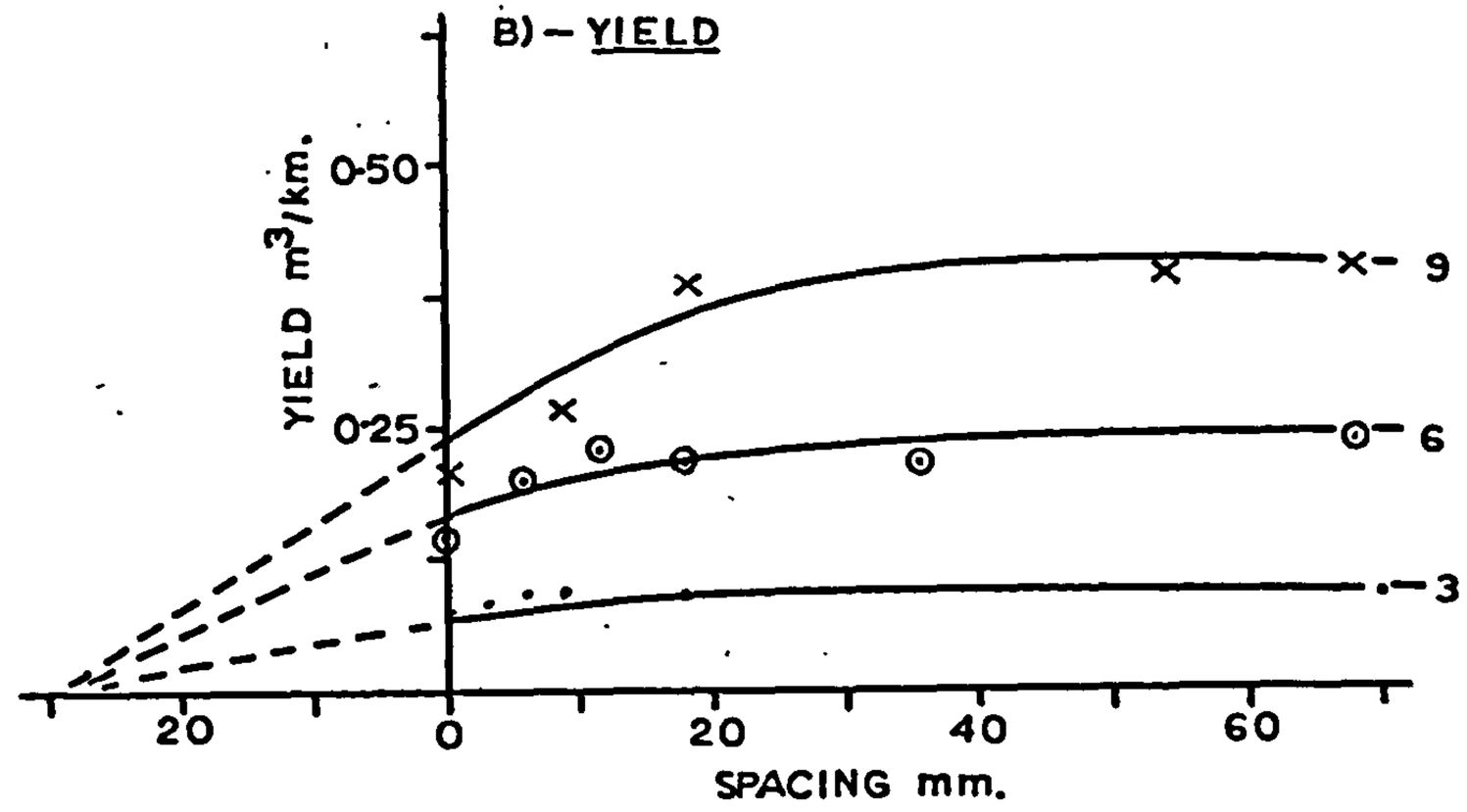

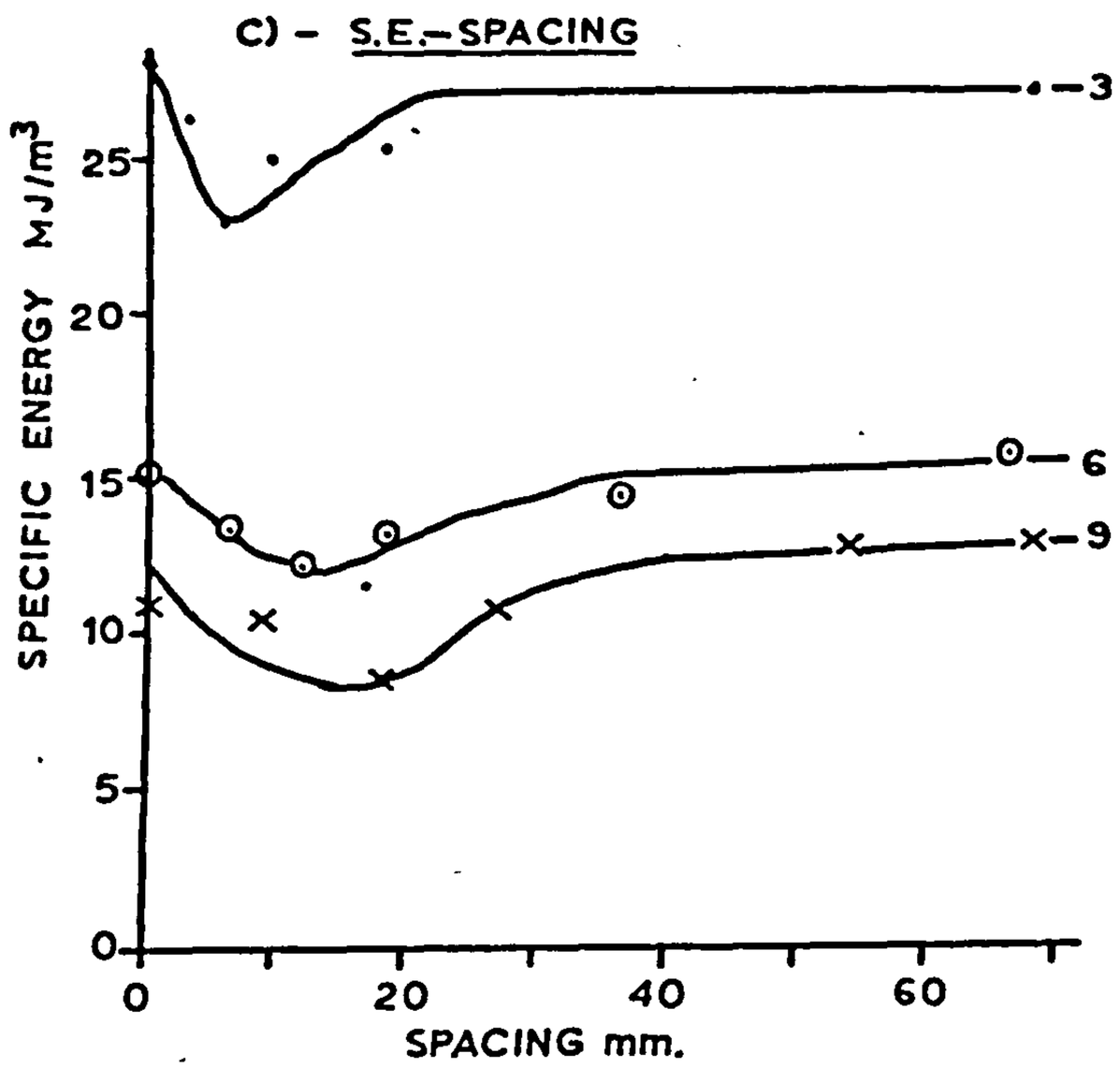

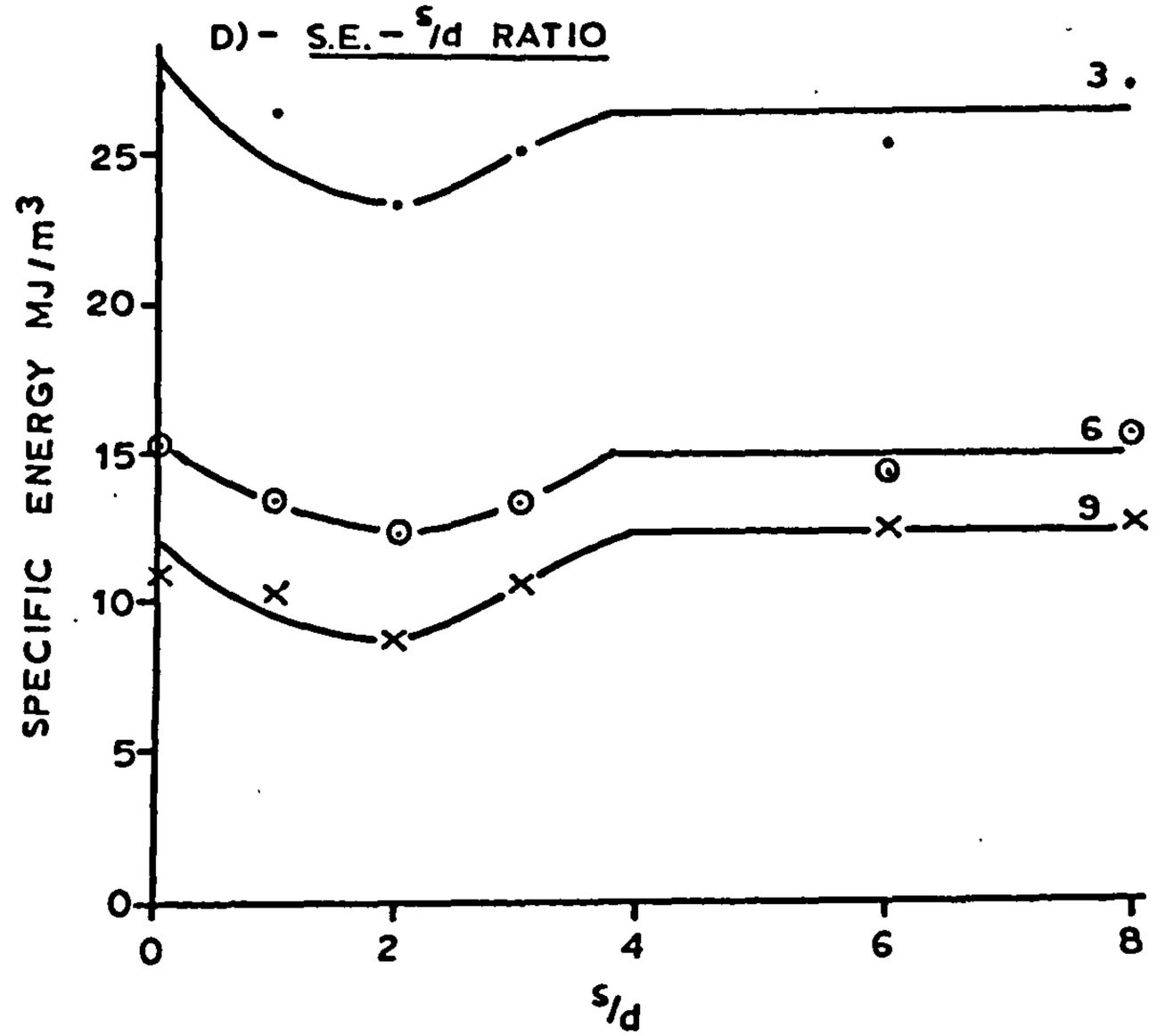

The spacing test results abstracted from Appendix III and shown in Figure 29 are at mean values of rake, width and depth. The geometrical interactions between depth, width and spacing, complicated by a sometimes modified breakout, produces a scatter of results in the spacing experiments and leads to values which cannot be directly equated to the unrelieved cutting results.

To assess the effects of these sources of error and thereby gain a more accurate spacing relationship, the supplementary experiments were undertaken in which the only variables were depth and spacing. Width was maintained throughout at 30mm, which is equivalent to the mean level provided in the partial factorial programme. Similarly, rake angle was at a fixed value of $+10^{\circ}$.

The results are shown in Figures 31 and 32. Peak and mean cutting and normal forces increase with spacing at all depths of cut, originating at $s = -w$ and increasing smoothly to constant values at spacings greater than $2d \tan \theta$.

The specific energy relationships are presented in two ways. Figures 31C and 32C show the direct effect of spacing with the minimum specific energy occurring at close spacings for the shallow cuts and increasing spacings as the depth of cut becomes larger. The locus of minimum specific energy, as shown in Figure 31, is of similar form to the unrelieved relationship between specific energy and depth. When spacing is expressed as a multiple of cutting depth, as shown in Figures 31 and 32D, the minimum specific energy values all occur at the same s/d ratio of between 2 and 2.5

In effect, this is the same conclusion as was reached from the partial factorial results in Figure 29. There is, however, a marked reduction in the scatter of results obtained in this latter experiment. It is interesting to observe the absolute energy levels for each depth of cut. The 6mm depth shows a marked overall increase in efficiency over 3mm, but between the largest depths, the improvement is negligible. This fact re-inforces the dominant role of cutting depth in establishing minimum specific energy.

7.4 Core Cutting Tests

A core cutting test has been developed at Newcastle University which is carried out on core specimens and makes use of a 12.7mm wide chisel tool. The tool has a front rake angle of -5^{o} and a back clearance angle of $+5^{o}$.

As described in 6.1 the core is clamped in a vice and slots, nominally 5mm deep are cut along the axial surface of the core. Figure 33 shows the schematic arrangement. After taking the first cut, the core sample is rotated axially through 90^{o} and a second cut is made. Thereafter two similarly disposed tests are undertaken on the same core giving four replications. Measurements of forces and yield, and the determination of specific energy are made in the same way as for cuts in a large block.

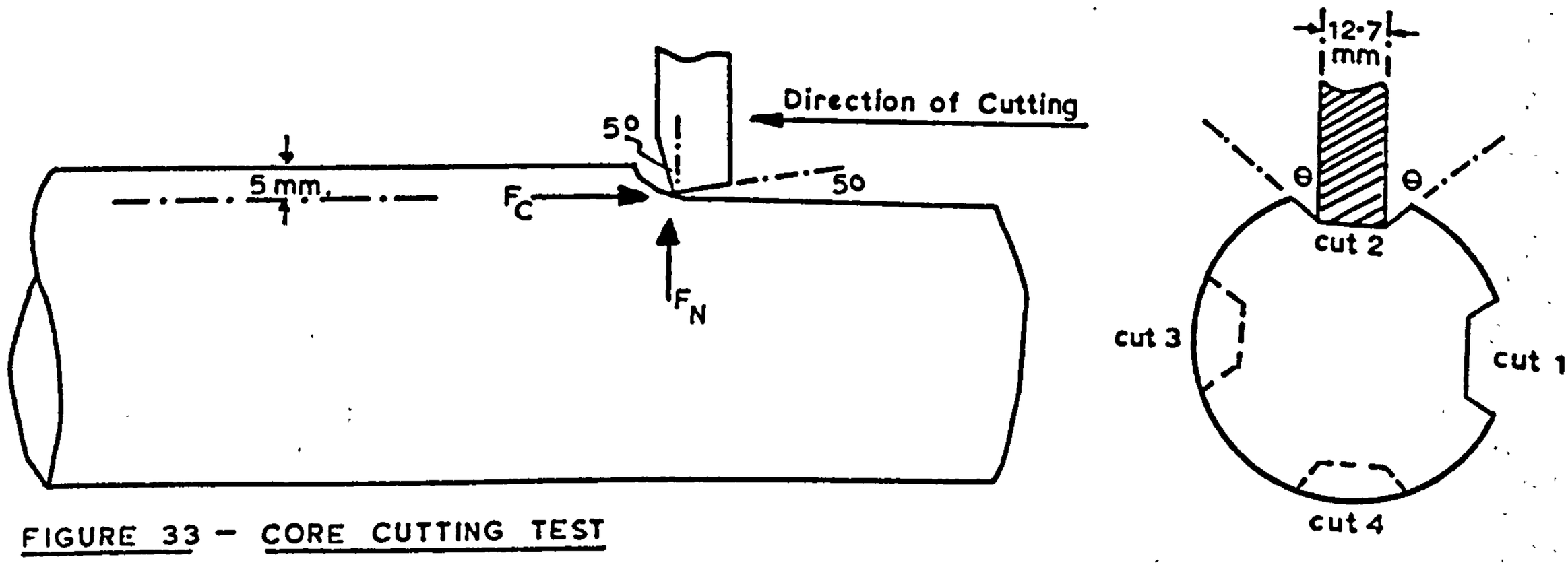

FIGURE 33 - CORE CUTTING TEST

Results from core cutting tests undertaken on dry and saturated specimens prepared from large blocks of Bunter and Magnesian Limestone are given in Tables 23 and 24.

TABLE 23

RESULTS OF CORE CUTTING IN BUNTER SANDSTONE

Parameter	Dry (± s.d.)	Saturated (± s.d.)
Number of tests	10	8
Mean Cutting Force kN ($\overline{Fc}$)	0.81 ± 0.11	0.93 ± 0.24
Peak Cutting Force kN (Fc)	2.29 ± 0.29	2.70 ± 0.35
Mean Normal Force kN ($\overline{F_N}$)	0.63 ± 0.13	0.62 ± 0.21
Peak Normal Force kN (F_N)	1.42 ± 0.15	1.32 ± 0.17
Yield m^3/km (Q)	0.08 ± 0.01	0.08 ± 0.01
Specific Energy MJ/m^3 (S.E.)	9.64 ± 1.80	10.94 ± 2.15
Coarseness Index	370	397
Breakout Angle (^{o})	65	65
Cutting Wear mg/m	2.54	3.16
Abrasive Wear mg/m	0.96	1.35

TABLE 24

RESULTS OF CORE CUTTING IN MAGNESIAN LIMESTONE

Parameter	Dry (± s.d.)	Saturated (± s.d.)
Number of Tests	16	16
Mean Cutting Force kN ($\overline{Fc}$)	3.61 ± 0.29	3.76 ± 0.42
Peak Cutting Force kN (Fc)	10.17 ± 1.82	11.28 ± 1.50
Mean Normal Force kN ($\overline{F_N}$)	3.58 ± 0.61	3.21 ± 0.56
Peak Normal Force kN (F_N)	7.93 ± 2.06	8.10 ± 1.76
Yield m^3/km (Q)	0.08 ± 0.01	0.09 ± 0.02
Specific Energy MJ/m^3 (S.E.)	43.17 ± 4.82	42.95 ± 8.71
Coarseness Index	——	——
Breakout Angle (^{o})	67	67

To assess the effects of curvature of the cutting surface, in the core test, the same test was carried out on the flat surface of a block of dry Bunter. The results are given below alongside the dry core values from Table 23.

	Core Test	Block Test
$\overline{F}_C$ (kN)	0.81 ± 0.11	0.72 ± 0.04
F_C (kN)	2.29 ± 0.29	1.99 ± 0.15
$\overline{F}_N$ (kN)	0.63 ± 0.13	0.56 ± 0.04
F_N (kN)	1.42 ± 0.15	1.22 ± 0.13
Q (m^3/km)	0.08 ± 0.01	0.12 ± 0.01
S.E. (MJ/m^3)	9.64 ± 1.80	6.07 ± 0.6

Curvature naturally has a big effect on yield. This will, however, reduce as the core diameter increases. For a constant breakout angle of 65^o, the theoretical yield from the core is 0.087 m^3/km which compares very favourably with the observed value of 0.084 m^3/km. At the same angle of breakout the expected yield is 0.115 m^3/km and that observed was 0.118 m^3/km.

This indicates that the equivalent yield from a flat surface can be obtained from the core yields by geometrical adjustment.

7.5 The Empirical Equations

The procedure outlined in Chapter 5 for the development of equations relating the parameters to the variables, has been applied to the 3 unrelieved partial factorial experiments.

These, together with appropriate constants, are listed in Appendix IV.

The empirical equations have been used to predict force and energy values for a level of each variable, different in each case, to those selected for the experimental programme. These levels were deliberately chosen as rake angle -5^o, width 12.7mm and depth 5mm, to coincide with the standard core cutting and flat surface test levels referred to in the

previous section. There were two main reasons for doing this. First to provide a measure of the value of the equations for purposes of prediction and secondly to establish a relationship between the full scale laboratory test results and the core cutting values.

The results for the flat surface test, carried out in conjunction with the core cutting test are given in Table 25 alongside the values predicted from the empirical equations.

TABLE 25

PREDICTED AND MEASURED CUTTING VALUES - DRY BUNTER

($\alpha = -5^{o}$, w = 12.7mm, d = 5mm)

Parameter	Predicted Value	Measured Result (± s.d.)	Difference
Mean Cutting Force (kN)	0.65	0.72 ± 0.04	- 1.75 s.d.
Peak Cutting Force (kN)	1.99	1.99 ± 0.15	0 s.d.
Mean Normal Force (kN)	0.72	0.56 ± 0.04	+ 4.00 s.d.
Peak Normal Force (kN)	1.78	1.22 ± 0.13	+ 4.00 s.d.
Yield (m^3/km)	0.116	0.118 ± 0.01	+ 0.20 s.d.
Specific Energy (MJ/m^3)	5.60	6.07 ± 0.60	+ 0.78 s.d.

The difference column in both tables expresses the difference between the predicted and measured values as a multiple of the observed standard deviation.

The data presented in the above table supports the validity of the empirical equations, which can be used to predict forces and energies appropriate to different combinations of variables.

7.6 The Effect of Cutting Speed

Results of previous research from all known sources, indicate that, in non-abrasive rocks, cutting speed within the range of 0 - 5 m/s has no influence on tool performance.

The Bunter Sandstone is, however, known to be highly abrasive and although a pristine pick was used for each test, a supplementary experiment was undertaken to assess the difference between the standard testing speed of 152 mm/s and the higher level of 456 mm/s.

The results, which are given in Table 26, involve the use of 3 different combinations of experimental variable. Each experiment was repeated 4 times in dry rock.

TABLE 26

EFFECT OF SPEED ON CUTTING PARAMETERS

	TEST A		TEST B		TEST C	
Speed mm/s	152	456	152	456	152	456
$\bar{F}_c$	1.68 ± 0.20	1.59 ± 0.22	0.98 ± 0.07	0.91 ± 0.12	0.76 ± 0.10	0.85 ± 0.08
F_c	4.15 ± 0.70	4.69 ± 0.57	2.57 ± 0.21	2.59 ± 0.29	2.40 ± 0.40	2.28 ± 0.34
$\bar{F}_N$	1.47 ± 0.25	1.35 ± 0.16	0.78 ± 0.10	0.76 ± 0.08	0.97 ± 0.20	1.07 ± 0.15
F_N	3.18 ± 0.41	3.58 ± 0.32	1.89 ± 0.31	1.97 ± 0.25	2.30 ± 0.36	2.31 ± 0.28
Q	0.82 ± 0.18	0.70 ± 0.12	0.54 ± 0.08	0.39 ± 0.06	0.55 ± 0.01	0.57 ± 0.07
S.E.	2.09 ± 0.60	2.27 ± 0.58	1.88 ± 0.39	2.29 ± 0.44	1.38 ± 0.21	1.50 ± 0.23

Test A : $\alpha = 0^{\circ}$, w = 10mm, d = 15mm

Test B : $\alpha = 10^{\circ}$, w = 10mm, d = 12mm

Test C : $\alpha = 30^{\circ}$, w = 40mm, d = 9mm

These results, which cover a wide range of rake angle, pick width and depth of cut, support the expectation that cutting speed has no significant effect on performance parameters.

The possible interaction of speed with pick wear rate was deliberately suppressed in these tests by using a new pick for each cut.

7.7 The Effect of Tool Wear

The high quartz content of the Bunter Sandstone makes it an abrasive rock, a property which is of fundamental concern to its excavation. Quartz is the hardest of the common rock forming minerals and extensive contact between a tool and a quartzitic rock surface, during the cutting process, leads to rapid erosion of the tool.

The stresses generated when cutting Magnesian Limestone with picks have, in some cases (see 7.2.1.), been high enough to cause chipping and gross failure of the carbide inserts.

While the chipping of tools is not a convenient topic for controlled laboratory experimentation, the abrasive wear of carbide picks is the subject of a current research project within the Department of Mining Engineering, University of Newcastle (88). The results of wear testing in Bunter Sandstone are reproduced from a paper by Harle and Fowell (89) and compared with a similar test in Magnesian Limestone.

Continuous cutting runs in excess of 500 metres were arranged using 0.5m diameter rock specimens rotating in a vertical borer. The depth of cut for all tests was 2.5mm and the cutting speed was maintained at 152 mm/s.

Specifications for the 3 carbide grades used (CH, CM and CPM) are given in Table 21 of Chapter 6. The picks were all of chisel configuration having a width of 10mm, front rake angle of 10° and a back clearance of 10°. Each grade of carbide was assessed in dry Bunter and one series of tests with the CH grade was undertaken in wet Bunter. As a very low rate of wear was anticipated from the Magnesian Limestone, only the softest (CPM) grade was tested.

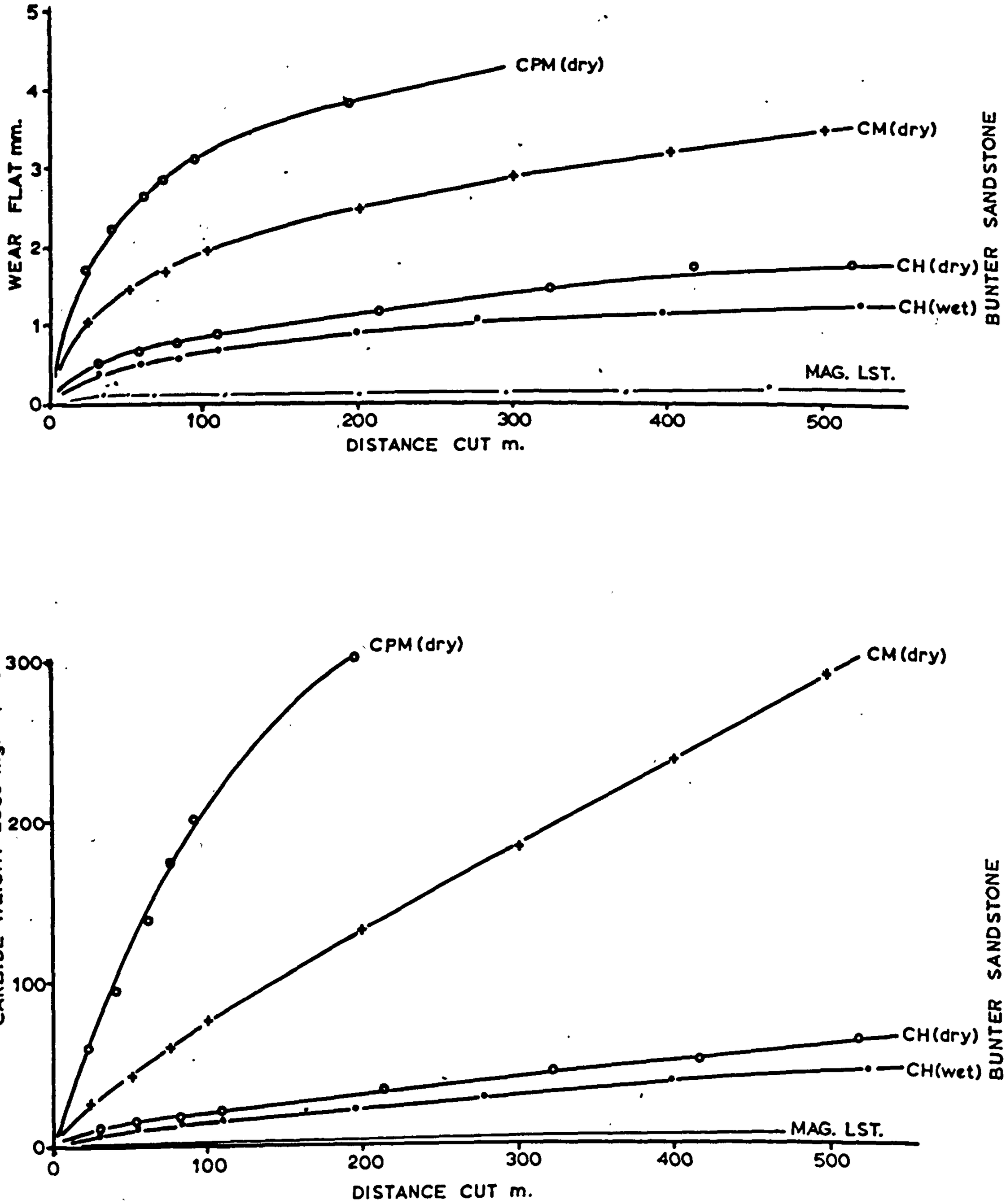

FIGURE 34 - EFFECT OF CUTTING DISTANCE ON PICK WEAR

Pick wear was monitored at intervals throughout each test by microscopic measurement of the wear flat generated. A second measure of wear was taken as the weight loss of the pick. To assess the change of pick performance as wear proceeded, indexing cuts were made from time to time on the instrumented shaping machine. This consisted of measuring the principal cutting parameters initially for the pristine tool condition and again on completion of the wear test. A further series of indexing cuts was arranged for the CH grade at 3 intermediate stages of the test. These indexing tests were undertaken at the same cutting depth (2.5 mm) as the wear test.

The results of the wear testing programme are given in Appendix V.

It is clear from Figure 34 that wear occurs most rapidly over the first 100 metres of cutting, beyond which a steady state condition is approached where the rate of wear is tending towards a constant value. It can also be seen that the wear in Magnesian Limestone is negligible in comparison to that in Bunter. After 200 metres of cutting the wear flat on a CPM tool operating in Bunter is 22 times that of a tool in Magnesian Limestone, while the corresponding figure for weight loss is 75.

Figure 35 shows the increase in mean cutting and normal forces with wear flat. Since increase in pick force with wear must be due to a modification of the geometry of the cutting edge, wear flat is likely to be a more meaningful measure than carbide weight loss. Figure 35 contains all the results from the Bunter tests, irrespective of carbide grade. The indexing cuts in Magnesian Limestone showed no significant increase in forces after the completion of 600 metres of cutting and are therefore not included.

The cutting force increases quite rapidly up to a wear flat of 2mm in width beyond which the rate of force increase diminishes quite markedly. The normal force increases much more rapidly than the cutting force, but the initial rapid rate of increase does not extend much beyond the 2mm wear flat.

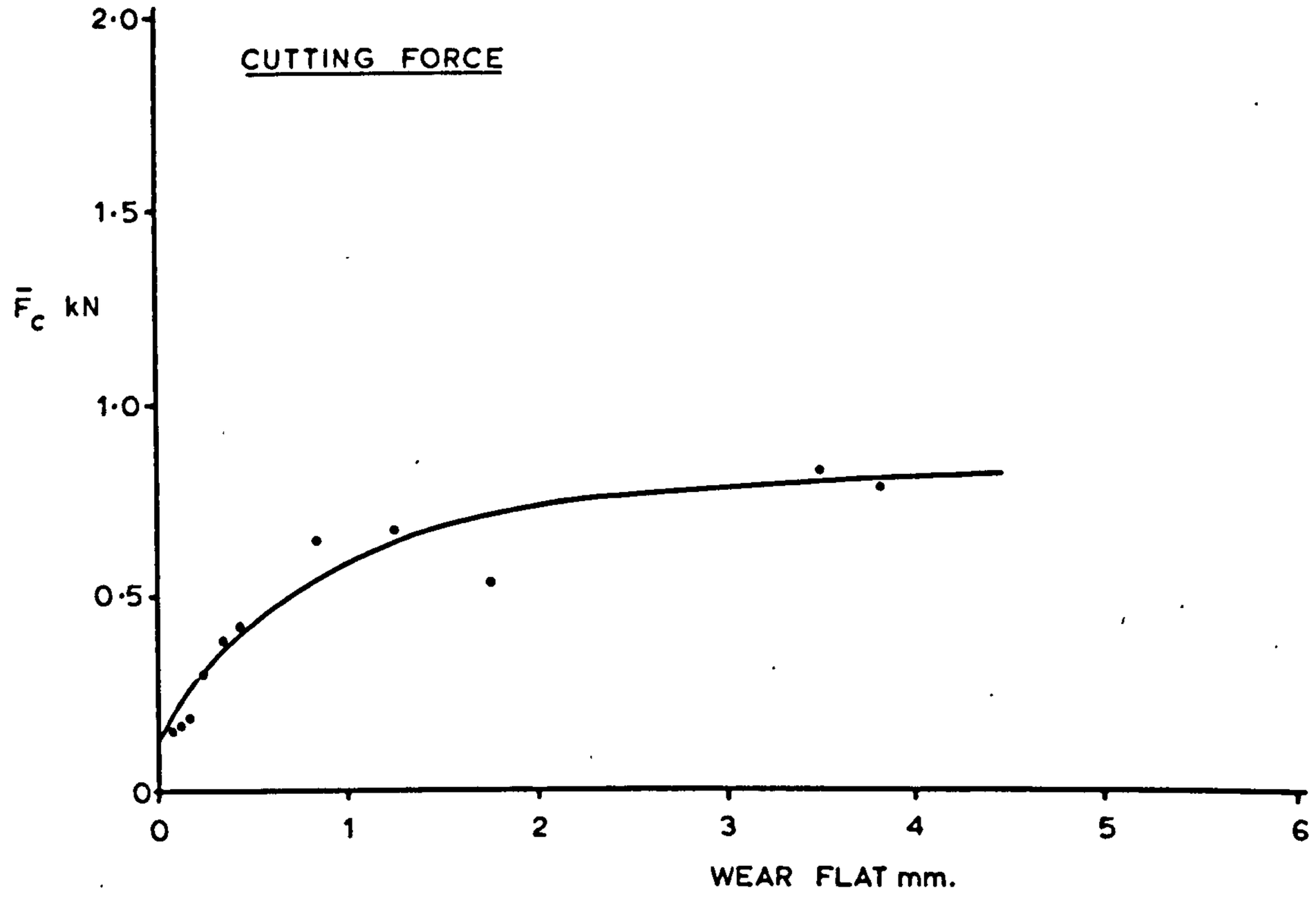

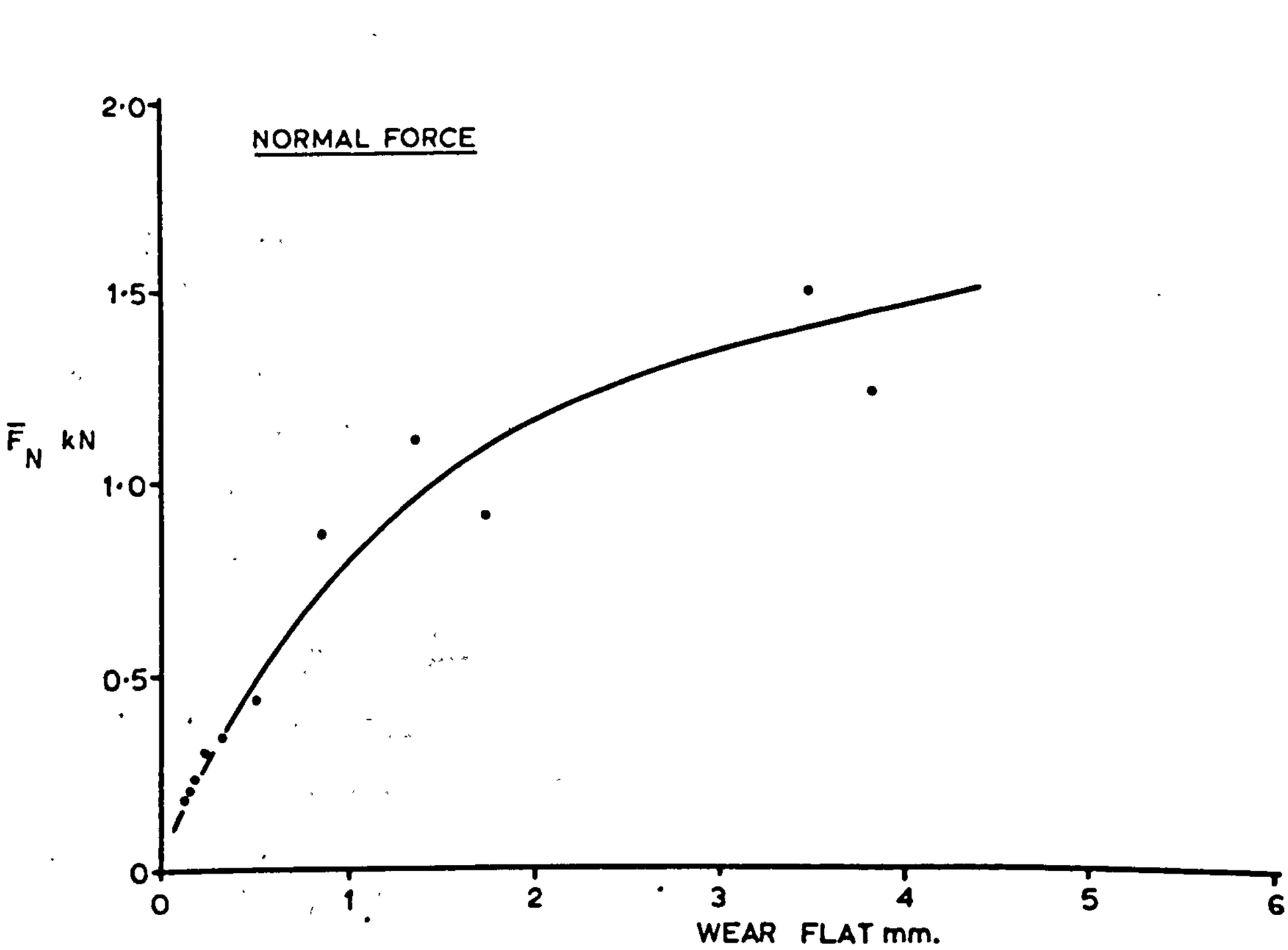

FIGURE 35 - EFFECT OF WEAR ON PICK FORCES

Figure 36 shows how yield and the normal to cutting force ratio changes with wear. Yield is quite clearly independent of wear, providing that sufficient normal force can be supplied to resist the tool moving out of the rock. Doubtless a stage of wear would eventually be reached where the tool could not be maintained at its prescribed depth, when the yield would quickly fall to zero.

The normal to cutting force ratio shows the disproportionate increase in normal force up to a wear flat of 2mm. Thereafter it tends towards a constant value of about 1.8. This represents a dramatic shift in pick force distribution from the practical pristine value of approximately 0.5 and emphasises the importance of stiffness in machine construction to withstand the large increase in normal force associated with pick wear.

Specific energy follows the same trend as cutting force. This is shown in Figure 37. The rapid initial increase in specific energy is tending to level off at a wear flat of around 2mm, but this constitutes between a three and fourfold increase in energy requirements. So that, in the practical reality of cutting an abrasive rock of only modest strength, the pick is seen to quickly attain a stable wear rate at which point its level of efficiency is little better than 25% of that for the pristine pick. In fact it just overlaps the most efficient of the pristine disc operations.

The persistent emergence of the 2mm wear flat, as a point of transition to a more stable tool performance, is worth further interpretation on the basis of carbide grade. Figure 34 shows that a 2mm wear flat is reached for each of the carbide grades after the following distances:-

Rock	Grade	CPM	CM	CH (dry)	CH (wet)
Bunter	Cutting Distance	30m	110m	1000m	1500m
Limestone	Cutting Distance	13km	-	-	-

Although none of these distances represent a very long cutting time it would be wrong to assume that, in reality, there is nothing to choose

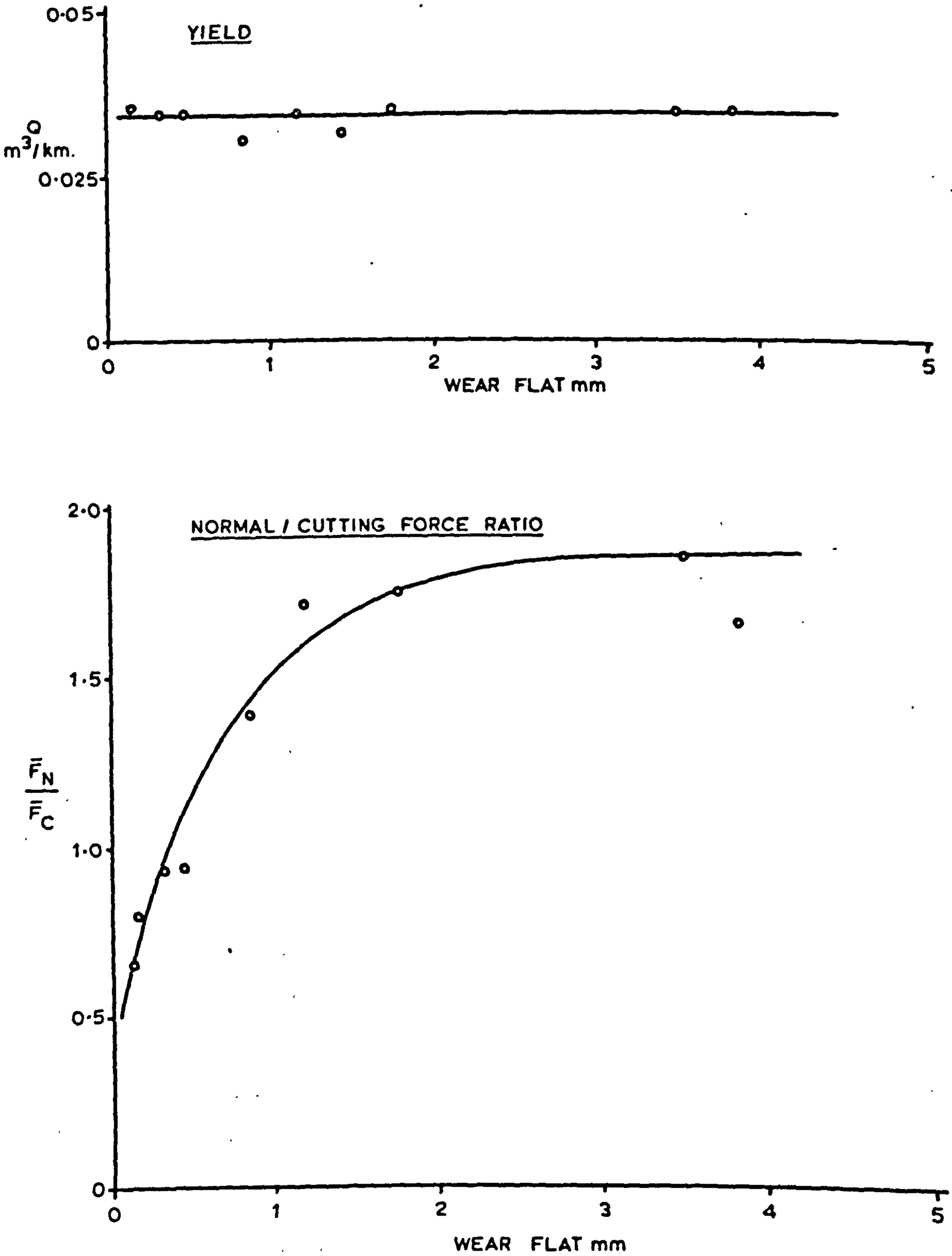

FIGURE 36 -EFFECT OF WEAR ON YIELD & NORMAL/CUTTING FORCE RATIO

between them. A "steady state" wear rate after the initial 2mm wear flat does not mean that all grades continue wearing at the same rate. As Figure 34 shows, not only does the CH grade take 50 times longer than CPM to achieve the 2mm wear flat, its rate of wear beyond the 2mm point is considerably lower than that for CPM. The clear implication is that the CH pick has a considerably longer ultimate life than both the CPM and CM grade tools.

In conclusion it must be emphasised that the foregoing experiments have dealt exclusively with abrasive wear. The harder grades of carbide such as CH, being more brittle, are susceptible to chipping and gross failure when exposed to high stress cutting conditions. Due to the random nature of this mode of tool failure the subject must be treated statistically and thereby involve the destruction of several hundred carbide tools.

7.8 A Comparison Between the Forces and Energies Required to Cut Magnesian Limestone and Bunter Sandstone

In order to compare the cutting characteristics of the two rocks the ratios between the measured parameters in each rock have been calculated. These ratios, which take the results in dry Bunter Sandstone as a base, are tabulated in Appendix I K. The average of the ratios for the mean cutting and mean normal forces are 4.6 and 3.5 respectively. The effects of each variable (rake angle, width and depth of cut) on the ratios have been isolated and the appropriate grouped data appears in Appendix I L. The increase in both cutting and normal force when excavating Magnesian Limestone is seen to be independent of each of the three variables.

Rock yield is consistently lower in Magnesian Limestone. The average value of the ratio of yields is 0.85 and since yield is measured on a volumetric rather than a graviametric basis it is dependent on the geometry of the groove and not on the density of the material.

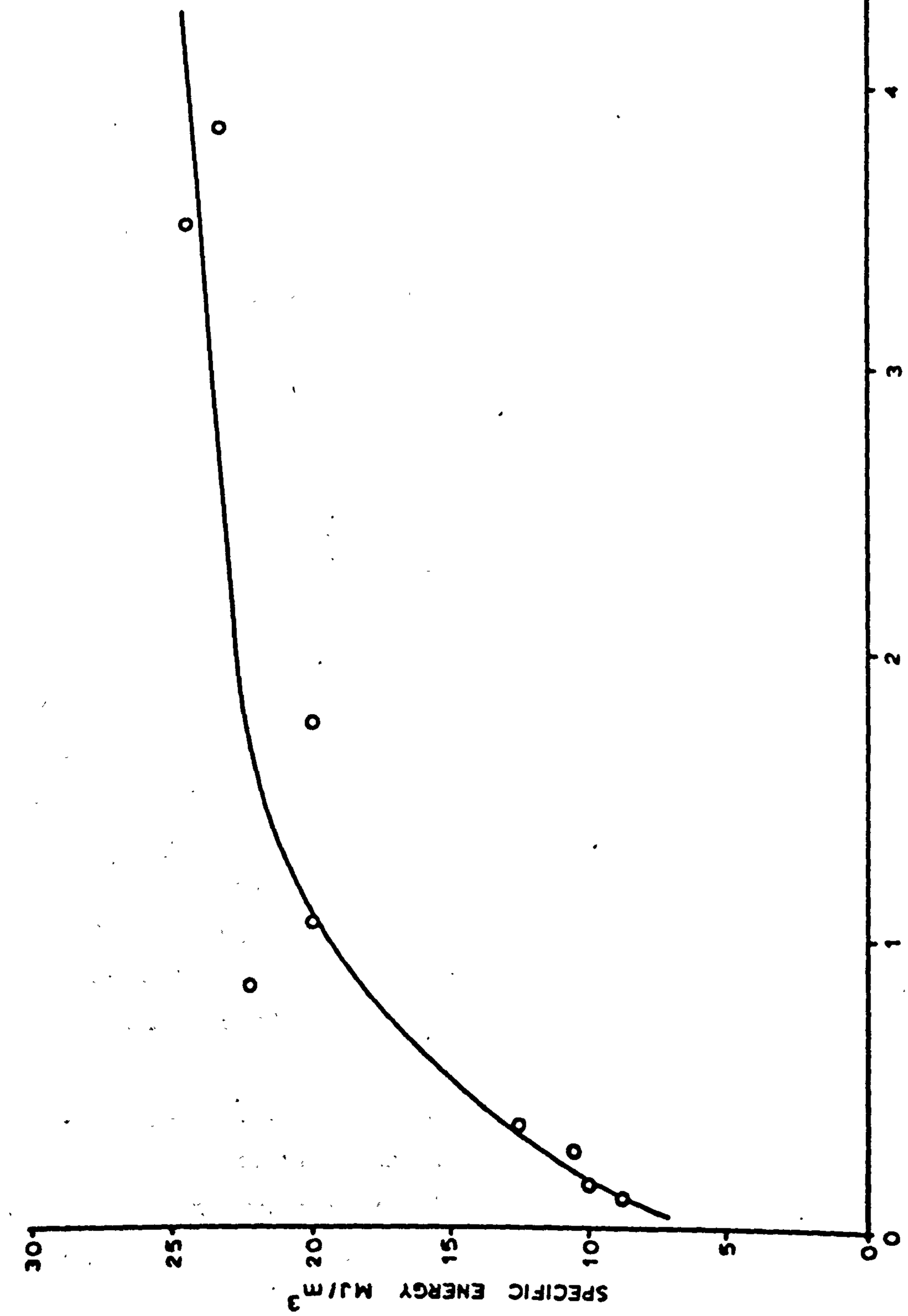

FIGURE 37 - EFFECT OF WEAR ON SPECIFIC ENERGY

The grouped data shows that rake angle and width of tool have no effect on the ratio of yields. At shallow depths of cut the yield in Magnesian Limestone and Bunter is nearly the same but, as depth increases this ratio falls until at a penetration of 15mm the yield from the Limestone is only 75% of that from an identical cut in Bunter. Equation 12 of section 7.2.2 expressed the yield as:-

$$Q = w\,d + d^2 \tan\theta \qquad \ldots\ldots\ldots (12)$$

where θ is the breakout angle defined in Figure 25. This breakout angle has been calculated for each of the unrelieved pick cutting tests and the results are given in Appendix I M. The appropriate grouped data appears in Appendix I N.

Figure 38 shows the variations in breakout angle with rake, width and depth of cut. Rake angle, as expected, has no effect on the breakout. The breakout does, however, decrease with width of tool. Inspection of Appendix I M shows this to be especially true at low depths of cut where the 40 and 50mm wide tools sometimes produce no breakout at all. This has only a minimal effect on rock yield since, with wide tools, the swept area is many times greater than the area of the breakout.

The Specific Energy required to cut Magnesian Limestone with the range of tools tested is, on average, 5.7 times that for Bunter. Rake angle and width of tool have no influence on this ratio but, reflecting the trend with yield, Specific Energy rises with increasing depth of cut.

For any given cutting situation the ratios between mean and mean peak forces could be influenced by rock strength or by the "brittleness" of the material being cut. Some of the ratios between the four principal forces have been calculated and are listed in Appendix I (P, Q and R). The average value of each ratio appears in Table 27.

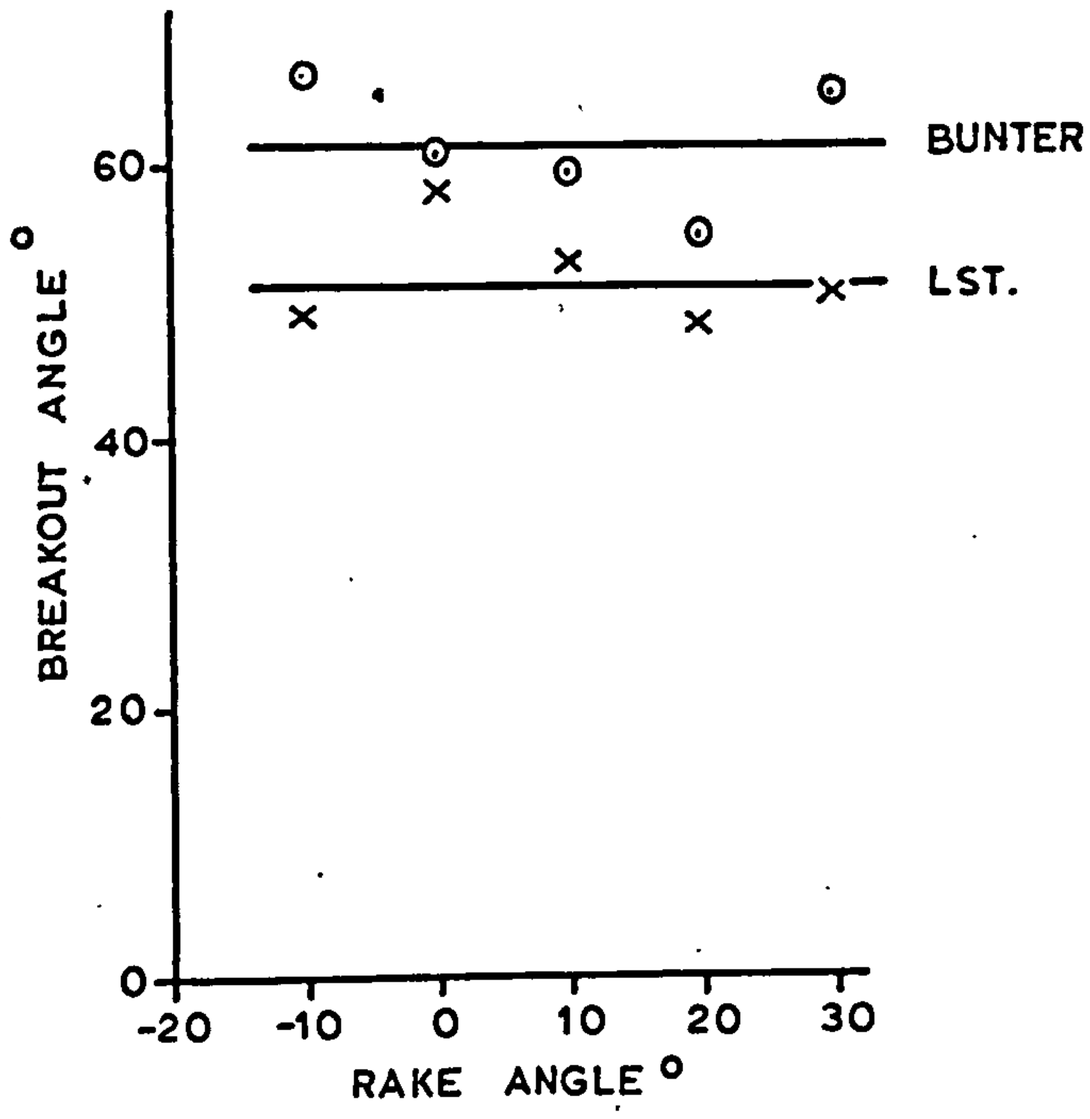

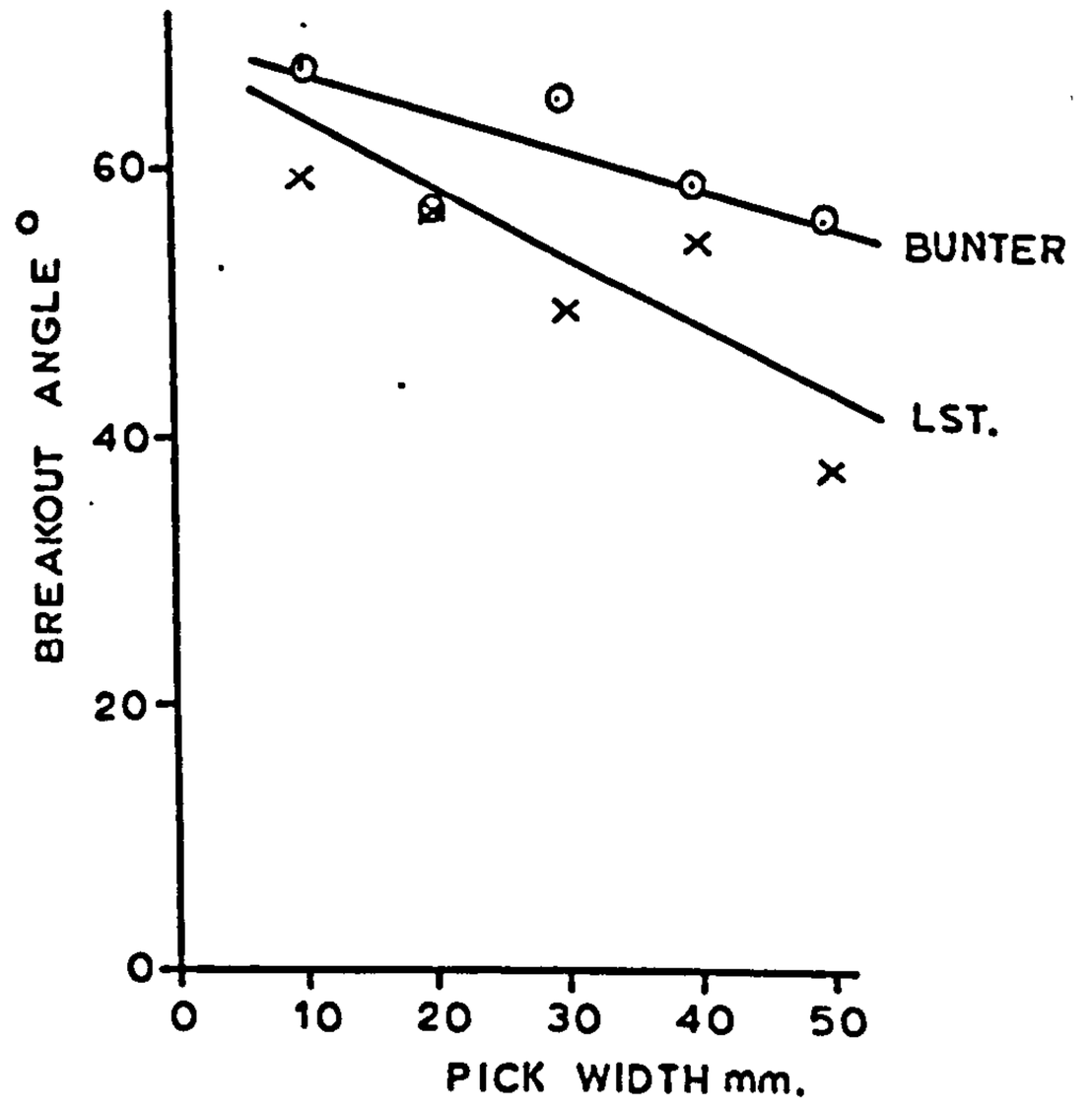

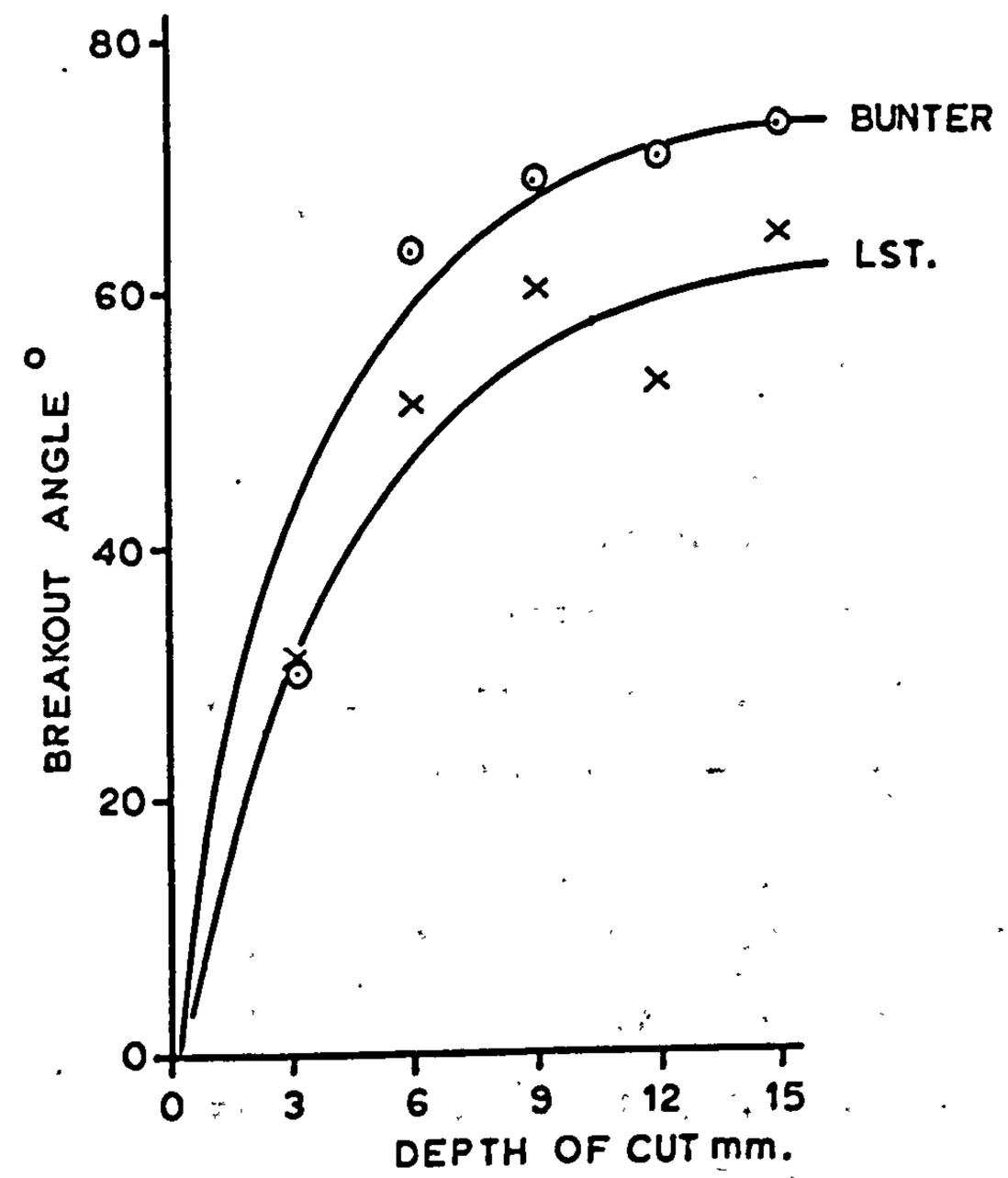

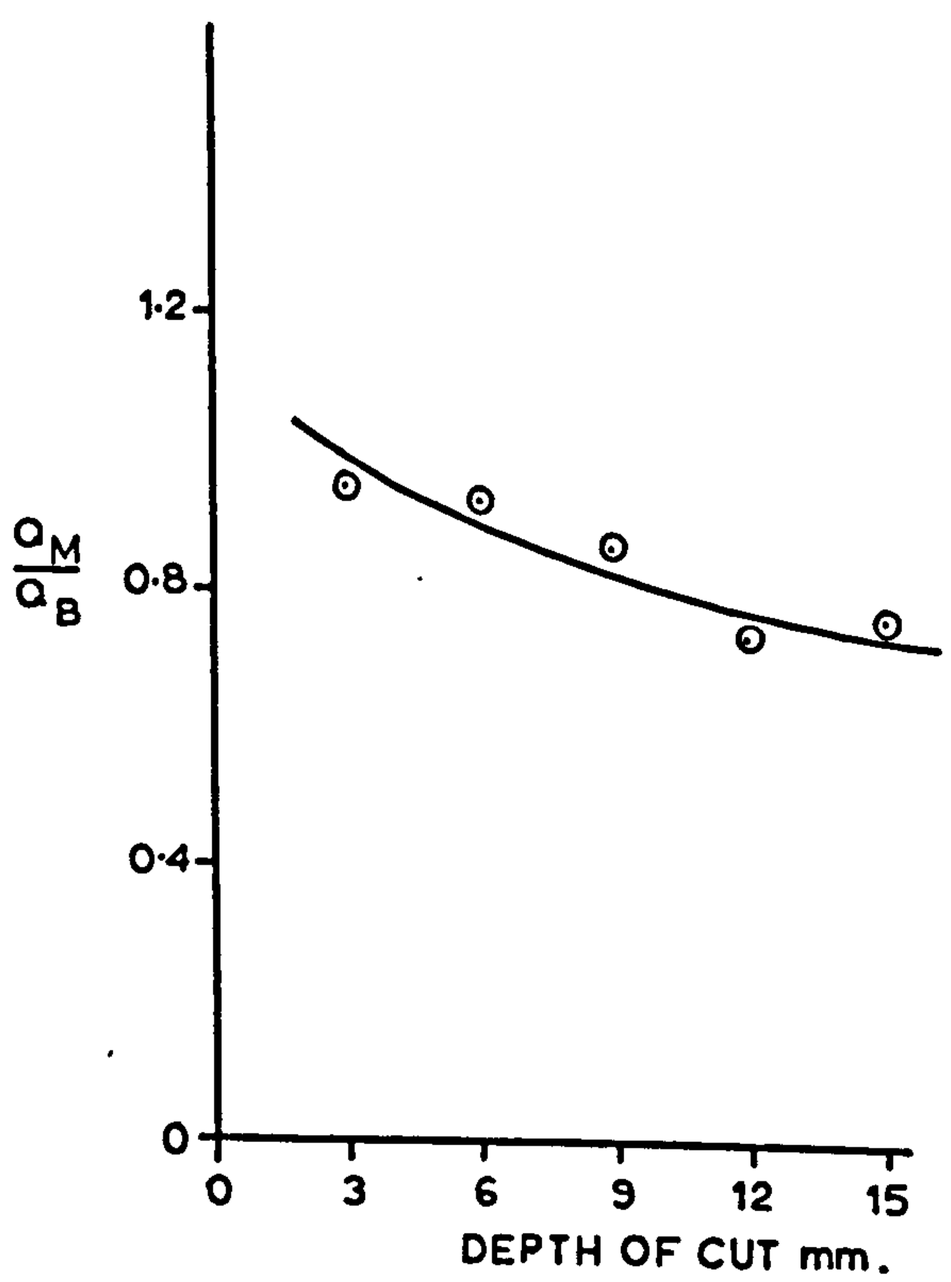

FIGURE 38 – VARIATIONS IN BREAKOUT ANGLE

TABLE 27

MEAN VALUES OF FORCE RATIOS

Ratio	Dry Bunter	Wet Bunter	Magnesian Limestone
$F_C/\overline{F}_C$	2.56	2.39	2.46
$F_N/\overline{F}_N$	2.13	2.18	1.88
$\overline{F}_C/\overline{F}_N$	0.93	1.05	1.22
F_C/F_N	1.14	1.14	1.58

The ratio between the mean and mean peak cutting forces remains virtually constant for both rocks. The relative abrasivity of the rocks may be deduced from the changes in mean cutting to mean normal force ratio. In dry Bunter, the most highly abrasive of the rocks, the normal force is greater than the cutting force. In wet Bunter the forces are approximately equal and in the non-abrasive Magnesian Limestone mean normal force is only 81% of the mean cutting force.

8. CUTTING WITH COMPLEX SHAPED PICKS

Most symmetrical picks having a shape other than that of a simple wedge can be described using the two shape variables i) Front Ridge Angle and ii) Vee-Bottom Angle. Some tools, however, have a rounded base profile which can be taken as an intermediate somewhere between the simple wedge and ridged picks.

Asymmetry is not a common feature of picks since it implies an unbalanced lateral force which, in practice, may be difficult to control. Modifying a chisel shaped tool to include a side rake angle is, however, believed to have beneficial effects in an array by directing lateral breakage forces towards an adjacent groove (90).

These three shape features, which are defined in Figure 17, have been investigated in both Bunter Sandstone and Magnesian Limestone. The levels of the variables under consideration, which were listed in Table 22 of Chapter 6, appear below. All tools were of width 20mm, front rake $+10^{\circ}$ and 10° back clearance angle.

Front Ridge Angle	(γ)	-	90°	120°	150°	180°
Vee-Bottom Angle	(λ)	60°	90°	120°	120°	180°
Side Rake Angle	(ν)	0°	10°	20°	30°	-

Although every effort was made to maintain a consistent quality of rock throughout all experiments, including the physical test work, picks and discs, it was found impossible to avoid some variation. Consequently the least variable material was used for the main multivariate pick, disc and physical test programmes in order to provide a reliable basis for comparison.

Unfortunately, therefore, the Bunter used for the complex shape experiments, although of good quality and virtually identical strength to the main blocks, did originate from a slightly lower geological horizon with a coarser grain size and occasional quartz pebbles. By and large the difference in quality is of little consequence to the main body of results, its effects sometimes showing at the shallowest depths of cut.

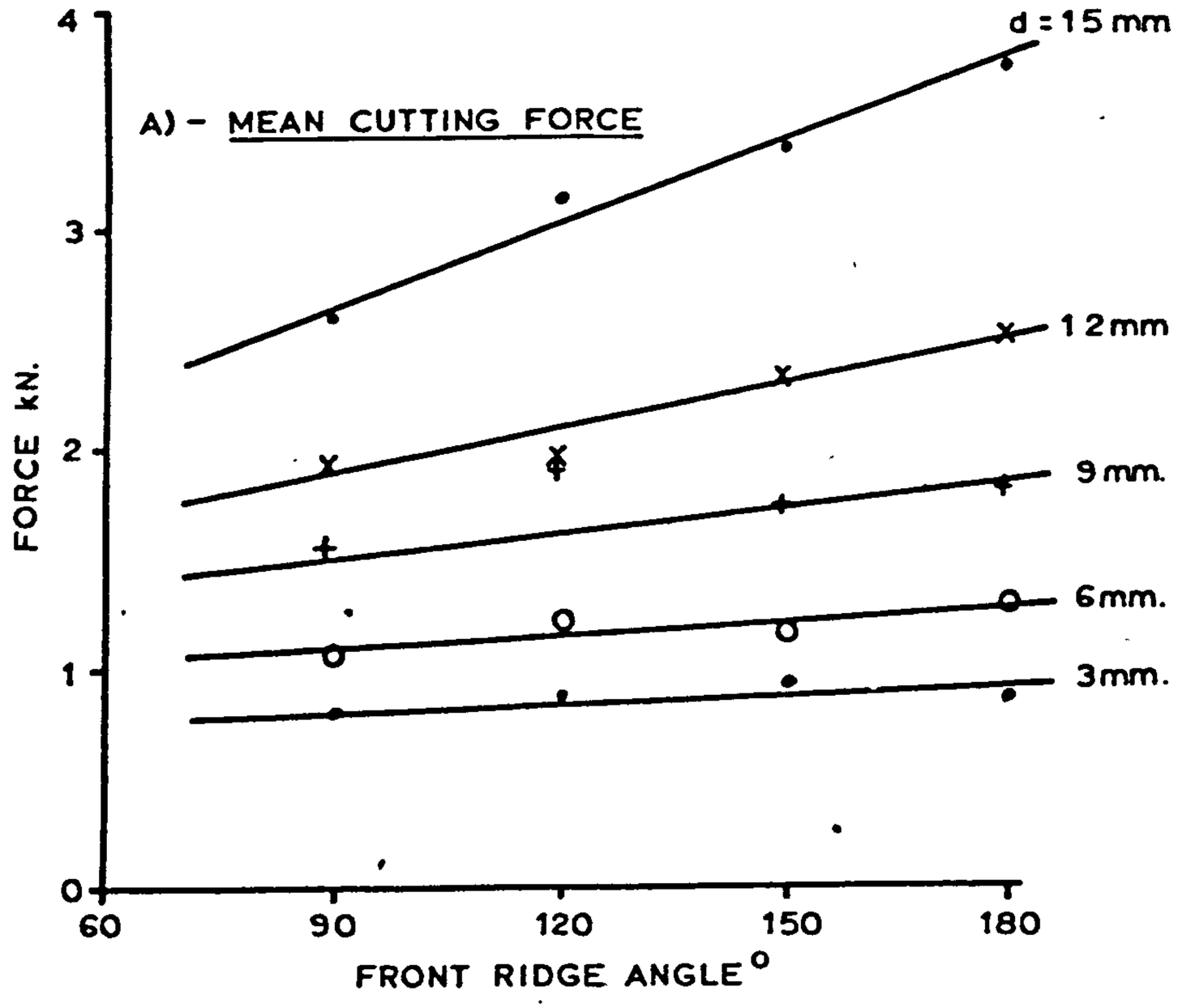

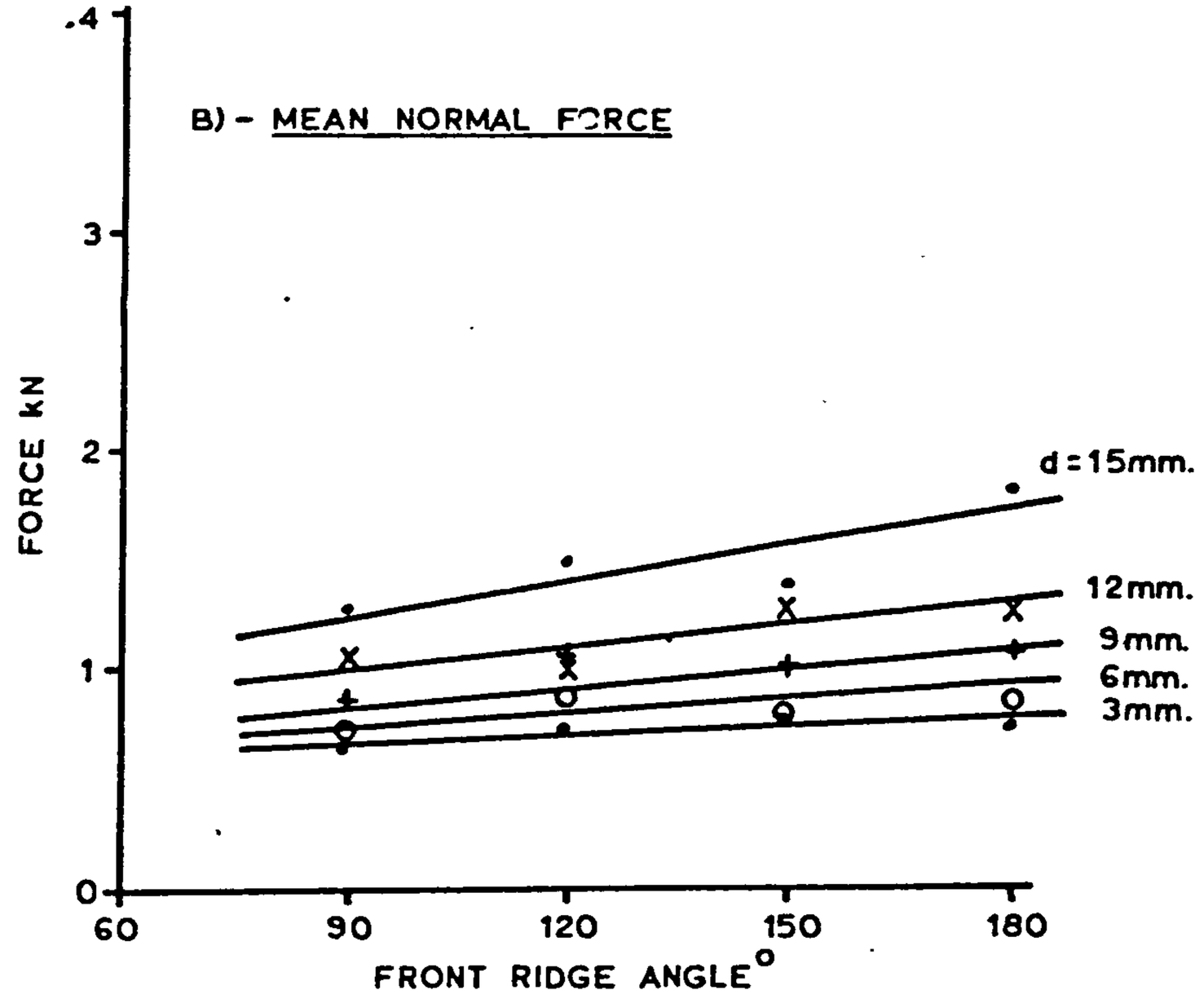

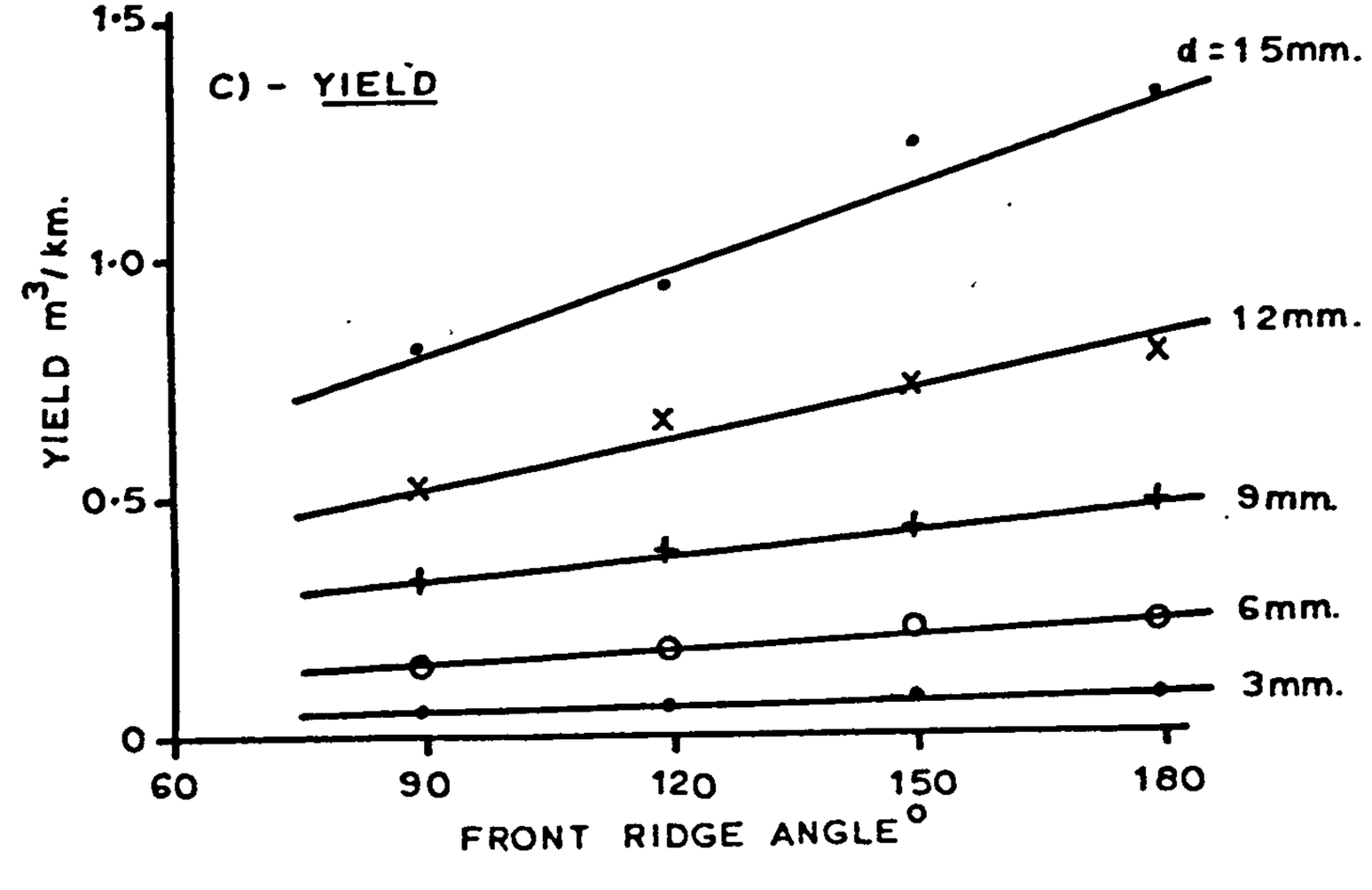

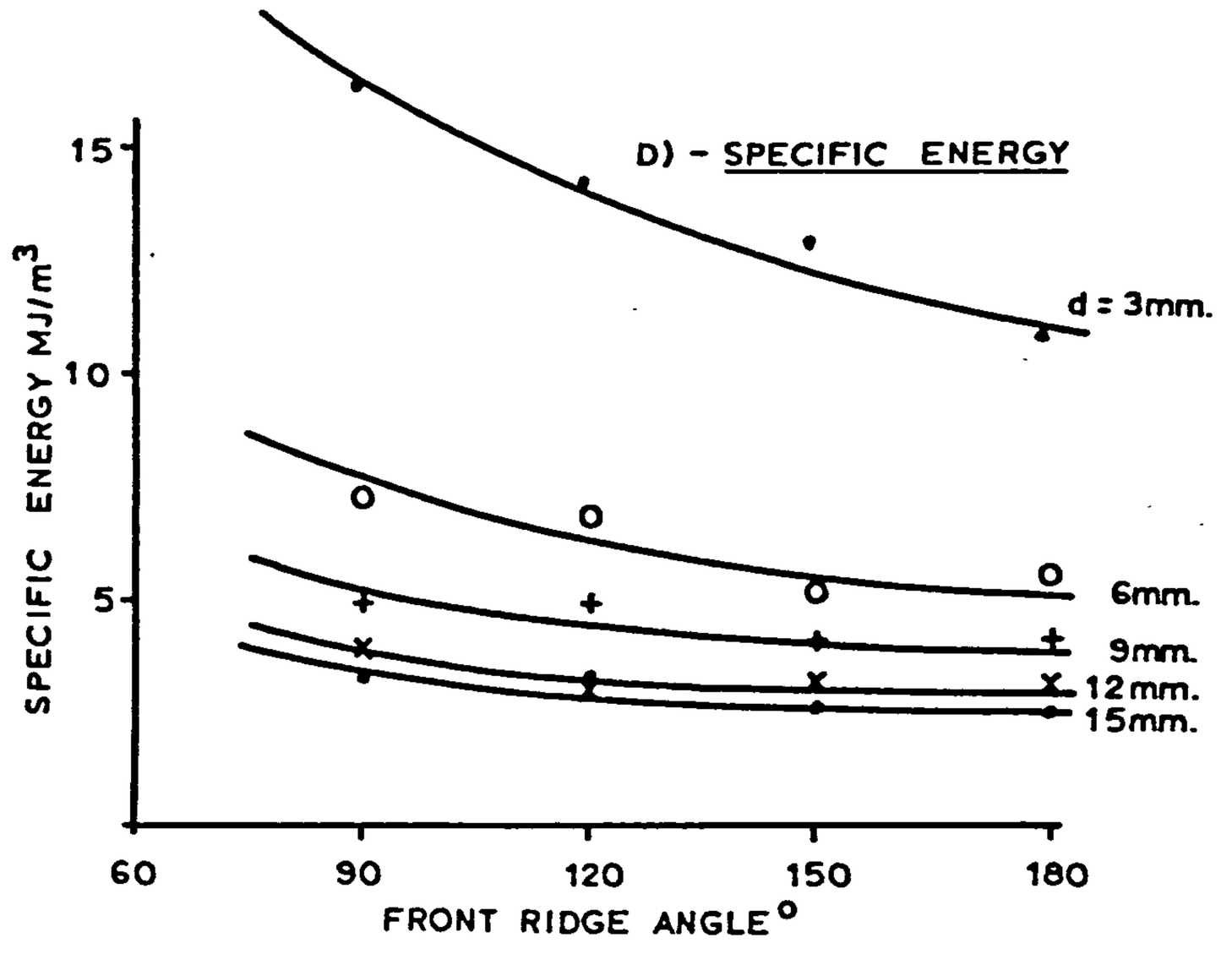

FIGURE 39 - EFFECT OF FRONT RIDGE ANGLE - BUNTER SANDSTONE

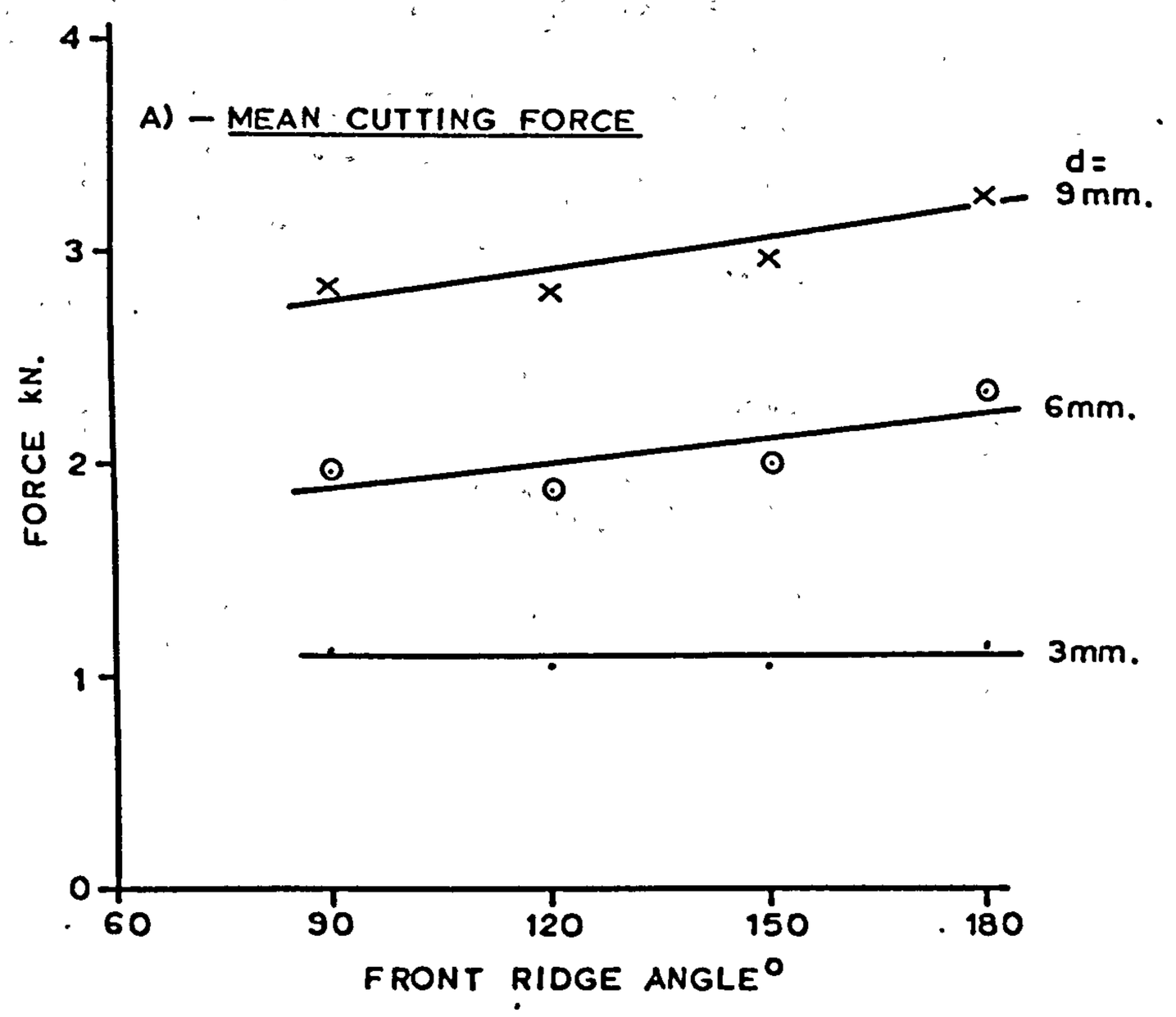

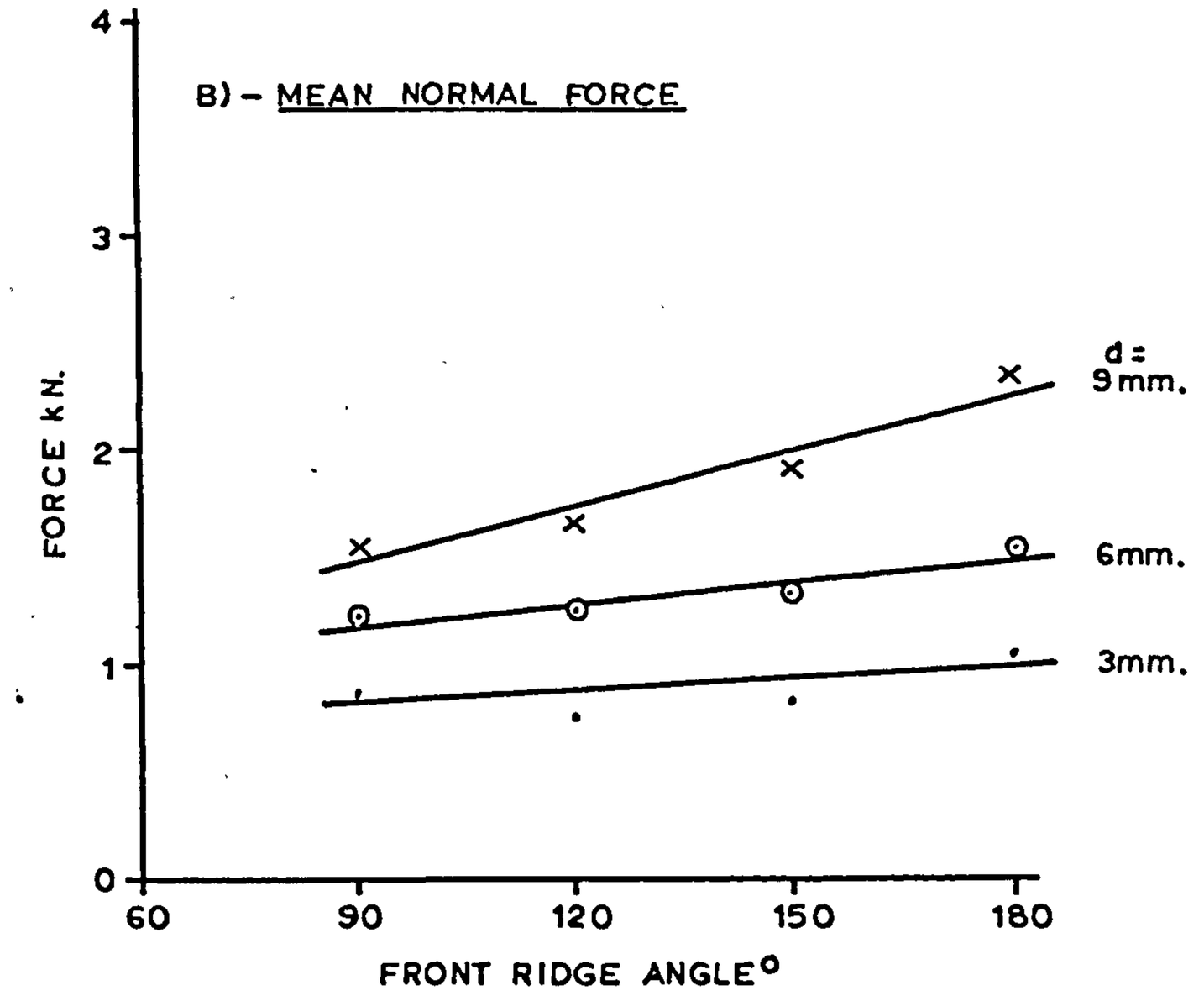

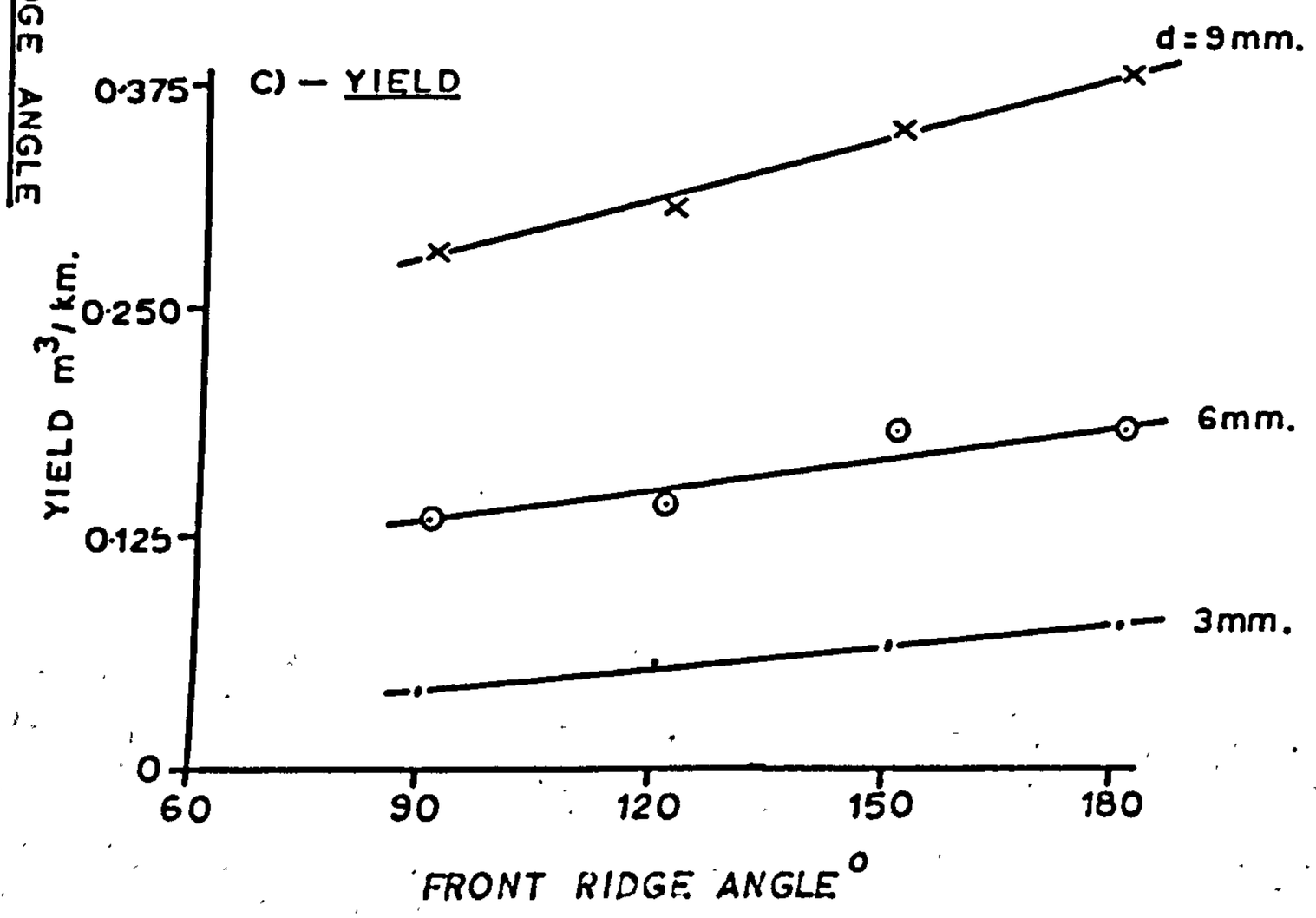

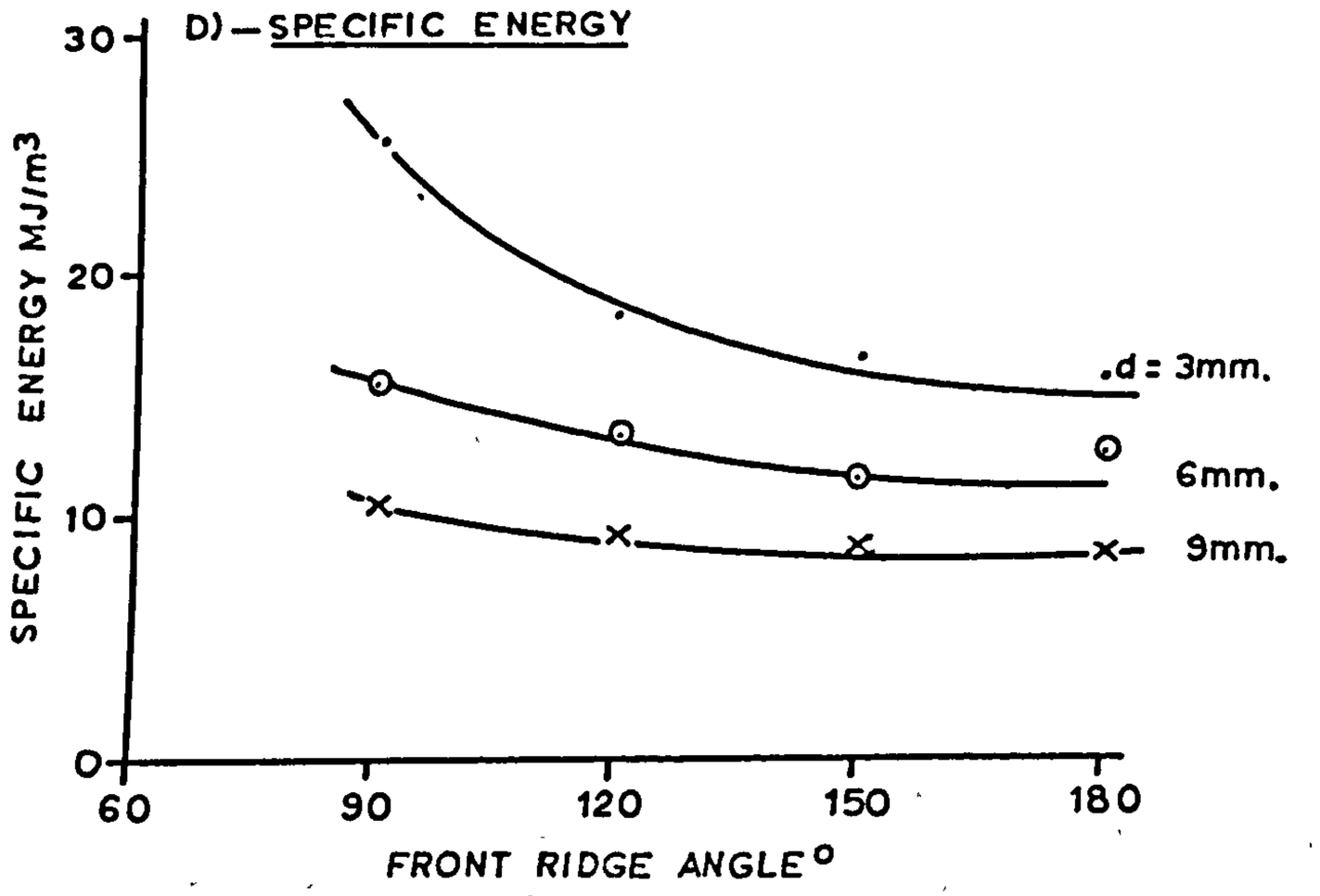

FIGURE 40 — EFFECT OF FRONT RIDGE ANGLE — MAGNESIAN LIMESTONE

8.1 Effect of Front Ridge Angle (γ)

Results for the tests, which are tabulated in Appendix VI, are shown graphically in Figures 39 and 40.

Mean cutting and normal force values increase linearly with ridge angle up to 180^{o}. Bearing in mind that 180^{o} is a flat front and thereby represents a chisel pick, it can be concluded that the provision of a front ridge angle reduces the forces acting on the tool and that the benefits in this respect are greatest at the higher cutting depths. Clearly the presence of a front ridge to the tool improves its forward penetrating capabilities.

On the other hand, the amount of rock cut also increases with front ridge angle, reaching a maximum at 180^{o}*. Since the swept volume of a tool, in this experiment, is independent of front ridge angle, it is clear that the amount of breakout produced is being affected. This implies that breakout is a function of the in-line cutting force and not some component of it deployed laterally. This is consistant with observations made of 3 dimensional breakage under idealised conditions which has shown that all breakage, including side splay, occurs ahead of the tool and as a consequence of the in-line cutting force (91). Whereas it may be argued that a front ridged tool, with its trailing cutting faces, will generate lateral force components, these can play little if any part of the production of breakout since they have no displacement in that direction.

Consequently the specific energy falls with increasing ridge angle and achieves a minimum at the simple wedge configuration. The disadvantage of a front ridge angle in terms of cutting efficiency is mostpronounced at shallow depths of cut. At large cutting depths the totally dominating effect of depth on efficiency is again evident and almost wholly overshadows the influence of a front ridge.

---

* A front ridge angle in excess of 180^{o} creates a tool having a central vee-shaped recess. This is equivalent to two side rake tools.

Although it is indisputable that the chisel pick is more efficient than a front ridged tool, there appears to be evidence supporting the view that the introduction of this tool design feature can provide some benefit, in practice, at little cost to cutting efficiency, providing the depth of cut is large. When cutting Bunter Sandstone at a depth of 15mm, a sacrifice of 14% in cutting efficiency leads to a cutting and normal force saving of more than 30%, when using a 90^{o} ridge angle in contrast to a simple chisel of otherwise similar shape. With the lower tool forces generated by a ridged tool, it appears that a larger depth of cut would be easier to achieve and maintain with this type of tool. It must, however, be borne in mind that the yield from a ridged pick is also much lower than for the chisel and, therefore, to excavate a given surface area would require a proportionate increase in the number of ridged picks on a cutting head. Specific energy alone determines the machine cutting torque and thereby the aggregate mean cutting force. It seems reasonable to suppose that the aggregate normal force on a cutting head will be related to the overall cutting force and that machine reaction forces will be higher than with chisel picks.

This analysis does show reasons why picks having a ridged front have found wide acceptance in industry. The substantial force reductions on a simple pick will doubtless have been reflected in fewer incidents of mechanical damage to picks and their mountings.

8.2 Effect of Vee-Bottom Angle (λ)

The force, yield and energy results are given in Appendix VI (C and Dλ.

Consideration is first given to the mean cutting force and rock yield relationships which are presented graphically in Figures 41 and 42. The effect of a vee-bottom angle is to reduce both the cutting force and the rock yield. Unlike the front ridged tool, these reductions both appear to be exponentially related to the vee-angle (λ).

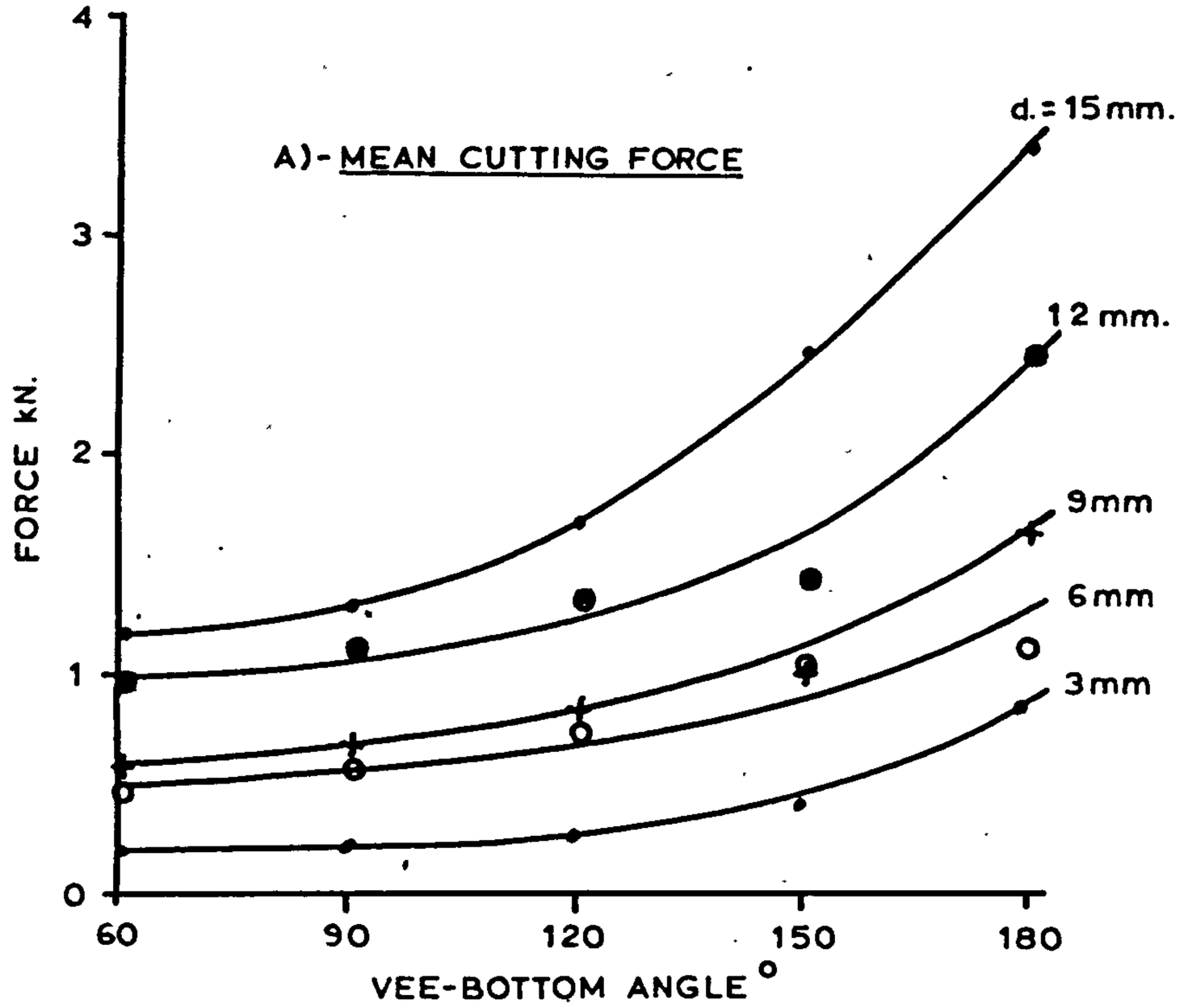

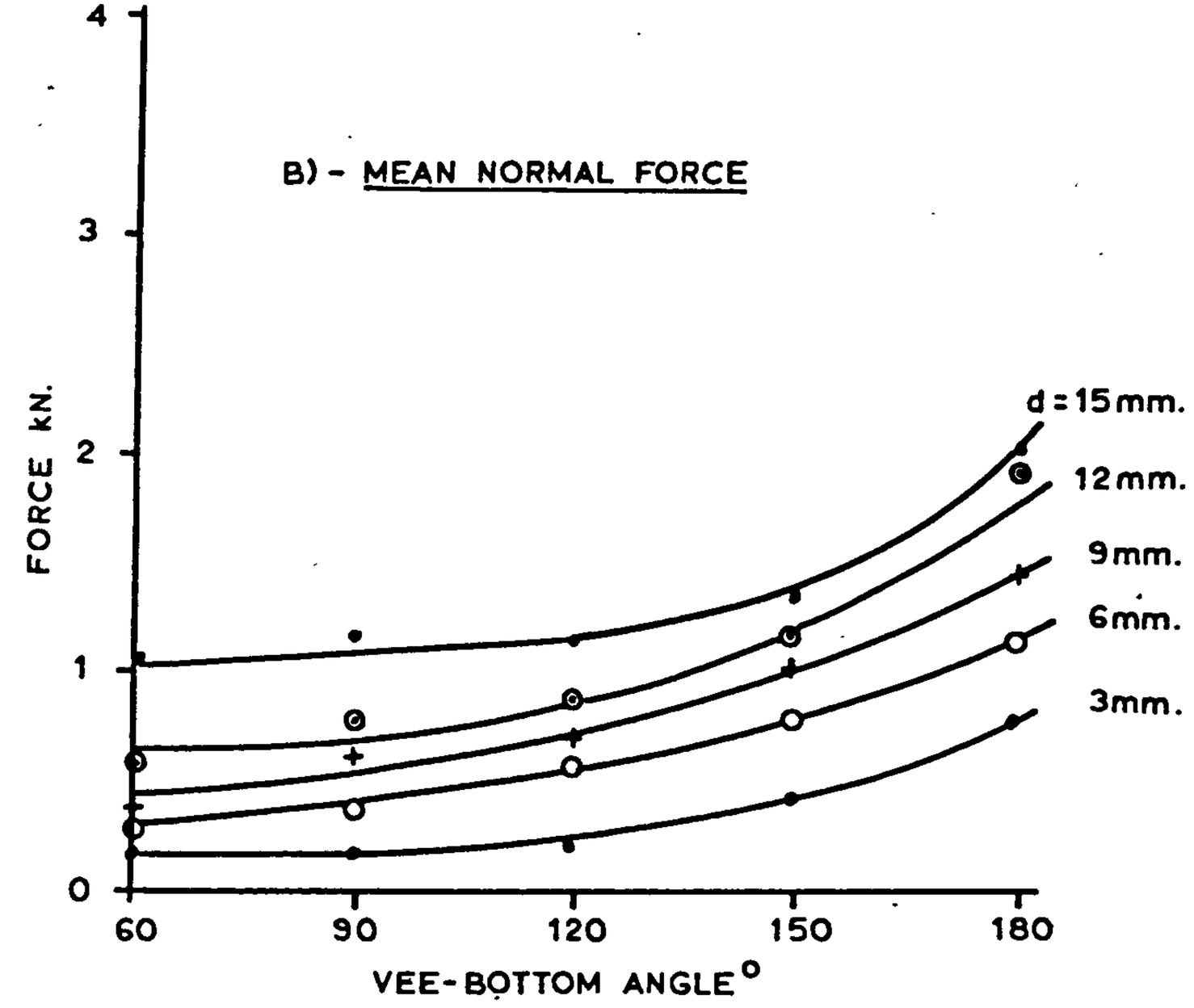

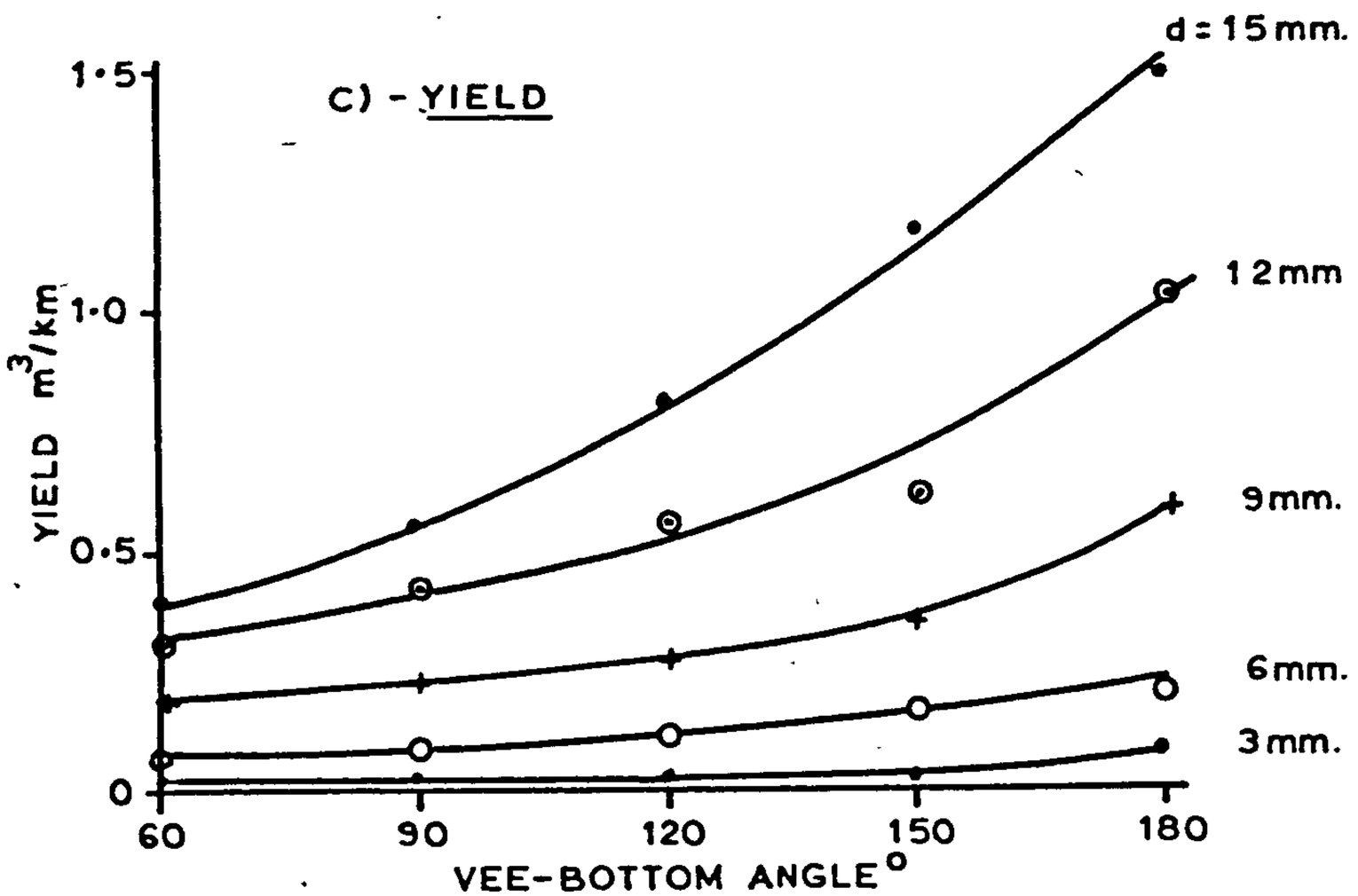

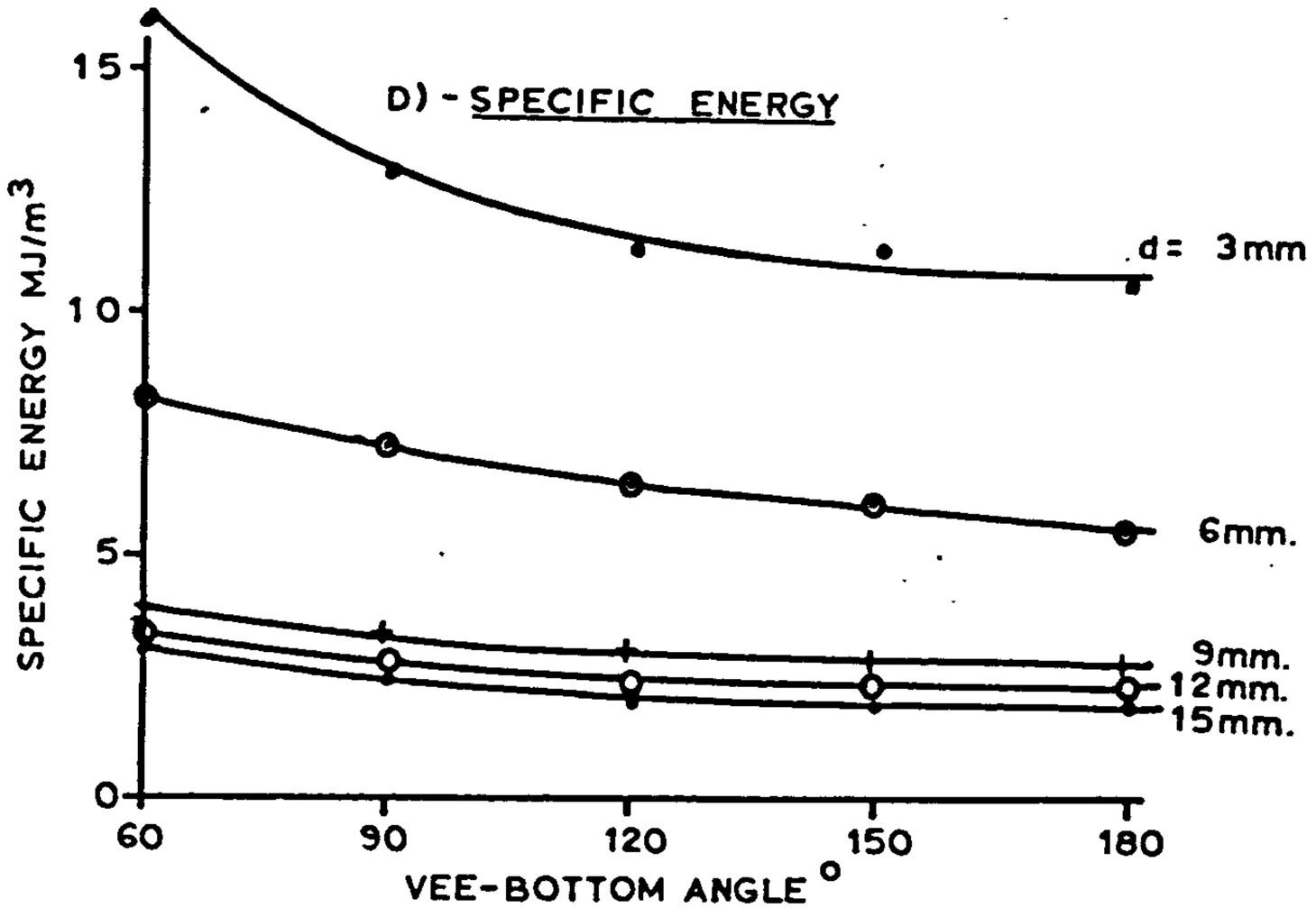

FIGURE 41 - EFFECT OF VEE-BOTTOM ANGLE - BUNTER SANDSTONE

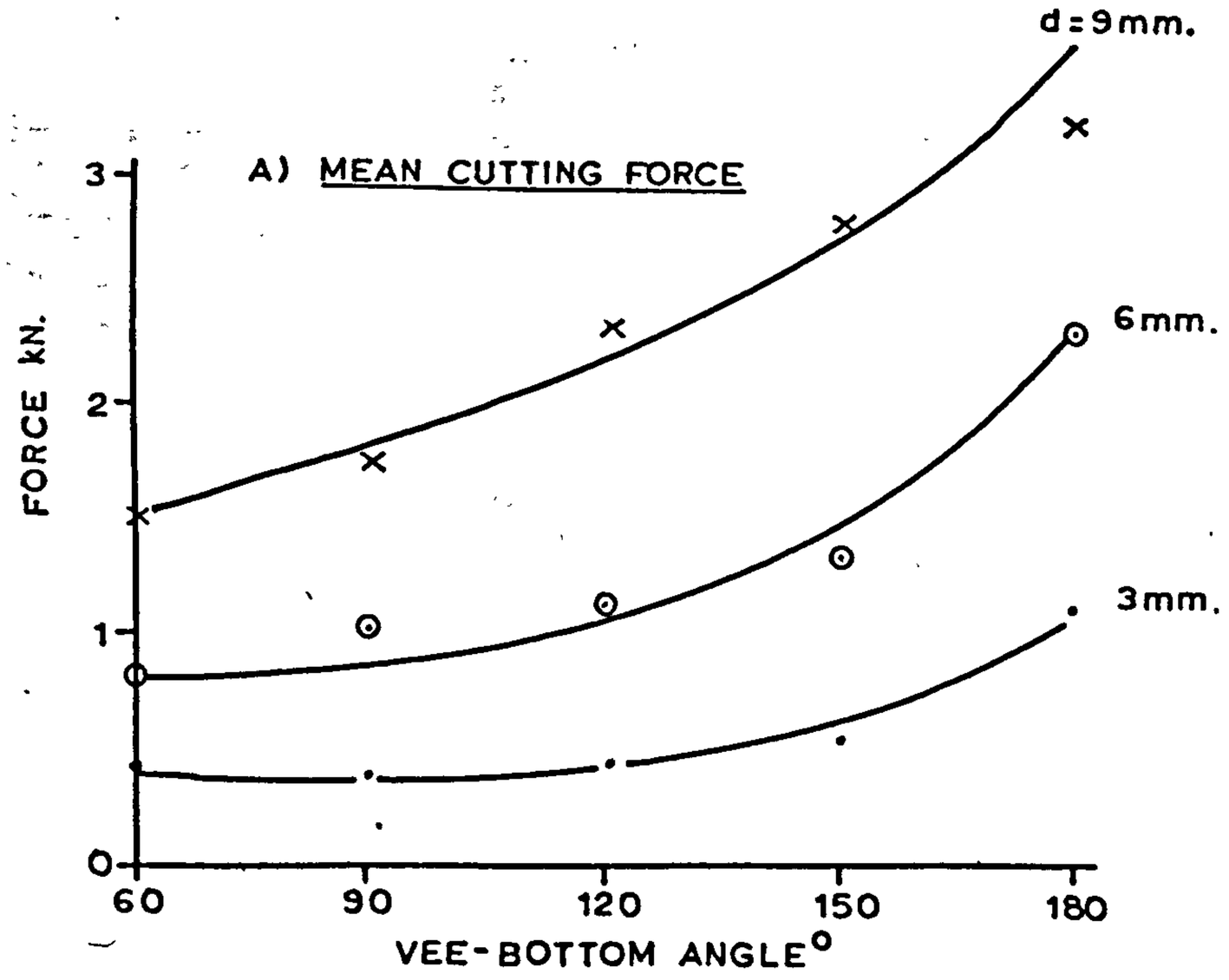

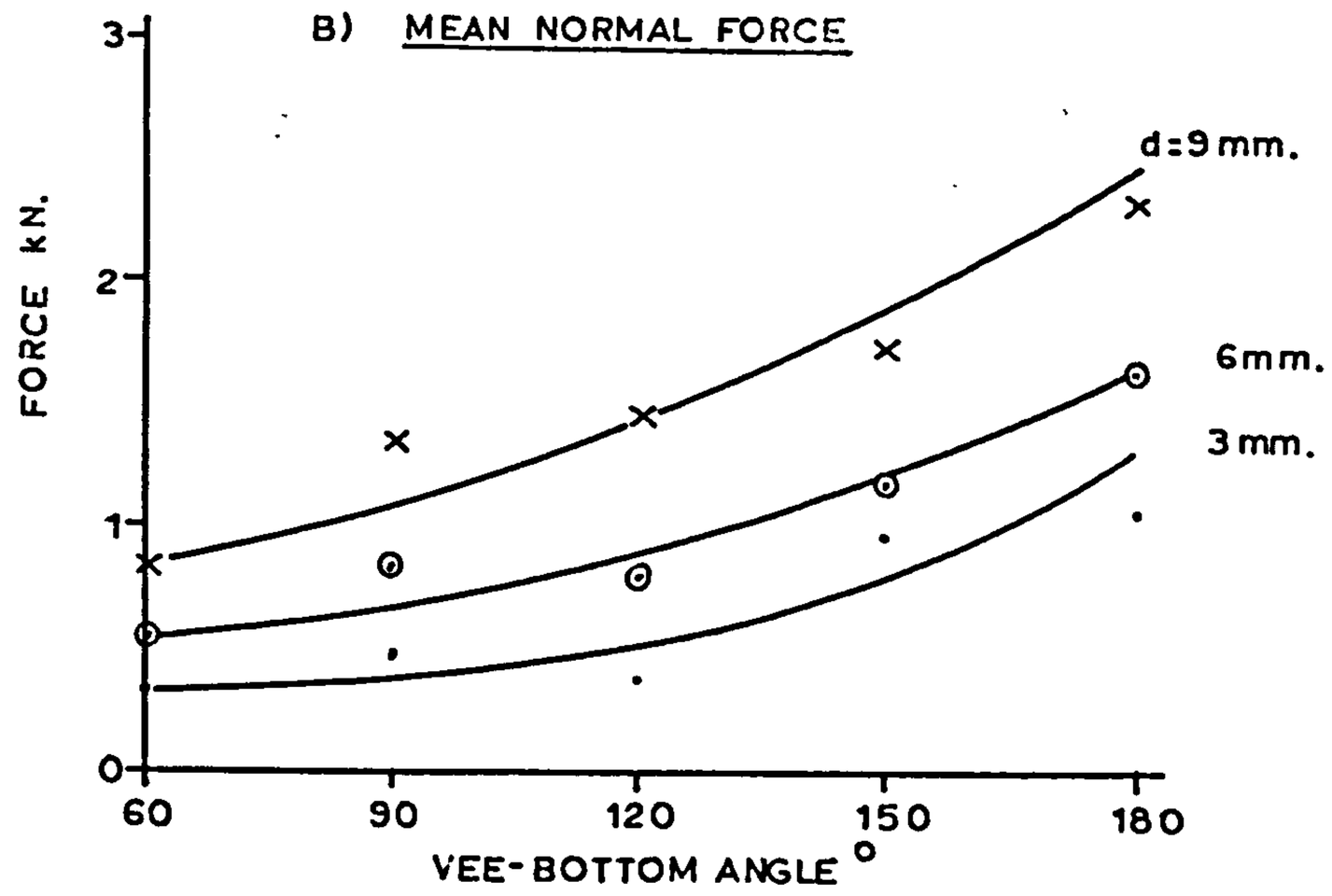

FIGURE 42 – EFFECT OF VEE BOTTOM ANGLE – MAGNESIAN LIMESTONE

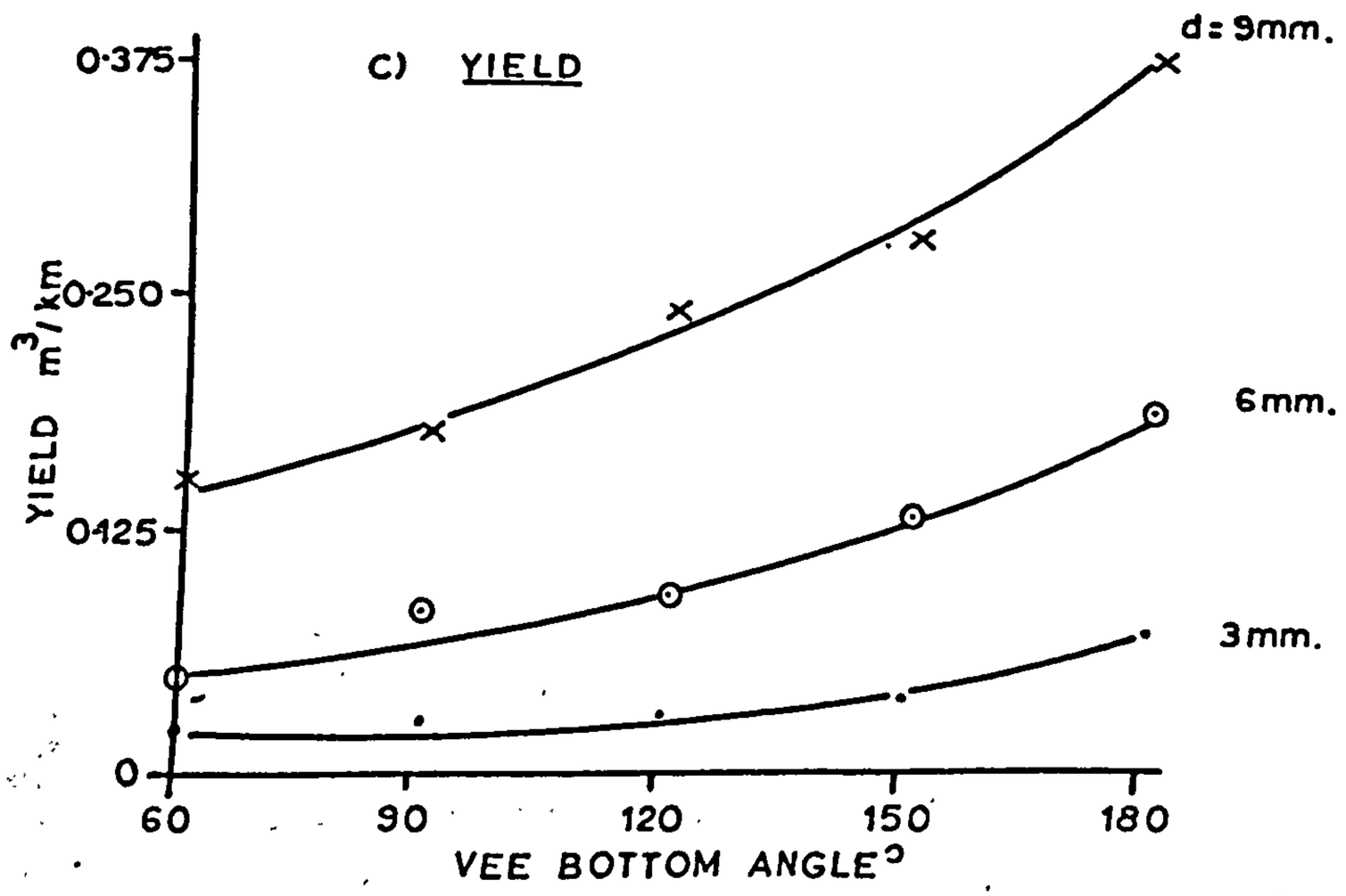

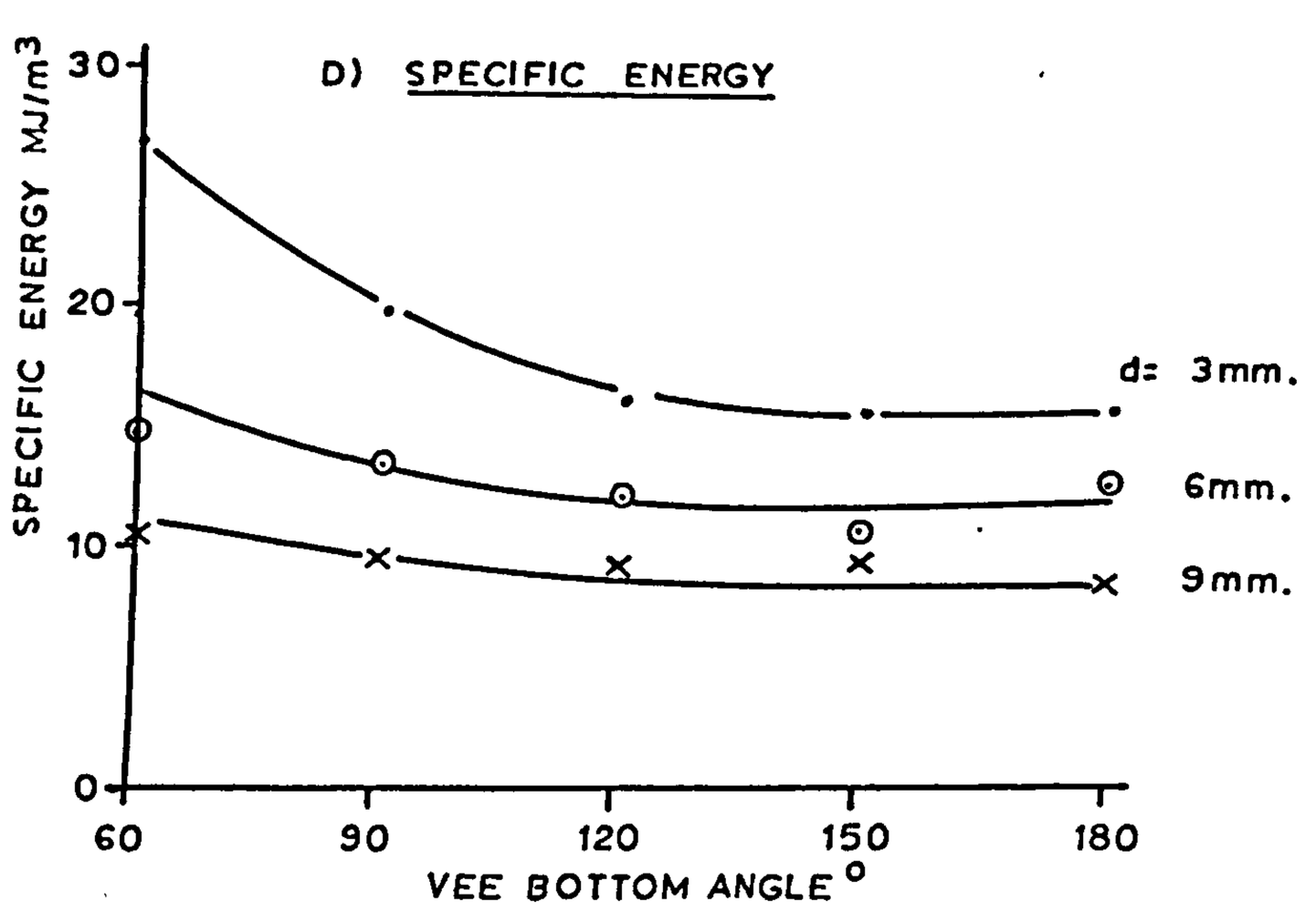

The reasons for this shape of curve emerge from considerations of the relationship between tool profile and consequential groove geometry, which is complex. This complexity was evident from differences in breakage patterns observed during the experiment.

Considering the front face geometry of a vee-bottom tool, as shown in the sketch below, lateral breakout in some cases was observed to originate from the point P and in all other situations from the side edge S.

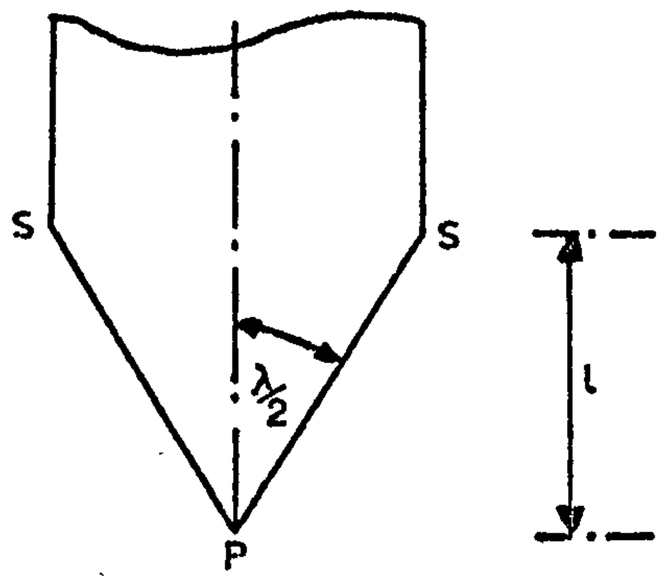

The half vee-angle is denoted by $\lambda/2$ and the reach of the point from the tool shank as ℓ.

A statement of the origins of breakout for all experiments is given in Table 28.

TABLE 28

SUMMARY OF BREAKAGE PATTERNS
(for 20mm tool shank width)

Depth of Cut d mm	Vee Angle λ°				
	60	90	120	150	180
3	P	P	P	S	S
6	P	P	S	S	S
9	P	P	S	S	S
12	P	S	S	S	S
15	P	S	S	S	S

There are only 4 possible combinations of tool and groove geometry and these inter-relate $\lambda/2$ and θ (breakout angle) with ℓ and d, as shown in Figure 43. The situations represented by diagrams A, B and C cover all cases met in Table 28. Situation D was not achieved in the experiment nor is it likely to occur in practice, since the implied very low value of the reach ℓ must always be larger than the depth of cut d.

The inequalities defining each situation are stated in Figure 43 and each combination of λ and d covered in the experiment can be described by situation A, B or C. For example, $\lambda = 60$, $d = 3$ is covered by situation A, similarly $\lambda = 120^{\circ}$, $d = 15$ corresponds to situation C.

All combinations of variables are similarly categorised in Table 29.

TABLE 29

GROOVE GEOMETRY - TOOL SHAPE SITUATIONS
(for 20mm tool shank width)

Depth of Cut	Vee Angle λ°				
d mm	60	90	120	150	180
3	A	A	A	B	B
6	A	A	C	B	B
9	A	A	C	B	B
12	A	C	C	B	B
15	A	C	C	B	B

for any breakout angle θ where $60^{\circ} < \theta < 75^{\circ}$

and where A = $d < \ell$, $\lambda/2 < \theta$

B = $d > \ell$, $\lambda/2 > \theta$

C = $d > \ell$, $\lambda/2 < \theta$

A comparison of Tables 28 and 29 now reveals a remarkable consistency in the patterns of breakage, thus:

a) When the reach of the tool is greater than the depth of cut, breakout always occurs from the point of the tool. There were 64 individual cuts made in this condition, <u>all</u> of which produced this type of breakage.

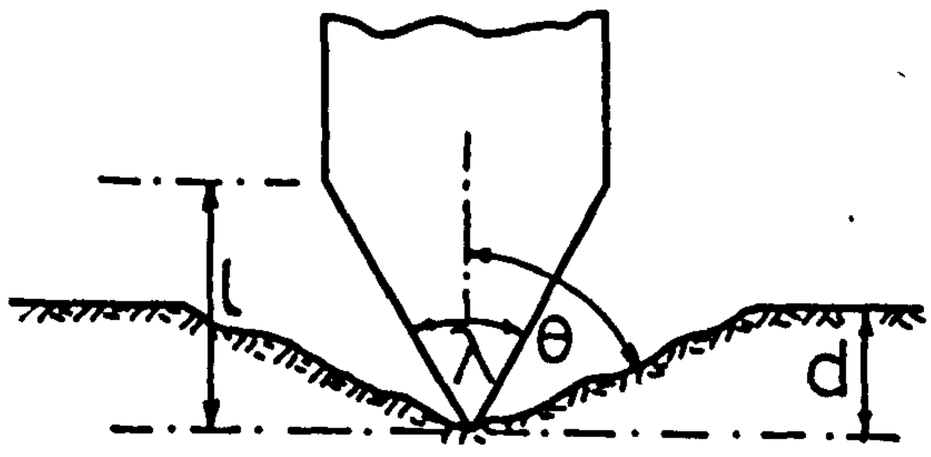

A) breakage pattern for
$d < l$
$\lambda/2 < \theta$

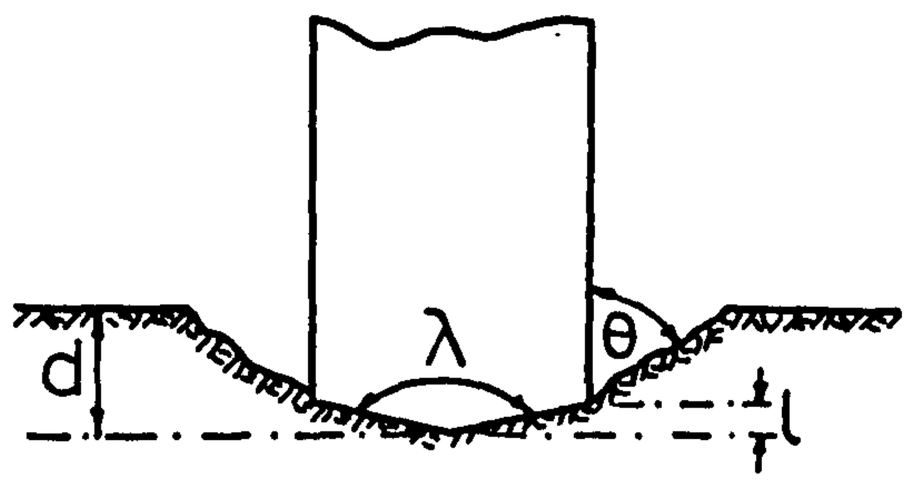

B) breakage pattern for
$d > l$
$\lambda/2 > \theta$

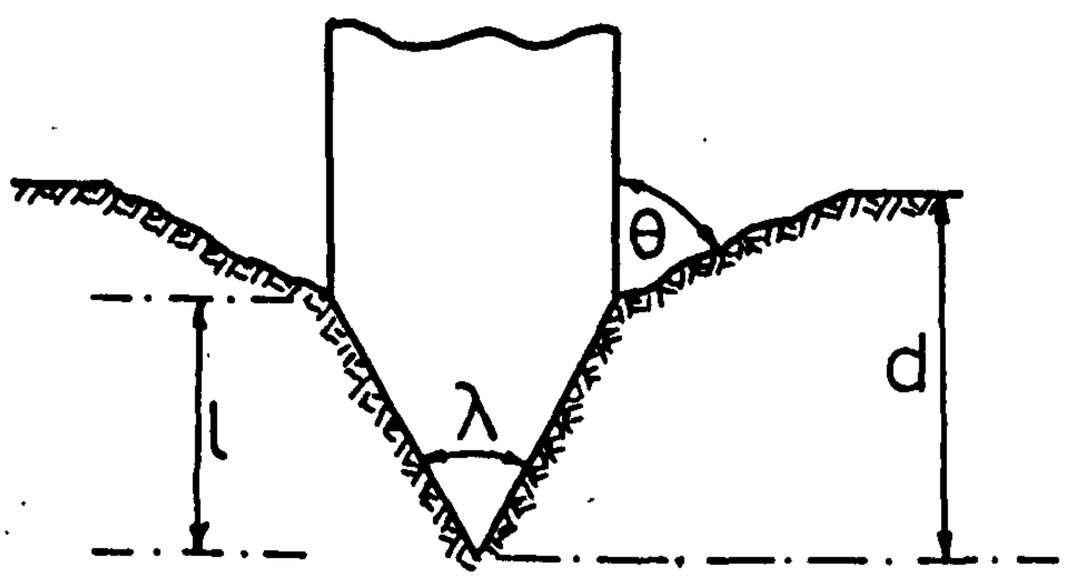

C) breakage pattern for
$d > l$
$\lambda/2 < \theta$

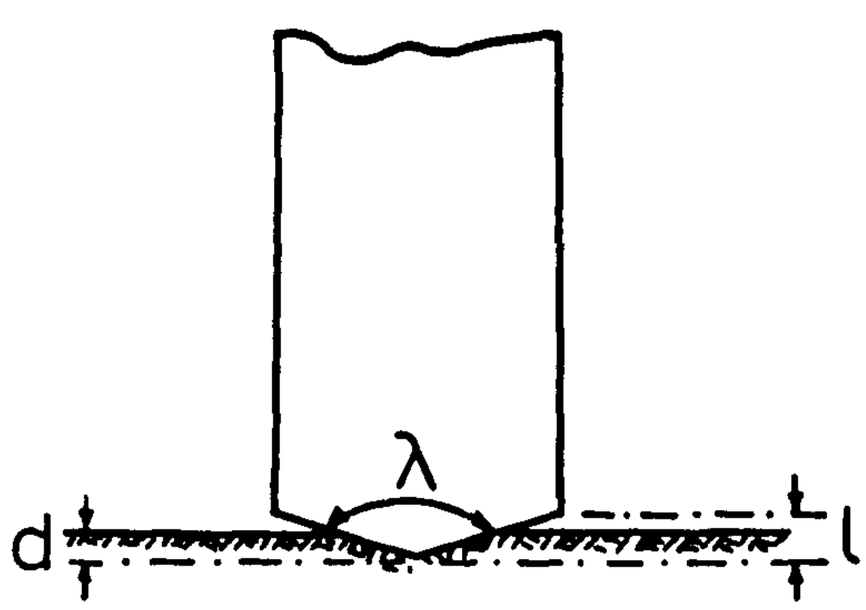

D) breakage pattern for
$d < l$
$\lambda/2 > \theta$

FIGURE 43 - BREAKAGE PATTERNS FOR VEE-BOTTOM PICKS

b) When the depth of cut was greater than the reach of the tool, breakout always originated from the upper edge of the tool side. There were 96 experiments carried out in this condition and <u>all</u> produced the type of breakage described by diagrams B or C in Figure 43.

c) When the depth of cut is greater than the reach of the tool, the relative magnitude of vee angle and breakout angle is of no significance. Breakout always emanates from the side of the tool.

d) It is axiomatic that situation D cannot produce a natural breakout and therefore the area cut by the tool will be the same as its swept area.

e) Natural breakout, whether originating from the point or the edge, produced an irregular rough surface. Those parts of the groove conforming to the shape of the tool (i.e. when $d > \ell$) always had smooth machined surfaces.

f) For situations where the tool reach was greater than the depth of cut, there was some evidence that the natural breakout angle varied with both vee angle and depth of cut. There was however insufficient data on which to base meaningful relationships.

It should be emphasised that the foregoing measurements all involved a tool shank width of 20mm and rake angle $+10^{\circ}$. Since the tool reach ℓ is a function of vee angle and shank width, the situations defined in Tables 28 and 29 are unique and would require re-evaluation for other widths.

As a general conclusion it is not surprising to find that rock yield is not linearly related to vee angle. Since, however, the regularity of groove shape has been defined, yield equations appropriate to situations A, B and C in Figure 43 can now be written. Algebraically situations B and C are identical.

i) Cross Sectional Area of Groove Type A:

$$\text{Area} = d^2 \tan\theta \qquad \ldots\ldots\ldots\ldots\ldots (15)$$

ii) Cross Sectional Area of Grooves Type B and C:

$$\text{Area} = \ell^2 \tan\frac{\lambda}{2} + 2\ell(d-\ell) \tan\frac{\lambda}{2} + (d-\ell)^2 \tan\theta \qquad \ldots\ldots\ldots\ldots\ldots (16)$$

Since $\ell = \frac{w}{2 \tan \lambda/2}$ where w = shank width = 20mm

equation (16) reduces to

$$\text{Area} = 20\left[d - \frac{5}{\tan \lambda/2}\right] + \left[d - \frac{10}{\tan \lambda/2}\right]^2 \tan\theta \text{ mm}^2 \ldots\ldots\ldots (17)$$

Theoretical yields, calculated using equations (15) and (17) as appropriate and assuming $\theta = 70^\circ$, provide the relationships shown in Figure 44.

Contrasting these theoretical yields with the measured values taken from Figures 41 and 42, it is found that the shape of curves is the same. At shallow depths the predicted and measured results are identical. At the largest depths of cut, however, the actual yields obtained are significantly higher than those anticipated. The reason for this difference lies in the fact that small variations in breakout angle θ when in the region of 70°, have a large effect on solutions to equations (15) and (17).

The specific energy and normal force relationships with vee-bottom angle are also shown in Figures 41 and 42. Normal force increases with vee-angle in similar fashion to the cutting force. Specific energy is found to increase with vee-angle acuteness. This is most pronounced at shallow depths of cut. For a 3mm deep cut in Bunter the specific energy at vee-angle 180° is 10.6 MJ/m^3 which increases to 15.8 MN/m^3 at 60°. This corresponds to an increase of almost 50%. The proportionate increase at 15mm depth is, nevertheless, a significant 36%. Corresponding savings in mean cutting force, as a consequence of providing a vee angle, are 76% at 3mm depth of cut and 64% at 15mm.

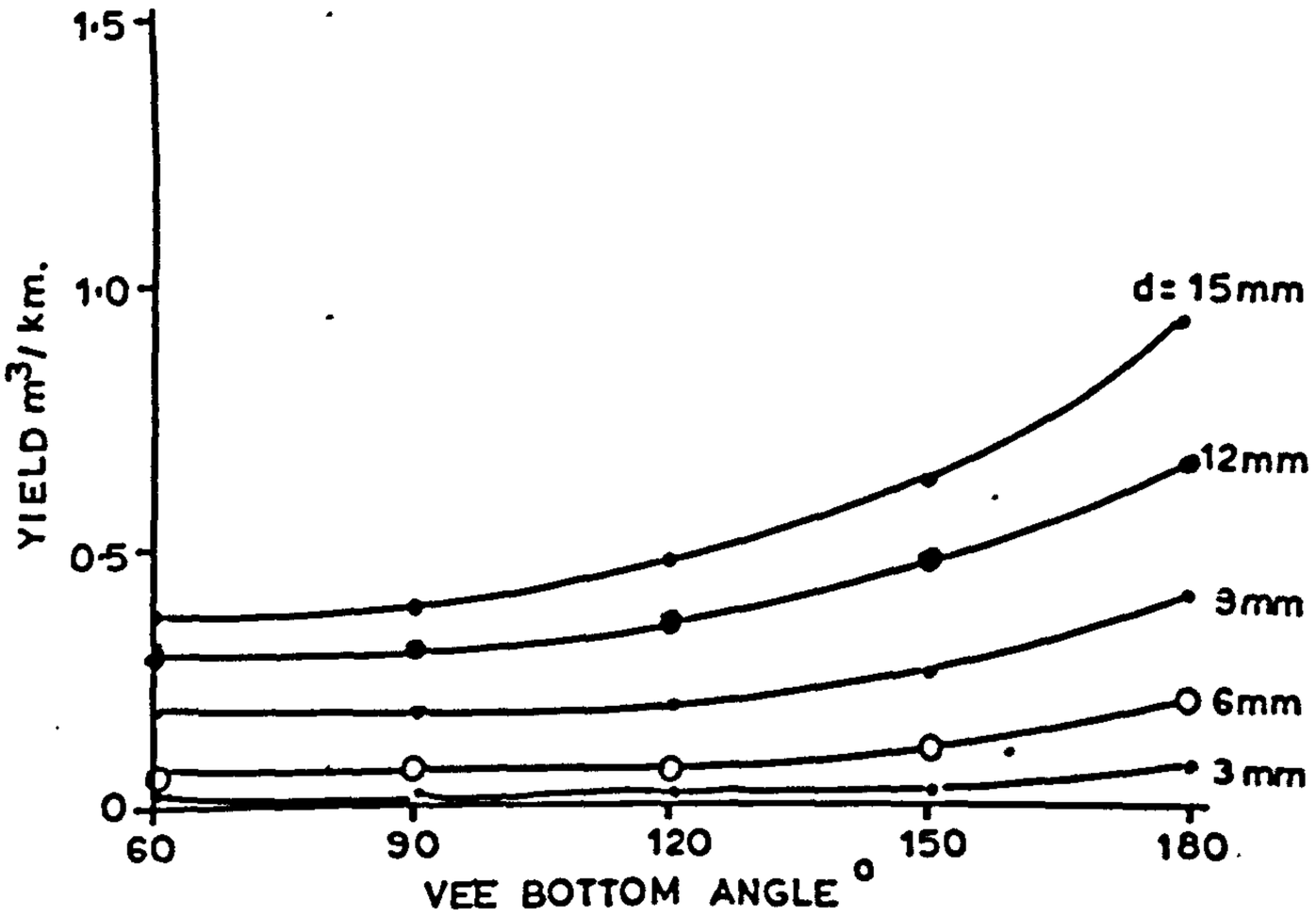

FIGURE 44- THEORETICAL YIELD - VEE BOTTOM PICKS

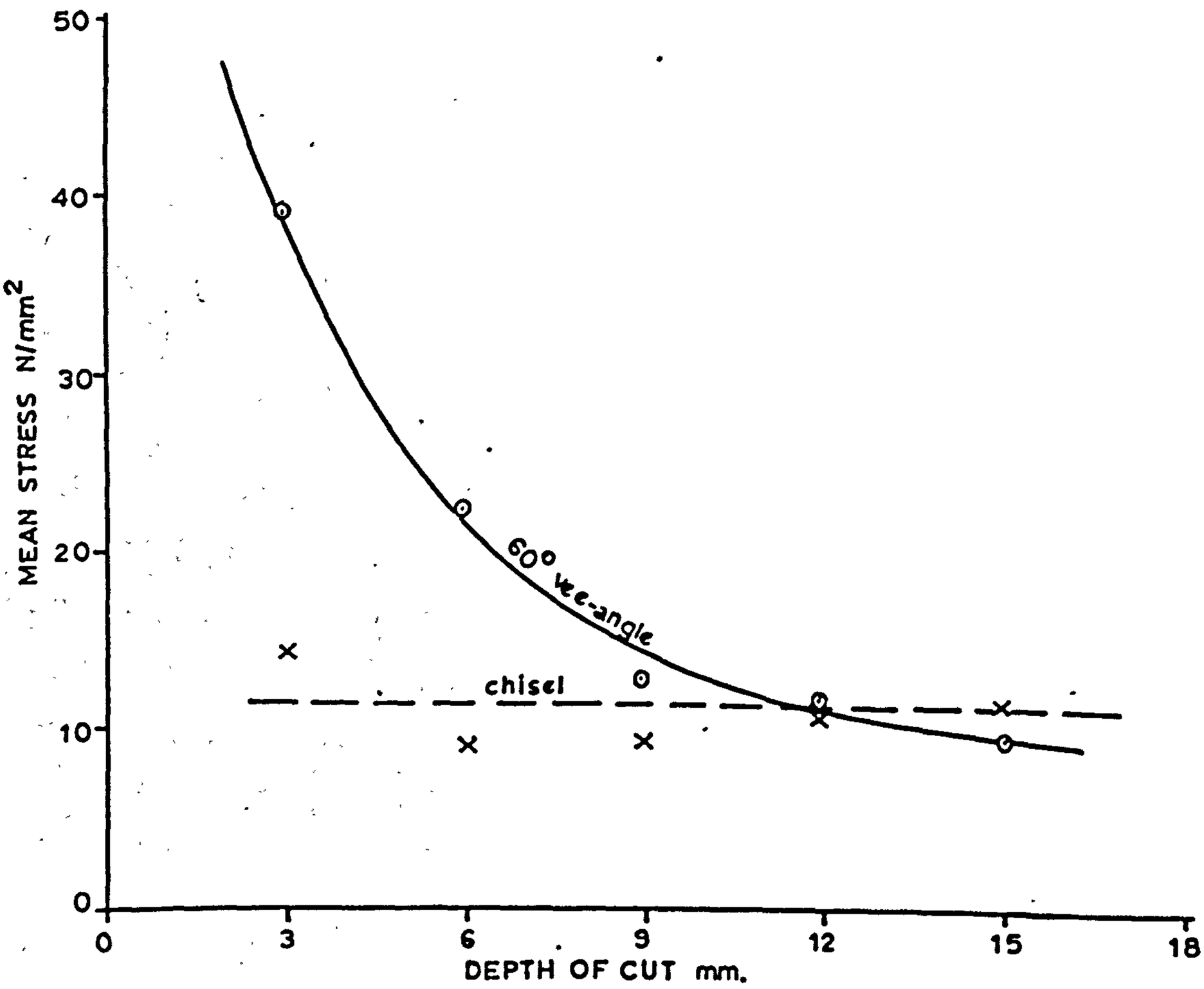

FIGURE 45 AVERAGE STRESS ON TOOL CUTTING FACE - BUNTER SANDSTONE

Like the ridged front angle, such large savings in force even at the expense of a significant loss of cutting efficiency, may appear attractive. It must, however, be borne in mind that the yield characteristics of vee bottom picks are even worse than those for the front ridged pick. Conclusions on the value of a vee bottom angle must therefore be similar to those reached in the case of front ridged picks.

A further important consideration affecting the issue of complex tool shape, is that the introduction of a front ridge angle alone is unlikely to have much significant effect on the mechanical strength of the tool nor to the degree of protection that can be offered to a tungsten carbide insert. Furthermore, the ridged pick presents a longer cutting edge than the equivalent chisel and this, together with the lower in-line cutting force, means that the ridge fronted tool is stressed to a much lower level than the chisel. For a 90^{o} ridge, the cutting edge is 1.41 times that for a chisel of the same width. At a width of 20mm and depth of 15mm, this results in a cutting edge loading of 92 N/mm for the ridged pick and 187 N/mm for the chisel.

On the other hand, the vee bottom pick must be much more susceptible to damage than either the ridged or chisel pick.

The frontal area of the tool, being triangular, must be appreciably less than the other tool types at the same depth of cut. The situation is most aggravated at the highest vee angle. At 60^{o}, for example, and at a depth of 15mm, the area of tool over which the cutting force is distributed will be 130 mm^2 in contrast to the chisel's 300 mm^2. Using the cutting forces in Bunter Sandstone the corresponding stress levels for each tool are in fact found to be 9.25 N/mm^2 and 11.2 N/mm^2. At shallower depths, however, this is not the case and the vee point becomes stressed to a much higher value. Mean stress levels assumed to be evenly distributed over the buried frontal area of the vee bottom and chisel picks are shown in Figure 45. The mean stress level for a chisel pick should be independent of depth since both mean cutting force and buried frontal area

of the tool are directly proportional to depth. This is found to be the case. On the other hand there is an exponential growth in mean stress level for the vee bottom pick as cutting depth decreases. This implies a high level of stress near the point at all cutting depths.

The mechanics of penetration with a vee bottom tool of positive rake, involves an initial entry of the point into the rock surface, which at any depth of cut will lead to very high stresses. A tungsten carbide insert, or for that matter any tool material, is at its most vulnerable near the point where the stress is highest and the transverse rupture strength of the carbide is at a minimum. Mechanical failure at the point of an acute angled tool is therefore inevitable in rocks of any appreciable strength. Whereas all pick points survived experimental work in the Bunter Sandstone, which is a relatively low strength rock, damage to the vee bottom picks confined the tests in Magnesian Limestone to the three shallowest levels of depth. Similar tests in a Carboniferous Limestone of uniaxial compressive strength 150 MN/m^2 (22,000 p.s.i.) caused all pointed tools to shatter.

8.3 Effect of Side Rake Angle (ν)

Although the benefits of introducing side rake to a chisel tool are believed to be restricted to relieved cutting, experiments have been undertaken for both unrelieved and relieved conditions.

In relieved cutting, the lateral component of force caused by asymmetry, if directed towards an adjacent groove, might improve breakthrough of rock between the grooves and thereby permit wider tool spacings. A lateral force will, however, be similarly generated in the unrelieved situation, which could be detrimental to control of the cutting path of the tool.

a) Unrelieved Cutting

The results of these tests are given in Appendix VI (E and F). Figures 46 and 47 show the effect of side rake angle on the principal cutting forces. Mean cutting and normal forces show no significant change with increasing side rake. This behaviour is consistent with

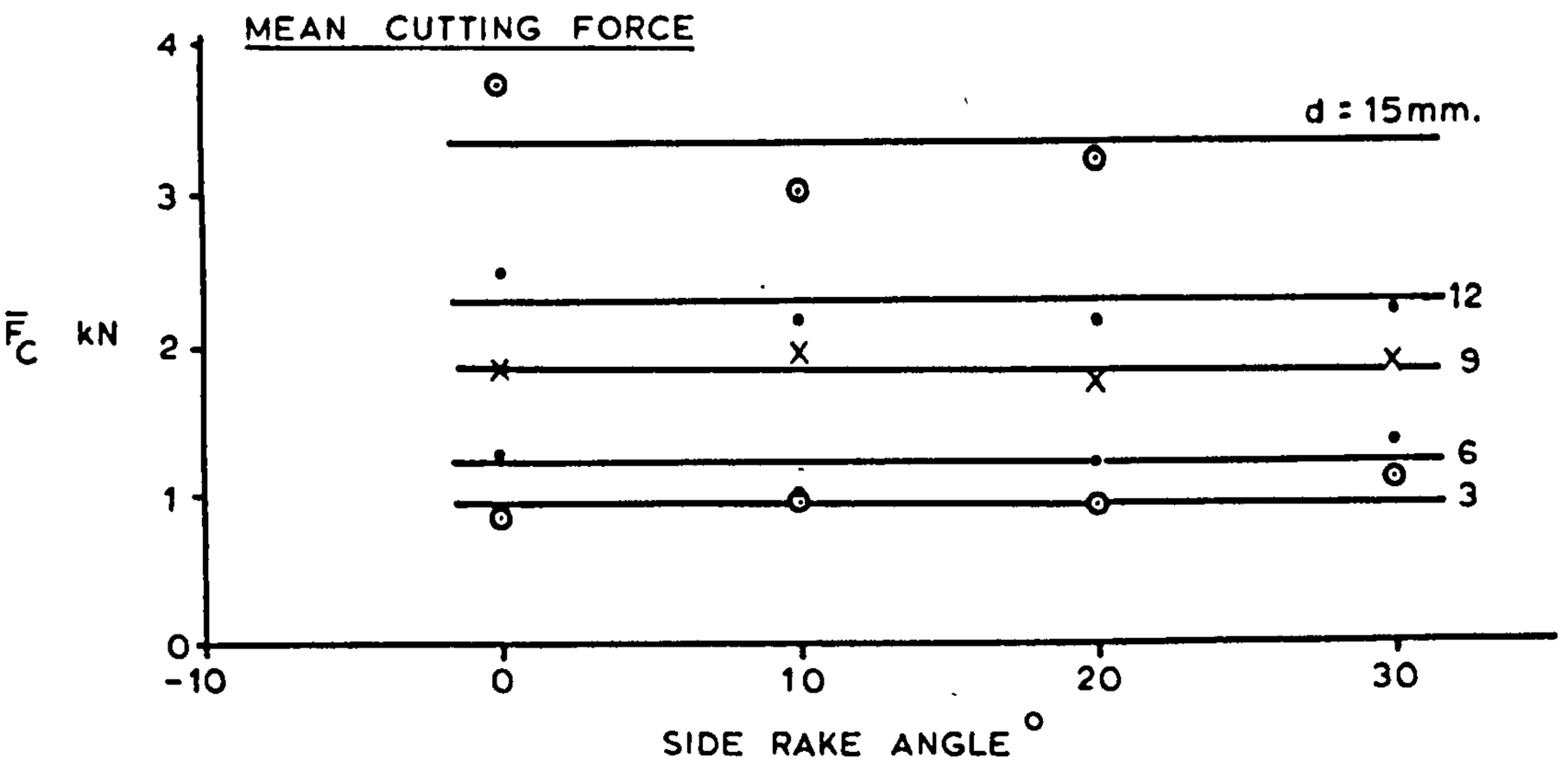

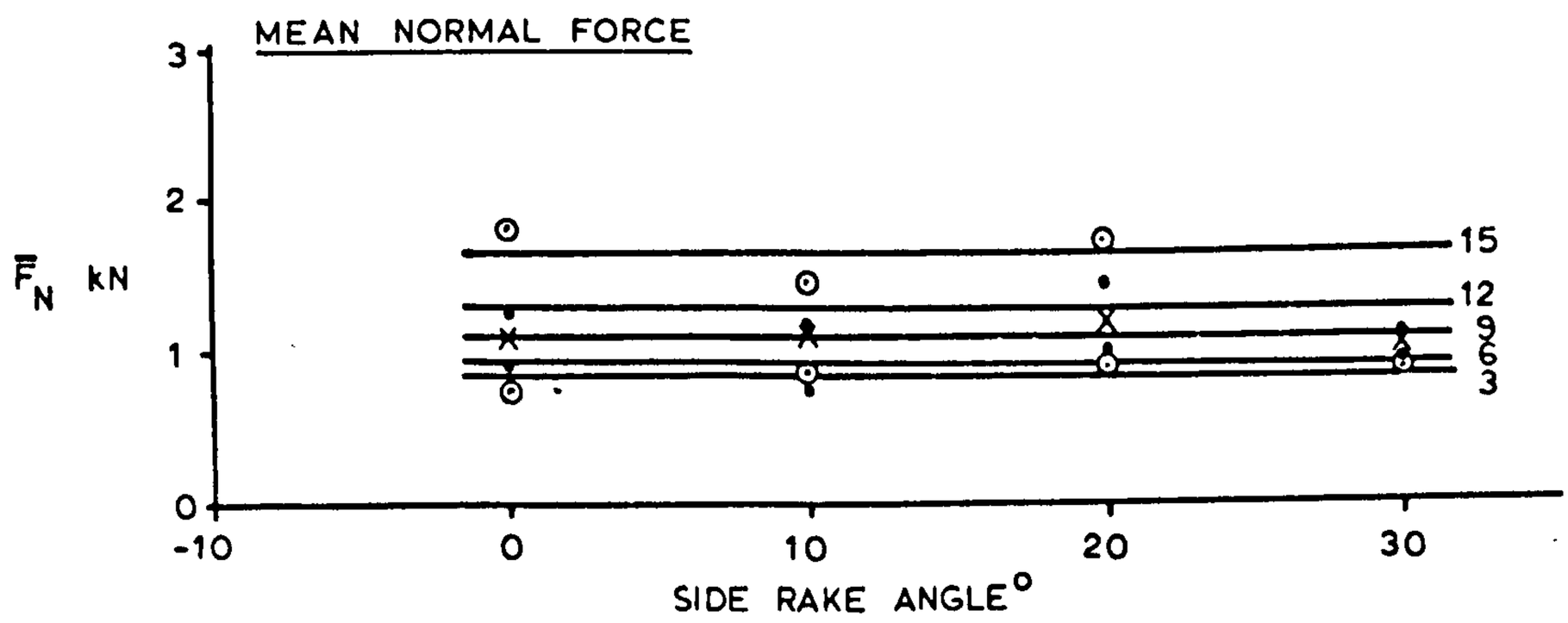

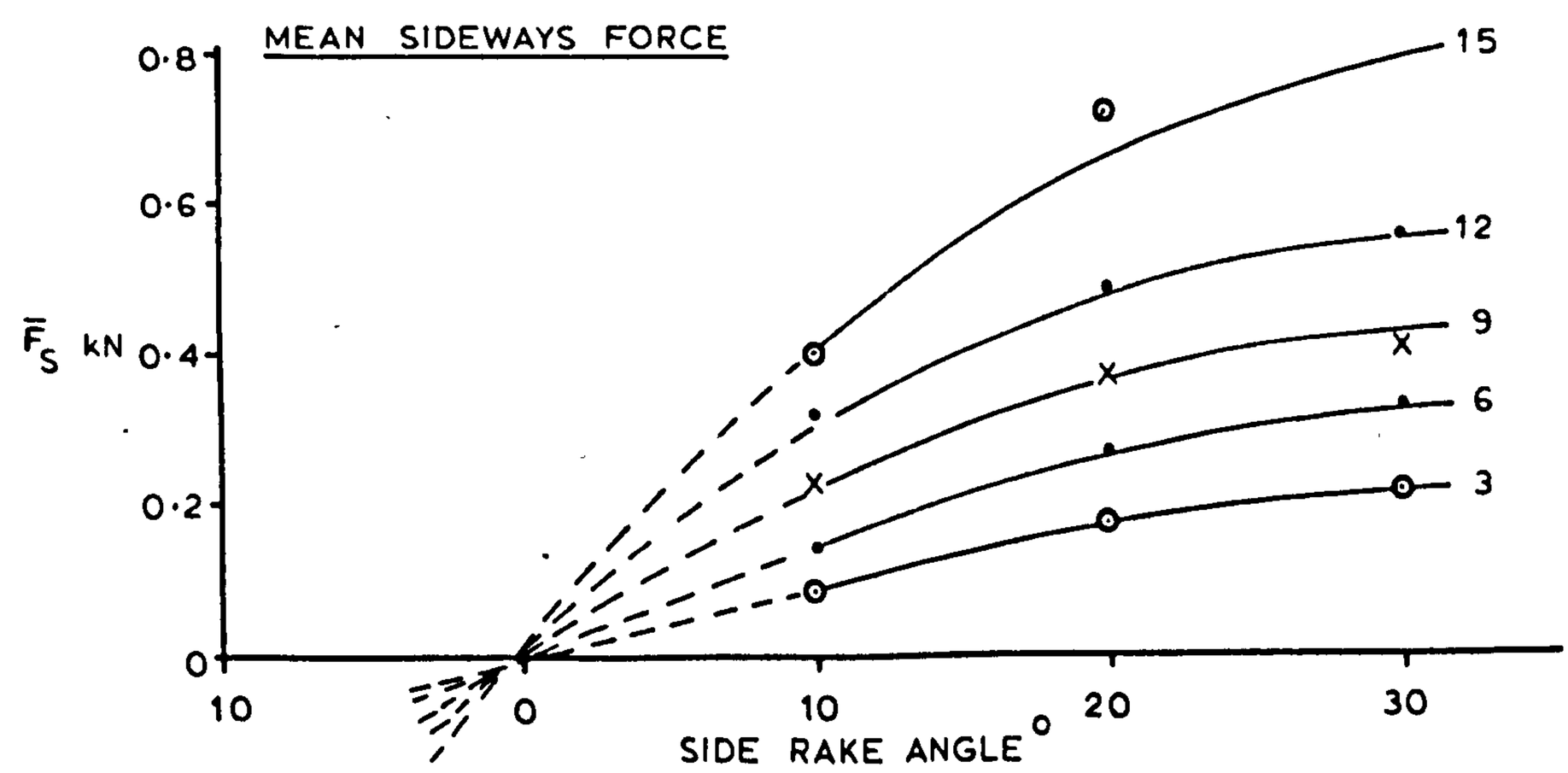

FIGURE 46 - EFFECT OF SIDE RAKE ANGLE ON FORCES (UNRELIEVED)

- BUNTER SANDSTONE

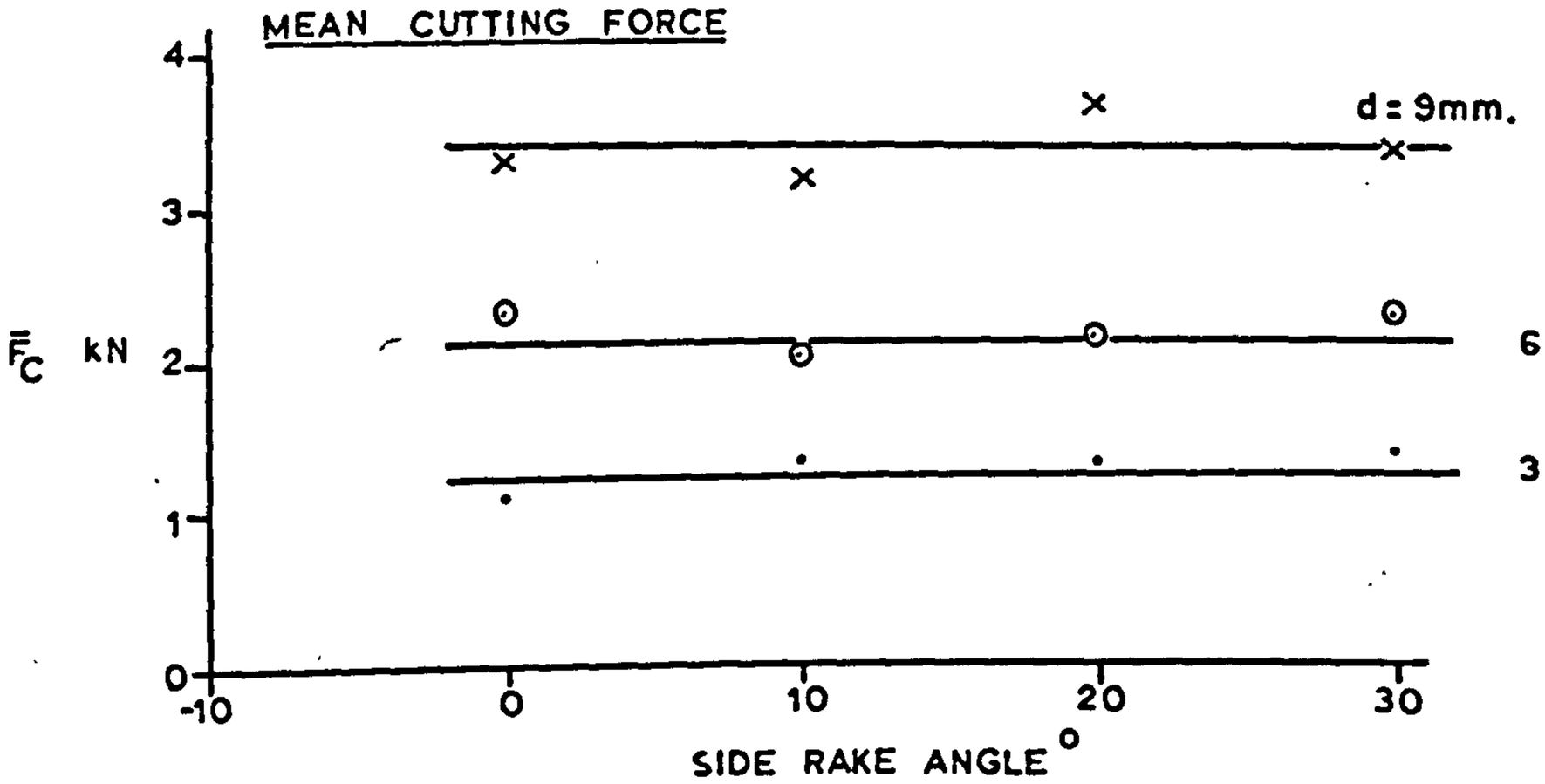

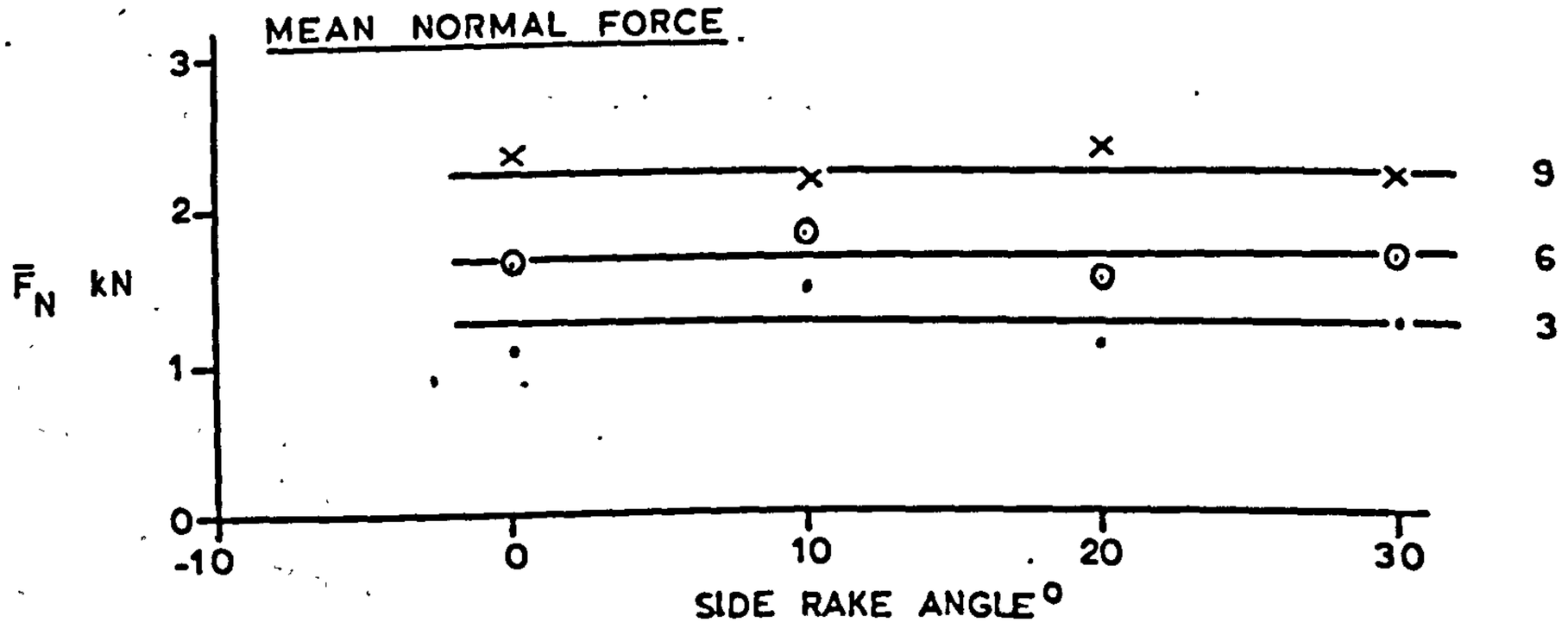

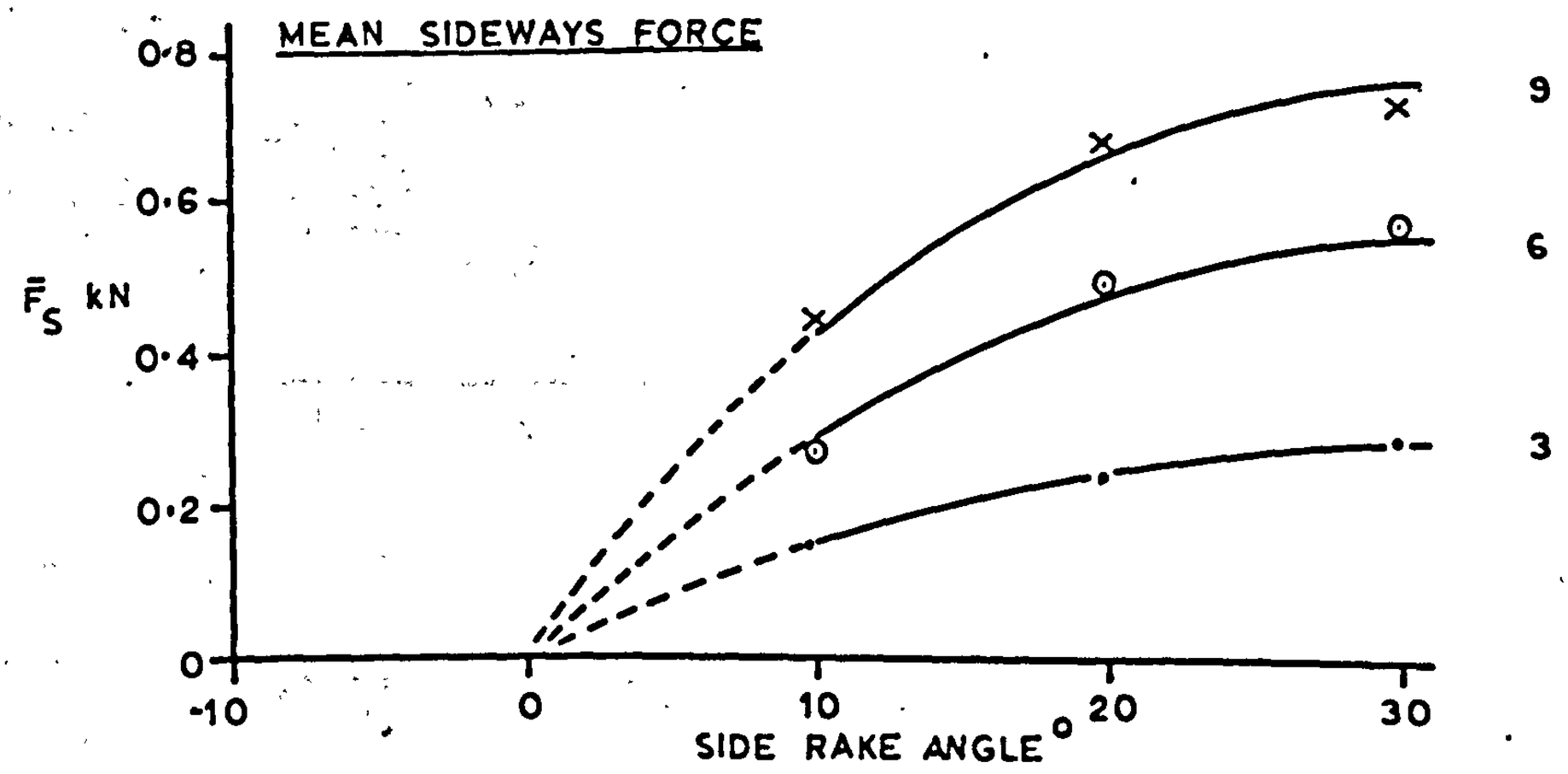

FIGURE 47 — EFFECT OF SIDE RAKE ANGLE ON FORCES (UNRELIEVED)
— MAGNESIAN LIMESTONE

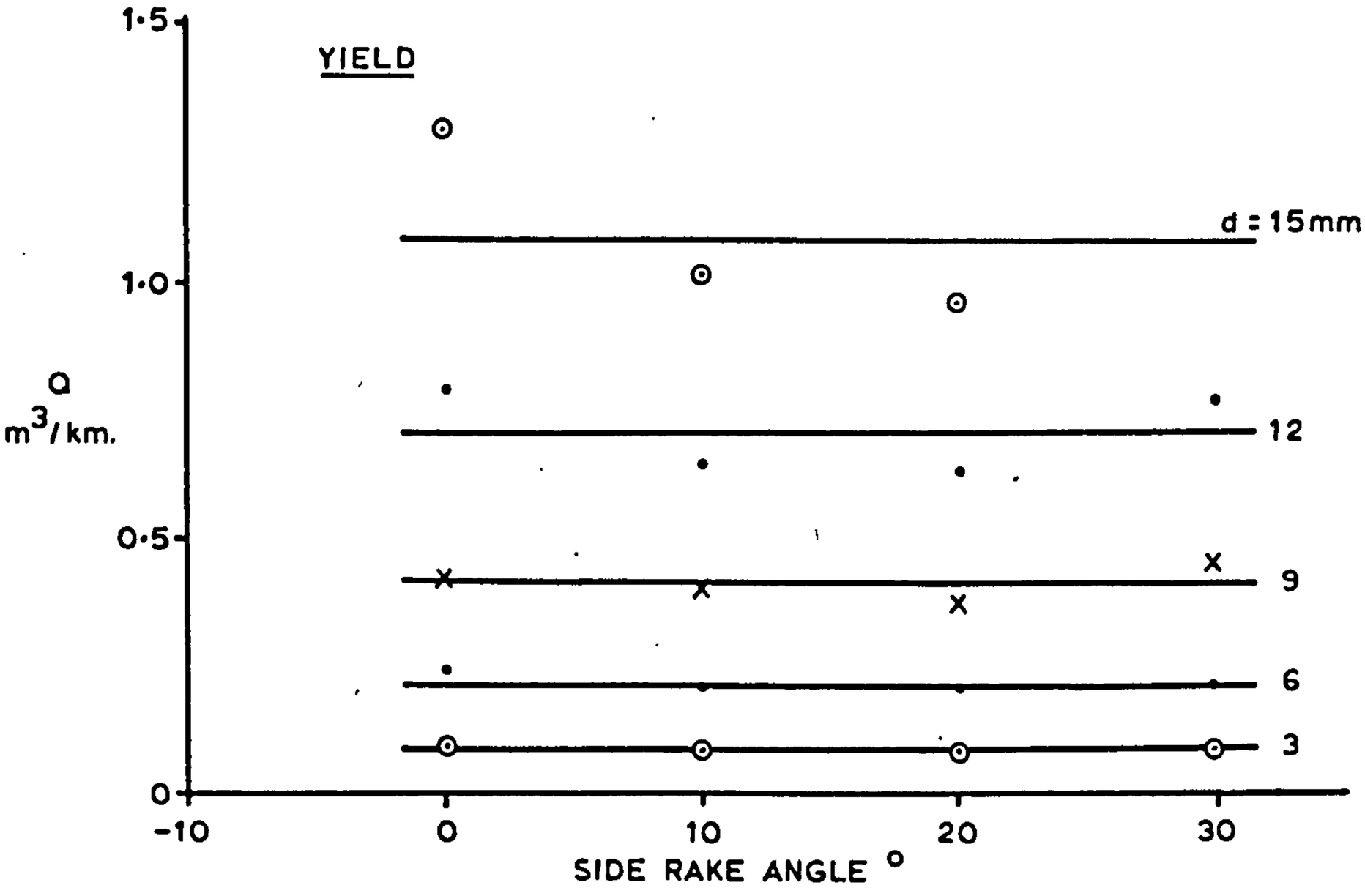

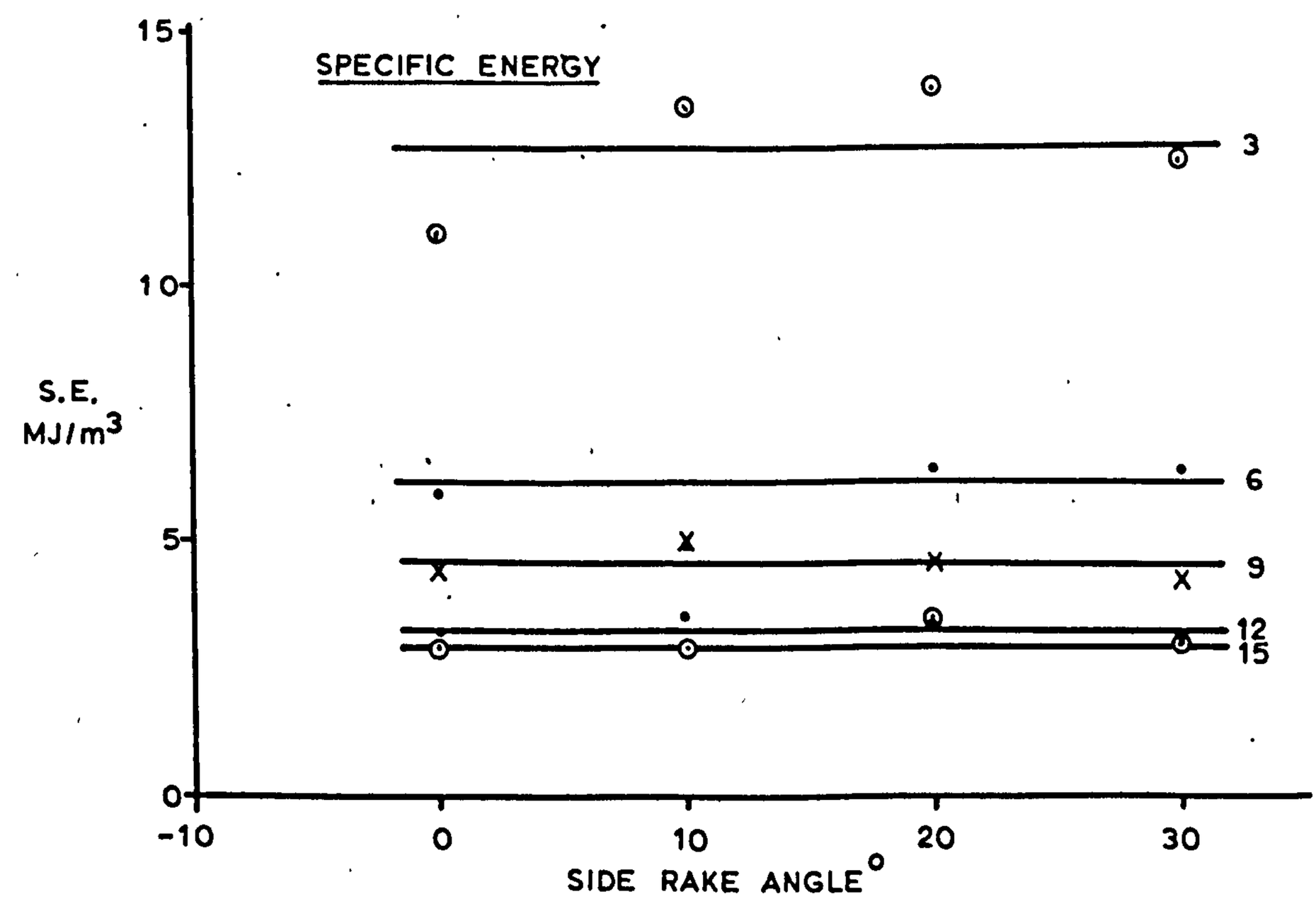

FIGURE 48 - EFFECT OF SIDE RAKE ANGLE ON YIELD & ENERGY (UNRELIEVED)
- BUNTER SANDSTONE

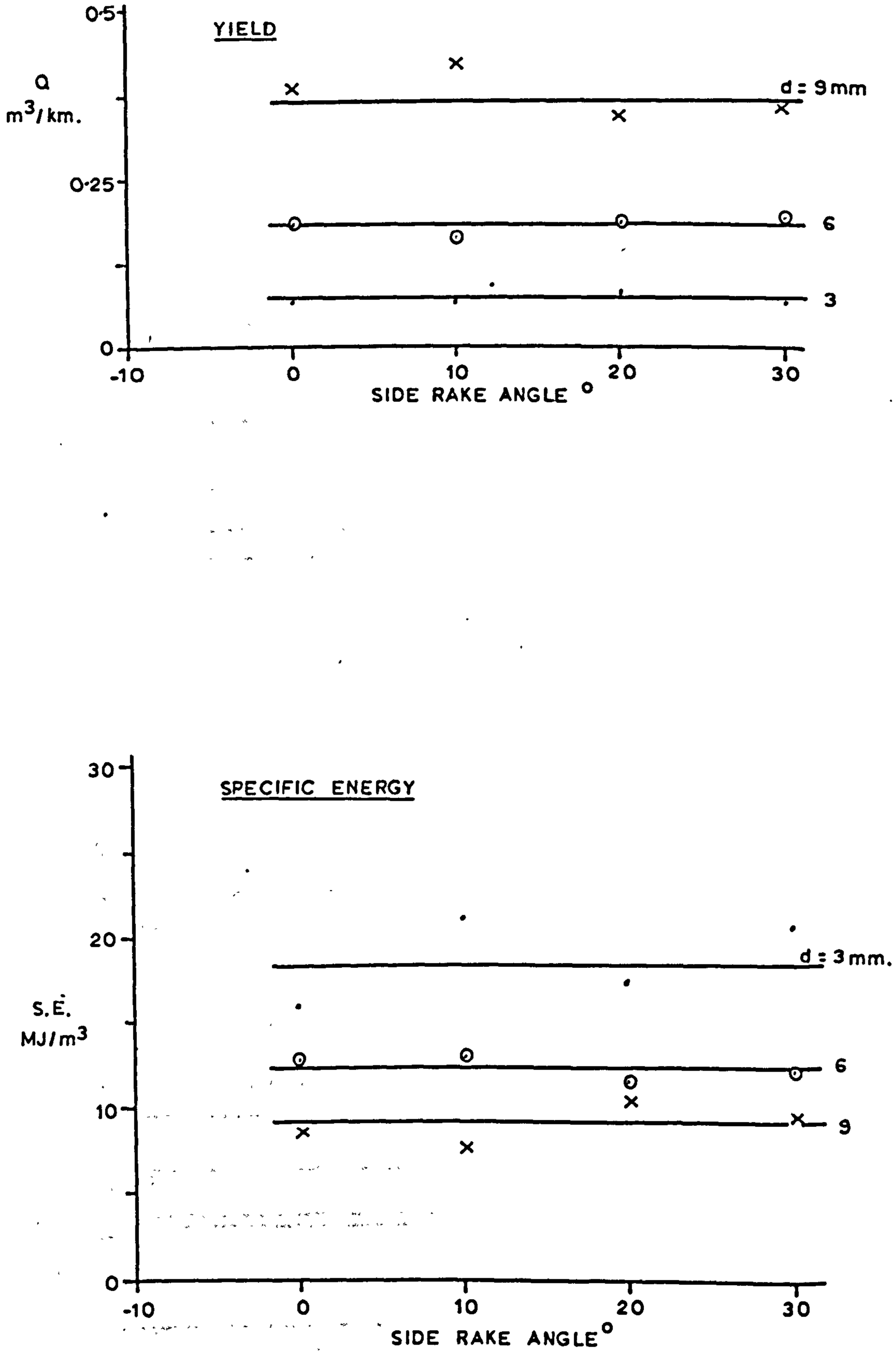

FIGURE 49 — EFFECT OF SIDE RAKE ANGLE ON YIELD & ENERGY (UNRELIEVED) — MAGNESIAN LIMESTONE

Evans' comparative analysis of forces acting on complex and equivalent wedge shaped tools (19). Although this analysis related to symmetrical pointed tools, the conclusion that penetrating force in the cutting direction is independent of side rake is equally valid. Bearing in mind that no change in front rake angle was permitted as a consequence of introducing a side rake, then the force in the direction of cutting should be the same for the side rake tool as it is for a wedge of the same front rake angle.

Unlike the simple chisel a measurable lateral force component is generated by a side rake angle. In comparison to the cutting force it is of low order being between 20 and 25% at the highest side rake value. Lateral force should be a function of the sine of the side rake angle.

The curves appear to follow a sine law for the measured values and furthermore must, as indicated, go through the origin and appear in the third quadrant. Adopting the convention that these measured forces and side rakes are both positive, then the mirror image situation will give negative rake angles and forces of the same value.

Rock yield is found, in Figures 48 and 49 to be unaffected by side rake and since cutting force is similarly unaffected, specific energy is found to be independent of side rake.

b) Relieved Cutting

The results of the spacing tests, which were all undertaken in dry Bunter are tabulated in Appendix VI G.

In the case of relieved cutting it was possible to generate 7 levels of side rake with the 4 tools, but only 6 of these were investigated. The additional 2 levels were arranged by undertaking tests with the side rake presented to the relieving cut as shown in Figure 50. The sign convention used is indicated by the diagram.

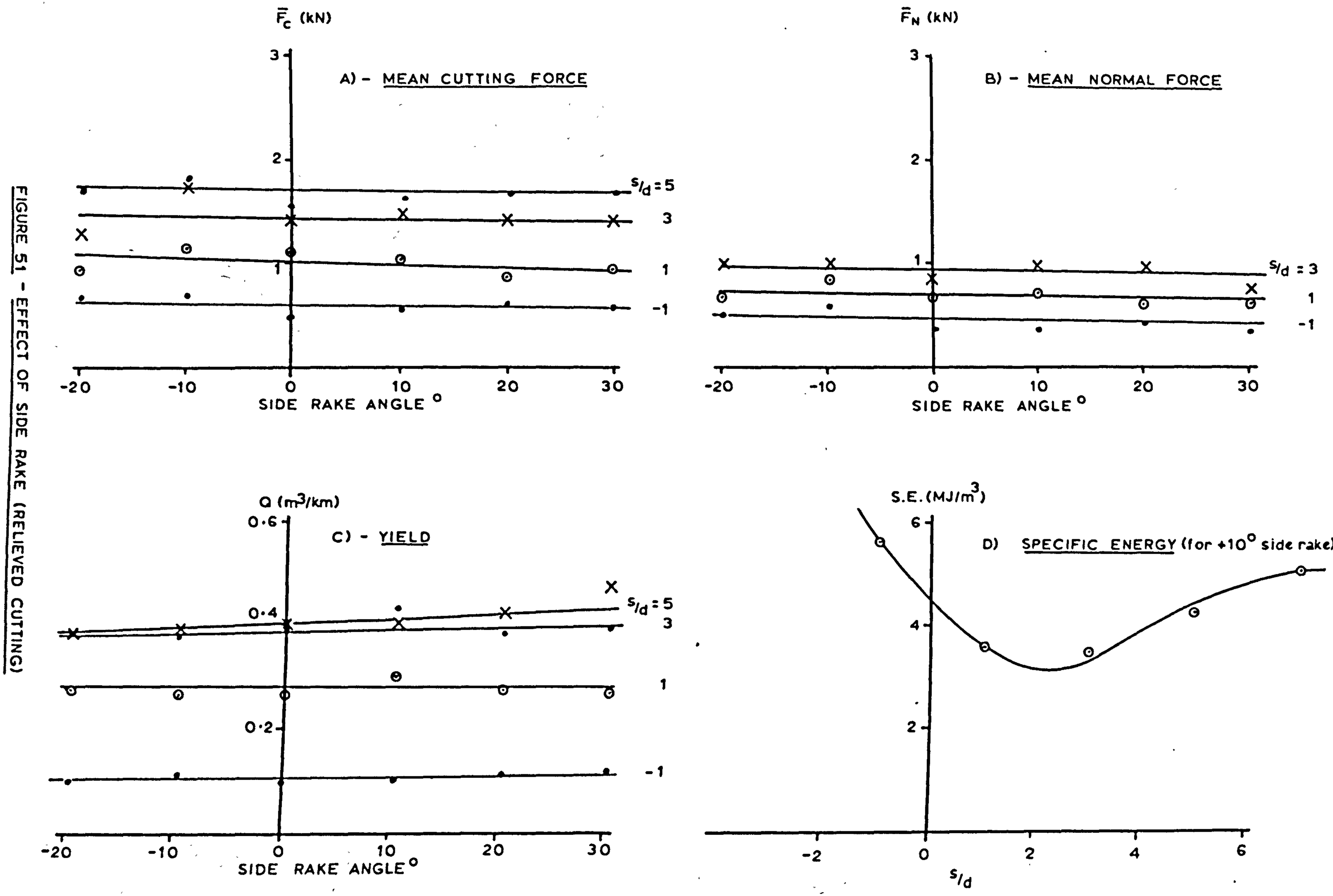

FIGURE 51 - EFFECT OF SIDE RAKE (RELIEVED CUTTING)

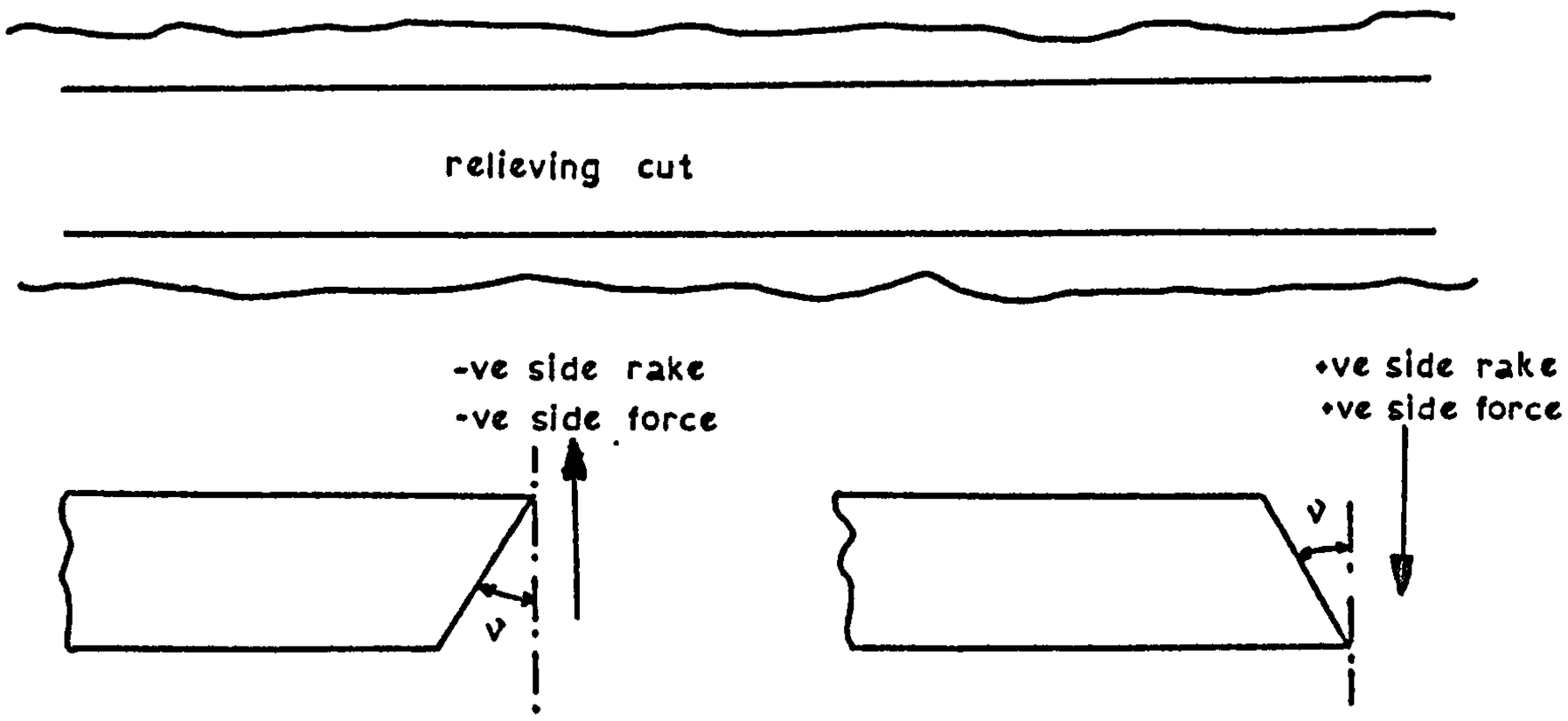

FIGURE 50. ANGULAR DISPOSITION OF SIDE RAKE.

Figure 51 shows the effect of side rake on cutting and normal forces, and rock yield. The specific energy-spacing relationship, which is also included, is for one value of side rake only. The influence of side rake on specific energy in the relieved situation requires separate and special attention as does sideways force.

The provision of a side rake on a chisel pick is found to have no appreciable effect on the in-line cutting force, normal force nor the amount of rock produced. At the lowest values of spacing theremight be a slight reduction in cutting force with increasing positive side rake and possibly sufficient of an increase in rock yield for both parameters to reflect a detectable change in specific energy.

Figure 52 shows specific energy plotted against side rake angle for the 6 values of spacing. In this case this is a more revealing method of presentation than the usual type of energy - spacing graph, an example of which was given in Figure 51. At the narrowest spacing, there is found to be a significant improvement in specific energy with increasing positive side rake. (The section of rock actually being cut by the tool is shown as the shaded area in the small illustration accompanying each graph). As spacing increases, the improvement in specific energy with side rake becomes progressively less, until there is found to be no change when s/d is 9 and above. This behaviour is readily understood by considering the cross sectional area of rock being cut at each of the

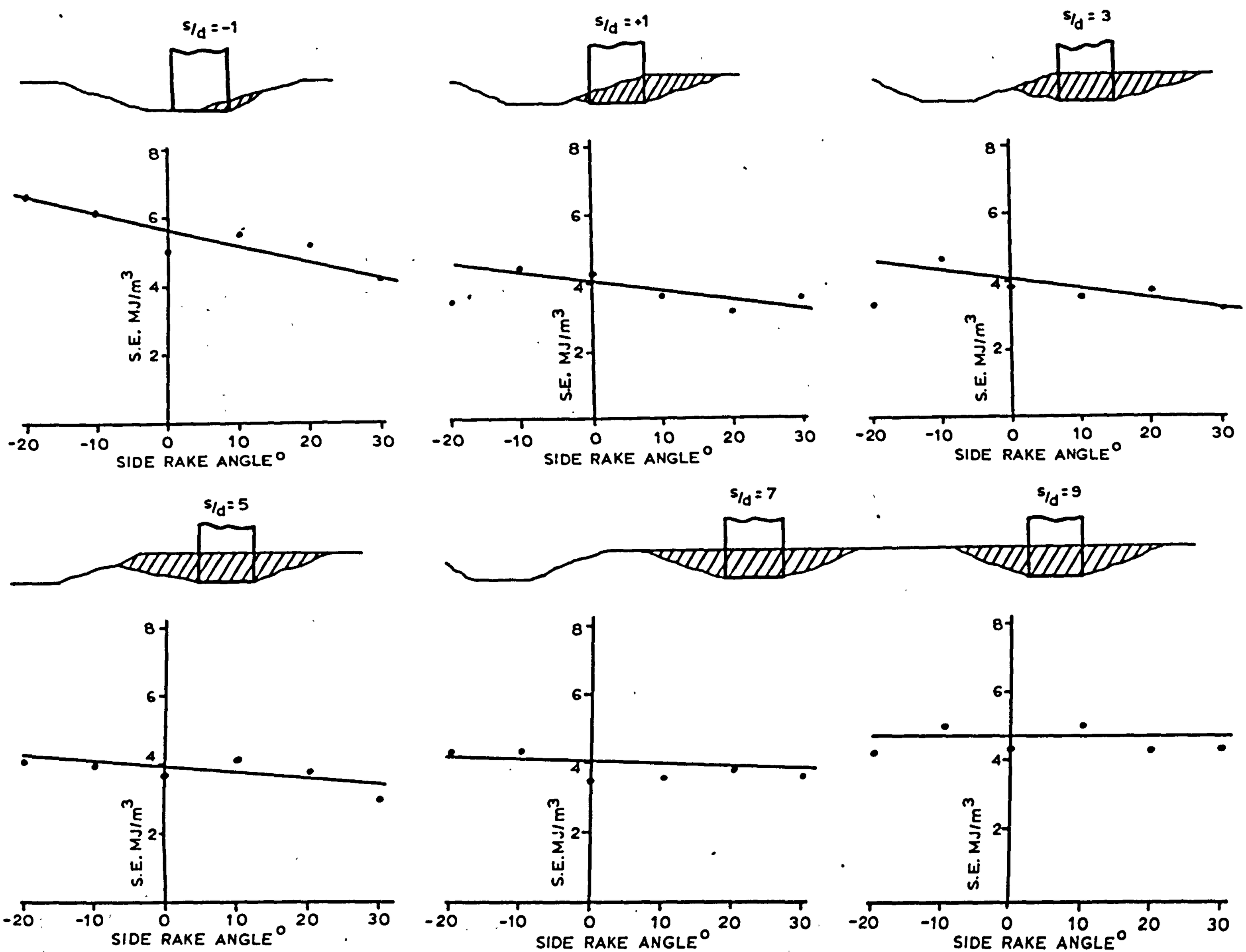

FIGURE 52 – SIDE RAKE / SPACING EFFECTS ON ENERGY

spacings. At s/d = -1, the tool is required to do no more than scour a small triangular section at one side. It is reasonable to expect, in this situation, that the point provided by the highest side rake will produce the most effective means of prising out this corner of rock. Conversely, the negative side rake tool is cutting this rock only at its trailing edge with the main body of the tool inhibiting lateral breakage. Similar lines of reasoning apply to the other spacing levels until a situation equivalent to unrelieved cutting is reached, beyond which specific energy is unaffected by side rake. It is important to note that the levels of specific energy are still greatest at the closest spacings and achieve a minimum at s/d between 1 and 3. The benefit of a $+30^{o}$ side rake in contrast to a simple chisel is approximately a 20% saving in specific energy at optimum spacing. It would be wrong at this stage to conclude that side rake tools are preferable to chisels even in an optimised array. This undeniably higher efficiency is at the cost of introducing a significant lateral force, which in some cutting systems could be difficult to control.

The sideways forces generated by a side rake tool operating in the relieved situation are presented graphically in Figure 53. At optimum spacing, represented by the s/d = 3 curve, the lateral force increases markedly with the first increment of positive and negative side rake. Thereafter further increases in side rake angle show the force to rise less dramatically and in fact to stabilise at values above 30^{o} or thereabouts. The same general shape of curve is evident at all levels of spacing, with the closest producing the lowest order of force.

It is interesting to note that the chisel pick, represented by 0^{o} side rake, has in fact a lateral force component in relieved cutting. This force, as shown in Figure 53 is always negative, which is appropriate to the tool being naturally forced towards the adjacent groove. Referring back to the small descriptive tool/groove sketches given in Figure 52, the origins of lateral force on a relieved chisel pick are evident. Some indication in the expected change in magnitude of this sideways force at

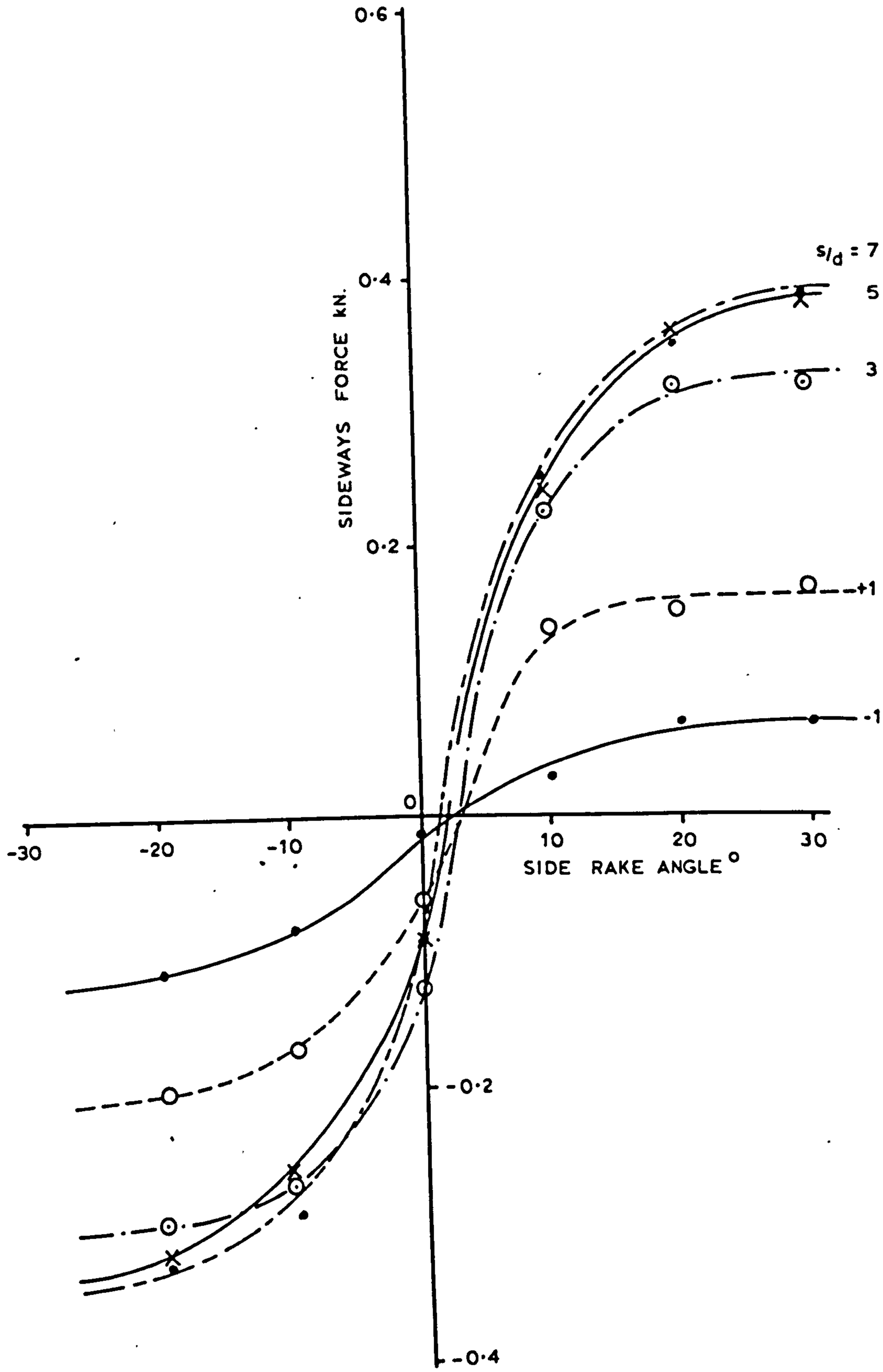

FIGURE 53 - LATERAL FORCE DUE TO SIDE RAKE

different spacings can be derived from these same sketches. As spacing increases from the lowest level, lateral force will increase to a maximum and then reduce gradually to zero as the spacing achieves a level equivalent to unrelieved cutting. The force intercepts on the 0^{o} side rake ordinate are found to follow such a sequence.

In circumstances where the generation of a lateral force could lead to instability (not uncommon with machines using cutting chains), balance may be achieved by introducing a positive side rake angle of $2\text{-}3^{o}$.

9.. CUTTING WITH DISC AND ROLLER CUTTERS

This chapter deals with tools which, during the excavation process, rotate passively about their axes. The performance of discs, in both the relieved and unrelieved cutting situations, is investigated in six partial factorial experiments. As any disc malfunction causing a loss of free rotation is likely to introduce fundamental changes in disc behaviour, a supplementary experiment using a stalled disc was undertaken. This test, which was in dry Bunter only, used a 200mm diameter tool having a 60° peripheral edge angle.

A limited programme of experiments with a single roller cutter was conducted in dry Bunter and Magnesian Limestone. The tool tested was 110mm in diameter and 25.4mm wide, having 12 teeth, each with a 60° tip angle and a root angle of 90°. The only variables available, penetration and spacing, were each studied at five levels.

9.1 Design of the Disc Cutting Experiments

The planning techniques used for the six partial factorial experiments were discussed in Chapter 5. The unrelieved cutting experiments in Bunter also included a study of the effects of cutting speed and so the appropriate plan was that shown in Figure 11. This was for a 4 variable, 5 level experiment. To avoid having the worst combination of edge angle, diameter and penetration the order of appearance of penetration level has been reversed. The experimental programme, including the appropriate levels of the variables, appears in Appendix VII (A-D).

Analysis of the results in Bunter Sandstone showed that, at the highest levels of penetration, thrust forces were approximately 80% of the design maxima of the dynamometer. Bearing in mind the reported increase in pick forces when cutting the Limestone, a 25% reduction was made in the numerical value attributed to each level of penetration, i.e. in Bunter the five levels of penetration were 2,4,6,8 and 10mm and in Magnesian Limestone the corresponding values were 1.5, 3, 4.5, 6 and 7.5mm. The plan for the unrelieved Magnesian Limestone experiment is shown in Appendix VII (E and F).

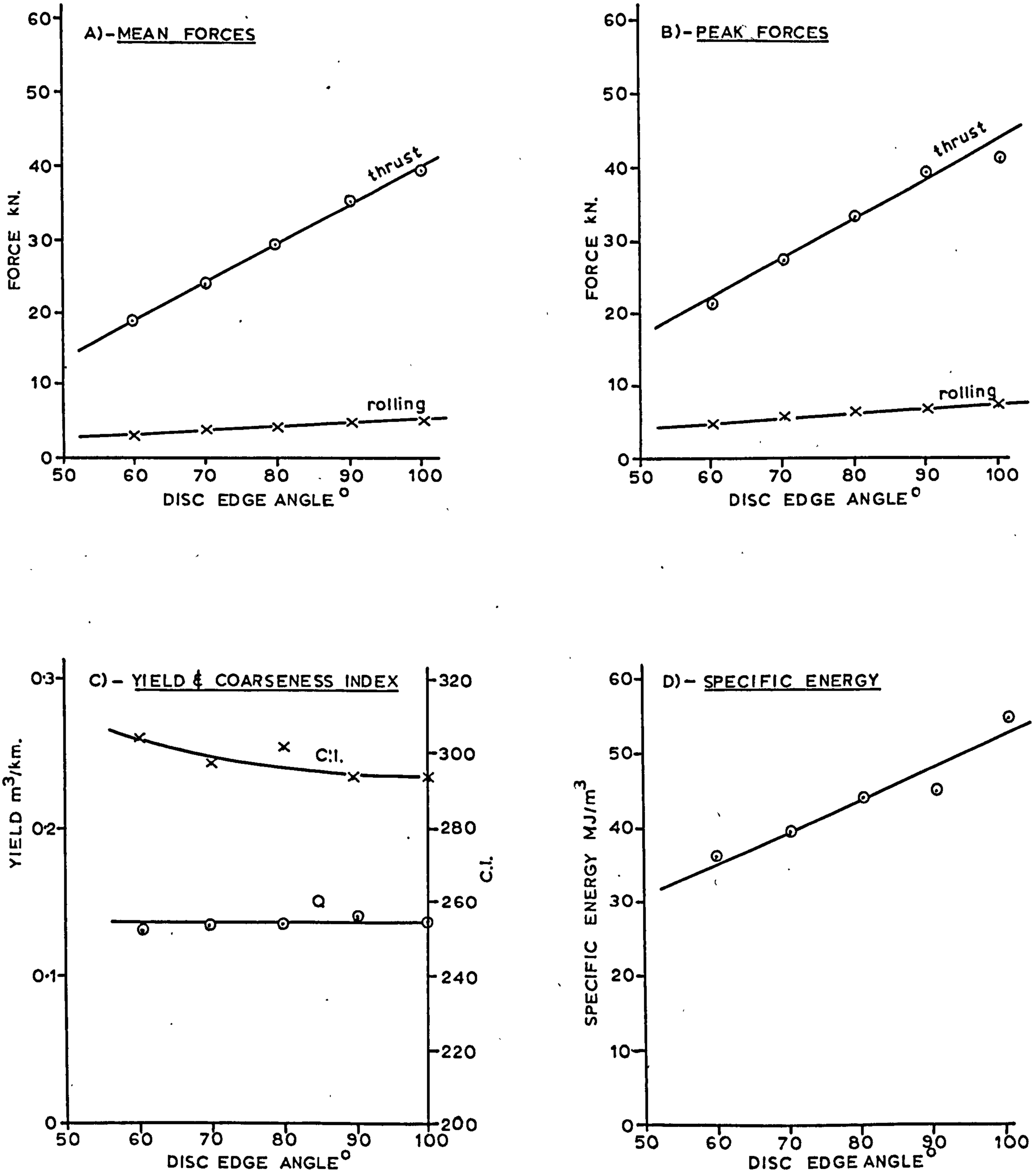

FIGURE 54 — EFFECT OF DISC ANGLE
— DRY BUNTER SANDSTONE

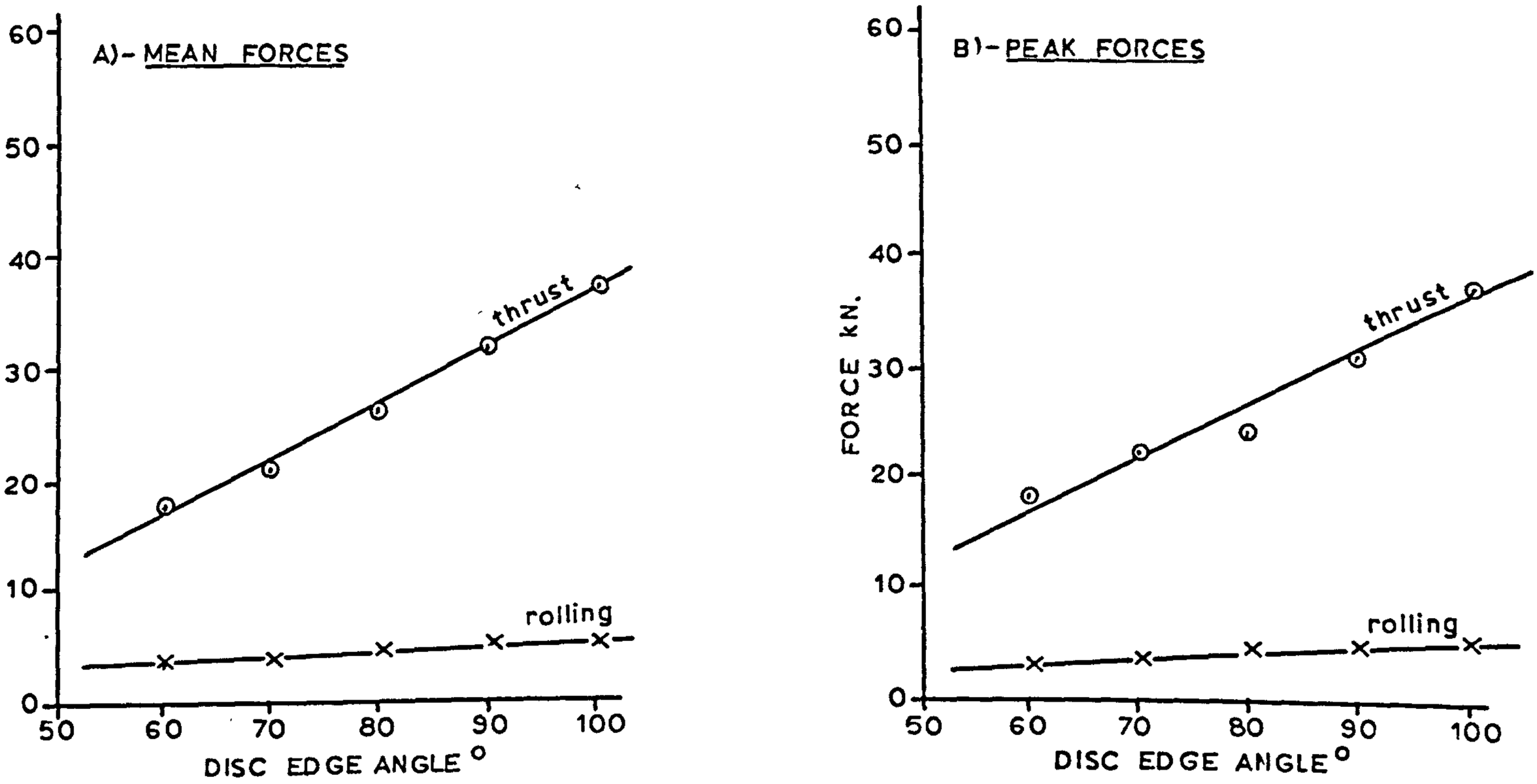

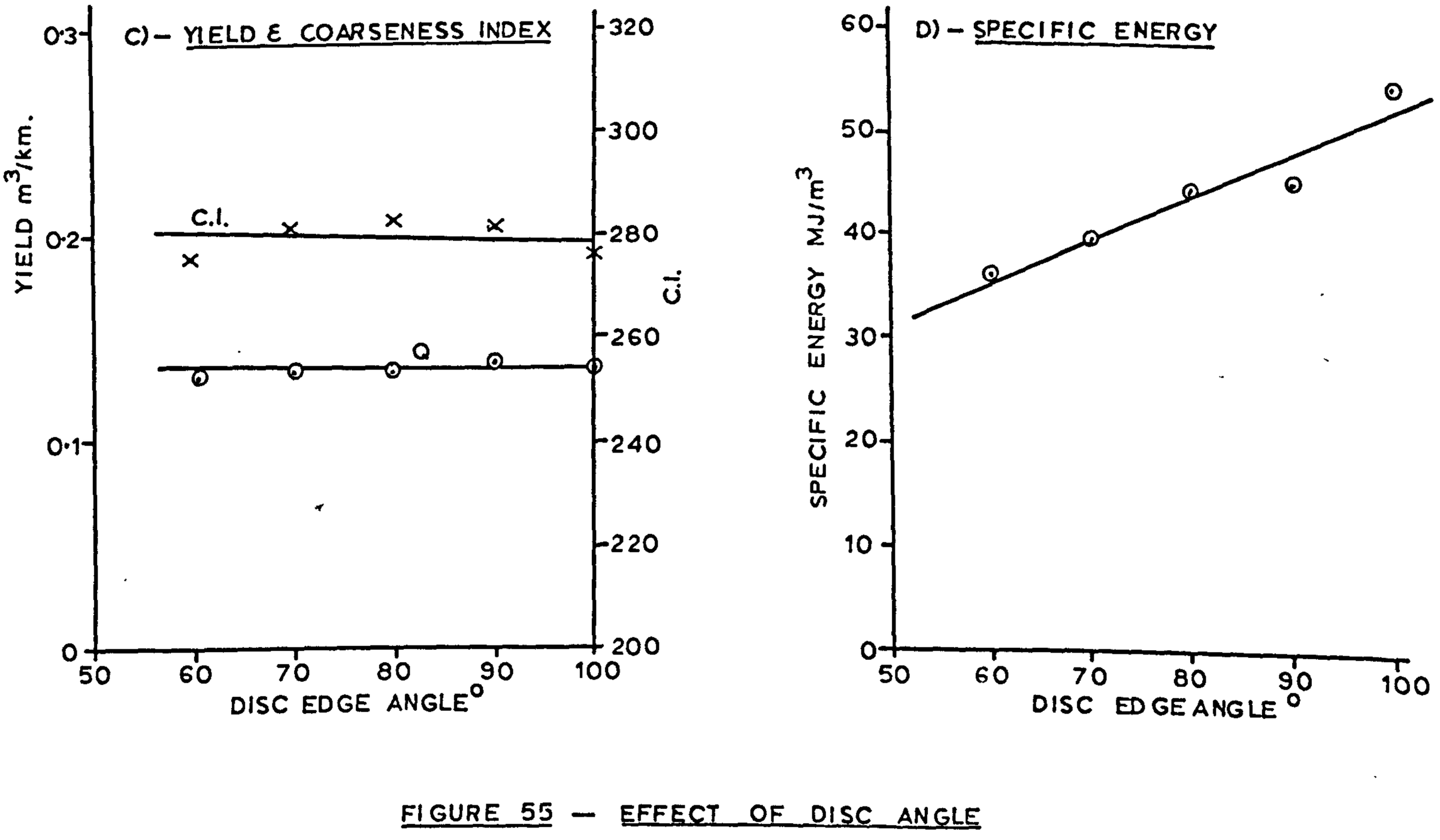

FIGURE 55 — EFFECT OF DISC ANGLE
— WET BUNTER SANDSTONE

The three spacing experiments followed the same four variable, five level plan. The precise values given to each level are shown in the tables of Appendix VIII. Although rock penetration was reduced in the Magnesian Limestone the same range of s/p ratios was maintained throughout by a reduction in the corresponding values of spacing.

9.2 Unrelieved Cutting

The effect of each variable has been presented in graphical form using data abstracted from the tabulated results which appear in Appendix VII (A-F). This same data, grouped according to variable, is given in Appendix VII (G,H and J).

From this tabulated data, it is found that peak forces are only marginally greater than the equivalent mean values. The absence of the transcient peaks, which were so evident in cutting with picks, was a consistent feature of all disc cutting work. Preliminary analysis revealed, for all variables, that the peak force curve was always close to, and followed the same trend as, the appropriate mean. While it was possible to display peak and mean pick forces on the same graph, it is advantageous to separate the peak and mean curves when representing the disc forces graphically.

1. Effect of Disc Edge Angle

All forces increase with edge angle as shown in Figures 54, 55 and 56. Over the range of angles examined the trend is effectively linear, but obviously the rate of increase must diminish as the angle increases, and force must reach a maximum at 180°. The rate of increase of both forces is very nearly constant in all three rock conditions studied, with thrust increasing more rapidly than the rolling force. At an edge angle of 100° the thrust force is, on average, 112% of the thrust at an angle of 60°, while the corresponding figure for rolling force is only 69%.

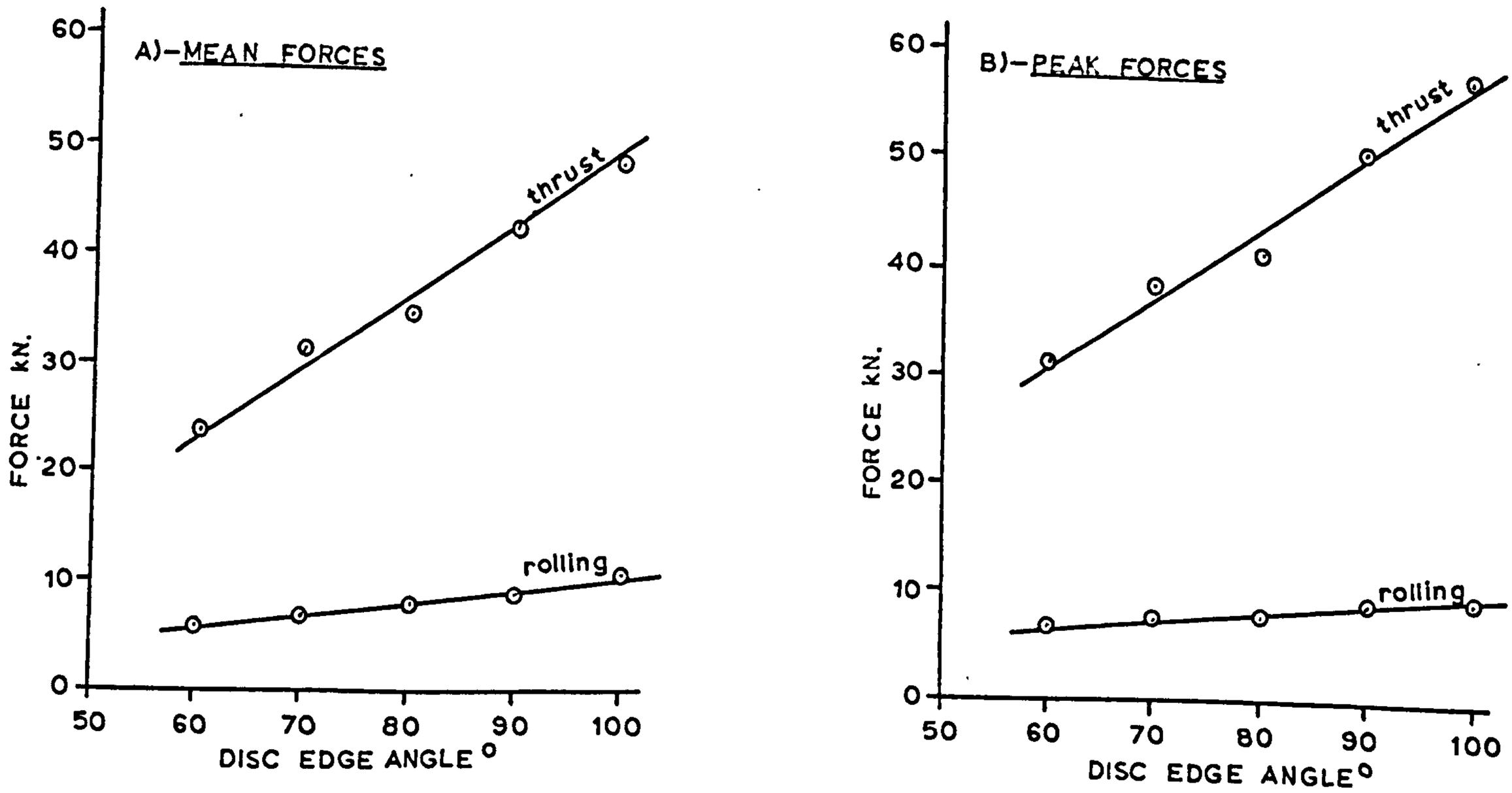

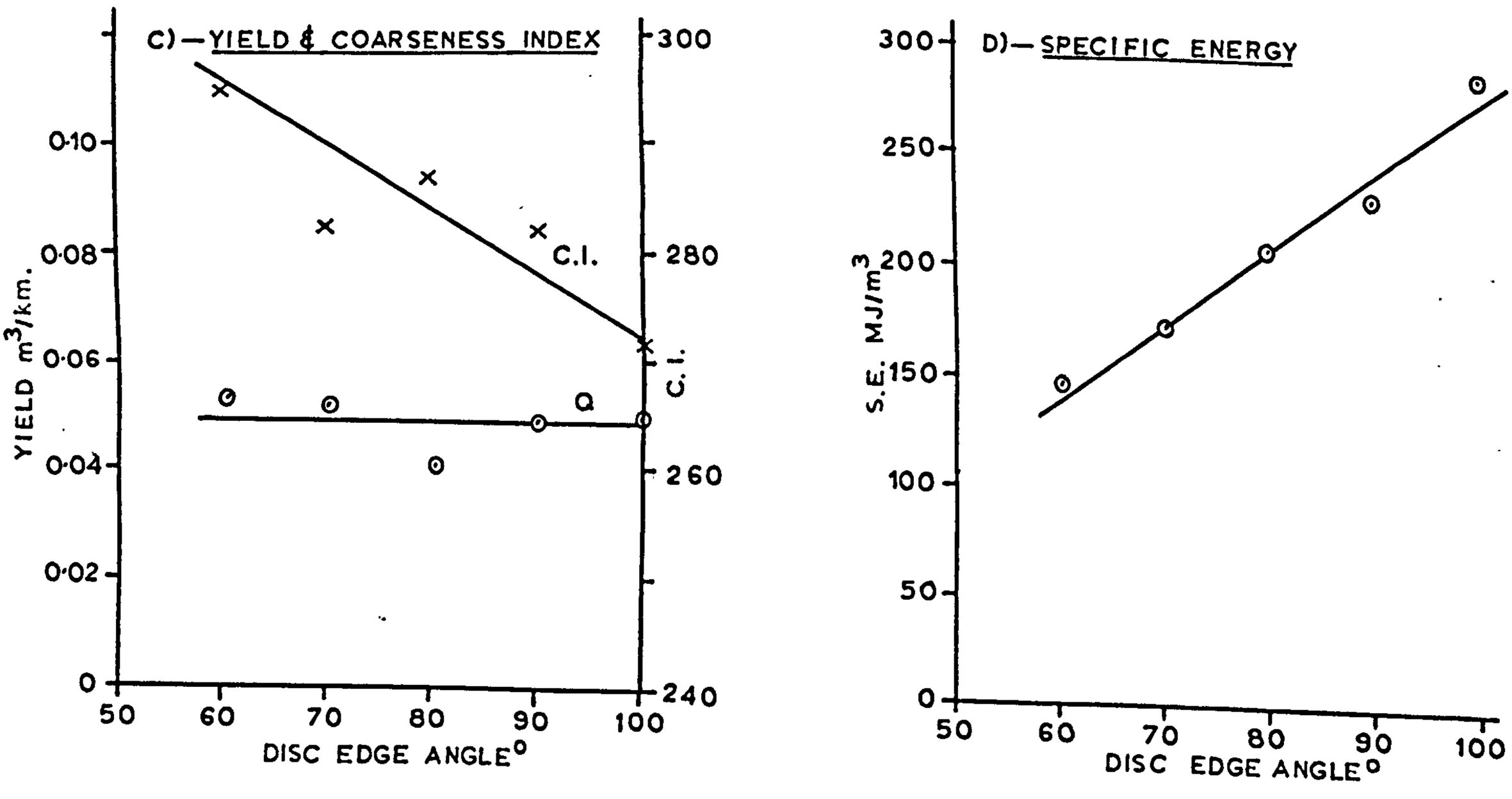

FIGURE 56 — EFFECT OF DISC ANGLE
— MAGNESIAN LIMESTONE

It should be borne in mind that no direct comparison between the forces and energies in Bunter and Magnesian Limestone can be obtained from these graphs. Although all three graphs show the variation in the measured parameters they are at mean penetration, mean speed and mean diameter. The mean penetration for Bunter is 6mm while for Magnesian Limestone it is only 4.5mm.

Edge angle appears to have no effect on rock yield. This is not unexpected since the maximum half edge angle of 50° is always less than the eventual angle of breakout.

Specific energy increases with disc edge angle, with the average increase over the range studied being 72%. Although specific energy is sensitive to edge angle, a disc of less than 60° would probably only provide improvement in efficiency at a disproportionately high loss of mechanical strength and wear resistance. Coarseness indeces decrease with increasing edge angle, showing that a higher proportion of crushed rock is produced by a blunt disc.

2. Effect of Disc Diameter

Thrust force is found to increase with diameter as indicated by Figures 57, 58 and 59. Rolling force, however, remains constant for all diameters.

This different effect of diameter on the principal forces is not difficult to understand. Rolling force is likely to be directly related to the projected area of the disc normal to the direction of movement. This area, while being dependent on disc edge angle and penetration, is clearly independent of disc diameter.

Conversely the thrust force will be related to the area of contact between the disc and the surface of the rock which, in turn, is a function of disc diameter.

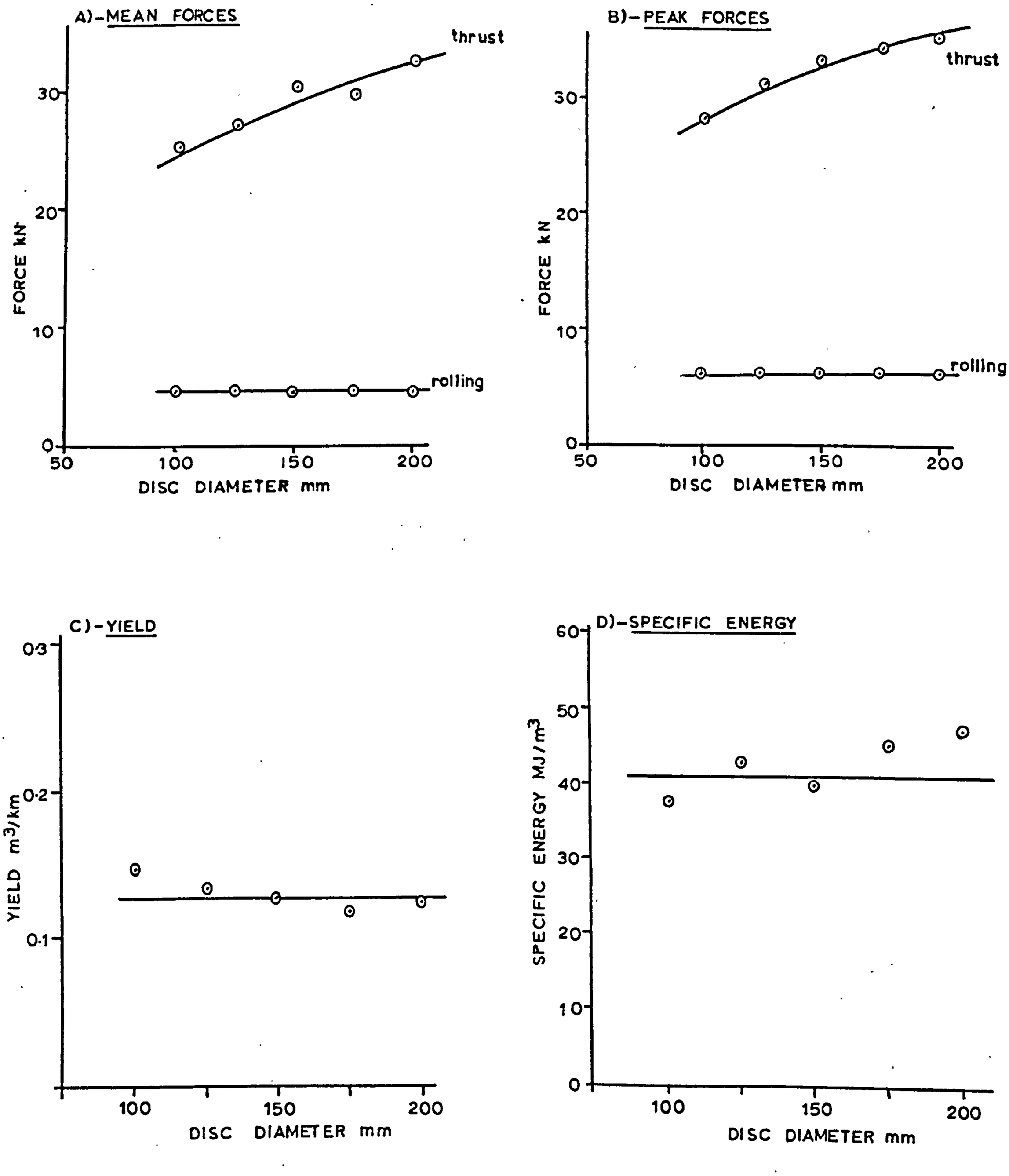

FIGURE 57 — EFFECT OF DISC DIAMETER
— DRY BUNTER SANDSTONE

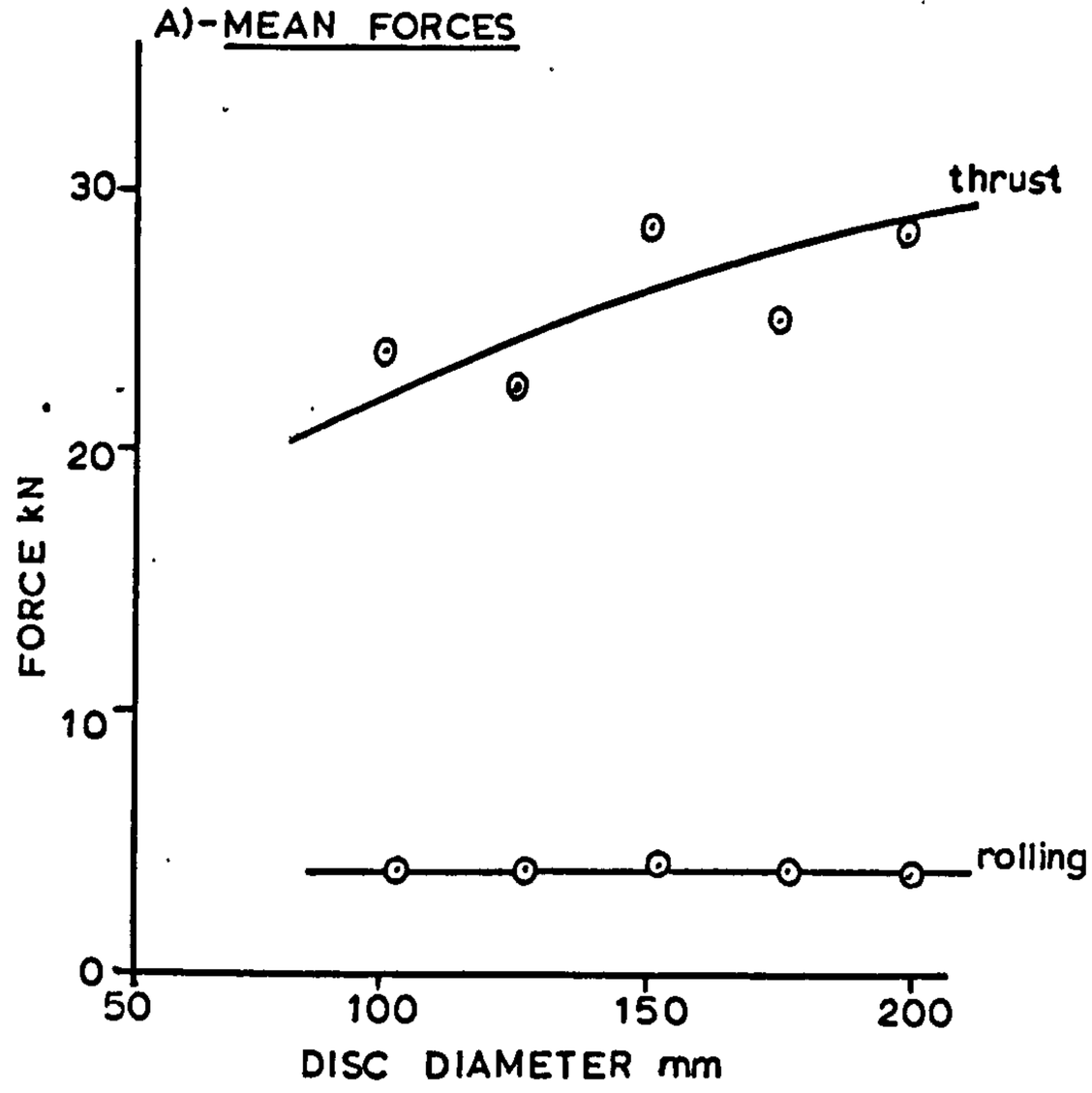

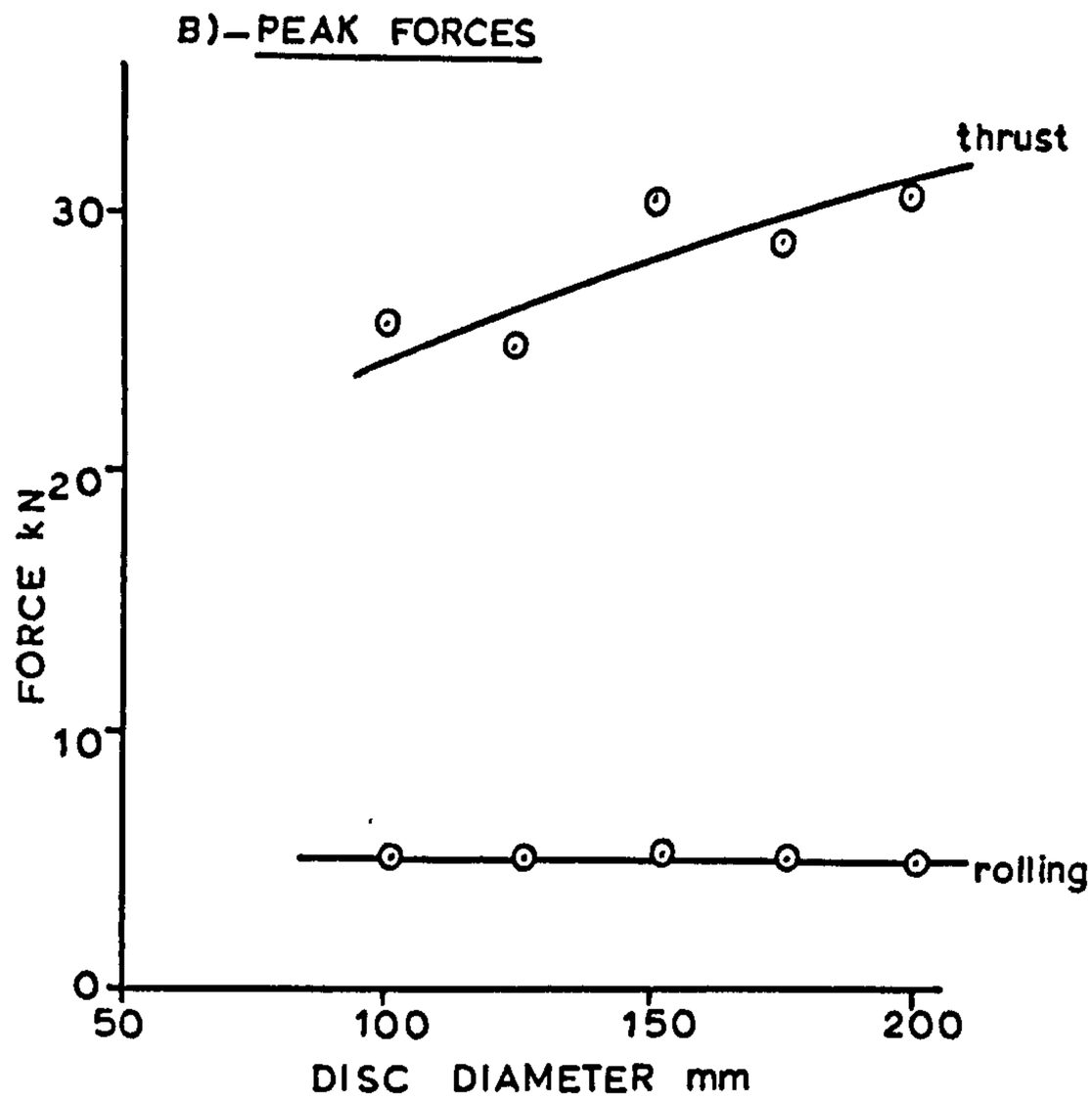

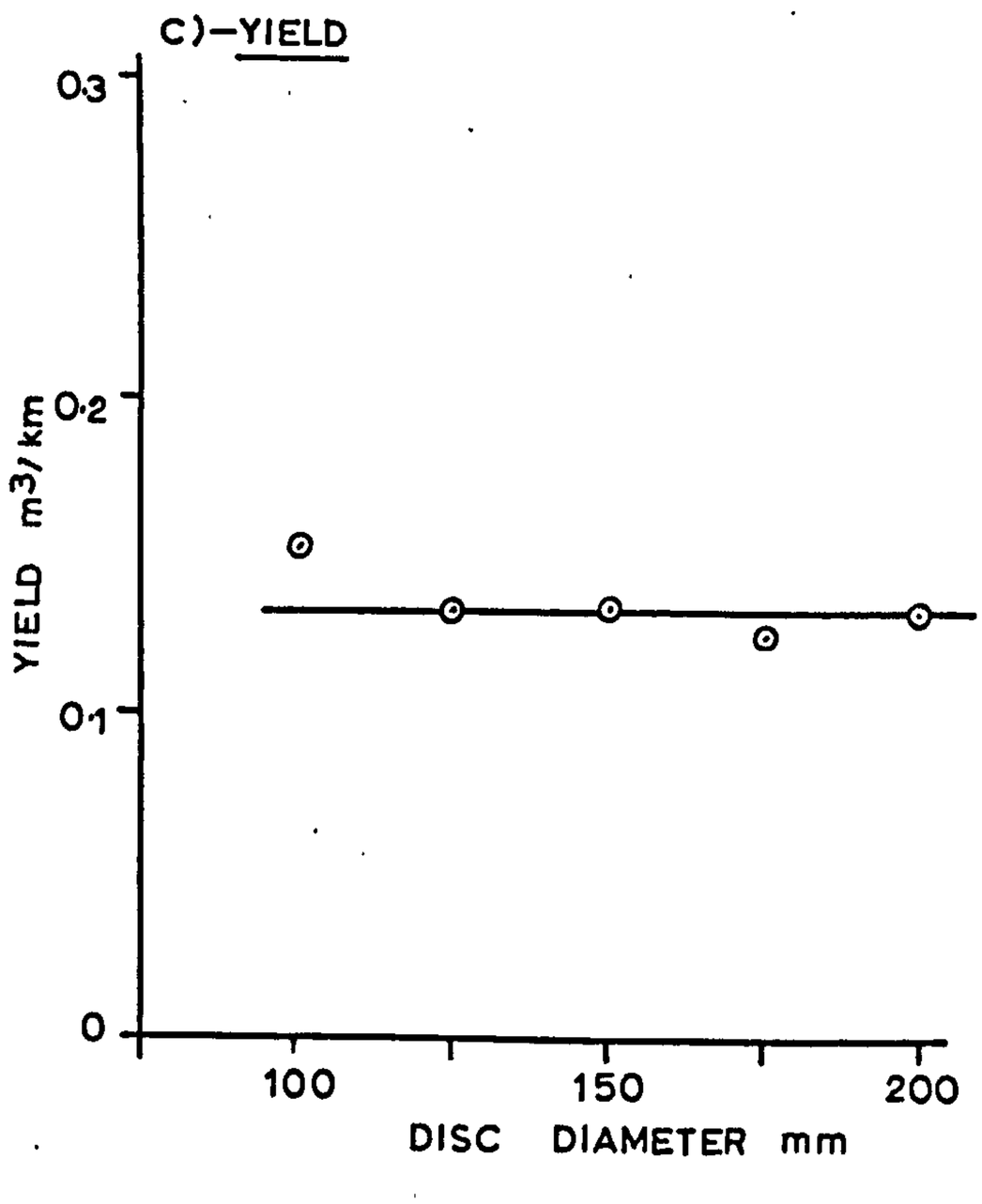

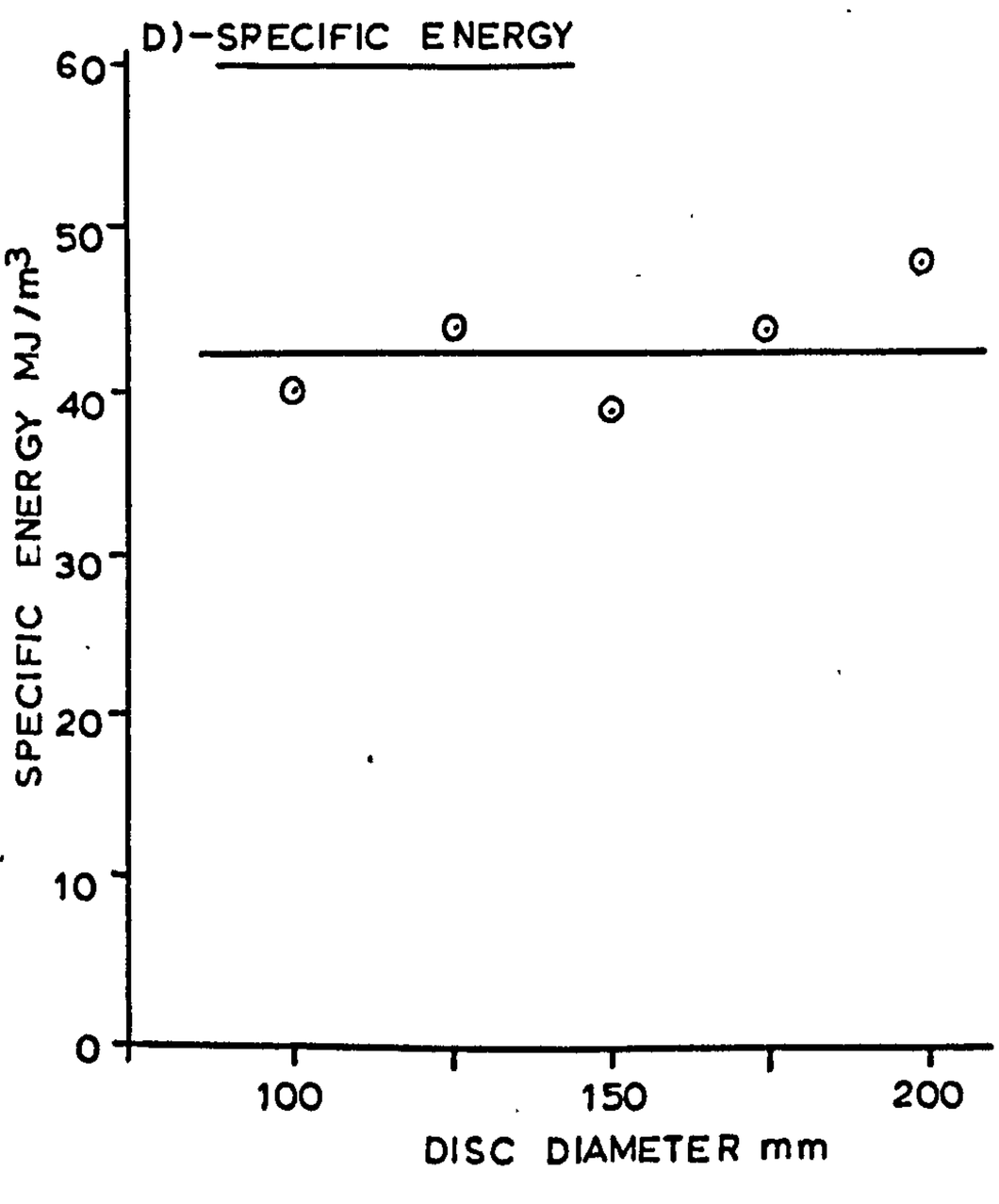

FIGURE 58 — EFFECT OF DISC DIAMETER
— WET BUNTER SANDSTONE

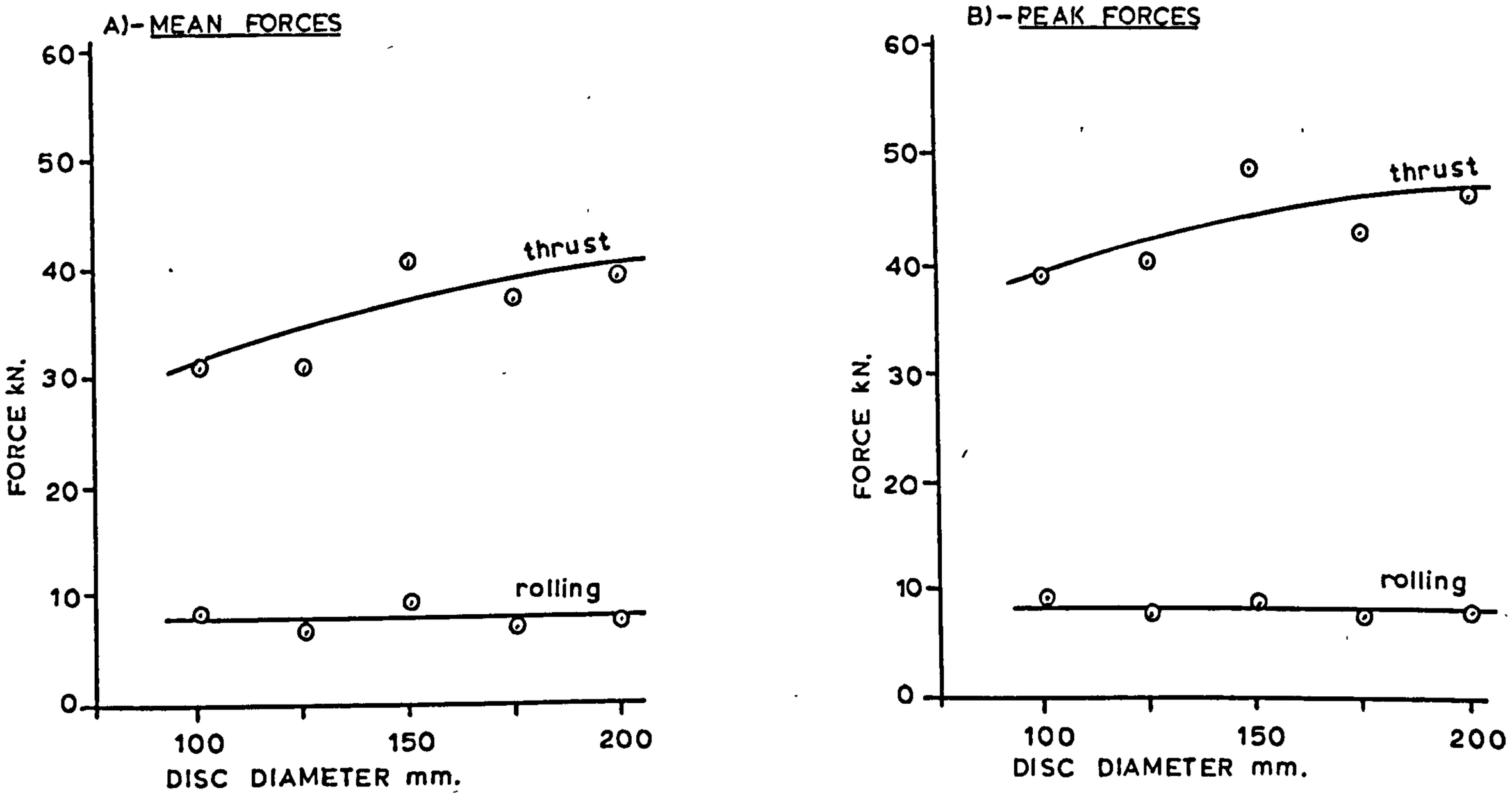

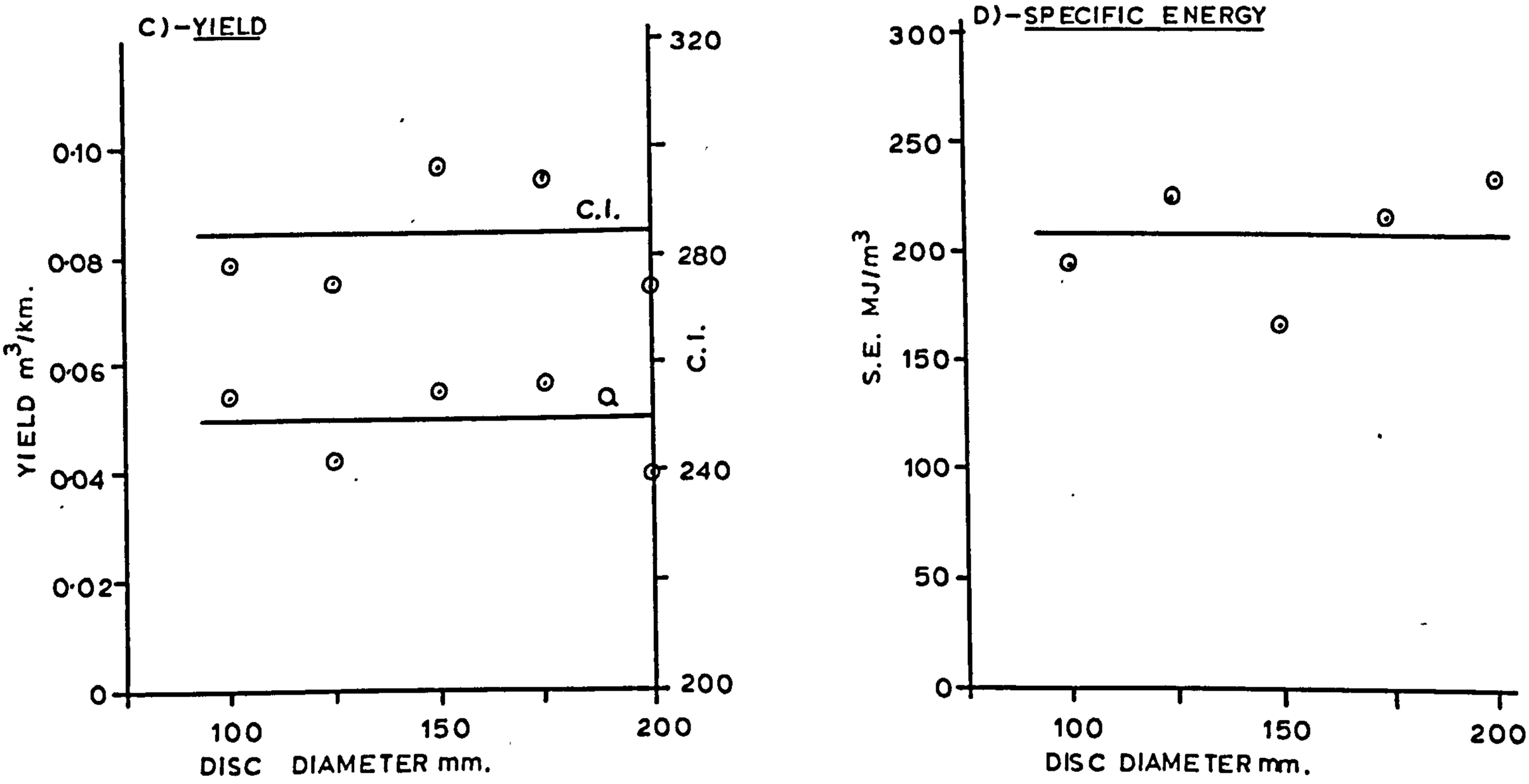

FIGURE 59 — EFFECT OF DISC DIAMETER
— MAGNESIAN LIMESTONE

Rock yield is independent of diameter and in Bunter Sandstone is not affected by rock moisture content. This complies with the supposition that the shape of incision and thereby the rolling force is unaffected by disc diameter.

Specific energies calculated from individual, rather than average, values for rolling force and yield are presented graphically in Figures 57, 58 and 59 D. Although the scatter of these results suggest the possibility of an increase in energy with diameter, the energy must, in fact, be independent of disc diameter, since both rolling force and yield are unaffected by this variable. The points on these graphs are, as shown, quite amenable to this interpretation. Further evidence to support this comes from the graphs of coarseness index, which on all previous occasions, both for picks and discs, have followed the inverse of the specific energy trend.

3. Effect of Penetration

Penetration, which is equivalent to depth of cut for a pick, is likely to be the most dominant variable in disc cutting. Figures 60, 61 and 62 show the variation in disc parameters with penetration, at mean edge angle and diameter.

Mean thrust and rolling forces both increase rapidly, but not linearly, with penetration. Since the range of edge angles and disc diameters was the same for all three experiments, these graphs provide the first opportunity to assess the differences caused by rock type. Interpolation of the graphs for Bunter has yielded the data quoted in Table 30.

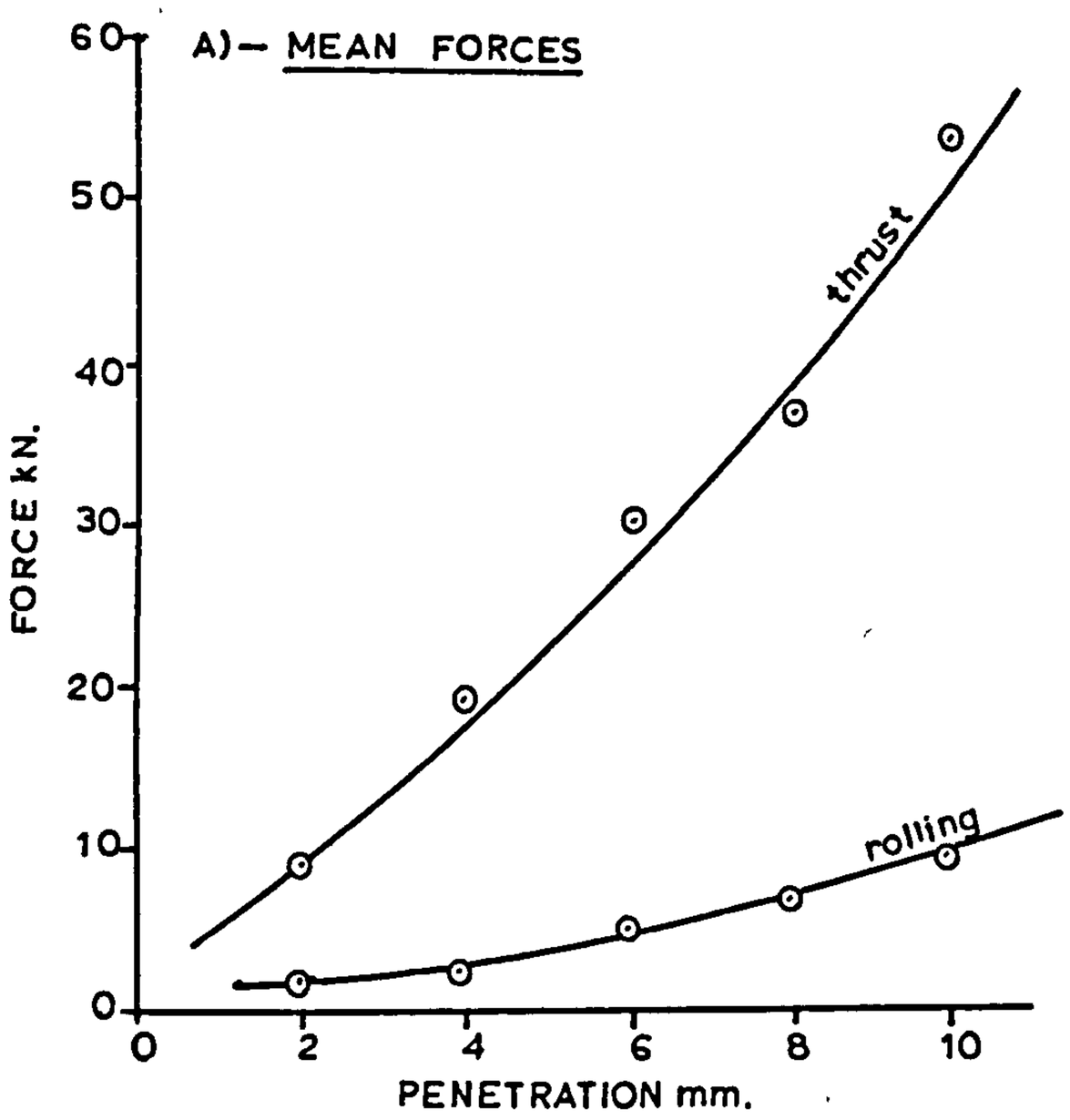

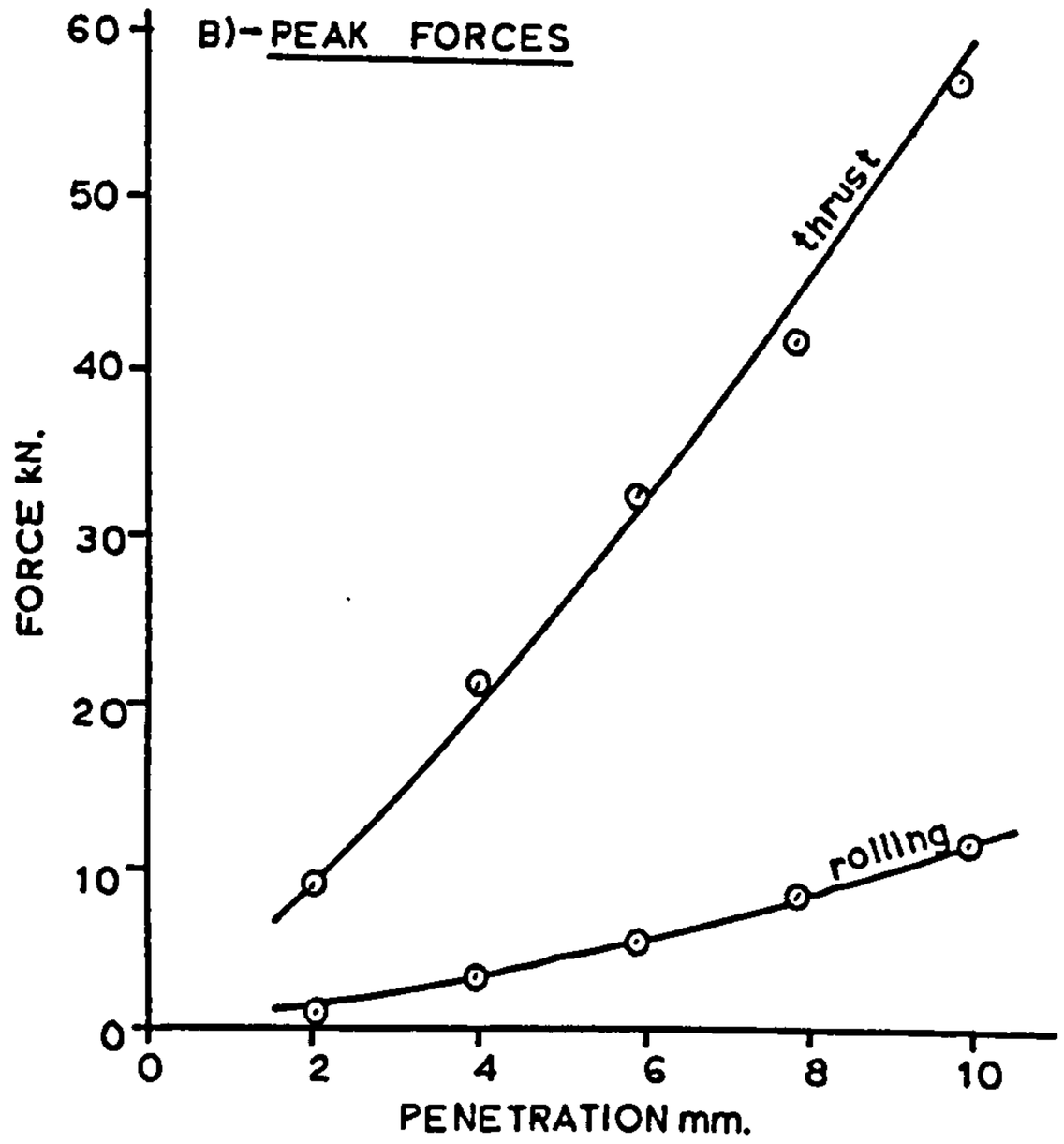

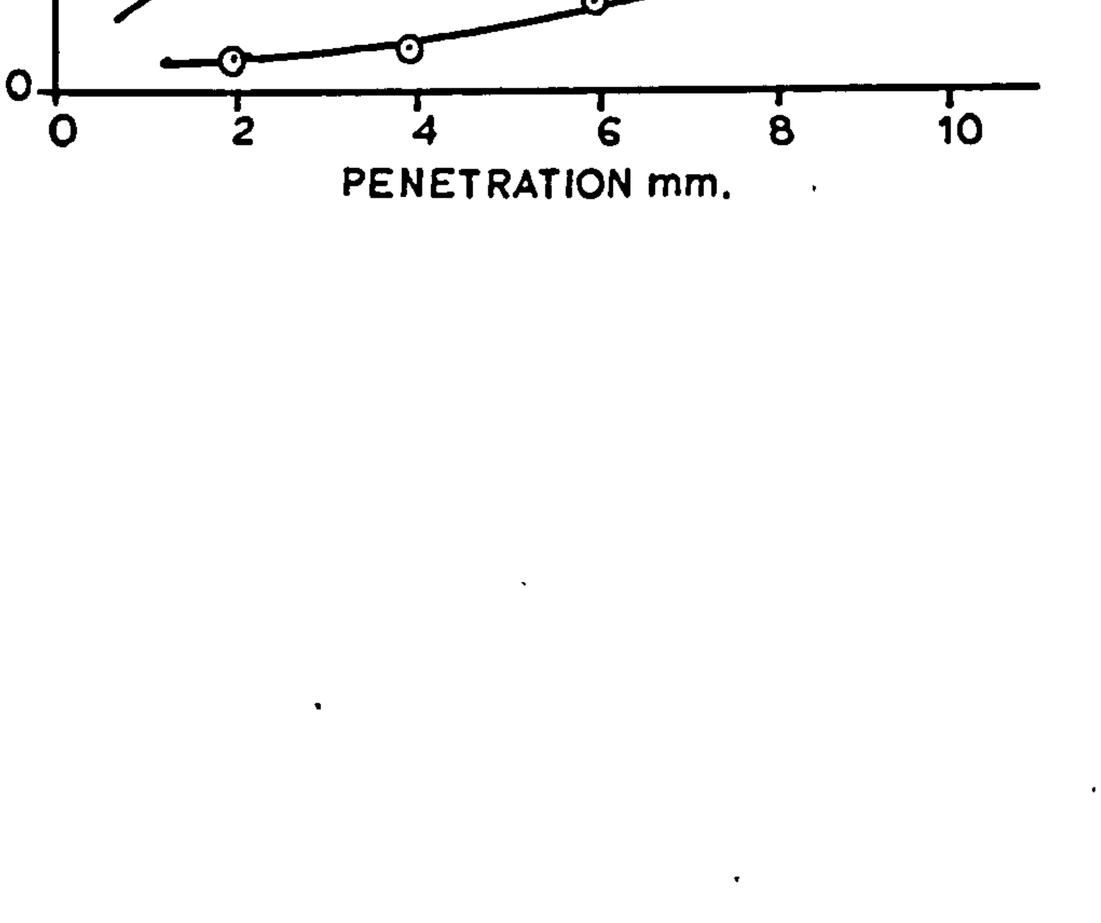

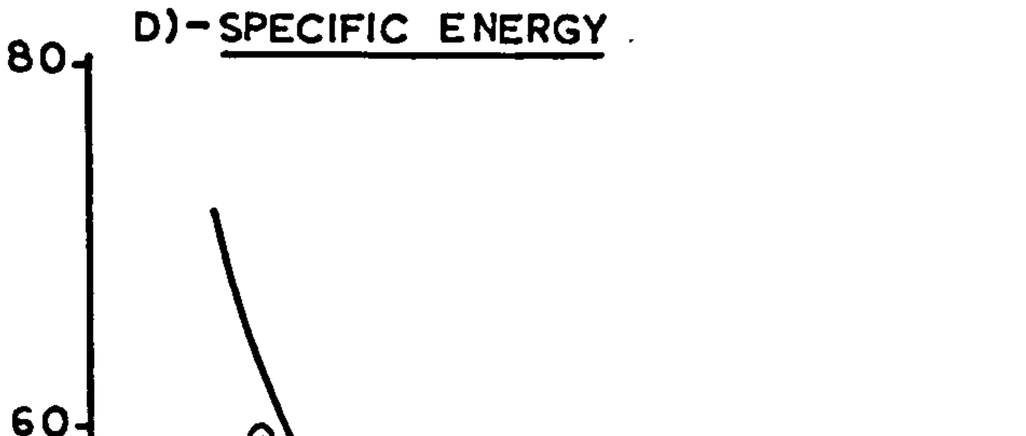

FIGURE 60 — EFFECT OF DISC PENETRATION
— DRY BUNTER SANDSTONE

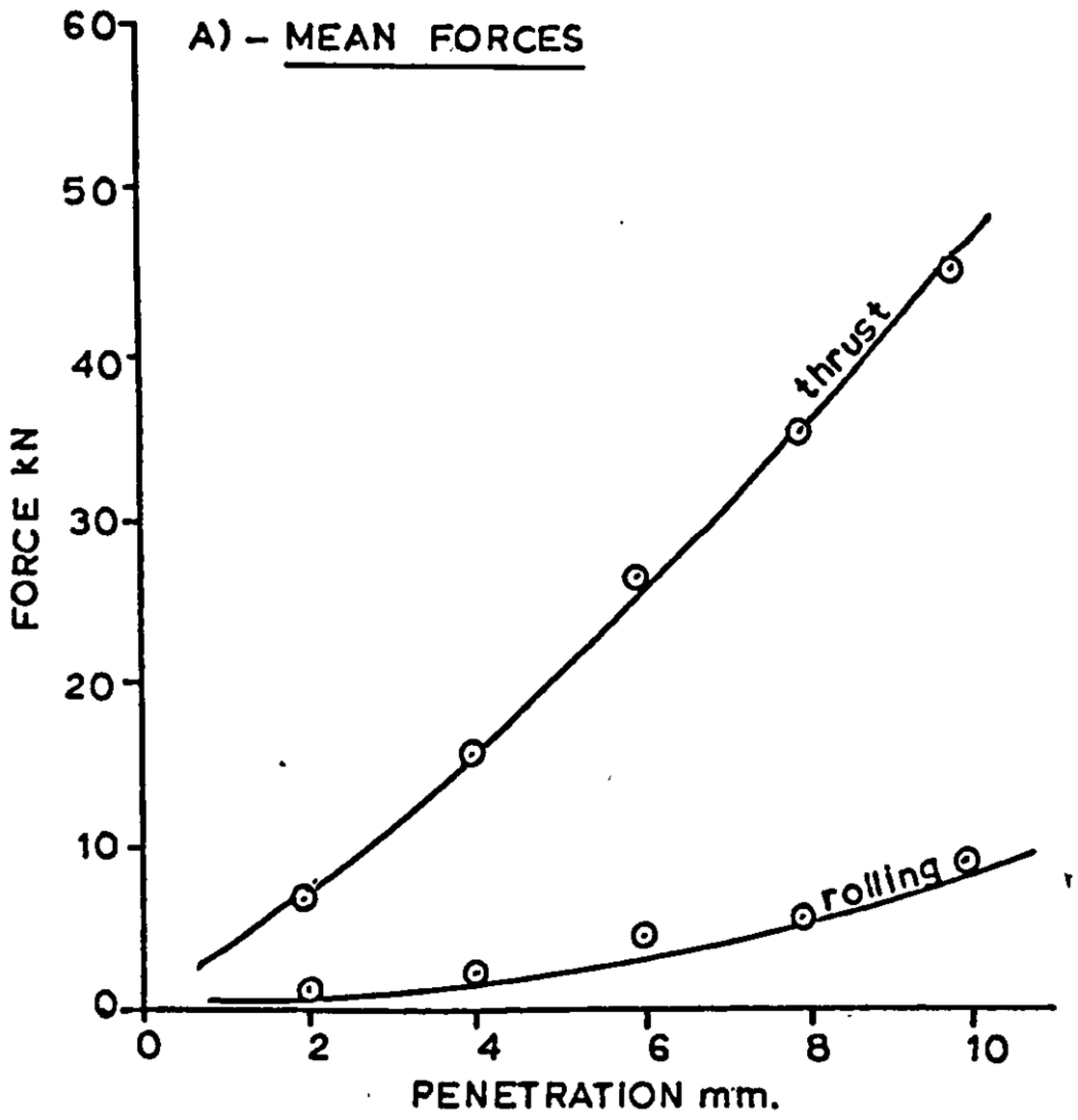

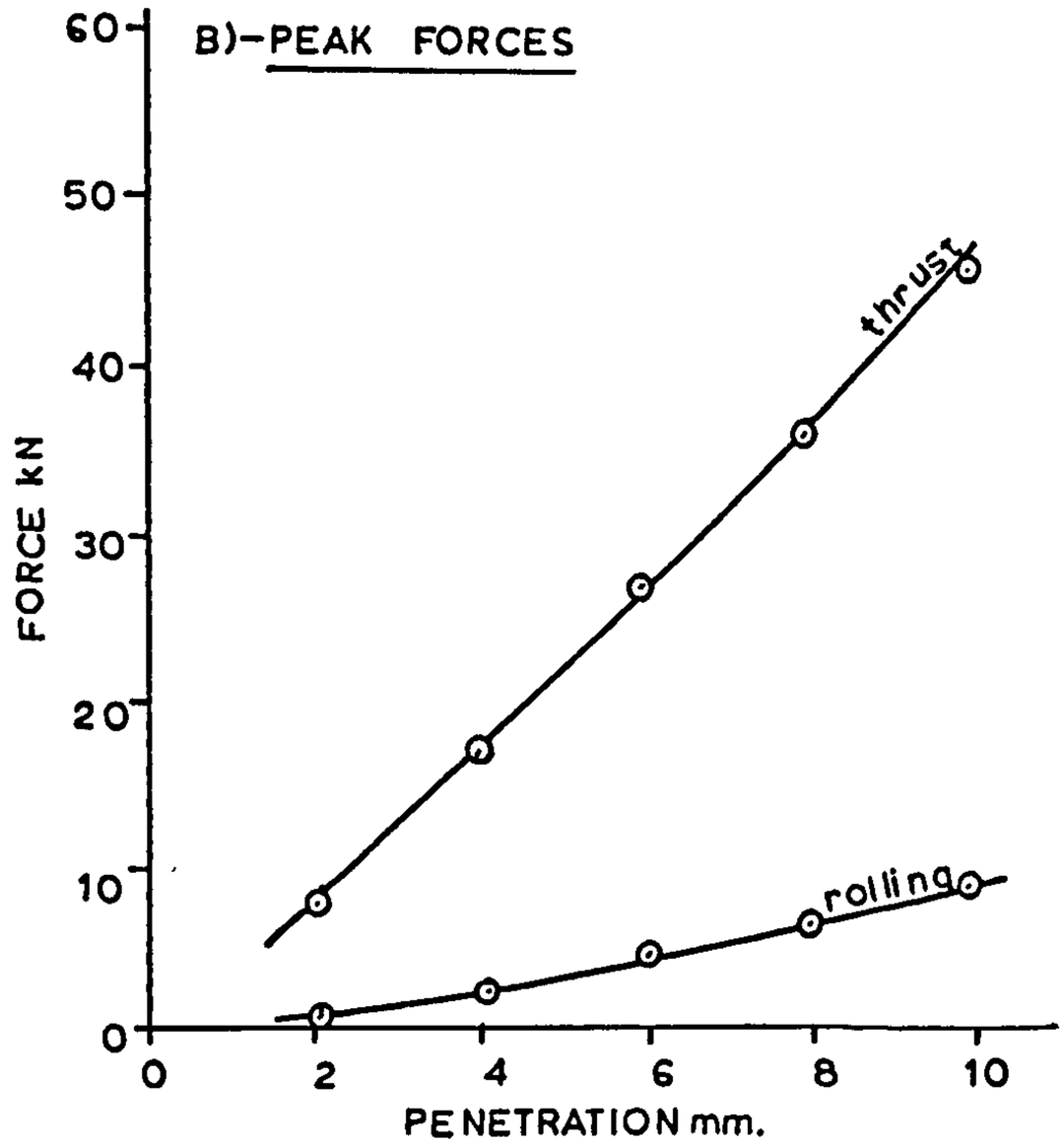

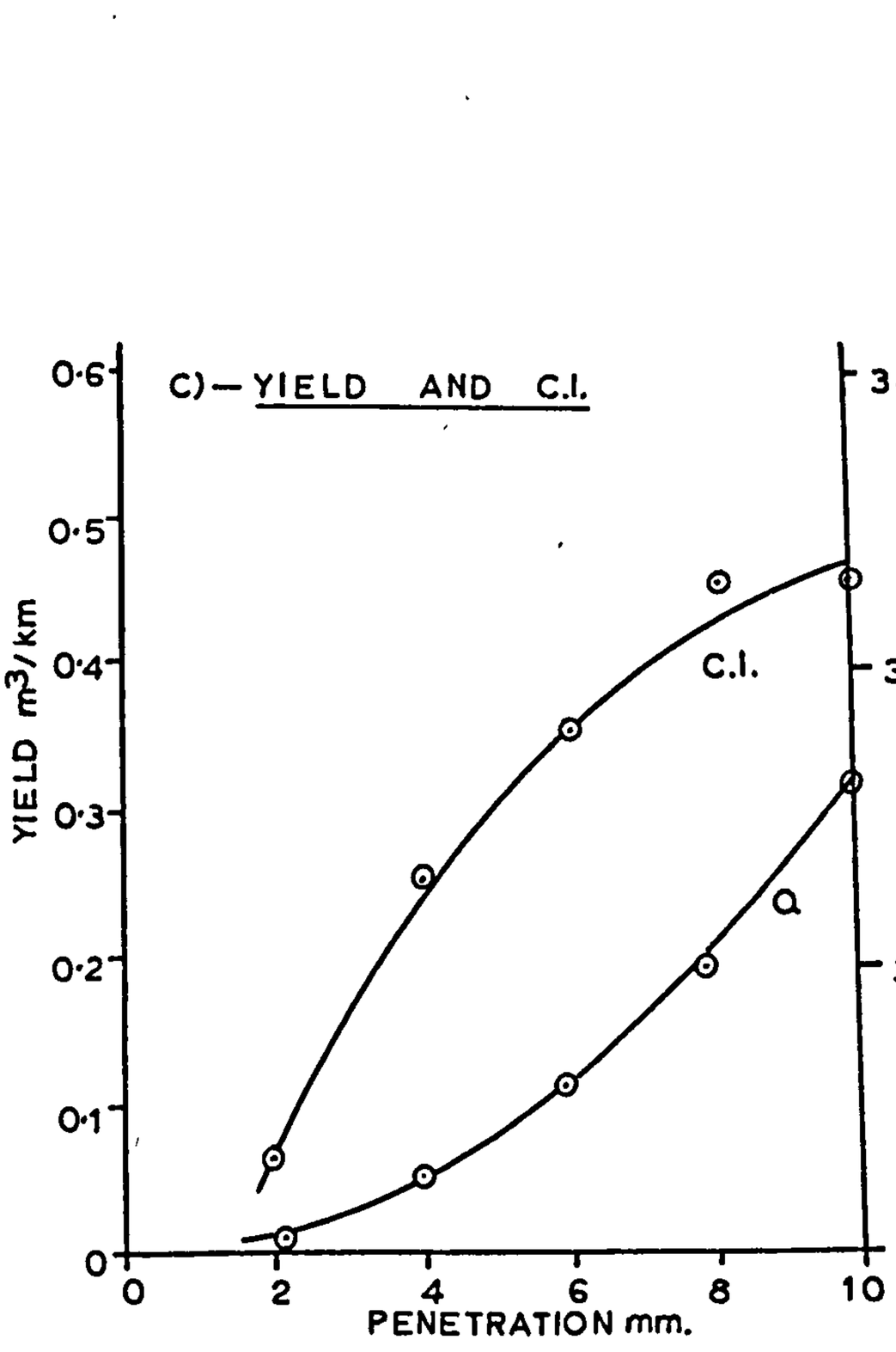

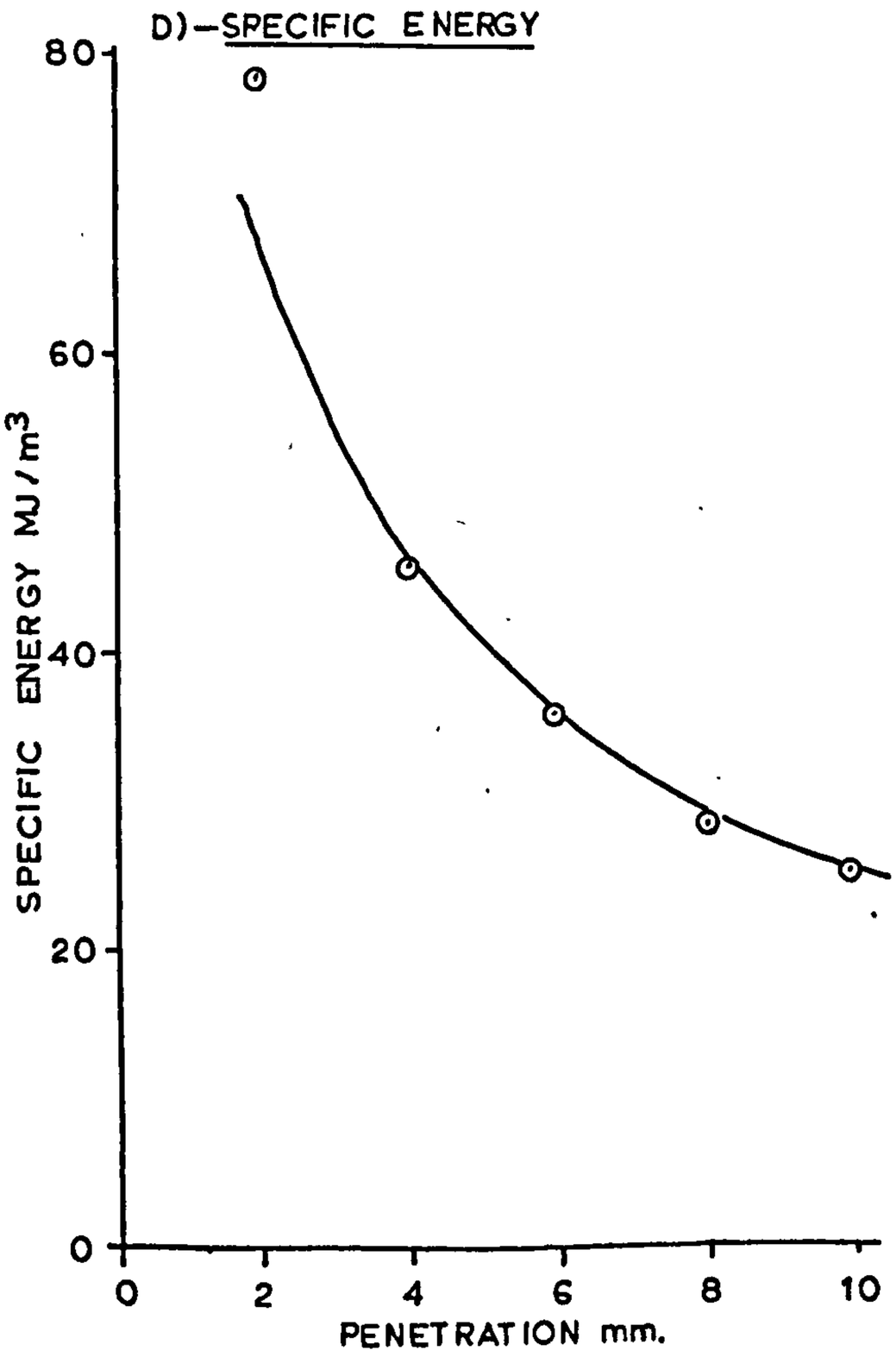

FIGURE 61 – EFFECT OF DISC PENETRATION
– WET BUNTER SANDSTONE

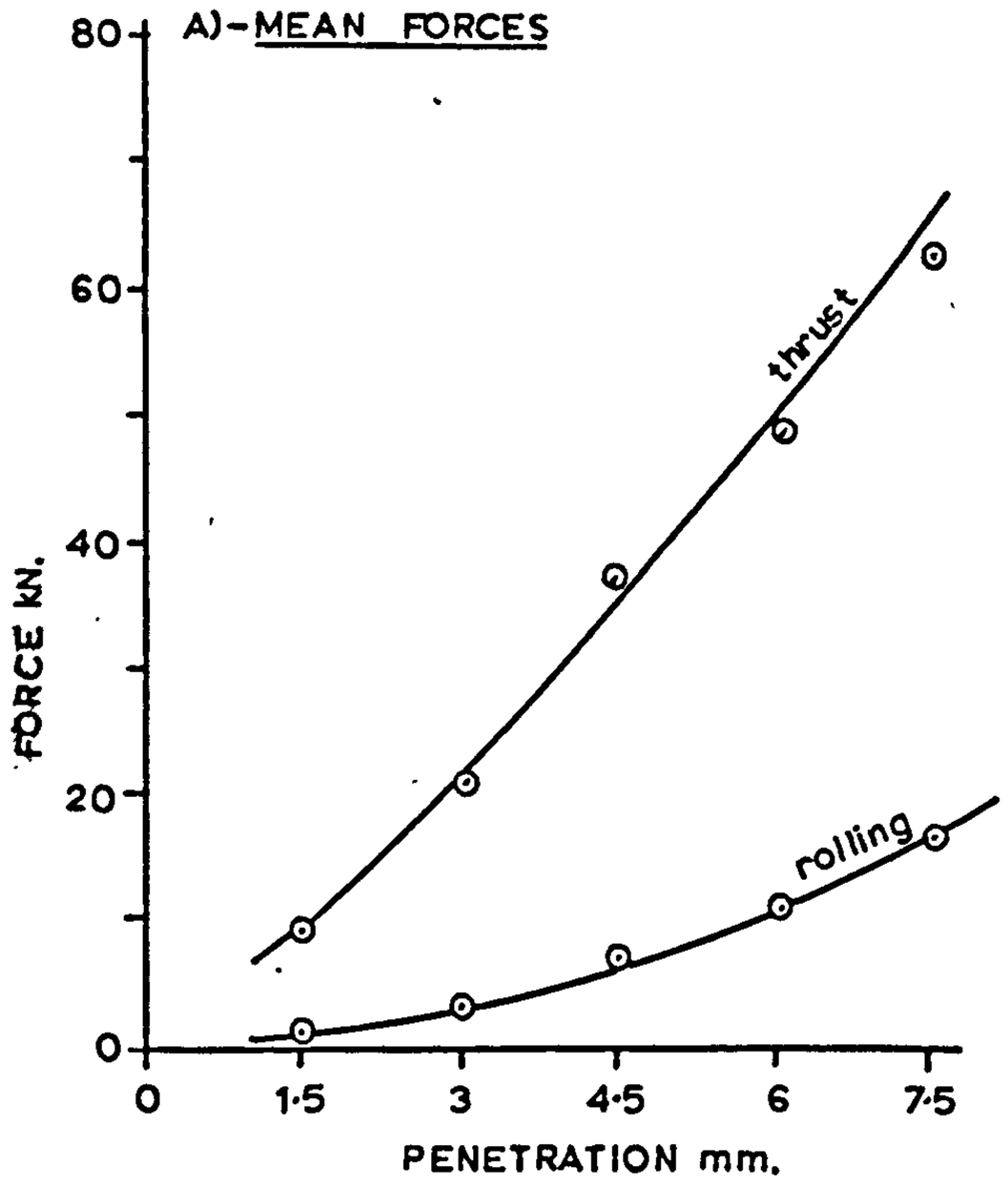

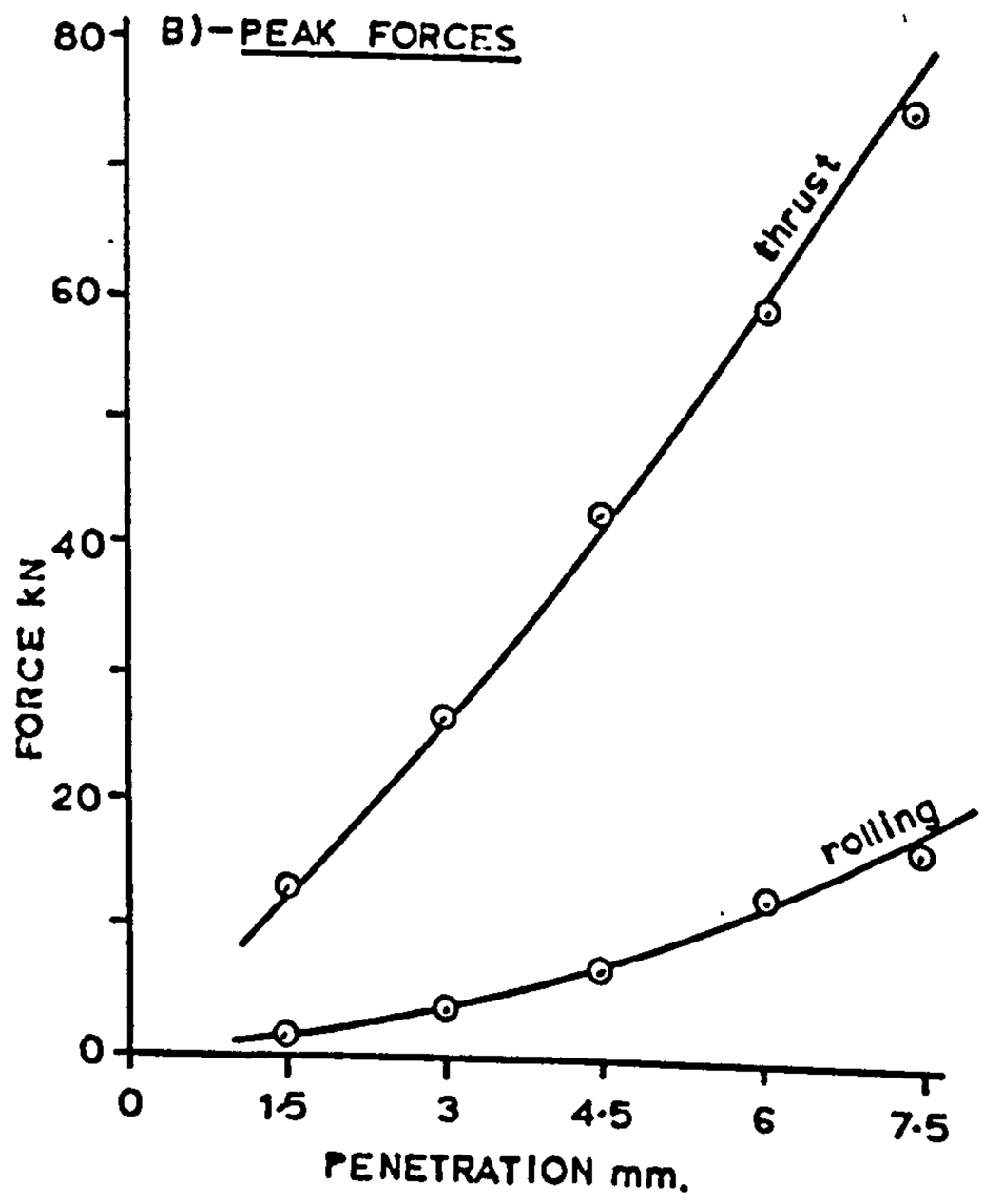

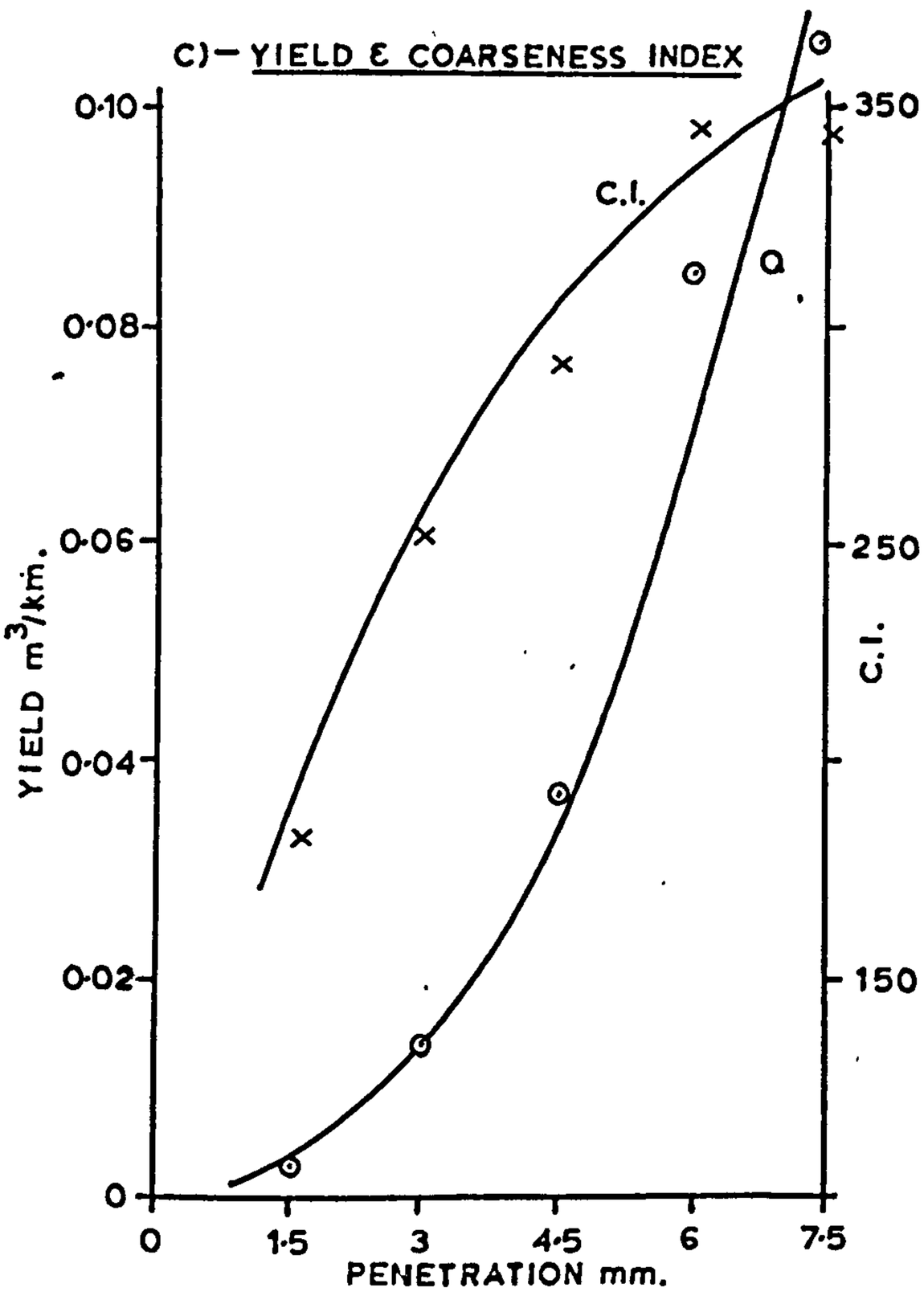

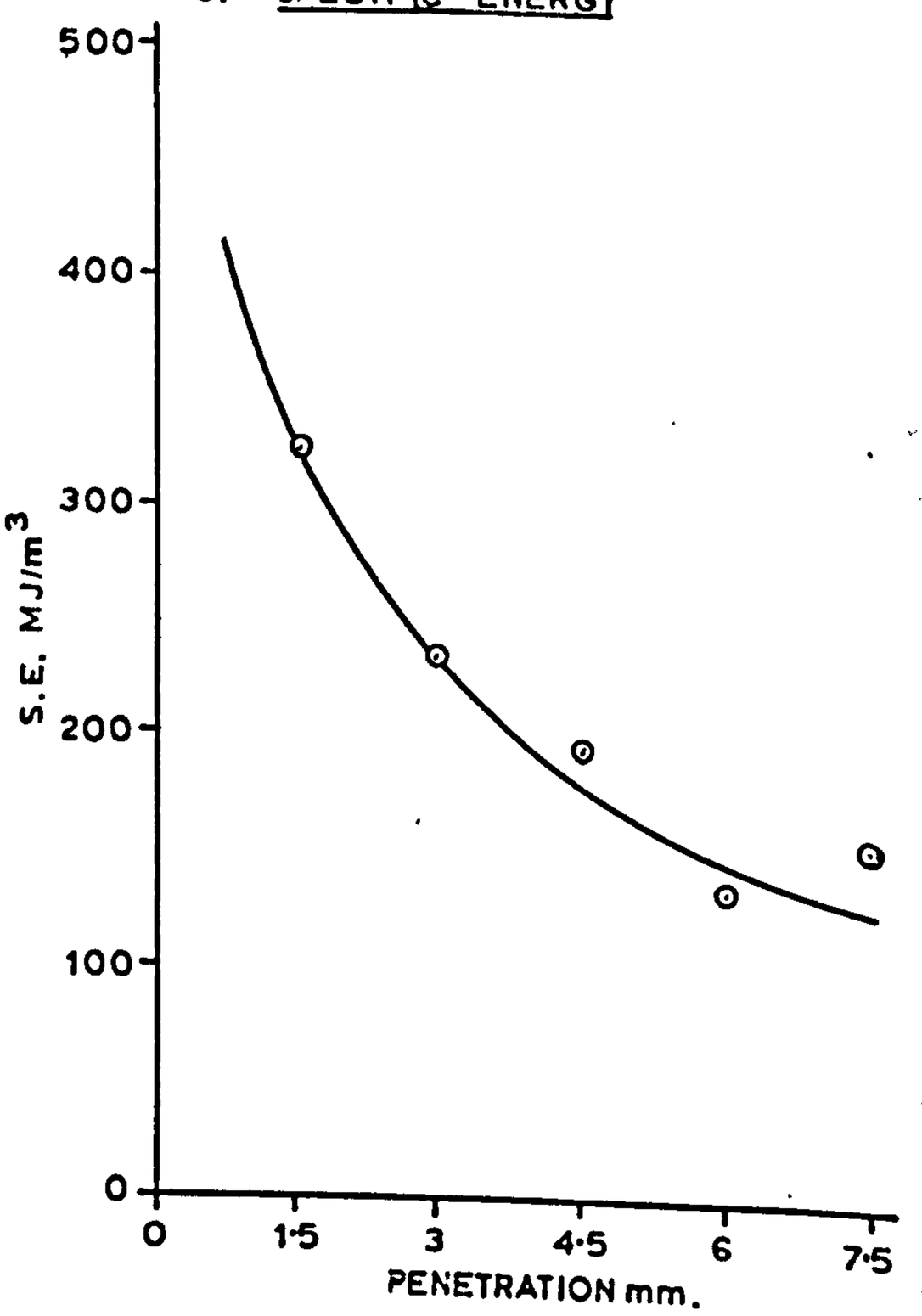

FIGURE 62 - EFFECT OF DISC PENETRATION
- MAGNESIAN LIMESTONE

TABLE 30

A COMPARISON OF THRUST FORCE IN THE THREE ROCKS

Penetration mm	$\overline{F_T}$ (kN)		
	Dry Bunter	Wet Bunter	Magnesian Limestone
1.5	6.16	5.19	9.65
3.0	13.49	11.44	21.42
4.5	21.45	18.72	37.24
6.0	29.51	27.02	48.81
7.5	34.60	33.55	63.29

If the values for dry Bunter are taken as a base, then the ratios between the forces are as listed in Table 31.

TABLE 31

RATIOS BETWEEN THRUST FORCES

Penetration mm	Dry Bunter	Wet Bunter	Magnesian Limestone
1.5	1	0.84	1.57
3.0	1	0.85	1.59
4.5	1	0.87	1.74
6.0	1	0.91	1.65
7.5	1	0.97	1.83
Mean	1	0.89	1.68

If it is assumed that resistance to penetration is essentially compressive then the mean thrust force should be proportional to the compressive strength of the material being excavated. The compressive strengths of the three materials, as given by Table 4 of Chapter 4, are 49.2 MN/m^2 for dry Bunter, 40.97 MN/m^2 for wet Bunter and 84.9 MN/m^2 for Magnesian Limestone. These figures give rise to ratios of 1, 0.83 and 1.73, which are not dissimilar to the mean values in Table 31 and give

credence to the concept that thrust force is proportional to compressive strength.

Rock yield increase dramatically with penetration and appears to follow a square law. This is not unexpected since the cross-section of all observed incisions was triangular. Hence $Q = p^2 \tan \theta$, where θ is the angle of breakout. This angle has been calculated for each unrelieved disc test and the values so obtained are tabulated in Appendix VII K. The appropriate grouped results are given in Appendix VII L. Breakout angle is not significantly affected by any of the variables, the only recognisable trend being a slight decrease at the higher levels of disc diameter.

Specific energy is found to be greatly influenced by penetration. The improvement in cutting efficiency is most pronounced over the first few levels of penetration and, whereas this improvement continues, the rate falls at higher penetrations. A tentative extrapolation of this trend suggests that an ultimate minimum specific energy might be achieved at a penetration of between 15 and 20mm. The effect of penetration, in Bunter, is seen to be similar for both moisture conditions with the energy requirements being approximately the same.

Coarseness index increases rapidly with penetration. This trend, being the converse of specific energy, is in compliance with the new surface area concept of energy dissipation.

4. Effect of Speed

In section 5.1 attention was drawn to the fact that previously reported research in the field indicated that cutting speed had no effect on the principal cutting parameters, with the possible exception of tool wear rate. This work had, however, been exclusively concerned with drag picks.

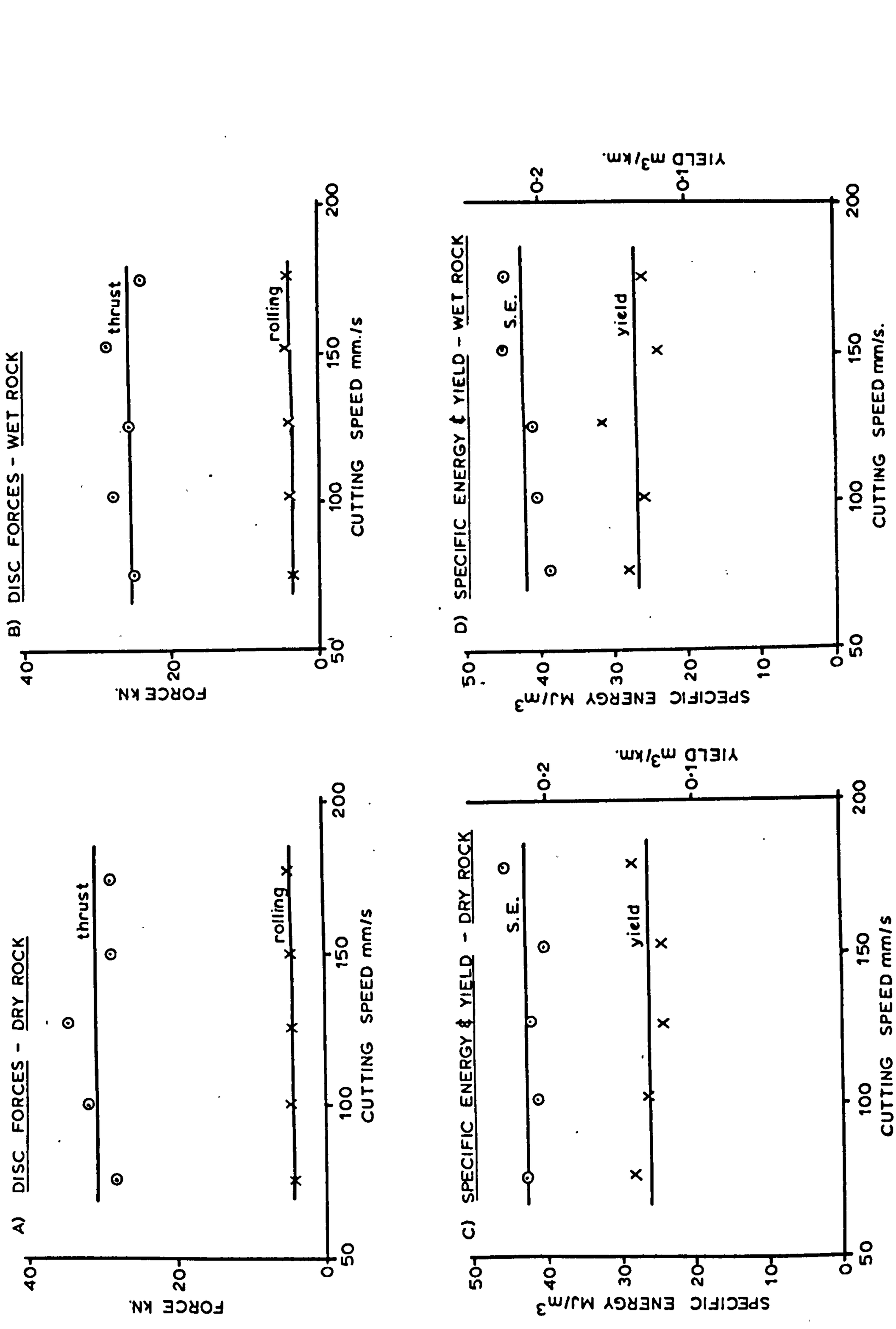

FIGURE 63 - EFFECT OF DISC CUTTING SPEED

As indicated by Figure 63, thrust force, rolling force, rock yield and specific energy show no discernable change with cutting speed over the range 50 - 200 mm/s. This fact is equally true for both conditions of rock moisture.

These results, taken in conjunction with the wealth of data for picks, encourages the general conclusion that, within normal operational limits, the performance of a cutting tool is not affected by the speed of cutting.

9.3 Relieved Cutting

In the case of relieved cutting with discs, spacing is defined as the distance between the peripheral edges of adjacent discs (i.e. groove centre-lines) as shown in Figure 64.

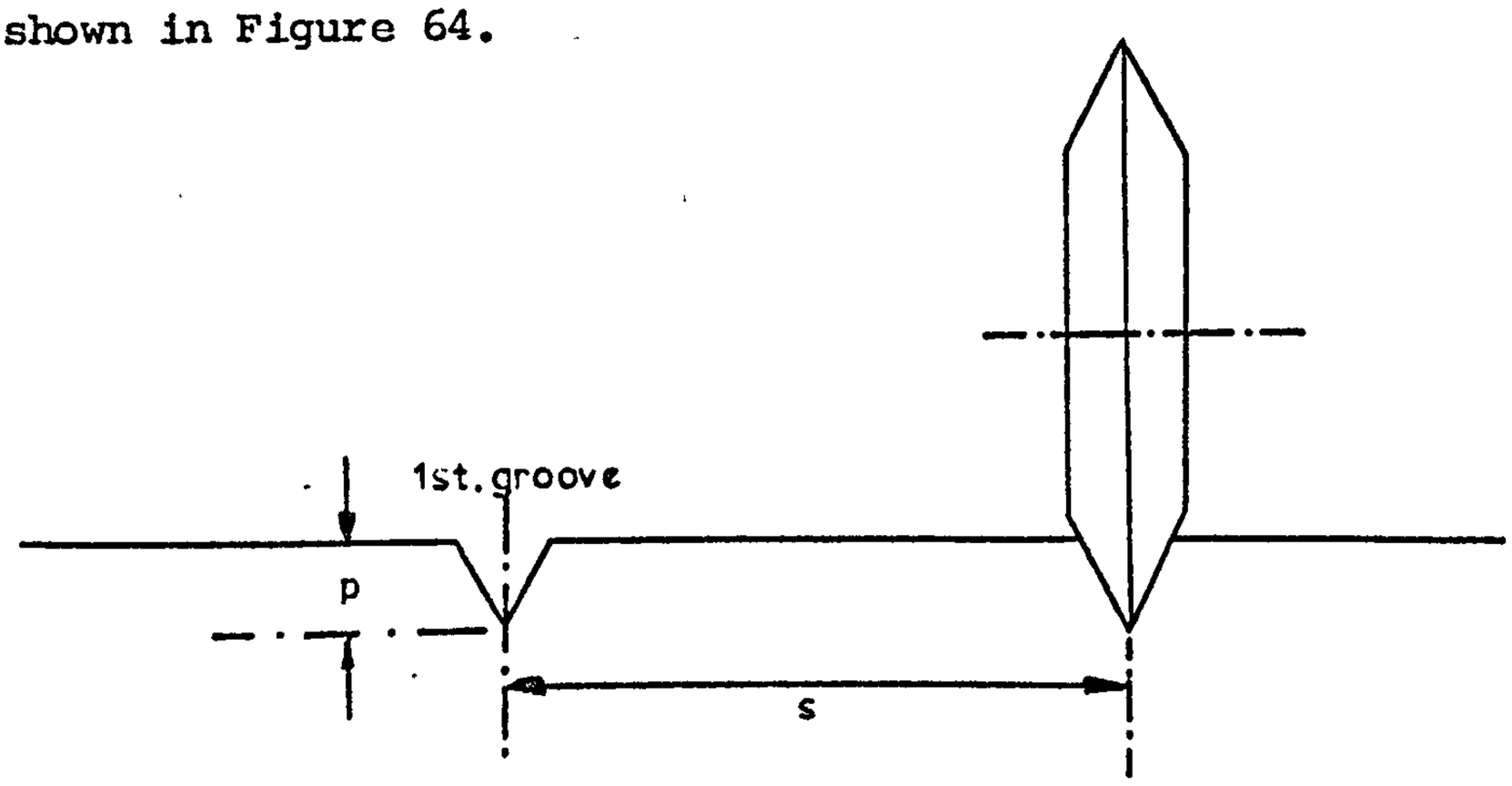

FIGURE 64 DISC SPACING NOTATION.

Preliminary experiments were undertaken to determine the most useful values of spacing appropriate to the levels of the other variables adopted for the disc cutting work. The levels of spacing so established provided a s/p range of 1.2 to 30.0. Although this broad range considerably exceeds the expected limit of interaction between adjacent tools, the majority of the 100 cuts made in each experiment were at s/p values of less than 8.

Data for all the relieved cutting tests with discs are given in Appendix VIII.

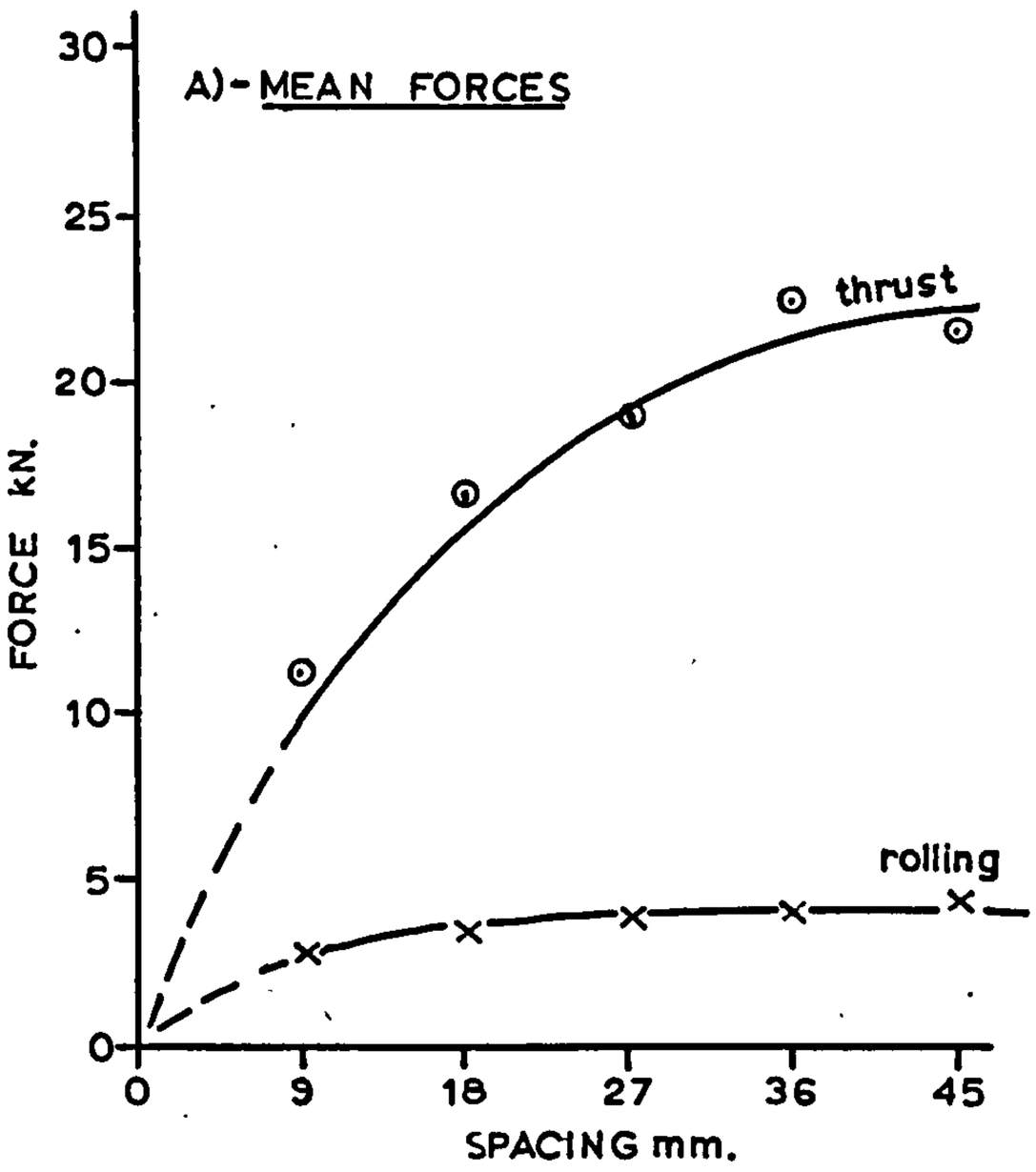

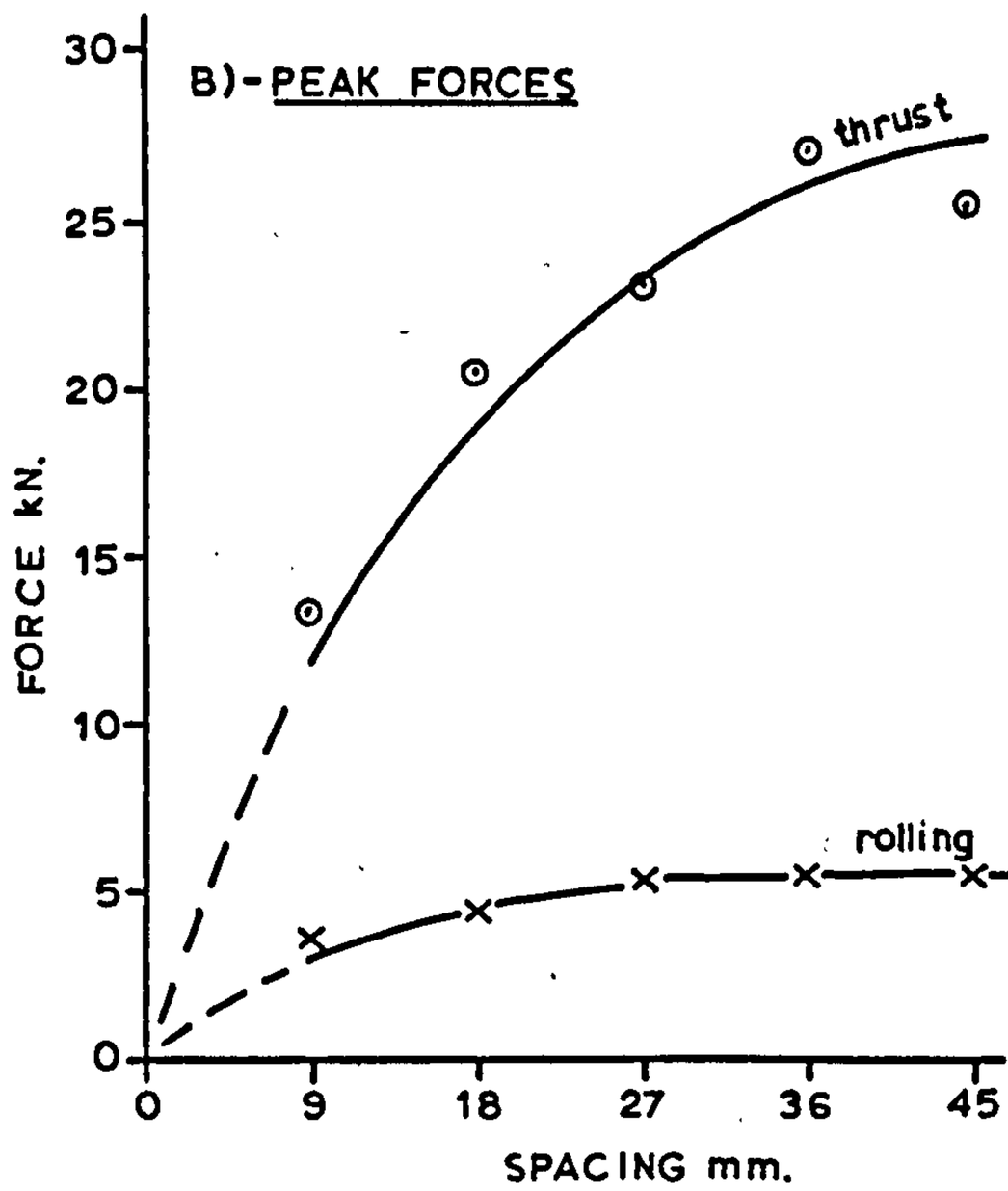

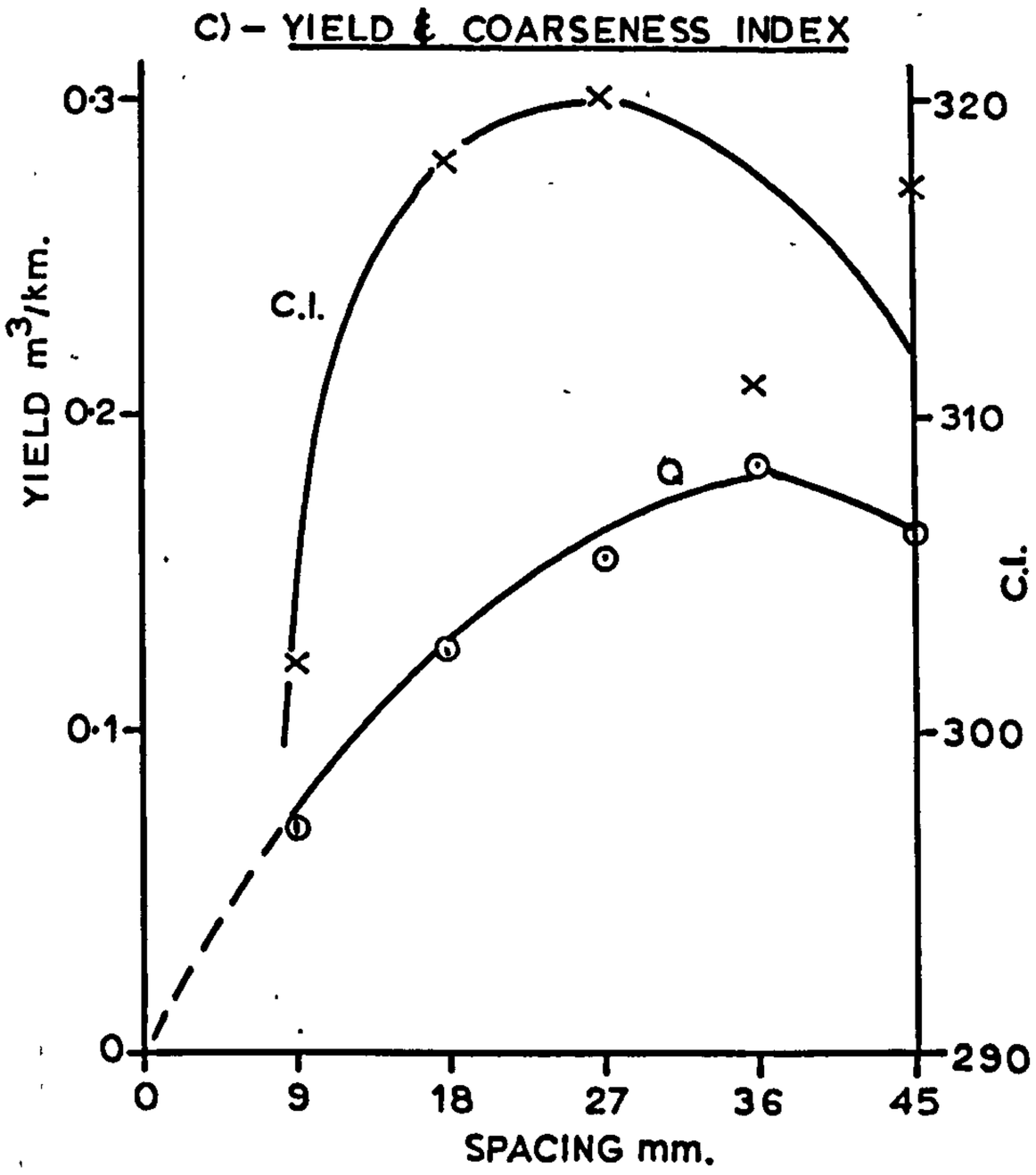

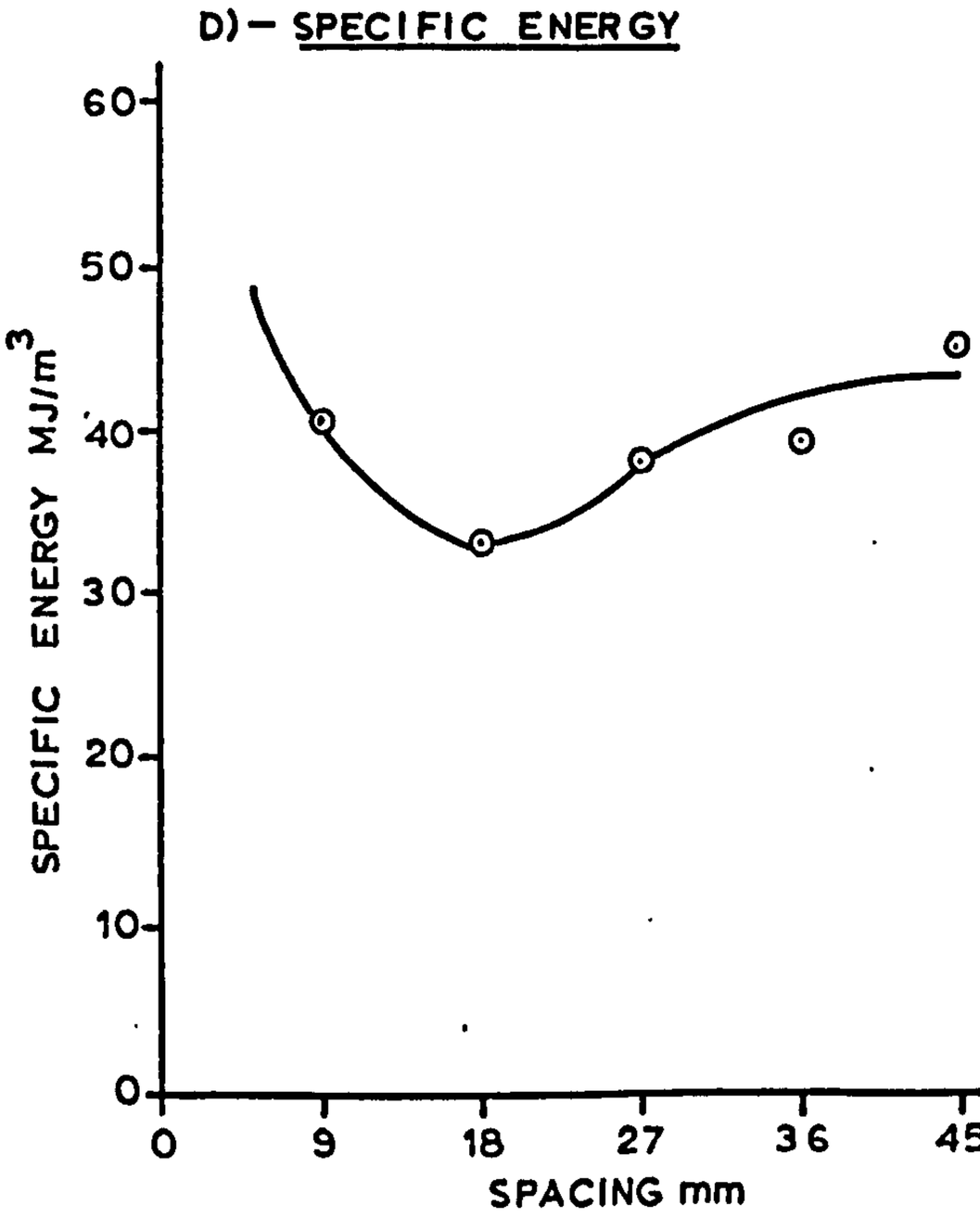

FIGURE 65 — EFFECT OF SPACING
— DRY BUNTER SANDSTONE

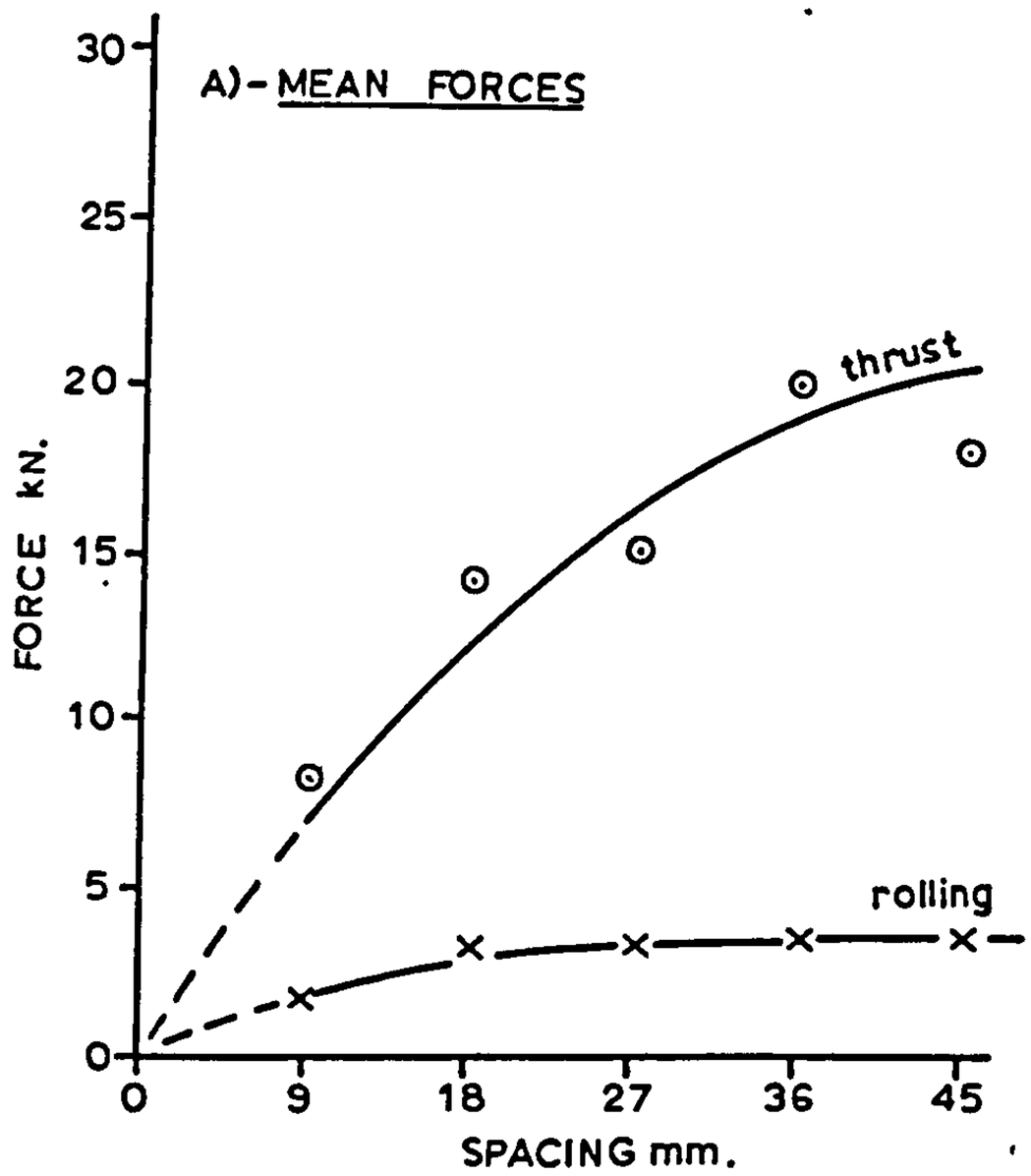

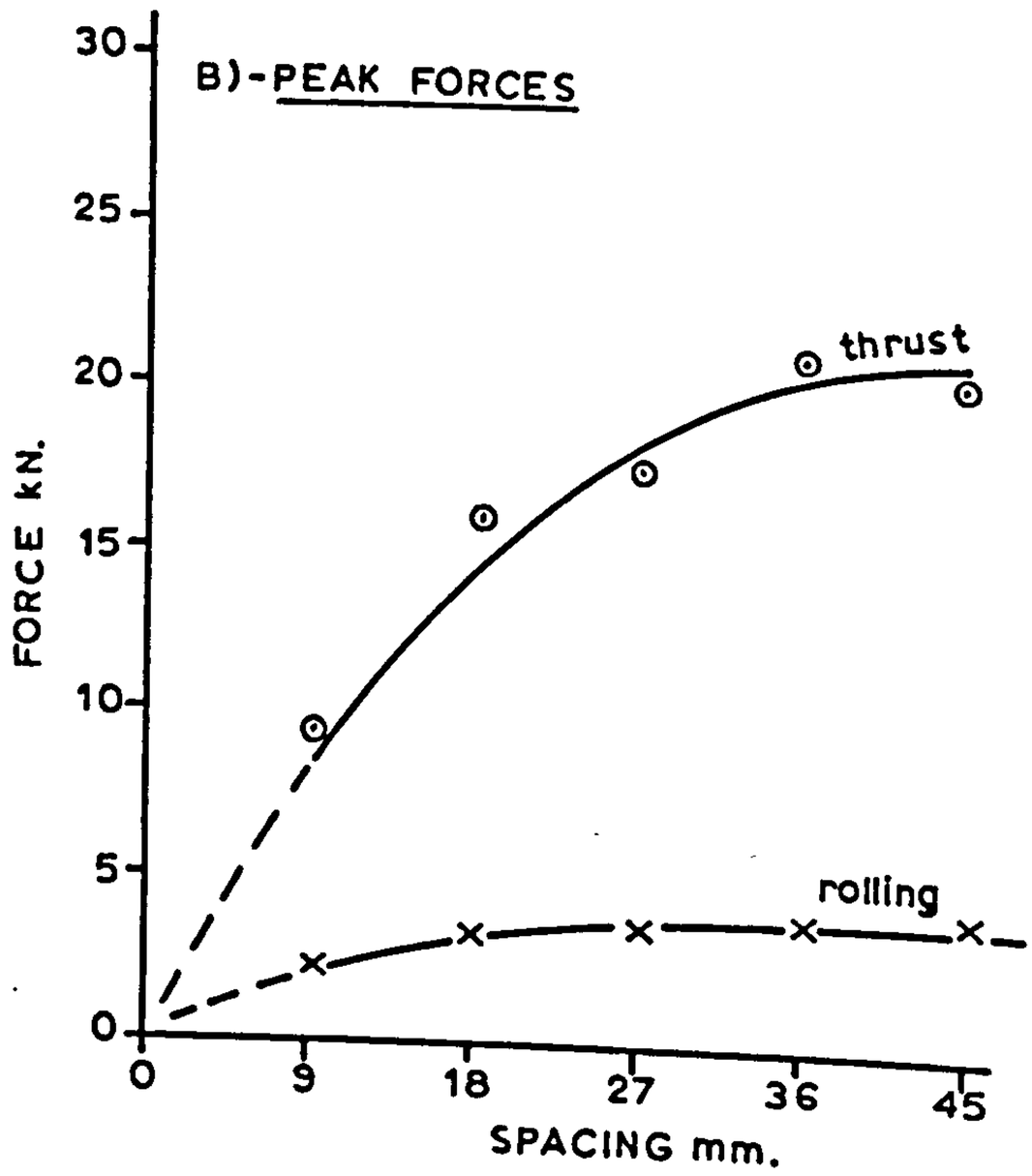

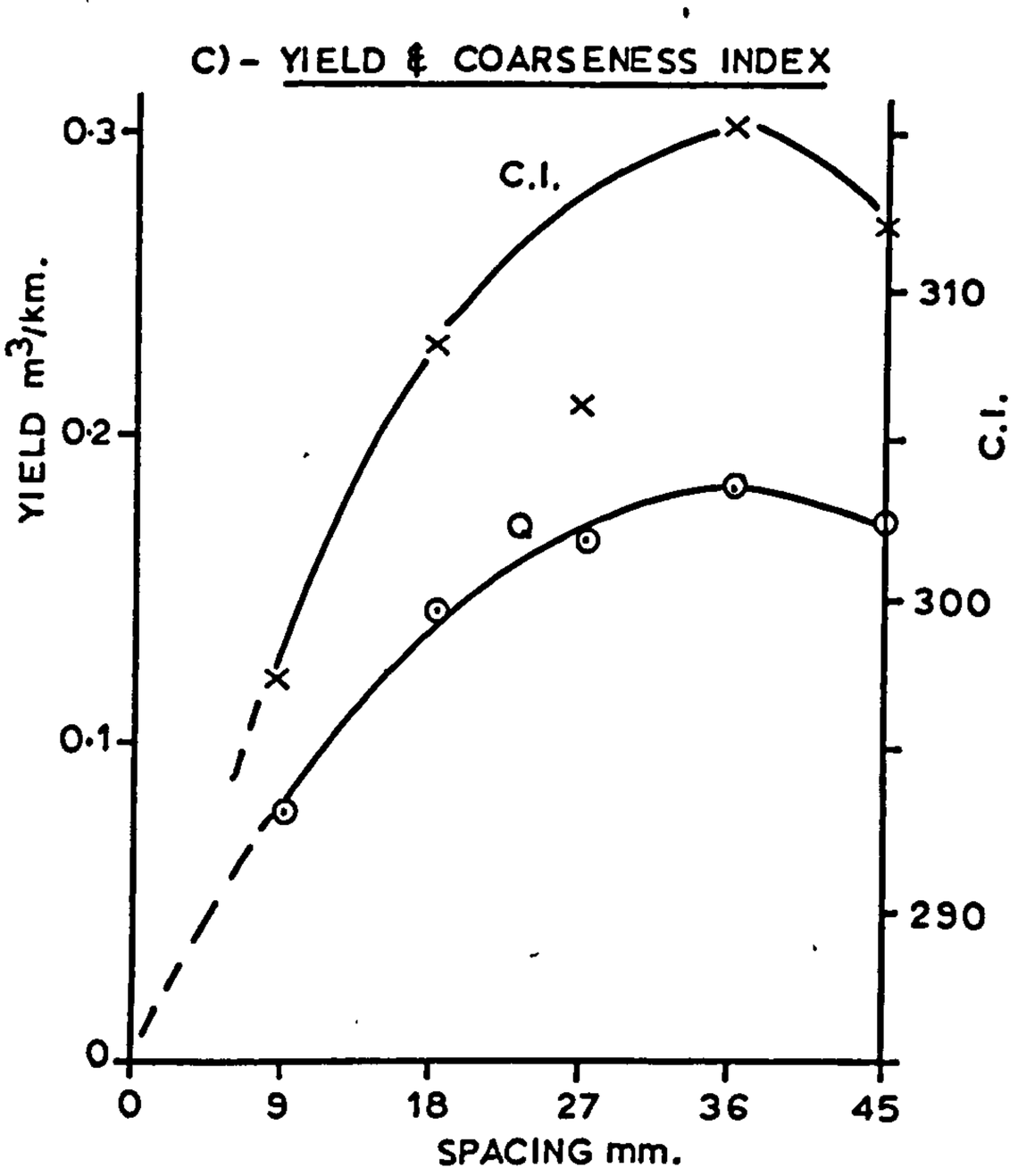

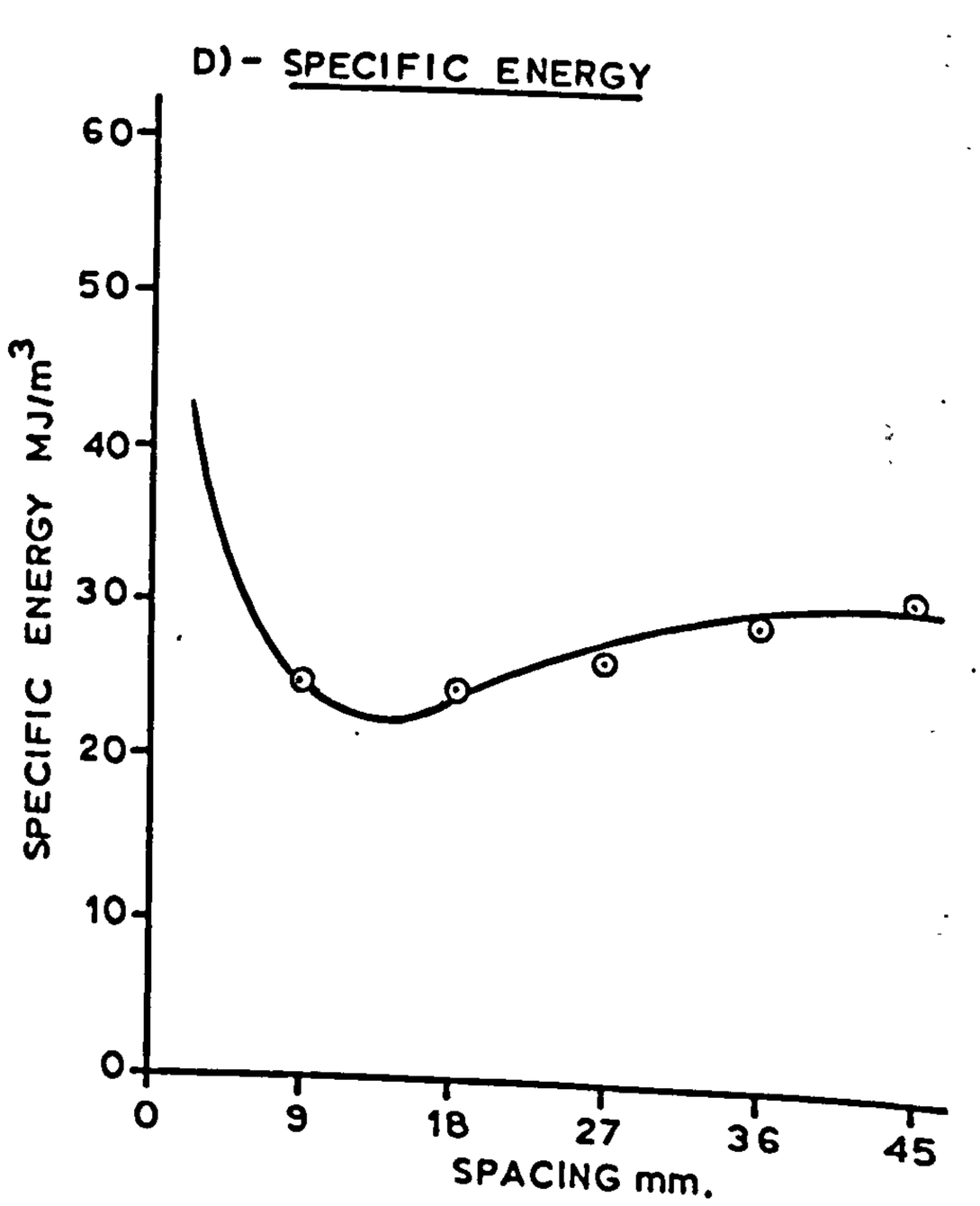

FIGURE 66 – EFFECT OF SPACING
– WET BUNTER SANDSTONE

1. Effect of Spacing on Disc Forces

Figures 65, 66 and 67 show the effect of spacing on all measured parameters. It is reasonable to expect all forces to be zero at zero spacing, which is equivalent to a disc cutting exactly in the shadow of the tool producing the relieving groove.

As spacing increases from this limiting situation so do thrust and rolling forces. Initially the rate of increase in force is high but, as the spacing becomes larger, the forces all tend towards a constant value. In Bunter Sandstone this is reached, for both moisture conditions, at a spacing of between 40 and 50mm, beyond which interaction ceases and the disc is effectively operating in isolation. It should be emphasised that this limit of interaction at 40 to 50mm is peculiar to the mean depth of penetration, which was 6mm. In Magnesian Limestone the limit occurs at spacings of between 30 and 40mm, for a mean depth of cut of 4.5mm. The s/p ratio for this cut-off point lies, for both rocks, between 6.6 and 8.8.

2. Effect of Spacing on Rock Yield

Yield increases rapidly with spacing but, unlike force, reaches a maximum value before decreasing to a stable level. It is of considerable importance to recognise that this maximum yield is significantly and consistently higher than the equivalent yields obtained in unrelieved cutting. Furthermore it was observed, whilst undertaking the experiments, that when unusually large quantities of rock were produced the debris consisted of slabs of rock. The width of the parallel sides of these slabs was measured and found to equal the spacing between adjacent tools. This observation will be further analysed in Chapter 10.

3. Effect of Spacing on Specific Energy

All three curves of specific energy against spacing conform to the expected shape. The large yields produced at spacings of up to 7 times the depth of penetration create a broad trough in the energy curve. Optimum spacing is, therefore, difficult to define accurately, but occurs at an s/p ratio of between 5.5 and 7. The improvement in specific energy at optimum spacing is of the order of 30%.

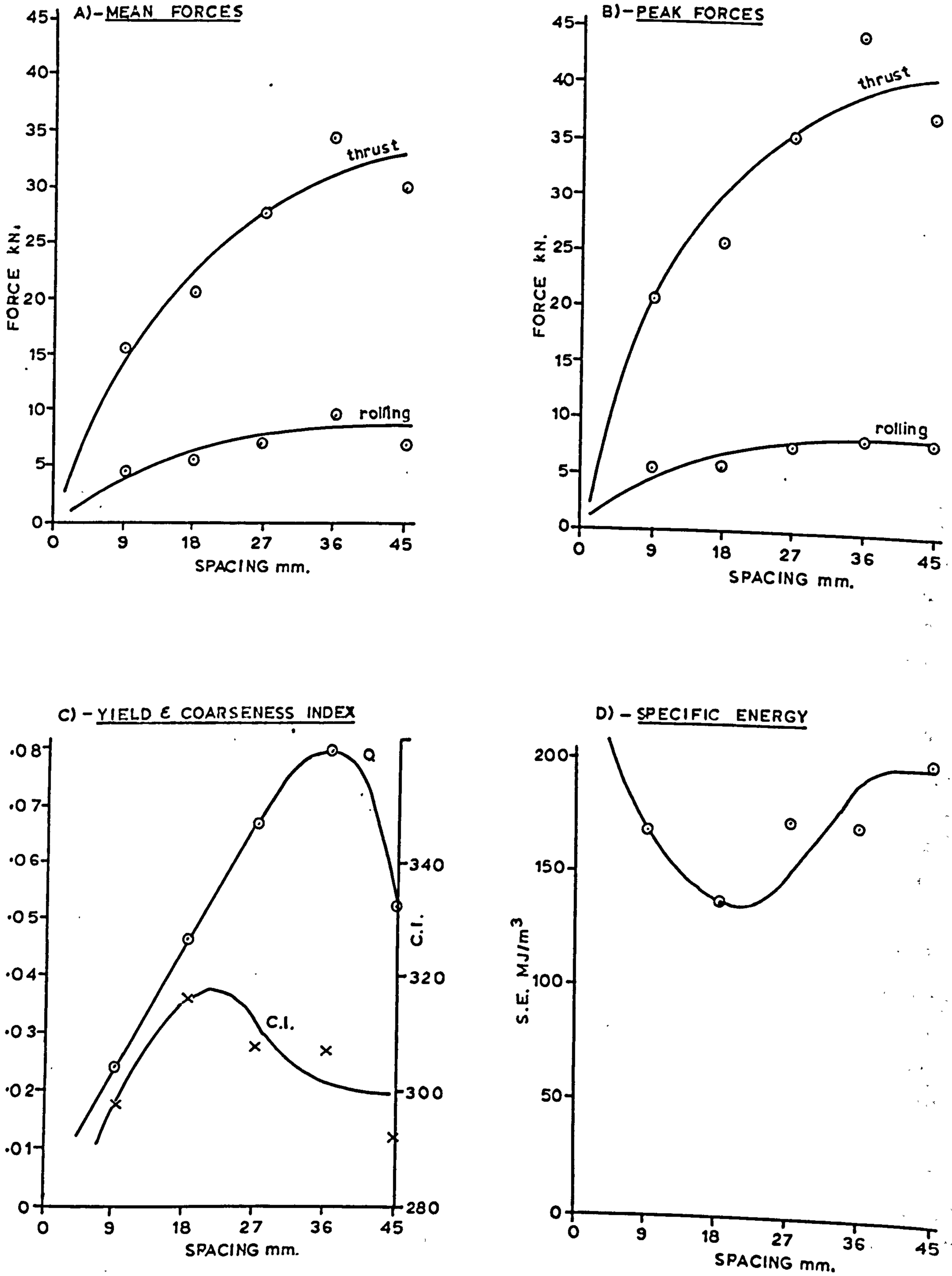

FIGURE 67 – EFFECT OF SPACING
– MAGNESIAN LIMESTONE

Empirical equations for all six disc experiments have been derived by the method outlined in Chapter 5. These, together with the appropriate constants, are given in Appendix IX.

9.4 Stalled Discs

These tests, which were only undertaken in dry Bunter, used a 60^{o} disc of 200mm diameter. One series was performed in the unrelieved condition and another at a constant spacing-penetration level of 5. The full results are tabulated in Appendix X.

Figure 68 shows the effect of stalling the disc on thrust and rolling forces. Although all forces increase with penetration, the thrust requirement for a stalled disc is considerably lower than for the free rolling condition. Conversely, the rolling force is significantly higher with the stalled tool.

The behaviour of the stalled disc seems, therefore, to resemble that of a pick, albeit an inefficient one. Indeed, when stalled, the disc can be likened to a pick having either a vee-bottom angle operating with a curved negative clearance or a ridged front of very high negative rake, the value of which varies according to penetration. With this analogy, thrust force is equivalent to pick normal force and rolling force becomes cutting force. Thrust force, when translated into a normal force, can be expected to fall because the new edge presented to the rock surface during rotation is not now required to be forced into the surface. As a normal force, it is merely required to hold the "pick" at its prescribed depth of cut. The force will of course be higher than for a normal pick due to the negative curved clearance, which will give a higher tendency for the tool to climb out of the rock. On the other hand, rolling force being replaced by a cutting force, shows significant increase for stalled cutting.

Figure 69 shows that in the relieved cutting situation the change of disc behaviour when stalled is the same.

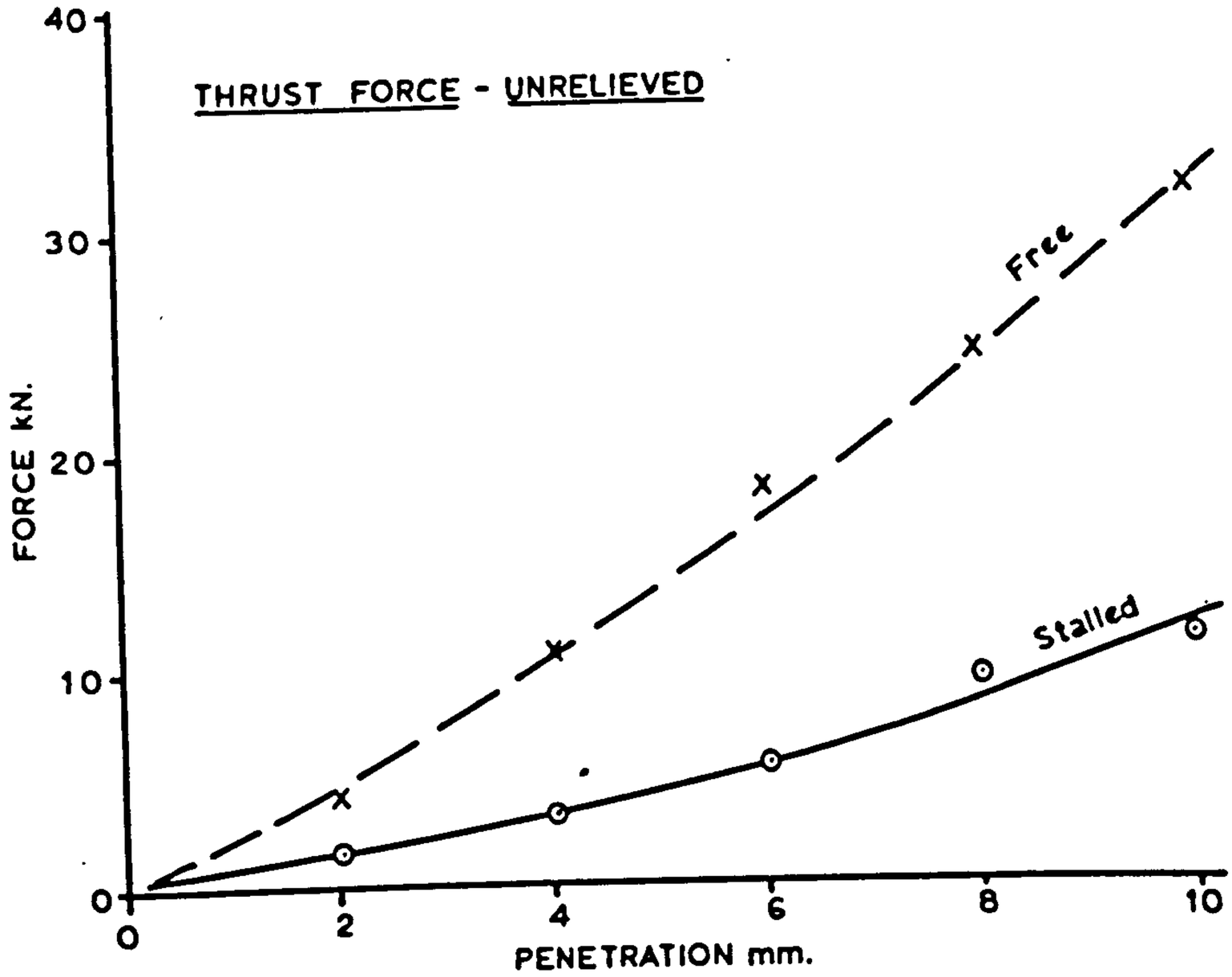

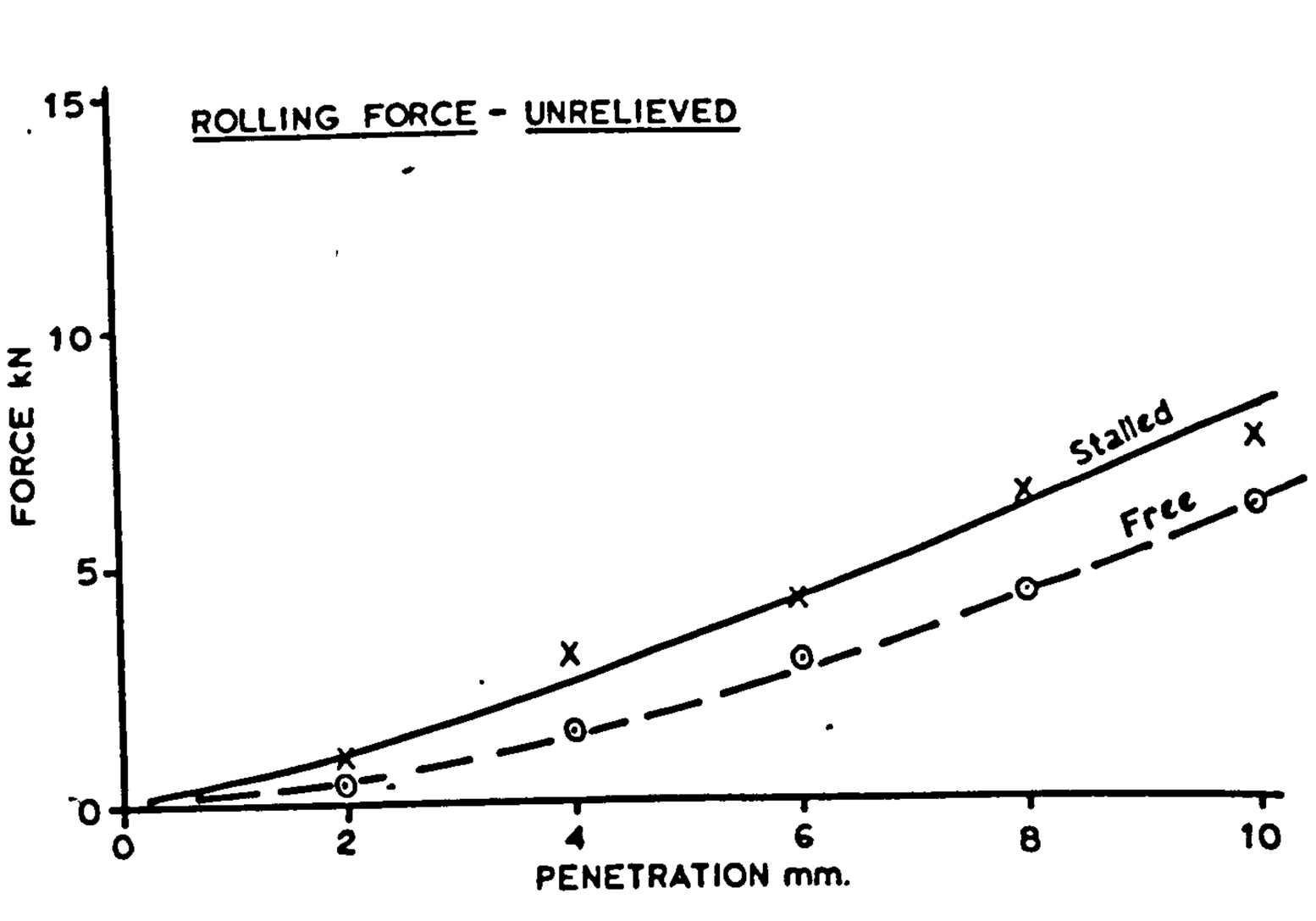

FIGURE 68 - EFFECT OF STALLING DISC ON FORCES (UNRELIEVED)

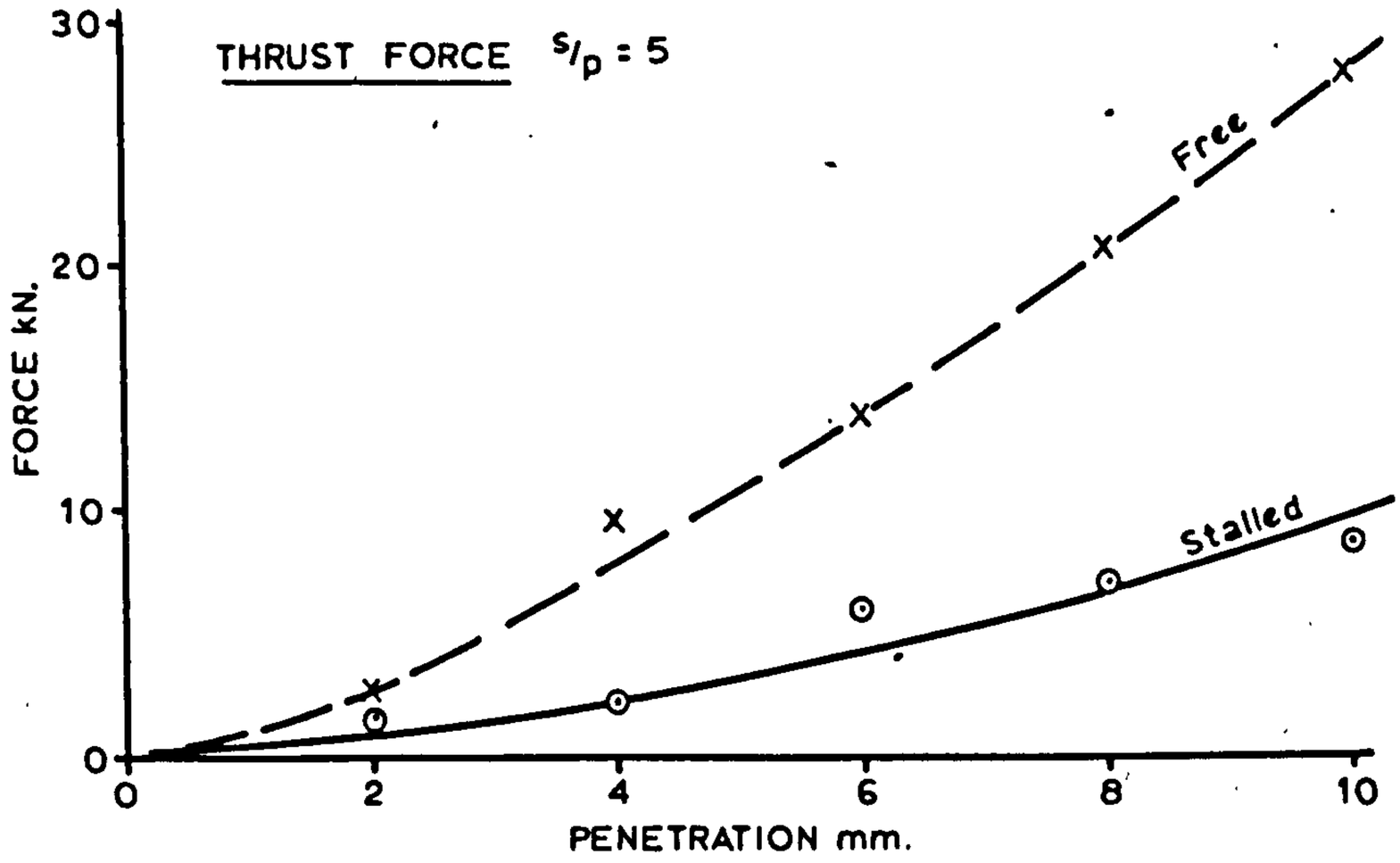

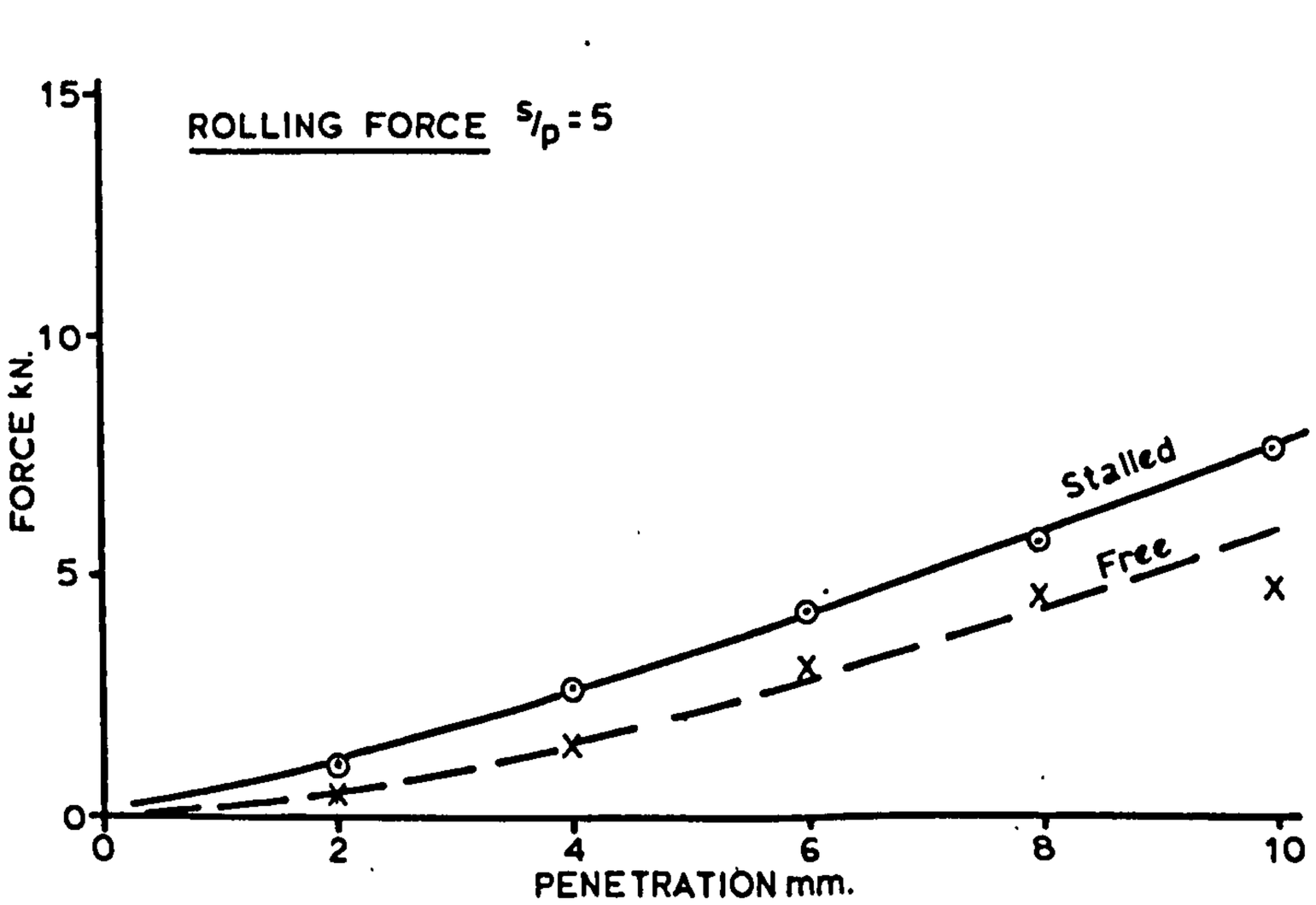

FIGURE 69 – EFFECT OF STALLING DISC ON FORCES (RELIEVED)

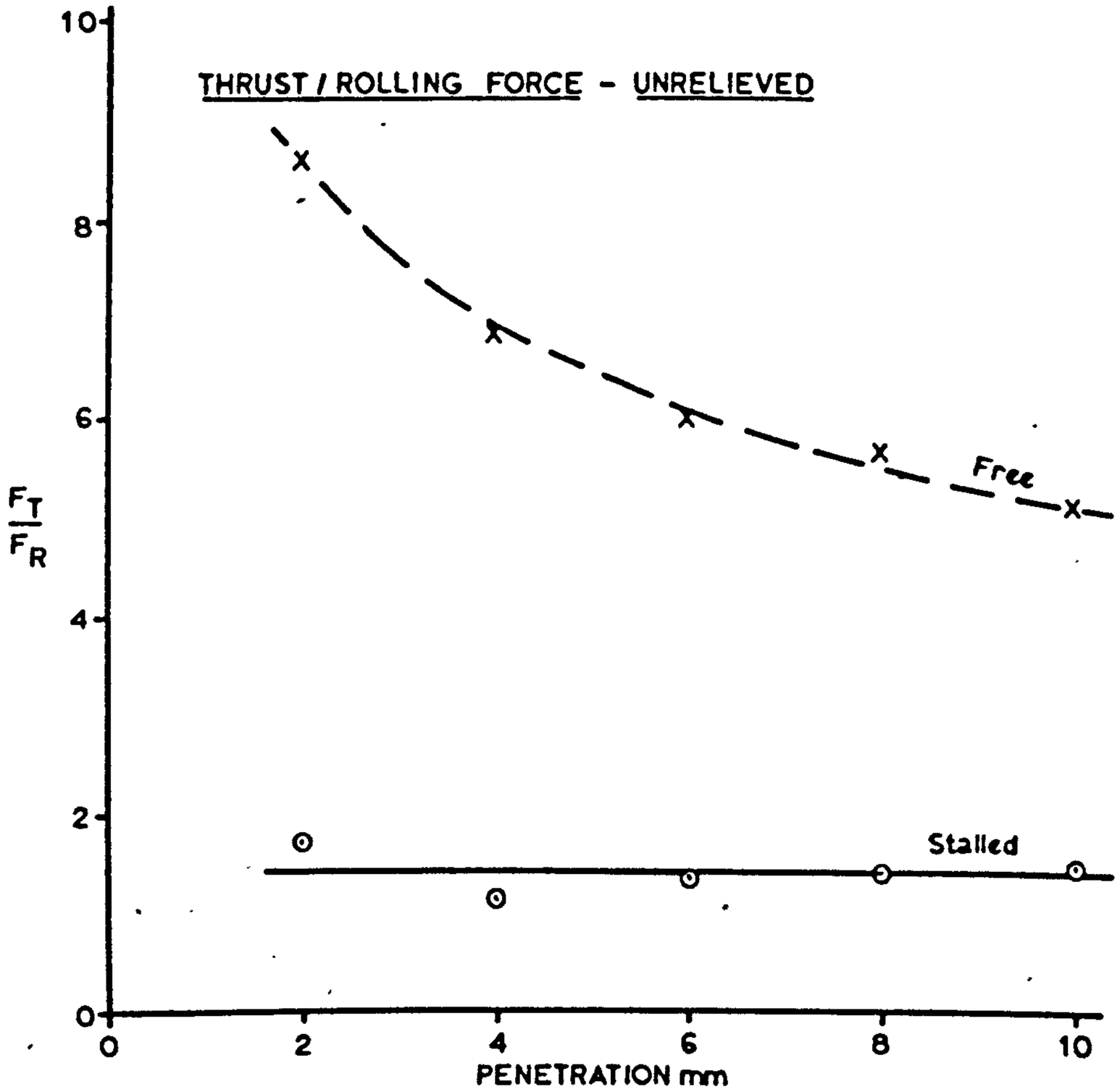

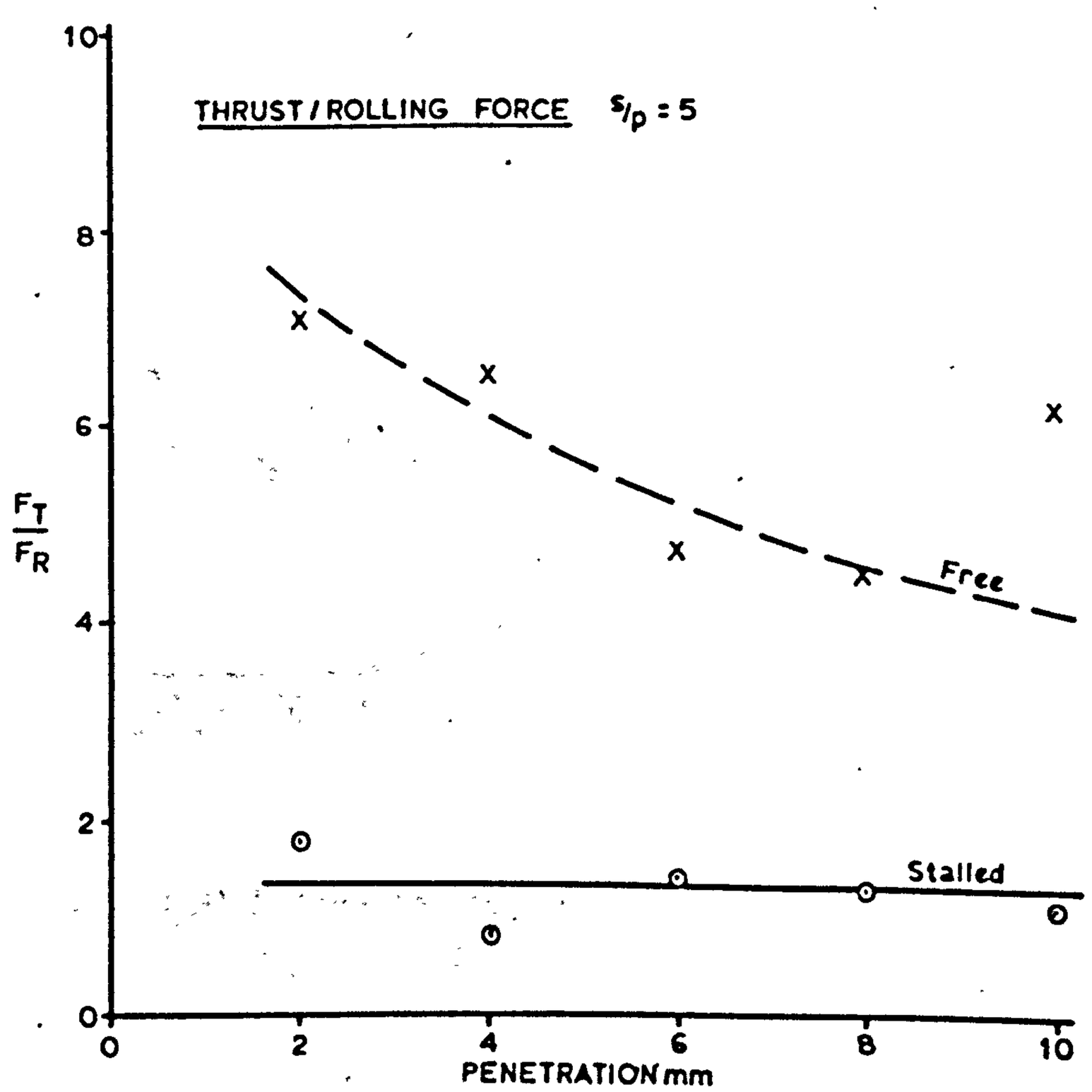

FIGURE 70 - STALLED DISC EFFECT ON $\frac{F_I}{F_R}$

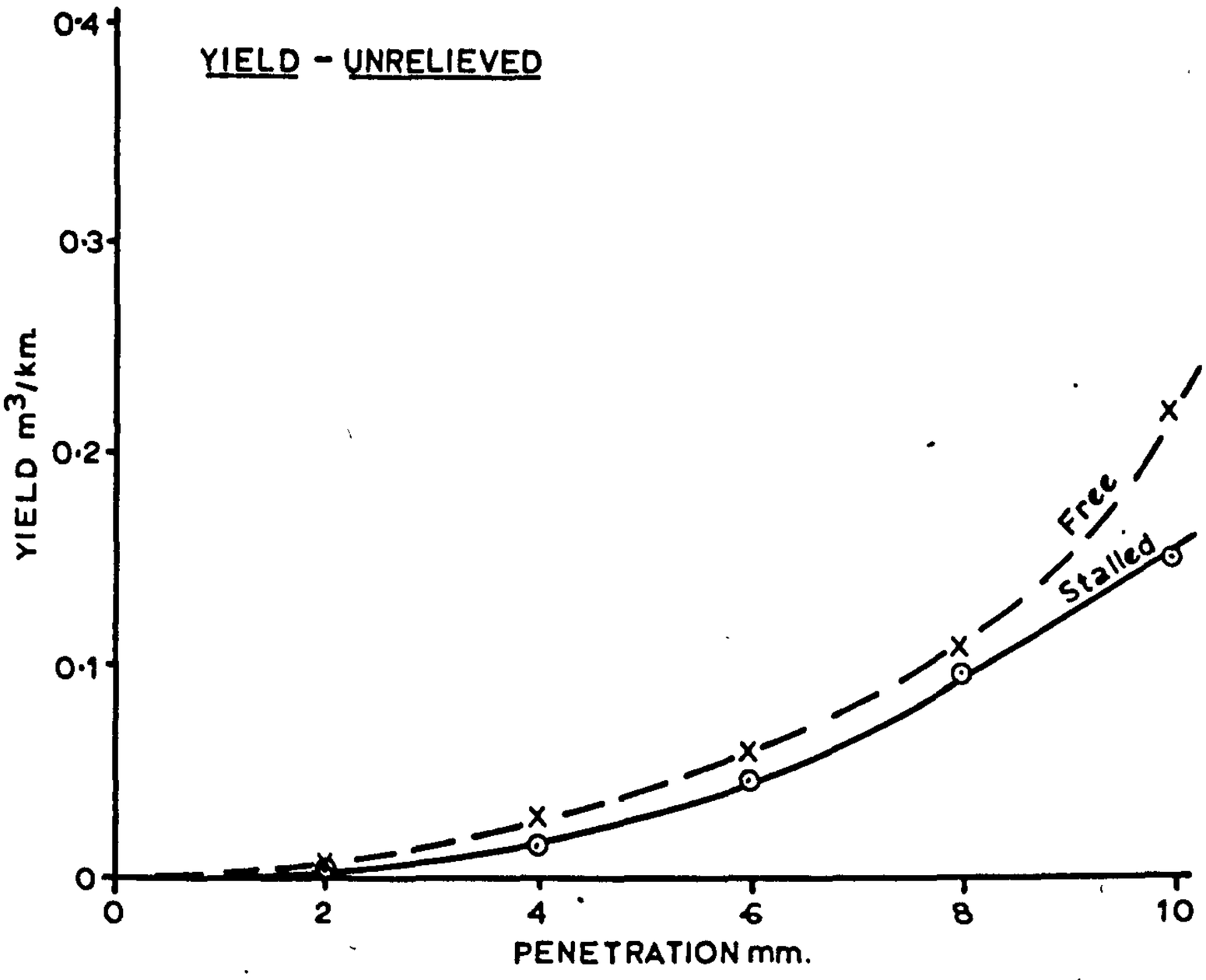

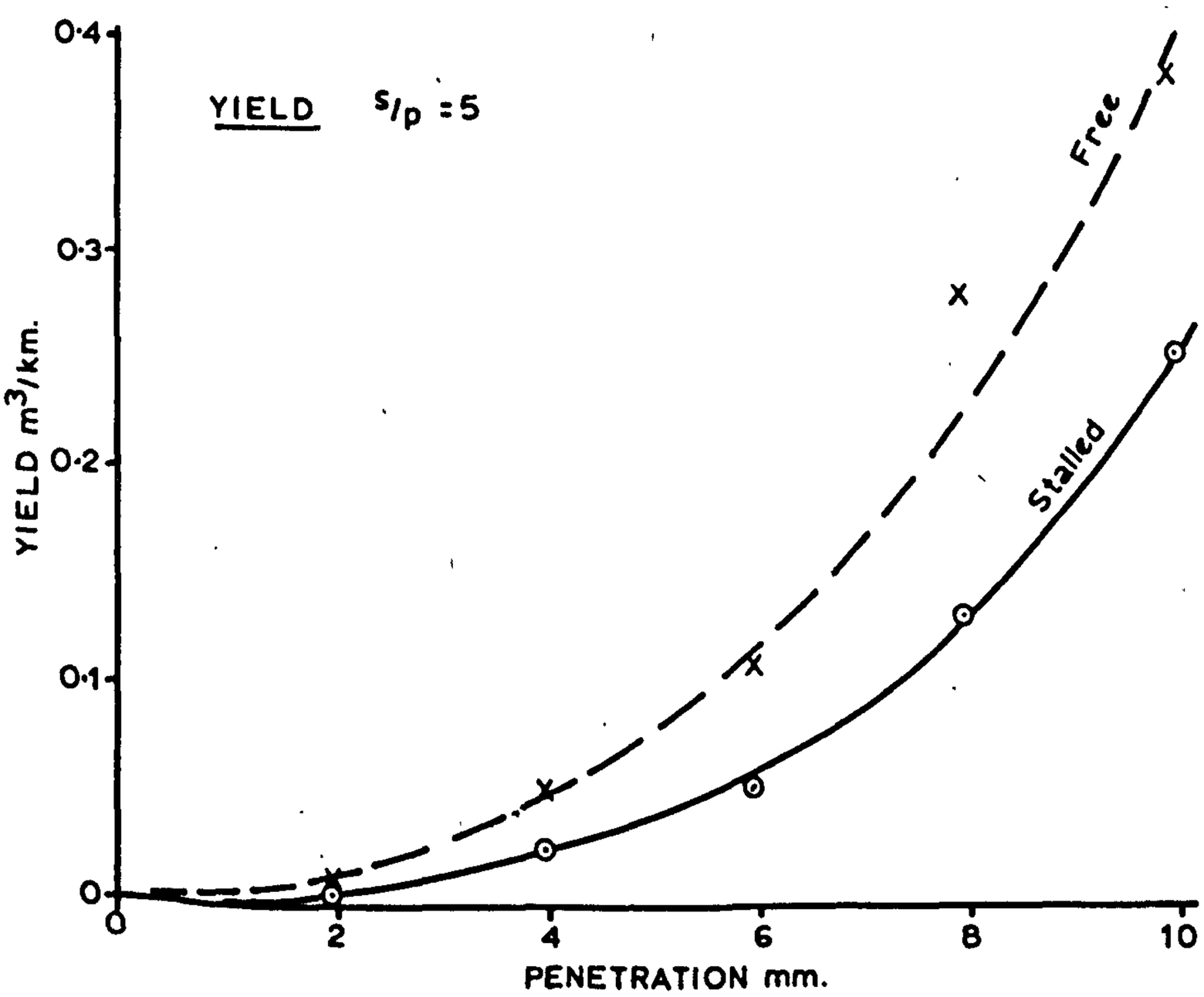

FIGURE 71 - EFFECT OF STALLING DISC ON ROCK YIELD

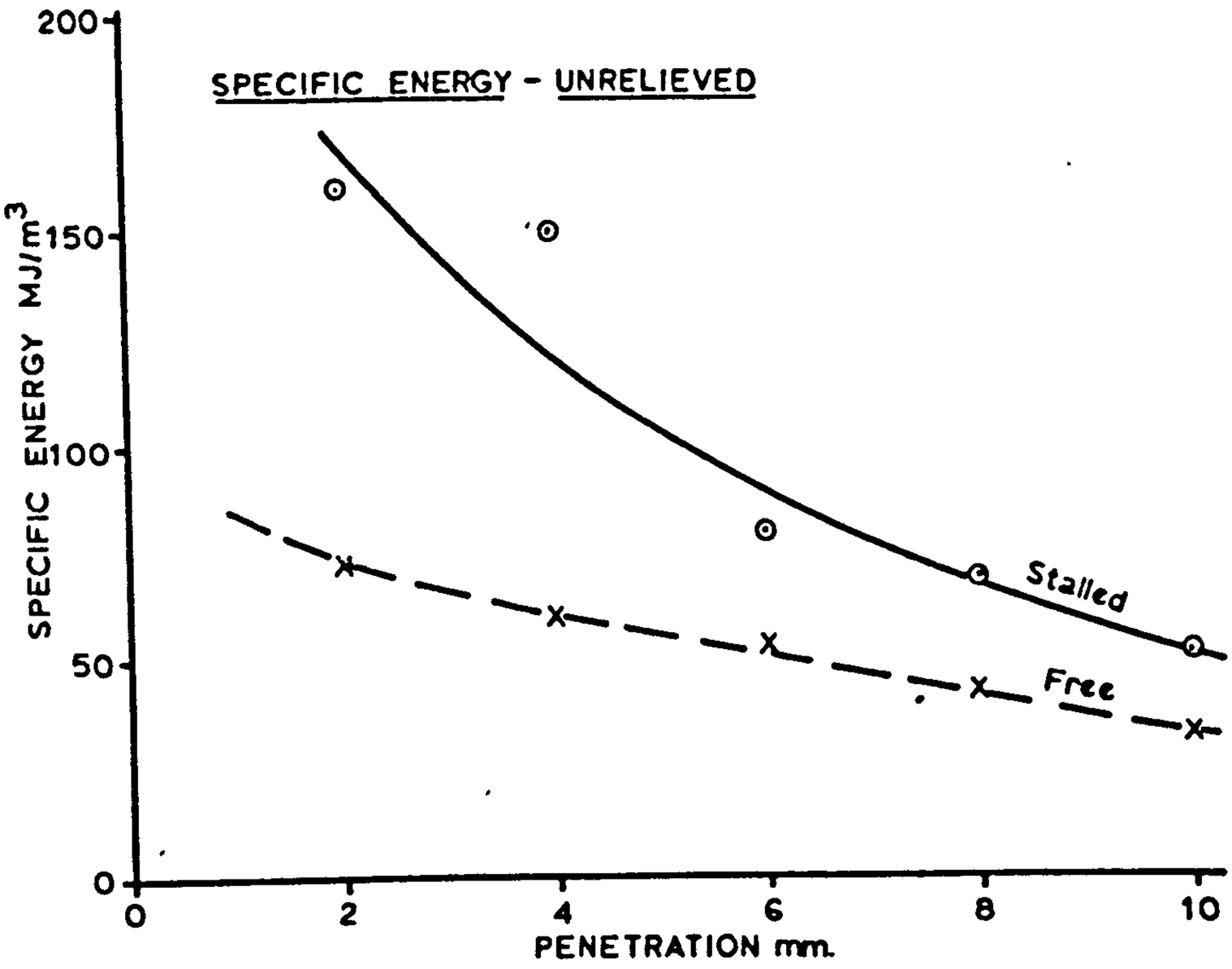

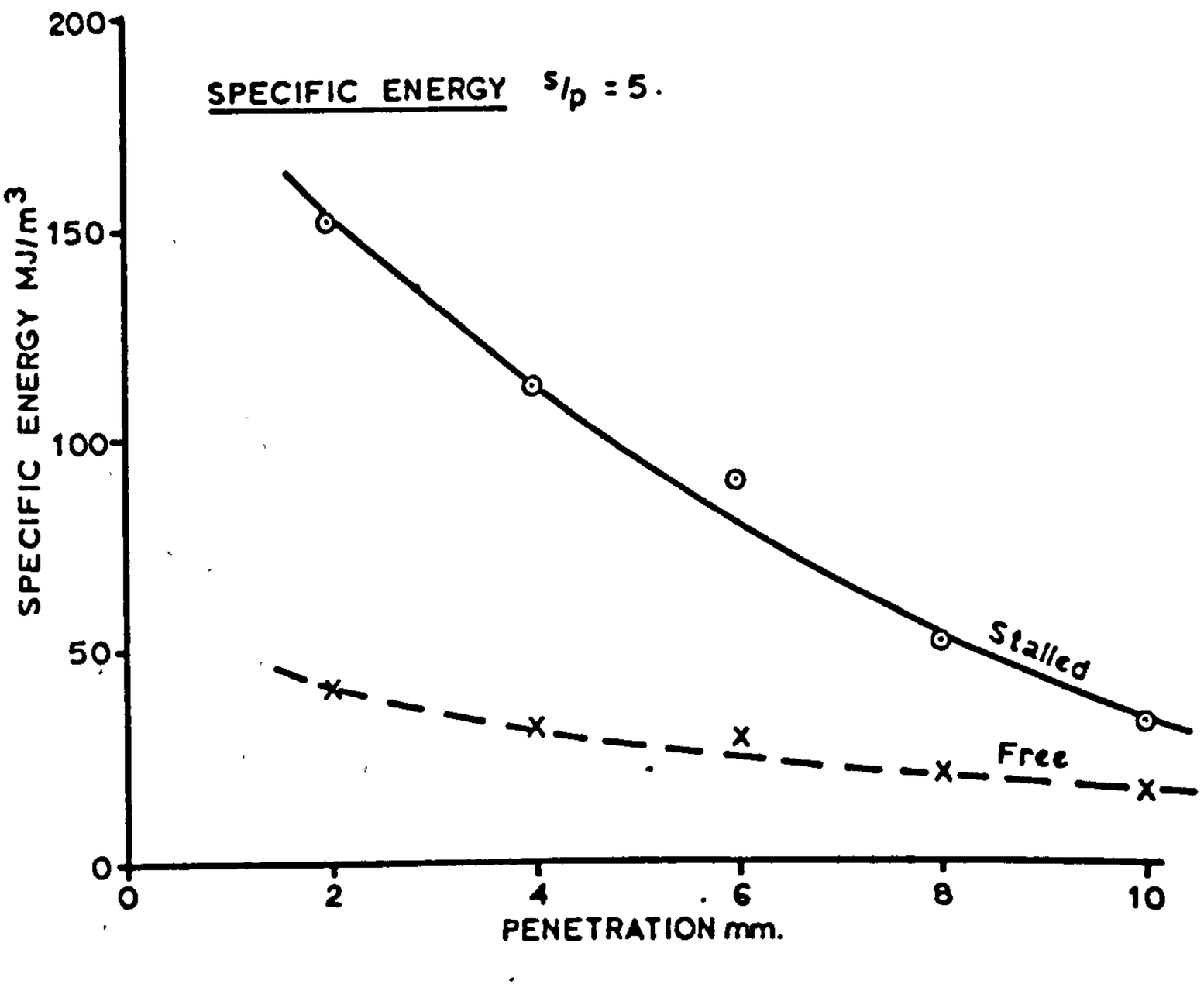

FIGURE 72 - EFFECT OF STALLING DISC ON ENERGY

It is of interest to note at this juncture that the traditionally low peak to mean force ratio for rolling discs which averaged 1.21, increased to 1.52 when the disc was stalled, which is much more in accordance with the value for pick cutting.

The thrust-rolling force ratio for normally functioning discs is always found to be high. Again, as shown in Figure 70, this ratio assumes values ranging from 4 to 8 according to penetration and state of relief. On the other hand the same ratio for stalled discs, which is now equivalent to the normal-cutting force ratio, is very much lower and seen to be independent of penetration level. This is also in accordance with expected pick behaviour, but the ratios are higher than for a sharp pick. The effect of tool wear, however, as was shown in Chapter 7, is to cause an increase in this ratio. Since the effect of wear is to produce a negative clearance, the similarity between a badly worn pick and a stalled disc is readily appreciated.

The respective rock yields for stalled and free discs are shown in Figure 71. In all cases there is a quadratic relationship between yield and penetration. The stalled disc, however, cuts less rock than the free rolling tool and as expected more rock is produced in the relieved cutting situation.

These different yields when related with the appropriate rolling and cutting forces, produce the specific energies given in Figure 72. It is these graphs which emphasise the gross inefficiency of operating discs in a stalled condition. In some cases, energies are in excess of 150 MJ/m^3, which is something like 25 times greater than an "average" pick at the same cutting depth or 2 to 3 times greater than the same disc rolling freely.

9.5 Roller Cutters

These tests were all undertaken using one cutter. This was constructed from mild steel, which was subsequently treated to achieve a surface hardness of 60 RC.

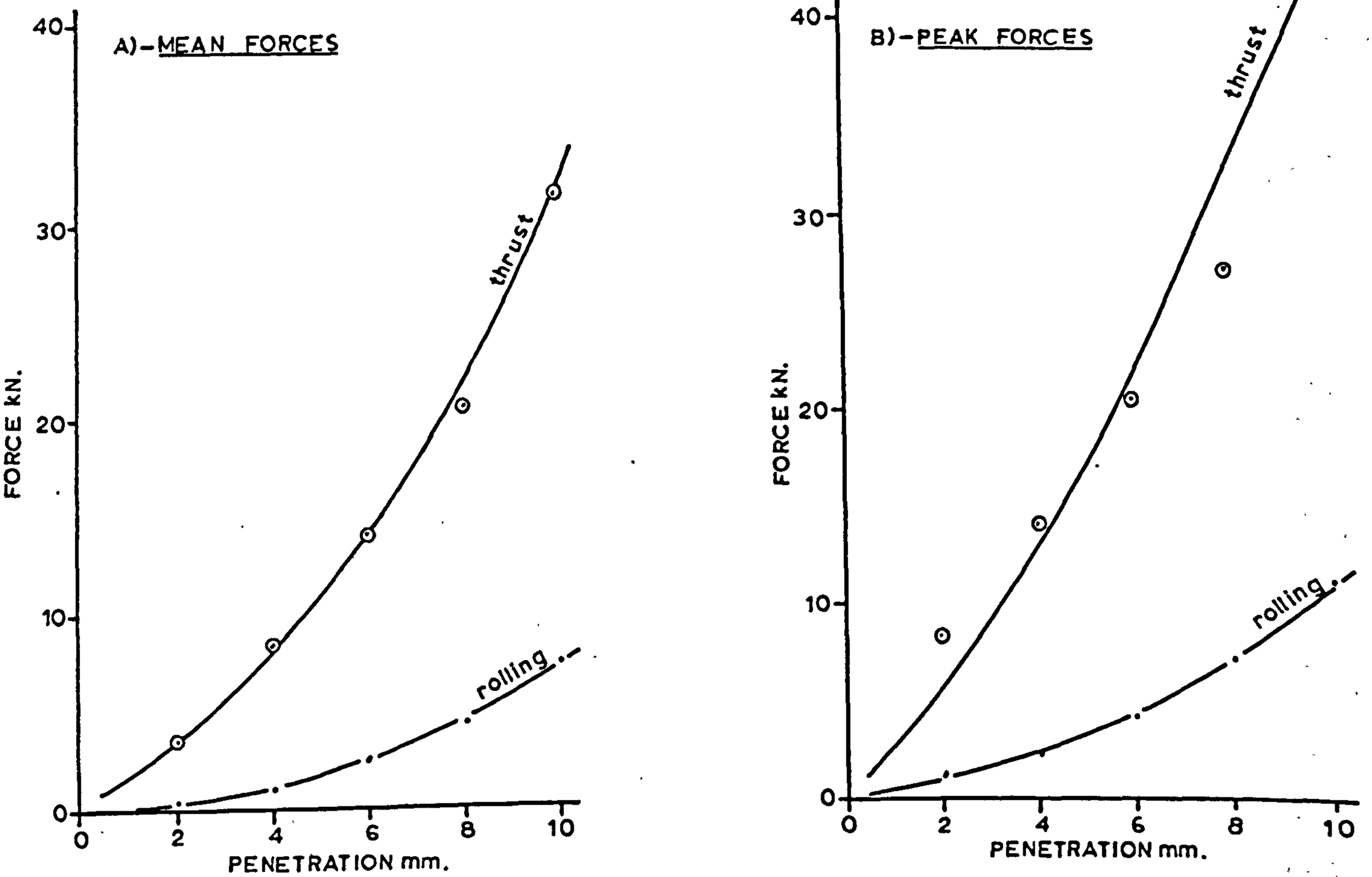

FIGURE 73 – EFFECT OF PENETRATION FOR A ROLLER CUTTER IN BUNTER SANDSTONE

During the relieved and unrelieved cutting tests in dry Bunter the tool showed no significant signs of wear. However, when cutting Magnesian Limestone, the stress concentrations at the apeces of the teeth werehigh enough to cause the metal to flake.

As the roller cutter was so badly damaged by the unrelieved cutting, no spacing tests were undertaken in Magnesian Limestone.

The results of all tests are given in Appendix XI.

1. Unrelieved Cutting

The thrust and rolling forces, as can be seen from Figures 73 and 74, increase rapidly with penetration. The relationship is not linear and appears to be governed by a square law. For the range of penetrations studied the force curves are continuous, but a roller cutter has a maximum reach beyond which the roots of the teeth come into contact with the surface of the rock. At this point the force curves will be discontinuous. The tool tested had a reach of 18mm which was well above the maximum penetration attempted.

At shallow penetrations each tooth is only briefly in contact with the rock and U.V. traces of these cuts show a series of abrupt peaks as each tooth touches the rock. As penetration increases so the duration of these peaks becomes longer. This is reflected in an analysis of ratios of peak to mean forces.

These ratios are much higher than the equivalent values for disc cutters and are more akin to those obtained for drag picks.

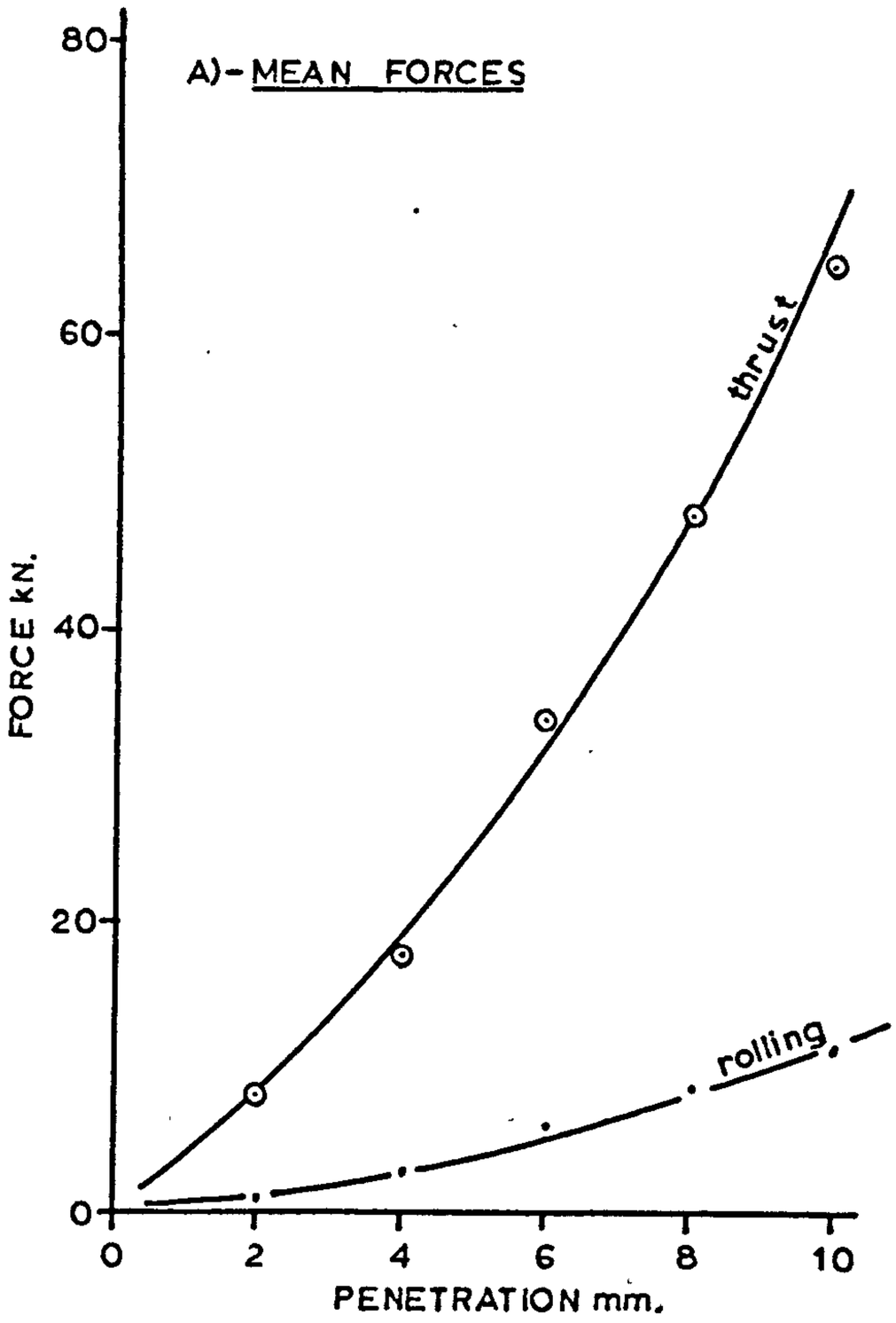

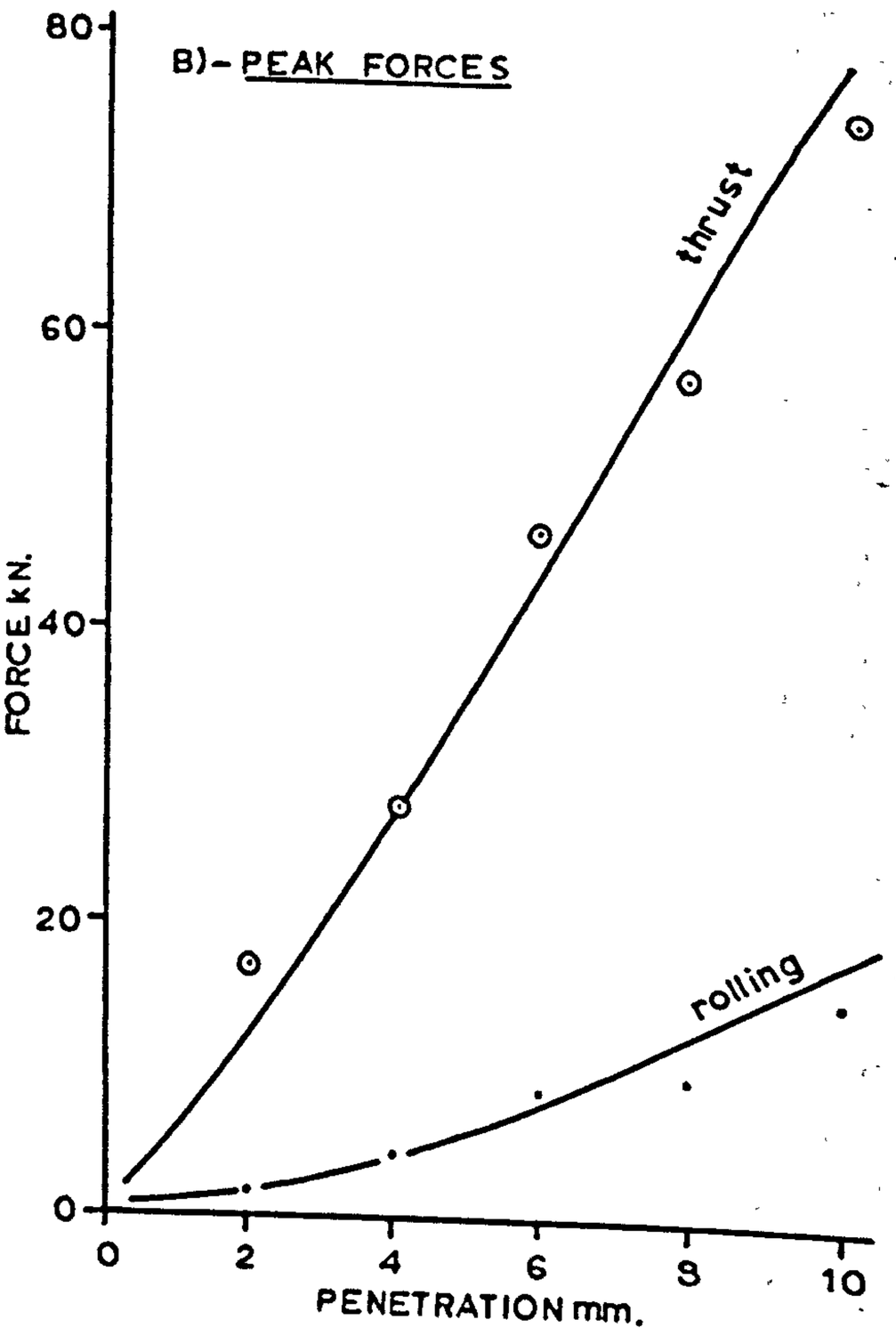

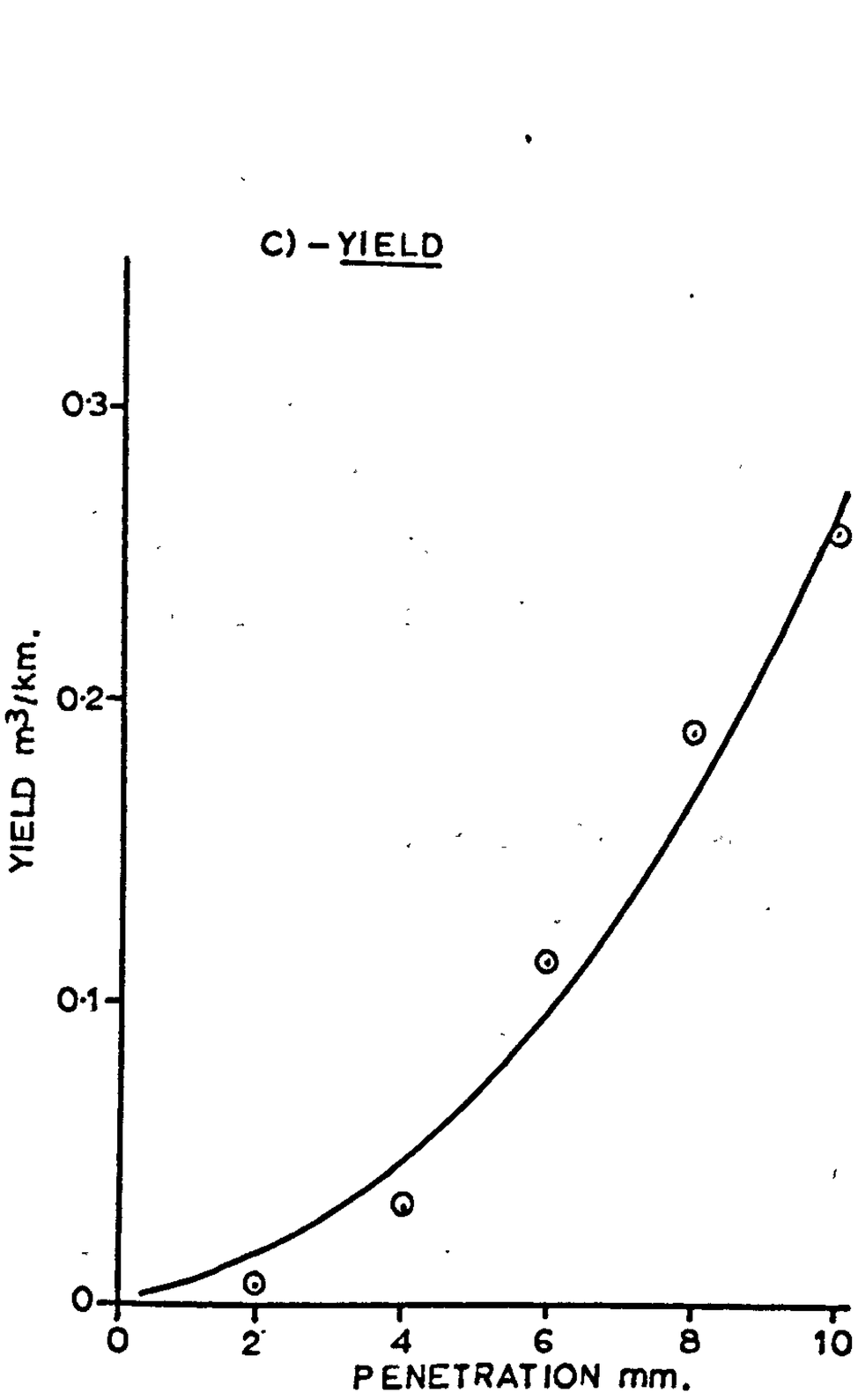

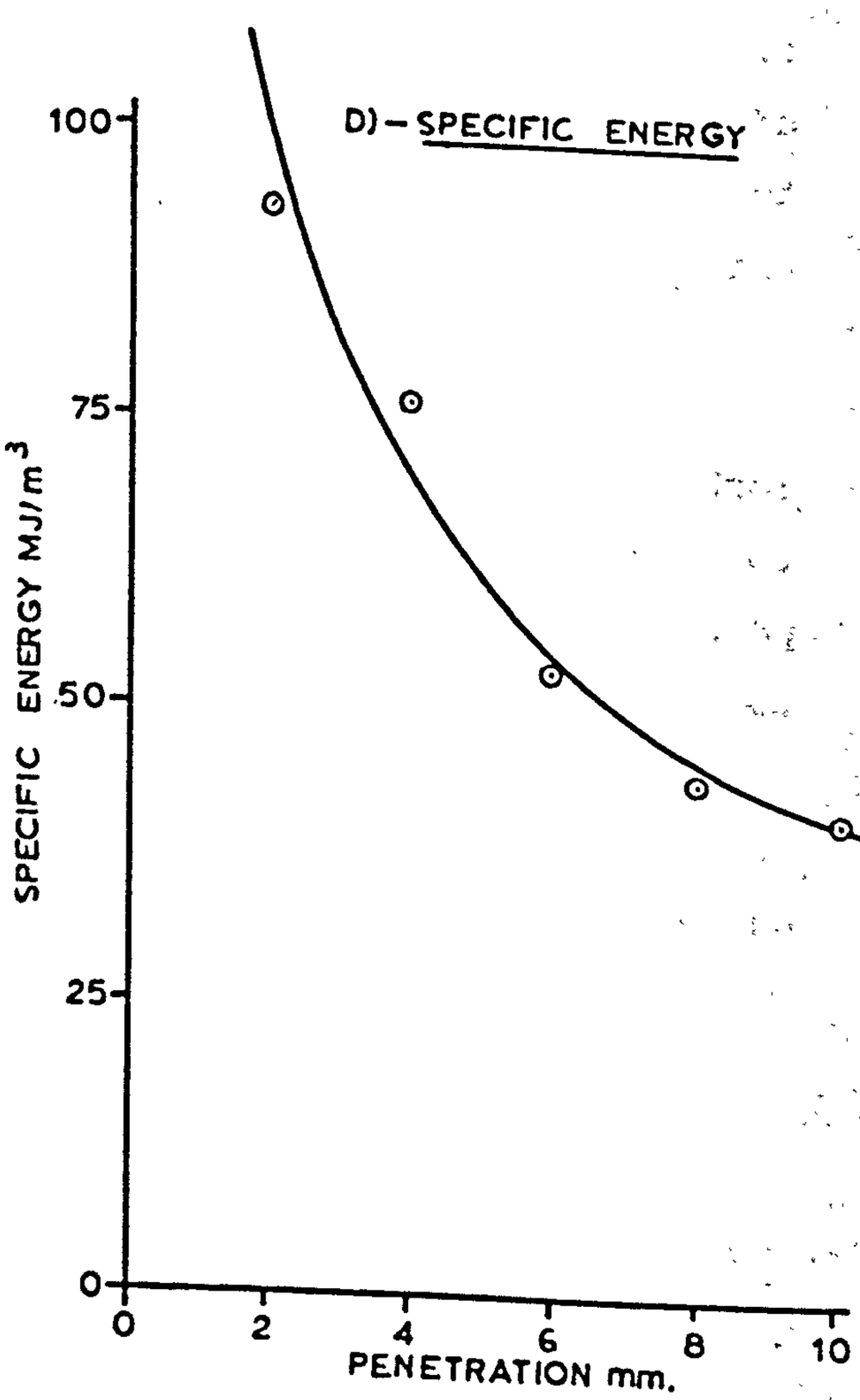

FIGURE 74 – EFFECT OF PENETRATION FOR A ROLLER CUTTER IN MAGNESIAN LIMESTONE

TABLE 32

RATIOS OF PEAK TO MEAN FORCES - ROLLER CUTTER

Penetration mm	Bunter		Magnesian Limestone	
	Thrust	Rolling	Thrust	Rolling
2	2.22	2.75	2.13	2.84
4	1.72	1.91	1.57	1.85
6	1.48	1.69	1.37	1.45
8	1.31	1.66	1.20	1.16
10	1.35	1.55	1.13	1.49

Yield, as may be anticipated, increases with the square of penetration. The breakout angle could not be calculated since the tests undertaken did not produce a continuous groove but rather a series of cavities were excavated in the rock. It was observed, however, that the breakout on either side of the tool was small. This is to be expected since, in the case of roller cutters, the thrust force cannot have any lateral components.

At shallow penetrations the volume of rock excavated was no greater than the volume swept by the tool, but as penetration increased more rock was broken in front of, and behind each tooth. It is obvious that for maximum cutting efficiency the penetration should be large enough to cause the excavated cavities to break into each other.

The specific energy curves show that although the improvement in efficiency is most marked at the lowest levels of penetration, specific energy may be expected to continue to fall at penetrations beyond the experimental range.

2. Relieved Cutting

The definition of spacing adopted for roller cutters is the same as that for drag picks. This is illustrated in Figure 25 of Chapter 7.

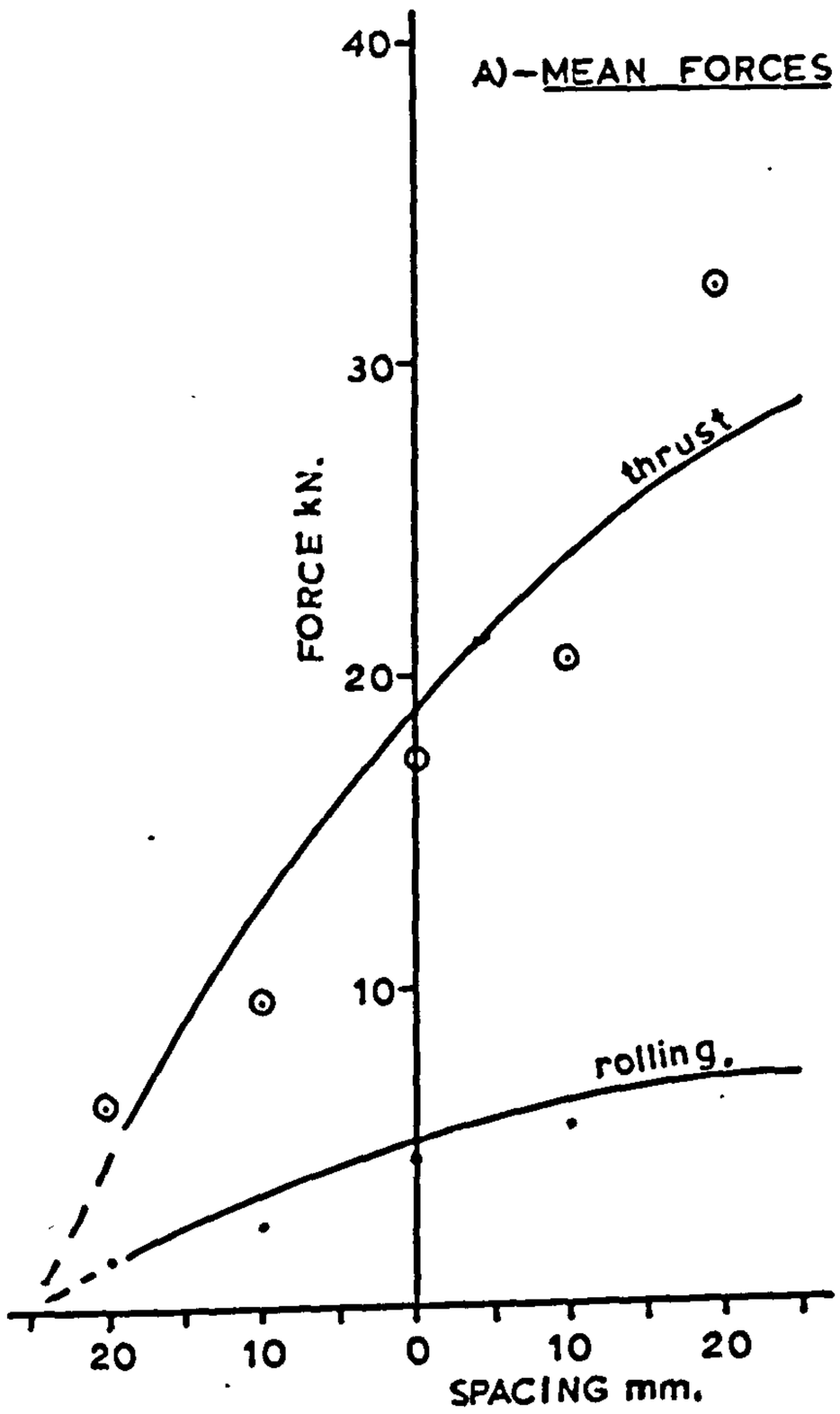

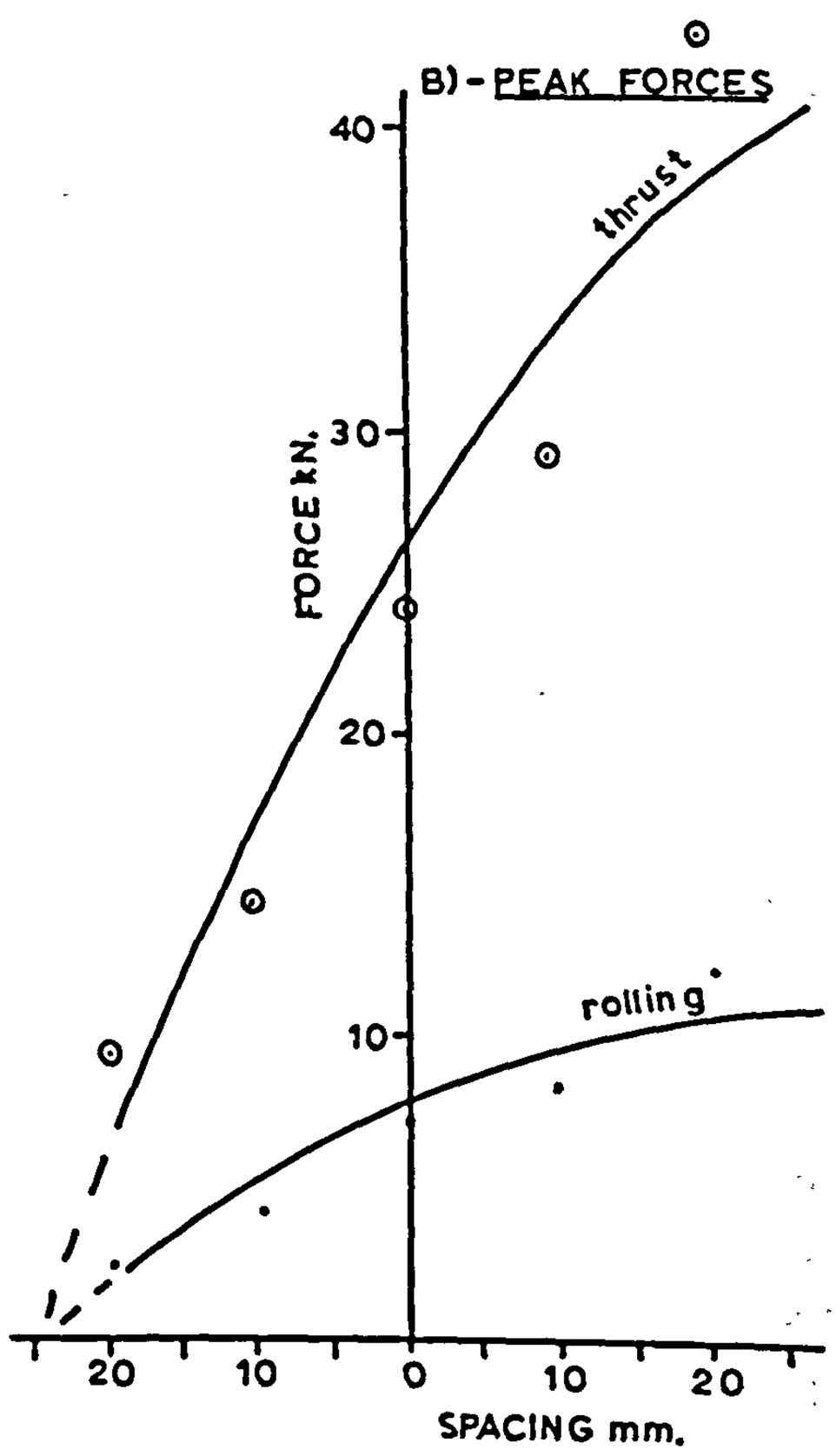

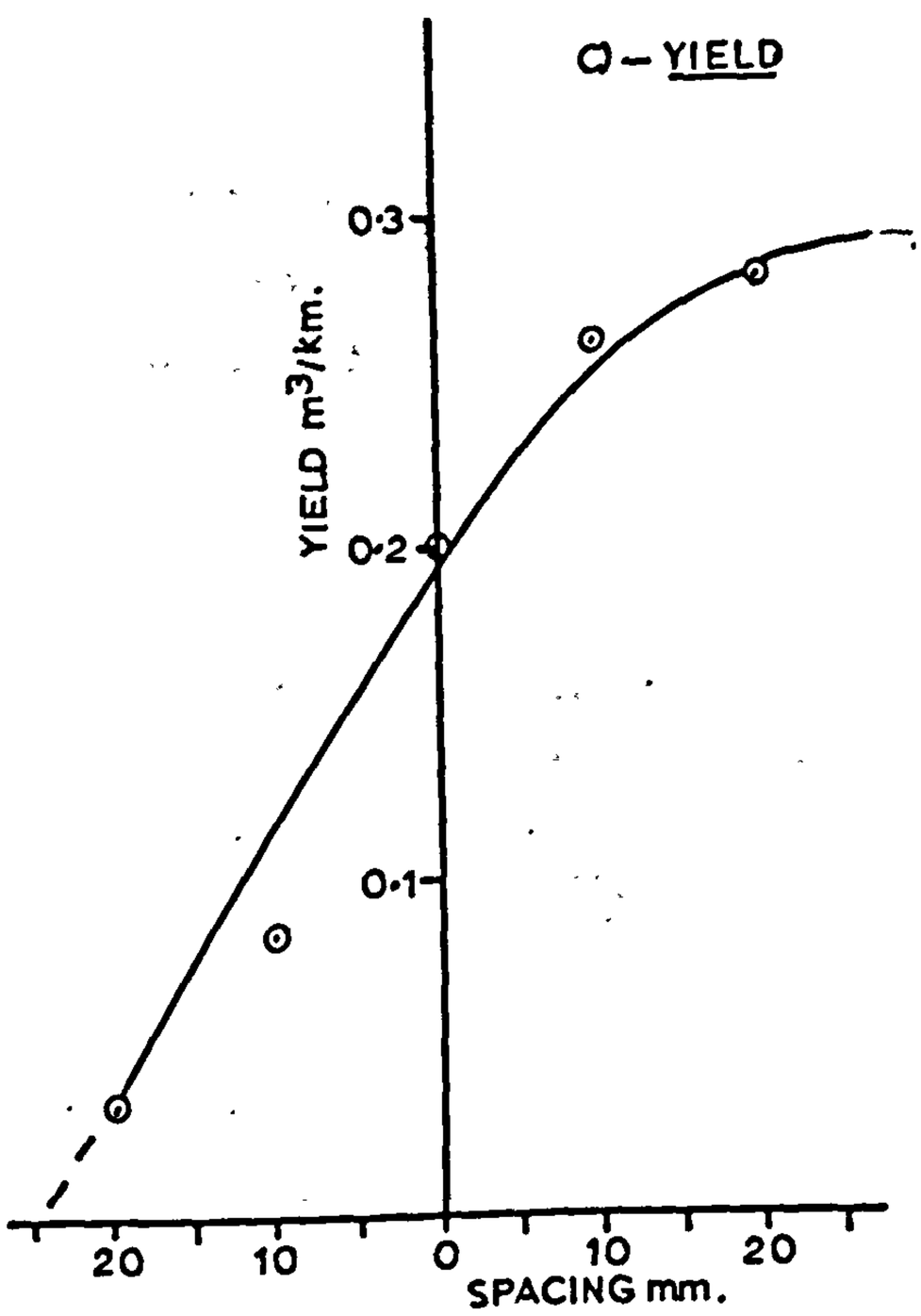

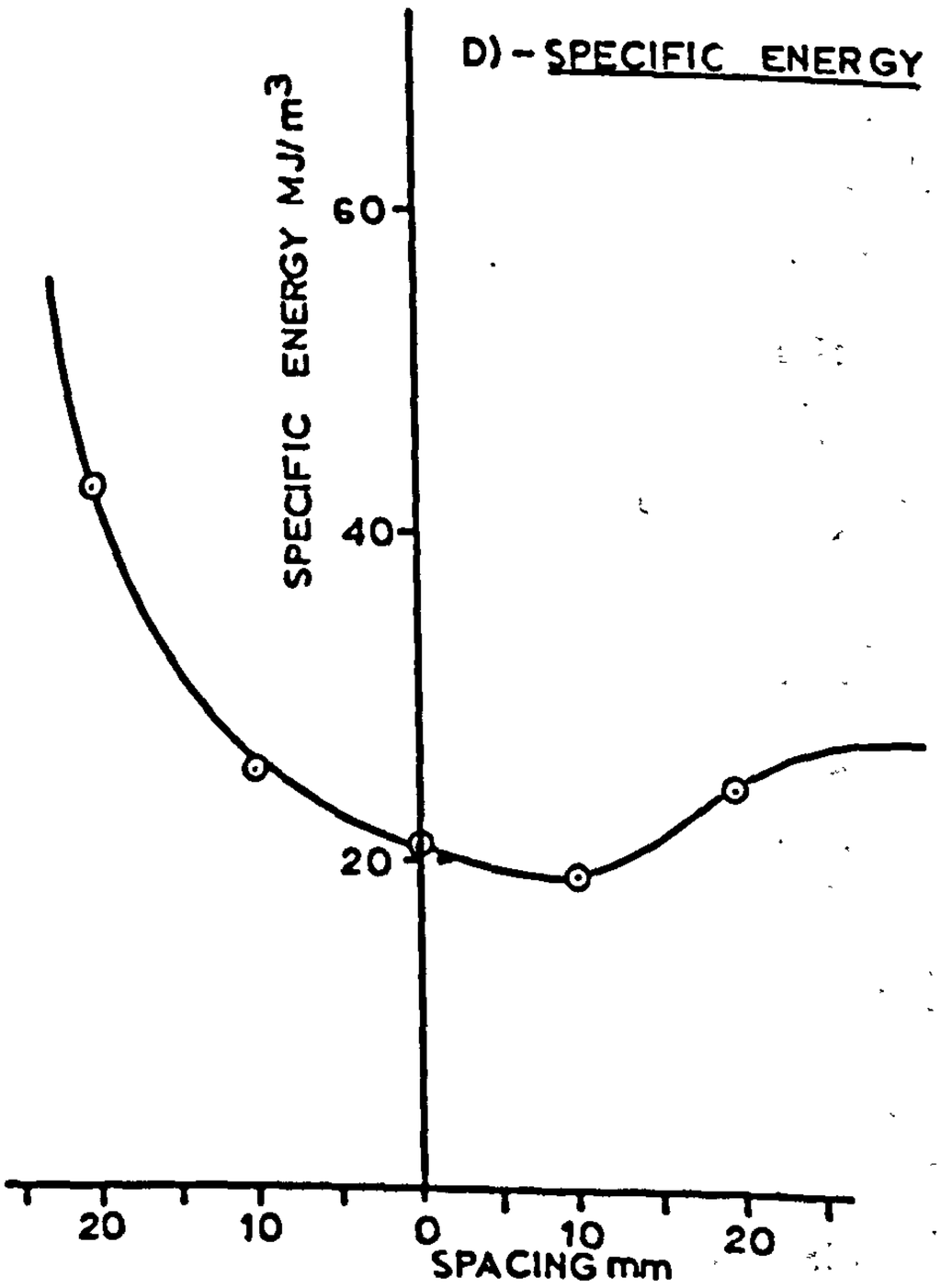

FIGURE 75 — EFFECT OF SPACING FOR A ROLLER CUTTER IN BUNTER SANDSTONE

Although no attempt was made to position the teeth of the roller cutter at the start of each spacing cut, it was observed that as the tool travelled through the rock it rotated in such a way that points of maximum penetration in adjacent cuts coincided.

The effects of varying the spacing between tools operating at a penetration of 10mm in Bunter Sandstone are shown in Figure 75.

All forces and yield increase rapidly with spacing until a plateau level is reached. This occurs at a spacing of approximately 20mm. If the angle of breakout is denoted by θ, then

$2p \tan \theta = 20mm$, when $p = 10mm$

Hence $\theta = 45^{o}$

This angle of 45^{o}, when compared with the 70^{o} achieved by picks and discs, again reflects the poor breakout achieved by roller cutters.

The specific energy curve shows that a minimum occurs at a spacing of about 10mm. This spacing/penetration ratio of 1 is much lower than that for either picks or discs. Hence, for an array of roller cutters to operate at optimum efficiency it must contain many more tools than an array of discs cutting at the same penetration.

10 SOME THEORETICAL ASPECTS OF ROCK CUTTING

All data previously presented in this thesis has been the result of experimental work and empirical analysis. There are, however, several theories relating the performance of drag picks to a strength attribute of the material being excavated. The three most widely accepted models are discussed and their theoretical predictions contrasted with the practical results of Chapter 7.

A theoretical model of the action of a disc cutter is developed and compared with the reported experimental data.

10.1 A Summary of Merchant's Theory

This, the earliest of the cutting theories (33), predicts the force required to cut a continuous strip from the plane surface of a block of metal. The geometry of Merchant's model is illustrated in Figure 76.

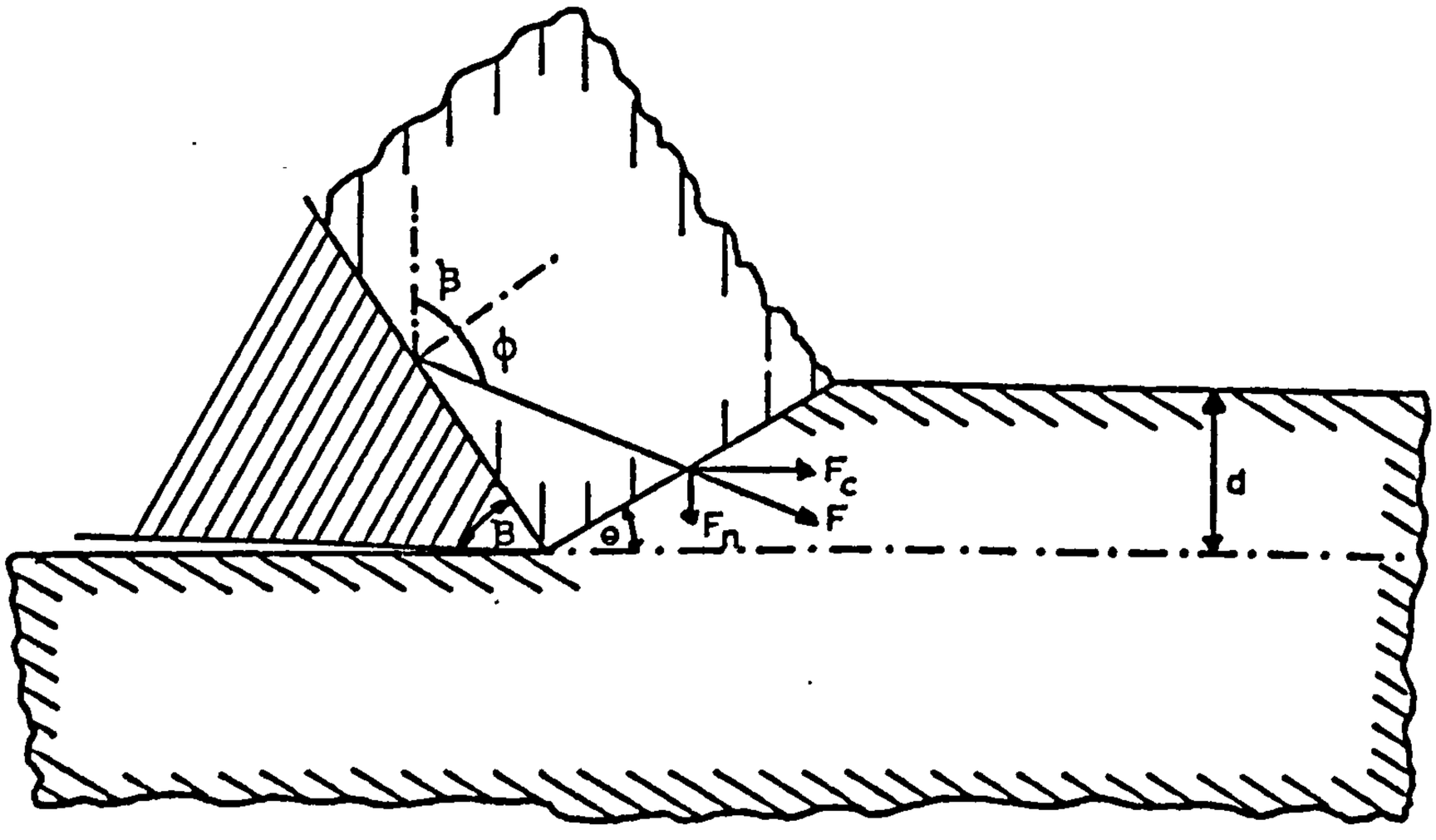

FIGURE 76. ILLUSTRATION OF MERCHANT'S THEORY OF METAL CUTTING

This theory is based on the two assumptions that:-

a) depth of cut will, in general, be small compared with the width of tool and hence a condition of plane strain will exist and b) shear failure takes place over a straight line, rising from the tip of the tool, and making an angle θ with the direction of cutting.

The material being cut is defined by its uniaxial shear strength Ss and by the coefficient of friction between the material and the cutting tool. This acceptance of a single value of shear strength implies the assumption that normal stress across a shear plane has no effect on this parameter. This is known to be untrue in rock.

Merchant achieves his solution by considering the equilibrium of a "chip" lying against the tool. If F is the resultant force exerted on the chip by the tool, with F_C and F_N its components in the cutting and normal directions respectively then

$$\frac{F_N}{F_C} = \cot(\pi - \beta - \phi) = -\cot(\beta + \phi) \qquad \ldots\ldots\ldots (18)$$

where β is the complement of α, the tool rake angle.

If F_C and F_N are resolved along the plane of shear then for the equilibrium of unit width of chip

$$F_C \cos\theta - F_N \sin\theta = \frac{d}{\sin\theta} \cdot Ss \qquad \ldots\ldots\ldots (19)$$

combining (18) and (19) gives

$$F_C \left(\cos\theta + \frac{\sin\theta}{\tan(\beta + \phi)}\right) = \frac{d \cdot Ss}{\sin\theta}$$

$$F_C = \frac{d \cdot Ss \cdot \sin(\beta + \phi)}{\sin\theta \cdot \sin(\beta + \theta + \phi)} \qquad \ldots\ldots\ldots (20)$$

If it is now assumed that the direction of the shear plane is such that the cutting force, and hence the work done in cutting, will be a minimum i.e. a hypothesis of minimum work

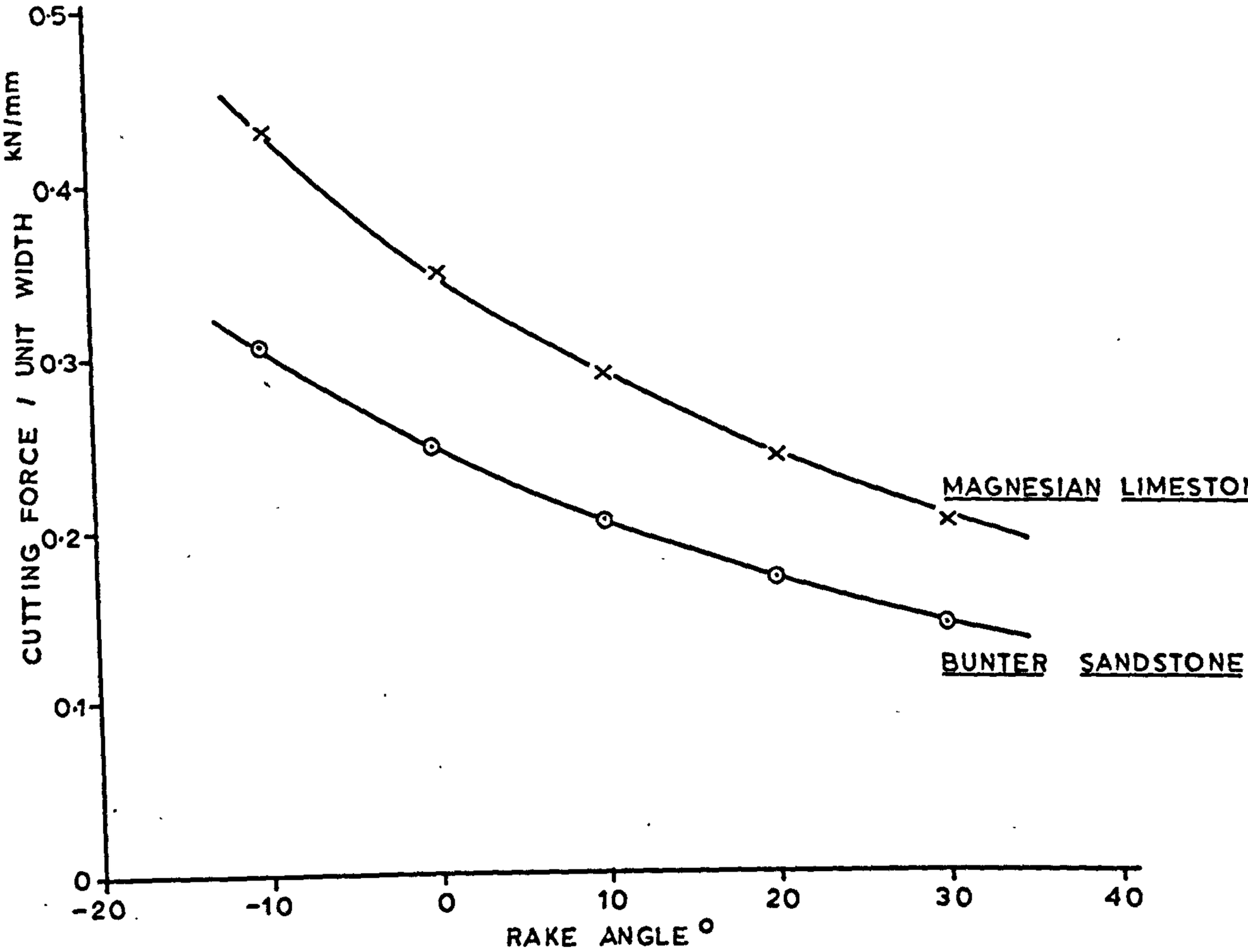

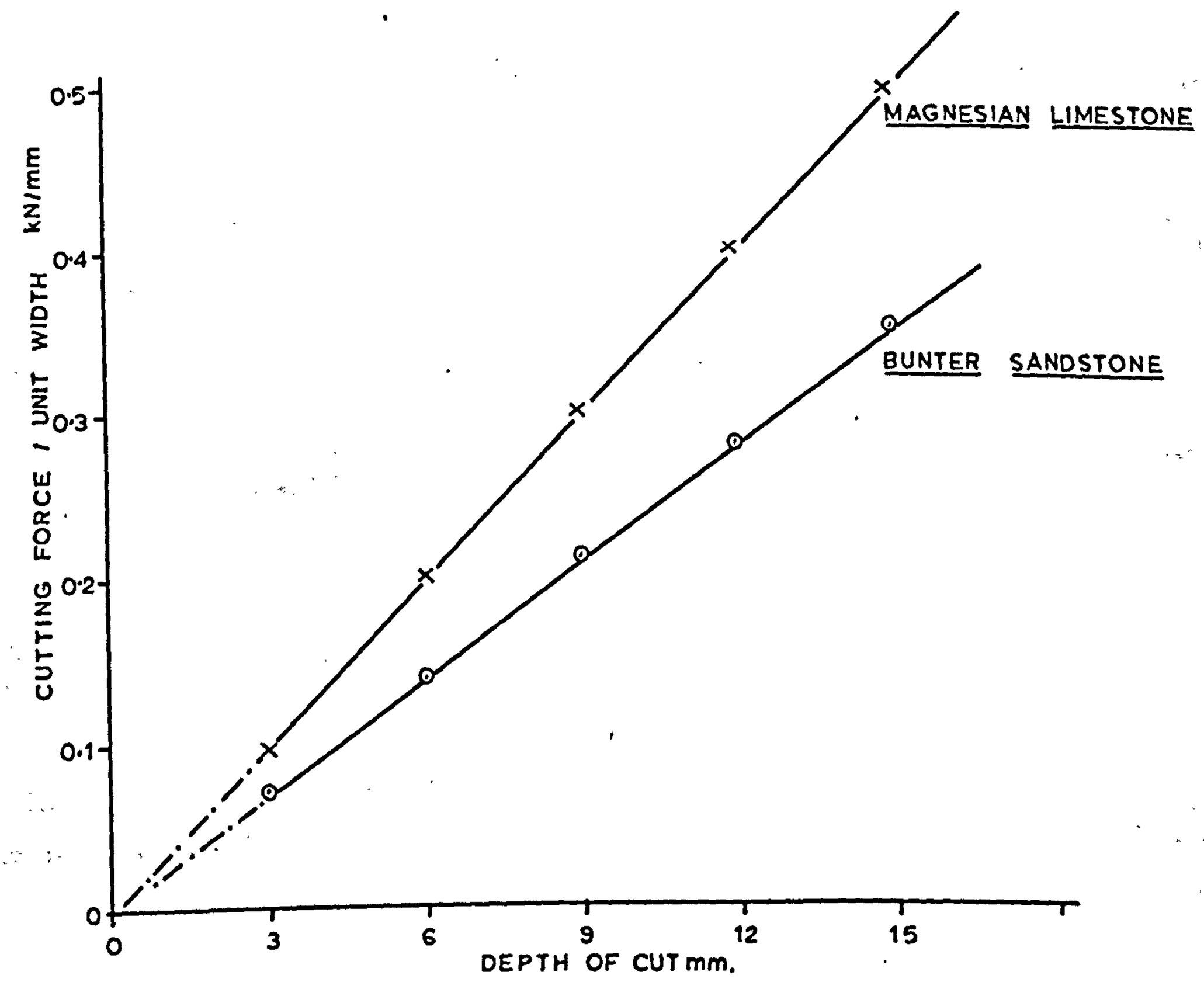

FIGURE 77 — CUTTING FORCE PREDICTIONS OF MERCHANT'S THEORY

then $\frac{d F_C}{d \theta} = 0$

this condition gives $\theta = \frac{\pi}{2} - \frac{1}{2}(\beta + \phi)$ i.e. the minimum value of F_C which causes failure is given by

$$F_C = 2 \cdot d \cdot Ss \cdot \tan \frac{1}{2}(\beta + \phi) \quad \ldots\ldots\ldots (21)$$

Values of Ss and ϕ, for both Bunter Sandstone and Magnesian Limestone, were given in Chapter 4. For convenience these have been abstracted and are tabulated below.

	Bunter	Magnesian Limestone
Shear Strength	7.34 N/mm^2	12.00 N/mm^2
Angle of Friction	33^o	26^o

Equation (21) has been used to obtain theoretical predictions of F_C for the same combinations of rake angle and depth of cut as those used in Experiments I and III of Chapter 7. The forces predicted by this equation will represent the peak and not the mean values since they represent the force at the moment of failure of each chip. These values of force/unit width are tabulated and, together with the appropriate grouped data, appear in Appendix XII (A and B).

It can be seen from Figure 77 that depth of cut has the same effect on the theoretical values of F_C as it had on the measured values reported in section 7.2.2. Similarly the effect of rake angle is identical to that observed in the experimental work recorded in 7.2.1.

The term force/unit width implies that the force for any given width may be obtained by a simple multiplication. This would, however, be at variance with the reported behaviour of picks (see 7.2.3), where a finite value of force, attributed to the effects of breakout, occurs at zero width of tool.

i.e. $F_C = a\,w + b$

Merchant's theory gives no indication of how these two constants may be determined. It is, however, possible to obtain them from the results of a very limited programme of rock cutting. If tests are undertaken using the five tools of different widths, all having a rake angle of 10^{o}, and operating at the mean depth of cut of 9mm., then the two constants associated with width can be found. Theoretical predictions of the cutting force for each test in the full matrix can now be made. These, together with the appropriate measured values are listed in Appendix XII C.

It can be seen that the predictions are realistic and that the grouped data given in Appendix XII D shows none of the variables to have undue influence on the discrepancies between measured and predicted values.

While an agreement exists between theory and practice it should be remembered that the constants in the final theoretical expression were established from cutting tests. In addition, it should be noted that the values of force/unit width in Magnesian Limestone are, on average, 1.42 times the equivalent value in Bunter. The corresponding ratio of 4:1 for the measured forces suggests that shear strength is not a valid parameter on which to base a cutting theory.

10.2 The Rock Cutting Theory of Nishimatsu

Nishimatsu (35) has proposed a model, based on the metal cutting theory of Merchant, to describe the action of a drag pick in rock. Whereas Merchant used a single value for the shear strength of the material, Nishimatsu invokes Mohr's failure envelope to define the strength of the rock.

The theory proposes a failure process involving the primary and secondary crushed zones associated with coarse chip formation and assumes that shear failure will occur along a line from the tip of the tool to the surface of the rock. It is further assumed that the stress at any point on this line will be proportional to its distance from the surface raised to some power, n.

i.e. stress is zero at the surface of the rock and a maximum at the tip of the tool.

The stress distribution and cutting forces are shown in Figure 78.

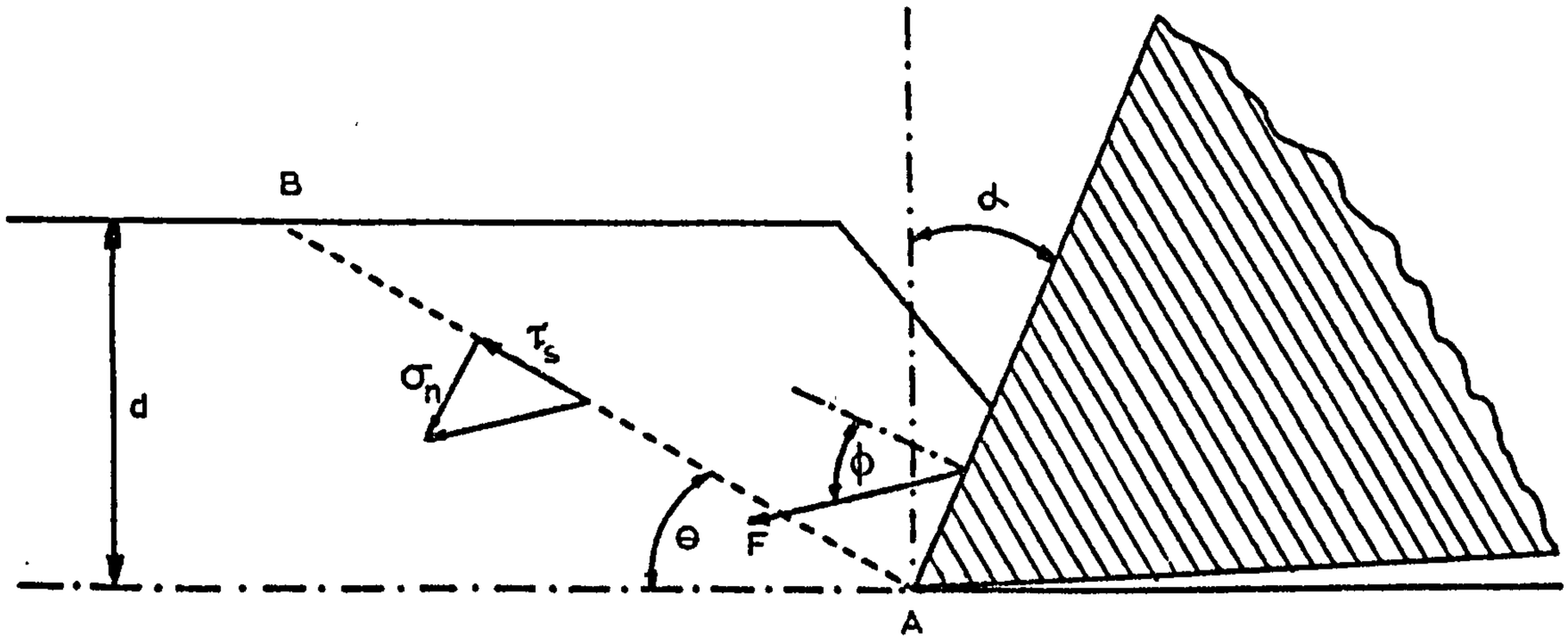

FIGURE 78 ILLUSTRATION OF NISHIMATSU'S THEORY OF ROCK CUTTING

Hence the resultant stress acting on a unit length of line AB is given by

$$p = p_o \left(\frac{d}{\sin \theta} - \lambda\right)^n \qquad \ldots\ldots\ldots (22)$$

where p_o is a constant

θ is the angle between the direction of cutting and the failure plane

$\frac{d}{\sin \theta} = AB$

λ is the distance from the tip of the tool

n is termed the stress distribution factor.

If F is the resultant force applied by the tool then for equilibrium

$$F + p_o \int_o^{d/\sin \theta} \left(\frac{d}{\sin \theta} - \lambda\right)^n d\lambda = o \qquad \ldots\ldots\ldots (23)$$

hence $p = F \cdot (n + 1) \cdot (\frac{\sin \theta}{d})^{n+1} \cdot (\frac{d}{\sin \theta} - \lambda)^{n}$

the maximum will occur when $\lambda = 0$

hence $p_{max} = F \cdot (n + 1) \cdot \frac{\sin \theta}{d}$ ..... (24)

and resolving this stress into its components gives

$$\sigma_{no} = F. (n + 1) \cdot \frac{\sin \theta}{d} \cdot \sin (\theta - \alpha + \phi) \quad \text{..... (25)}$$

and $\tau_{so} = f. (n + 1) \frac{\sin \theta}{d} \cdot \cos (\theta - \alpha + \phi)$ ..... (26)

Also, from the straight line portion of Mohr's envelope

$$\tau_s = Ss + \sigma_n \tan k \quad \text{..... (27)}$$

where τ_s is the shear stress and k the angle of internal friction of the rock

Combining equations (25), (26) and (27) gives:-

$$F = \frac{-1}{(n + 1) \cdot \sin \theta} \cdot \frac{d\ Ss}{\tan k \cdot \sin (\theta + \phi - \alpha) - \cos (\theta + \phi - \alpha)} \quad \text{... (28)}$$

This theory again invokes the hypothesis of minimum work, i.e. the requirement that $\frac{d F}{d \theta} = 0$

Hence the final equation for the resultant tool force becomes

$$F = \frac{2}{n + 1} \cdot Ss \cdot d \cdot \frac{\cos k}{1 - \sin (k - \alpha + \phi)} \quad \text{..... (29)}$$

Values of shear strength and angle of internal friction have been obtained from both rocks and these are recorded in Chapter 4. In order to follow the calculations of Nishimatsu the predictor equations for Bunter Sandstone, which were developed in Chapter 7, have been used to calculate peak cutting and normal forces for tools of five rake angles operating at a range of depths in dry Bunter Sandstone. Although these

values are derived from the empirical equations, they will be referred to as experimental values to distinguish them from the theoretical predictions of Nishimatsu. These values of cutting and normal forces are given in Appendix XII E.

It can be seen from Figure 78 that the ratio of normal to cutting forces is equal to tan $(\phi - \alpha)$. Value of ϕ have been calculated for each of the five levels of α and the relationships between ϕ and α was found to be linear and defined by the equation:-

$$\phi = 32.5 + 1.21\ (\alpha + 10) \qquad \ldots\ldots\ldots (30)$$

From an analysis of his own results, Nishimatsu concludes that the stress distribution factor is independent of rock type and varies only with rake angle, following the relationship

$$n = 11.3 - 0.18\alpha \qquad \ldots\ldots\ldots (31)$$

As all the factors in equation (25) are now known, theoretical prediction of the cutting force/unit width for a range of rake angles and depths of cut can now be made. These, together with the equivalent experimental values, are tabulated in Appendix XII F. It can be seen that the correlation between the two sets of data is very poor and the grouped values given in Appendix XII G show that, while the trends for depth of cut are similar, those for rake angle are totally at variance. In fact this may be deduced from equations (29) and (31). Equation (29) shows that n decreases as α increases and equation (30) shows that F is inversely proportional to n. Hence this theory indicates that force rises as the rake of a tool is increased. A more plausible solution is that the stress distribution factor is not independent of rock type and so the five values of n, corresponding to the five levels of rake angle studied in the Bunter, have been calculated. The values of n are found to increase with α, the relationship being

$$n = 0.15\ (\alpha + 10)^2 + 6.50 \qquad \ldots\ldots\ldots (32)$$

If, as it appears from this analysis, the stress distribution factor varies not only with rake angle but also with rock type the application of this theory becomes little more than a curve fitting exercise to be carried out after the practical work has been concluded.

10.3 Evans' Tensile Theory of Rock Breakage

In contrast to the two theories already discussed, Evans' theory is based on the observation that wedge penetration of a rock produces cracks attributed to tensile failure (83). The basic theory is for the penetration of a buttock of rock by a simple symmetrical wedge, as shown in Figure 79.

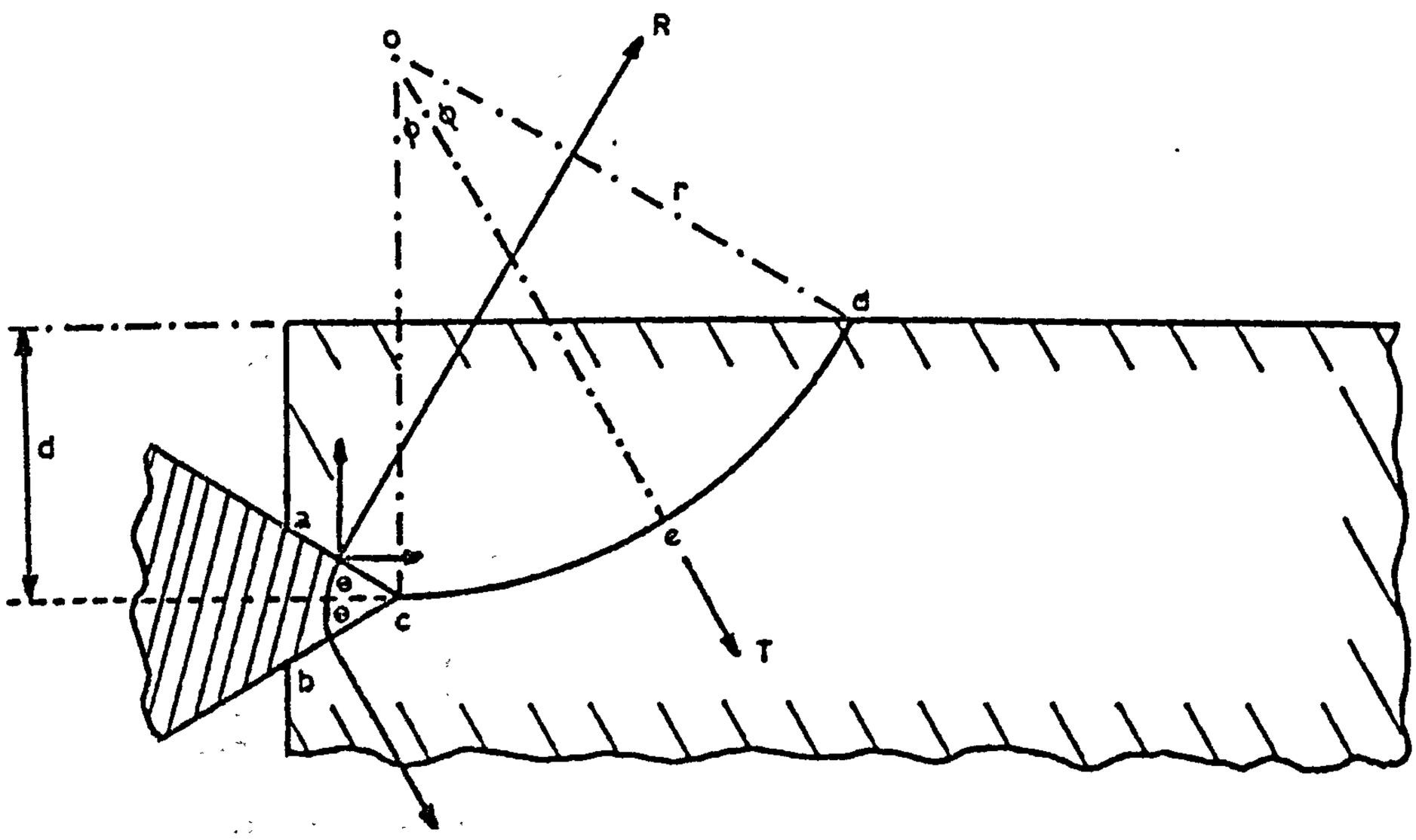

FIGURE 79. ILLUSTRATION OF EVANS' THEORY

Evans assumes that failure takes place along a circular arc and, since width of tool is likely to be much greater than depth of cut, that a state of plane strain exists.

The total tensile force required to tear the rock is given by:-

$$T = \sigma_t \cdot r \cdot \int_{-\phi}^{\phi} \cos w \, d w = 2 \sigma_t \cdot r \cdot \sin \alpha \qquad \ldots\ (33)$$

where r . d w is any element of the arc cd making an angle w with Oe.

By taking moments about d, R and T may now be equated

$$R \cdot \frac{d}{\sin \phi} \cdot \cos (\phi + \theta) = Tr \sin \phi \qquad \ldots\ldots\ldots (34)$$

and from the geometry of Figure 79 it can be seen that

$$r \sin \phi = \frac{d}{2 \sin \phi} \qquad \ldots\ldots\ldots (35)$$

Hence

$$R = \frac{\sigma_t \cdot d}{2 \sin \phi \cos (\theta + \phi)} \qquad \ldots\ldots\ldots (36)$$

and

$$F_C = 2 R \sin \theta = \frac{\sigma_t \cdot d \cdot \sin \theta}{\sin \phi \cos (\theta + \phi)} \qquad \ldots\ldots\ldots (37)$$

The assumption is now made that ϕ will be such as to make F_C a minimum i.e.

$$\frac{d F_C}{d\phi} = 0$$

This gives

$$\cos \phi \cos (\theta + \phi) - \sin \phi \sin (\theta + \phi) = 0$$

$$\text{i.e.} \quad \phi = \frac{1}{2} \left(\frac{\pi}{2} - \theta\right)$$

Hence

$$F_C = \frac{2 \sigma_t d \sin \theta}{1 - \sin \theta} \qquad \ldots\ldots\ldots (38)$$

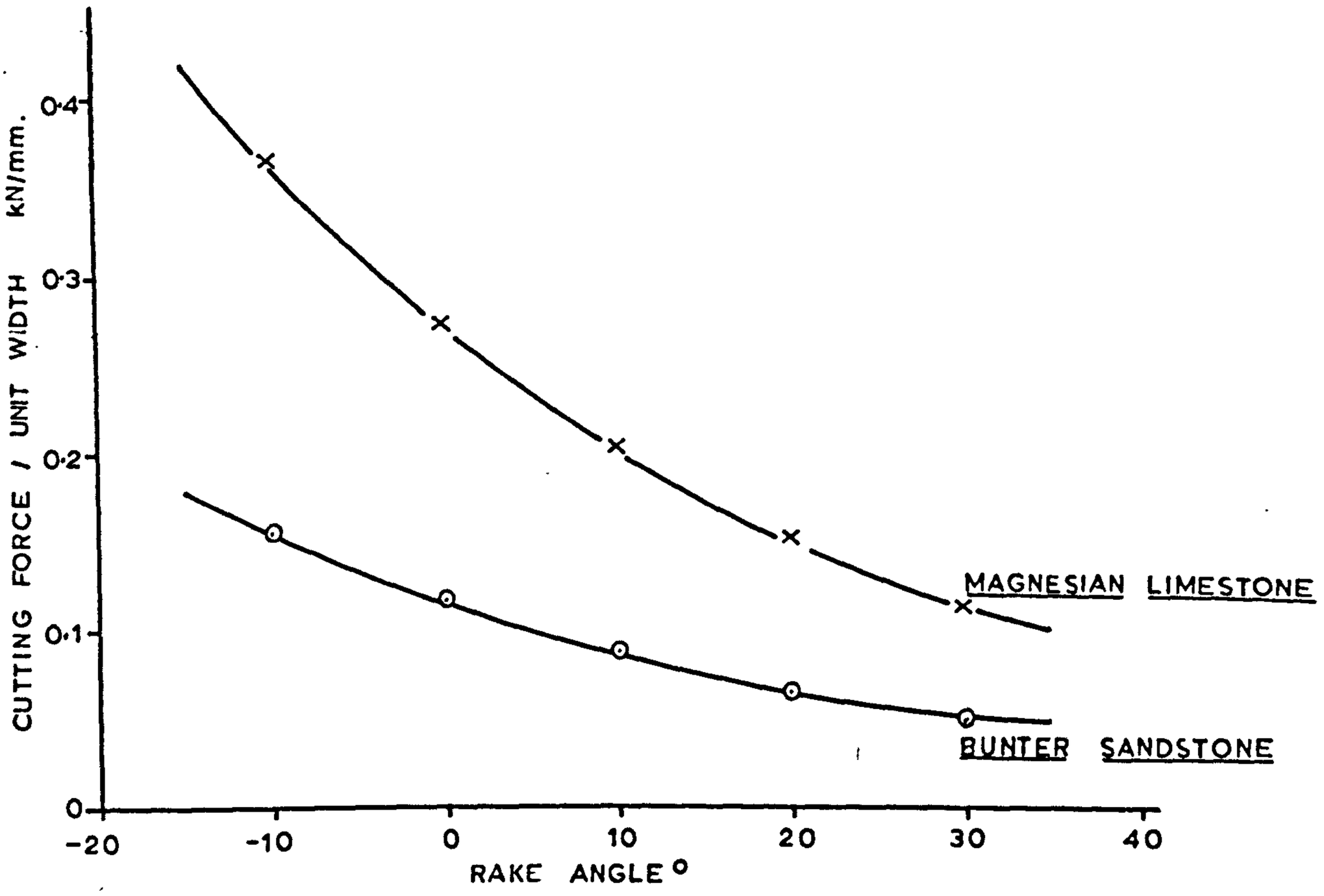

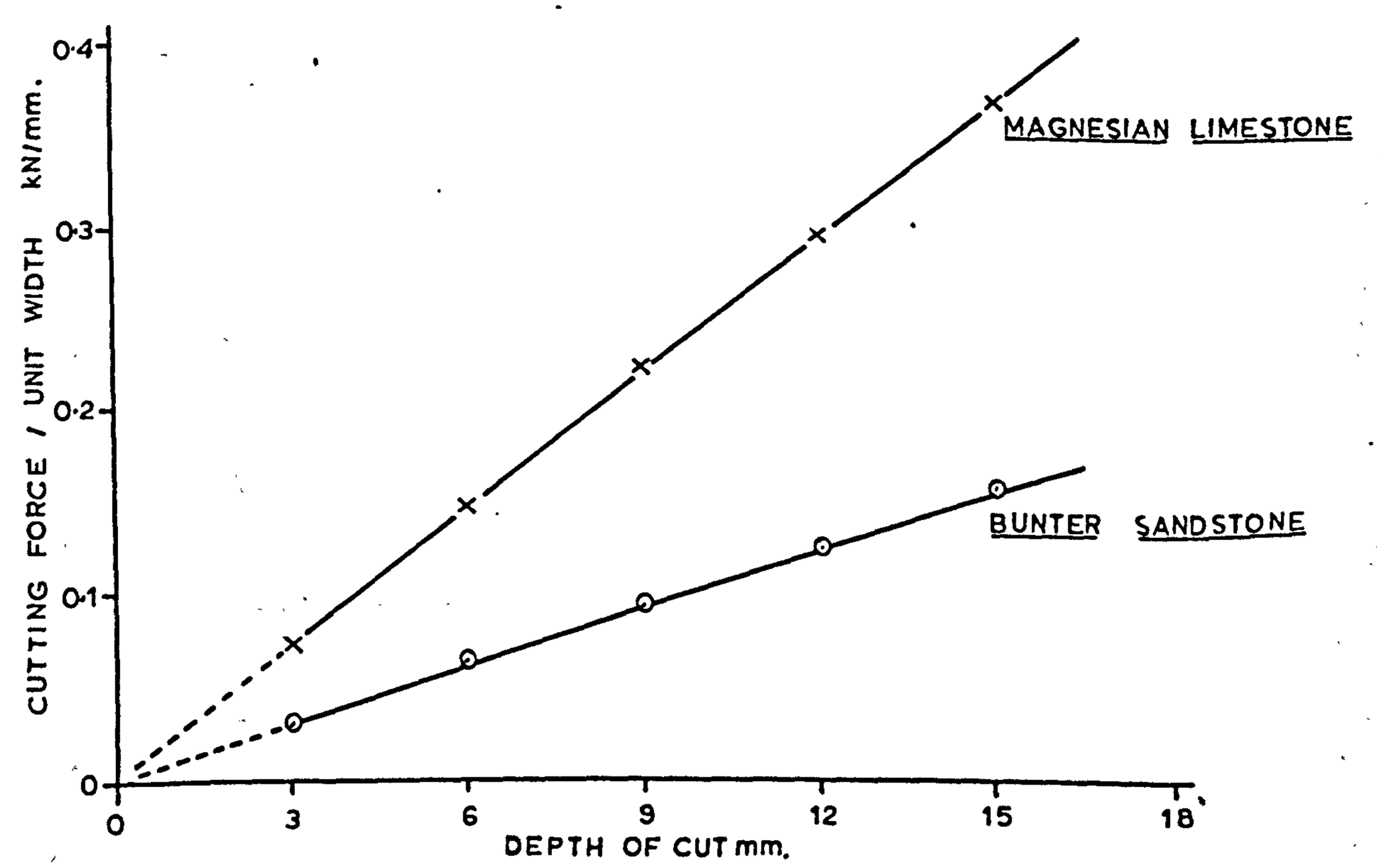

FIGURE 80 — CUTTING FORCE PREDICTIONS OF EVANS' THEORY

Roxborough (76) has shown that equation (38) may be adapted for chisel picks of the geometry illustrated by Figure 25. If it is assumed that the circular arc of failure is tangential to the bisector of $\frac{\pi}{2} - \alpha$, where α is the rake angle then the following equation can be derived:-

$$F_C = \frac{2\ \sigma_t\ d\ \sin\frac{1}{2}\ (\frac{\pi}{2} - \alpha)}{1 - \sin\frac{1}{2}\ (\frac{\pi}{2} - \alpha)} \qquad \ldots\ldots\ldots (39)$$

This equation has been used to calculate theoretical values of mean cutting force/unit width for the combinations of rake angle and depth of cut used in the experimental programme. These are listed in Appendix XII H. The grouped data of Appendix XII J, which is also displayed graphically in Figure 80, shows the correct relationships to exist between the variables and the force/unit width exerted by the tool.

The effects of width have been predicted by the method outlined in section 10.1 and the resulting values of theoretical force are listed in Appendix XII (K and L). The grouped data shows rake angle to have a greater effect on Evans' theoretical predictions than it has on experimental data.

Equation (39) also shows tool forces to be directly proportional to the tensile strength of the material. Hence the ratio of theoretical force in Magnesian Limestone to that in Bunter will be 2.4:1. Since the equivalent ratio for measured forces is 4:1 and for forces derived from Merchant's theory is 1.4:1 it would seem that cutting forces cannot be predicted accurately from theories based on the rock failing in either simple shear or tension. Picks do, in fact, apply a complex system of loading to the rock and the model of Nishimatsu, involving primary and secondary crushed zones, must provide a more realistic representation than do other, simpler, models.

10.4 A THEORETICAL MODEL OF THE ACTION OF DISC CUTTERS

It was shown in section 9.2.3 that the forces involved in cutting with a disc are influenced by the compressive strength of the rock it is required to penetrate. Similarly, it is to be expected that the forces will be affected by the disc geometry.

An elementary analysis of the mechanics of disc operation can be provided by invoking several assumptions and approximations, none of which depart too far from reality, but the introduction of which simplifies the mathematics.

Consider, as shown in Figure 81, a disc of edge angle ϕ and diameter D, penetrating the plane surface of a rock to a depth 'p' under the action of a Force F_T.

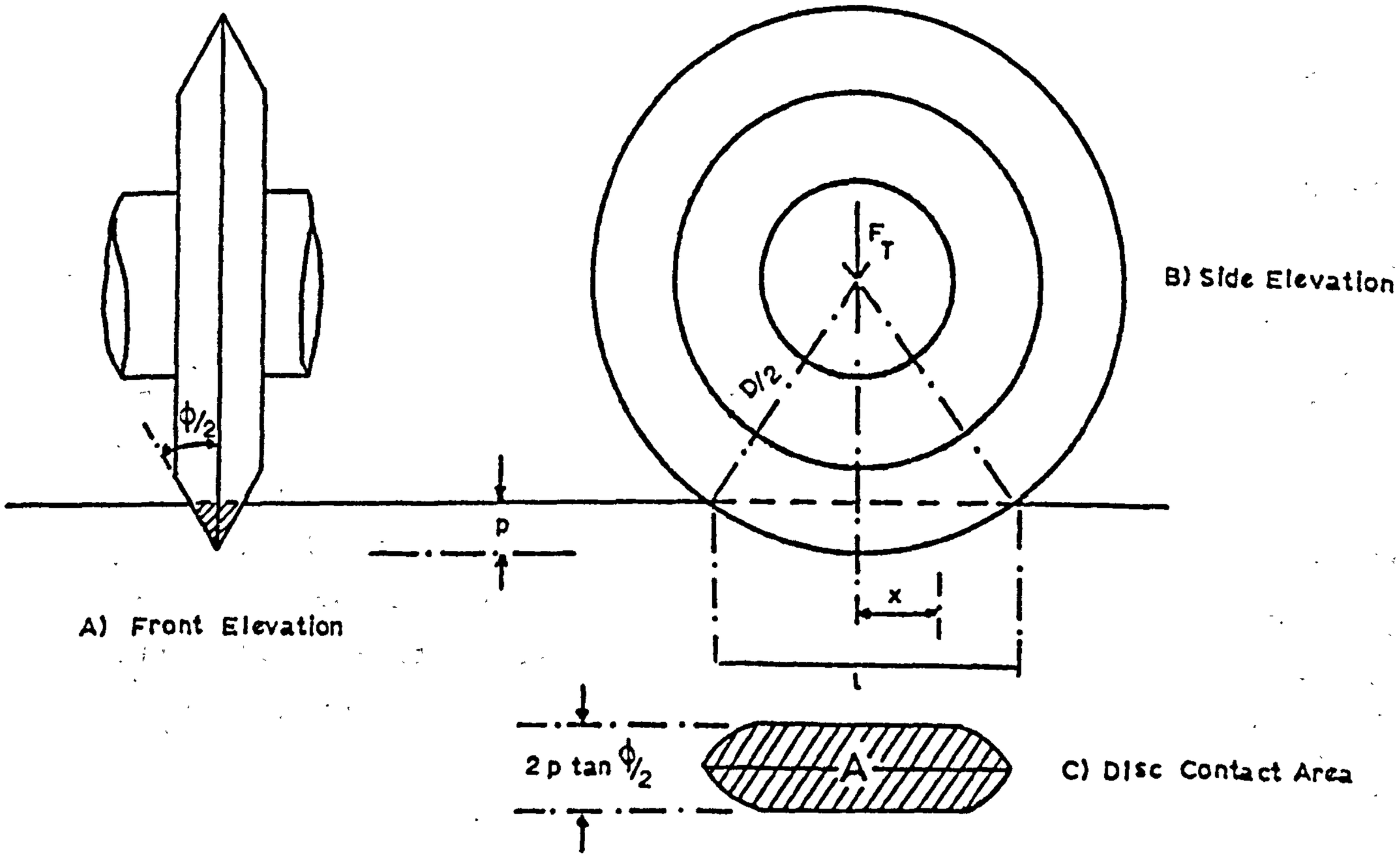

FIGURE 81. GEOMETRY OF DISC PENETRATION

Since it would appear that the resistance to penetration is essentially compressive then the force F_T is equivalent to a compressive stress acting

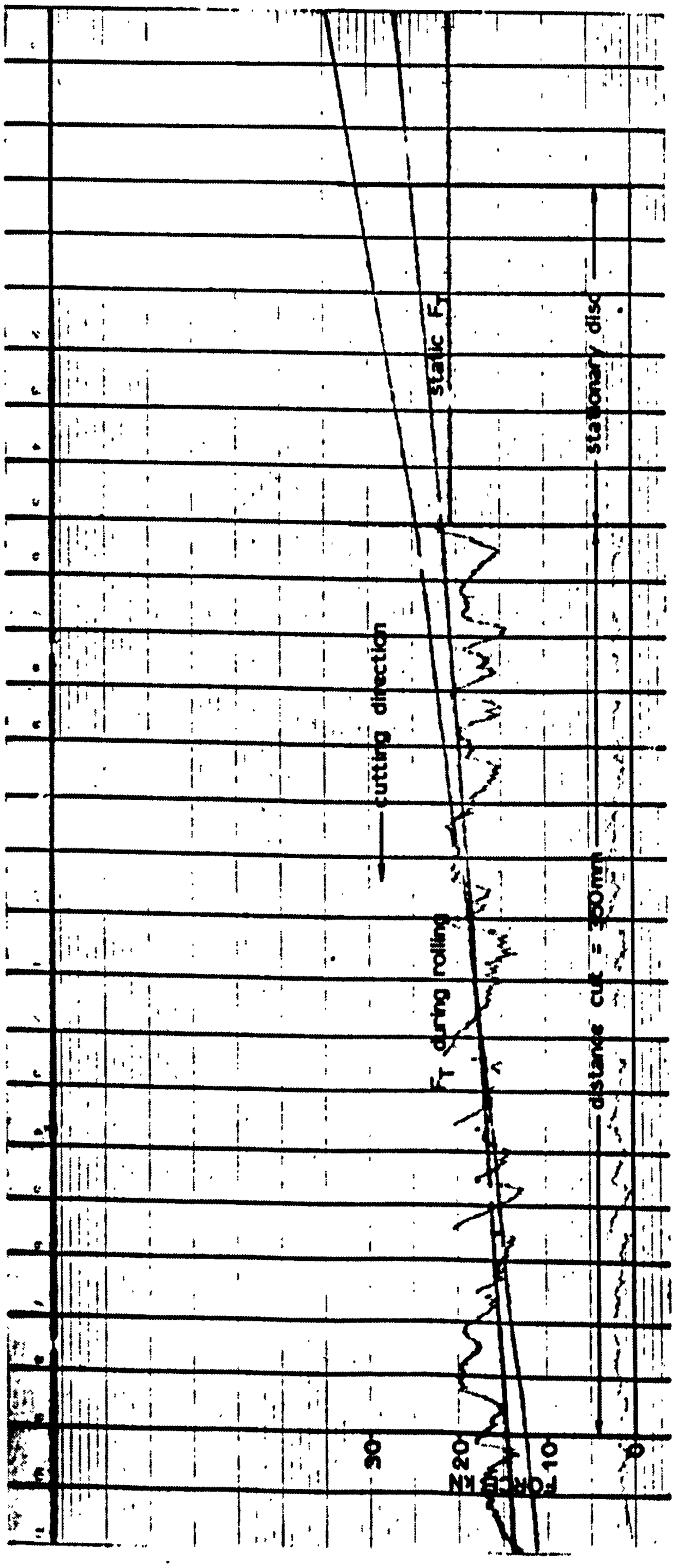

FIGURE 82. U.V. TRACE OF THRUST FORCE FOR STATIONARY AND ROLLING CONDITIONS

over the projected area of disc contact 'A'. As penetration increases, so does the chord length of contact 'ℓ' such that

$$\ell = 2\sqrt{Dp - p^2} \qquad \ldots\ldots\ldots (40)$$

A precise determination of area 'A' involving an equation of the form

$$\int_0^{\ell/2} f\ (\tan\phi,\ D,\ p,\ x)\ d\,x \qquad \ldots\ldots\ldots (41)$$

is given in Appendix XIII A.

As a first approximation, this may be simplified to give

$$A = 2\ p\ \ell\ \tan\ \phi/2 \qquad \ldots\ldots\ldots (42)$$

The thrust force to effect a penetration 'p' may, therefore, be written:-

$$F_T = 4\ \sigma_c\ \tan\ \phi/2\sqrt{Dp^3 - p^4} \qquad \ldots\ldots\ldots (43)$$

Further analysis depends on the observation that the value of F_T remains constant when the disc is made to roll.

Figure 82 shows an analog trace of the static penetration force and thereafter the same force measured while the disc is rolling. It shows peak values of F_T to be substantially the same for the static and rolling conditions.

An equation for the rolling force F_R may now be obtained by considering the forces acting on the disc, as shown by Figure 83.

If it is assumed that the stress acting along the arc of contact $\overline{ab}$ is constant then Evans (92) has shown that the line of action of the resultant can be determined as follows.

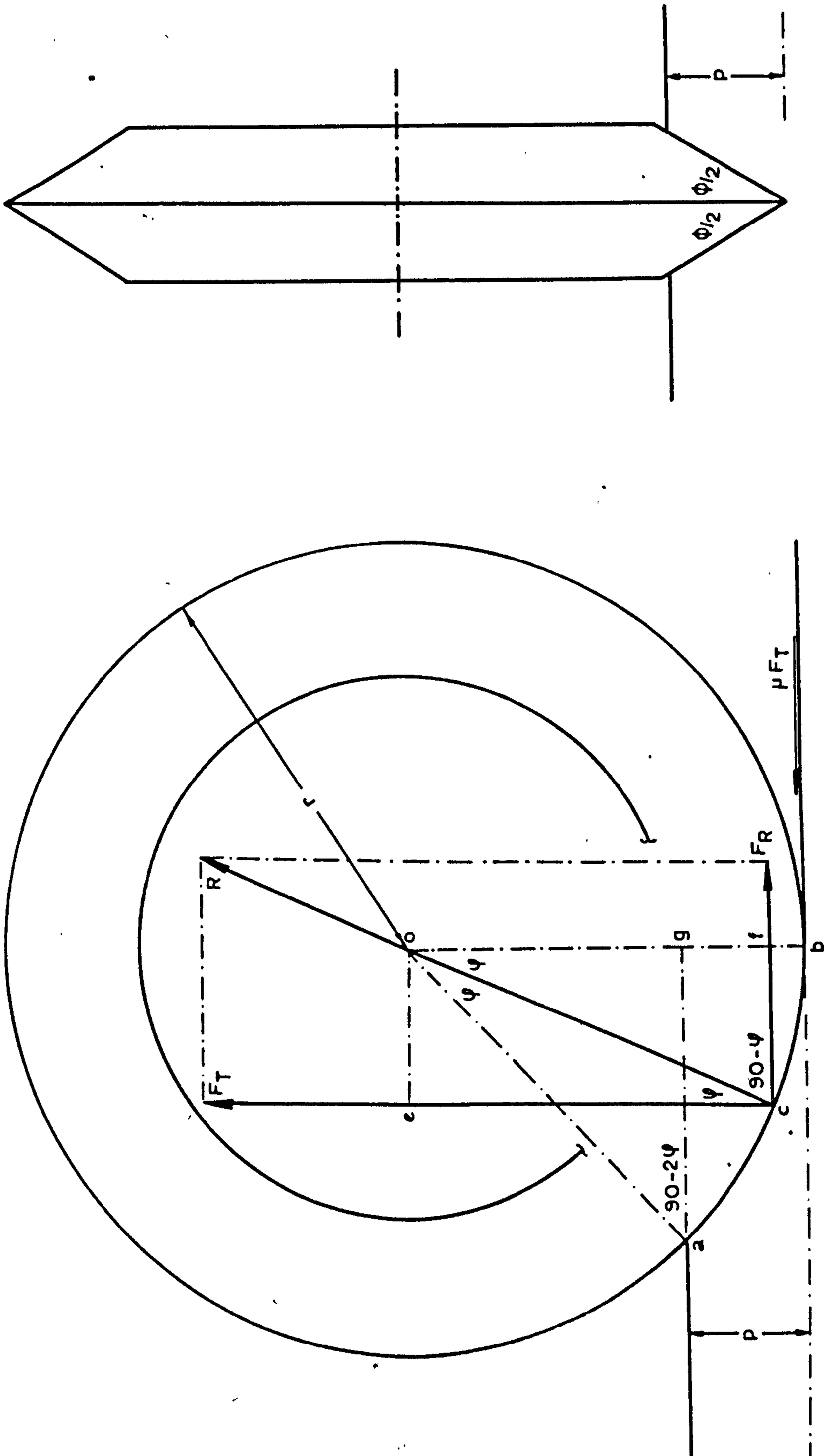

FIGURE 83 - ORTHOGONAL FORCES ACTING ON A DISC

If the resultant force makes an angle α with the vertical $\overline{ob}$ then the moment of F_T about O is

$$F_T \cdot r \cdot \sin \alpha$$

If the force per unit length is δT then the moment of the force on an element of length at any point x, where angle xob is β is $r \cdot \delta\beta \cdot \delta T \cdot r \cdot \sin \beta$

Hence $F_T \cdot r \cdot \sin \alpha = r^2 \, \delta T \int_0^{2\psi} \sin \beta d\beta$ ..... (44)

and $F_T = 2r\psi \cdot \delta T$ ..... (45)

Combining equations (44) and (45) gives

$$\sin \alpha = \frac{1 - \cos 2\psi}{2\psi}$$

and for small angles $\psi \simeq \sin \psi$*

hence $\sin \alpha = \sin \psi$

$$\alpha = \psi$$

and the resultant force bisects the arc of contact.

The above analysis is based on a frictionless system with the line of action of the resultant R passing through the centre of rotation in order that the zero nett torque condition be satisfied.

Again, for zero torque

$$F_R \cdot \overline{of} = F_T \cdot \overline{oe}$$

$$\text{so that } \frac{F_T}{F_R} = \cot \psi \quad \text{..... (46)}$$

---

* The largest value of ψ encountered in the experimental matrix was 18°. The approximation $18^\circ = \sin 18^\circ$ gives rise to a 1.6% error.

From the geometry of Figure 83 it can be seen that

$$\frac{\overline{og}}{\overline{oa}} = \frac{r - p}{r}$$

$$= \cos 2\psi$$

$$= \frac{1 - \tan^2 \psi}{1 + \tan^2 \psi}$$

hence $\tan^2 \psi = \frac{p}{2r - p}$

or $\frac{F_T}{F_R} = \sqrt{\frac{D - p}{p}}$ ..... (47)

Combining equations (43) and (47) gives

$$F_R = 4 \sigma_c p^2 \tan \phi/2 \quad \text{..... (48)}$$

If friction were to be considered equation (47) would become

$$\frac{F_T}{F_R} = \frac{\sqrt{\frac{D - p}{p}}}{1 + \mu \sqrt{\frac{D}{p}}} \quad \text{..... (49)}$$

Since rolling friction is likely to be the most appropriate coefficient and this is reported (85) to have values of less than 0.02, the inclusion of a friction term is of little consequence to equation (48).

In order to check the validity of this model theoretical predictions of the performance of discs working in Bunter Sandstone and Magnesian Limestone have been made. These, together with the appropriate experimental results abstracted from Chapter 9, are tabulated in Appendix XIII (B, C and D). The data for Bunter Sandstone, grouped for each variable, is given in Appendix XIII (E and F) while the equivalent grouped values for Magnesian Limestone are given below.

TABLE 33 A

VARIATION IN DISC FORCES WITH EDGE ANGLE

D = 150mm : p = 4.5mm

Edge Angle ^{o}	Thrust Force (kN)		Rolling Force (kN)	
	Theoretical	Measured	Theoretical	Measured
60	23.09	23.56	4.85	5.81
70	30.48	31.24	5.89	6.64
80	35.21	34.53	7.05	7.26
90	43.68	42.41	8.41	8.69
100	46.81	48.67	10.02	10.14

TABLE 33 B

VARIATION IN FORCES WITH DISC DIAMETER

$\phi = 80^{o}$: p = 4.5mm

Disc Diameter mm	Thrust Force (kN)		Rolling Force (kN)	
	Theoretical	Measured	Theoretical	Measured
100	29.40	31.05	7.12	8.18
125	30.45	31.17	6.59	6.94
150	40.86	40.78	8.67	9.07
175	36.23	37.73	6.47	7.04
200	42.33	39.69	7.37	7.31

TABLE 33 C

VARIATION IN FORCES WITH DISC PENETRATION

D = 150mm : $\phi = 80^{o}$

Penetration mm	Thrust Force (kN)		Rolling Force (kN)	
	Theoretical	Measured	Theoretical	Measured
1.5	6.61	9.65	0.66	0.98
3.0	18.05	21.42	2.63	3.04
4.5	33.45	37.24	5.93	6.70
6.0	50.29	48.81	10.53	11.52
7.5	70.88	63.29	16.46	16.30

These theoretical values of Thrust and Rolling Force show good agreement in both trend and magnitude with the experimental data. The theoretical values of thrust force in Bunter Sandstone also show good agreement with the experimental results but the rolling forces are somewhat at variance. Since Bunter Sandstone has been shown to be abrasive and to possess a high coefficient of friction it is likely that the exclusion of the friction term in equation (49) will have some effect.

It is however difficult to determine a value for μ appropriate to disc cutting since, in addition to the coefficient of rolling friction already mentioned, it will have a sliding component. Generally values of rolling friction are very low ranging from 0.02 to 0.001 and it is a difficult quantity to measure accurately. Rolling friction will of course be a function of F_T but the sliding component will vary with the resolved part of F_T acting normal to the groove sides. This will, therefore, change with edge angle and penetration.

The effects of friction can be assessed empirically by linearly regressing the measured and theoretical values of rolling force for each rock type. This has yielded the following equations

Dry Bunter

$$F_{R\ (MEASURED)} = 0.443 \cdot F_{R\ (THEORETICAL)} + 1.067$$

Wet Bunter

$$F_{R\ (MEASURED)} = 0.495 \cdot F_{R\ (THEORETICAL)} + 0.989$$

Mangesian Limestone

$$F_{R\ (MEASURED)} = 0.961 \cdot F_{R\ (THEORETICAL)} + .747$$

The similarity of the two equations for Bunter gives credence to the belief that differences between theoretical and experimental values of rolling force may be attributed to the coefficient of friction, a material property.

The published results of other workers in this field provide a further opportunity to examine the validity of the disc force analysis. Morrell, Bruce and Larson (39) and the Wolfson Research Group (93) have published experimental results on disc performance in a range of sedimentary and metamorphic rocks.

Figure 84 shows the variation of F_T with penetration for two 178mm diameter discs in A) Tennessee Marble, a rock having a quoted unconfined compressive strength of 116 MN/m^2 and B) Indiana Limestone - Type 2 which has a compressive strength of 69 MN/m^2. Figure 84 (C and D) shows the force/penetration characteristics for Mansfield Sandstone (σ = 67) and Anhydrite (σ = 113 MN/m^2).

In all cases the theoretical curves, drawn in broken line, agree quite well in both trend and magnitude with the experimental relationships.

10.5 A theoretical Derivation of the Maximum Effective Separation Between Discs

It was reported in section 9.3.2 that in some of the experimental tests rock breakage occurred between adjacent grooves. This slabbing effect has also been observed elsewhere (94).

Such breakage implies a shearing of the rock across a surface extending between the centre of each groove and at the full depth of penetration.

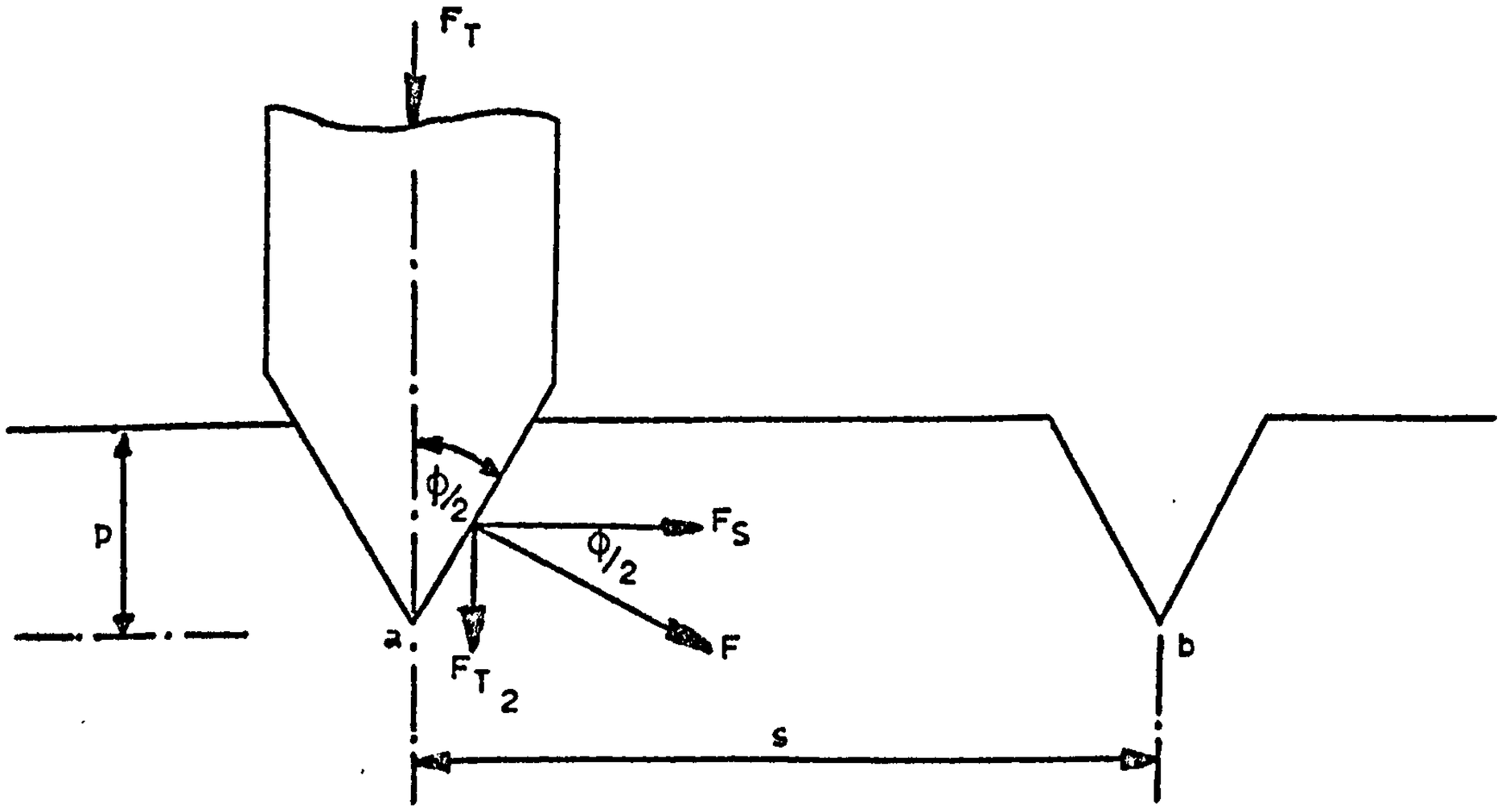

FIGURE 85. SHEARING FORCE BETWEEN DISC GROOVES

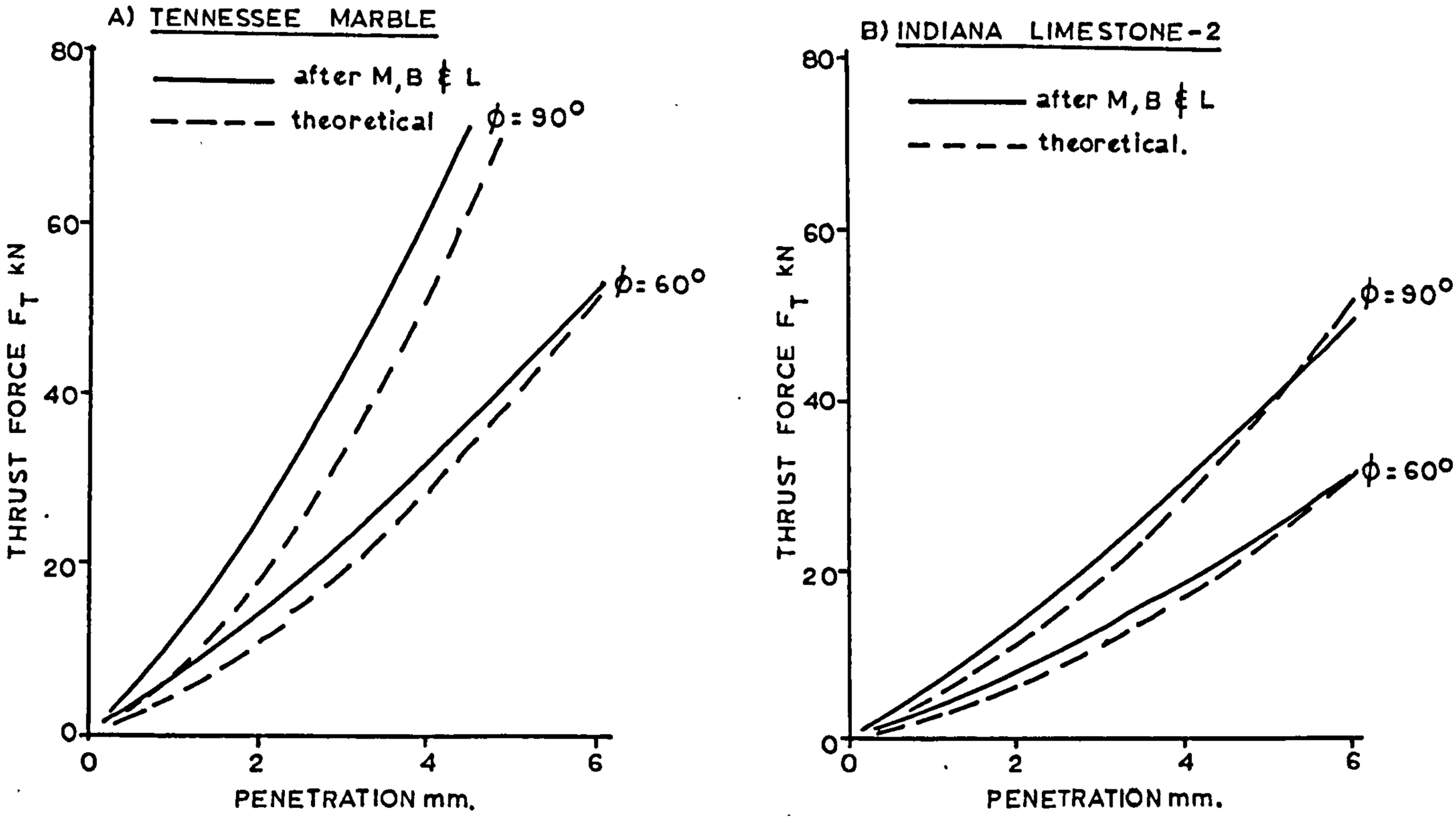

FIGURE 84 — DISC FORCE ANALYSIS

If, as indicated by Figure 85, the rock shears across the horizontal plane bounded by $\overline{ab}$ then if F_S is the shearing force

$$F_S = F \cos \frac{\phi}{2}$$

and $$F_T = 2F \sin \frac{\phi}{2}$$

so that $$F_S = \frac{F_T}{2 \tan \frac{\phi}{2}} \quad \ldots\ldots\ldots (50)$$

Assuming as for equation (43) that F_T is equivalent to a compressive stress acting over the projected surface area and for disc contact length 'ℓ':

$$F_T = 2\, p \tan \frac{\phi}{2} \cdot \ell \cdot \sigma_c \quad \ldots\ldots\ldots (51)$$

where σ_c is the compressive strength of the rock.

Combining (50) and (51)

$$F_S = \frac{2 \cdot p \cdot \tan \frac{\phi}{2} \cdot \ell \cdot \sigma_c}{2 \tan \phi/2}$$

so that $$F_S = p\, \ell\, \sigma_c \quad \ldots\ldots\ldots (52)$$

Also, if the rock fails in simple shear, due to F_S, then

$$F_S = s \cdot \ell \cdot \tau \quad \ldots\ldots\ldots (53)$$

equating (52) and (53) gives

$$s/p = \sigma_c/\tau \quad \ldots\ldots\ldots (54)$$

So the force F generated by penetrating a disc to a depth of p will cause shearing between adjacent grooves up to a maximum spacing defined by equation (54). The uniaxial compressive and shear strengths of the test rocks are given in Chapter 4 and summarized below

	Dry Bunter	Wet Bunter	Magnesian Limestone
σ_c (MN/m^2)	49.2	41.0	84.9
τ (MN/m^2)	7.3	6.9	12.00
Ratio	6.7	5.9	7.1

These ratios show reasonable agreement with the observed limit of breakthrough at s/p values of around 7.

11. GENERAL CONCLUSIONS

The conclusions reached in each discrete part of this thesis have already been discussed under appropriate headings in the preceding chapters. The findings of the individual sections do, however, interrelate and some general conclusions, based on an overall appraisal of the results, may be drawn.

Fundamental differences in the cutting characteristics of picks and discs are illustrated in Figure 20, which shows typical cutting force diagrams for both types of tool. The high frequency transcient stresses so evident with picks are almost absent from recordings of disc forces. This must, in part, explain why picks are much less able to survive the rigours of a hard and abrasive rock environment. The free rolling action of the disc has the further benefit of less rubbing contact between the tool and rock thereby suffering significantly less abrasive wear than the pick. Although disc diameter was not found, nor was it expected, to have an effect on specific energy, a large diameter tool has the advantage of distributing any wear over a longer continuous cutting edge.

While disc and roller cutters were found to have almost identical specific energy requirements, picks were undoubtedly the most efficient of the three tool types investigated. This superiority of the pick against the disc, operating unreleived, may be greatly diminished when both are operating in optimally spaced arrays and the telling effects of wear on picks have been taken into account. For instance, a 10^{o} rake, 30mm wide pick cutting at a depth of 9mm in Bunter Sandstone, with a generated wear flat of 2mm and optimally spaced, would have a specific energy of around 8 MJ/m^3. This would compare with a specific energy requirement of about 16 MJ/m^3 for a 80^{o} edge angle, 150mm diameter disc operating at a penetration of 9mm in an optimised array. The figures for the pristine unrelieved situation are correspondingly 3.2 and 42 MJ/m^3. Although a full matrix of spacing tests was not undertaken with the roller cutter it is obvious that no significant lateral forces can be generated by this tool and the dramatic reductions of specific energy so apparent for discs in array, will not be achieved.

The study of complex shaped picks has produced results which, by and large, agree with those of Pomeroy and Evans. The reduction of forces and improved penetration capabilities associated with pointed picks are more than off-set by the loss of rock yield and the potentially damaging stress levels generated at the point. The provision of a side rake angle does lead to a reduction in specific energy when the tools are working in an optimised array. In all other situations no benefit is obtained and the significant lateral forces generated by this shape of tool can be difficult to control. Although the simple chisel represents the most efficient shape of pick, reasons have been shown why picks of a more recondite geometry have found wide acceptance in industry.

The moisture content has been shown to have an apparently inconsistent influence on the physical properties and cutting characteristics of the rock. In general forces and energies for disc cutting decrease when the rock is wet and this is quite consistent with the general change in physical properties of the rock. With picks, however, the situation is different, and rather puzzling. Forces and specific energies are invariably higher when cutting Bunter in the wet condition. By all accounts rock is weakened by water yet it requires large forces and greater energies to cut it with a pick. The care taken to avoid minor inconsistencies of rock quality from affecting a single group of the tests in Bunter Sandstone, together with the wealth of experimental data confirming this particular effect of moisture, means that the phenomenon is real and cannot be dismissed as a chance event.

The reason for this behaviour is not fully understood but two factors are thought to have a bearing on the issue. If the rock failure mechanism under the action of a pick is dependent on its shear strength, then since shear strength has been shown to be largely unaffected by moisture content, it would be reasonable to expect pick forces and energies to be similarly unaffected. But even if acceptable, this reasoning does not explain the higher forces and energies. To account for this, it is necessary to hypothesise on the role of pore water in the rock. When cutting with a pick, rock failure originates near the cutting edge and is initiated due to high stress concentrations at the boundaries of suitably orientated

natural flaws or cracks in the rock. Evans and Pomeroy provide a plausible description of the influence of such Griffith cracks on failure mechanisms for coal (19). The presence of water in the rock might, however, cause a state of hydrostatic loading in the vicinity of such flaws thereby reducing the levels of point stresses. To attain the failure stress under such circumstances would require a higher cutting force. Because the cutting force and line of failure are both in the direction of pick travel, then the water has no opportunity to disperse and a 'bow wave' effect is conceivable. In the case of discs, however, rock breakage is predominantly lateral with little occurring in the direction of rolling. And breakage is in any case dependent on the general stress level generated over the contact area of the flanks of the disc and thereby probably insensitive to the presence of water. This hypothesis appears to be consistent with the performance of both discs and picks in wet and dry rock.

The influence of water in increasing the demands on a pick is not confined to Bunter Sandstone. The same was found with Chalk, although probably for different reasons (24)(86), and core cutting tests undertaken at Newcastle in a variety of sedimentary rocks have shown that a majority involve higher forces and energies when saturated despite reductions in the rock's mechanical strength (95).

The experiments undertaken on deliberately stalled discs have been most revealing. The results show that a collapsed or siezed bearing may cause a three-fold increase in the energy required by a disc to excavate unit volume of rock.

The general trends with all three tools were qualitatively similar in both the rocks investigated. In the experiments with drag picks the ratio of forces in Bunter Sandstone to those in Magnesian Limestone could not be equated directly to any similar ratio between the measured physical properties of the two rocks. It was concluded from this that theories based on the rock failing in either simple shear or tension are unlikely to provide accurate predictions of pick forces. However, a comparison

of disc forces in the two rocks revealed them to be directly proportional to the compressive strength ofthe rock and a simple model based on this fact has been shown to be equally valid in respect of the reported work of others in this field.

The work described in this thesis has been an attempt to provide a better fundamental understanding of the mechanics of rock breakage under the action of the three prevailing cutting techniques. In addition it provides data basic to the design of a cutting head and enables realistic estimates to be made of the excavation rates likely to be achieved from a given level of input power.

REFERENCES

1. BRE/TRRL Committee on Tunnelling — "Future Tunnelling in Britain". BRE Report, CP39/74.

2. MUIRHEAD, I.R. and GLOSSOP, L.G. — "Hard Rock Tunnelling Machines". Trans. Inst. Min. & Met., Vol. 77. January, 1968, p. A1-A21.

3. PROTODYAKONOV, M.M. and TEDER, R.I. — "Application of Statistical Curves to Laboratory Experiments". Nuaka, Moscow, 1970. (Russian Text).

4. DODDS, G.S. and McKENZIE, J.C. — "Mersey Kingsway Tunnel : Construction". Proc. Inst. Civil Engrs. Vol. 51, March, 1972. p.503.

5. LYONS, A.C. and SCOFIELD, J. — "Great Charles Street Road Tunnel". Tunnels & Tunnelling, Vol.1, No.1. May-June, 1969. p.23.

6. "Mersey Loop Extension". Tunnels & Tunnelling. Vol.4, No.2. March-April, 1972. p.131.

7. ALLINGTON, A.V. — "The Machining of Rock Materials". Ph.D. Thesis, University of Newcastle upon Tyne. Oct. 1969.

8. HAY, J.D., HUGHES, H.M. and WRATHALL, R.W. — "The Bretby Tunnelling Machine". Proc. Inst. Civil Engrs. Vol. 30, April, 1965. pp.649-674.

9. BARKER, J.S., POMEROY, C.D. and WHITTAKER, D. — "The M.R.E. Large Pick Shearer Drum". The Mining Engineer. Feb. 1966. p.323.

10. POTTS, E.L.J., ROXBOROUGH, F.F. and WHITTAKER, B.N. — "Experiments with the Automatic Variable Geometry Coal Plough". The Mining Engineer. May, 1967. p.539.

11. WILSON, J.W. and GRAHAM, P.C. — "Raise-boring Experiences in the Gold Mines of the Anglo American Corporation Group". Trans. Inst. Min. & Met. (Sect. A) 82, 1973, p.A.142.

12. POMEROY, C.D. and BROWN, J.H. — "Laboratory Investigations of Cutting Processes Applied to Coal Winning Machines". J. of Strain Analysis, 1968. Vol.3. No.3. p.232.

13. EVANS, I. and POMEROY, C.D. "The Strength, Fracture and Workability of Coal". Pergamon, London. 1966. page 254.

14. RISPIN, A. "An Investigation into the Application of Linear Cutting Tools to the Machining of Strong and Abrasive Rock Materials". Ph.D. Thesis, University of Newcastle upon Tyne, Oct. 1970.

15. O'DOGHERTY, M.J. "A Laboratory Examination of the Effect of Rake Angle and Back Clearance Angle on Cutter Pick Performance in Barnsley Hards". N.C.B./M.R.E. Report No. 2217, 1962.

16. ROBINSON, D.J. and POMEROY, C.D. "Laboratory Tests with Picks of Different Profile". N.C.B./M.R.E. Report No. 2244, 1963.

17. DALZIEL, J.A. "The Effect on the Performance of a Cutter Pick of Ridging the Rake and Clearance Faces". N.C.B./M.R.E. Report No. 2291, 1965.

18. BARKER, J.S. "A Laboratory Investigation of Rock Cutting using Large Picks". Int. J. of Rock Mech. Min. Sci., Vol.1. Pergamon, p.519-34

19. EVANS, I. and POMEROY, C.D. "The Strength, Fracture and Workability of Coal". Pergamon, London. 1966. pps.277.

20. POTTS, E.L.J. and SHUTTLEWORTH, P. "A Study on the Ploughability of Coal .....". Trans. Inst. Min. Engrs. Vol.117. No.8. May, 1959, p.512.

21. ROXBOROUGH, F.F. "The Effect of Sub-sectional Strength Variations on Full Seam Ploughability". Ph.D. Thesis, University of Durham. May, 1961.

22. ALLINGTON, A.V. "The Machining of Rock Materials". Ph.D. Thesis, University of Newcastle upon Tyne, 1969.

23. OSBURN, H.J. "Wear of Rock Cutting Tools". Powder Metallurgy. 1969. Vol.12. No.24. p.471.

24. ROXBOROUGH, F.F. and RISPIN, A. "The Mechanical Cutting Characteristics of the Lower Chalk". Report to T.R.R.L., May 1972. Department of Mining Engineering, University of Newcastle upon Tyne.

25. HIGNETT, H.J. and HOWARD, T.R.
"A Pilot Scale Machine for Tunnel Boring Research".
T.R.R.L. Report 632. 1974.

26. HIGNETT, H.J.
"Laboratory and Pilot Scale Studies Related to the Design of Tunnel Boring Machines".
M.Sc. Thesis, University of Newcastle upon Tyne. Oct. 1974.

27. HIGNETT, H.J. and BODEN, J.B.
"Chinnor Tunnelling Trials - Background and Progress".
Tunnels & Tunnelling, Vol.6. No.6. Nov.-Dec, 1974. p.65.

28. COOK, N.G.W., JOUGHIN, N.C. and WIEBOLS, G.A.
"Rock Cutting and its Potentialities as a New Method of Mining".
J. of S.A. Inst. Min. & Met. Vol.68. May 1968. p.435.

29. EVANS, I.
"A Theory of the Basic Mechanics of Coal Ploughing".
Int. Symp. of Mining Research. Vol.2. Pergamon Press, London 1962. p.761.

30. DALZIEL, J.A. and DAVIES, E.
"Initiation of Cracks in Coal Specimens by Blunted Wedges".
The Engineer. Vol.217. Jan. 1964, p.217.

31. EVANS, I.
"The Force Required to Cut Coal with Blunt Wedges".
Int. J. Rock Mech. Min. Sci. Vol.2. Pergamon, 1965. p.1.

32. EVANS, I.
"Line Spacing of Picks for Effective Cutting".
Int. J. Rock Mech. Min. Sci. Vol.9. No.3. 1972. p.335.

33. MERCHANT, M.E.
"Basic Mechanics of the Metal Cutting Process".
"J. Appl. Mech. Vol.11. 1945. p.A.168.

34. SHUTTLEWORTH, P.
"An Investigation into the Design Factors Influencing the Ploughability of Coal Seams".
Ph.D. Thesis, University of Durham. June, 1958.

35. NISHIMATSU, Y. "The Mechanics of Rock Cutting". Int. J. Rock Mech. Min. Sci. Vol.9. 1972. p.261.

36. HARDY, M.P. and FAIRHIRST, C. "Chip Formation by Drag Cutters". Proc. 6th Conference on Drilling and Rock Mechanics. 1973. A.I.Min., Met., & Petroleum Engs., Inc.

37. DALZIEL, J.A. "A Laboratory Examination of Disc Cutters for Rock Cutting". N.C.B./M.R.E. Report No. 2354.

38. TEALE, R. "The Mechanical Excavation of Rock-Experiments with Roller Cutters". Int. J. Rock Mech. Min. Sci. Vol.1. No.1. 1964. p.63.

39. MORRELL, R.J., BRUCE, W.E. and LARSON, D.A. "Disc Cutter Experiments in Sedimentary and Metamorphic Rocks". U.S. Bureau of Mines. RI 7410, 1970. pp.32.

40. MORRELL, R.J. and LARSON, D.A. "Disc Cutter Experiments in Metamorphic and Igneous Rocks". U.S. Bureau of Mines. RI 7961, 1974. pp.50.

41. RAD, P.F. and OLSON, R.C. "Tunnelling Machine Research - Interaction between Disc Cutter Grooves in Rock". U.S. Bureau of Mines, RI 7881, 1974. pp.21.

42. RAD, P.F. "Muck Evaluates Machines". Tunnels & Tunnelling. Vol.7. No.1. Jan. 1975. p.30.

43. ROSS, N. and HUSTRALID, W. "Development of a Tunnel Boreability Index". Report REC-ERC-72-7, Bureau of Reclamation, Denver, Colorado 80225. Feb. 1972.

44. TAKAOKA, S., HAYAMIZU, H. and MISAWA, S. "Studies on the Cutting of Rock by Disc Cutters". Tunnels & Tunnelling. Vol.5. No.2. March, 1973. p.181.

45. EVANS, I. and MURRELL, S.A.F.
"Wedge Penetration into Coal". Colliery Engineer. Vol.39. No.445. 1962. p.11.

46. PAUL, B. and SIKARSKIE, D.L.
"A Preliminary Theory of Static Penetration by a Rigid Wedge into a Brittle Material". A.I.M.E. Trans. Vol.232. 1965. p.372.

47. GAYE, F.
"Efficient Excavation - Part 1". Tunnels & Tunnelling. Vol.4. No.1. Jan-Feb., 1972. p.39.

48. ROSS, N.A. and HUSTRALID, W.A.
"Some Comments on the Design of Medium to Hard Rock Tunnel Boring Machines". Dynamic Rock Mechanics. Proc. of 12th Symposium of Rock Mechanics. Society of Mining Engineers. New York. 1971. p.977.

49. SHEPHERD, R. and O'DOGHERTY, M.J.
"A Study of the Forces Acting on a Model Star Wheel Cutter". N.C.B./M.R.E. Report No. 2099.

50. SHEPHERD, R. and PRICE, N.J.
"Roller Bit Penetration Experiments in Concretes". N.C.B./M.R.E. Report No. 2095.

51. TAKAOKA, S., HAYANIZU, H., MISAURA, S. and KURIYAGAWA, M.
"Studies on the Cutting of Rock by Rotary Cutters - Part II". Tunnels and Tunnelling. Vol.5. No.3. May, 1973. p.276.

52. BLYTH, F.G.H.
"A Geology for Engineers". Edward Arnold, London, 1974. pps.351.

53. RAYNER, D.H.
"The Stratigraphy of the British Isles". Cambridge University Press. 1967. pps. 453.

54. SMITH, E.G., RHYS, G.H. and EDEN, R.A.
"Geology of the Country around Chesterfield, Matlock and Mansfield". Memoirs of the Geological Survey of Great Britain. Vol.112. H.M.S.O., 1967.

55. MITCHELL, G.H., et al
"Geology of the Country around Barnsley". Memoirs of the Geological Survey of Great Britain. Vol.87. H.M.S.O., 1947.

56. HEWITT, K.S. "Aspects of the Design and Application of Cutting Systems for Rock Excavation". Ph.D. Thesis. University of Newcastle upon Tyne. August, 1975.

57. CHEN, P.Y. "A Modification of Sandstone Classification". J. Sed. Petrol. 1968. Vol.38. p.54.

58. HARVEY, P.K. et al "An Accurate Fusion Method for the Analysis of Rocks & Chemically Related Materials by X-Ray Fluorescence Spectrometry". J. X-Ray Spectr. 1973. Vol.2. p.33.

59. LEAKE, B.E. et al "The Chemical Analysis of Rock Powders by Automatic X-Ray Fluorescence". Chem. Geol. 1969. Vol.5. p.7.

60. DUNCAN, N. "Engineering Geology and Rock Mechanics". Vol. 1. Leonard Hill, London. 1969. pps. 252.

61. "Directives for Rock Testing". Proc. of I.B.R.M. Symp. Nov. 1963. (German Text).

62. OBERT, L. and DUVALL, W.I. "Rock Mechanics & The Design of Structures in Rock". John Wiley & Sons, Inc. 1967. pps.650.

63. COATES, D.F. "Rock Mechanics Principles". Mines Branch Monograph, 875. 1963. Dept. of Energy, Mines and Resources, Ottowa, Canada. pps.320.

64. JAEGER, J.C. and COOK, N.G.W. "Fundamentals of Rock Mechanics". Chapman & Hall Ltd., London. 1971. pps.515.

65. ROXBOROUGH, F.F. and WHITTAKER, B.N. "Roof Control and Coal Hardness". Colliery Engineering. Dec. 1964. p.511.

66. TONKINSON, W.D. "Drilling & Rock Hardness". Kings Coll. Min. Soc. Bull. (University of Durham). Vol.3. Bull. No.3. Series:Mech. No.22.

67. GAYE, F. "Efficient Excavation - with Particular Reference to Cutting Head Design of Hard Rock Tunnelling Machines". Pt. 2, Tunnels & Tunnelling. Vol.4. No.2. March-April, 1972. p.135.

68. PROTODYAKONOV, M.M. (Jr). "The Determination of Strength of Coal in Mines". Ugol. Vol.25. Sept. 1950. p.20. (N.C.B. Transl. A.347).

69. FIELD-FOSTER, P. "Mechanical Testing of Metals and Alloys". Pitmans, London 1948. pps.319.

70. FOWELL, R.J. "A Simple Method of Assessing the Machineability of Rocks". Tunnels & Tunnelling. Vol.2. No.2. July-Aug. 1970. p.251.

71. PROTODYAKONOV, M.M. (Sr). "Compilation of Mining Norms and Their Use". Moscow, Leningrad, Novosibisk, 1932. (Russian Text).

72. PROTODYAKONOV, M.M. (Jr) and Teder, R.I. "Rational Methods of Planning Experiments". Dynamic Rock Mechanics. Proc. of 12th Symposium of Rock Mechanics Society of Mining Engineers, New York. 1971. p.129.

73. FEDERER, W.T. "Experimental Design - Theory and Application". McMillan & Co., New York. 1755. pps.543.

74. FISHER, SIR R.A. "Statistical Methods for Research Workers". Oliver & Boyd. 1970. pps.332.

75. PROTODYAKONOV, M.M. (Jr). Private Communication.

76. ROXBOROUGH, F.F. "Cutting Rock with Picks". The Mining Engineer. June 1973. p.445.

77. O'DOGHERTY, M.J. and WHITTAKER, D. "An Examination of the Characteristics of a Solid Plate Dynamometer Designed for Triaxial Force Measurements". N.C.B./M.R.E. Technical Memorandum. No.197. Nov. 1965.

78. DALZIEL, J.A., JORDAN, D.W. and WHITTAKER, D. "Force Dynamometers for Coal and Rock Cutting Research". J. Strain Analysis. Vol.3. No.2. 1968. p.81.

79. RYDER, J.D. "Engineering Electronics". McGraw Hill. 1957. pps.665.

80. POTTS, E.L.J., ROXBOROUGH, F.F. RISPIN, A. and COOPER, I.
Second Progress Report to the Wolfson Foundation. Department of Mining Engineering, University of Newcastle upon Tyne. Oct. 1972.

81. DUNN, P.L.
"An Investigation into the Mechanical Cutting of Hard Rock Materials in Relation to the Design of Effective Tunnelling Systems". Ph.D. Thesis, University of Newcastle upon Tyne. Feb. 1975.

82. DUNN, P.L.
"The Analysis of Rock Cutting Research Data by Computer". Conf. Application of New Technical Solutions and Modern Mathematical Methods in Mining. Polytechnic University Miskole, Hungary. Sept. 1972.

83. EVANS, I. and MURRELL, S.A.F.
"The Forces Required to Penetrate a Brittle Material with a Wedge Shaped Tool". Proc. of Conf. on Mech. Props. of Non-Metallic Brittle Materials. Pergamon, London. 1958. p.432.

84. POMEROY, C.D.
"Mining Applications of the Deep Cut Principle". The Mining Engineer. June 1968. p.506.

85. COOK, N.G.W.
"Analysis of Hard Rock Cuttability for Machines". (Rapid Excavation-Problems & Progress). Proc. of the Tunnel & Shaft Conf. Minneapolis. May 1968. p.39.

86. ROXBOROUGH, F.F. and RISPIN, A.
"A Laboratory Investigation into the Application of Picks for Mechanized Tunnel Boring in the Lower Chalk". The Mining Engineer. Oct. 1973. p.1.

87. POMEROY, C.D.
Private Communication.

88.
"Rock Cutting Research - An Investigation of Tool Wear - A Proposal to Hoy Carbides". Department of Mining Engineering, University of Newcastle upon Tyne.

89. HARLE, M. and FOWELL, R.J.
"The Effect of Abrasion on the Performance of Drag Picks in Bunter Sandstone". To be published.

90. BARKER, J.S. — Private Communication.

91. HARLE, M. — "An Investigation of some Fundamental Aspects of Three Dimensional Chip Formation in Rock Cutting". M.Sc. Dissertation, University of Newcastle upon Tyne. Aug. 1973.

92. EVANS, I. — Private Communication.

93. POTTS, E.L.J., ROXBOROUGH, F.F., RISPIN, A. and COOPER, I. — Fourth Progress Report to the Wolfson Foundation. Department of Mining Engineering, University of Newcastle upon Tyne, October, 1974.

94. GAYE, F. — Private Communication .

95. CROZIER, A. — "The Assessment of Rock Machineability and Abrasivity from Borehole Samples". M.Sc. Dissertation, University of Newcastle upon Tyne. Aug. 1972.

APPENDIX IA

EXPERIMENT I - DRY BUNTER SANDSTONE

Test No	Levels of α, w, d	$\overline{F}_C$ kN	F_C kN	$\overline{F}_N$ kN	F_N kN
1	-10, 10, 3	0.374	1.236	0.363	0.956
2	-10, 20, 9	1.890	3.759	1.669	3.103
3	-10, 30, 15	4.230	8.393	3.964	7.830
4	-10, 40, 6	1.285	3.293	1.824	3.630
5	-10, 50, 12	3.856	6.837	3.945	5.350
6	0, 20, 6	0.722	2.217	0.667	1.692
7	0. 30, 12	2.432	5.441	1.763	4.016
8	0. 40, 3	0.740	2.186	1.383	2.739
9	0, 50, 9	1.440	3.214	1.190	2.607
10	0, 10, 15	1.650	4.151	1.466	3.175
11	10, 30, 9	1.048	2.792	1.495	2.989
12	10, 40, 15	2.320	5.300	2.280	4.646
13	10, 50, 6	1.518	3.558	2.440	5.107
14	10, 10, 12	0.975	2.567	0.779	1.889
15	10, 20, 3	0.371	1.046	0.443	0.972
16	20, 40, 12	1.860	4.367	2.020	3.966
17	20, 50, 3	0.813	1.765	1.481	2.685
18	20, 10, 9	0.520	1.464	0.576	1.267
19	20, 20, 15	1.154	3.394	1.008	2.365
20	20, 30, 6	0.714	1.988	1.190	2.373
21	30, 50, 15	1.474	3.778	1.085	2.273
22	30, 10, 6	0.358	1.001	0.449	1.031
23	30, 20, 12	0.933	2.388	1.034	2.231
24	30, 30, 3	0.537	1.389	0.922	1.767
25	30, 40, 9	0.758	2.400	0.967	2.305

APPENDIX IB

EXPERIMENT I - DRY BUNTER SANDSTONE

Test No	Levels of α, w, d	Q m^3/km	S.E. MJ/m^3	C.I.
1	-10, 10, 3	0.050	7.598	287
2	-10, 20, 9	0.352	5.409	394
3	-10, 30, 15	1.150	3.683	489
4	-10, 40, 6	0.305	4.206	356
5	-10, 50, 12	0.965	4.011	461
6	0, 20, 6	0.187	3.853	365
7	0, 30, 12	0.763	3.189	455
8	0, 40, 3	0.124	5.944	279
9	0, 50, 9	0.736	1.953	436
10	0, 10, 15	0.819	2.093	521
11	10, 30, 9	0.524	2.024	459
12	10, 40, 15	1.395	1.704	546
13	10, 50, 6	0.386	3.979	406
14	10, 10, 12	0.538	1.876	466
15	10, 20, 3	0.062	5.991	274
16	20, 40, 12	0.866	2.152	530
17	20, 50, 3	0.150	5.480	297
18	20, 10, 9	0.298	1.744	458
19	20, 20, 15	1.107	1.043	566
20	20, 30, 6	0.249	2.891	396
21	30, 50, 15	1.454	1.049	559
22	30, 10, 6	0.130	2.753	400
23	30, 20, 12	0.711	1.317	518
24	30, 30, 3	0.101	5.330	301
25	30, 40, 9	0.553	1.372	461

APPENDIX IC

EXPERIMENT II - WET BUNTER SANDSTONE

Test No	Levels of α, w, d	$\overline{F}_C$ kN	F_C kN	$\overline{F}_N$ kN	F_N kN
1	-10, 10, 3	0.325	0.989	0.349	0.959
2	-10, 20, 9	1.649	3.914	1.613	3.198
3	-10, 30, 15	5.353	9.743	4.772	8.280
4	-10, 40, 6	1.548	3.339	1.436	2.938
5	-10, 50, 12	5.227	9.744	4.673	8.632
6	0, 20, 6	0.917	2.554	0.914	2.094
7	0, 30, 12	2.237	5.052	1.749	4.031
8	0, 40, 3	1.072	2.316	1.137	2.643
9	0, 50, 9	2.406	5.554	2.336	5.884
10	0, 10, 15	2.409	4.393	1.716	3.226
11	10, 30, 9	1.170	2.923	1.185	2.453
12	10, 40, 15	2.637	5.016	2.334	4.386
13	10, 50, 6	1.616	3.727	2.236	5.109
14	10, 10, 12	1.081	2.936	0.663	1.617
15	10, 20, 3	0.355	0.950	0.452	0.977
16	20, 40, 12	1.746	4.088	1.914	4.106
17	20, 50, 3	1.086	2.497	1.903	3.471
18	20, 10, 9	0.598	1.632	0.533	1.173
19	20, 20, 15	1.436	3.480	0.934	2.242
20	20, 30, 6	0.823	2.019	1.127	2.124
21	30, 50, 15	1.559	3.551	0.948	2.357
22	30, 10, 6	0.362	1.033	0.408	1.051
23	30, 20, 12	1.028	2.713	1.071	2.418
24	30, 30, 3	0.574	1.299	0.863	1.563
25	30, 40, 9	0.969	2.735	0.972	2.389

APPENDIX ID

EXPERIMENT II - WET BUNTER SANDSTONE

Test No	Levels of α, w, d	Q m^3/km	S.E. MJ/m^3	C.I.
1	-10, 10, 3	0.041	7.924	308
2	-10, 20, 9	0.390	4.305	442
3	-10, 30, 15	1.061	5.237	492
4	-10, 40, 6	0.274	5.701	386
5	-10, 50, 12	0.958	5.505	481
6	0, 20, 6	0.196	4.715	434
7	0, 30, 12	0.880	2.559	509
8	0, 40, 3	0.113	9.465	282
9	0, 50, 9	0.635	3.932	448
10	0, 10, 15	0.652	3.722	497
11	10, 30, 9	0.472	2.492	477
12	10, 40, 15	1.303	2.103	588
13	10, 50, 6	0.354	4.570	406
14	10, 10, 12	0.414	2.661	465
15	10, 20, 3	0.060	5.934	273
16	20, 40, 12	0.944	1.900	546
17	20, 50, 3	0.137	8.009	282
18	20, 10, 9	0.337	1.792	484
19	20, 20, 15	1.225	1.206	589
20	20, 30, 6	0.247	3.364	401
21	30, 50, 15	1.728	0.920	555
22	30, 10, 6	0.144	2.533	419
23	30, 20, 12	0.702	1.484	565
24	30, 30, 3	0.097	5.925	275
25	30, 40, 9	0.576	1.689	491

APPENDIX IE

EXPERIMENT III - MAGNESIAN LIMESTONE

Test No	Levels of α, w, d	$\overline{F}_C$ kN	F_C kN	$\overline{F}_N$ kN	F_N kN
1	-10, 10, 3	1.340	3.895	1.297	2.759
2	-10, 20, 9	4.341	17.756	3.948	8.792
3	-10, 30, 15	15.786	22.540	14.070	15.200
4	-10, 40, 6	6.033	8.338	6.403	8.721
5	-10, 50, 12	16.889	23.847	16.194	18.517
6	0, 20, 6	3.243	9.813	2.574	5.692
7	0, 30, 12	8.599	12.791	5.511	8.214
8	0, 40, 3	3.341	6.414	3.763	6.156
9	0, 50, 9	9.697	23.308	7.902	15.138
10	0, 10, 15	9.652	17.418	5.304	7.593
11	10, 30, 9	5.254	16.435	5.934	13.317
12	10, 40, 15	12.429	20.173	8.531	11.764
13	10, 50, 6	4.460	12.458	3.687	8.193
14	10, 10, 12	3.923	9.717	1.921	3.703
15	10, 20, 3	1.355	4.395	1.299	2.825
16	20, 40, 12	7.540	16.785	8.054	15.484
17	20, 15, 3	4.151	8.435	3.525	9.015
18	20, 10, 9	2.656	9.511	2.666	5.735
19	20, 20, 15	5.444	13.337	2.739	4.874
20	20, 30, 6	3.254	10.031	3.562	8.744
21	30, 50, 15	5.777	12.147	3.696	5.661
22	30, 10, 6	1.551	5.221	1.661	3.874
23	30, 20, 12	6.495	15.305	5.924	9.957
24	30, 30, 3	2.898	7.057	2.914	5.830
25	30, 40, 9	4.274	12.101	3.495	6.834

APPENDIX IF

EXPERIMENT III - MAGNESIAN LIMESTONE

Test No	Levels of α, w, d	Q m^3/km	S.E. MJ/m^3	C.I.
1	-10, 10, 3	0.043	31.33	382
2	-10, 20, 9	0.350	12.58	469
3	-10, 30, 15	0.839	24.82	510
4	-10, 40, 6	0.275	21.94	440
5	-10, 50, 12	0.660	25.55	472
6	0, 20, 6	0.173	18.77	433
7	0, 30, 12	0.677	16.86	498
8	0, 40, 3	0.133	25.26	380
9	0, 50, 9	0.552	17.54	487
10	0, 10, 15	0.566	17.11	506
11	10, 30, 9	0.468	11.34	530
12	10, 40, 15	1.042	11.90	554
13	10, 50, 6	0.336	13.30	447
14	10, 10, 12	0.312	12.58	546
15	10, 20, 3	0.067	20.10	392
16	20, 40, 12	0.724	10.42	525
17	20, 50, 3	0.129	32.09	379
18	20, 10, 9	0.257	10.38	504
19	20, 20, 15	0.874	6.30	476
20	20, 30, 6	0.223	14.65	459
21	30, 50, 15	1.344	4.60	581
22	30, 10, 6	0.135	11.43	460
23	30, 20, 12	0.491	13.15	525
24	30, 30, 3	0.091	31.87	387
25	30, 40, 9	0.468	9.49	500

APPENDIX IG

GROUPED DATA FOR EXPERIMENT I

	$\overline{F}_C$ kN	$\overline{F}_N$ kN	F_C kN	F_N kN	Q m^3/km	S.E. MJ/m^3	C.I.
$P_{1\alpha}$	2.33	2.35	.470	4.17	0.56	4.98	397
$P_{2\alpha}$	1.40	1.29	3.44	2.85	0.53	3.41	411
$P_{3\alpha}$	1.25	1.49	3.05	3.12	0.58	3.12	430
$P_{4\alpha}$	1.01	1.26	2.60	2.53	0.53	2.66	450
$P_{5\alpha}$	0.81	0.89	2.19	2.01	0.59	2.36	448
P_{1W}	0.78	0.61	2.08	1.66	0.37	3.21	426
P_{2W}	1.01	0.96	2.56	2.07	0.48	3.52	423
P_{3W}	1.79	1.87	4.00	3.80	0.56	3.42	420
P_{4W}	1.39	1.70	3.51	3.46	0.65	3.08	434
P_{5W}	1.82	2.03	3.83	3.69	0.74	3.30	432
P_{1d}	0.57	0.92	1.52	1.82	0.10	6.07	288
P_{2d}	0.92	1.31	2.41	2.77	0.25	3.54	385
P_{3d}	1.13	1.18	2.73	2.45	0.49	2.50	441
P_{4d}	2.01	1.91	4.32	3.49	0.77	2.51	486
P_{5d}	2.17	1.96	5.00	4.15	1.19	1.92	536

APPENDIX IH

GROUPED DATA FOR EXPERIMENT II

	$\overline{F}_C$ kN	$\overline{F}_N$ kN	F_C kN	F_N kN	Q m^3/km	S.E. MN/m^3	C.I.
$P_{1\alpha}$	2.82	2.57	5.55	4.80	0.55	5.73	422
$P_{2\alpha}$	1.81	1.57	3.97	3.58	0.50	4.88	434
$P_{3\alpha}$	1.37	1.37	3.11	2.91	0.52	3.55	442
$P_{4\alpha}$	1.14	1.28	2.74	2.62	0.58	3.25	450
$P_{5\alpha}$	0.90	0.85	2.27	1.96	0.65	2.51	448
P_{1W}	0.96	0.73	2.20	1.61	0.32	3.73	434
P_{2W}	1.08	1.00	3.16	2.19	0.52	3.53	460
P_{3W}	2.03	1.94	4.21	3.69	0.55	3.92	431
P_{4W}	1.59	1.56	3.50	3.29	0.64	4.17	459
P_{5W}	2.38	2.42	5.02	5.09	0.76	4.59	435
P_{1d}	0.68	0.94	1.61	1.92	0.09	7.45	284
P_{2d}	1.05	1.22	2.53	2.66	0.24	4.18	409
P_{3d}	1.36	1.33	3.35	3.02	0.48	2.84	469
P_{4d}	2.26	2.01	4.91	4.16	0.78	2.82	513
P_{5d}	2.68	2.14	5.24	4.10	1.19	2.64	544

APPENDIX IJ

GROUPED DATA FOR EXPERIMENT III

	$\overline{F}_C$ kN	F_C kN	$\overline{F}_N$ kN	F_N kN	Q m^3/km	S.E. MJ/m^3	C.I.
$P_{1\alpha}$	8.88	15.28	8.38	10.80	0.433	23.24	455
$P_{2\alpha}$	6.91	13.95	5.01	8.56	0.426	19.11	461
$P_{3\alpha}$	5.48	12.64	4.27	7.96	0.445	13.84	494
$P_{4\alpha}$	4.61	11.63	4.11	8.77	0.441	14.77	469
$P_{5\alpha}$	4.20	10.37	3.54	6.43	0.506	14.11	490
$P_{1\omega}$	3.82	9.16	2.57	4.73	0.263	16.57	480
$P_{2\omega}$	4.18	12.12	3.30	6.43	0.391	14.18	459
$P_{3\omega}$	7.16	13.77	6.40	10.26	0.370	19.91	477
$P_{4\omega}$	6.72	12.76	6.05	9.79	0.528	15.80	480
$P_{5\omega}$	8.19	16.04	7.00	11.30	0.604	18.61	473
P_{1d}	2.62	6.04	2.56	5.32	0.093	28.13	384
P_{2d}	3.71	9.17	3.57	7.04	0.228	16.02	448
P_{3d}	5.24	15.83	4.79	9.96	0.419	12.27	498
P_{4d}	8.69	15.69	7.52	11.18	0.573	15.71	513
P_{5d}	9.82	17.12	6.87	9.02	0.933	12.94	525

APPENDIX IK

RATIOS OF MEASURED PARAMETERS IN MAGNESIAN LIMESTONE TO EQUIVALENT VALUES IN DRY BUNTER SANDSTONE

Test No	Levels of d, w, d	$\bar{F}_C$ Ratio	$\bar{F}_N$ Ratio	Q Ratio	S.E. Ratio	C.I. Ratio
1	-10, 10, 3	3.583	3.573	0.86	4.123	1.331
2	-10, 20, 9	2.297	2.365	0.99	2.283	1.190
3	-10, 30, 15	3.732	3.549	0.73	6.739	1.043
4	-10, 40, 6	4.695	3.510	0.90	5.216	1.236
5	-10, 50, 12	4.380	4.105	0.68	6.370	1.024
6	0, 20, 6	4.492	3.859	0.93	4.872	1.186
7	0, 30, 12	3.536	3.126	0.89	5.287	1.095
8	0, 40, 3	4.515	2.721	1.07	4.250	1.362
9	0, 50, 9	6.734	6.640	0.75	8.981	1.117
10	0, 10, 15	5.849	3.618	0.69	8.175	0.971
11	10, 30, 9	5.013	3.969	0.89	5.603	1.155
12	10, 40, 15	5.357	3.742	0.75	6.984	1.015
13	10, 50, 6	2.938	1.511	0.87	3.343	1.101
14	10, 10, 12	4.024	2.466	0.58	6.706	1.172
15	10, 20, 3	3.652	2.932	1.08	3.355	1.431
16	20, 40, 12	4.054	3.987	0.84	4.842	0.991
17	20, 50, 3	5.106	2.380	0.86	5.856	1.276
18	20, 10, 9	5.108	4.628	0.86	5.952	1.100
19	20, 20, 15	4.718	2.717	0.79	6.040	0.841
20	20, 30, 6	4.557	2.993	0.90	5.067	1.159
21	30, 50, 15	3.919	3.406	0.92	4.385	1.039
22	30, 10, 6	4.332	3.699	1.04	4.152	1.150
23	30, 20, 12	6.961	5.729	0.69	9.985	1.014
24	30, 30, 3	5.397	3.161	0.90	5.979	1.286
25	30, 40, 9	5.639	3.614	0.85	6.917	1.085

APPENDIX IL

GROUPED DATA FOR RATIOS BETWEEN MEASURED PARAMETERS IN MAGNESIAN LIMESTONE AND DRY BUNTER SANDSTONE

	$\overline{F}_C$	$\overline{F}_N$	Q	S.E.	C.I.
$P_{1\alpha}$	3.74	3.42	0.83	4.95	1.16
$P_{2\alpha}$	5.03	3.99	0.86	6.31	1.15
$P_{3\alpha}$	4.20	2.92	0.83	5.20	1.17
$P_{4}\alpha$	4.71	3.34	0.85	5.55	1.07
$P_{5\alpha}$	5.25	3.92	0.88	6.28	1.11
$P_{1\omega}$	4.58	3.60	0.81	5.82	1.14
$P_{2\omega}$	4.42	3.52	0.90	5.31	1.13
$P_{3\omega}$	4.45	3.36	0.86	5.74	1.15
$P_{4\omega}$	4.85	3.51	0.88	5.64	1.14
$P_{5\omega}$	4.62	3.61	0.82	5.79	1.11
P_{1d}	4.45	2.95	0.95	4.71	1.34
P_{2d}	4.20	3.11	0.93	4.53	1.17
P_{3d}	4.96	4.24	0.87	5.95	1.13
P_{4d}	4.59	3.88	0.74	6.64	1.06
P_{5d}	4.72	3.41	0.78	6.46	0.98

APPENDIX IM

BREAKOUT ANGLE (θ^{o}) WHEN CUTTING WITH PICKS

Test No	Levels of α, w, d	Dry Bunter	Wet Bunter	Magnesian Limestone
1	-10, 10, 3	64.5	50.7	55.3
2	-10, 20, 9	64.8	74.9	64.5
3	-10, 30, 15	72.2	69.8	59.9
4	-10, 40, 6	61.0	43.4	44.2
5	-10, 50, 12	68.5	68.1	22.6
6	0, 20, 6	61.8	64.7	55.8
7	0, 30, 12	70.3	74.5	65.6
8	0, 40, 3	24.0	0.0	55.3
9	0, 50, 9	74.2	66.4	51.5
10	0, 10, 15	71.2	65.9	61.6
11	10, 30, 9	72.3	68.1	67.8
12	10, 40, 15	74.2	72.3	63.0
13	10, 50, 6	67.3	56.3	45.0
14	10, 10, 12	71.0	63.9	53.1
15	10, 20, 3	10.7	0.0	37.9
16	20, 40, 12	69.5	72.8	59.4
17	20, 50, 3	0.0	0.0	0.0
18	20, 10, 9	68.7	71.1	64.1
19	20, 20, 15	74.4	76.3	68.6
20	20, 30, 6	62.4	61.8	50.0
21	30, 50, 15	72.3	77.0	69.3
22	30, 10, 6	62.1	66.8	64.3
23	30, 20, 12	73.0	72.7	60.1
24	30, 30, 3	50.7	37.9	6.3
25	30, 40, 9	67.2	69.4	53.1

APPENDIX IN

GROUPED DATA FOR BREAKOUT ANGLE (θ^{o})

	Dry Bunter	Wet Bunter	Magnesian Limestone
$P_{1\alpha}$	66.2	61.4	49.3
$P_{2\alpha}$	60.3	54.3	58.0
$P_{3\alpha}$	59.1	52.1	53.4
$P_{4\alpha}$	55.0	56.4	48.4
$P_{5\alpha}$	65.1	64.8	50.6
$P_{1\omega}$	67.5	63.7	59.7
$P_{2\omega}$	56.9	57.7	57.4
$P_{3\omega}$	65.6	62.4	49.9
$P_{4\omega}$	59.2	51.6	55.0
$P_{5\omega}$	56.4	53.6	37.7
P_{1d}	30.0	17.7	31.0
P_{2d}	62.9	58.6	51.9
P_{3d}	69.4	70.0	60.2
P_{4d}	70.5	70.4	52.2
P_{5d}	72.9	72.3	64.5

APPENDIX IP

RATIOS OF FORCES - DRY BUNTER SANDSTONE

Test No	Levels of α, w, d	$F_C/\bar{F}_C$	$F_N/\bar{F}_N$	$\bar{F}_C/\bar{F}_N$	F_C/F_N
1	-10, 10, 3	3.305	2.634	1.030	1.293
2	-10, 20, 9	1.989	1.859	1.132	1.211
3	-10, 30, 15	1.984	1.975	1.067	1.072
4	-10, 40, 6	2.563	1.990	0.704	0.907
5	-10, 50, 12	1.773	1.356	0.977	1.277
6	0, 20, 6	3.071	2.537	1.082	1.310
7	0, 30, 12	2.237	2.278	1.379	1.354
8	0, 40, 3	2.954	1.980	0.535	0.798
9	0, 50, 9	2.232	2.191	1.210	1.233
10	0, 10, 15	2.516	2.166	1.126	1.308
11	10, 30, 9	2.664	1.999	0.701	0.934
12	10, 40, 15	2.284	2.038	1.018	1.139
13	10, 50, 6	2.344	2.093	0.622	0.697
14	10, 10, 12	2.633	2.425	1.252	1.359
15	10, 20, 3	2.819	2.194	0.837	1.075
16	20, 40, 12	2.348	1.963	0.921	1.102
17	20, 50, 3	2.171	1.813	0.548	0.656
18	20, 10, 9	2.815	2.200	0.903	1.155
19	20, 20, 15	2.941	2.346	1.145	1.435
20	20, 30, 6	2.784	1.994	0.600	0.838
21	30, 50, 15	2.563	2.510	1.359	1.388
22	30, 10, 6	2.796	2.296	0.797	2.228
23	30, 20, 12	2.559	2.158	0.902	1.070
24	30, 30, 3	2.587	1.916	0.582	0.702
25	30, 40, 9	3.166	2.384	0.784	1.036

APPENDIX IQ

RATIOS OF FORCES - WET BUNTER SANDSTONE

Test No	Levels of α, w, d	$F_C/\overline{F}_C$	$F_N/\overline{F}_N$	$\overline{F}_C/\overline{F}_N$	F_C/F_N
1	-10, 10, 3	3.043	2.748	0.931	1.031
2	-10,.20, 9	2.374	1.983	1.022	1.224
3	-10, 30, 15	1.820	1.735	1.122	1.177
4	-10, 40, 6	2.127	2.046	1.078	1.136
5	-10, 50, 12	1.864	1.847	1.119	1.129
6	0, 20, 6	2.785	2.287	1.003	1.220
7	0, 30, 12	2.258	2.305	1.279	1.253
8	0, 40, 3	2.160	2.325	0.943	0.876
9	0, 50, 9	2.308	2.519	1.030	0.944
10	0, 10, 15	1.823	1.880	1.404	1.362
11	10, 30, 9	2.498	2.070	0.987	1.192
12	10, 40, 15	1.902	1.879	1.130	1.144
13	10, 50, 6	2.306	2.285	0.723	0.729
14	10, 10, 12	2.716	2.439	1.630	1.816
15	10, 20, 3	2.676	2.162	0.785	0.972
16	20, 40, 12	2.341	2.145	0.912	0.996
17	20, 50, 3	2.299	1.824	0.571	0.719
18	20, 10, 9	2.729	2.200	1.122	1.391
19	20, 20, 15	2.423	2.400	1.537	1.552
20	20, 30, 6	2.453	1.885	0.730	0.951
21	30, 50, 15	2.278	2.486	1.645	1.507
22	30, 10, 6	2.854	2.576	0.887	0.982
23	30, 20, 12	2.639	2.258	0.960	1.122
24	30, 30, 3	2.263	1.811	0.665	0.831
25	30, 40, 9	2.822	2.458	0.997	1.145

APPENDIX IR

RATIOS OF FORCES - MAGNESIAN LIMESTONE

Test No	Levels of α, w, d	$F_C/\bar{F}_C$	$F_N/\bar{F}_N$	$\bar{F}_C/\bar{F}_N$	F_C/F_N
1	-10, 10, 3	2.907	2.127	1.033	1.412
2	-10, 20, 9	4.090	2.227	1.100	2.020
3	-10, 30, 15	1.428	1.080	1.122	1.483
4	-10, 40, 6	1.382	1.362	0.942	0.956
5	-10, 50, 12	1.412	1.143	1.043	1.288
6	0, 20, 6	3.026	2.211	1.260	1.724
7	0, 30, 12	1.487	1.490	1.560	1.557
8	0, 40, 3	1.920	1.636	0.888	1.042
9	0, 50, 9	2.404	1.916	1.227	1.540
10	0, 10, 15	1.805	1.432	1.820	2.294
11	10, 30, 9	3.128	2.244	0.885	1.234
12	10, 40, 15	1.623	1.379	1.457	1.715
13	10, 50, 6	2.793	2.222	1.210	1.521
14	10, 10, 12	2.477	1.928	2.042	2.624
15	10, 20, 3	3.244	2.175	1.043	1.556
16	20, 40, 12	2.226	1.923	0.936	1.084
17	20, 50, 3	2.032	2.557	1.178	0.936
18	20, 10, 9	3.604	2.151	0.996	1.669
19	20, 20, 15	2.450	1.779	1.988	2.736
20	20, 30, 6	3.083	2.455	0.914	1.147
21	30, 50, 15	2.103	1.532	1.563	2.146
22	30, 10, 6	3.366	2.332	0.934	1.348
23	30, 20, 12	2.356	1.681	1.096	1.537
24	30, 30, 3	2.435	2.001	0.995	1.210
25	30, 40, 9	2.831	1.955	1.223	1.771

APPENDIX IS

GROUPED DATA FOR RATIOS BETWEEN FORCES - BUNTER SANDSTONE

	DRY BUNTER			WET BUNTER		
	$\overline{F}_C/\overline{F}_N$	F_C/F_C	$F_N/\overline{F}_N$	$\overline{F}_C/\overline{F}_N$	F_C/F_C	$F_N/\overline{F}_N$
$P_{1\alpha}$	0.98	2.32	1.96	1.05	2.25	2.07
$P_{2\alpha}$	1.07	2.60	2.23	1.13	2.27	2.26
$P_{3\alpha}$	0.89	2.55	2.15	1.05	2.42	2.17
$P_{4\alpha}$	0.82	2.61	2.06	0.97	2.45	2.09
$P_{5\alpha}$	0.88	2.73	2.25	1.03	2.57	2.32
$P_{1\omega}$	1.02	2.81	2.34	1.19	2.63	2.37
$P_{2\omega}$	1.02	2.68	2.22	1.06	2.58	2.22
$P_{3\omega}$	0.87	2.45	2.03	0.96	2.26	1.96
$P_{4\omega}$	0.79	2.66	2.07	1.01	2.27	2.17
$P_{5\omega}$	0.94	2.22	1.99	1.02	2.21	2.19
P_{1d}	0.71	2.77	2.11	0.78	2.49	2.17
P_{2d}	0.76	2.71	2.18	0.88	2.51	2.22
P_{3d}	0.95	2.57	2.13	1.03	2.55	2.25
P_{4d}	1.28	2.31	2.04	1.18	2.36	2.20
P_{5d}	1.14	2.46	2.21	1.37	2.05	2.08

APPENDIX IT

GROUPED DATA FOR RATIOS BETWEEN FORCES - MAGNESIAN LIMESTONE

	$\overline{F}_C/\overline{F}_N$	$F_C/\overline{F}_C$	$F_N/\overline{F}_N$	F_C/F_N
$P_1\alpha$	1.05	2.24	1.59	1.43
$P_2\alpha$	1.35	2.13	1.74	1.63
$P_3\alpha$	1.33	2.65	1.99	1.73
$P_4\alpha$	1.20	2.68	2.17	1.51
$P_5\alpha$	1.16	2.62	1.90	1.60
$P_1\omega$	1.37	2.83	1.99	1.87
$P_2\omega$	1.30	3.03	2.01	1.91
$P_3\omega$	1.10	2.31	1.85	1.33
$P_4\omega$	1.09	2.00	1.65	1.31
$P_5\omega$	1.24	2.15	1.87	1.49
P_1d	1.03	2.51	2.10	1.23
P_2d	1.05	2.73	2.12	1.34
P_3d	1.09	3.21	2.10	1.65
P_4d	1.34	1.99	1.63	1.62
P_5d	1.59	1.88	1.44	2.07

APPENDIX IIA

ROCK MOISTURE CONTENT AND DENSITY - BUNTER SANDSTONE

	Experiment II		Experiment V	
Test No	Moisture Content	Density	Moisture Content	Density
1	6.99 %	2.168g/cc	8.23 %	2.193g/cc
2	7.20	2.172	7.33	2.175
3	5.75	2.142	7.53	2.179
4	7.11	2.170	7.44	2.177
5	7.10	2.170	7.04	2.169
6	6.90	2.166	7.95	2.187
7	7.23	2.172	6.89	2.166
8	8.20	2.192	7.84	2.185
9	7.33	2.175	7.01	2.168
10	7.25	2.173	6.89	2.166
11	6.68	2.161	6.89	2.166
12	7.03	2.168	7.40	2.176
13	7.19	2.172	7.39	2.176
14	7.98	2.188	7.43	2.177
15	9.59	2.220	6.07	2.149
16	6.69	2.162	6.07	2.149
17	8.25	2.193	8.04	2.189
18	7.23	2.172	7.14	2.171
19	7.30	2.174	7.60	2.180
20	7.08	2.169	6.90	2.166
21	8.11	2.190	6.24	2.152
22	7.29	2.174	6.37	2.155
23	7.69	2.182	6.02	2.148
24	8.26	2.193	6.61	2.160
25	6.60	2.160	6.79	2.164
Mean	7.36	2.175	7.07	2.170
± s.d.	0.74	0.015	0.65	0.013

APPENDIX IIB

ROCK MOISTURE CONTENT AND DENSITY - BUNTER SANDSTONE

	Experiment VII		Experiment X	
Test No	Moisture Content	Density	Moisture Content	Density
1	7.51 %	2.178g/cc	6.72 %	2.162g/cc
2	8.33	2.195	7.79	2.184
3	7.74	2.183	9.23	2.213
4	6.66	2.161	7.24	2.173
5	8.42	2.197	6.33	2.154
6	7.01	2.168	6.98	2.167
7	10.27	2.238	6.93	2.166
8	7.33	2.175	7.27	2.173
9	5.36	2.136	11.60	2.261
10	7.34	2.175	7.02	2.168
11	8.96	2.208	7.80	2.184
12	6.08	2.149	8.39	2.196
13	7.63	2.181	7.47	2.177
14	8.11	2.190	7.27	2.173
15	6.22	2.152	7.31	2.174
16	8.78	2.204	6.93	2.166
17	6.25	2.153	6.84	2.165
18	9.76	2.224	9.18	2.212
19	6.93	2.166	9.13	2.211
20	7.63	2.181	7.57	2.179
21	8.30	2.194	10.59	2.241
22	7.93	2.187	7.78	2.184
23	7.32	2.174	6.36	2.155
24	7.11	2.170	7.32	2.174
25	8.97	2.208	7.80	2.184
Mean	7.68	2.181	7.79	2.184
± s.d.	1.16	0.024	1.27	0.026

APPENDIX IIIA

EXPERIMENT IV - DRY BUNTER SANDSTONE

Test No	Levels of α, w, d, s	$\overline{F}_C$ kN	F_C kN	$\overline{F}_N$ kN	F_N kN
1	-10, 10, 3, -6	0.154	0.521	0.114	0.422
2	-10, 20, 9, 30	1.910	4.474	1.424	3.004
3	-10, 30, 15, 6	1.683	3.997	1.363	3.274
4	-10, 40, 6, 42	1.971	4.064	1.917	3.348
5	-10, 50, 12, 18	3.012	5.988	2.936	6.358
6	0, 20, 6, 6	0.879	2.921	0.841	2.265
7	0, 30, 12, 42	1.573	3.515	1.331	3.305
8	0, 40, 3, 18	1.027	2.707	1.422	2.992
9	0, 50, 9, -6	1.724	4.319	2.013	4.138
10	0, 10, 15, 30	1.468	4.203	0.960	2.340
11	10, 30, 9, 18	1.102	3.277	1.926	4.157
12	10, 40, 15, -6	1.281	4.296	1.218	3.230
13	10, 50, 6, 30	1.473	3.509	2.005	4.127
14	10, 10, 12, 6	0.354	1.084	0.405	1.076
15	10, 20, 3, 42	0.360	1.106	0.509	1.141
16	20, 40, 12, 30	1.419	2.884	1.850	3.651
17	20, 50, 3, 6	0.718	1.931	1.271	2.118
18	20, 10, 9, 42	0.854	2.353	0.671	1.598
19	20, 20, 15, 18	1.043	3.080	1.029	2.462
20	20, 30, 6, -6	0.540	1.615	0.748	1.624
21	30, 50, 15, 42	2.270	5.673	1.997	4.721
22	30, 10, 6, 18	0.405	1.151	0.480	1.127
23	30, 20, 12, -6	0.377	1.210	0.463	1.234
24	30, 30, 3, 30	0.749	1.765	1.117	2.032
25	30, 40, 9, 6	1.333	3.671	1.397	3.099

APPENDIX IIIB

EXPERIMENT IV - DRY BUNTER SANDSTONE

Test No	Levels of a, w, d, s	Q m^3/km	S.E. MJ/m^3	C.I.
1	-10, 10, 3, -6	0.011	13.060	249
2	-10, 20, 9, 30	0.390	4.933	437
3	-10, 30, 15, 6	0.554	3.142	486
4	-10, 40, 6, 42	0.279	7.070	388
5	-10, 50, 12, 18	0.805	3.770	468
6	0, 20, 6, 6	0.154	5.740	391
7	0, 30, 12, 12	0.754	2.099	494
8	0, 40, 3, 18	0.136	7.527	311
9	0, 50, 9, -6	0.391	4.419	441
10	0, 10, 15, 30	0.469	3.154	495
11	10, 30, 9, 18	0.396	2.770	453
12	10, 40, 15, -6	0.433	3.181	481
13	10, 50, 6, 30	0.387	3.817	417
14	10, 10, 21, 6	0.133	3.148	449
15	10, 20, 3, 42	0.069	5.183	312
16	20, 40, 12, 30	0.797	1.803	513
17	20, 50, 3, 6	0.147	4.897	309
18	20, 10, 9, 42	0.270	3.191	488
19	20, 20, 15, 18	0.517	2.091	503
20	20, 30, 6, -6	0.139	3.798	419
21	30, 50, 15, 42	1.227	1.852	555
22	30, 10, 6, 18	0.133	3.077	430
23	30, 20, 12, -6	0.130	3.777	454
24	30, 30, 3, 30	0.097	7.695	322
25	30, 40, 9, 6	0.430	3.110	481

APPENDIX IIIC

EXPERIMENT V - WET BUNTER SANDSTONE

Test No	Levels of α, w, d, s	$\overline{F}_C$ kN	F_C kN	$\overline{F}_N$ kN	F_N kN
1	-10, 10, 3, -6	0.088	0.329	0.078	0.264
2	-10, 20, 9, 30	1.430	3.682	1.045	2.432
3	-10, 30, 15, 6	1.354	3.668	1.087	2.379
4	-10, 40, 6, 42	1.767	4.058	1.480	2.855
5	-10, 50, 12, 18	3.105	6.587	2.454	4.528
6	0, 20, 6, 6	0.613	1.767	0.500	1.148
7	0, 30, 12, 42	1.715	4.439	1.050	2.442
8	0, 40, 3, 18	0.970	2.260	1.255	2.210
9	0, 50, 9, -6	1.052	2.744	0.832	1.767
10	0, 10, 15, 30	1.764	4.263	0.823	1.700
11	10, 30, 9, 18	1.059	2.885	1.064	2.254
12	10, 40, 15, -6	1.066	3.124	0.732	1.787
13	10, 50, 6, 30	1.693	4.143	2.231	4.438
14	10, 10, 12, 6	0.612	1.768	0.393	1.032
15	10, 20, 3, 42	0.588	1.472	0.417	0.891
16	20, 40, 12, 30	2.282	5.289	1.902	3.911
17	20, 50, 3, 6	1.320	2.824	1.982	3.277
18	20, 10, 9, 42	0.595	1.720	0.432	1.109
19	20, 20, 15, 18	1.089	3.041	0.808	1.876
20	20, 30, 6, -6	0.493	1.503	0.512	1.303
21	30, 50, 15, 42	2.288	4.596	1.504	3.156
22	30, 10, 6, 18	0.355	1.062	0.262	0.709
23	30, 20, 12, -6	0.559	1.683	0.457	1.205
24	30, 30, 3, 30	0.775	1.790	0.924	1.763
25	30, 40, 9, 6	0.957	2.161	0.880	1.685

APPENDIX IIID

EXPERIMENT V - WET BUNTER SANDSTONE

Test No	Levels of α, w, d, s	Q m^3/km	S.E. MJ/m^3	C.I.
1	-10, 10, 3, -6	0.011	7.750	253
2	-10, 20, 9, 30	0.389	3.676	411
3	-10, 30, 15, 6	0.505	2.776	465
4	-10, 40, 6, 42	0.335	5.335	359
5	-10, 50, 12, 18	0.768	4.030	442
6	0, 20, 6, 6	0.154	3.943	376
7	0, 30, 12, 42	0.771	2.294	500
8	0, 40, 3, 18	0.123	7.914	296
9	0, 50, 9, -6	0.403	2.645	466
10	0, 10, 15, 30	0.541	3.262	521
11	10, 30, 9, 18	0.372	2.950	457
12	10, 40, 15, -6	0.516	2.263	495
13	10, 50, 6, 30	0.340	5.009	360
14	10, 10, 12, 6	0.530	4.143	430
15	10, 20, 3, 42	0.070	8.357	300
16	20, 40, 12, 30	0.705	3.247	532
17	20, 50, 3, 3	0.159	8.292	301
18	20, 10, 9, 42	0.292	2.060	460
19	20, 20, 15, 18	0.428	2.633	571
20	20, 30, 6, -6	0.137	3.617	385
21	30, 50, 15, 42	1.218	1.881	589
22	30, 10, 6, 18	0.123	2.888	384
23	30, 20, 12, -6	0.150	3.914	441
24	30, 30, 3, 30	0.083	9.320	274
25	30, 40, 9, 6	0.438	2.175	434

APPENDIX IIIE

GROUPED DATA FOR EXPERIMENT IV

	$\overline{F}_C$ kN	$\overline{F}_N$ kN	F_C kN	F_N kN	Q m^3/km	S.E. MJ/m^3	C.I.
$P_{1\alpha}$	1.75	1.55	3.81	3.28	0.41	6.40	405
$P_{2\alpha}$	1.33	1.31	3.53	3.01	0.38	4.59	426
$P_{3\alpha}$	0.91	1.21	2.65	2.75	0.28	3.62	422
$P_{4\alpha}$	0.91	1.11	2.37	2.29	0.37	3.15	446
$P_{5\alpha}$	1.03	1.09	2.69	2.44	0.40	3.76	448
P_{1W}	0.64	0.53	1.86	1.31	0.20	5.13	422
P_{2W}	0.91	0.85	2.56	2.02	0.25	4.20	419
P_{3W}	1.13	1.30	2.83	2.88	0.39	3.90	435
P_{4W}	1.15	1.56	3.52	3.26	0.42	4.54	435
P_{5W}	1.84	2.04	4.28	4.29	0.59	3.75	438
P_{1d}	0.60	0.89	1.61	1.74	0.09	7.67	300
P_{2d}	1.05	1.20	2.65	2.50	0.22	4.70	409
P_{3d}	1.39	1.49	3.62	3.20	0.38	3.69	460
P_{4d}	1.35	1.40	2.94	3.13	0.52	2.78	4.76
P_{5d}	1.55	1.31	4.25	3.21	0.64	2.68	504
P_{1s}	0.82	0.91	2.39	2.13	0.22	5.51	409
P_{2s}	0.99	1.06	2.72	2.37	0.28	4.01	423
P_{3s}	1.32	1.56	3.24	3.42	0.40	3.85	433
P_{4s}	1.40	1.47	3.37	3.03	0.43	4.28	437
P_{5s}	1.41	1.29	3.34	2.83	0.52	3.88	447

APPENDIX IIIF

GROUPED DATA FOR EXPERIMENT V

	$\overline{F}_C$ kN	$\overline{F}_N$ kN	F_C kN	F_N kN	Q m^3/km	S.E. MJ/m^3	C.I.
$P_{1\alpha}$	1.55	1.23	3.66	2.49	0.40	4.72	386
$P_{2\alpha}$	1.22	0.89	3.10	1.85	0.40	3.97	432
$P_{3\alpha}$	1.00	0.97	2.68	2.08	0.29	4.54	409
$P_{4\alpha}$	1.16	1.13	2.88	2.30	0.34	3.97	450
$P_{5\alpha}$	0.99	0.81	2.26	1.70	0.40	4.04	424
P_{1W}	0.68	0.40	1.82	0.96	0.22	4.02	410
P_{2W}	0.68	0.65	2.21	1.51	0.24	3.22	420
P_{3W}	1.08	0.93	2.86	2.21	0.37	4.19	416
P_{4W}	1.41	1.25	3.38	2.49	0.42	4.19	423
P_{5W}	1.89	1.80	4.18	3.43	0.58	4.37	432
P_{1d}	0.75	0.93	1.74	1.68	0.09	8.33	285
P_{2d}	0.98	1.00	2.51	2.09	0.22	4.16	373
P_{3d}	1.02	0.85	2.64	1.85	0.38	2.70	446
P_{4d}	1.66	1.04	3.95	2.62	0.61	3.53	469
P_{5d}	1.51	0.99	3.74	2.18	0.64	2.56	528
P_{1s}	0.65	0.52	1.88	1.27	0.22	4.04	408
P_{2s}	0.97	0.97	2.44	1.90	0.31	4.27	401
P_{3s}	1.32	1.17	3.17	2.32	0.36	4.08	430
P_{4s}	1.59	1.39	3.83	2.85	0.41	4.90	420
P_{5s}	1.39	0.98	3.26	2.09	0.54	3.99	442

APPENDIX IIIG

RESULTS OF THE SUPPLEMENTARY SPACING TESTS IN BUNTER SANDSTONE

	S mm	$\overline{F}_C$ kN	$\overline{F}_N$ kN	F_C kN	F_N kN	Q m^3/km	S.E. MJ/m^3
d = 3mm	0	0.59	0.56	1.61	1.19	0.096	6.15
	12	0.75	0.75	1.97	1.58	0.109	6.88
	24	0.76	0.75	2.00	1.60	0.109	7.00
	36	0.76	0.75	2.00	1.60	0.109	7.00
	48	0.76	0.75	2.00	1.60	0.109	7.00
d = 6mm	0	0.67	0.56	2.01	1.37	0.192	3.48
	12	0.82	0.70	2.52	1.70	0.260	3.07
	24	0.94	0.73	2.39	1.56	0.279	3.37
	36	1.00	0.72	2.56	1.53	0.281	3.56
	48	1.05	0.73	2.58	1.55	0.276	3.80
d = 9mm	0	0.67	0.35	1.88	0.93	0.227	2.95
	12	0.87	0.40	2.41	1.12	0.400	2.18
	24	0.97	0.42	2.88	1.20	0.501	1.94
	36	1.13	0.47	2.85	1.21	0.530	2.12
	48	1.57	0.67	3.04	1.62	0.542	2.89
d = 12mm	0	0.71	0.43	2.08	1.08	0.294	2.41
	12	0.92	0.45	3.07	1.12	0.440	2.10
	24	1.12	0.43	3.35	1.15	0.652	1.71
	36	1.33	0.56	3.51	1.30	0.750	1.77
	48	1.48	0.77	3.73	1.81	0.728	2.03
d = 15mm	0	0.94	0.48	2.76	1.25	0.404	2.32
	12	1.14	0.60	2.94	1.32	0.508	2.24
	24	1.31	0.65	1.93	1.30	0.804	1.63
	36	1.28	0.72	3.57	1.52	0.889	1.44
	48	1.90	0.98	3.91	1.83	0.891	2.13

APPENDIX IIIH

RESULTS OF SUPPLEMENTARY SPACING TESTS IN MAGNESIAN LIMESTONE

	S mm	$\overline{F}_C$ kN	F_C kN	$\overline{F}_N$ kN	F_N kN	Q m^3/km	S.E. MJ/m^3	C.I.
d = 3mm	0	2.09	5.86	2.73	6.36	0.075	27.82	378
	3	2.12	5.26	3.38	5.98	0.080	26.34	366
	6	2.11	5.68	3.29	7.24	0.092	23.02	388
	9	2.32	6.71	3.80	7.66	0.095	25.18	288
	18	2.26	6.79	3.65	8.29	0.089	25.41	361
	∞	2.56	6.88	4.03	8.39	0.090	27.27	369
d = 6mm	0	2.20	7.18	3.05	6.73	0.146	15.09	484
	6	2.64	8.90	3.76	8.36	0.202	13.21	450
	12	2.74	9.70	4.06	8.26	0.235	12.04	440
	18	3.18	10.29	4.39	8.22	0.215	13.04	446
	36	3.06	10.18	4.61	8.18	0.213	14.39	449
	∞	3.52	10.95	4.84	8.09	0.226	15.56	443
d = 9mm	0	2.39	8.90	2.47	6.74	0.218	10.92	487
	9	2.73	8.16	2.83	6.35	0.266	10.25	473
	18	3.21	10.68	3.61	8.52	0.380	8.45	500
	27	3.90	10.76	3.92	9.15	0.370	10.54	467
	54	4.75	13.64	4.74	9.86	0.389	12.23	492
	∞	4.87	13.40	4.90	10.13	0.387	12.58	470

APPENDIX IV

EMPIRICAL EQUATIONS FOR THE PRIMARY PARAMETERS

UNRELIEVED PICK CUTTING

$$F = (w + A) \cdot (\varepsilon^{B\alpha + C} + D) \cdot d$$

$$Q = (Aw + B) \cdot d^2$$

$$C.I. = (d + A)\ (B\alpha + C)$$

	Parameter	A	B ($\times 10^{-2}$)	C	D ($\times 10^{-2}$)
EXPERIMENT I	$\bar{F}_C$	19.158	-3.438	-6.059	0.13
	$\bar{F}_N$	6.138	-2.297	-5.737	0.25
	F_C	34.482	-2.320	-5.319	0.18
	F_N	12.943	-5.070	-6.146	0.74
	Q	1.48×10^{-4}	0.245	-	-
	C.I.	12.408	6.260	19.306	-
EXPERIMENT II	$\bar{F}_C$	9.821	-2.702	-5.421	0.10
	$\bar{F}_N$	2.313	-0.538	-4.123	-0.93
	F_C	16.751	-6.120	-5.733	0.66
	F_N	3.905	-1.830	-4.541	0.30
	Q	1.40×10^{-4}	0.248	-	-
	C.I.	12.33	4.02	20.361	-
EXPERIMENT III	$\bar{F}_C$	14.721	-3.568	-5.013	1.00
	$\bar{F}_N$	11.093	-0.033	-0.661	-50.00
	F_C	43.657	-0.561	-3.909	0.20
	F_N	15.679	-9.317	-5.829	0.20
	Q	1.27×10^{-4}	0.219	-	-
	C.I.	31.811	1.874	11.416	-

APPENDIX VA

WEAR TESTING OF TUNGSTEN CARBIDE PICKS

DRY BUNTER					
CPM GRADE			CM GRADE		
Distance Cut (m)	Wear Flat (mm)	Weight Loss (mg)	Distance Cut (m)	Wear Flat (mm)	Weight Loss (mg)
0.44	0.284	3.45	0.44	0.234	2.93
0.89	0.353	6.13	0.88	0.270	3.83
1.33	0.421	8.33	1.32	0.302	4.35
1.76	0.465	10.98	1.76	0.321	5.53
23.15	1.669	60.40	25.00	1.054	25.30
41.91	2.238	96.85	50.00	1.411	42.78
60.35	2.699	138.00	75.00	1.634	59.03
76.52	2.850	172.18	100.00	1.985	75.53
90.98	3.213	201.18	200.00	2.450	131.58
195.90	3.841	302.20	300.00	2.914	181.65
			400.00	3.206	239.65
			500.00	3.497	292.35

DRY MAGNESIAN LIMESTONE CPM GRADE		
Distance Cut (m)	Wear Flat (mm)	Weight Loss (mg)
17.91	0.130	1.4
34.91	0.156	2.3
51.19	0.156	2.5
67.30	0.156	2.8
83.62	0.161	3.4
114.33	0.169	4.0
198.40	0.177	4.0
294.12	0.182	4.5
371.73	0.195	5.0
465.38	0.210	5.5
581.61	0.221	5.8

APPENDIX VB

WEAR TESTING OF TUNGSTEN CARBIDE PICKS

CH GRADE					
DRY BUNTER			WET BUNTER		
Distance Cut (m)	Wear Flat (mm)	Weight Loss (mg)	Distance Cut (m)	Wear Flat (mm)	Weight Loss (mg)
0.44	0.096	0.65	0.44	0.079	0.525
0.86	0.111	1.15	0.89	0.096	1.10
1.30	0.135	1.45	1.33	0.124	1.15
1.85	0.144	2.00	1.77	0.131	1.25
30.60	0.480	7.35	30.59	0.377	4.80
56.80	0.640	11.55	58.84	0.501	8.48
82.80	0.770	15.70	85.80	0.592	11.08
108.90	0.860	19.55	110.50	0.696	13.48
214.10	1.140	33.15	196.30	0.874	21.83
321.80	1.410	43.80	277.80	1.064	28.63
417.20	1.750	50.15	394.50	1.151	38.65
519.20	1.760	63.23	524.40	1.273	46.45

INDEXING CUTS

Tool Material	Distance Cut (m)	$\overline{F}_C$ (kN)	$\overline{F}_N$ (kN)	$\frac{\overline{F}_N}{\overline{F}_C}$	Q (m^3/km)	S.E. (MN/m^3)
CH	0.86	0.286	0.230	0.80	0.032	8.83
	1.82	0.360	0.241	0.67	0.036	10.00
	96.98	0.645	0.882	1.37	0.029	23.30
	189.52	0.656	1.137	1.73	0.033	19.85
	519.20	0.678	1.336	1.97	0.034	19.94
CM	0.88	0.367	0.341	0.93	0.034	10.50
	500.00	0.811	1.497	1.85	0.033	24.87
CPM	0.89	0.415	0.397	0.96	0.033	12.34
	195.90	0.754	1.222	1.62	0.033	23.45

APPENDIX VIA

FORCE, YIELD AND ENERGY RESULTS FOR RIDGED FRONT PICKS IN BUNTER SANDSTONE

	γ °	$\overline{F}_C$ kN	F_C kN	$\overline{F}_N$ kN	F_N kN	Q m^3/km	S.E. MJ/m^3	C.I.
d = 3mm	90	0.78	1.78	0.63	1.12	0.05	16.3	296
	120	0.82	1.85	0.76	1.36	0.06	14.4	309
	150	0.91	2.30	0.85	1.94	0.07	13.2	327
	180	0.85	2.20	0.72	1.45	0.08	11.0	323
d = 6mm	90	1.06	2.61	0.71	1.42	0.15	7.25	387
	120	1.21	3.03	0.89	1.87	0.18	6.90	404
	150	1.14	3.13	0.76	1.93	0.22	5.21	427
	180	1.29	3.42	0.81	1.73	0.23	5.80	421
d = 9mm	90	1.55	3.59	0.82	1.64	0.33	4.74	454
	120	1.93	4.57	1.02	2.27	0.39	4.95	454
	150	1.72	4.07	0.96	2.24	0.42	4.12	475
	180	1.78	4.23	1.01	2.08	0.49	4.34	482
d = 12mm	90	1.95	4.50	1.06	1.99	0.52	3.78	466
	120	1.93	4.69	0.89	2.11	0.67	2.98	525
	150	2.35	6.34	1.27	3.06	0.72	3.35	522
	180	2.51	6.36	1.21	2.97	0.79	3.24	542
d = 15mm	90	2.59	6.00	1.26	2.71	0.81	3.25	523
	120	3.14	7.39	1.50	3.23	0.93	3.40	522
	150	3.34	7.41	1.31	2.93	1.23	2.74	564
	180	3.74	7.95	1.81	3.42	1.31	2.85	583

APPENDIX VIB

FORCE, YIELD AND ENERGY RESULTS FOR RIDGED FRONT PICKS IN MAGNESIAN LIMESTONE

	γ_o	$\bar{F}_C$ kN	F_C kN	$\bar{F}_N$ kN	F_N kN	Q m^3/km	S.E. MJ/m^3	C.I.
d = 3mm	90	1.13	2.67	0.88	2.15	0.04	25.32	320
	120	1.08	3.17	0.77	1.80	0.06	18.47	356
	150	1.08	3.35	0.80	1.93	0.06	16.78	363
	180	1.14	3.99	1.04	2.53	0.07	15.76	387
d = 6mm	90	1.99	4.87	1.21	2.73	0.13	15.39	418
	120	1.88	5.32	1.24	2.75	0.14	13.36	432
	150	2.01	5.28	1.31	3.20	0.18	11.59	447
	180	2.34	4.95	1.60	3.33	0.18	12.97	468
d = 9mm	90	2.87	8.15	1.55	3.78	0.28	10.34	501
	120	2.81	9.27	1.65	4.51	0.31	9.29	500
	150	3.02	10.27	1.88	4.65	0.35	8.73	514
	180	3.31	7.42	2.36	4.67	0.38	8.58	508

APPENDIX VIC

FORCE, YIELD AND ENERGY RESULTS FOR VEE-BOTTOM PICKS IN BUNTER SANDSTONE

	λ o	$\overline{F}_C$ kN	F_C kN	$\overline{F}_N$ kN.	F_N kN	Q m^3/km	S.E. MN/m^3
d = 3mm	60	0.203	0.577	0.165	0.367	0.013	15.84
	90	0.219	0.643	0.180	0.427	0.017	12.88
	120	0.235	0.628	0.205	0.401	0.020	11.41
	150	0.403	0.803	0.415	0.649	0.032	11.43
	180	0.868	1.569	0.745	1.127	0.082	10.58
d = 6mm	60	0.463	1.084	0.261	0.599	0.058	8.09
	90	0.609	1.437	0.372	0.708	0.084	7.20
	120	0.770	1.794	0.689	1.029	0.118	6.55
	150	1.054	1.863	1.053	1.519	0.171	6.17
	180	1.051	2.369	1.116	1.885	0.192	5.50
d = 9mm	60	0.591	2.177	0.330	1.017	0.161	3.66
	90	0.699	2.832	0.659	1.984	0.215	3.26
	120	0.819	2.855	0.562	1.494	0.276	2.98
	150	0.978	3.242	0.775	1.637	0.346	2.82
	180	1.608	3.869	1.447	2.878	0.573	2.81
d = 12mm	60	0.968	3.543	0.550	1.584	0.301	3.21
	90	1.151	3.237	0.741	1.745	0.417	2.76
	120	1.336	5,009	0.838	2.403	0.561	2.38
	150	1.384	4.865	1.129	2.246	0.601	2.30
	180	2.450	5.962	1.904	3.680	1.053	2.33
d = 15mm	60	1.202	3.232	1.042	2.515	0.390	3.08
	90	1.350	4.338	1.161	2.919	0.560	2.43
	120	1.684	5.529	1.117	1.558	0.821	2.06
	150	2.468	6.334	1.319	3.221	1.177	2.18
	180	3.345	7.894	2.075	4.325	1.478	2.26

APPENDIX VID

FORCE, YIELD AND ENERGY RESULTS FOR VEE-BOTTOM PICKS IN MAGNESIAN LIMESTONE

	λ o	$\bar{F}_C$ kN	F_C kN	$\bar{F}_N$ kN	F_N kN	Q m^3/km	S.E. MJ/m^3	C.I.
d = 3mm	60	0.43	1.74	0.34	1.11	0.02	26.88	328
	90	0.40	2.12	0.49	1.42	0.02	19.99	380
	120	0.43	2.14	0.37	1.33	0.03	15.96	346
	150	0.55	3.73	0.97	2.62	0.04	15.57	342
	180	1.14	3.99	1.04	2.53	0.07	15.76	387
d = 6mm	60	0.81	3.47	0.56	1.75	0.05	14.99	432
	90	1.02	3.86	0.80	2.06	0.08	13.47	445
	120	1.12	3.92	0.79	1.81	0.09	12.07	453
	150	1.38	5.09	1.10	3.74	0.13	10.62	432
	180	2.34	4.95	1.60	3.33	0.18	12.97	468
d = 9mm	60	1.53	5.37	0.86	2.58	0.15	10.42	479
	90	1.79	5.91	1.35	3.23	0.18	9.88	472
	120	2.37	6.44	1.45	3.29	0.25	9.63	469
	150	2.86	7.55	1.71	4.04	0.29	9.87	484
	180	3.31	7.42	2.31	4.67	0.38	8.58	508

APPENDIX VIE

FORCE, YIELD AND ENERGY RESULTS FOR SIDE RAKE PICKS - UNRELIEVED CUTTING IN BUNTER SANDSTONE

	ν_o	$\overline{F}_C$ kN	$\overline{F}_N$ kN	$\overline{F}_S$ kN	Q m^3/km	S.E. MJ/m^3
d = 3mm	0	0.85	0.72	-	0.08	11.0
	10	0.95	0.84	0.10	0.07	13.7
	20	0.97	0.94	0.18	0.07	14.0
	30	1.11	0.91	0.22	0.09	12.6
d = 6mm	0	1.29	0.82	-	0.23	5.80
	10	0.96	0.72	0.14	0.20	4.84
	20	1.20	1.01	0.27	0.19	6.32
	30	1.30	0.89	0.33	0.21	6.31
d = 9mm	0	1.79	1.01	-	0.42	4.34
	10	1.97	1.11	0.24	0.39	5.07
	20	1.73	1.18	0.38	0.37	4.67
	30	1.86	0.94	0.40	0.45	4.20
d = 12mm	0	2.51	1.21	-	0.79	3.24
	10	2.18	1.17	0.32	0.64	3.57
	20	2.14	1.31	0.48	0.63	3.36
	30	2.20	1.02	0.55	0.77	2.89
d = 15mm	0	3.74	1.81	-	1.31	2.85
	10	3.02	1.45	0.40	1.02	2.97
	20	3.18	1.74	0.73	0.95	3.38
	30	-	-	-	-	-

APPENDIX VIF

FORCE, YIELD AND ENERGY RESULTS FOR SIDE RAKE PICKS - UNRELIEVED CUTTING IN MAGNESIAN LIMESTONE

	ν_o	$\overline{F}_C$ kN	$\overline{F}_N$ kN	$\overline{F}_S$ kN	Q m^3/km	S.E. MJ/m^3	C.I.
d = 3mm	0	1.14	1.04	-	0.07	15.76	387
	10	1.38	1.50	0.15	0.07	21.07	373
	20	1.36	1.15	0.24	0.08	17.48	378
	30	1.41	1.24	0.29	0.07	20.81	379
d = 6mm	0	2.34	1.60	-	0.18	12.97	468
	10	2.00	1.79	0.27	0.16	13.01	463
	20	2.10	1.49	0.49	0.18	11.63	469
	30	2.32	1.61	0.56	0.19	11.96	462
d = 9mm	0	3.31	2.31	-	0.38	8.58	508
	10	3.17	2.19	0.44	0.42	7.68	513
	20	3.57	2.37	0.68	0.34	10.64	492
	30	3.34	2.19	0.72	0.35	9.60	523

APPENDIX VIG

FORCE, YIELD AND ENERGY RESULTS FOR SIDE RAKE PICKS - RELIEVED CUTTING

	ν_o	$\overline{F}_C$ kN	F_C kN	$\overline{F}_N$ kN	F_N kN	$\overline{F}_S$ kN	F_S kN	Q m^3/km	S.E. MJ/m^3
s/d = -1	-20	0.68	1.92	0.49	1.19	0.11	0.33	0.10	6.61
	-10	0.69	1.88	0.60	1.36	0.08	0.26	0.11	6.16
	0	0.47	1.49	0.33	0.87	0.01	0.11	0.10	4.90
	10	0.56	1.86	0.35	1.11	0.03	0.26	0.10	5.58
	20	0.60	1.74	0.43	1.04	0.07	0.34	0.11	5.26
	30	0.52	1.77	0.27	0.81	0.07	0.37	0.13	4.12
s/d = +1	-20	0.91		0.60		0.20		0.28	3.33
	-10	1.13	3.25	0.83	2.18	0.17	0.47	0.26	4.42
	0	1.09	2.84	0.64	1.66	0.06	0.23	0.26	4.22
	10	1.02	2.79	0.71	1.82	0.14	0.41	0.29	3.55
	20	0.85	2.41	0.59	1.53	0.15	0.52	0.27	3.12
	30	0.93	2.67	0.61	1.50	0.17	0.73	0.27	3.54
s/d = 3	-20	1.26	3.11	0.77	1.78	0.29	0.68	0.38	3.30
	-10	1.76	3.88	1.05	2.41	0.27	0.63	0.38	4.68
	0	1.45	3.42	0.78	1.92	0.13	0.27	0.39	3.73
	10	1.48	3.84	0.93	2.35	0.23	0.62	0.43	3.47
	20	1.39	3.45	0.96	2.06	0.32	0.76	0.38	3.74
	30	1.35	3.29	0.78	1.77	0.32	0.70	0.39	3.55
s/d = 5	-20	1.55	3.84	0.98	2.23	0.32	0.83	0.39	4.01
	-10	1.79	4.36	1.06	2.56	0.26	0.70	0.38	4.95
	0	1.45	3.62	0.79	1.85	0.05	0.25	0.40	3.66
	10	1.66	3.98	1.03	2.45	0.24	0.59	0.40	4.19
	20	1.58	3.71	0.98	2.14	0.36	0.84	0.42	3.78
	30	1.33	3.29	0.67	1.68	0.38	0.90	0.48	2.83
s/d = 7	-20	1.64	3.87	1.05	2.30	0.32	0.84	0.38	4.37
	-10	1.78	4.31	1.03	2.42	0.29	0.68	0.41	4.38
	0	1.85	3.61	0.72	1.91	0.09	0.29	0.43	4.90
	10	1.61	3.78	0.88	2.09	0.24	0.57	0.48	3.52
	20	1.68	3.86	1.04	2.19	0.35	0.88	0.44	3.79
	30	1.65	4.05	0.85	2.06	0.39	1.07	0.48	3.49

APPENDIX VIIA

EXPERIMENT VI - DRY BUNTER SANDSTONE

Test No	Levels of ϕ, D, p, ν	$\overline{F}_T$ kN	F_T kN	$\overline{F}_R$ kN	F_R kN
1	60, 100, 10, 76	29.424	32.431	6.363	8.519
2	60, 125, 6, 152	15.350	18.963	2.653	3.859
3	60, 150, 2, 102	5.350	6.032	0.559	0.766
4	60, 175, 8, 178	28.964	35.969	5.115	7.312
5	60, 200, 4, 127	13.657	15.997	1.583	2.181
6	70, 125, 8, 102	26.776	31.630	5.497	7.407
7	70, 150, 4, 178	13.942	16.859	1.836	2.717
8	70, 175, 10, 127	43.311	48.933	7.976	10.862
9	70, 200, 6, 76	29.891	32.768	3.887	5.071
10	70, 100, 2, 152	5.772	6.773	0.708	0.994
11	80, 150, 6, 127	29.486	33.663	4.461	5992
12	80, 175, 2, 76	8.106	9.049	0.716	0.960
13	80, 200, 8, 152	34.482	46.727	5.184	7.597
14	80, 100, 4, 102	14.119	17.079	2.107	3.076
15	80, 125, 10, 178	57.512	61.924	10.090	13.151
16	90, 175, 4, 152	24.139	27.525	2.411	3.472
17	90, 200, 10, 102	71.690	82.945	9.750	12.775
18	90, 100, 6, 178	28.816	32.096	4.862	6.515
19	90, 125, 2, 127	8.698	9.855	0.890	1.323
20	90, 150, 8, 76	42.192	44.721	6.304	8.415
21	100, 200, 2, 178	13.190	13.033	0.942	1.294
22	100, 100, 8, 127	49.063	51.204	7.751	10.627
23	100, 125, 4, 76	27.923	29.121	3.229	4.203
24	100, 150, 10, 152	63.114	64.376	9.061	12.190
25	100, 175, 6, 102	43.992	47.335	5.476	6.846

APPENDIX VIIB

EXPERIMENT VI - DRY BUNTER SANDSTONE

Test No	Levels of ϕ, D, p, ν	Q m^3/km	S.E. MJ/m^3	C.I.
1	60, 100, 10, 76	0.333	19.283	346
2	60, 125, 6, 152	0.088	30.295	296
3	60, 150, 2, 102	0.012	44.082	235
4	60, 175, 8, 178	0.163	31.591	333
5	60, 200, 4, 127	0.048	33.720	301
6	70, 125, 8, 102	0.178	30.820	313
7	70, 150, 4, 178	0.047	39.288	271
8	70, 175, 10, 127	0.250	31.170	335
9	70, 200, 6, 76	0.085	45.877	312
10	70, 100, 2, 152	0.015	46.416	245
11	80, 150, 6, 127	0.095	47.769	305
12	80, 175, 2, 76	0.013	55.466	268
13	80, 200, 8, 152	0.169	30.668	321
14	80, 100, 4, 102	0.050	42.386	263
15	80, 125, 10, 178	0.336	30.220	378
16	90, 175, 4, 152	0.043	56.351	269
17	90, 200, 10, 102	0.282	34.709	356
18	90, 100, 6, 178	0.122	39.718	293
19	90, 125, 2, 127	0.014	61.659	228
20	90, 150, 8, 76	0.204	30.927	321
21	100, 200, 2, 178	0.010	89.203	245
22	100, 100, 8, 127	0.212	36.768	306
23	100, 125, 4, 76	0.051	63.511	269
24	100, 150, 10, 152	0.262	36.063	366
25	100, 175, 6, 102	0.111	50.674	278

APPENDIX VIIC

EXPERIMENT VII - WET BUNTER SANDSTONE

Test No	Levels of ϕ, D, p, ν	$\overline{F}_T$ kN	F_T kN	$\overline{F}_R$ kN	F_R kN
1	60, 100, 10, 76	28.680	26.362	5.607	6.328
2	60, 125, 6, 152	16.310	17.189	2.953	3.532
3	60, 150, 2, 102	4.526	5.709	0.650	0.763
4	60, 175, 8, 178	23.918	28.145	4.111	4.989
5	6 0, 200, 4, 127	13.090	14.782	1.759	2.171
6	70, 125, 8, 102	26.162	29.277	5.034	5.482
7	70, 150, 4, 178	11.432	13.817	1.616	2.090
8	70, 175, 10, 127	35.152	39.830	6.831	7.685
9	70, 200, 6, 76	23.901	23.895	3.325	3.764
10	70, 100, 2, 152	3.971	5.380	0.769	0.942
11	80, 150, 6, 127	25.343	25.570	3.949	4.667
12	80, 175, 2, 76	6.679	7.375	0.718	0.802
13	80, 200, 8, 152	38.000	41.878	5.995	6.940
14	80, 100, 4, 102	12.523	13.639	2.076	2.387
15	80, 125, 10, 178	42.140	41.997	8.219	9.592
16	90, 175, 4, 152	19.794	21.660	2.376	2.809
17	90, 200, 10, 102	55.376	55.219	8.293	9.571
18	90, 100, 6, 178	29.119	28.829	4.706	5.598
19	90, 125, 2, 127	7.290	8,761	0.983	1.139
20	90, 150, 8, 76	43.109	40.604	6.013	6.687
21	100, 200, 2, 178	12.143	12.346	0.965	1.124
22	100, 100, 8, 127	47.447	40.704	7.073	7.995
23	100, 125, 4, 76	22.930	22.893	2.668	3.017
24	100, 150, 10, 152	66.459	67.255	10.133	11.913
25	100, 175, 6, 102	40.419	43.350	4.892	5.350

APPENDIX VIID

EXPERIMENT VII - WET BUNTER SANDSTONE

Test No	Levels of ϕ, D, p, ν	Q m^3/km	S.E. MJ/m^3	C.I.
1	60, 100, 10, 76	0.321	17.836	249
2	60, 125, 6, 152	0.095	31.230	288
3	60, 150, 2, 102	0.010	58.570	221
4	60, 175, 8, 178	0.134	30.987	312
5	60, 200, 4, 127	0.044	40.568	306
6	70, 125, 8, 102	0.179	28.533	324
7	70, 150, 4, 178	0.041	38.997	243
8	70, 175, 10, 127	0.342	20.410	323
9	70, 200, 6, 76	0.106	32.300	297
10	70, 100, 2, 152	0.011	72.612	230
11	80, 150, 6, 127	0.113	35.145	293
12	80, 175, 2, 76	0.010	72.507	220
13	80, 200, 8, 152	0.177	34.770	316
14	80, 100, 4, 102	0.044	46.605	270
15	80, 125, 10, 178	0.315	26.158	351
16	90, 175, 4, 152	0.044	51.646	259
17	90, 200, 10, 102	0.327	25.474	317
18	90, 100, 6, 178	0.129	36.298	290
19	90, 125, 2, 127	0.012	84.485	257
20	90, 150, 8, 76	0.222	21.459	312
21	100, 200, 2, 178	0.008	109.713	236
22	100, 100, 8, 127	0.266	26.736	295
23	100, 125, 4, 76	0.053	50.409	282
24	100, 150, 10, 152	0.276	37.513	309
25	100, 175, 6, 102	0.109	44.897	280

APPENDIX VIIE

EXPERIMENT VIII - MAGNESIAN LIMESTONE

Test No	Levels of ϕ, D, p	$\overline{F}_T$ kN	F_T kN	$\overline{F}_R$ kN	F_R kN
1	60, 100, 7.5	35.059	48.114	12.055	14.190
2	60, 125, 4.5	23.185	30.714	5.058	5.662
3	60, 150, 1.5	6.760	9.140	0.730	0.890
4	60, 175, 6	36.964	47.157	8.964	8.627
5	60, 200, 3	15.855	21.494	2.258	2.878
6	70, 125, 6	39.256	53.340	9.651	10.779
7	70, 150, 3	18.102	24.052	2.770	3.457
8	70, 175, 7.5	58.514	62.537	14.368	16.141
9	70, 200, 4.5	31.860	38.706	5.242	5.564
10	70, 100, 1.5	8.459	11.561	1.176	1.469
11	80, 150, 4.5	37.411	42.414	6.401	6.640
12	80, 175, 1.5	9.217	13.008	0.910	1.213
13	80, 200, 6	53.526	59.530	10.627	11.755
14	80, 100, 3	18.349	23.441	3.190	3.836
15	80, 125, 7.5	54.171	68.424	15.172	16.281
16	90, 175, 3	25.872	30.385	3.183	3.549
17	90, 200, 7.5	83.648	95.115	17.346	17.608
18	90, 100, 4.5	35.667	43.261	9.029	9.387
19	90, 125, 1.5	10.285	14.146	1.011	1.333
20	90, 150, 6	56.564	69.415	12.893	14.849
21	100, 200, 1.5	13.548	17.142	1.066	1.241
22	100, 100, 6	57.729	70.379	15.471	17.412
23	100, 125, 3	28.938	35.680	3.811	4.487
24	100, 150, 7.5	85.043	101.445	22.566	17.500
25	100, 175, 4.5	58.073	61.340	7.777	7.788

APPENDIX VIIF

EXPERIMENT VIII - MAGNESIAN LIMESTONE

Test No	Levels of ϕ, D, p	Q m^3/km	S.E. MJ/m^3	C.I.
1	60, 100, 7.5	0.106	113.0	349
2	60, 125, 4.5	0.038	131.5	298
3	60, 150, 1.5	0.004	198.3	202
4	60, 175, 6	0.104	86.2	374
5	60, 200, 3	0.011	199.8	253
6	70, 125, 6	0.069	139.1	324
7	70, 150, 3	0.018	155.4	261
8	70, 175, 7.5	0.137	104.8	373
9	70, 200, 4.5	0.032	166.3	294
10	70, 100, 1.5	0.004	288.7	160
11	80, 150, 4.5	0.041	156.4	317
12	80, 175, 1.5	0.003	313.8	209
13	80, 200, 6	0.063	171.1	327
14	80, 100, 3	0.014	231.9	249
15	80, 125, 7.5	0.086	175.8	334
16	90, 175, 3	0.013	263.6	253
17	90, 200, 7.5	0.086	201.2	325
18	90, 100, 4.5	0.049	182.4	294
19	90, 125, 1.5	0.003	370.1	179
20	90, 150, 6	0.094	137.2	360
21	100, 200, 1.5	0.002	437.4	167
22	100, 100, 6	0.097	159.8	344
23	100, 125, 3	0.012	326.8	240
24	100, 150, 7.5	0.116	193.7	344
25	100, 175, 4.5	0.024	327.8	261

APPENDIX VIIG

GROUPED DATA FOR EXPERIMENT VI - DRY BUNTER SANDSTONE

	$\overline{F}_T$ kN	$\overline{F}_R$ kN	F_T kN	F_R kN	Q m^3/km	S.E. MJ/m^3	C.I.
$P_{1\phi}$	18.55	3.255	21.88	4.527	0.129	31.79	302
$P_{2\phi}$	23.94	3.945	27.39	5.410	0.115	38.71	295
$P_{3\phi}$	28.74	4.512	33.69	6.155	0.133	41.30	307
$P_{4\phi}$	35.11	4.843	34.93	6.500	0.133	44.67	293
$P_{5\phi}$	39.46	5.292	41.01	7.032	0.129	55.24	293
P_{1D}	25.44	4.358	27.92	5.946	0.146	36.91	291
P_{2D}	27.25	4.472	30.30	5.989	0.133	43.30	297
P_{3D}	30.82	4.444	33.13	6.016	0.124	39.63	300
P_{4D}	29.70	4.303	33.76	5.890	0.116	45.05	297
P_{5D}	32.58	4.269	38.29	5.783	0.119	46.84	307
P_{1P}	8.22	0.763	8.95	1.07	0.013	59.37	244
P_{2P}	18.76	2.233	21.32	3.13	0.048	47.05	275
P_{3P}	29.51	4.268	32.97	5.66	0.100	42.87	297
P_{4P}	36.30	5.970	42.05	8.27	0.185	32.16	319
P_{5P}	53.01	8.612	58.12	11.50	0.293	30.29	326
P_{1V}	27.51	4.100	29.62	5.433	0.137	43.01	303
P_{2V}	32.39	4.678	37.00	6.170	0.127	40.53	289
P_{3V}	35.32	4.496	31.93	6.197	0.124	42.22	295
P_{4V}	28.57	4.003	32.87	5.662	0.115	39.96	299
P_{5V}	28.48	4.569	31.98	6.198	0.136	46.00	304

APPENDIX VIIH

GROUPED DATA FOR EXPERIMENT VII - WET BUNTER SANDSTONE

	$\overline{\overline{F_T}}$ kN	$\overline{F_R}$ kN	F_T kN	F_R kN	Q m^3/km	S.E. MJ/m^3	C.I.
$P_{1\phi}$	17.30	3.016	18.44	3.557	0.121	35.84	275
$P_{2\phi}$	20.12	3.515	22.44	3.993	0.136	38.57	283
$P_{3\phi}$	24.94	4.191	26.09	4.878	0.132	43.04	290
$P_{4\phi}$	30.93	4.474	31.01	5.161	0.147	43.87	287
$P_{5\phi}$	37.88	5.146	37.31	5.880	0.142	53.85	280
P_{1D}	24.35	4.046	22.98	4.650	0.154	40.02	267
P_{2D}	22.97	3.971	24.02	4.552	0.131	44.16	300
P_{3D}	30.17	4.472	30.59	5.224	0.132	38.34	276
P_{4D}	25.18	3.786	28.07	4.327	0.128	44.09	279
P_{5D}	28.50	4.067	29.62	4.714	0.132	48.57	294
P_{1P}	6.92	0.817	7.91	0.495	0.010	79.58	233
P_{2P}	15.95	2.099	17.36	2.495	0.045	45.65	272
P_{3P}	27.02	3.965	27.77	4,582	0.110	35.97	290
P_{4P}	35.73	5.645	36.12	6.419	0.196	28.50	312
P_{5P}	45.56	7.817	46.13	9.018	0.316	25.48	310
P_{1V}	25.06	3.666	24.22	3.516	0.142	38.90	272
P_{2V}	27.80	4.189	29.44	4.711	0.134	40.82	282
P_{3V}	25.66	4.119	25.93	4.731	0.155	41.47	295
P_{4V}	28.90	4.445	30.67	5.227	0.121	45.55	280
P_{5V}	23.75	3.923	25.03	4.679	0.125	48.43	286

APPENDIX VIIJ

GROUPED DATA FOR EXPERIMENT VIII - MAGNESIAN LIMESTONE

	$\overline{F}_T$ kN	F_T kN	$\overline{F}_R$ kN	F_R kN	Q m^3/km	S.E. MJ/m^3	C.I.
$P_{1\phi}$	23.56	31.32	5.81	6.45	0.053	145.8	295
$P_{2\phi}$	31.24	38.04	6.64	7.48	0.052	170.9	282
$P_{3\phi}$	34.53	41.36	7.26	7.95	0.041	209.8	287
$P_{4\phi}$	42.41	50.46	8.69	9.35	0.049	231.0	282
$P_{5\phi}$	48.67	57.20	10.14	9.69	0.050	289.1	271
P_{1D}	31.05	39.35	8.18	9.26	0.054	195.3	279
P_{2D}	31.17	40.46	6.94	7.71	0.042	228.6	275
P_{3D}	40.78	49.29	9.07	8.67	0.055	168.2	297
P_{4D}	37.73	42.89	7.04	7.46	0.056	219.2	294
P_{5D}	39.69	46.60	7.31	7.81	0.039	235.1	273
P_{1p}	9.65	13.00	0.98	1.23	0.003	321.6	183
P_{2p}	21.42	27.01	3.04	3.64	0.014	235.5	251
P_{3p}	37.24	43.29	6.70	7.01	0.037	193.0	293
P_{4p}	48.81	59.96	11.52	12.68	0.085	138.6	346
P_{5p}	63.29	75.31	16.30	16.34	0.106	157.7	345

APPENDIX VIIK

BREAKOUT ANGLE (θ°) WHEN CUTTING WITH DISCS

Test No	Levels of ϕ, D, p	Dry Bunter	Wet Bunter	Magnesian Limestone
1	60, 100, 5	73.3	72.7	62.0
2	60, 125, 3	67.8	69.2	61.9
3	60, 150, 1	71.6	68.2	60.6
4	60, 175, 4	68.6	64.5	70.9
5	60, 200, 2	71.6	70.0	50.7
6	70, 125, 4	70.2	70.3	62.4
7	70, 150, 2	71.2	68.7	63.4
8	70, 175, 5	68.2	73.7	67.7
9	70, 200, 3	67.0	71.2	57.7
10	70, 100, 1	75.1	70.0	60.6
11	80, 150, 3	69.2	72.3	63.7
12	80, 175. 1	72.9	68.2	53.1
13	80, 200, 4	69.3	70.1	60.3
14	80, 100, 2	72.3	70.0	57.3
15	80, 125, 5	73.4	72.4	56.8
16	90, 175, 2	69.6	70.0	55.3
17	90, 200, 5	70.5	73.0	56.8
18	90, 100, 3	73.6	74.4	67.5
19	90, 125, 1	74.0	71.6	53.1
20	90, 150, 4	72.6	73.9	69.0
21	100, 200, 1	68.2	63.4	41.6
22	100, 100, 4	73.2	76.5	69.6
23	100, 125, 2	72.6	73.2	53.1
24	100, 150, 5	69.1	70.0	64.1
25	100, 175, 3	72.0	71.7	49.8

Level of Penetration	1	2	3	4	5
Bunter	2	4	6	8	10mm
Magnesian Limestone	1.5	3	4.5	6	7.5mm

APPENDIX VIIL

GROUPED DATA FOR BREAKOUT ANGLE (θ^{o})

	Dry Bunter	Wet Bunter	Magnesian Limestone
$P_{1\phi}$	70.6	68.9	61.2
$P_{2\phi}$	70.3	70.8	42.4
$P_{3\phi}$	71.4	70.6	58.2
$P_{4\phi}$	72.0	72.6	60.3
$P_{5\phi}$	71.0	71.0	55.6
P_{1D}	73.5	72.7	63.4
P_{2D}	71.6	71.3	57.5
P_{3D}	70.7	70.6	64.2
P_{4D}	70.3	69.6	59.4
P_{5D}	69.3	49.5	53.4
P_{1p}	72.4	68.3	53.8
P_{2p}	71.5	70.4	56.0
P_{3p}	69.9	71.8	60.1
P_{4p}	70.8	71.0	66.4
P_{5p}	70.9	72.4	61.5

APPENDIX VIIIA

EXPERIMENT IX - DRY BUNTER SANDSTONE

Test No	Levels of ϕ, D, p, s	$\bar{F}_T$ kN	F_T kN	$\bar{F}_R$ kN	F_R kN
1	60, 100, 10, 12	11.332	14.170	4.328	5.372
2	60, 125, 6, 48	14.044	17.281	3.062	3.624
3	60, 150, 2, 24	3.711	5.238	0.569	0.697
4	60, 175, 8, 60	24.937	28.907	4.810	5.882
5	60, 200, 4, 36	12.200	14.390	1.673	1.978
6	70, 125, 8, 24	16.672	20.040	4.375	5.786
7	70, 150, 4, 60	13.611	16.084	2.122	2.463
8	70, 175, 10, 36	26.098	32.967	5.875	8.638
9	70, 200, 6, 12	9.886	11.962	2.101	2.574
10	70, 100, 2, 48	4.336	5.925	0.804	1.005
11	80, 150, 6, 36	19.819	24.913	3.947	4.787
12	80, 175, 2, 12	4.700	6.948	0.762	0.979
13	80, 200, 8, 48	33.797	43.189	5.937	9.107
14	80, 100, 4, 24	11.281	14.535	2.260	2.888
15	80, 125, 10, 60	35.097	43.753	7.963	11.800
16	90, 175, 4, 48	20.444	21.915	2.574	2.894
17	90, 200, 10, 24	29.547	37.137	5.045	7.596
18	90, 100, 6, 60	24.367	27.471	5.034	5.947
19	90, 125, 2, 36	6.592	8.276	0.925	1.041
20	90, 150, 8, 12	19.170	22.863	4.507	5.947
21	100, 200, 2, 60	9.553	11.602	1.005	1.150
22	100, 100, 8, 36	30.180	36.094	6.634	10.371
23	100, 125, 4, 12	10.990	12.778	2.255	2.569
24	100, 150, 10, 18	41.784	48.180	7.435	10.951
25	100, 175, 6, 24	22.765	27.012	4.326	5.156

APPENDIX VIIIB

EXPERIMENT IX - DRY BUNTER SANDSTONE

Test No	Levels of ϕ, D, p, ν	Q m^3/km	S.E. MN/m^3	C.I.
1	60, 100, 10, 12	0.127	33.996	370
2	60, 125, 6, 48	0.086	35.643	295
3	60, 150, 2, 24	0.010	55.525	205
4	50, 175, 8, 60	0.168	28.036	337
5	50, 200, 4, 36	0.040	41.693	266
6	70, 125, 8, 24	0.194	22.707	363
7	70, 150, 4, 60	0.045	47.244	279
8	70, 175, 10, 36	0.302	19.798	395
9	70, 200, 6, 12	0.057	36.784	299
10	70, 100, 2, 48	0.012	67.044	209
11	80, 150, 6, 36	0.163	24.274	362
12	80, 175, 2, 12	0.021	36.675	266
13	80, 200, 8, 48	0.334	18.666	426
14	80, 100, 4, 24	0.082	27.444	346
15	80, 125, 10, 60	0.471	17.178	452
16	90, 175, 4, 48	0.043	59.189	248
17	90, 200, 10, 24	0.209	26.210	360
18	90, 100, 6, 60	0.117	43.302	302
19	90, 125, 2, 36	0.011	79.403	204
20	90, 150, 8, 12	0.098	47.119	309
21	100, 200, 2, 60	0.011	88.110	216
22	100, 100, 8, 36	0.253	26.510	372
23	100, 125, 4, 12	0.049	46.055	268
24	100, 150, 10, 48	0.448	16.688	378
25	100, 175, 6, 24	0.131	33.516	318

APPENDIX VIIIC

EXPERIMENT X - WET BUNTER SANDSTONE

Test No	Levels of ϕ, D, p, s	$\overline{F}_T$ kN	F_T kN	$\overline{F}_R$ kN	F_R kN
1	60, 100, 10, 12	7.950	8.937	2.881	3.482
2	60, 125, 6, 48	12.458	13.494	2.299	2.724
3	60, 150, 2, 24	3.524	4.464	0.452	0.560
4	60, 175, 8, 60	21.807	23.988	4.053	4.908
5	60, 200, 4, 36	8.364	10.203	1.172	1.430
6	70, 125, 8, 24	12.178	13.810	3.291	3.890
7	70, 150, 4, 60	8.836	11.245	1.513	1.863
8	70, 175, 10, 36	21.866	25.691	5.050	6.134
9	70, 200, 6, 12	8.892	9.969	1.812	2.207
10	70, 100, 2, 48	3.856	4.854	0.677	0.836
11	80, 150, 6, 36	17.071	20.140	3.147	3.852
12	80, 175, 2, 12	4.051	5.333	0.540	0.708
13	80, 200, 8, 48	27.970	30.384	4.603	5.575
14	80, 100, 4, 24	7.407	9.903	1.774	2.180
15	80, 125, 10, 60	28.935	33.143	7.030	8.310
16	90, 175, 4, 48	17.176	17.704	1.962	2.313
17	90, 200, 10, 24	25.558	28.030	5.852	6.735
18	90, 100, 6, 60	22.608	23.801	4.159	4.881
19	90, 125, 2, 36	5.621	6.543	0.710	0.848
20	90, 150, 8, 12	12.959	14.146	2.563	3.586
21	100, 200, 2, 60	8.485	9.202	0.653	0.768
22	100, 100, 8, 36	23.612	26.796	5.975	6.929
23	100, 125, 4, 12	7.820	9.375	1.738	2.051
24	100, 150, 10, 48	45.432	40.762	8.022	9.116
25	100, 175, 6, 24	22.394	23.845	3.848	4.658

APPENDIX VIIID

EXPERIMENT X - WET BUNTER SANDSTONE

Test No	Levels of ϕ, D, p, s	Q m^3/km	S.E. MJ/m^3	C.I.
1	60, 100, 10, 12	0.150	19.302	303
2	60, 125, 6, 48	0.099	23.563	317
3	60, 150, 2, 24	0.011	42.105	218
4	60, 175, 8, 60	0.188	21.500	357
5	60, 200, 4, 36	0.040	29.251	271
6	70, 125, 8, 24	0.206	18.337	331
7	70, 150, 4, 60	0.048	31.819	264
8	70, 175, 10, 36	0.299	16.952	352
9	70, 200, 6, 12	0.071	25.418	296
10	70, 100, 2, 48	0.013	52.132	228
11	80, 150, 6, 36	0.193	16.448	344
12	80, 175, 2, 12	0.026	20.976	313
13	80, 200, 8, 48	0.306	15.655	379
14	80, 100, 4, 24	0.096	18.516	344
15	80, 125, 10, 60	0.485	14.885	381
16	90, 175, 6, 48	0.050	39.146	284
17	90, 200, 10, 24	0.235	25.045	346
18	90, 100, 6, 60	0.128	32.470	268
19	90, 125, 2, 36	0.014	51.200	231
20	90, 150, 8, 12	0.087	32.158	287
21	100, 200, 2, 60	0.011	60.525	223
22	100, 100, 8, 36	0.288	21.067	331
23	100, 125, 4, 12	0.062	28.207	285
24	100, 150, 10, 48	0.440	18.625	369
25	100, 175, 6, 24	0.161	23.948	301

APPENDIX VIIIE

EXPERIMENT XI - MAGNESIAN LIMESTONE

Test No	Levels of ϕ, D, p, s	$\overline{F}_T$ kN	F_T kN	$\overline{F}_R$ kN	F_R kN
1	60, 100, 7.5, 9	13.064	21.171	7.716	8.998
2	60, 125, 4.5, 36	23.185	30.714	5.058	5.662
3	60, 150, 1.5, 18	6.760	9.140	0.730	0.890
4	60, 175, 6 , 45	34.254	41.270	8.262	9.121
5	60, 200, 3 , 27	15.855	21.494	2.258	2.878
6	70, 125, 6 , 18	23.219	35.376	6.895	8.491
7	70, 150, 3 , 45	18.102	24.052	2.770	3.457
8	70, 175, 7.5, 27	38.780	51.143	11.712	12.453
9	70, 200, 4.5, 9	13.369	17.386	3.302	3.816
10	70, 100, 1.5, 36	8.459	11.561	1.176	1.469
11	80, 150, 4.5, 27	29.421	34.704	5.651	6.00
12	80, 175, 1.5, 9	9.013	11.606	0.867	1.128
13	80, 200, 6 , 36	52.365	63.528	11.512	13.045
14	80, 100, 3 , 18	16.291	23.415	3.154	4.151
15	80, 125, 7.5, 45	48.362	60.588	13.217	14.900
16	90, 175, 3 , 36	25.872	30.385	3.183	3.549
17	90, 200, 7.5, 18	49.648	53.992	13.564	13.244
18	90, 100, 4.5, 45	35.667	43.261	9.029	9.387
19	90, 125, 1.5, 27	10.285	14.146	1.011	1.333
20	90, 150, 6 , 9	28.978	34.962	8.131	9.114
21	100, 200, 1.5, 45	13.548	17.142	1.066	1.241
22	100, 100, 6 , 27	45.142	58.058	13.442	14.516
23	100, 125, 3 , 9	13.652	19.000	2.358	3.321
24	100, 150, 7.5, 36	62.949	85.208	16.831	16.713
25	100, 175, 4.5, 18	7.776	7.898	1.011	1.049

APPENDIX VIIIF

EXPERIMENT XI - MAGNESIAN LIMESTONE

Test No	Levels of ϕ, D, p, s	Q m^3/km	S.E. MJ/m^3	C.I.
1	60, 100, 7.5, 9	0.062	125.6	363
2	60, 125, 4.5, 36	0.038	131.5	298
3	60, 150, 1.5, 18	0.004	198.3	202
4	60, 175, 6 , 45	0.084	98.3	374
5	60, 200, 3 , 27	0.011	199.8	253
6	70, 125, 6 , 18	0.093	74.1	389
7	70, 150, 3 , 45	0.018	155.4	261
8	70, 175, 7.5, 27	0.142	82.6	390
9	70, 200, 4.5, 9	0.003	131.4	309
10	70, 100, 1.5, 36	0.004	288.7	160
11	80, 150, 4.5, 27	0.054	106.7	346
12	80, 175, 1.5, 9	0.004	217.6	227
13	80, 200, 6 , 36	0.115	101.6	409
14	80, 100, 3 , 18	0.002	133.0	316
15	80, 125, 7.5, 45	0.107	133.8	364
16	90, 175, 3 , 36	0.013	263.6	253
17	90, 200, 7.5, 18	0.078	173.6	344
18	90, 100, 4.5, 45	0.049	182.8	294
19	90, 125, 1.5, 27	0.003	370.1	179
20	90, 150, 6 , 9	0.036	225.2	327
21	100m 200, 1.5, 45	0.002	437.4	167
22	100, 100, 6 , 27	0.126	106.1	371
23	100, 125, 3 , 9	0.016	147.3	266
24	100, 150, 7.5, 36	0.228	73.7	414
25	100, 175, 4.5, 18	0.053	107.4	330

APPENDIX VIIIG

GROUPED DATA FOR EXPERIMENT IX

	$\overline{F}_T$ kN	$\overline{F}_R$ kN	F_T kN	F_R kN	Q m^3/km	S.E. MJ/m^3	C.I.
$P_{1\phi}$	13.24	2.888	16.00	3.511	0.086	38.98	295
$P_{2\phi}$	14.12	3.055	17.40	4.093	0.122	38.72	309
$P_{3\phi}$	20.94	4.174	26.67	5.912	0.214	24.85	370
$P_{4\phi}$	20.02	3.617	23.53	4.685	0.096	51.04	285
$P_{5\phi}$	23.05	4.331	27.13	6.039	0.178	42.18	310
P_{1D}	16.30	3.812	19.64	5.117	0.118	39.66	320
P_{2D}	16.68	3.716	20.43	4.964	0.162	40.20	316
P_{3D}	19.62	3.716	23.46	4.969	0.153	38.17	307
P_{4D}	19.79	3.669	23.55	4.710	0.133	35.44	313
P_{5D}	19.00	3.152	23.66	4.481	0.130	42.29	313
P_{1P}	5.78	0.813	7.60	0.974	0.013	65.35	220
P_{2P}	13.71	2.177	15.94	2.558	0.052	44.33	281
P_{3P}	18.18	3.694	21.73	4.418	0.111	34.70	315
P_{4P}	24.95	5.253	30.22	7.419	0.209	28.61	361
P_{5P}	28.77	6.129	35.24	8.871	0.311	22.77	391
P_{1S}	11.22	2.791	13.74	3.488	0.070	40.13	302
P_{2S}	16.80	3.315	20.79	4.425	0.125	33.08	318
P_{3S}	18.98	3.811	23.33	5.363	0.154	38.34	320
P_{4S}	22.88	3.962	27.30	5.516	0.185	39.45	311
P_{5S}	21.51	4.187	25.56	5.448	0.162	44.77	317

APPENDIX VIIIH

GROUPED DATA FOR EXPERIMENT X

	$\overline{F}_T$ kN	$\overline{F}_R$ kN	F_T kN	F_R kN	Q m^3/km	S.E. MJ/m^3	C.I.
$P_{1\phi}$	10.82	2.171	12.22	2.262	0.098	27.14	293
$P_{2\phi}$	11.13	2.469	13.11	2.986	0.127	28.93	294
$P_{3\phi}$	17.09	3.419	19.78	4.125	0.221	17.30	352
$P_{4\phi}$	16.78	3.049	18.04	3.672	0.103	36.00	283
$P_{5\phi}$	21.54	4.047	22.00	4.704	0.192	30.47	302
P_{1D}	13.09	3.093	14.86	3.661	0.135	28.70	295
P_{2D}	13.40	3.014	15.27	3.565	0.173	27.24	309
P_{3D}	17.56	3.139	18.15	3.795	0.156	28.23	296
P_{4D}	17.46	3.091	19.31	4.978	0.145	24.50	342
P_{5D}	15.85	2.818	17.56	3.343	0.133	31.18	303
P_{1P}	5.10	0.606	6.08	0.744	0.015	45.39	243
P_{2P}	9.92	1.632	11.69	1.967	0.059	29.39	290
P_{3P}	16.68	3.053	18.25	3.664	0.130	24.37	305
P_{4P}	19.71	4.097	21.82	4.978	0.215	21.74	337
P_{5P}	25.95	5.767	27.31	6.755	0.322	19.86	290
P_{1S}	8.33	1.907	9.55	2.407	0.079	25.21	297
P_{2S}	14.21	3.043	16.01	3.605	0.142	25.59	308
P_{3S}	15.31	3.211	17.87	3.839	0.167	26.98	306
P_{4S}	21.38	3.513	21.44	4.113	0.182	29.82	315
P_{5S}	18.13	3.482	20.28	4.146	0.172	32.24	298

APPENDIX VIIIJ

GROUPED DATA FOR EXPERIMENT XI

	$\overline{F}_T$ kN	F_T kN	$\overline{F}_R$ kN	F_R kN	Q m^3/km	S.E. MJ/m^3	C.I.
$P_{1\phi}$	18.62	24.76	4.80	5.50	0.040	150.7	298
$P_{2\phi}$	20.39	27.90	5.17	5.94	0.052	146.4	302
$P_{3\phi}$	31.09	38.77	6.88	7.84	0.056	138.5	332
$P_{4\phi}$	30.09	35.35	6.98	7.33	0.036	243.1	279
$P_{5\phi}$	28.61	37.46	6.94	7.37	0.085	174.4	310
P_{1D}	23.72	31.49	6.90	7.70	0.049	167.2	301
P_{2D}	23.74	31.96	5.71	6.74	0.051	171.4	299
P_{3D}	29.24	37.61	6.82	7.23	0.068	151.9	310
P_{4D}	23.14	28.46	5.00	5.46	0.059	153.9	315
P_{5D}	28.96	34.71	6.34	6.84	0.042	208.8	296
P_{1p}	9.61	12.72	0.97	1.21	0.003	302.4	187
P_{2p}	17.95	23.67	2.74	3.47	0.012	179.8	270
P_{3p}	21.88	26.79	4.81	5.18	0.039	132.0	315
P_{4p}	36.79	46.64	9.65	10.86	0.091	121.1	374
P_{5p}	42.56	54.42	12.61	13.26	0.123	117.9	375
P_{1s}	15.62	20.83	4.47	5.28	0.024	169.4	298
P_{2s}	20.74	25.96	5.07	5.57	0.046	137.3	316
P_{3s}	27.90	35.91	6.81	7.44	0.067	173.1	308
P_{4s}	34.57	44.28	9.55	8.09	0.080	171.8	307
P_{5s}	30.00	37.26	6.87	7.62	0.052	201.5	292

APPENDIX IX A

EMPIRICAL EQUATIONS FOR THE PRIMARY PARAMETERS

DISC CUTTING UNRELIEVED

$$F = (p + A)\ (B\phi + C)\ (E.D + F)$$

$$Q = Ap^2 + B$$

$$C.I. = (Ap + B)\ (\phi + C)$$

Parameter		A	B	C	E ($\times 10^{-4}$)	F ($\times 10^{-2}$)
EXPERIMENT VI	$\bar{F}_T$	-0.556	1	-28.047	2.826	6.197
	F_R	-1.504	1.347×10^{-2}	-1.445×10^{-2}	-	-
	F_T	-0.511	1	-18.3	2.771	5.525
	F_R	-1.443	1.648×10^{-2}	7.932×10^{-2}	-	-
	Q	2.912×10^{-3}	-3.266×10^{-4}	-	-	-
	C.I.	13.412	217.7	-	-	-
EXPERIMENT VII	$\bar{F}_T$	-0.594	0.1	-3.166	-	-
	F_R	-1.362	1.138×10^{-2}	2.673×10^{-2}	-	-
	F_T	-0.315	1	-22.43	2.362	4.733
	F_R	-1.319	1.2×10^{-2}	0.102	-	-
	Q	3.163×10^{-3}	-3.049×10^{-3}	-	-	-
	C.I.	9.69	225.1	-	-	-
EXPERIMENT VIII	$\bar{F}_T$	-0.240	1	-20.271	3.024	9.323
	F_R	-1.535	3.613×10^{-2}	-28.77×10^{-2}	-	-
	F_T	-0.164	1	-9.946	1.851	11.44
	F_R	-1.467	2.713×10^{-2}	$+49.24\times10^{-2}$	-	-
	Q	2.029×10^{-3}	-1.206×10^{-3}	-	-	-
	C.I.	3.723×10^{-4}	21.175×10^{-2}	668.4	-	-

APPENDIX IX B

B. EMPIRICAL EQUATIONS FOR THE PRIMARY PARAMETERS - DISC CUTTING RELIEVED

$$F = (p + A)\frac{(s + B)}{(s + C)} \cdot (E\phi + F)\,(G \cdot D + H)$$

$$Q = p^2 \{A + B(\frac{s}{p}) + C(\frac{s}{p})^2 + E(\frac{s}{p})^3\}$$

$$C.I. = Ap + B$$

	Parameter	A	B	C	E	F	G ($\times 10^{-2}$)	H ($\times 10^{-2}$)
EXPERIMENT IX	$\overline{F}_T$	0.387	0.141	19	1	-11.158	1.545	4.34
	$\overline{F}_R$	-0.729	0.105	9	9.139×10^{-3}	0.159	-	-
	F_T	0.367	9.356×10^{-2}	15	1	-2.502	1.514	-4.412
	F_R	-1.306	-0.150	7	1.454×10^{-2}	0.198	-	-
	Q	1.254×10^{-4}	4.901×10^{-4}	2.487×10^{-4}	-3.480×10^{-5}	-	-	-
	C.I.	21.108	187.14	-	-	-	-	-
EXPERIMENT X	$\overline{F}_T$	1.296×10^{-2}	-0.157	22	7.463×10^{-2}	-1.539	-	-
	$\overline{F}_R$	-1.259	-0.280	7	1.015×10^{-2}	2.332×10^{-2}	-	-
	F_T	0.475	-0.156	17	1	-9.08	1.55	3.46
	F_R	-1.182	3.137×10^{-2}	7	1.096×10^{-2}	8.416×10^{-2}	-	-
	Q	7.2×10^{-4}	1.026×10^{-4}	3.697×10^{-4}	-4.45×10^{-5}	-	-	-
	C.I.	13.135	226.13	-	-	-	-	-

APPENDIX IX C

EMPIRICAL EQUATIONS FOR THE PRIMARY PARAMETERS

- DISC CUTTING RELIEVED

CONSTANTS AS GIVEN IN APPENDIX IX B

	Parameter	A	B	C	E	F	G	H
EXPERIMENT XI	$\overline{F}_T$	6.035×10^{-2}	-2.023	10.0	1	16.935	1.601×10^{-4}	0.071
	$\overline{F}_R$	-1.440	-1.636	5.0	2.499×10^{-2}	4.421	-	-
	F_m	0.132	0.522	14.0	1	31.743	5.536×10^{-5}	0.102
	F_T	-1.262	-0.381	6.0	1.583×10^{-2}	2.164	-	-
	F_R	9.054×10^{-2}	-1.248×10^{-2}	0.477×10^{-2}	-5×10^{-6}	-	-	-
	Q	32.013	160.18	-	-	-	-	-
	C.I.							

APPENDIX XA

RESULTS OF STALLED DISC TESTS

A. MEAN THRUST FORCE, $\overline{F}_T$ (kN)

d	s/d = ∞		s/d = 5	
mm	Rolling	Stalled	Rolling	Stalled
2	4.04	1.61	2.95	1.85
4	10.67	3.08	9.49	2.03
6	17.90	5.30	13.81	6.07
8	24.06	9.26	20.52	6.98
10	31.39	10.92	27.58	8.26

B. MEAN ROLLING FROCE, $\overline{F}_R$ (kN)

d	s/d = ∞		s/d = 5	
mm	Rolling	Stalled	Rolling	Stalled
2	0.47	0.96	0.42	1.02
4	1.57	2.91	1.46	2.65
6	3.00	3.96	2.96	4.26
8	4.29	6.40	4.51	5.59
10	6.12	7.50	4.45	7.58

C. PEAK THRUST FORCE, F_T (kN)

d	s/d = ∞		s/d = 5	
mm	Rolling	Stalled	Rolling	Stalled
2	5.89	2.60	4.36	3.46
4	14.09	6.88	11.79	5.94
6	20.06	7.10	18.87	6.81
8	25.50	11.92	24.26	10.76
10	33.65	12.30	26.34	11.84

APPENDIX XB

D. PEAK ROLLING FORCE, F_R (kN)

d	s/d = ∞		s/d = 5	
mm	Rolling	Stalled	Rolling	Stalled
2	0.65	1.92	0.57	2.34
4	2.10	4.48	2.01	3.48
6	3.27	4.77	3.81	4.49
8	4.89	8.20	5.33	6.72
10	6.44	10.34	7.74	9.72

E. YIELD, Q (m^3/km)

d	s/d = ∞		s/d = 5	
mm	Rolling	Stalled	Rolling	Stalled
2	0.007	0.006	0.011	0.005
4	0.028	0.019	0.050	0.024
6	0.063	0.048	0.107	0.050
8	0.112	0.098	0.282	0.132
10	0.218	0.153	0.378	0.250

F. SPECIFIC ENERGY, S.E. (MJ/m^3)

d	s/d = ∞		s/d = 5	
mm	Rolling	Stalled	Rolling	Stalled
2	71.36	160.75	39.47	151.95
4	60.12	150.71	30.84	111.56
6	53.16	82.99	29.63	90.73
8	42.18	67.67	17.51	49.90
10	31.76	50.83	13.10	32.86

APPENDIX XIA

ROLLER CUTTERS IN BUNTER SANDSTONE

1. Unrelieved Cutting

p mm	$\overline{F}_T$ kN	F_T kN	$\overline{F}_R$ kN	F_R kN	Q m^3/km	S.E. MJ/m^3
2	3.719	8.262	0.373	1.025	0.006	68.18
4	8.151	14.041	1.076	2.056	0.024	46.91
6	14.067	20.813	2.500	4.218	0.086	29.67
8	20.692	27.125	4.315	7.163	0.128	33.48
10	32.726	44.098	7.266	11.234	0.272	27.33

2. Spacing Tests - Depth = 10mm

s mm	$\overline{F}_T$ kN	F_T kN	$\overline{F}_R$ kN	F_R kN	Q m^3/km	S.E. MJ/m^3
-20	6.286	9.373	1.432	2.768	0.033	42.741
-10	9.785	14.580	2.130	4.040	0.084	25.381
0	17.788	24.272	4.228	7.084	0.198	21.213
10	20.782	29.812	5.013	8.498	0.261	19.161
20	32.128	43.455	7.142	12.235	0.284	25.163

APPENDIX XIB

ROLLER CUTTERS IN MAGNESIAN LIMESTONE

Unrelieved Cutting

p mm	$\overline{F}_T$ kN	F_T kN	$\overline{F}_R$ kN	F_R kN	Q m^3/km	S.E. MJ/m^3
2	7.992	17.036	0.671	1.906	0.006	93.7
4	17.846	28.027	2.450	4.534	0.032	77.0
6	34.025	46.771	5.996	8.706	0.114	53.2
8	48.453	57.974	8.410	9.763	0.190	44.1
10	65.983	74.516	10.617	15.848	0.256	41.3

APPENDIX XIIA

CUTTING FORCE PREDICTIONS USING MERCHANT'S THEORY

Test No	Levels of α, d	Bunter Sandstone F_C/unit width kN/mm	Magnesian Limestone F_C/unit width kN/mm
1	-10, 3	0.101	0.141
2	-10, 9	0.304	0.424
3	-10, 15	0.506	0.706
4	-10, 6	0.203	0.283
5	-10, 12	0.405	0.565
6	0, 6	0.162	0.230
7	0, 12	0.324	0.461
8	0, 3	0.081	0.115
9	0, 9	0.243	0.346
10	0, 15	0.406	0.576
11	10, 9	0.200	0.287
12	10, 15	0.333	0.478
13	10, 6	0.133	0.191
14	10, 12	0.266	0.382
15	10, 3	0.067	0.095
16	20, 12	0.221	0.320
17	20, 3	0.055	0.080
18	20, 9	0.166	0.240
19	20, 6	0.111	0.160
21	30, 15	0.232	0.336
22	30, 6	0.093	0.134
23	30, 12	0.186	0.269
24	30, 3	0.046	0.067
25	30, 9	0.139	0.201

APPENDIX XIIB

GROUPED VALUES OF THEORETICAL PREDICTIONS - MERCHANT'S THEORY

	Bunter F_C/unit width (kN/mm)	Magnesian Limestone F_C/unit width (kN/mm)
$P_{1\alpha}$	0.304	0.424
$P_{2\alpha}$	0.243	0.346
$P_{3\alpha}$	0.200	0.287
$P_{4\alpha}$	0.166	0.240
$P_{5\alpha}$	0.139	0.200
P_{1d}	0.070	0.100
P_{2d}	0.140	0.200
P_{3d}	0.210	0.300
P_{4d}	0.281	0.399
P_{5d}	0.351	0.499

APPENDIX XIIC

THEORETICAL AND MEASURED VALUES OF CUTTING FORCE - EMPIRICAL RELATIONSHIP BASED ON MERCHANT'S THEORY

Test No	Levels of α, w, d	Bunter Sandstone		Magnesian Limestone	
		F_C (kN)	F_C (kN)	F_C (kN)	F_C (kN)
1	-10, 10, 3	1.236	1.139	3.895	4.909
2	-10, 20, 9	3.759	4.028	17.756	16.997
3	-10, 30, 15	8.393	7.699	22.540	32.022
4	-10, 40, 6	3.293	3.488	8.338	14.327
5	-10, 50, 12	6.837	7.758	23.847	31.581
6	0, 20, 6	2.217	2.147	9.813	9.220
7	0, 30, 12	5.441	4.930	12.791	20.909
8	0, 40, 3	2.186	1.392	6.414	5.822
9	0, 50, 9	3.214	4.655	23.308	19.340
10	0, 10, 15	4.151	4.578	17.418	20.055
11	10, 30, 9	2.792	3.043	16.435	13.017
12	10, 40, 15	5.300	5.723	20.173	23.200
13	10, 50, 6	3.558	2.548	12.458	10.676
14	10, 10, 12	2.567	2.999	9.717	13.300
15	10, 20, 3	1.046	0.888	4.395	3.808
16	20, 40, 12	4.367	3.798	16.785	16.201
17	20, 50, 3	1.765	1.063	8.435	4.472
18	20, 10, 9	1.464	1.872	9.571	8.356
19	20, 20, 15	3.394	3.670	13.337	16.035
20	20, 30, 6	1.988	1.689	10.031	7.257
21	30, 50, 15	3.778	4.444	12.147	18.781
22	30, 10, 6	1.001	1.049	5.221	4.665
23	30, 20, 12	2.388	2.465	15.305	10.783
24	30, 30, 3	1.389	0.700	7.057	3.039
25	30, 40, 9	2.400	2.385	12.101	10.176

APPENDIX XIID

GROUPED VALUES, OBTAINED FROM APPENDIX XIIC

	Bunter Sandstone		Magnesian Limestone	
	F_C Measured	F_C Theoretical	F_C Measured	F_C Theoretical
$P_{1\alpha}$	4.70	4.82	15.28	19.97
$P_{2\alpha}$	3.44	3.54	13.95	15.07
$P_{3\alpha}$	3.05	3.04	12.64	13.00
$P_{4\alpha}$	2.60	2.42	11.63	10.46
$P_{5\alpha}$	2.19	2.21	10.37	9.49
P_{1W}	2.08	2.33	9.16	10.26
P_{2W}	2.56	2.64	12.12	11.37
P_{3W}	4.00	3.61	13.77	15.25
P_{4W}	3.51	3.36	12.76	14.15
P_{5W}	3.83	4.09	16.04	16.97
P_{1d}	1.52	1.04	6.04	4.41
P_{2d}	2.41	2.18	9.17	9.23
P_{3d}	2.73	3.20	15.83	13.58
P_{4d}	4.32	4:39	15.69	18.55
P_{5d}	5.00	5.22	17.12	22.21

APPENDIX XIIE

PEAK CUTTING AND NORMAL FORCES - DRY BUNTER

F_C (w = 30mm)

α \ d	3 mm	6 mm	9 mm	12 mm	15 mm
-10°	1.543	3.086	4.269	6.172	7.716
0°	1.296	2.591	3.887	5.183	6.479
10°	1.100	21.99	3.299	4.398	5.498
20°	0.944	1.888	2.831	3.775	4.719
30°	0.821	1.641	2.462	3.282	4.103

F_N (w = 30mm)

α \ d	3 mm	6 mm	9 mm	12 mm	15 mm
-10°	1.412	2.824	4.236	5.648	7.060
0°	1.229	2.459	3.688	4.917	6.146
10°	1.120	2.239	3.359	4.478	5.598
20°	1.054	2.108	3.161	4.215	5.269
30°	1.014	2.208	3.042	4.056	5.069

APPENDIX XIIF

CUTTING FORCE PREDICTIONS USING NISHIMATSU'S THEORY

Test No	Levels of α, d	F_C (N/mm) Experimental	F_C (N/mm) Theoretical
1	-10, 3	51.4	27.4
2	-10, 9	154.3	82.1
3	-10, 15	257.2	136.8
4	-10, 6	102.9	54.7
5	-10, 12	205.7	109.4
6	0, 6	86.4	67.6
7	0, 12	172.8	135.2
8	0, 3	43.2	33.8
9	0, 9	129.6	101.4
10	0, 5	216.0	169.0
11	10, 9	110.0	139.5
12	10, 15	183.3	232.5
13	10, 6	73.3	93.0
14	10, 12	146.6	186.0
15	10, 3	36.7	46.5
16	20, 12	125.8	284.7
17	20, 3	31.5	71.2
18	20, 9	94.4	213.5
19	20, 15	157.3	355.9
20	20, 6	62.9	142.3
21	30, 15	136.8	612.3
22	30, 6	54.7	244.9
23	30, 12	109.4	490.4
24	30, 3	27.4	122.5
25	30, 9	82.1	367.3

APPENDIX XIIG

GROUPED DATA FOR NISHIMATSU'S THEORY

	F_C/unit width Experiment	F_C/unit width Theoretical
$P_{1\alpha}$	154.3	82.1
$P_{2\alpha}$	129.6	101.4
$P_{3\alpha}$	110.0	139.5
$P_{4\alpha}$	94.4	213.5
$P_{5\alpha}$	82.1	267.3
P_{1d}	38.0	60.3
P_{2d}	76.0	120.5
P_{3d}	114.1	180.8
P_{4d}	152.1	241.1
P_{5d}	190.1	301.3

APPENDIX XIIH

CUTTING FORCE PREDICTIONS USING EVANS' THEORY

Test No	Levels of α, d	Bunter Sandstone Force/unit width N/mm	Magnesian Limestone Force/unit width N/mm
1	-10, 3	51.86	122.58
2	-10, 9	155.59	367.76
3	-10, 15	259.32	612.94
4	-10, 6	103.73	245.18
5	-10, 12	207.46	490.36
6	0, 6	76.48	180.77
7	0, 12	152.96	361.54
8	0, 3	38.24	90.39
9	0, 9	114.72	271.16
10	0, 15	191.21	451.95
11	10, 9	85.51	202.11
12	10, 15	142.52	336.87
13	10, 6	57.00	134.73
14	10, 12	114.01	269.48
15	10, 3	28.50	67.36
16	20, 12	85.22	201.43
17	20, 3	21.31	50.37
18	20, 9	63.92	151.08
19	20, 15	106.53	251.80
20	20, 6	42.61	100.71
21	30, 15	79.20	187.20
22	30, 6	31.68	74.88
23	30, 12	63.36	149.76
24	30, 3	15.84	37.44
25	30, 9	47.52	112.32

APPENDIX XIIJ

GROUPED VALUES FOR EVANS' THEORY

	Bunter Sandstone Force/unit width N/mm	Magnesian Limestone Force/unit width N/mm
$P_{1\alpha}$	155.59	367.76
$P_{2\alpha}$	114.72	271.16
$P_{3\alpha}$	85.51	202.11
$P_{4\alpha}$	63.92	151.08
$P_{5\alpha}$	47.52	112.32
P_{1d}	31.15	73.63
P_{2d}	62.30	147.25
P_{3d}	93.45	220.88
P_{4d}	124.60	294.51
P_{5d}	155.76	368.16

APPENDIX XIIK

THEORETICAL AND MEASURED VALUES OF CUTTING FORCE - EMPIRICAL RELATIONSHIPS BASED ON EVANS' THEORY

Test No	Levels of α, w, d	Bunter Sandstone		Magnesian Limestone	
		F_C (kN)	F_C' (kN)	F_C (kN)	F_C' (kN)
1	-10, 10, 3	1.236	1.380	3.895	6.020
2	-10, 20, 9	3.759	5.070	17.756	19.211
3	-10, 30, 15	8.393	10.000	22.540	36.390
4	-10, 40, 6	3.293	4.620	8.338	16.292
5	-10, 50, 12	6.837	10.481	23.847	36.105
6	0, 20, 6	2.217	2.492	9.813	9.443
7	0, 30, 12	5.441	5.899	12.791	21.465
8	0, 40, 3	2.186	1.703	6.414	6.011
9	0, 50, 9	3.214	5.796	23.308	19.966
10	0, 10, 15	4.151	5.088	17.418	22.195
11	10, 30, 9	2.792	3.298	16.435	11.999
12	10, 40, 15	5.300	6.348	20.173	22.402
13	10, 50, 6	3.558	2.880	12.458	9.920
14	10, 10, 12	2.567	3.033	9.717	13.234
15	10, 20, 3	1.046	0.929	4.395	3.519
16	20, 40, 12	4.367	3.796	16.785	13.395
17	20, 50, 3	1.765	1.077	8.435	3.709
18	20, 10, 9	1.464	1.701	9.571	7.420
19	20, 20, 15	3.394	3.471	13.337	13.154
20	20, 30, 6	1.988	1.643	10.031	5.979
21	30, 50, 15	3.778	4.001	12.147	13.784
22	30, 10, 6	1.001	0.843	5.221	3.677
23	30, 20, 12	2.388	2.065	15.305	7.823
24	30, 30, 3	1.389	0.611	7.057	2.223
25	30, 40, 9	2.400	2.117	12.101	7.469

F_C is the measured value of Peak Cutting Force.

F_C' is the theoretical value of Peak Cutting Force.

APPENDIX XIIL

GROUPED DATA BASED ON APPENDIX XIIK

	Bunter Sandstone		Magnesian Limestone	
	F_C (kN) Measured	F_C (kN) Theoretical	F_C (kN) Measured	F_C (kN) Theoretical
$P_{1\alpha}$	4.70	6.31	15.28	22.80
$P_{2\alpha}$	3.44	4.20	13.95	15.82
$P_{3\alpha}$	3.05	3.30	12.64	12.21
$P_{4\alpha}$	2.60	2.34	11.63	8.73
$P_{5\alpha}$	2.19	1.93	10.37	7.00
P_{1W}	2.08	2.41	9.16	10.51
P_{2W}	2.56	2.81	12.12	10.63
P_{3W}	4.00	4.29	13.77	15.61
P_{4W}	3.51	3.72	12.76	13.11
P_{5W}	3.83	4.85	16.04	16.69
P_{1d}	1.52	1.14	6.04	4.30
P_{2d}	2.41	2.50	9.17	9.06
P_{3d}	2.73	3.60	15.83	13.21
P_{4d}	4.32	5.05	15.69	18.40
P_{5d}	5.00	5.78	17.12	21.59

APPENDIX XIII A

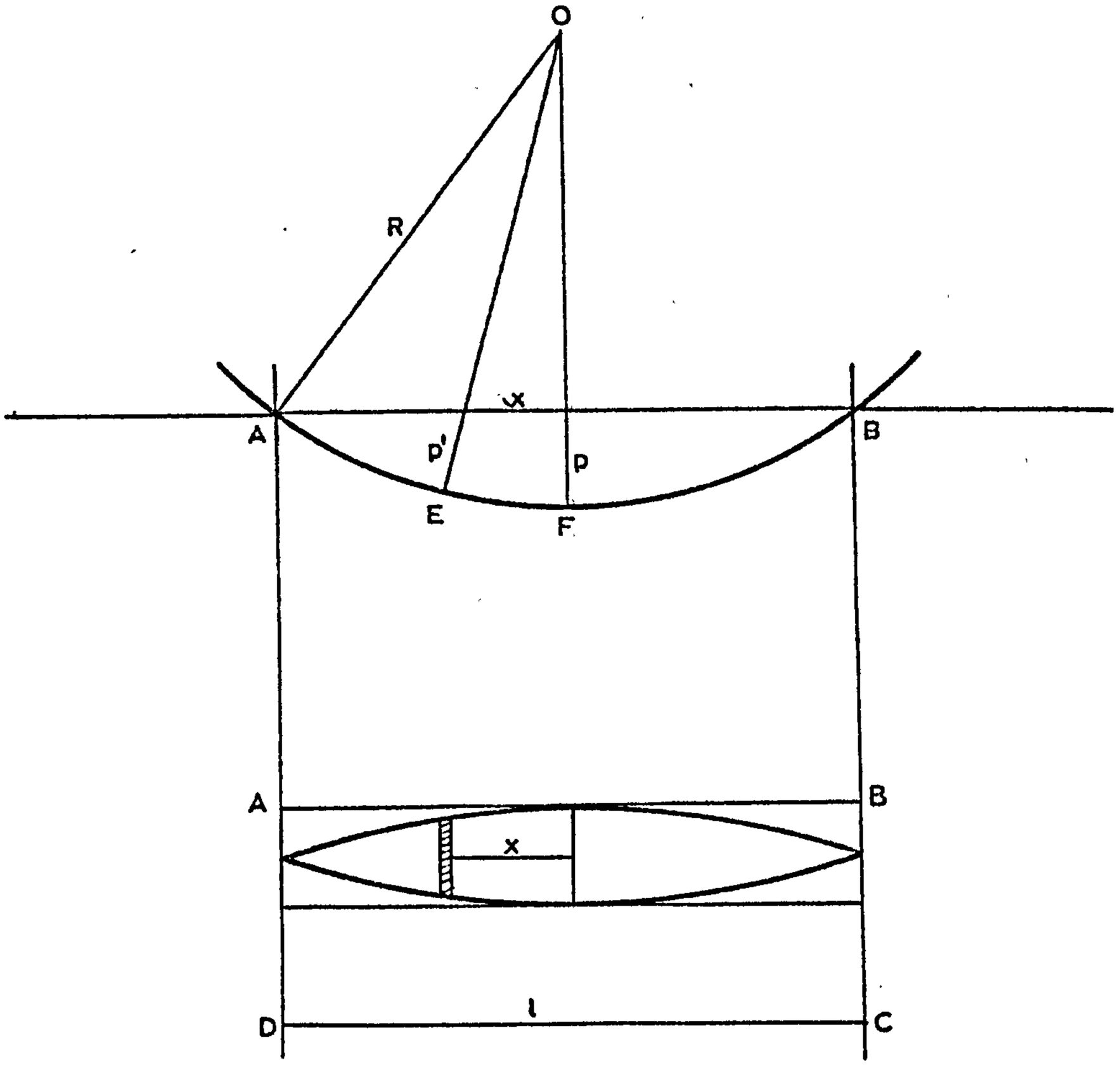

It can be seen from the above figure that

$$(R - p^1)^2 = x^2 + (R - p)^2$$

hence $p^1 = R - \sqrt{x^2 + (R - p)^2}$

Width of incision at a distance x from centre line OF = $2\ p^1 \tan \frac{\phi}{2}$

So that shaded increment of area = $2\ p^1 \tan \frac{\phi}{2}\ \delta x$

hence total area of incision = $2.2 \tan \phi/2 \int_0^{\frac{\ell}{2}} (R - x^2 + (R - p)^2)\ .\ \delta x$

If $(R - p) = a$

then using standard integrals

$$\text{Area} = 4 \tan \frac{\phi}{2} \left\{ \frac{R\ell}{2} - \frac{1}{2} \left(\frac{\ell}{2} \sqrt{a^2 + \frac{\ell^2}{4}} + a^2 \ln \left| \frac{\frac{\ell}{2} + \sqrt{\frac{\ell^2}{4} + a^2}}{a} \right| \right) \right\} \Bigg|_0^{\frac{\ell}{2}}$$

but from the geometry of the figure

$$(R - p)^2 + \frac{\ell^2}{4} = R^2$$

$$\text{Area} = 2 \tan \frac{\phi}{2} \left(\frac{R\ell}{2} - (R - p)^2 \ln \left| \frac{\frac{\ell}{2} + R}{R - p} \right| \right)$$

and by expanding the log term into a power series it can be shown that to a first approximation

$$\frac{R\ell}{2} - (R - p)^2 \ln \left| \frac{\frac{\ell}{2} + R}{R - p} \right| = \frac{2}{3} \cdot p \cdot \ell \cdot$$

APPENDIX XIIIB

THEORETICAL AND MEASURED FORCES FOR DRY BUNTER SANDSTONE

Test No	Levels of ϕ, D, p	Thrust Force		Rolling Force	
		Measured kN	Theoretical kN	Measured kN	Theoretical kN
1	60, 100, 10	28.42	34.09	6.36	11.36
2	60, 125, 6	15.35	18.22	2.65	4.09
3	60, 150, 2	5.35	3.91	0.56	0.45
4	60, 175, 8	28.96	33.32	5.12	2.27
5	60, 200, 4	13.66	12.73	1.58	1.82
6	70, 125, 8	26.78	34.12	5.50	8.82
7	70, 150, 4	13.94	13.32	1.84	2.20
8	70, 175, 10	43.31	55.97	7.80	13.78
9	70, 200, 6	29.89	28.21	3.89	4.96
10	70, 100, 2	5.77	3.86	0.71	0.55
11	80, 150, 6	29.49	29.12	4.46	5.94
12	80, 175, 2	8.11	6.14	0.72	0.66
13	80, 200, 8	34.48	51.78	5.18	10.57
14	80, 100, 4	14.12	12.94	2.11	2.64
15	80, 125, 10	57.51	56.00	10.09	16.51
16	90, 175, 4	24.14	20.59	2.41	3.15
17	90, 200, 10	71.69	85.78	9.75	19.68
18	90, 100, 6	28.82	28.04	4.86	7.08
19	90, 125, 2	8.70	6.17	0.89	0.79
20	90, 150, 8	42.19	53.06	6.30	12.60
21	100, 200, 2	13.19	9.33	0.94	0.94
22	100, 100, 8	49.06	50.90	7.75	15.01
23	100, 125, 4	27.92	20.64	3.23	3.75
24	100, 150, 10	63.11	87.76	9.06	23.45
25	100, 175, 6	43.99	44.81	5.48	8.44

APPENDIX XIIIC

THEORETICAL AND MEASURED FORCES FOR WET BUNTER SANDSTONE

Test No	Levels of ϕ, D, p	Thrust Force		Rolling Force	
		Measured kN	Theoretical kN	Measured kN	Theoretical kN
1	60, 100, 10	28.68	28.41	5.61	9.47
2	60, 125, 6	16.31	15.18	2.95	3.41
3	60, 150, 2	4.53	3.26	0.65	0.38
4	60, 175, 8	23.92	27.69	4.11	6.06
5	60, 200, 4	13.09	10.60	1.76	1.51
6	70, 125, 8	26.16	28.11	5.03	7.35
7	70, 150, 4	11.43	11.10	1.62	1.84
8	70, 175, 10	35.15	46.65	6.83	11.48
9	70, 200, 6	23.90	23.51	3.33	4.13
10	70, 100, 2	3.97	3.22	0.77	0.46
11	80, 150, 6	25.34	24.27	3.95	4.95
12	80, 175, 2	6.68	5.12	0.72	0.55
13	80, 200, 8	38.00	43.15	6.00	8.81
14	80, 100, 4	12.52	10.79	2.08	2.20
15	80, 125, 10	42.14	46.67	8.22	13.76
16	90, 175, 4	19.75	17.16	2.38	2.62
17	90, 200, 10	55.38	71.49	8.29	16.40
18	90, 100, 6	29.12	23.37	4.71	5.90
19	90, 125, 2	7.29	5.14	0.98	0.66
20	90, 150, 8	43.11	44.22	6.01	10.50
21	100, 200, 2	12.14	7.78	0.97	0.78
22	100, 100, 8	47.45	42.42	7.07	12.51
23	100, 125, 4	22.93	17.20	2.67	3.13
24	100, 150, 10	66.46	73.13	10.13	19.54
25	100, 175, 6	40.42	37.34	4.89	7.04

APPENDIX XIIID

THEORETICAL AND MEASURED FORCES FOR MAGNESIAN LIMESTONE

Test No	Levels of ϕ, D, p	Thrust Force		Rolling Force	
		Measured kN	Theoretical kN	Measured kN	Theoretical kN
1	60, 100, 7.5	35.06	38.73	12.06	11.03
2	60, 125, 4.5	23.19	20.55	5.06	3.97
3	60, 150, 1.5	6.76	4.39	0.73	0.44
4	60, 175, 6	36.96	37.46	8.96	7.06
5	60, 200, 3	15.86	14.30	2.26	1.76
6	70, 125, 6	39.26	38.12	9.65	8.56
7	70, 150, 3	18.10	14.98	2.77	2.14
8	70, 175, 7.5	58.51	63.21	14.37	13.38
9	70, 200, 4.5	31.86	31.74	5.24	4.82
10	70, 100, 1.5	8.46	4.34	1.18	0.54
11	80, 150, 4.5	37.41	32.81	6.40	5.77
12	80, 175, 1.5	9.22	6.90	0.91	0.64
13	80, 200, 6	53.53	58.33	10.63	10.25
14	80, 100, 3	18.35	14.58	3.19	2.56
15	80, 125, 7.5	54.17	63.44	15.17	16.03
16	90, 175, 3	25.87	23.14	3.18	3.06
17	90, 200, 7.5	83.65	96.78	17.35	19.10
18	90, 100, 4.5	35.67	31.68	9.03	6.88
19	90, 125, 1.5	10.29	6.93	1.01	0.76
20	90, 150, 6	56.56	59.89	12.89	12.23
21	100, 200, 1.5	13.55	10.48	1.07	0.91
22	100, 100, 6	57.73	57.67	15.47	14.57
23	100, 125, 3	28.94	23.23	3.81	3.64
24	100, 150, 7.5	85.04	92.23	22.57	22.76
25	100, 175, 4.5	58.07	50.45	7.78	8.20

APPENDIX XIIIE

GROUPED VALUES OF THRUST FORCE IN BUNTER SANDSTONE

	Dry Bunter		Wet Bunter	
	Measured	Theoretical	Measured	Theoretical
$P_{1\phi}$	18.55	20.43	17.30	17.03
$P_{2\phi}$	23.94	27.10	20.12	22.52
$P_{3\phi}$	28.74	31.20	24.94	26.00
$P_{4\phi}$	35.11	38.73	30.93	32.28
$P_{5\phi}$	39.46	42.69	37.88	35.57
P_{1D}	25.44	25.97	24.35	21.64
P_{2D}	27.25	27.03	32.97	22.46
P_{3D}	30.82	37.43	30.17	31.20
P_{4D}	29.70	32.15	25.18	26.79
P_{5D}	32.58	37.57	28.50	31.31
P_{1P}	8.22	5.88	6.92	4.90
P_{2P}	18.76	16.04	15.95	13.37
P_{3P}	29.51	26.69	27.02	24.73
P_{4P}	36.30	44.62	35.73	37.12
P_{5P}	53.01	63.92	45.56	53.27

APPENDIX XIIIF

GROUPED VALUES OF ROLLING FORCE IN BUNTER SANDSTONE

	Dry Bunter kN		Wet Bunter kN	
	Measured	Theoretical	Measured	Theoretical
$P_{1\phi}$	3.26	5.00	3.02	4.17
$P_{2\phi}$	3.95	6.06	3.52	5.05
$P_{3\phi}$	4.51	7.26	4.19	6.05
$P_{4\phi}$	4.84	8.66	4.47	7.22
$P_{5\phi}$	5.29	10.32	5.15	8.60
P_{1D}	4.36	7.33	4.05	6.11
P_{2D}	4.47	6.79	3.97	5.66
P_{3D}	4.44	8.93	4.47	7.44
P_{4D}	4.30	6.66	3.79	5.55
P_{5D}	4.27	7.59	4.07	6.33
P_{1P}	0.76	0.68	0.82	0.57
P_{2P}	2.23	2.71	2.10	2.26
P_{3P}	4.27	6.10	3.97	5.09
P_{4P}	5.97	10.85	5.65	9.05
P_{5P}	8.61	16.96	7.82	14.13

APPENDIX XIV

Several quantities are used to indicate the performance of a pick under different operational conditions.

a) Mean Cutting Force - the average force on the tool in the direction of cutting. Multiplying this by the distance cut gives the amount of work done.

b) Mean Peak Cutting Force - the average of the peak forces acting on the tool in the direction of cutting. This is relevant to the mechanical strength of the tool design and its holder.

c) Mean Normal Force - the average force acting normal to the direction of cutting, tending to push the tool into or out of the rock face. This value is the thrust required to maintain the tool at its required depth of cut.

d) Mean Peak Normal Force - the average of the peak forces acting as above.

e) Yield - the quantity of rock produced in either mass or volume per unit distance cut.

f) Spcific Energy - the work done per unit mass (or volume) of rock cut.

g) Coarseness Index - a comparative measure of the size distribution of the cut rock.

When disc and roller cutters are considered the nomenclature is somewhat different. The definition of rolling force is, however, the same as that for cutting force and similarly thrust force corresponds to normal force.